Synthesis, Antimalarial Evaluation, β-Hematin Inhibition, and *In Silico* and *In Vitro* ADMET Profiling of 4-Aminoquinoline-Hydroxypyridinone Hybrids

A thesis submitted to the University of Cape Town for the fulfillment of the requirement for the degree of Doctor of Philosophy

Warren Andrew Andayi

Supervisors: Prof. Kelly Chibale and Prof. Timothy J. Egan

September 2011

Department of Chemistry
University of Cape Town
Rondebosch, 7701,
Cape Town

ABSTRACT

With the aim of designing appropriate hybrid molecules as a strategy to fight drug resistant malaria parasites, 4-aminoquinoline-3,4-hydroxypyridinone hybrids were designed and synthesized. Their hypothesized mode of action was studied with respect to inhibition of hemozoin formation.

Precursor *N*-alkyl-3,4-hydroxypyridinones and selected gallium (III) complexes were synthesized and evaluated for *in vitro* antiplasmodial activity. The activity of the most potent *N*-alkyl-3,4-hydroxypyridinone **2h** had was IC_{50} = 2.38 μM and 1.8 μM against sensitive strain 3D7 and resistant strain K1 of *Plasmodium falciparum* respectively. *In vitro* antimalarial activity of these compounds was negated by blocking the chelator moiety via complexation with gallium (III) or protection by a benzyl group. None of these compounds inhibited β-hematin formation. Antiplasmodial activity of the combination of **2h** with chloroquine-diphosphate or dihydroartemisinin was studied using the isobologram method. The combination resulted in a synergistic effect in the K1 and the 3D7 strains, justifying the synthesis of antimalarial aminoquinoline-3,4-hydroxypyridinone hybrids.

The synthesis of the hybrid molecules involved the Michael addition of *N*-(7-chloro-4-quinolinyl)-diaminoalkanes to 3-benzyl or methoxy protected maltol or ethylmaltol, and by coupling of N-(7-chloro-4-quinolinyl)-diaminoalkane to 2-(chloromethyl)-5 (benzyloxy)-1-alkylpyridin-4-(*1H*)-one. Deprotection of the benzyl group was via hydrogenolysis or acid hydrolysis delivering the target hybrids.

The resistant strains of *P. falciparum* (K1 and W2) were more susceptible to the iron chelating hybrids. The presence of an amine group in the alkyl side chain enhanced activity against the resistant K1 strain presumably via enhanced accumulation in the parasitic food vacuole. Incorporation of a tertiary amino group enhanced antimalarial activity despite causing a decrease in β-hematin inhibition. Most of the compounds were more potent inhibitors β-hematin formation than chloroquine (IC_{50}/equiv. = 1.9μM), with

32 having the highest activity (IC_{50}/equiv. = 0.07μM). Correlation between antiplasmodial activity (against W2 or 3D7) and β-hematin inhibition was observed only for benzylated ethylmaltol/maltol derived hybrids (R^2 = 0.8). The most potent compounds against K1 and 3D7 respectively were **16** (0.08 μM and 0.007 μM); **32 (**0.001 μM and 0.123 μM); **13a** (0.03 μM and 0.07 μM) and **24a (**0.05 μM and 0.01μM). Blocking the chelator group by benzyl or methoxy protection or pre-complexation with iron (III) and gallium (III) did not negate nor alter significantly the antimalarial activity of these hybrids implying that iron abrogation is not their main mode of action. The dihydrochloride salt of Compound **16** (**16.HCl salt**) and its deprotected analogue **16a** were evaluated for *in vivo* activity in a mouse model of *P. berghei* and the percent survival observed after 15 days for animals treated with chloroquine**, 16.HCl salt** and **16a** was 80%, 40% and 0% respectively at a dosage of 2x day 50mg/kg administered intraperitoneally.

Only the ethylmaltol/maltol-derived hybrids were tested *in vitro* for CYP3A4 inhibition in the presence of testosterone as the substrate and 85% of the compounds tested showed potential to cause drug-drug interaction (IC_{50} < 10μM). *In vitro* data indicated that the protected hybrids were more potent inhibitors than their deprotected analogues, and a similar trend was predicted using *in silico* tools (AutoDock4.2.3, MoKa and Volsurf).

The predicted CYP4A4 affinity constants (K_i) correlated significantly (R^2=0.6) with the *in vitro* determined K_i values. For a number of compounds the predicted K_i values were close to the *in vitro* K_i values e.g. **16 (**K_i predicted = 0.79μM, *in vitro* K_i = 0.97μM). Significant correlations were observed between β-hematin inhibition and CYP3A4 inhibition (R^2>0.8) for the benzylated hybrids only. Some Weak hematin inhibitors were predicted to have high affinity for CYP3A4 confirming tentatively that strong hematin inhibitors are not necessarily potent CYP3A4 inhibitors. Unique docking modes in AutoDock4.2 that distinguished weak from strong CYP3A4 inhibitors were observed and from this, structural modification strategies to improve CYP3A4 inhibition profiles were proposed. Among the potent antimalarial hybrids **24a** and **13a** were predicted to have the best CYP3A4 inhibition profile hence preferable potential leads. Using experimental and

in silico predicted physicochemical data alongside the Lipinski guidelines, over 75% of the deprotected hybrids and about 30% of the benzyl protected hybrids were observed to have drug-like properties.

DECLARATION

I declare that the work in this thesis is my own unaided work submitted for the degree of Doctor of Philosophy (PhD), and it has not been submitted previously for a degree or examination at this or any other university. Relevant sources used and people that contributed are referenced and acknowledged.

……

Warren Andrew Andayi

September 2011

ACKNOWLEDGEMENTS

I am indebted to a number of people whose contribution towards this thesis was invaluable. My sincere thanks go to

To my supervisors: Prof. Kelly Chibale and Prof. Timothy Egan, for their guidance, support, patience and for teaching me professional and social etiquettes during the training.

Fellow group members from the Chibale's (medicinal chemistry) and Egan's (bioinorganic and bioanalytical) groups at the University of Cape Town for their support, encouragement and company in the laboratory, especially my friends Samkele Nsumiwa, Matshawendile Tukhulula, Dr Mahajan Aman, Dr. Dennis Ongarora, Dr. Eric Guantai among others. Many thanks to the people who have taught me and supported in upholding good laboratory practices, Dr. Aloysius Nchinda (Chief scientific officer Chibale's group) as well as Dr. Margaret Blackie and Dr Fredrick Doulle who at one point or another acted as scientific officers in the same group..

The University of Cape Town, in particular the staff, students in the departments of chemistry, pharmacology and botany.

Dr. Grace Mugumbate for teaching me how to use computational tools for *in silico* experiments. Dr. Khanyile Ncokazi for training and helping me to perform the phiβ-hematin inhibition assays. Noel Hendricks and Pete Roberts for running the NMR analyses, Pierro Benincasa for performing the microanalysis and low resolution mass spectrometry. The staff at botany department for allowing us to use their UV plate reader for β-hematin inhibition assay when ours had broken down. Staff and students at Professor Pete Smith's laboratory at the department of pharmacology, for performing the antiplasmodial tests against D10 and Dd2 strains.

Prof. Philip Rosenthal and Jiri Gut of the Department of Medicine San Francisco general Hospital, University of California, San Francisco, for antiplasmodial *in vitro* tests (against W2 and 3D7) and *in vivo* tests (against *P. berghei*). The staff at the London School of Hygiene and Tropical Medicine, for performing antiplasmodial tests against K1 and 3D7 strains. Roslyn Thelingwani for performing the solubility determinations, log D determination and CYP3A4 inhibition assay at the African Institute of Biomedical Science and Technology AiBST, Harare and Dr. Moolman of the Stellenbosch University for mass spectroscopy.

I am grateful to the National Research foundation (NRF) SARchI, Merck (Merck medicinal chemistry bursary), Oppenheimer memorial Trust, South African Malaria Initiative (SAMI), UCT (UCT conference travel grant) for financial support.

Lastly but not least to my family, my parents Shem Andayi and Anne Mulaa and my love Florence Njeri. Above all, I thank God for everything.

This thesis is dedicated to Cecilia Mulaa Andayi and Neville Davies Andayi -Papi

ABBREVIATIONS

ADMET	Absorption, distribution, metabolism, excretion and toxicity
AQ	amodiaquine
Bn	benzyl
CQ	chloroquine
CYPs	cytochrome P450 isozymes
DFO	desferroxamine
DFP	deferiprone
DHA	dihydroartemisinin
DNA	deoxyribonucleic acid
DMF	dimethyl formamide
DMSO	dimethylsulphoxide
DV	digestive vacuole
Equiv.	equivalents
EtOAc	ethylacetate
EtOH	ethanol
FGI	functional group interconversion
FV	food vacuole
HEPES	4-(2-hydroxyethyl)-1-piperazineethanesulphonic acid
3,4-HPOs	3,4-hydroxypyridinones
HR-MS	high resolution mass spectroscopy
IC_{50}	concentration needed to cause 50% inhibition in activity or growth
IR	infra red
MeOH	methanol
MHz	mega hertz
Min.	minutes
MMV	malaria medicine venture
m.p	melting point
MS	mass spectroscopy

m/z	mass to charge ratio
PD/PK	pharmacodynamics/pharmacokinetics
PfCRT	*Plasmodium falciparum* Chloroquine Resistance Transporter
PK/Tox	pharmacokinetics/toxicity
R_f	ratio of movement of solute to solvent in thin layer chromatography
R_t	retention time
RPMI 1640	a cell culture medium (Seromed, Munich)
SP	sulphadoxine-pyrimethamine
S_N	nucleophilic substitution reaction
THF	tetrahydrofuran
UV	ultra violet
WHO	World Health Organization
QD	quinidin
QN	quinine
QSAR	quantitative structure activity relationship
UV vis.	Ultra violet spectrum visible range

Nuclear Magnetic resonance (NMR) abbreviations

Ar	aromatic
br.	broad
$CDCl_3$	deuterated chloroform
CD_3CN	deuterated acetonitrile
^{13}C NMR	carbon 13 NMR
d	doublet
dd	doublet of doublets
D_2O	deuterated water
^{1}H NMR	proton NMR
J	coupling constant
m	multiplet

MeOD	deuterated methanol
ppm	parts per million
s	singlet
δ	chemical shift in ppm
t	triplet
TMS	tetramethylsilane

Infrared (IR) abbreviations

br	broad
m	medium
s	strong
ν_{max}	maximal velocity (cm^{-1})
w	weak

PUBLICATIONS AND CONFERENCE PRESENTATIONS

Oral presentation

Andayi, A.W, Chibale K, Egan T.J, Ncokazi K.K, Smith P.J, Rosenthal, P.J, and Gut J, 3,4-hydroxypyridinone-quinoline double drugs in combating drug resistant malaria: design, synthesis and biological evaluation. Oral Presentation at the 19th International conference on chelation (ICOC) for the treatment of Thalassaemia, Cancer and other Diseases related to Metal and Free Radical Imbalance and Toxicity November 15, 2009, London, UK.

TABLE OF CONTENTS

Chapter One: Introduction

Chapter Two:.Synthesis and Characterisation

Chapter Three: Biological activity

CHAPTER ONE
INTRODUCTION

1.1 Malaria

Malaria is the most lethal human parasitic infection with over 250 million annual cases reported worldwide in 2008; of this 86% were in Africa. The World Health Organization (WHO) estimated 0.881 million deaths due to malaria worldwide of which 90% were in the African region and 4% in each of the South East Asia and eastern Mediterranean regions (WHO, 2009). The disease is particularly fatal among children under the age of five, and pregnant women. The disease which is both a consequence and a cause of poverty has been reported by Gallup and Sachs (2001) to slow down economic growth in endemic countries by about 1.3% per annum, and it costs sub-Sahara Africa US$12 billion annually in gross domestic product (The World Bank, 2007).

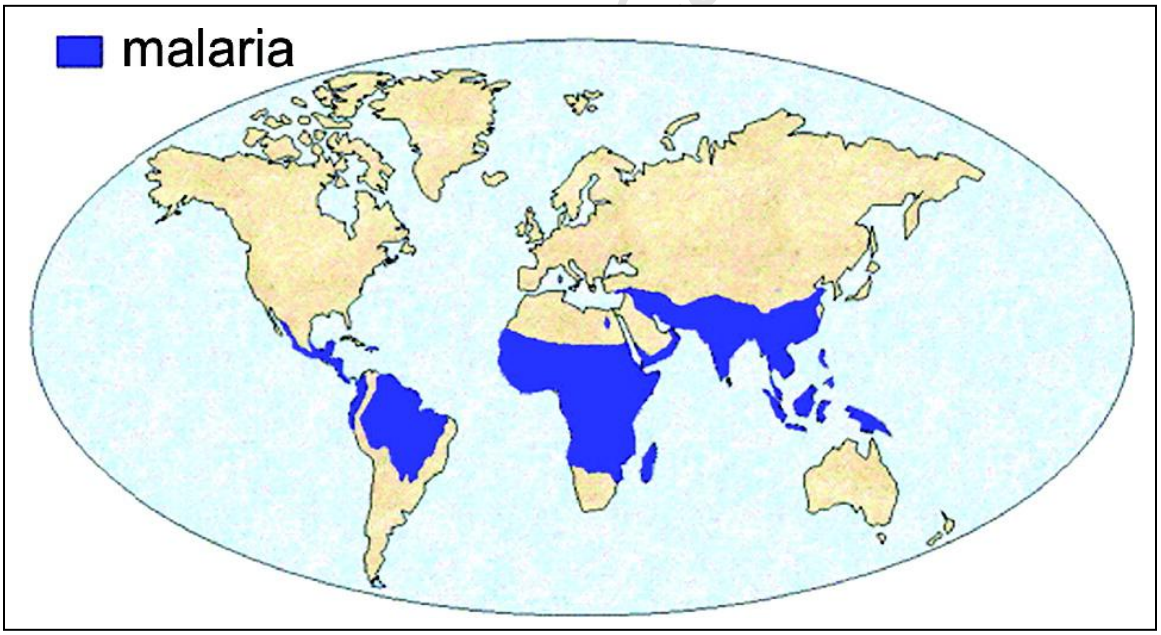

Figure 1.1: *Global distribution of malaria (CDC website 2010)*

The disease now threatens to affect over 40% of the population and even though it was primarily a tropical problem (Fig 1.1), it is now found in many temperate regions of the world (Nosten *et al.,* 1991).

The problem of endemic malaria has been exacerbated by the emergence of widespread resistance to the once effective first line treatment drugs such as chloroquine (CQ) and sulphadoxine-pyrimethamines (Wells *et al.,* 2009). Increasing resistance of *Anopheles* mosquito to insecticides has also been linked to the problem (Weissbuch and Leiserowitz, 2008). Ironically, at a time when exciting scientific advances are offering the opportunity to successfully manage previously untreatable diseases, our ability to reliably treat malaria has actually diminished over the last half century (Rosenthal and Miller, 2001).

Artemisinin based combination therapies, ACTs, have replaced the failed therapies and are the recommended first line treatments of *falciparum* malaria in all endemic countries. However, artemisinin monotherapy has been reported to be facing the prospects of declined efficacy due to the emergence of resistance. This has been reported on the Thai-Cambodian border, historically a site of emerging antimalarial resistance (Dondorp *et al.,* 2009, Wiwanitkit., 2010). With increasing resistance to available agents, intensive drug discovery efforts aimed at developing new antimalarial drugs or modifying existing ones are on going (Guantai *et al.,* 2010).

1.1.2 Biology of Malaria

Malaria is caused by protozoan parasites of the genus *Plasmodium* and is spread by the female *Anopheles* mosquito (Weissbuch and Leiserowitz, 2008). The parasites infect and destroy the red blood cells, leading to fever, severe anaemia and in some cases cerebral malaria and if untreated, death.

Human malaria is caused by five protozoan types of the genus *Plasmodium: P. falciparum, P. vivax, P. ovale P malariae and P. knowlesi. P. falciparum* is the most prevalent and virulent and it accounts for 95% of malaria related deaths (WHO, 2005). *Plasmodium* requires two hosts to complete its life cycle (Fig 1.2), namely, a mosquito vector and a vertebrate host (humans, rodents, monkeys, lizards or birds).

When a female *Anopheles* mosquito with *Plasmodium* bites humans, it transmits sporozoites into the human body. The sporozoites enter the blood circulatory system and infect liver cells within one hour (liver stage) where they develop into schizonts. After about one to two weeks, the schizonts rupture each releasing thousands of "daughter" parasites called merozoites into the blood stream (Weissbuch and Leiserowitz, 2008). The merozoites then invade the red blood cells (RBCs) inside which they mature to schizonts. Each new schizont contains several merozoites and it eventually ruptures to release the merozoites, which are then free to infect other RBCs. This process (blood stage) is responsible for the clinical symptoms of malaria. A small number of the merozoites differentiate into male and female gametocytes (sexual stages), which are ingested by a mosquito when it bites an infected person.

Inside the mosquito gut another cycle of growth and multiplication occurs, eventually resulting in sporozoites, which are liberated into the mosquito's salivary glands. From the salivary gland the parasite maybe transferred from the mosquito host to a human host via a bite.

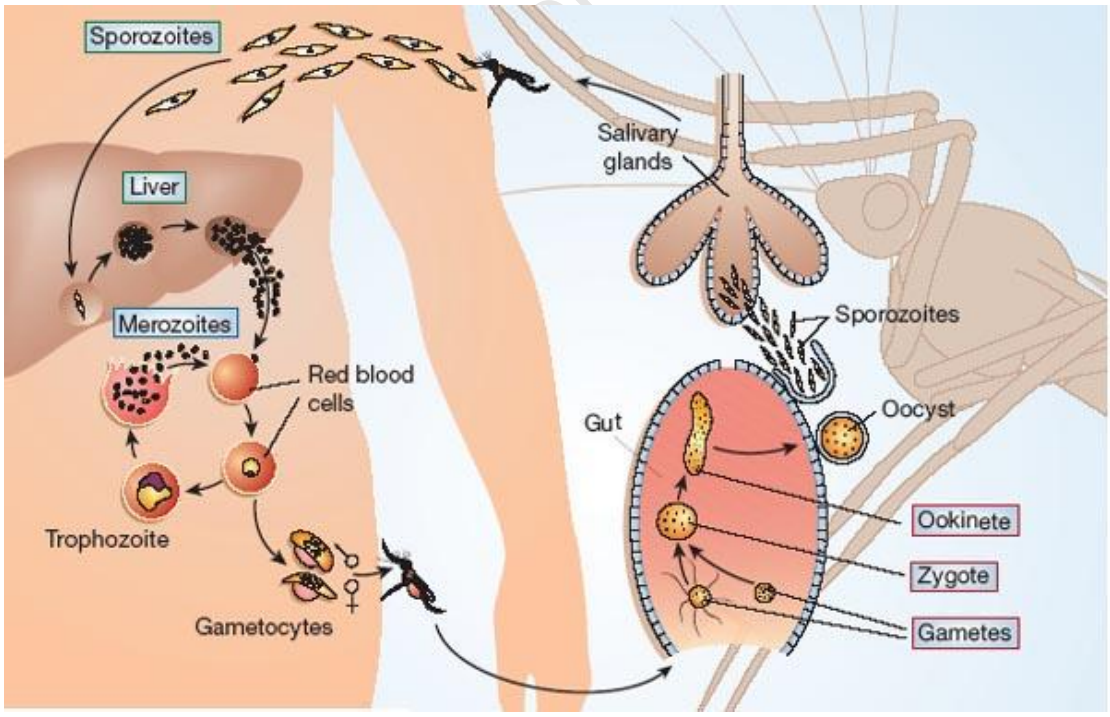

Figure 1.2: *Lifecycle of Plasmodium falciparum* (*www.tulane.edu/~wiser/malaria/mal)*

1.1.3 Clinical Symptoms of Malaria

The fever or flu-like symptoms associated with malaria are caused by the rapture of the infected RBCs to release the merozoites and starts around 8-30 days after infection. The resulting cell debris and toxins are released into the blood and this causes an immune response (fever) to promote other immune defences to combat the foreign material. The fever includes bouts of sudden chills followed by intense fever and sweating. Anaemia can result from repeated malaria parasite infections.

P. falciparum produces specific proteins that are transported and embedded in the cell membrane of the infected red blood cells. As a consequence, the erythrocytes stick to the walls of the pre-venous capillaries causing obstruction and inflammation of these vessels. This phenomenon occurs in brain vessels during cerebral malaria leading to loss of consciousness (coma and convulsions) and this is lethal if not treated immediately (Wiesner *et al.,* 2003). Other symptoms of malaria include glomerulonephritis (kidney inflammation), hypoglycaemia (low glucose levels), and accumulation of fluids in the lungs (pulmonary oedema), acute renal failure and metabolic acidosis (Winstanley, 2001; Wilairatana *et al.,* 2002). Humans in endemic areas who have survived an attack of malaria are semi-immune and in such cases the disease is characterised by headache and mild fever (Wilairatana *et al.,* 2002, Winstanley, 2001)

P. ovale and *P. vivax* can persist for up to 5 years as dormant stages in the liver (hypnozoites) and can cause clinical relapses at regular intervals. (Wiesner *et al.,* 2003)

1.1.4 Diagnosis

Diagnosis is mainly by microscopy and is used to determine the presence of the parasites in the RBCs. The method is documented in the WHO bench aids for the diagnosis of malaria (WHO, 2000). It is difficult to detect malaria in its early stages or if the parasitemia is low. The use of the polymerase chain reaction makes diagnosis accurate,

and the method works by detecting the replicating *Plasmodium* proteins or genetic material in a human host's blood.

1.2 Hemoglobin Catabolism in the *Plasmodium*

Haemoglobin is imported in transport vesicles into a specialised compartment in the parasite; the food vacuole FV, where it is degraded by four types of proteolytic enzymes (Fig. 1.3). The enzymes include four aspartic proteases plasmepsin I, II, IV and histoaspartic protease HAP (Omara-Opyene *et al.,* 2004), three cysteine proteases falcipain 1, 2 and 3 (Rosenthal *et al.,* 2002) and a zinc metalloproteases falcilysin (Banerjee and Goldberg, 2001).

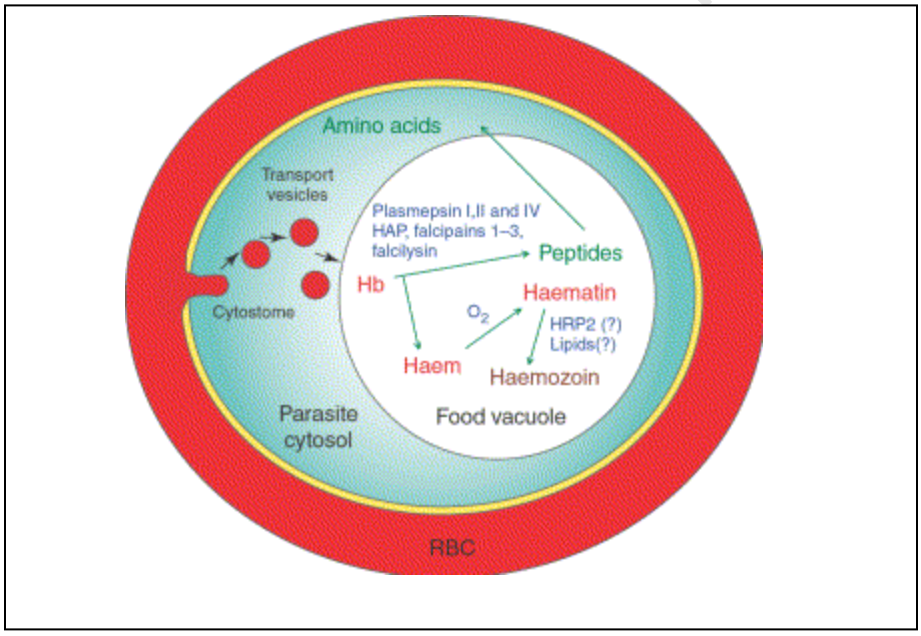

Figure 1.3: *Uptake and Degradation of haemoglobin by the parasite inside the RBC. Adapted from Egan, (2003)*

The FV is an acidic (pH 5.0-5.4) degradative organelle optimised for haemoglobin catabolism (Banerjee and Goldberg, 2001, Krogstad *et al.,* 1985, Yayon *et al*., 1984). It is a site of acidification, proteolysis, peptide transport, haemozoin formation, detoxification of oxygen radicals and quinoline antimalarial action.

During development inside the RBC, *P. falciparum* digests between 60-80% of the available haemoglobin in the FV (Egan *et al.,* 2002, Krogstad *et al.,* 1985, Hayward *et al.,* 2006). The digestion results in smaller peptides and free haem [Fe^{2+}-protoporphyrin IX] or [Fe(II)-PPIX] (Weissbuch and Leiserowitz, 2008). Fe(II)PPIX is released into an aqueous environment where the metal centre is irreversibly oxidised to Fe (III) presumably by molecular oxygen (de Villiers and Egan, 2009) to give HO-/H_2O-Fe(III)PPIX also referred to as hydroxo/aqua ferritoprotoporphyrin IX or haematin, which is toxic to the parasite (Chou *et al*., 1980).

Though insoluble in the acidic aqueous environment, haematin is soluble in a lipid environment and as such causes lipid peroxidation and membrane damage. Vertebrates detoxify haematin by catabolism using the haem oxygenase, which *P falciparum* lacks (Banerjee and Goldberg, 2001). The parasite detoxifies haematin by sequestering the free haematin into a microcrystalline form known as haemozoin or the malaria pigment (Brown 1911). The compact insoluble haemozoin has decreased pro-oxidant capability and hence is non toxic to the parasite (Oliveira *et al.,* 2002). It has been demonstrated that at least 95% of the haem released in the parasite is converted to haemozoin (Egan, 2008)

1.2.1 Mechanism of Haemozoin Formation

Haemozoin has been discovered in other blood feeding organisms including the insect *Rhodnius prolixus* ,(Oliveira *et al.,* 1999), helminth worms *Schistosoma mansoni* the causative agent for bilharzias (Oliveira *et al.,* 2000, Chen *et al.,* 2001), *Echinostoma trivolvis* (Pisciotta *et al.,* 2005) and the bird infecting protozoan *Haemoproteus columbae* (Chen *et al.,* 2001). The Figure below shows some of the haemozoin crystals retrieved from these organisms (Fig 1.4).

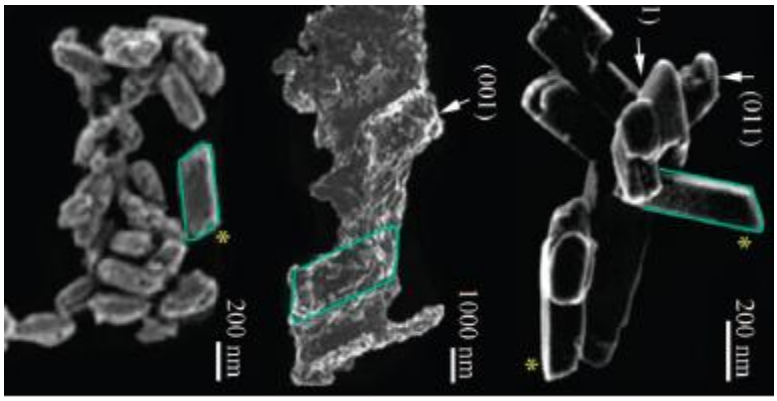

A B C

Figure 1.4: *Field emission inlens scanning electron microscopy micrographs of haemozoin purified from (A) Hemoproteus columbae (B) S. mansoni (C) P. falciparum (Buller et al., 2002)*

A primary cause of the re-emergence of malaria is a consequence of developing parasite resistance to antimalarial drugs in particular some of the widely used synthetic quinolines. Several workers have shown that antimalarial quinolines act by binding to haemozoin crystal faces, which would inhibit their growth and result in a build up of the toxic haematin and thus death of the parasite (Weissbuch and Leiserowitz, 2008). Thus, understanding the mechanisms of haemozoin formation *in vivo* and under biomimetic conditions is important in elucidating the modes of action of quinoline antimalarials.

Haemozoin is chemically and structurally identical to a synthetic haematin product called β-haematin (Slater *et al.,* 1999, Bohle *et al.,* 1997), which is a cyclic dimer of Fe(III)PPIX (Pagola *et al*., 2000). The dimer's structure consists of reciprocal coordination of the ionised haem-propionate side chain of one haem to the iron centre of the other haem (Fig. 1.5). CQ and structurally related antimalarial compounds are known to inhibit β-haematin and evidence shows that by the same mechanism these drugs exert their antimalarial activity by inhibiting haemozoin formation in the intraerythrocytic parasite. (Egan and Ncokazi, 2005, Sullivan *et al.,* 2002, Kaschula *et al.,* 2002, Dorn *et al.,* 1998, Egan *et al.,* 1994)

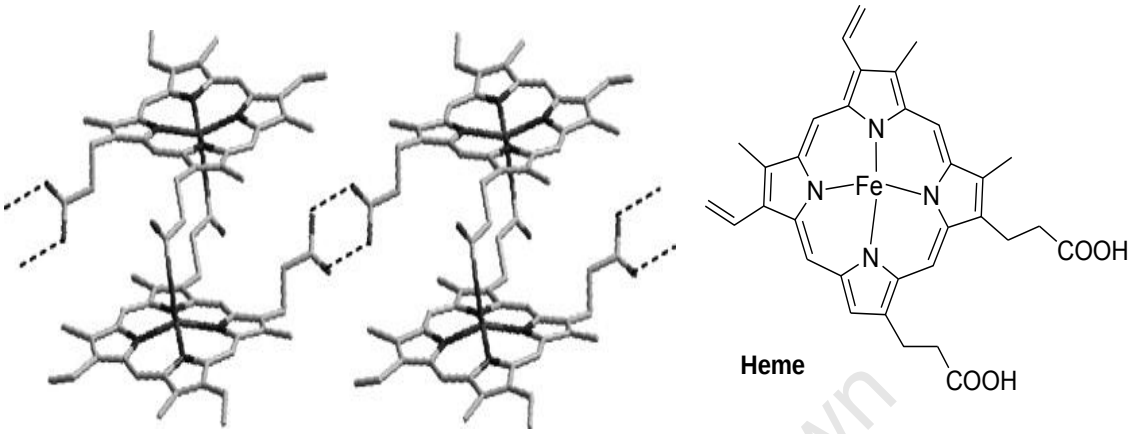

Figure 1.5: *Structure of β-haematin dimer on the left (Egan, 2008) and haem on the right*

The formation of β-haematin from haematin appears to be a thermodynamically spontaneous process under acidic conditions and requires the presence of a suitable catalyst eg acetic acid (Egan and Kanyile, 2005). Evidence from electron microscopy of three different haemozoin forming organisms *P. falciparum, S. mansoni* and *R. prolixus* provide strong evidence that the formation occurs in close association with lipids (Egan, 2008; Oliveira *et al*., 2005; Soares *et al*., 2007; Pisciotta *et al.,* 2007; Coppeus *et al.,* 2005)

Indeed in the case of *P. falciparum* and *S. mansoni,* the formation occurs within lipid bodies. Biomimetic studies by Hoang *et al* (2010) strongly support the hypothesis that haemozoin formation is caused by lipid droplets/nanospheres in the FV of *P. falciparum*. Supported by insights from molecular dynamic simulations, it has been suggested that the lipid/aqueous interface that these bodies present is key to the formation of haemozoin crystals (Egan, 2006)

1.3 Malaria Chemotherapy

Several antimalarial drugs are in use for the treatment or prevention of the disease. The drugs are classified according to their molecular structure and their mode of action. The most important antimalarials currently in clinical use include quinolines, antifolates, antibiotics, endoperoxides related to artemisinin and the hydroxynaphthoquinone atovaquone (Table 1.1)

Table 1.1. The *main antimalarial drugs in current use.*

Structure and name	Target	Drawbacks
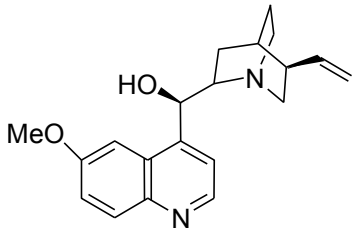 Quinine	Heme detoxification pathway (Egan, 2008)	Cannot control all stages of malaria
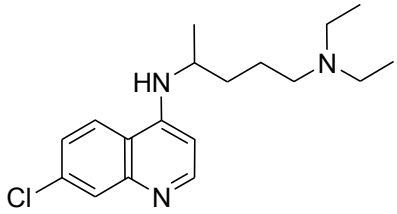 Chloroquine	Heme detoxification pathway (Egan, 2008)	Widespread resistance
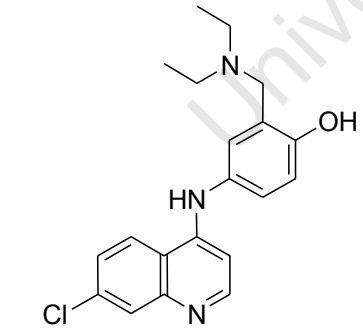 Amodiaquine	Heme detoxification pathway (Egan, 2008)	Cross resistance with CQ (Petersen, 2011)

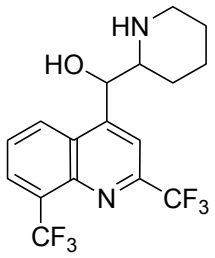 Mefloquine	unknown	Neuropsychiatric disorders
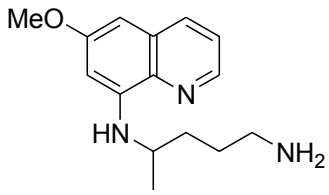 Primaquine	unknown	Resistance unknown Hemolysis in G6PD deficient individuals (Brueckner *et al*., 2008).
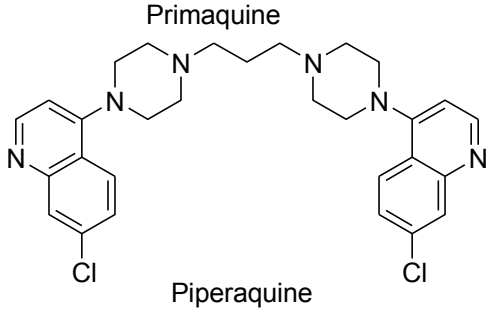 Piperaquine	unknown	Resistance when used in monotherapy
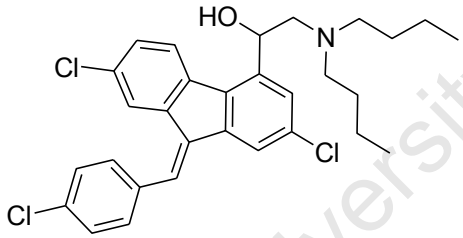 Lumefantrine	unknown	No high level resistance reported
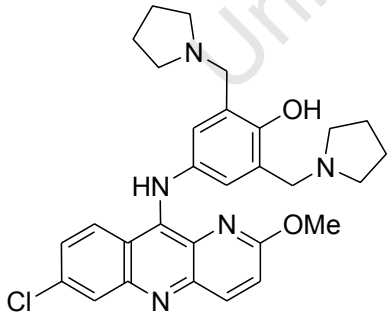 pyronaridine	unknown	No cross resistance with other drugs

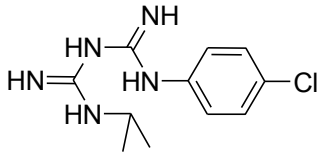 proguanil	Folate biosynthesis (Petersen *et al* 2011)	
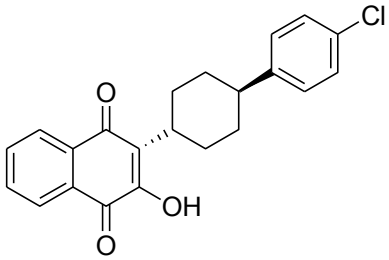 Atovaquone	Parasite mitochondria functions i.e. the cytochrome bc_1 complex (Painter *et al.,* 2007)	Resistance when used in monotherapy
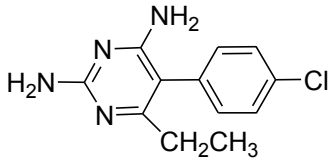 pyrimethamine	Folate biosynthesis	Resistance
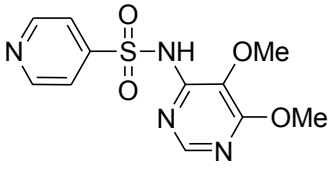 sulfadoxine	Folate biosynthesis (Petersen *et al*., 2011)	Resistance
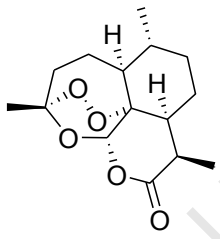 Artemisinin 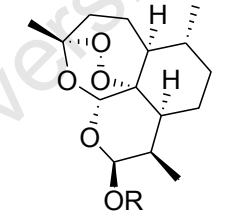 Artemisinin derivat	Alkylation of parasitic biomolecules (Bray *et al*., 2005; Meunier and Robert 2010)	Short plasma half life Recrudescence and resistance possibly emerging

.

1.3.1 Aminoquinolines and Arylmethanols

The first widely used antimalarial drug was quinine a natural product extracted from the bark of the tree *Cinchona calisaya* and it is classified as a quinoline methanol. Quinine

acts primarily as a blood schizonticide and has little effect on sporozoites (pre-erythrocytic) forms of malaria parasites hence cannot control all stages of malaria.

Arylmethanols were developed as alternatives to amodiaquine, which was considered to have some toxic side effects; they include mefloquine, halofantrine, pyronaridine, piperaquine and lumefantrine (Fig. 1.6), and are used to treat uncomplicated malaria (Wells *et al.,* 2010). All the aryl amino alcohols have side effects eg neuropsychiatric problems and arrhythmia associated with the use of mefloquine and halofantrine respectively (Wiesner *et al.,* 2003).

The 4-aminoquinolines have been proven to be the most successful class of compounds for malaria treatment and prophylaxis because they are cheap, easy to synthesize, have acceptable toxicity profiles, are well tolerated and effective against a number of chloroquine-resistant strains (O'Neill *et al.,* 1998).

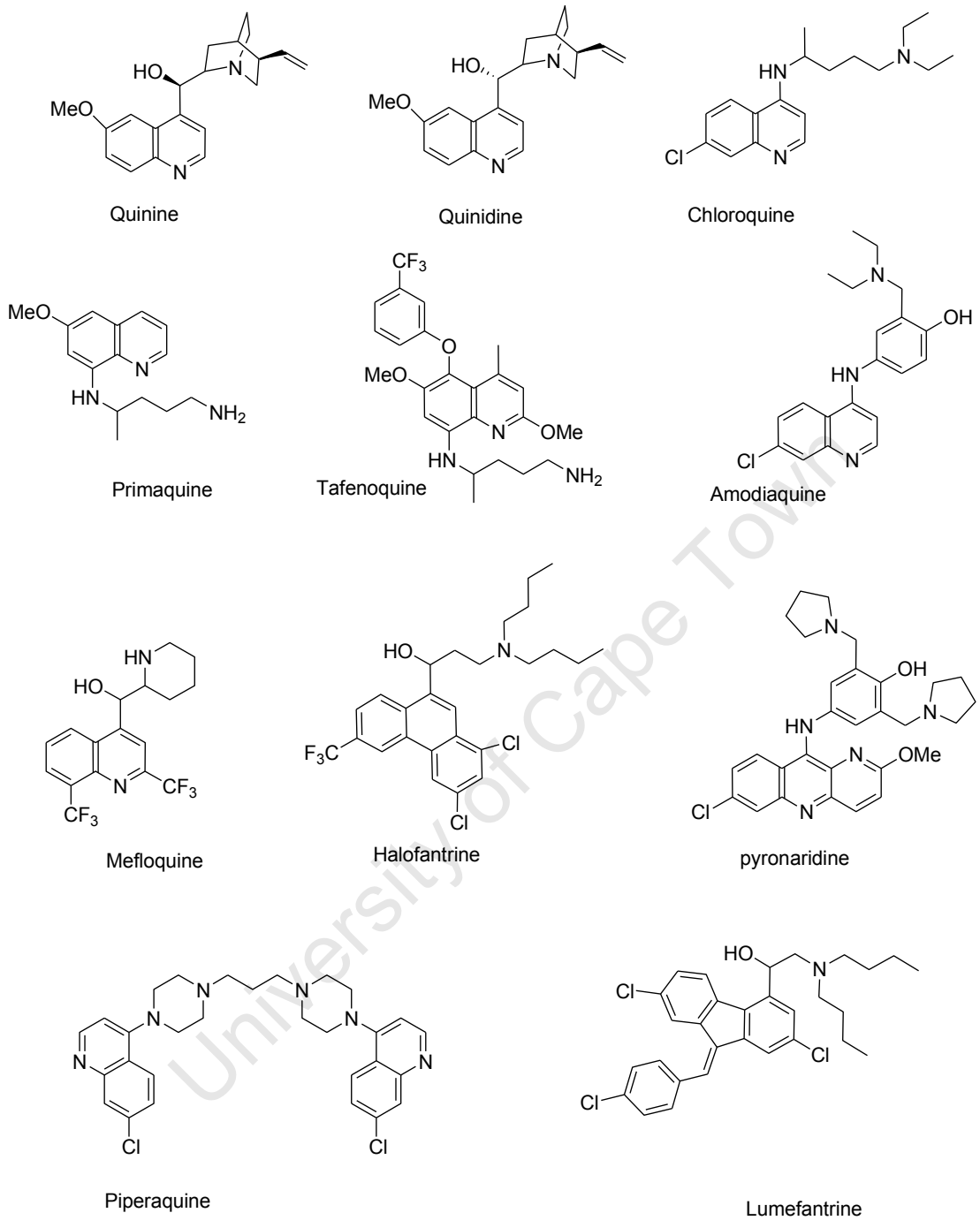

Figure 1.6: *Chemical structures of aminoquinoline and arylmethanols*

1.3.2 Antifolates

These antimalarials act by inhibiting the enzymes involved in folate metabolism in the parasite. The antifolates include sulfadoxine, pyrimethamine, commonly called SP drugs, and proguanil (Fig. 1.7). SP combination therapy has emerged as a cheap and effective drug against chloroquine-resistant strains of *P. falciparum* (Oketch-Rabah, 1996). However, excess use has caused development of resistance [Wiesner *et al.,* 2003]. Proguanil was developed during the Second World War by British scientists and later became the template for the synthesis of pyrimethamine. For effectiveness, proguanil is combined with chloroquine (Wiesner *et al.,* 2003) or with atovaquone [Malarone®] (Wells *et al.,* 2010).

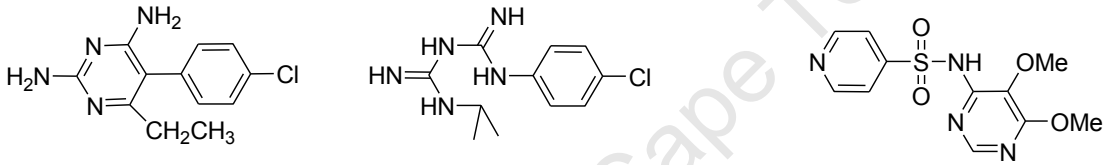

Figure 1.7: *Chemical structures of Antifolates*

1.3.3 Artemisinin Derivatives

The development of resistance and toxic side effects of some of the synthetic antimalarial drugs rejuvenated the interest in searching for antimalarials from natural sources. This is exemplified by the discovery of the sesquiterpene lactone artemisinin from the Chinese medicinal plant *Artemisia annua* (Asteraceae). The semi-synthetic artemisinin derivatives include artemether, arteether, artelinic acid, artelinate and artesunate (Fig. 1.8). Artemisinin and its derivatives are metabolized to dihydroartemisinin DHA, the main bioactive molecule. (Meshnick, 2002; Wiesner *et al.,* 2003)

This class of compounds acts faster than all the rest of the antimalarial drugs with an approximate parasite and fever clearance time of 32 hours, in contrast to 2-3 days required for conventional antimalarial drugs to resolve symptoms (Meshnick, 1998;

Price, 2000). Artemisinins are associated with high rates of recrudescence (treatment failures) when used in monotherapy. (Wongsrichanalai *et al.,* 2000)

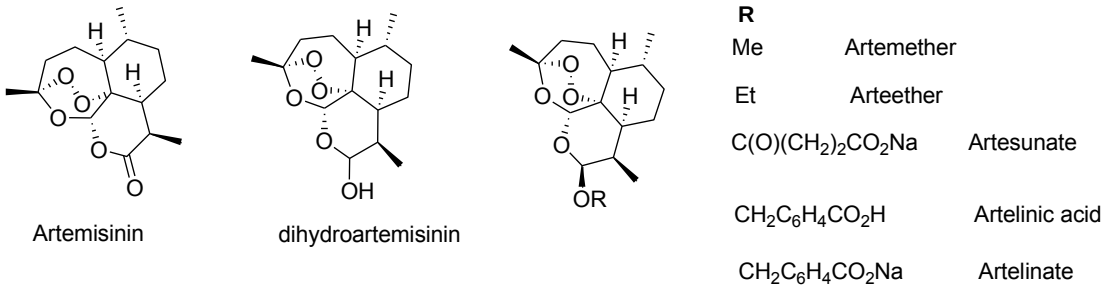

Figure 1.8: *Chemical structures of artemisinins*

Recrudescence occurs because of the rapid clearance of the drug from the blood stream (shorter plasma half life). To correct this, artemisinins are used in combination with other antimalarials that have longer plasma half life for example mefloquine– artesunate, artemether –lumefantrine combinations.

Some derivatives of artemisinin such as artelinic acid and its sodium salts have been synthesized to increase the plasma half-life of the artemisinins (Wilairatana, *et al.,* 2002; Meshnick, 2002; Wongsrichanalai *et al.,* 2001; Borsnick *et al.,* 2002) Much research is still going on with the sole purpose of generating more stable, less neurotoxic, simpler, more soluble and highly bioavailable derivatives of artemisinin (Oketch-Rabah, 1996; WHO, 1996; Ekthawatchai *et al.,* 2001).

1.3.4 Antibiotics

Several antibiotics that are known to be antibacterial act as antimalarials. An example is the tetracyclines such as doxycycline and tetracycline (Fig. 1.9). Antibiotics are applied as prophylactics, or in combination with other antimalarial drugs for the treatment. In practice doxycycline is the most frequently used antibiotic in antimalarial therapy, either on its own as a prophylactic or in combination with quinine or artesunate for treatment of multi-drug resistance (Wiesner *et al.,* 2003). Other commonly used antibiotics are clindamycin and azithromycin, with the latter being an effective prophylactic against *P.*

vivax (Wiesner *et. al.,* 2003; Taylor *et al.,* 1999), with clindamycin being the one recommended for expectant women and young children (Wiesner *et al.,* 2003)

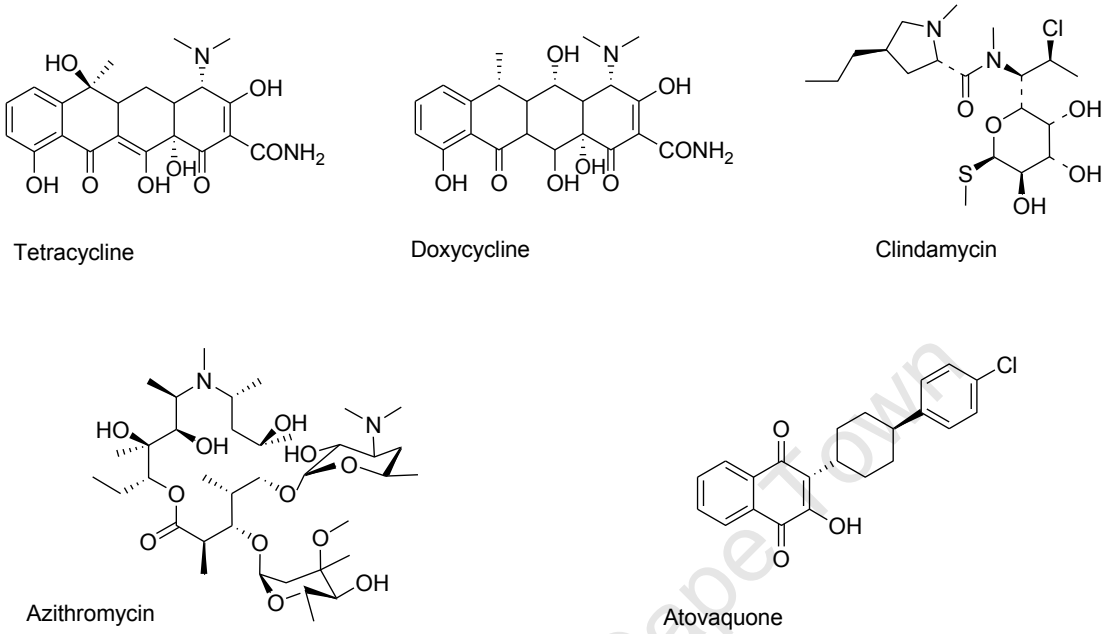

Figure 1.9: *Chemical structures of Antiplasmodial Antibiotics and Atovaquone*

Furthermore these antibiotics are under investigation for combination therapy with known antimalarial drugs. For instance combinations of oral quinine and antibiotics have been proposed in regions with declining quinine sensitivity. Proposals under investigation include quinine–clindamycin and quinine–azithromycin regimens in Africa, and the 7-day quinine–tetracycline regimen in Thai-Burma (Philippe and Milller, 2002)

1.4 Approaches to Discovery of New Antimalarial agents

The discovery of new antimalarial agents is important in the fight against drug resistance. Six approaches to discovery of new antimalarial agents have been identified namely combination therapy, structural modification of old drugs, use of natural products and their derivatives, use of compounds active against other diseases and use of resistance reversers and the use of compounds against new parasitic targets. Globally a number antimalarials have been developed using the above mentioned strategies, and most are in

the clinical phases (Olliaro and Wells 2009; Wells *et al.,* 2010). The majour one are depicted in Table 1.2.

Table 1.2. *Global malaria development pipeline of new antimalarial combinations and chemical entities by 2009.*

Derivative/active ingredient	Commercial name	Clinical phase and reference
Ozonide or artificial peroxide	OZ 439	II (Charman *et al.,* 2011)
4'-fluoro-*N*-tert-butylamodiaquine	Isoquine	I (O'Neil *et al.* 2009)
Tafenoquine	Tafenoquine	II (Olliaro and Wells, 2009)
A pyridone	4-pyridone	I (Olliaro and Wells 2009)
N^1 – (7- chloroquinolin-4-yl) - N^3, N^3- diethylpropane -1, 3- diamine.	AQ-13	I (Mzayek *et al,* 2007)
1, 2, 4 - trioxane	CDRI 97/78	I (O'Neil and Wells 2009)
Artemisone	Artemisone	II (Pooley *et al.,* 2011)
Fosmidomycin-clindamycin	Fosmidomycin-clindamycin	II (O'Neil and Wells 2009)
Ferroquine-artesunate	Ferroquine	II (O'Neil and Wells 2009)
1,12-Bis[5-(2-hydroxyethyl)-4-methyl-1,3-thiazol-3-ium]dodecane dibromide	SAR 97276	II (Margout *et al.,* 2009)
Methylene blue and amodiaquine	Methylene blue-amodiaquine	II (O'Neil and Wells 2009)
Tinidazole	Tinidazole	II (O'Neil and Wells 2009)
Dihydroartemisinin-piperaquine	Euratesim	III (O'Neil and Wells 2009)
Dihydroartemisinin-pyronaridine	Pyramax	III (O'Neil and Wells 2009)
Artesunate -mefloquine	ASMQ	III (O'Neil and Wells 2009)
Azithromycin-Chloroquine	Azithromycin-Chloroquine	III (O'Neil and Wells 2009)
Arterolane-piperaquine	Arterolane	III (Vennerstrom *et al*., 2011)
Arthemether-lumefantrine	Coartem D	Approved in 2009 (O'Neil and Wells 2009)
Artesunate - amodiaquine	Coarsucam	Approved in 2008 (O'Neil and Wells 2009)

The use of combination therapy is currently mandated by the WHO (WHO, 2001), as the best way to counter resistance. This is the only viable method for restoring or maintaining usefulness of antifolates and atovaquone, where resistance arises from mutations in the target proteins themselves (Egan and Kaschula, 2007). Evidence shows that combination therapies of drugs with different resistance mechanisms greatly reduces the chances of mutants resistant to any of the individual drugs surviving (White 1999) hence potent and long lasting combinations must constitute drugs that act by different modes and have different resistance mechanisms (White 1999, Berenbaum, 1977)

Examples of combination therapies in current use include suphadoxine-pyrimethamine (SP), atovaquone-proguanil (malarone®), chlorproguanil/dapsone (Lapdap ®), mefloquine-artesunate, ®), azithromycin-CQ with the latter being in phase three of clinical trials. Amodiaquine-sulphadoxine-pyrimethamine has shown encouraging clinical activity (Sendagire *et al.,* 2005). Non artemisinin combination therapies have been important to counteract resistance to artemisinin (Ohrt *et al.,* 2002, Dunne *et al.,* 2005) Fixed dose artemisinin combination therapies ACTs available or in late stage development include lumefantrine/artemether (Coartem), artesunate-pyronaridine (pyramax®), dihydroartemisin/piperaquine (eurarte sim), artesunate–amodiaquine (coarsucam®), artesunate-mefloquine (ASMQ), CQ-artemisisnin and CQ-azithromycin(Wells, 2010, MMV 2011; Weissbuch and Leiserowitz 2008).

Many of the current antimalarial agents were developed via new analogues of existing antimalarial drugs. CQ, mefloquine and primaquine were developed as synthetic analogues of quinine and the analogues have proven to be better against resistant strains of plasmodia than the parent drug (Rosenthal and Miller, 2001). Lumefantrine and pyronaridine were developed through such a strategy. New synthetic endoperoxides related to artemisinin have proven to be more potent than artemisinin (Wells *et al.,* 2010). Natural products and their derivatives present another major strategy. This method has identified the most important drugs currently available to treat severe *P. falciparum* malaria i.e. quinine and artemisinin (Rosenthal and Miller, Vipan *et al.,* 2010). The

approach involves screening plant extracts and the potential drugs isolated from these extracts.

The use of compounds active against other diseases is a viable strategy for discovery of new antimalarials. Folate inhibitors and other antibiotics were developed for their antibacterial activity and later found to be active against malaria eg doxycycline, azithromycin and atovaquone (Rosenthal and Miller, 2001). Iron chelators which were designed and used in treatment of iron overload were found to have antimalarial activity (Mabeza *et al.,* 1999; Weinberg *et al.,* 2009).

Combining effective antimalarial agents with compounds that reverse parasite resistance to these agents (resistance reversers or "chemosensitizers") is an important strategy. The activity of CQ against resistant parasites has been enhanced by a number of compounds including verapamil, despiramine, and chlorpheniramine (Martin *et al.,* 1987, Basco *et al.,* 1994, Bitonti *et al.,* 1988) *in vitro*, in animal models and in man. The mechanisms of these chemosensitizers is unclear although many appear to work by enhancing the accumulation of CQ (Bray and Ward 1998), or by interfering with the transmembrane proteins involved in drug efflux or uptake (Henry *et al.,* 2006). Some reversers are known to clearly increase drug susceptibility in CQ resistant parasites and not in sensitive ones (Millet *et al.,* 2004). The resistance reversers belong to different pharmacological classes such as calcium ion channel blockers, tricyclic antidepressants, antipsychotic calmodulin antagonists, histamine receptor antagonists and antifungals. In deed CQ-resistance reversers have been identified to have the key elements of a CQ resistance reverser pharmacophore i.e. hydrogen bond acceptor and two hydrophobic aromatic rings (Egan and van Schwalkwyk, 2006; Martin *et al.,* 2010) and this is irrespective of the class of compounds it belongs to.

The use of compounds against new targets involves identification of the new targets in *P. falciparum* and subsequent discovery of compounds that act on these targets. With the recent mapping of the *P. falciparum* genome (Gardner *et al.,* 2002), it is hoped that the identification of new targets will be expedited. An example of the new targets is the

Plasmodial proteases which are appealing targets for chemotherapy because they are critical for parasite survival. These enzymes are used in haemoglobin degradation and in the rupture of the red blood cells to release the schizonts (Rosenthal, 2001). The SP drugs are known to inhibit two of the five enzymes required for the folate synthesis that is dihydrofolate reductase and dihydropteroate synthase (Hyde 2005, Bzik *et al.,* 1987, Triglia *et al.,* 1994). Aspartyl proteases (Plasmepsins I, II and V) and cysteine proteases (Falcipains 1, 2, and 3) are potential targets for antimalarials (Russo *et al.,* 2010). New permeability pathways (NPPs) are induced into the hosts cell membrane, making the latter more permeable to a variety of low molecular weight compounds required by the invading *P. falciparum* and these are potentially good drug targets (Staines *et al.,* 2005). All pathogenic protozoan parasites do not synthesize their purines *de novo* and they rely on the host for this (Sherman *et al.*, 1979), thus the identification of the purine and nucleoside transporters and purine salvage enzymes, hypoxanthine phosphoribosyltransferase, HPRT, and purine nucleoside phosphorylase, PNP) from the genome project exposes the two as new drug targets (Gessner, 2009. Sherman *et.al.,* 1979).

1.5 Haemozoin and Antimalarial Quinolines

Quinolines and other antimalarials that target haemozoin are believed to inhibit haemozoin crystal nucleation and growth (Weissbuch and Leiserowitz, 2008). Over all the absence of indisputable structural evidence of the interaction of antimalrial drugs with haem has hampered the rational design of novel compounds (de Villiers and Egan, 2009). However, two set of proposals on the interaction of antimalarials with haem have been proposed.

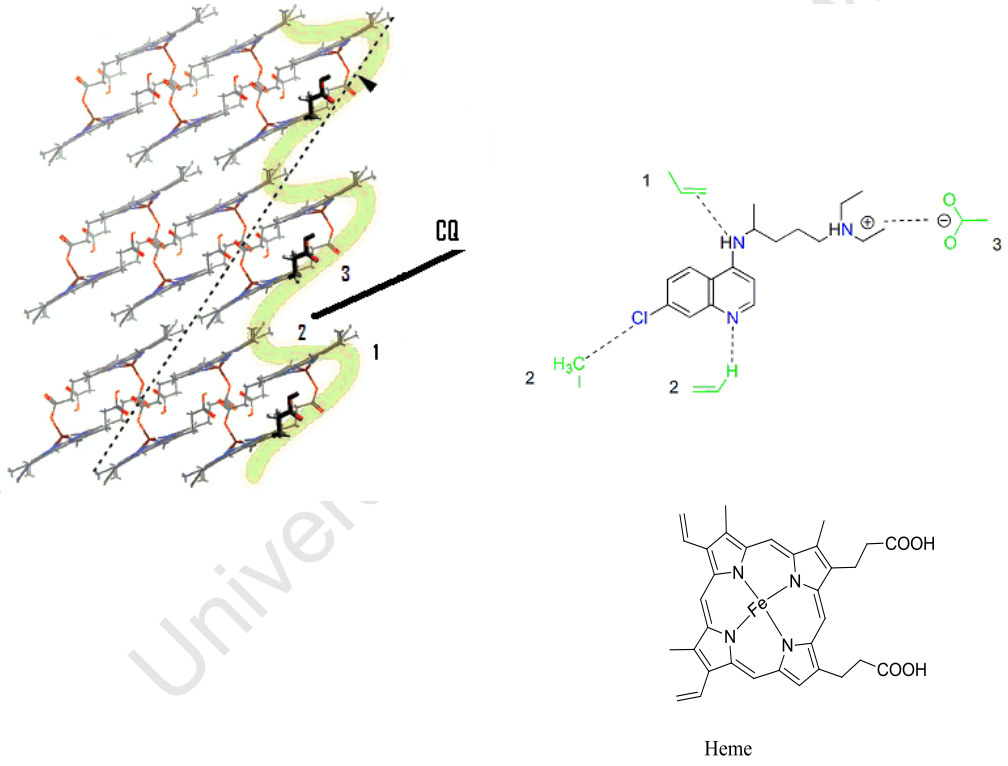

Figure 1.10: *The external morphology of the haemozoin crystal, the heme molecules are linked to each other via a carboxylate - iron coordination. The figure shows the corrugated face and its interaction with CQ as proposed by Leiserowitz and coworkers. The interaction is between the 4-amino group and the porphyrin vinyl group (**1**), the 7-Cl and the porphyrin methyl and quinoline N with the porphyrin vinyl group (**2**), and the positively charged amino group with the negatively charged propionate group forming a salt bridge (**3**).*

The first is a mechanism proposed by Buller *et al.,* 2002; it involves the interaction of the inhibiting compound (quinolines) with the fastest growing faces of the haemozoin crystal. Weissbuch and Leiserowitz (2010), further proposed that artemisinins interact with the slowest growing faces of the haemozoin crystal. On the corrugated surface of the haemozoin crystal the propionic acid and vinyl group of the Fe (III)PPIX are exposed and the antimalarials are thought to interact with these moieties as shown in Figure 1.10. A criticism levelled against this model is that CQ was modelled in its monoprotonated state; under the FV conditions where CQ is thought to accumulate and interact with haemozoin, the diprotonated form is the major species. With the discovery of lipid involvement in haemozoin formation, the monoprotonated species may be present in a lipid environment, thus this mechanism is plausible (Kuter, 2008)

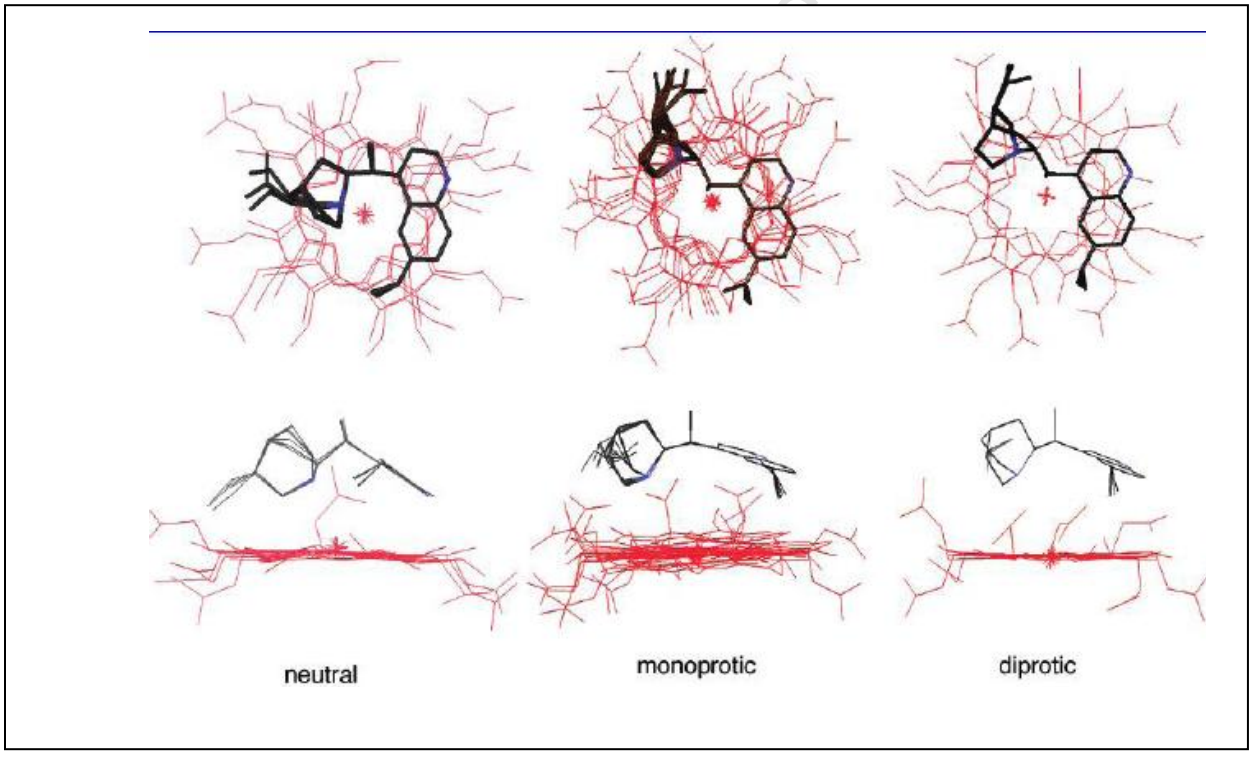

Figure 1.11: Interaction *of quinine with haematin (Leeds et al., 2002)*

In the second model or mechanism, it is assumed that the principle bonding interactions between the free haem and the quinoline haemozoin inhibitors comprises π-π stacking

forces of the quinoline ring over the porphyrin with possible weak electrostatic interactions between the protonated amino group of the quinoline and the carboxylate of the haem (Moreau *et al.,* 1982, O'Neil *et al.,* 1997). In the case of arylmethanol antimalarials such as quinine (QN) and quinidine (QD), it has been proposed that in addition to the π-π stacking, coordination to the iron centre of Fe(III)PPIX through the hydroxy occurs (Warhurst 1981; Behere and Goff 1984; Constantinidis *et al.,* 1988; Marques *et al.,* 1996).

UV Vis, NMR and X-ray crystallography data has been used to confirm these interactions. An example is from solution chemistry, NMR and computational studies done by Roepe and co-workers; Figure 1.11 illustrates the interaction between quinine and haem as proposed by the group (Leed *et al.,* 2002). The figure 1.11 shows there is π-π stacking interaction between the heme porphyrin ring and the quinoline nucleus for different species of CQ i.e.. CQ neutral, CQH^+ and $.CQH_2$

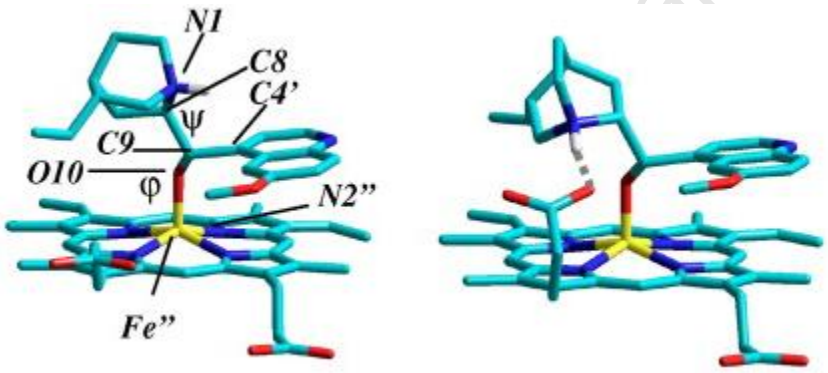

Figure 1.12: *Computational model of halofantrine – haem complex depicting the intramolecular H-bond that was proposed in the isolated complex [Fig. 1.13a] (de Villiers et al., 2008)*

The most convincing evidence was when the first crystal structure of an antimalarial-Fe (III)PPIX complex ie halofantrine-haem complex, was elucidated, as shown in Figures 1.13(a) and 1.12 (de Villiers *et al.,* 2008). It was shown that in addition to the envisaged ππ stacking of the phenanthrene ring of halofantrine over the porphyrin ring, the drug coordinates to the iron centre of the monomeric Fe(III)PPIX via its alcohol functionality (de Villiers and Egan, 2009).

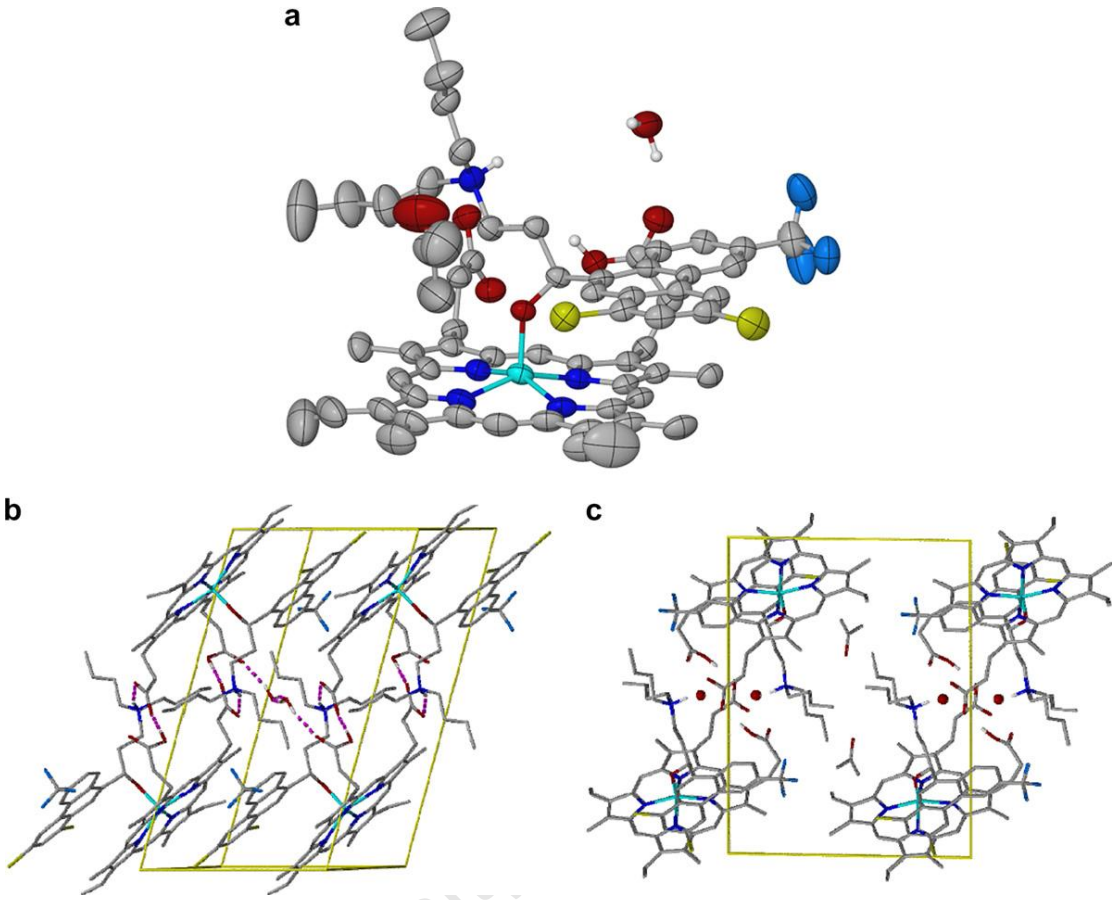

Figure 1.13: *(a) The halofantrine (Hf) - Fe(III)PPIX crystal structure. Thermal ellipses are drawn at 50% probability illustrating significant disorder in the Fe(III)PPIX vinyl group, butyl chain termini of Hf and the included acetone molecule. (b) A packing showing π-stacking and hydrogen bonding in the crystal. (c) a packing viewed down the a-axis of the unit cell emphasising the included acetone and water molecules in channels running down this axis. H-bonding was omitted for clarity. Atom colour coding: C, grey; H, white; Cl, lime green; F, Prussian blue; Fe, cyan; N, blue; O, red.(Adapted from de Villiers et al., 2008)*

An important intermolecular hydrogen bonding between the protonated terminal N atom of the halofantrine and the propionate group of a neighbouring Fe(III)PPIX molecule were observed (Fig. 1.13b; 1.13c). Using computational tools and spectroscopic investigation de Villiers *et al.,*(2008), showed that favourable formation of an intra molecular hydrogen bonding in the cases of QN and QD prevents dissociation of the drug

from the Fe(III)PPIX thus essentially blocking the iron centre from coordinating to a second molecule of Fe(III)PPIX and this was proposed to block haemozoin formation (Fig. 1.13).

On this basis the authors proposed a novel pharmacophore for haem targeting compounds. The model consisted of a 3-point interaction that involves ππ stacking, coordination and intramolecular hydrogen bonding. Thus the mechanism of action of halofantrine and related antimalarials in the inhibition of haemozoin involves firstly anchoring the molecule to haematin through coordination to the iron centre and ππ stacking with the protoporphyrin system.

This then allows the hydrogen bonding interactions with the propionate side chain to occur resulting in the inhibition of haemozoin formation (Kuter, 2008). The shortcoming of this second proposal is that the interactions observed were in aqueous/solid state and may not necessarily be the same as in the lipid (non-aqueous) environment in which haemozoin formation occurs (de Villiers and Egan, 2009)

1.6 Mechanisms of Quinoline Resistance-the Biochemical Basis of CQ Resistance

Chloroquine, a 4- aminoquinoline was the mainstay for treatment and prevention of malaria because of its low cost, safety and efficacy. CQ resistance by *P. falciparum* and *P. vivax* has been reported in every malaria endemic country and this drug is no longer considered appropriate for the treatment of malaria in many areas (Barat *et al.,* 1997, Whitby *et al.,* 1997). Despite massive drug pressure following its introduction in the 1940s, the resistance of *P. falciparum* to CQ was not recognised until in the late 1950s when treatment failures were reported from distinct foci in SE Asia and S America. Afterwards it spread to almost all malaria areas around the world (Barat *et al.,* 1997, Wernsdorfer, 1994). Gradual development of resistance to other aminoquinolines like mefloquine, quinine and quinidine has been reported (Grant *et al.,* 2001). Also some strains of *P. falciparum* from Cambodia and Thailand are resistant to all antimalarial drugs except artemisinin combined therapies (Dondorp *et al.,* 2009, Wiwanitkit., 2010, Barat *et al.,* 1997)

A wide range of drug transport studies using intact infected red blood cells, isolated malarial parasites, heterogenous expression systems and purified protein, combined with genetic experiments have suggested that CQ transport mechanism by the *Plasmodium falciparum* Chloroquine Resistance Transporter (PfCRT) is a key aspect of the molecular mechanism of quinoline antimalarial drug resistance (Roepe, 2011). Nearly all evidence has been in favour of a digestive vacuole (DV) membrane drug pump or drug channel explanation for CQ resistance and the digestive vacuole as the principle site of CQ accumulation because haem released via haemoglobin catabolism within the DV is the principle molecular target of CQ. So far it has been demonstrated that resistance is conferred by mutations of the CQ resistance transporter PfCRT, an integral protein membrane localised to the parasites internal digestive vacuole. The mutations were showed to cause a marked reduction in the accumulation of CQ by the parasite (Martin *et al.,* 2010).

CQ is a diprotic weak base (pKa of 8.1 and 10.2, where pKa is the acid dissociation constant) The relative proportions of the neutral, mono-protonated (CQH^+), and diprotonated (CQH_2^{2+}) species vary with pH. The neutral species enters the parasite and its acidic DV (pH~5) via diffusion. Inside the DV the equilibrium is shifted toward the CQH_2^{2+} species, which is unable to diffuse across the membrane and becomes trapped by accumulating to high concentrations within the DV (Klonis *et al.,* 2007). In side the DV chloroquine exerts its antimalarial activity via haemozoin inhibition. From a biochemical standpoint, CQ resistant parasites have been found to accumulate less CQ when compared to the sensitive parasites (Dorsey *et al.,* 2001).

Chemosensitizing agents such as verapamil are reported to reverse resistance by enhancing drug accumulation in the resistant parasites and not the sensitive ones hence cancelling out the difference in accumulation (Foley *et al.,* 1998).

From a genetic standpoint the goal has been to identify genes that encode proteins that play a role in CQ resistance (Wellems *et al.,* 1990; Su *et al.,* 1997; Fidock *et al.,* 2000)

and a number of hypotheses have been proposed to explain the differences in CQ accumulation between CQ resistant and sensitive parasites. Verdier *et al.,* (1985) and Krogstad *et al.,* (1987) proposed that CQ efflux occurs at a greatly enhanced rate in CQ resistant parasites and this prevents its accumulation in the parasitic FV. They proposed a mechanism similar to that mediated by P-glycoprotein molecules in drug resistant mammalian cancer cells (Martin *et al.,* 1987). They stated that the lack of accumulation is caused by a mutated membrane transport protein and this causes an increase in CQ efflux resulting in decreased concentration that is too low to inhibit haemozoin formation.

Initial studies were able to associate CQ resistance with point mutations in the gene PfCRT (Fidock *et al.*, 2000; Sidhu *et al.,* 2002). A direct proof of a casual relationship remained elusive therefore models prior to the work by Fidock and co-workers (2002), posited a multigenic basis of CQ resistance. Fidock and co-workers gave evidence that mutant halotypes of the PfCRT gene conferred resistance with characteristic verapamil reversibility and reduced accumulation. The PfCRT mediated resistance mechanism is structural specific and this has been underscored by findings that PfCRT-modified clones remain susceptible to amodiaquine a compound similar to CQ but with a modified aminoquinoline side chain. This promoted the use of amodiaquine and related compounds that have a modified aminoquinoline side chain in their structures for the treatment of CQ resistant *falciparum* malaria (Sidhu *et al.,* 2002).

A current model demonstrates that CQ resistance is due to direct transport of the drug via mutant PfCRT and that resistant reversers act by inhibiting the PfCRT transport mechanism (Martin *et al.,* 2010; Krogstad *et al,.* 1987). The mutant form of the transporter was found to transport CQ while the wild one (sensitive) did not. The experiment to demonstrate this involved the use of *Xenopus laevis* oocytes (frog eggs) to simulate the FV membrane of the *P. falciparum.* Localization of CQ sensitive and resistance forms of PfCRT ($PfCRT^{CQS)}$ and $PfCRT^{CQR}$ respectively) on the *Xenopus laevis* oocytes plasma afforded a method to study the differential efflux of CQ by the PfCRT in resistant and sensitive strains. The uptake of [^{3}H]CQ was measured in an acidic medium (pH 6) in which majority of the CQ was protonated. Oocytes expressing

PfCRT^{CQR} showed marked (5-10 fold) increase in the [^{3}H]CQ uptake relative to the non injected controls and the oocytes expressing PfCRT. This effect was demonstrated to be due to PfCRT^{CQR} but not PfCRT^{CQS} mediating the transport because the membrane potential and cytosolic pH in PfCRT^{CQR} expressing oocytes were the same as those in the PfCRT^{CQS} expressing oocytes. The main resistance conferring mutant in PfCRT (K76T) was found to be necessary but not sufficient for the transport of CQ via PfCRT and that other PfCRT mutations act in synergy with K76T to confer CQ resistance. The K76T is located in a region of the protein that is known to be involved in the recognition of the substrate (Martin *et al.,* 2004). It was demonstrated that the presence of a positive charge (K76 or R163) in the PfCRT substrate binding site prevents CQH_2^{2+} (or CQH^{+}) from interacting with the transporter. The K76T mutation removes the positive charge altering the substrate specificity of PfCRT to allow the transport of the protonated drug (Martin *et al.,* 2010). The presence of mutant PfCRT on the digestive vacuole was hypothesised to allow the protonated drug to be transported down its electrochemical gradient, out of the digestive vacuole, and thus away from the site of action and this was found to be consistent with previous reports (Bray *et al.,* 2006; Sanchez *et al.,* 2005; Sanchez *et al.,* 2005; Naude *et al.,* 2005). The work by Martin *et al*, 2010, provides a convincing evidence of the involvement of PfCRT in CQ resistance however, it is still important to consider alternative models because CQ resistance appears to be multifaceted.

Alternative findings show that CQ efflux rates in CQR and CQS parasites are similar and that the decreased steady state levels of CQ in the resistant strains are a result of a diminished accumulation rather than a drug export mechanisms (Bray *et al.,* 1994., Ginsburg 1991). The specific hypotheses also incorporated the concept that decreased CQ accumulation can be the result of diminished drug accumulation. Increases in the pH of the parasitic FV could explain the decreased accumulation of CQ in the resistant strain (Geary *et al.,* 1990, Bray *et al.,* 1992). It has been proven that that the FV pH is actually decreased in CQ resistant parasites by 0.4-0.5 pH units relative to CQ sensitive parasites (Dzekunov *et al.,* 2000). The proposal and results appear paradoxical if vacuolar accumulation were explained only by weak-base trapping (Dorsey *et al.,* 2001). However, CQ accumulation in the FV is known to be additionally driven by binding to

soluble haem (Bray *et al.,* 1998, Fitch *et al.,* 1970). Given that there is a steep effect of pH on the conversion of soluble haem to insoluble haemozoin, and that the formation of haemozoin is much more efficient at the low FV pH value of CQR parasites, then vacuolar acidification would leave significantly less free haem available for the formation of toxic complexes with CQ (Dzekunov *et al.,* 2000). The result would be reduced accumulation of CQ in CQR parasites and this is consistent with experimental data which shows a reduction in high affinity drug receptor sites (Dorsey *et al.,* 2001, Dzekunov *et al.,* 2000, Bray *et al.,* 1998, Fitch *et al.,* 1970).

Diminished drug accumulation has also been explained in terms of differences in drug susceptibility between CQR and CQS parasites (Bray *et al.,* 1996). For instance, parasites demonstrating a 4-fold to 5-fold difference in CQ accumulation were found to exhibit a 10-fold to 20-fold difference in susceptibility (Bray *et al.,* 1996). This shows that CQ resistance may be mediated by a reduction in target site sensitivity/affinity or accessibility (Dorsey *et al.,* 2001, Bray *et al.,* 1998)

Alternative explanations for the decreased accumulation of CQ in the resistant parasite proposes the loss or alteration of a protein involved in the CQ uptake or alteration in the intracellular "receptor" (Bray *et al.,* 1998, Hawley *et al.,* 1996, Warhurst *et al.,* 1986, , Chou *et al.,* 1980). An amiloride-sensitive Na^+/H^+ exchanger was proposed to actively transport CQ into the FV (Sanchez *et al.,* 1997, Wunsch *et al.,* 1998), and that this activity is decreased in CQR parasites. More evidence, however, implicates indirect involvement of Na^+/H^+ in the resistance mechanism (Dorsey *et al.,* 2001)

1.6.1 Drug Molecular Structure and Resistance Mechanisms

It appears that CQ resistance mechanisms recognize the aminoalkyl side of CQ (Egan, 2001), and this is indicated by the fact that CQ analogues with side chains much shorter (2-3 carbon atoms long) or much longer (10-12 carbon atoms long) maintain full activity against resistant strains (De *et al.,* 1996).

CQ analogues with chain lengths closer to that of CQ have intermediate activities between that of CQ and the fully active compounds. This change of activity has been related to the distance between aminoquinoline amine group and the terminal tertiary amino group of the side chain (De *et al.,* 1996). To affirm this, amodiaquine which has a similar N-N atomic separation to CQ shows marked cross resistance (Egan, 2001)

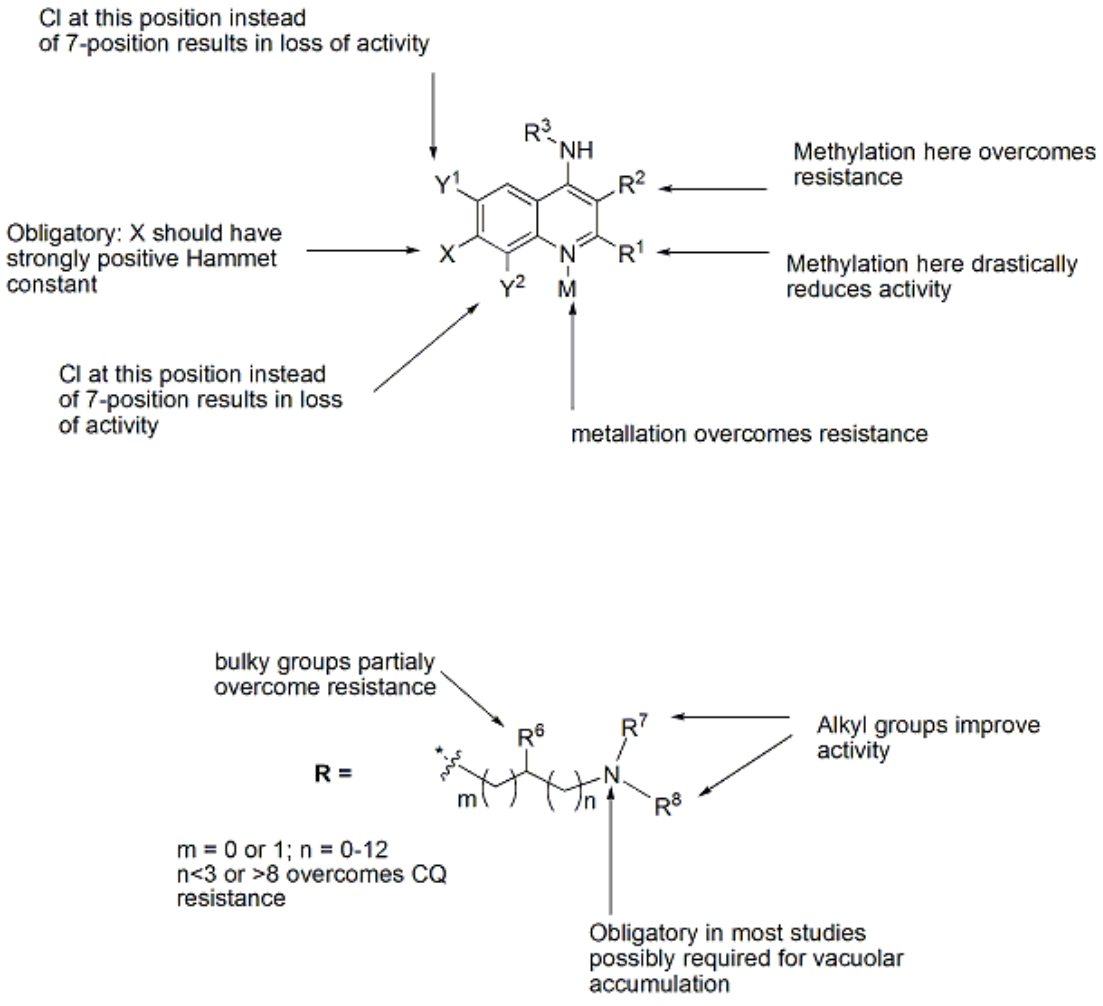

Figure 1.14: *A summary of findings regarding the roles of various substituents on 4-aminoquinolines with respect to antiplasmodial activity and activity against CQ resistant strains.* (Egan, 2001)

Even minor alteration of the side chain of 4-amino-7-chloroquinolines restores activity against CQR parasites. For example the incorporation of ferrocenyl groups, replacement of the ethyl groups with bulky butyl groups or incorporation of additional quinoline nucleus to form bisquinolines (Biot 2007, Raynes *et al.,* 1999, Biot, 1997)

By contrast, changes solely in the aminoquinoline nucleus, only restores activity marginally as exemplified by the replacement of the Cl with a Br or I (Vippagunta *et al.,* 1999; De *et al.,* 1998). Despite this, replacements of Cl with 7-CF_3 and the insertion of 3-CH_3 seem to restore some degree of activity (De *et al.,* 1998). Metallation of the quinoline N with a variety metals seems to restore activity (Navarro, 2009; Ajibade *et al,* 2008, Navarro *et al.,* 1997). Figure 1.14 summarises the effect of modifications of the substituents on the activity of quinolines against CQ resistant strains.

This suggests that the aminoalkyl side chain and the quinoline N may be involved in the molecular recognition associated with CQ resistance (Egan, 2001)

1.7 Iron Chelators and Malaria

1.7.1 Iron Loading as a Risk Factor for Malaria

Clinicians have reported that elevated host iron is a serious risk factor for human malaria (Weinberg *et al.,* 2009), for example, during the third trimester of pregnancy, a 9-fold increase in the quantity of absorbed dietary iron provides a sufficient amount of the growth essential metal to the rapidly developing foetus (Barret *et al.,* 1994) As gestation proceeds latent malarial protozoa in pregnant women become active especially in the iron rich placenta. This in one way explains why pregnant women are more vulnerable to malaria. Indeed during the later half of gestation, women are advised to forego travel to malarial regions (Diro and Beydoun, 1982; Bruce-Chwatt, 1983).

In malaria regions, iron loading in non-pregnant persons likewise increases the risk of developing malaria. Iron supplements in adults and feeds for children have been observed to increase vulnerability to malaria (Berger *et al.,* 2000; Gebresselassie, 1996; Murray *et al.,* 1978)

1.7.2. Iron chelators as antimalarials

One important strategy for fighting malaria drug resistance is the development of drugs with new mechanisms of action. Iron chelators have been proposed as potential antimalarial agents because of the central role of iron for the rapid proliferation of the malaria parasite and the arrest of parasite growth by iron chelators *in vivo* and *in vitro* (Cabantchik *et al,* 1996; Hershko *et al*, 1991a, b; Heppner *et al,* 1988; Raventos-Saurez *et al*, 1982). An example is deferiprone (DFP) and desferrioxamine (DFO), (Figure 1.15), which have been evaluated *in vitro* for activity against a chloroquine (CQ) resistant strain (FCR-3) and *P. berghei* in rat models. The activities are shown in Figures 1.16 and 1.17 respectively (Hershko *et al,* 1991b). Clinical trials have even been conducted for DFO (Gordeuk *et al,* 1993 and Mabeza *et al,* 1999) and for DFP (Thuma *et al,* 1998).

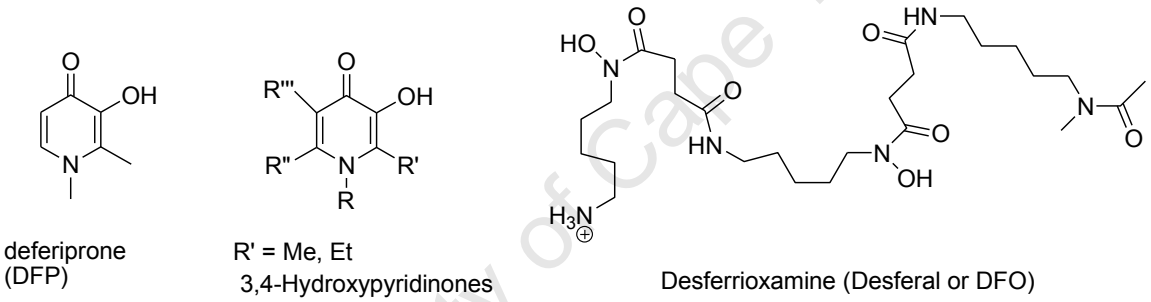

Figure 1.15: Some common iron chelators

DF and DFO are used in the treatment of iron overload in β-thalassaemia. DFO, the most widely used iron chelator in haematology over the past 30 years, has a major disadvantage of being orally inactive, unlike hydroxypyridinones, specifically DFP.

Hershko and co-workers (1991a) demonstrated that DFP has optimal combination of limited toxicity and effective antimalarial activity for *in vivo* tests in animal models (Fig. 1.16). This came after studies on the *in vitro* activities of the 3,4-hydroxypyridinones (3,4-HPOs). 3,4-HPOs exhibit a dose-related suppression of *P. falciparum* growth *in vitro* with IC_{50} values in the range 5-100μM, (Figure 1.17), when the parasites are exposed to the drug continuously (Heppner 1988 *et al,*, Hershko *et al,* 1991).

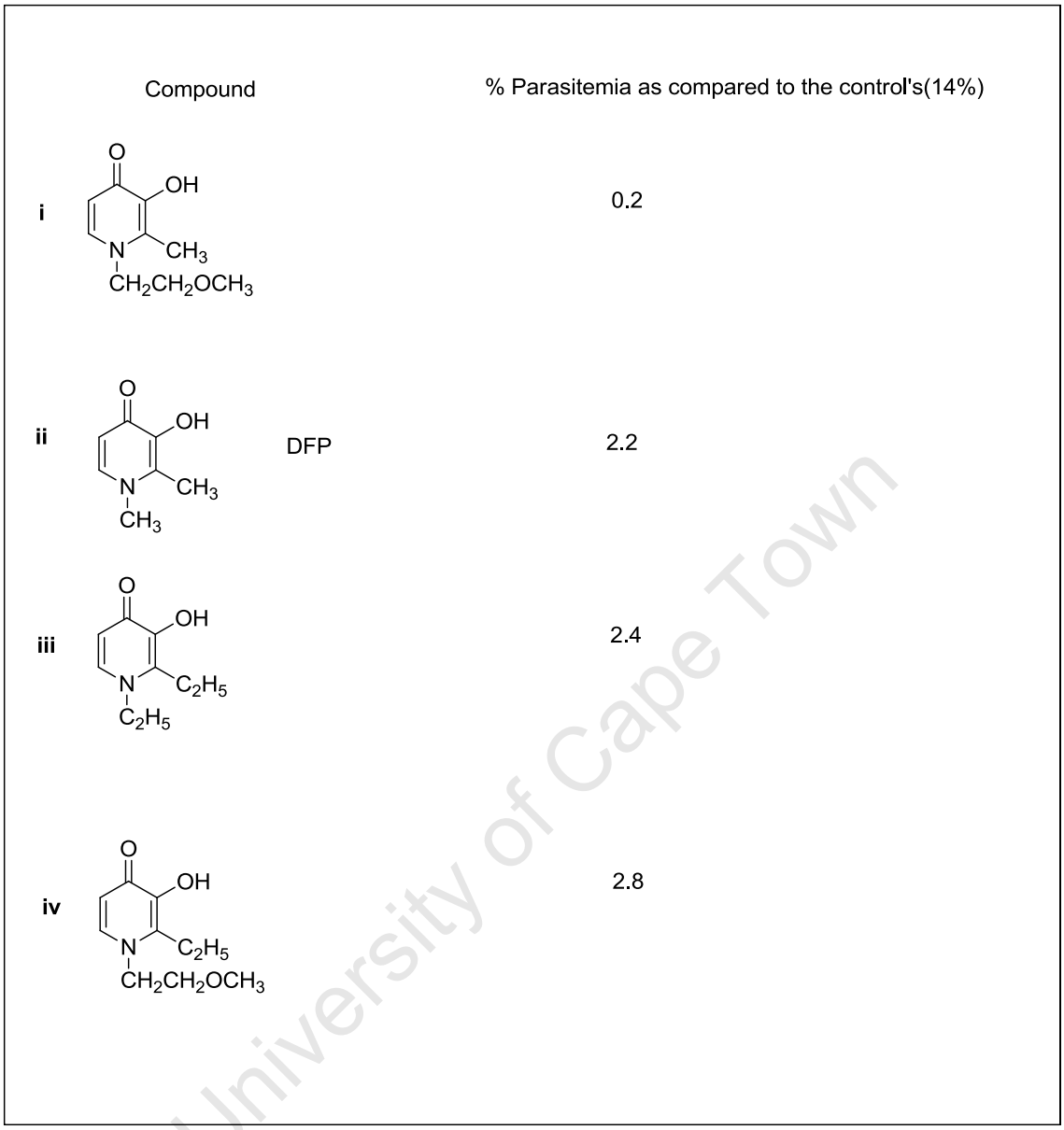

Figure 1.16: *In vivo antimalarial activity of 3,4-hydroxypyridinones (Hershko et al., 1991)*

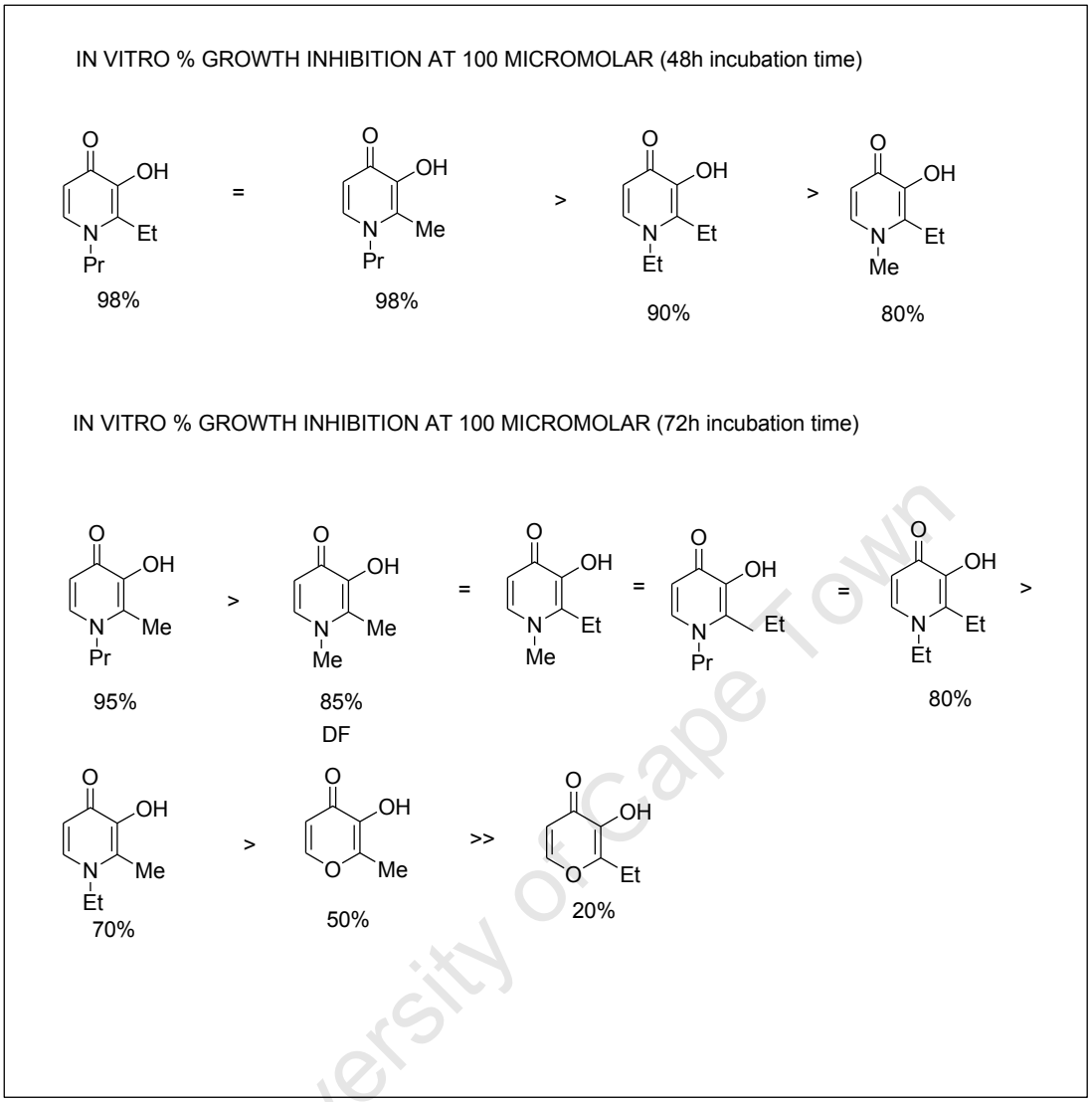

Figure 1.17: *In vitro activity of 3,4-hydroxypyridinones (Heppner et al., 1988)*

It is important to note that iron chelators were initially designed to treat iron overload, therefore iron chelation may not achieve a defined role in the treatment of malaria until new agents are designed specifically with antimalarial properties (Loyevsky and Gorduek 2001).

1.7.3. Sources of Iron for the Malaria Parasite

The intraerythrocytic *P. falciparum* degrades haemoglobin for nutrition (amino acids, probably for iron) and to create space for itself (Ginsburg *et al,* 1990; Sherman *et al,* 1977, Francis *et al,* 1997; Kolakovich *et al,* 1997). The haem liberated by the proteolysis of haemoglobin is crystallized in the parasite food vacuole to form the non toxic haemozoin and the process is probably lipid mediated (Egan *et al* 2006, Slater *et al,* 1992).

How the intraerythrocytic phase parasite acquires iron has not been determined. However, several possible sources have been postulated, these include plasma transferin bound iron (Pollack *et al,* 1988a; 1984, Van Zyl *et al,* 1993); iron derived from red blood cell host ferritin (Gabay *et al,* 1993, Cazzola *et al,* 1983); Iron liberated from catabolism of host haemoglobin in the food vacuole of the parasite (Gamboa de Dominguez *et al,* 1966, Francis 1997, Kolakovich *et al,* 1997) and labile intraerythrocytic iron pool (Hershko *et al,* 1988). Studies show that labile iron pools of the host red blood cells may be either utilized or stored during plasmodial growth (Loyevsky *et al,* 1999). This is because parasitized erythrocytes have lower concentrations of iron than normal erythrocytes.

Abrogation of the labile iron by the introduction of iron chelators into the cytoplasm of the erythrocyte but not into the parasite compartment did not result in growth inhibition of the parasite (Loyevsky *et al,* 1993b, Scott *et al,* 1990). It is possible that both the host labile iron and another source such as the haemoglobin iron are used by the parasite and the abrogation of only one source of iron will not prevent parasite growth (Loyevsky and Gorduek 2001).

1.7.4 Mechanisms of Antimalarial Activity of Iron Chelators

Several classes of iron chelators have been shown to suppress the growth of the malaria parasite *P. falciparum*. The antimalarial iron chelators are classified into two broad groups based on the mode of activity.

The first group consists of iron chelators that act by withholding iron from the plasmodial metabolic pathways. They include hydroxamate siderophores and derivatives; (Loyevsky *et al,* 1993, Fritsch *et al,* 1987) 3,4-hydroxypyridinones (α-ketohydroxypyridinones) (Heppner *et al,* 1988) catecholamide and catecholate siderophores; dihydroxycoumarins; polyanionic amines; acylhydrazones; aminothiols; aminophenols and bis-cyclic imides (Loyevsky and Gorduek 2001).The inhibitory action of these compounds on malaria cultures is fully abrogated upon pre-complexation with iron.

The second class of antimalarial iron chelators acts by forming toxic complexes with iron. They include 2',2-bipyridyls (Loyevsky *et al.,*1999) and 8-hydroxyquinolines and alkylthiocarbamates (Scheibel *et al,* 1989) and certain aminophenols (Ocheskey *et al,* 2005, Loyevsky *et al,* 1999). The inhibitory effect of this class of chelators cannot be abrogated by precomplexation with iron before addition to the cultures (Loyevsky and Gorduek 2001).

Since the utilization of identified scaffolds does not necessarily depend on prior knowledge of action or the biological target of the drug from which the scaffold is derived (Biot and Chibale, 2006), iron chelators still have a great potential for development into antimalarial drugs.

The degree of antimalarial activity of iron chelators correlates with the degree of lipophilicity (ability to cross cell membranes) of the compound (Cabantichik *et al,* 1996, Yinnon *et al,* 1989, Shanzer *et al,* 1991, Hershko *et al,* 1991a). The lipophilicity-

hydrophilicity balance in this type of molecule is important for the effective transportation of the chelators across the cell bilayer membranes to reach the site of action. This has been improved by the use of certain metal (III) complexes of the chelators (Ocheskey *et al,* 2005). Lipophilicity has also been identified as an important factor in antimalarial drug resistance (Chibale, 2002)

Iron withholding may cause the malfunction of certain enzymes for which iron is indispensable. These enzymes include those involved in DNA synthesis (ribonucleotide reductase); pyridine synthesis (dihydoorotate dehydrogenase); CO_2 fixation (phosphoenol pyruvate carboxykinase); haem synthesis (delta- aminolevulinate synthase) and mitochondrial electron transport (cytochrome oxidase, cytochrome b) (Loyevsky and Gorduek 2001). Thus antimalarial iron chelators may affect the host or the parasite by interacting with the iron dependent enzymes.

1.7.5. Physical Properties that Affect the Antimalarial Activity of Iron Chelators

The site of action of iron chelators is in the parasitic compartment of the infected red blood cell (Scott *et al,* 1990, Hershko *et al,* 1988, Loyevsky *et al,* 1993). An effective iron chelator therefore must be lipophilic, have high affinity for iron and have selectivity for iron versus other cations and have an effective number of coordination sites.

Lipophilicity directly correlates to the chelator's inhibitory action against malaria as demonstrated for reversed sidereophores, N-alkyl derivatives of 3,4-hydroxypyridinones and aminothiols (Shanzer *et al,* 1991, Hershko *et al,* 1991, Loyevsky *et al,* 1996). The 3,4-HPOs iron (III) chelates carry no net charge therefore can penetrate membranes easily (Neufeld, 2006)

Maltol Ethylmaltol

Figure 1.18: *Synthetic precursors of 3,4-HPOs*

Selectivity for iron versus other cations is important because (1) *P. falciparum* has limited capability to recover after deprivation compared to mammalian cells (Cabantchik 1995). Hence it is reasonable to target iron as compared to other essential metals for which the ability to recover from deprivation has not been studied. (2) Removal by iron chelators of the other essential biometals (zinc, calcium and magnesium) may be detrimental for the mammalian host as well. In this regard the hydroxamate siderophores have a favourable profile because their affinity for iron is at least one order of magnitude higher than for calcium (Lytton 1994). The synthetic precursor of 3,4-hydroxypyridinones, maltol (Fig 1.18), has an affinity for zinc, and there are studies under way to develop it for diabetes therapy as a vanadium complex (Sakurai and Adachi 2005). However, this does not rule out the suitability of these compounds as antimalarial iron chelators because the iron affinity constants of antimalarial iron chelators are in the range 10^{24} to 10^{38}, with the 3,4-HPOs and 8-hydroxyquinolines having the highest affinities of 10^{36} and 10^{38} respectively (Gorduek and Loyevsky 2001)

1.7.6. DFP and DFO in Antimalarial Clinical Trials

Clinical trials have been conducted in Zambia on subjects with asymptomatic *P. falciparum* parasitemia using DFP (Thuma *et al.,* 1998). No reduction in asexual intraerythrocytic parasites was observed during or after DFP treatment. The failure was attributable to short plasma half life and short time taken to reach plasma peak. The remedy could have been prolonged use, but this resulted in neutropenia and other side effects. Neutropenia is abnormal low count of the type of white blood cells responsible for defence against bacterial infection (Hsieh *et al,* 2007). In the same study using DFO,

success was recorded in that DFO treatment significantly enhanced the rate of parasite clearance.

In symptomatic uncomplicated *P. falciparum* and *P. vivax* malaria, DFO as a single agent was administered continuosly for 3 days at 100 mg/kg/d, i.v, parasitemia reduced to zero after 57 h and 105 h for the *falciparum* and *vivax* groups respectively. However, recrudescence was observed and the study failed to achieve radical cure (Gorduek *et al,* 1992b). The addition of DFO to standard antimalarial drugs (sulfadoxine-pyrimethamine or quinine) shortened the rate of clearance of parasitemia and the recovery to full consciousness in children with deep coma by about two fold. Further clinical studies in which DFO was added to quinine in a regimen that included a loading dose of quinine were conducted (Gorduek *et al,* 1992a). Surprisingly this yielded negative results (higher mortality rates and poor parasite clearance were recorded).

Combination of 3,4-HPOs with standard antimalarials (chloroquine, mefloquine, artesunate, tetracycline, atovaquone) showed addition or mild antagonism and this is similar to what has been reported about combinations involving DFO and other iron chelators (Pattanapanyasat *et al,*, 2001, Loyevsky and Gorduek 2001). Combination therapies of artemisinins and iron chelators including 3,4-HPOs have been unsuccessful because of antagonism. Meshnick *et al.,* 1993 showed that there is specific need for iron (III) in addition to haem (III) or free iron (III) to activate artemisinins and it is assumed that iron chelators interfere with this process (Weinberg *et al.,* 2009).

DFO, desferrithiocin and dexrazoxane were reported to inhibit growth of exoerythrocytic hepatic phases of *P. falciparum* and *P. yoelii* (Loyevsky *et al,* 1991, Stahel *et al,* 1988). This demonstrated that iron chelators represent a potential antimalarial strategy with effectiveness against blood and liver phases of the parasite. In addition prodrugs of iron chelators have been found to be effective in hepatic activity (Loyevsky and Gorduek 2001, Hasinoff *et al,* 1991).

1.7.7. Suitability of 3,4-HPOs for Antimalarial Chemotherapy

In addition to thalasaemia treatment, 3,4-HPOs have been investigated for a variety medicinal applications; enzyme inhibitors, cell probes and labelling (Ellis 1996, Loyevsky *et al,* 1999b), HIV treatment (Barral *et al,* 2006), antidiabetic therapy (Thompson *et al,* 2003), aluminium detoxification (Amelia-Santos *et al,* 2005), antioxidants (Bebbington *et al,* 2002), imaging agents and diagnostics (Thompson *et al,* 2006), removal of excess metal irons in neurodegenerative diseases i.e. Parkinsons and Alzheimers diseases (Bebbington *et al,* 2002; 2000).

There are a number of reasons why 3,4-HPOs stand a better chance of being developed to better antimalarial agents. The 3,4-hydroxypyridinones are neutral bidentate ligands with high affinity for ferric iron and they form stable iron complexes. For instance DFP iron complexes have a stability constant = 37, which is six orders of magnitude higher than that of DFO (Loyevsky and Gorduek 2001). Therefore, 3,4-HPOS may effectively sequestrate iron from the parasite.

These small ligands have a clear advantage over larger hexadentate ligands (eg DFO) with respect to oral bioavailability. Though DFO has been in use in haematology for the past 30 years, it has a disadvantage of being orally inactive as already mentioned (Liu *et al,* 2000).

In combination therapy clinical studies where iron chelators were used to arrest microbial growth and cancer, DFO acted as a siderophore for the growth of invading cells instead of assisting the host cells. It was observed that DFO promoted the growth of *Yersinia* (a rare intestinal bacterial infection) and *Mucormycosis* (fungal infection of the brain, sinuses, lungs common in patients with immune disorder eg HIV-AIDS), (Kontoghiorghes *et al.,* 2004). In contrast DFP and related derivatives did not appear to assist the growth of these or related bacteria or fungal strains at the doses used for treating the patients.

3,4-HPOs do not inhibit haem containing enzymes or iron sulfhur cluster proteins but do interfere with enzymes containing mono-iron and bis-iron centres coordinated to oxygen ligands including lipoxygenases and aromatic amino acid hydroxylases (Liu *et al,* 2002). More lipophilic HPOs are better enzyme inhibitors (Kayyali *et al,* 1997, Hider *et al,* 1989). Hence they may be used against targets in *P. falciparum* eg proteases.

1.7.8. Metal Complexes for Antimalarial Chemotherapy

Metal (III) as well as metal (II) complexes have been studied for various chemotherapeutic uses. Metal complexes have been successfully used in cancer chemotherapy. However, little attention has been paid so far to their uses in the treatment in tropical diseases (Sanchez *et al,* 2004).

Zinc (II) metal complexes of DFO are known to result in increased *in vivo* activity of DFO due to transmetallation reactions with iron (III) and enhanced membrane permeation, (Chevion *et al,* 1995). Chloroquine-metal complexes of ruthenium and gold have been studied as well (Sharma *et al,* 1999; Ajibade *et al,* 2008, Navarro *et al.,* 1997) and have been shown to have improved activity against chloroquine resistant strains. It has been postulated that high valent iron-oxo species may mediate the molecular mechanism of action of artemisinin (Posner *et al,* 1995).

A number of antimalarial aminophenol metal (III) complexes of gallium, iron, and aluminium have been synthesized (Goldberg *et al,* 1997, Ocheskey *et al,* 2005; 2003, Sharma *et al,* 1997), to enhance activity of antimalarial aminophenols (Fig. 1.19). The gallium complexes were found to be selectively toxic against the CQ-resistant strain Dd2 in a verapamil insensitive manner but less active against the sensitive strains HB3 (Goldberg *et al,* 1997) in the nanomolar range. Incorporation of quinoline into the aromatic part of the organic scaffold of these complexes resulted in increased activity against the sensitive strain (>33 fold) but an insignificant effect on the potency against the resistant strain (Ocheskey *et al,* 2005). Their mode of action was postulated to be via

inhibition of haemozoin formation. These iron chelators contain the N_4O_2 donor core and the gallium complexes are thought to have increased membrane permeability (Ocheskey *et al,* 2003). Some inactive metal complexes have been reported to have enhanced activity against resistant strains as well as sensitive strains when coupled to quinolines. For example ferrocene is known to be stable, non-toxic but inactive on its own. However, when linked with a CQ-like nucleus (Fig. 1.19), the hybrid molecule acts against resistant parasites (Biot C., *et. al.,* 2006; Beagley *et. al.,* 2003). Metal porphyrins have been shown to have a synergistic effect on artemisinins and the mechanism is via haem binding through π-π interactions (Sanchez *et al,* 2004; Kelly *et al,* 2000).

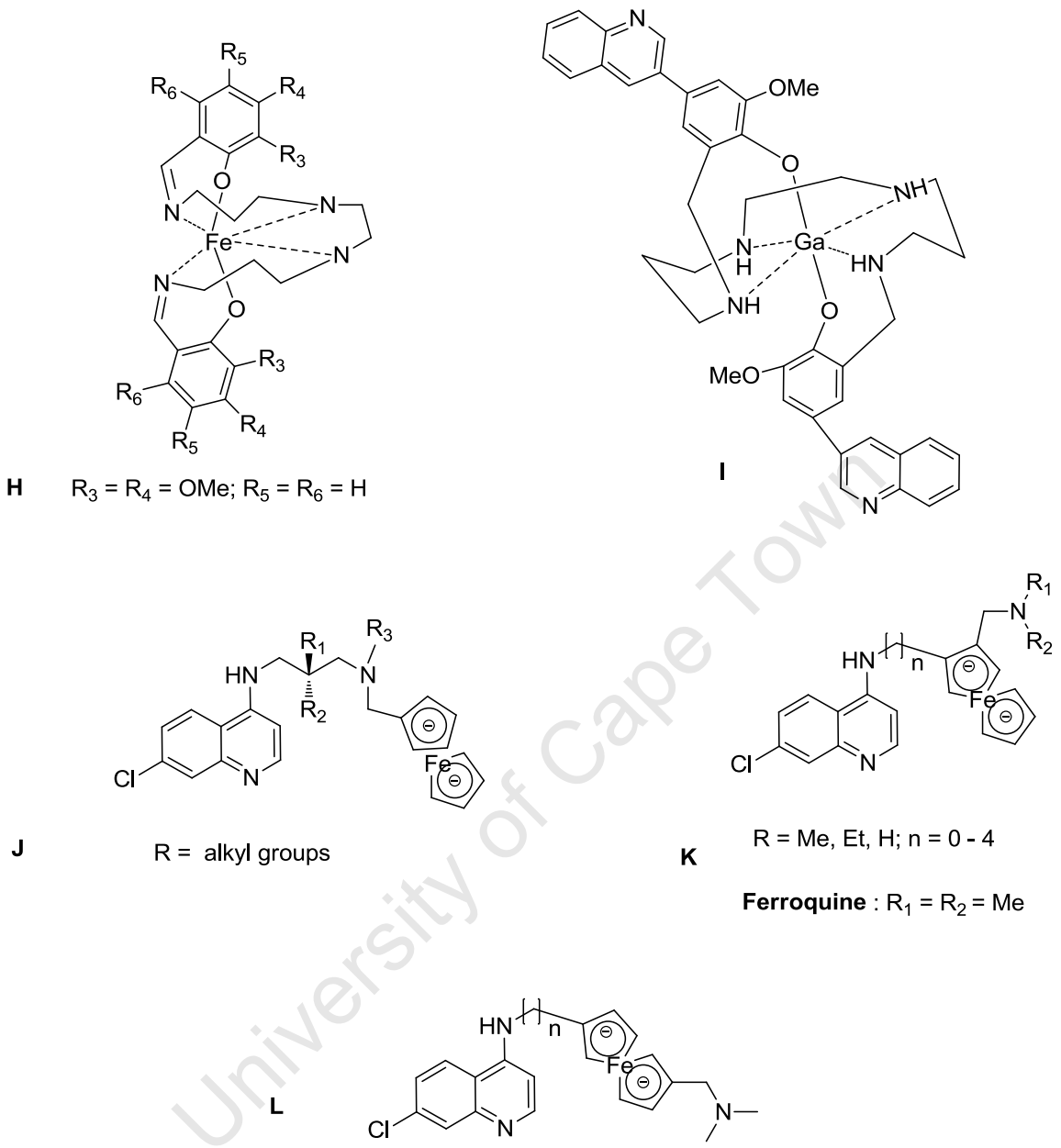

Figure 1.19. *Structures of some antimalarial aminophenol iron (III) and gallium (III) complexes (**H** and **I**) and ferrocene-aminoquinoline conjugates (**J**, **K** and **L**)*

1.7.9. HPO Metal Complexes in Medicinal Chemistry

Heppner *et al* 1988, showed that pre-formation of HPO-iron complexes completely obliterates the antimalarial activity of this type of iron chelator. No studies have been performed on antimalarial activities of 3,4-HPO-metal (III) complexes of other metals, nor the coupling of these complexes to standard antimalarial molecules to form „covalent bitherapies. However a lot of work has been conducted on HPO metal (III) complexes for other medicinal chemistry applications (Thompson *et al,* 2006).

Maltol, the synthetic precursor of a number of 3,4-HPOs and its analogs have high affinity for a variety of metal ions ie trivalent ions of Al, Fe, Ga, and In, and the divalent ions of Zn, Ru, $[VO]^{2+,}$ $[MoO_2]^{2+}$. Hence these ligands are used in applications that involve removal of excess metal ions while their complexes are used in absorption or redistribution of metal ions.

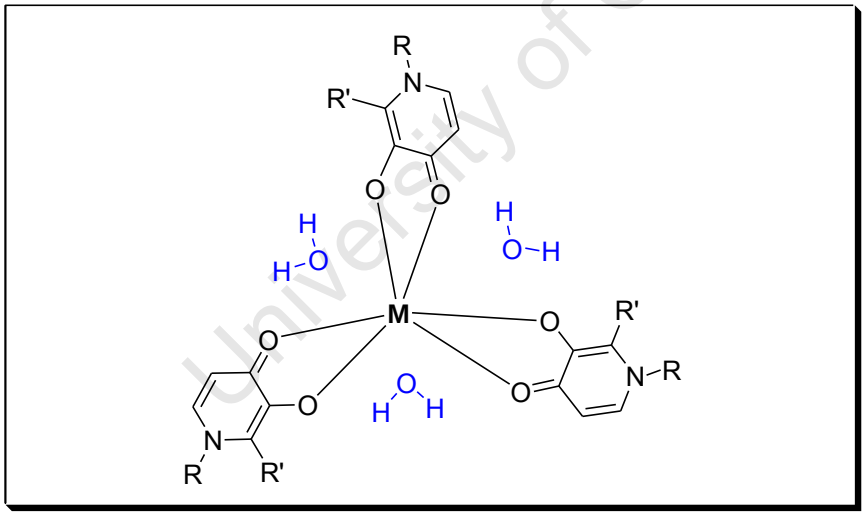

Figure 1.20: *Geometry of the 3,4-HPO metal (III) complexes*

The metal complexes of 3,4-HPOs are neutral and stable and form extensive hydrogen bonding with water and amines and with compounds with hydroxyl and ketone functionalities. Also the ligands are non toxic and the high affinity for iron is desirable because this prevents catalytic formation of reactive oxidative species. These complexes

usually assume a distorted octahedral geometry (Fig. 1.20), with all the six chelating O atoms hydrogen bonded to $3H_2O$ molecules by a three-fold axis ie (ML_3)**.** $3H_2O$; M = Fe, Ga, Al (Thompson *et al* 2006, Xiao *et al*, 1992).

3,4-HPOs tend to be insoluble in water. Their aqueous solubility is several hundred fold enhanced at the physiologically relevant temperature of 37 ^{o}C. In addition under physiological conditions, they presented highest affinity for the hard trivalent metal ions of group 13 (Thompson *et al* 2006) and are resistant to acid catalysed and enzyme catalysed cleavage (Amelia-Santos *et al* 2004).The functionalizable ring nitrogen allows variation of lipophilicity without the sacrifice of thermodynamic stability of the complexes (Thompson *et al* 2006). Substitution at C-2 has an effect on iron affinity and bioavailability as seen in the enhancement of the two properties of 2-amido substituted 3,4-HPOs. Also this modification affects enzyme inhibition as mentioned earlier. Therefore, the role of side chain modification is to tune physicochemical properties like molecular weight, hydrophilicity-lipophilicity balance and to improve interactions with biological receptors (Thompson *et al* 2004).

Novartis has produced a range of bidentate HPO ligands, which possess an aromatic substitutent at the 2-position (Liu *et al* 2001). The aromatic ring is reported to stabilize the resulting iron complex (Liu *et al* 2001). The 1'-hydroxyalkyl groups on the ring N in the Novartis HPO ligands enhances the stability of iron complexes formed *in vivo* via intramolecular hydrogen bonding (Liu *et al* 2001).

The deferiprone iron complex was found to exchange its iron with apotransferrin and other proteins of iron metabolism much more readily than the DFO iron complex. Thus the physiological processes involving iron containing proteins may be affected by chelating drugs and their complexes (Kontoghiorghes *et al* 2004). However the extent of effect depends on many factors such as affinity for iron, iron accessibility, the form of interaction, the rate of reaction and the concentration of the chelator or its iron complex at the site where the enzyme or protein resides (Kontoghiorghes *et al* 2004). Possibly the cell can balance out the side effects of iron chelators to some extent.

1.7.10. Hydroxypyridinone Hybrid Molecules

Multitherapies associating long acting and short acting compounds with different modes of action potentially offer efficient treatment though they tend to be expensive (Biot and Chibale, 2006). Other multitherapies combine two or more biological characteristics in one hybrid molecule. For instance Bebbington and co-workers (2000) synthesized antioxidant-3,4-HPO hybrid molecules (Fig. 1.21), the purpose of which was to bestow more lipophilicity to the iron chelators as well as counteract the formation of reactive oxidative species in their medicinal applications.

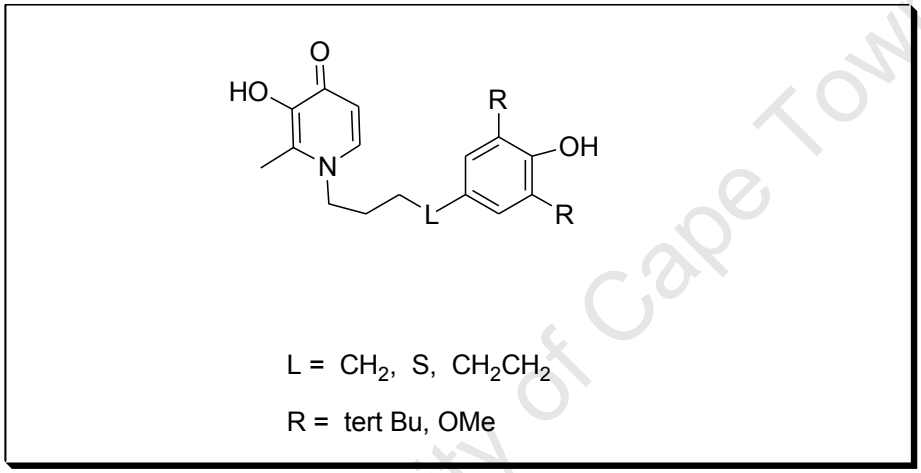

Figure 1.21: *3,4-HPOs-antioxidant hybrid molecules*

It has been verified that hybrid molecules have higher activity than the dual administration of the constituent molecules (Bebbington *et al.,* 2000).

1.8 Catecholate Siderophores

Siderophores are compounds produced by bacteria, fungi and graminaceaous plants for scavenging iron from the environment (Hider and Xiaole, 2010). Catecholate siderophores are considered of importance herein because they are bioisoteres of 3,4-hydroxypyridinones (Von Kohler *et al.,* 1970; Von Wallensfels, 1966). Although iron chelators have antimalarial activity, all have been developed more specifically either for cancer chemotherapy or for treatment of iron overload. The catecholate siderophores are

unique in that they have been developed specifically for their antimalarial activity and this work was pioneered by Pradines and coworkers, 1996.

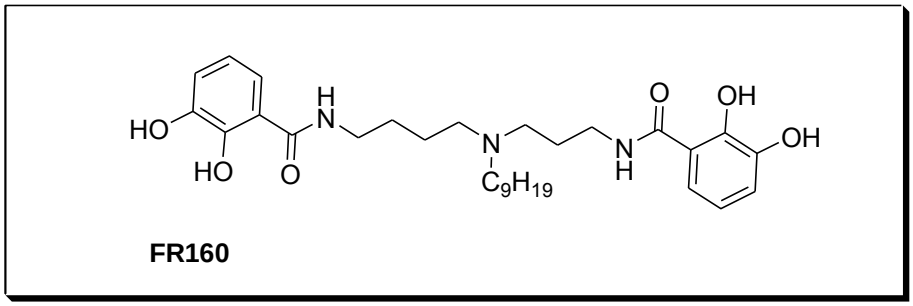

FR160

Figure 1.22: ***FR160*** *First iron chelator specifically developed with antimalarial properties.*

One of the compounds referred to as **FR160** (Fig 1.22), was 7-60 times more potent than CQ against CQR and CQS strains of *P. falciparum* (Hammadi *et al*., 2003; Pradines *et al.,* 1996). When **FR160** was incubated with iron (III) chloride, its antimalarial activity was suppressed, while no effect was observed with the incubation of **FR160** with copper (II) sulphate nor zinc (II) sulphate, suggesting that iron deprivation may be the main mechanism of action of **FR160** against malarial parasites (Weinberg *et al.,* 2009). **FR160** was found to affect the trophozoite stage of the parasite. This suggests that it acts presumably by inhibition of ribonucleotide reductase and inhibition of DNA synthesis as was previously suggested for other antimalarial iron (III) chelators (Pradines *et al*., 1996).

Mono and tris acylated catecholates were investigated for antimalarial activity and were found to be more active than DFO and its derivatives (Rotheneder *et al.,* 2002). The acylated catecholates were found to be more lipophilic than the free catecholates, and the former were assumed to be cleaved by esterases before iron chelation. An example of these compounds is shown in Figure 1.23.

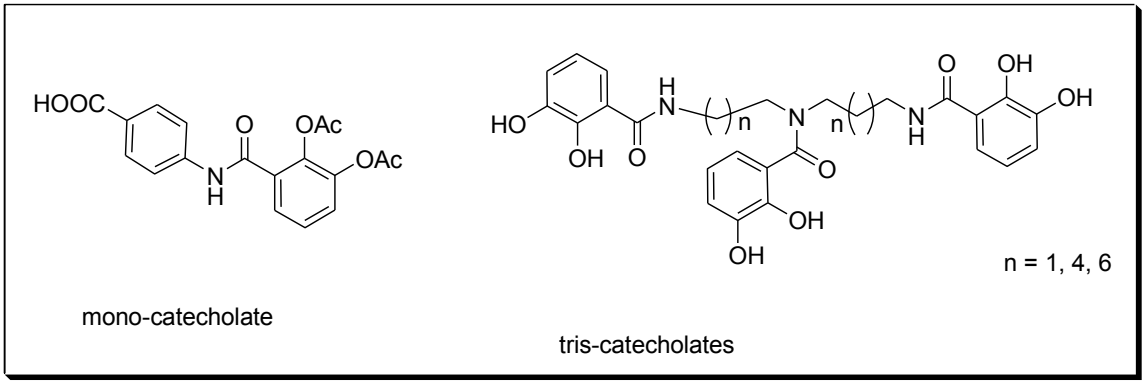

Figure 1.23: *Examples of mono and tris-catecholate compounds*

The antiparasitic effect of most of the triscatecholates was reversed by low concentrations of Fe (III) salts, suggesting that their antiparasitic effect maybe due to the iron abrogation. In contrast, the toxicity towards *P. falciparum* exerted by most monocatecholate compounds was not affected by exogenous iron salts. This indicated that the antiplasmodial effect was independent of chelation of intracellular iron and instead could be via other mechanisms like inhibition of parasitic enzymes or interference with iron release from haem (Weinberg *et al.,* 2009).

1.8.1 Siderophore Antibiotics or Sideromycins

Sideromycins are natural products in which the antibiotic component is covalently attached to a siderophore (Hider and Xiaole, 2010). These compounds are actively transported into bacteria and they have the effect of lowering the minimum inhibitory concentration (MIC) of the antibiotic by more than 100-fold. The sideromycins were discovered simultaneously with hydroxamate siderophores, with ferrimycin (Figure 1.24) being the first to be reported in 1960 and was isolated from *Streptomyces grieso-flavus* (Gross *et al.,* 1992; Bicket, 1960). Ferrimycin A consists of ferrioxamine B linked via a bridging aminohydroxy benzoic acid, to an iminoester substituted lactam. Siderophores that are structurally related to ferrimycin, ie salymycin A, danomycins A and B and succinimycin exclusively inhibit Gram positive bacteria and gain access into the cells via the ferrioxamine B transporter (Hider and Xiaole, 2010)

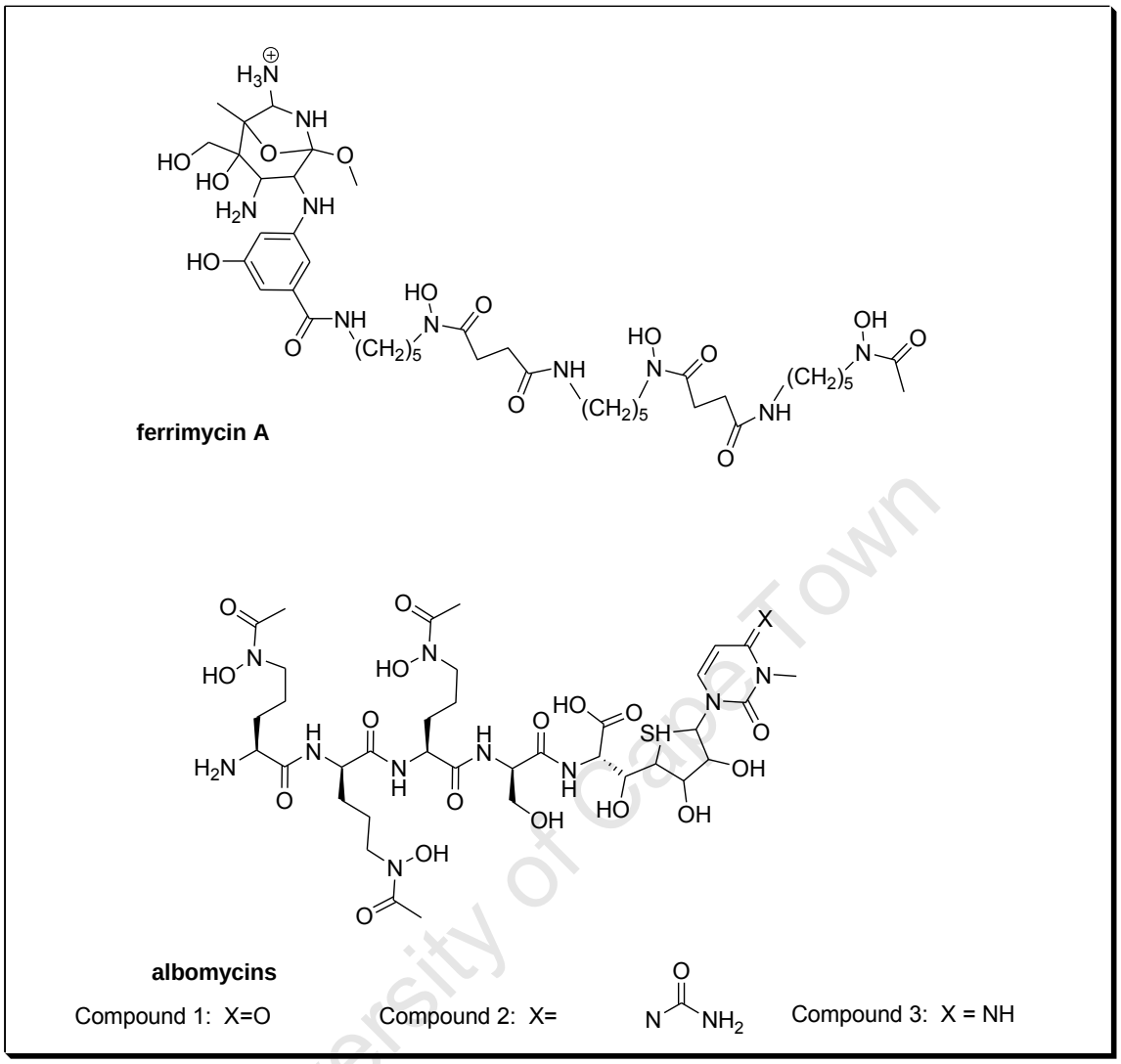

Figure 1.24: *Ferrimycin and albomycins; (compound 1= albomycin δ_1 , compound 2= albomycin δ_2, compound 3 = albomycin ε_1)*

Albomycin is another iron containing antibiotic from Streptomyces species and has activity against Gram negative organisms unlike the ferrimycin group (Fig. 1.24). The albomycin-like siderophores (eg albomycin δ_1, albomycin δ_2, albomycin and albomycin ε_1) gain access into the cell via the ferrichrome transporter (Braun *et al.,* 2009).

1.8.2 Siderophore Based Double Drugs

On the basis of the properties of the sideromycins a range of siderophore drug conjugates have been designed and synthesised and the design was based on the template in Figure 1.25 (Miller *et al.,* 1993; Mollmann *et al.,* 2009). The double drug was designed to act by dual mechanism i.e. iron chelation or deprivation and by the mode action similar to the attached drug moiety (chloroquinolinyl). Assuming a „Trojan horse' mechanism (Braun *et al.,* 2009; Mollmann *et al.,* 2009; Heinisch *et al.,* 2002) then the siderophore group will enhance the uptake or transport of the attached drug across the microbial cell membrane hence this may improve the drug accessibility to the intra cellular targets.

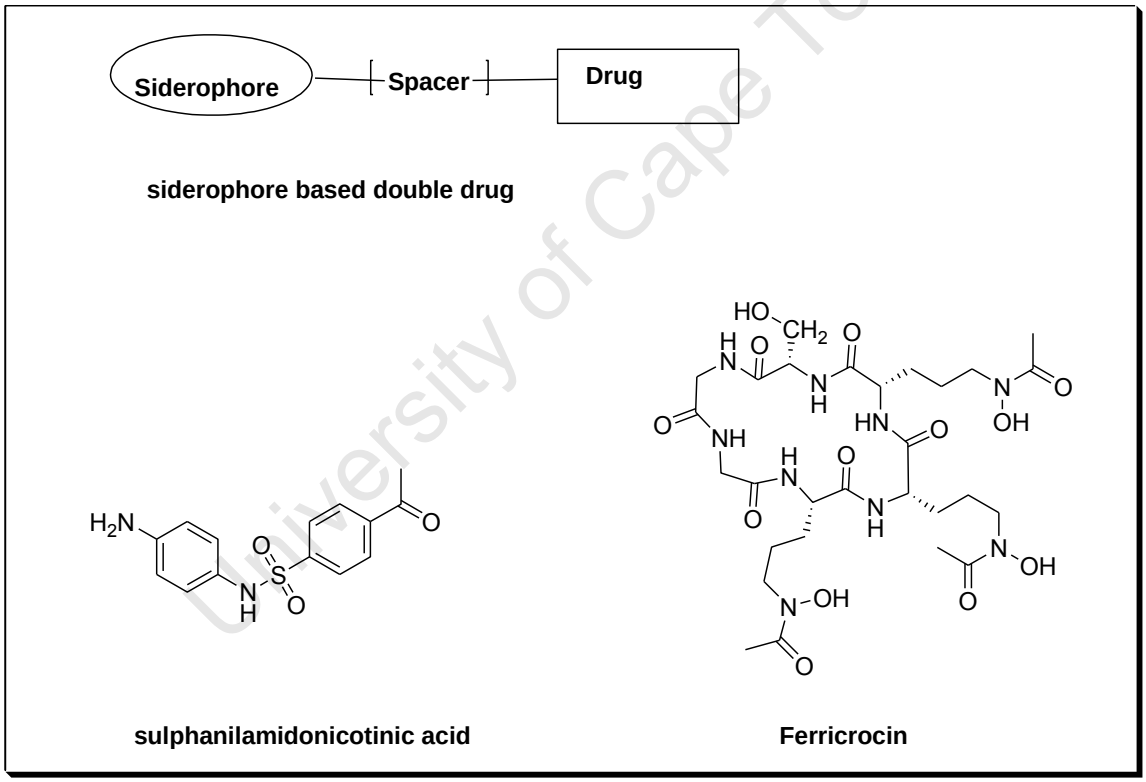

Figure 1.25: *Siderophore based double drug template and structures of sulphanilamidonicotinic acid and Ferricrocin.*

Initially sulfonamides were prepared by attaching sulfanilamidonicotinic acid to either DFO (Ferrioxamine B) or Ferricrocin, the resulting conjugates were found to be active against *S. aureus* and not *B. subtilis* or *E. coli* (Zahner *et al.,* 1977). Intense work on

siderophore-β-lactam conjugates has been reported and has involved coupling of β-lactams to hexadentate, tetradentate and bidentate iron (III) chelating ligands and out of these the biscatecholate conjugates were found to be potent (Miller *et al.,* 1993; Watanabe *et al.,* 1987; Imap *et al.,* 1993; Miller *et al.,* 1989). The structure of one of the dichatecholates is shown below (Fig. 1.25). Mutant bacteria were found to lack hydroxamate and catechol receptors required for the uptake of drugs-siderophores and siderophores, and it is clear that conjugation promoted the transport of the antibiotics (Miller 1993).

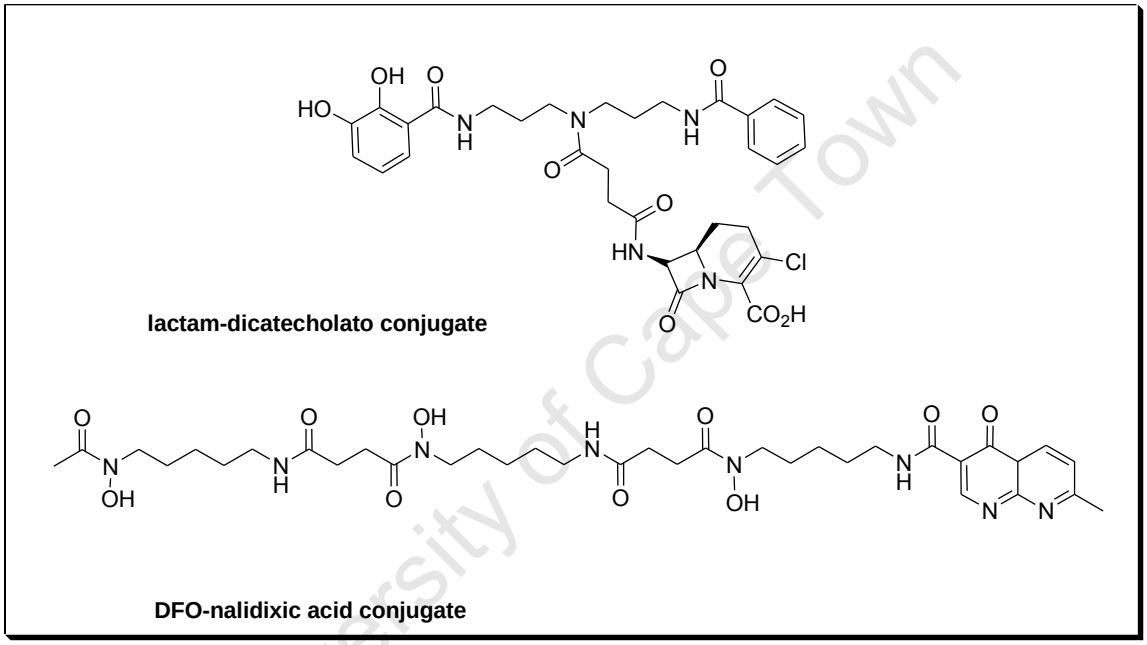

Figure 1.26: β-*lactam-dicatecholato and DFO-nalidixic acid drug conjugates*

The fundamental challenge associated with this approach is that most pathogenic organisms possess multiple routes for iron uptake, and the higher the number of genes involved in iron transport the higher the frequency of resistance (Hider and Xiaole, 2010).

1.8.3 Antimalarial Siderophore Drug Conjugates

A conjugate was prepared by coupling desferal/ferrioxamine (DFO) an antimalarial siderophore to nalidixic acid a DNA intercalator as illustrated in Figure 1.26 above, (Ghosh *et al.,* ., 1995) The conjugate was found to have antimalarial activity against multidrug resistant strains of *P .falciparum* D6 and N2 (IC_{50} =0.6µg/mL for both strains). It was assumed that the conjugate killed the parasite via DNA intercalation (Hider *et al.,* ., 1997; Roosenberg II *et al.,* 2000)

1.9 ADMET Properties: Absorption, Distribution Excretion and Toxicity.

After administration, a drug undergoes adsorption, distribution, metabolism and finally excretion as illustrated below (Fig. 1.27). The drug also may impart toxic effects on the organism.

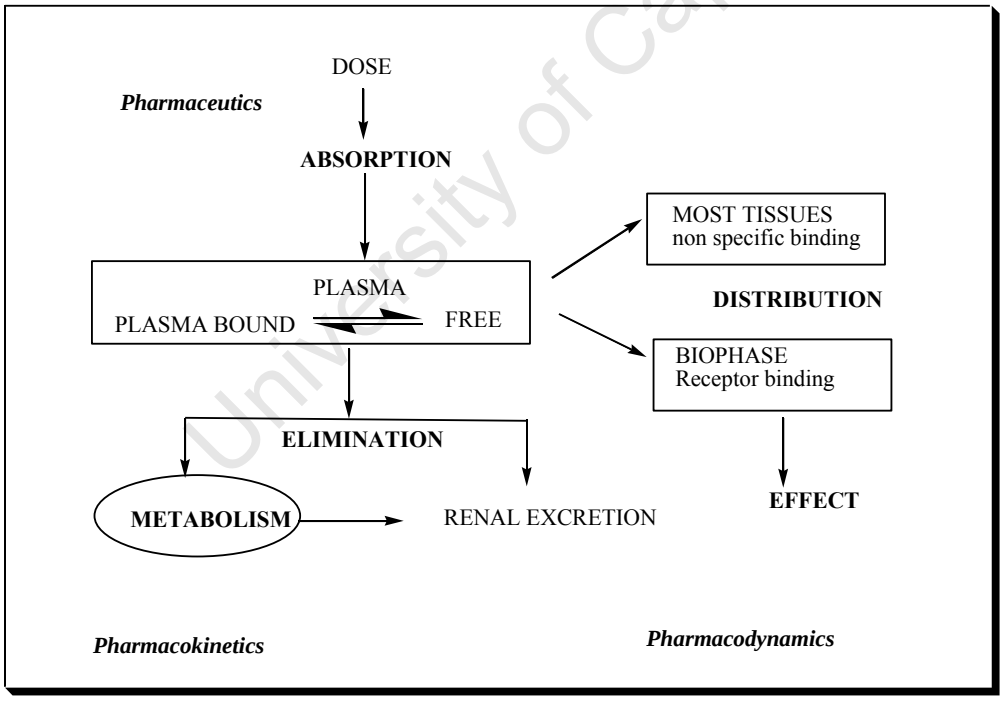

Figure 1.27: *Fate of a Drug (Adopted from Evans and Relling, 1999)*

Studies in the 1990s show that poor pharmacokinetics and toxicity (PK-Tox), were the most important causes of costly late stage failures in drug development (Van de

Waterbeemd and Gifford, 2003). It is therefore important to consider the PK-Tox as early as possible in the drug discovery process.

ADMET data may be obtained from *in vitro* assays, *in silico* models and from predictive models. The ADMET data helps to inform whether to continue with synthesis or not and whether to modify the compounds to optimize its properties before proceeding to clinical studies.

An orally administered drug will first dissolve in the gastrointestinal tract, and then will be absorbed through the gut wall passing the liver to get into the blood circulation. The percentage of the dose reaching circulation is referred to as its bioavailability (Fig. 1.28). The systemic circulation will distribute the drug to various tissues and organs. The extent of distribution will depend on the structure and physicochemical characteristics of the compound. Finally the drug will bind to its molecular target eg a receptor or ion channel and exert the desired effect (Evans and Riley, 1999). Alternatively it may bind to undesired sites and cause toxicity.

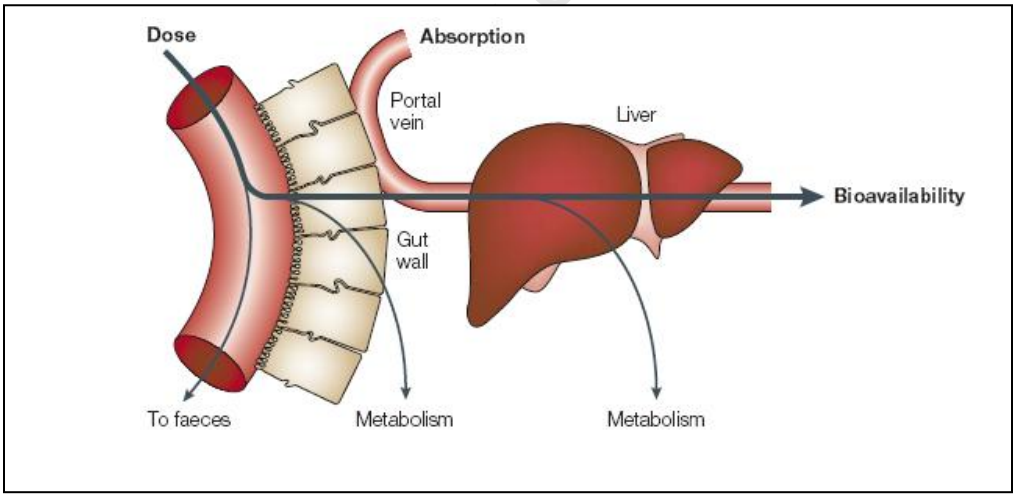

Figure 1.28: *The path of an orally administered drug and processes in respective organs (Van de Waterbeemd and Gifford, 2003)*

1.9.1 Drug Physicochemical Properties that Affect ADMET

1 1.9.1.Lipophilicity

The gold standard for expressing lipophilicity is the partition coefficient P or log P in the octanol/water system. The calculated or predicted partition coefficient (cLog P) depends on molecular size/weight, polarity and hydrogen bonding. Poor aqueous solubility and slow dissolution rate can lead to poor oral absorption hence low oral bioavailability. In general poor solubility is related to high lipophilicity i.e.. high log P or clog P. Hydrophilic compounds (highly soluble compound) generally have poor permeability and thus low absorption. It is clear that solubility and lipophilicity as well as ionization constant, pKa, affect permeability and absorption of a drug (Fig 1.29). A moderate log P (0-3) is desirable for good gastrointestinal absorption or for good oral bioavailability (Di and Kerns, 2008). Calculated or predicted log P values can be obtained by use of programs such as MetaSite, MoKa and Volsurf.

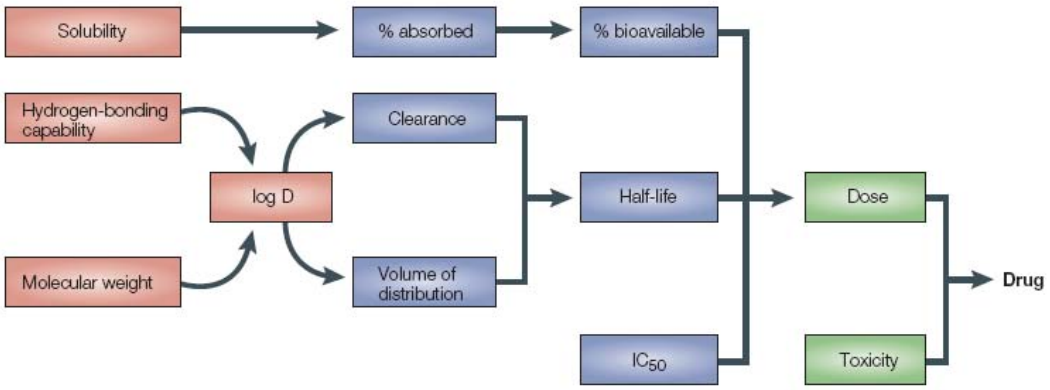

Figure 1.29: *Relationships between some physicochemical and ADMET properties (Adopted from Van de Waterbeemd and Gifford, 2003)*

1.9.1.2. Distribution Coefficient Log D

Distribution coefficient is determined experimentally at pH 7.4 (blood pH) or pH 6.5 (intestinal pH). It often provides a more meaningful description of lipophilicity especially for ionizable compounds. Log D affects clearance and volume of distribution of a drug which influence plasma half life (Fig 1.29). Programs that can reliably predict log D are scarce (Van de Waterbeemd and Gifford, 2003)

1.9.1.3. Solubility

Low solubility is detrimental to good oral absorption, so early measurement of solubility is important in drug discovery especially for antimalarials. The main experimental measurements rely on turbidimetry and nephelometry (Di and Kerns 2008). Solubility can be improved by preparation of salts or by structural modification. The structural modifications may involve inclusion of polar groups, decreasing the molecular weight, increasing the hydrogen bonding capability, increasing the ionizability and incorporating structures that will decrease crystal stacking (Di and Kerns, 2008).

1.9.1.4 Ionizability (pKa)

Ionizability or pKa is the negative log of the ionization or dissociation constant of a compound. A majority of drugs contain ionisable groups and ionization of a drug is known to affect its solubility, lipophilicity, permeability and absorption. It can be determined experimentally or by use of computer programs.

1.9.1.5. Hydrogen Bonding

The hydrogen bonding capacity is a determinant of permeability. In order to cross cell membranes a drug molecule needs to break hydrogen bonds within its aqueous environment. The more potential hydrogen bonding a molecule can make the more energy it will require to break them. Higher number of hydrogen bonds leads to low

permeability and poor absorption. Computational methods have been used to determine hydrogen bonding capacity ie by counting the hydrogen bond acceptors and donors and by using free energy factors and the polar surface area (PSA) (Stenberg *et al.,* 2001)

1.9.1.6. Permeability

Permeability of compounds through the Caco-2 cells is used to model for human intestinal absorption. This is referred to as membrane quantitative structure activity relationship MI-QSAR (Kulkami *et al.,* 2002). Hence permeability helps predict the degree of absorption after oral administration. A drug must be sufficiently permeable through the biological membranes present in order to enter the systemic circulation.

1.9.2 ADMET Properties

The ADMET properties are closely related or dependent upon the physicochemical properties of a drug (Fig. 1.30). Several researchers have used physicochemical properties to predict ADMET properties, notable examples are Lipinski (1997; 2004) and Gleeson (2008).

1.9.2.1. Absorption

Lipinski and coworkers formulated minimum physicochemical requirements for orally bioavailable drugs. The Lipinski rule of 5 which was derived from a database of clinical candidates reaching phase II trials identifies several critical properties that should be considered for compounds meant for oral administration, sometimes these rules are referred to as the drug-like properties (Di and Kerns, 2008). These guidelines are molecular weight < 500 daltons (Da), calculated octanol/water partition coefficient (clogP) < 5, number of hydrogen bond acceptors < 10 and number of hydrogen bond donors < 5 (Lipinski, 1997; Lipinski *et al.,* 2004). Drugs that do not comply often have poor absorption and permeability.

1.9.2.2. Distribution or Promiscuity

Distribution of a drug in the organism depends largely on lipophilicity ie log P. It is known that log P influences drug potency, pharmacokinetics and toxicity (Leeson and Springthorpe, 2007). If lipophilicity is too high there is an increased likelihood of binding to multiple targets and resultant pharmacologically based toxicity as well as poor solubility and metabolic clearance. The risk of unwanted pharmacology increases with lipophilicity and is dependent on ionization class (Azzaoui *et al.,* 1997). However, promiscuity becomes less important if the selectivity for the desired target is high. Distribution can be measured by the volume of distribution V_D which together with the clearance determines the plasma half life and thus affects the dosing.

1.9.2.3. Metabolism

The rate and extent of metabolism (turn over), the enzymes involved and the products formed are the main concerns when one refers to drug metabolism. The extent and rate of metabolism affects clearance whereas the involvement of a particular enzyme might lead to issues related to the polymorphic nature of some enzymes and to drug-drug interactions, (DDIs) (Van de Waterbeemd and Gifford, 2003). DDIs are possible when CYP induction or inhibition occur when drugs are co-administered. CYP induction increases metabolism of one of the drugs while CYP inhibition slows down the metabolism of one of the drugs (Zhou, 2008).

Compounds with good solubility and permeability may have low oral bioavailability if the *in vivo* plasma/blood clearance is too high (Gleeson, 2008). *In vivo* clearance affects the half life of the compound and in turn the latter together with V_D affects the dosing regimen. Clearance is via hepatic, renal and bilary processes and is considered to be the most difficult ADMET process to predict because it strongly depends on structural aspects rather than the physicochemical properties (Madden and Cronin, 2006)

In silico approaches have an increasingly important role as alternatives to in vitro metabolic studies. The *in silico* tools for predicting metabolism can be divided into QSAR and 3D-QSAR studies, protein pharmacophore models (eg AutoDock and MetaSite programs) and predictive databases eg Volsurf (Ekins *et al.,* 2000, 2001, 2003, 2007; De Groot *et al.,* 1999). Early prediction of the vulnerability of metabolism of certain positions in the molecule might help to eliminate molecular liabilities and this is possible with programs like MetaSite.

1.9.2.4. Toxicity

Toxicity is responsible for many compounds failing to reach the market and for the withdrawal of a significant number of compounds from the market once they have been approved (Waterbeemd and Gifford, 2003). In vitro assays to determine toxicity include DDIs (due to CYP inhibition), hERG channel blocking, mutagenicity/genotoxicity, cytotoxicity, teratogenicity, selectivity and reactivity screens (Di and Kerns, 2008).

A number of *in silico* toxicity methods are in use and are broadly classified into two. First are knowledge based expert systems. These methods use expert systems that derive models on the basis of abstracting and codifying knowledge from human experts and scientific literature (Di and Kerns, 2008; Van de Waterbeemd and Gifford, 2003). Second are the statistically based *in silico* toxicity methods which rely on the generation of descriptors of chemical structures and statistical analysis of the relationships between these descriptors and the toxicological endpoint (Di and Kerns, 2008; Waterbeemd and Gifford, 2003).

1.9.2.5. Drug-Drug Interactions

Patients often receive several medications at the same time and if the drugs involved compete for the same enzymes to be metabolized or if the same transporters are involved in transporting the drugs across the membranes, this can lead to undesired effects with possible fatal results (Van de Waterbeemd and Gifford, 2003). This can be explained

using the victim perpetrator concept. One drug (the perpetrator) binds to the isozyme and the other drug (the victim) is excluded from metabolism, thus increasing toxic concentrations. A major cause of DDI is CYP3A4 inhibition.

1.9.3. CYP3A4 Inhibition

CYP3A4 belongs to the superfamily of P450 enzymes (CYPs) that is involved in the metabolism of endogenous and exogenous substrates in living organisms. They control oxidative metabolism clearance of drug molecules and other xenobiotics (Mao *et al.,* 2006). CYP3A4 is the predominant metabolic monooxygenase in intestinal and hepatic drug metabolism and is involved in clearance of more than 50% of all marketed drugs (Egan *et al*., 2004; Guengerich, 1997). The liver is frequently the target of toxic chemicals and since it lies between the portal and systemic circulation the liver will receive drugs entering via the portal system during oral absorption (Yan *et al.,* 2001)

To date the identified clinically important CYP3A4 inhibitors include macrolide antibiotics, anti-HIV agents, antidepressants, calcium channel blockers, steroids and their modulators and several herbal and dietary components (Zhou, 2008). Structural features associated with CYP3A4 inhibition are illustrated in Figure 1.30 and they include terminal olefins and acetylenes, quinolines, amines, hydrazines, hydrazones and methylene dioxy phenyls (Zlokarnik *et al.,* 2005; Riley and Kenna, 2004).

The large variety of structurally diverse drugs that are metabolized by CYP3A4 suggests a broad enzyme binding pocket (and thus a broad range of possible intermolecular interactions) for this enzyme (Mao, 2006). The non competitive inhibition of CYP3A4 shows that multiple substrates or inhibitors can bind simultaneously in the enzyme pocket (Mao, 2006) and experimental and modeling evidence supports this (Ekins *et al.,* 2003; Ekroos and Sjogren, 2006).

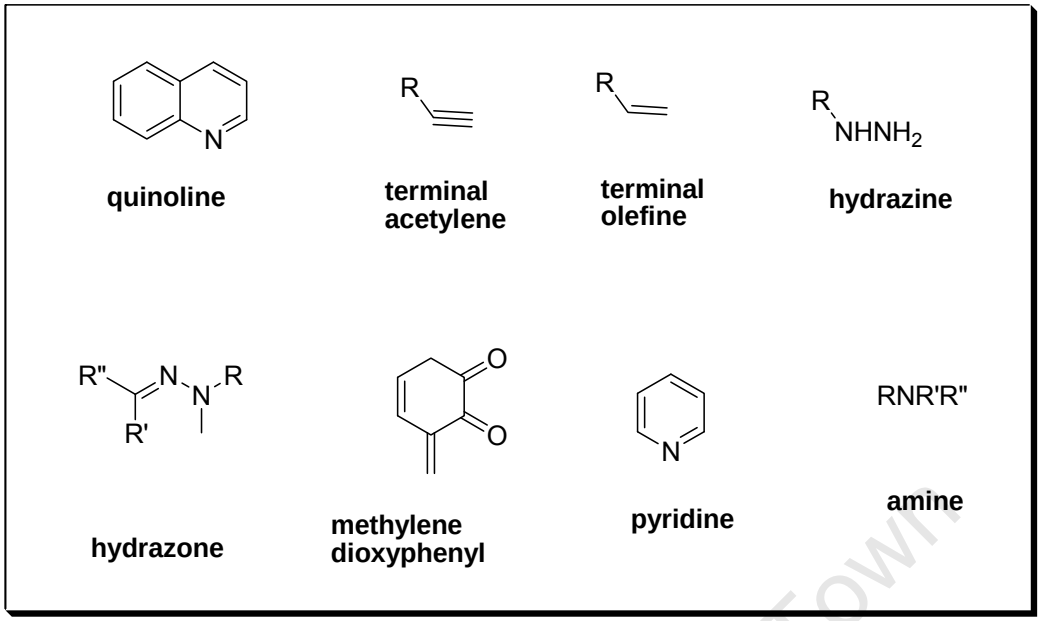

Figure 1.30: *Structural features associated with CYP3A4 inhibition*

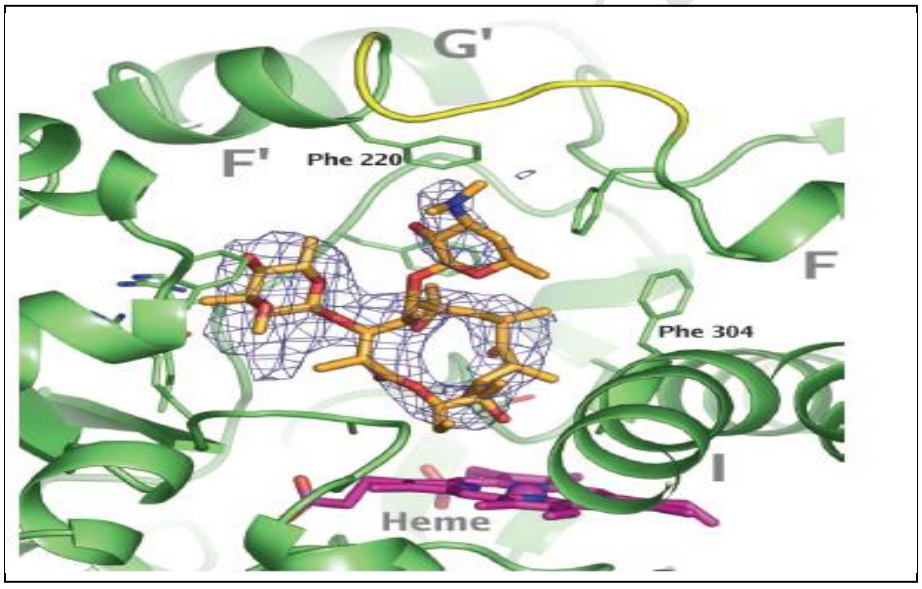

Figure 1.31: *Crystal structures of erythromycin bound in CYP3A4 (Ekroos and Sjogren, 2006)*

Recently the 3D structure of CYP3A4 has been determined by X-ray crystallography and it has been confirmed that a large binding site exists near the haem (Sevrioukova and Poulos, 2010; Ekroos and Sjogren, 2006; Yano *et al.,* 2004; Williams *et al.,* 2004). Figure

1.31 show the crystal structures of erythromycin bound in the CYP3A4; note the large binding pocket in the haem's vicinity

P450s are known to contain a ferriprotoporphyrin IX (haem) prosthetic group and a polypeptide encoded by a single gene. The haem moiety acts as an oxidation reaction centre and the apoprotein determines the substrates specificity and the binding affinity of individual isozymes (Yan *et al.,* 2001). In the hepatic microsomal membrane, the haem is in the ferric form Fe^{3+} and functions as an electron pair acceptor in oxidation reactions. Although CYPs have been detected in various tissues, the hepatic CYPs play the most important role in drug metabolism (Yan *et al.,* 2001).

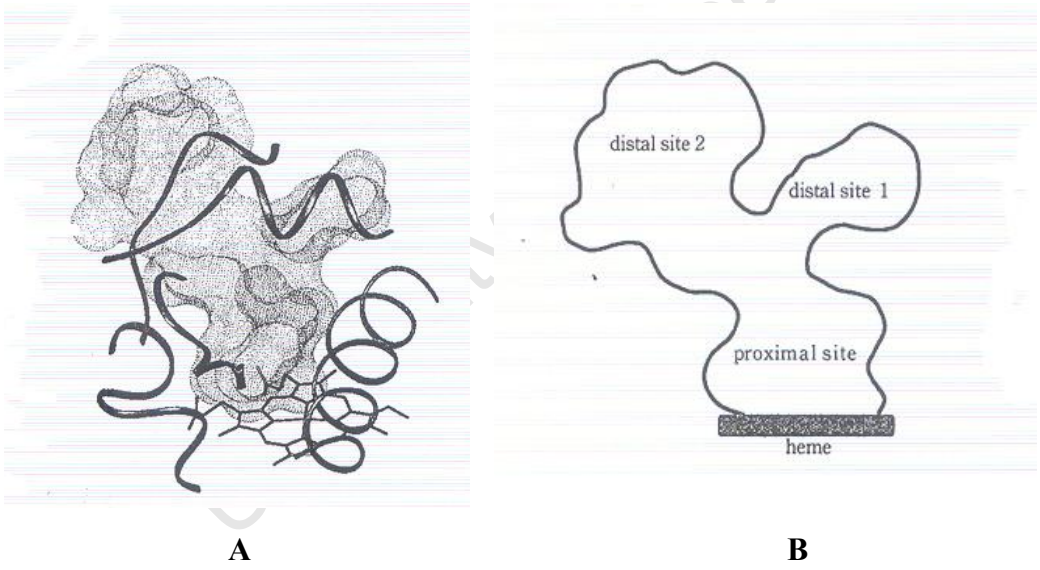

A **B**

Figure 1.32: *(A) Model of the Binding pocket of CYP3A4 (B) Sketch of the three putative parts of the active site (Tanaka et al., 2004)*

Experimental evidence shows that there are two substrate binding sub-pockets and one effector binding region in the CYP3A4 active site (Domanski *et al.,* 2001). These sub-pockets may be described as two distal binding sites and one proximal binding site with respect to the active site see Figure 1.32, (Tanaka, *et al.,* 2004), Hydrogen bonding and hydrophobicity dominate the ligand-CYP3A4 interactions. The hydrophobic pocket

residues include Phe 108, Leu 210, Leu 211, Phe 241, Ile 301, Phe 304 while the polar pocket residues include Arg 106, Arg 372 and Glu 374 among others (Sevrioukova and Poulos, 2010; Ekroos and Sjogren., 2006; Tanaka *et al.,* 2004).

A growing body of evidence shows that the interactions between CYP3A4 and its substrates and inhibitors are complex (Yan *et al.,* 2000). Atypical kinetic profiles (Kronbach *et al.,* 1989), positive cooperativity (Ueng *et al.,* 1997), and multiple apparent K_m values (Bloomer *et al.,* 1997) as well as substantial probe-substrate dependent qualitative and quantitative differences in the extent of inhibition of CYP3A4 have been reported (Kenworthy *et al.,* 1999; Wang *et al.,* 2000).

The classical approach for *in vitro* P450 inhibition analysis is to use a drug as a probe substrate and measure inhibition over a range of substrate and inhibitor concentrations (Stresser *et al.,* 2000). To reduce attrition of otherwise promising lead candidates due to toxicity liabilities from DDIs, in vitro screening tests of new chemical entities (NCEs) for the inhibition of drug metabolizing CYPs is important (Mao *et al.,* 2006)

In silico tools have been used to predict binding modes, sites of metabolism and affinities of NCEs in CYPs. Docking techniques are increasingly used to support lead optimization efforts (Kitchen, 2004). Accurate predictions of binding affinities critically depend on finding correct binding conformations (Verdonk, 2006), thus docking programs need to produce reliable binding modes to obtain good enrichment in virtual screening (Kellenberger, 2004).

1.10 OBJECTIVES

To identify novel antimalarial 4-aminoquinoline-3,4-hydroxypyridinone hybrid compounds with *in vitro* and *in vivo* potency

To elucidate the mechanism of action with respect to haemozoin inhibition in *P. falciparum*

1.11 HYPOTHESES

Is it possible to enhance the *in vitro* and *in vivo* antimalarial activity of 3-hydroxypyridin-4-ones (3,4-HPOs) and other iron chelators by covalently linking them with standard antimalarial drugs.

1.12 AIMS

2. Synthesis and studies of 3,4-HPOs as antimalarial inhibitors of haemozoin formation.
3. Synthesis of hybrid structures of 3,4-HPOs with 4-aminoquinolines.
4. Screening of the synthesized compounds for biological activity: *in vitro* and *in vivo* antimalarial activity, β-haematin inhibition and toxicity.

1.13 JUSTIFICATION

The resistance of *P. falciparum* to standard antimalarial drugs is still a problem hence the necessary search for new drugs with different or better modes of action. Most of the current antimalarial iron chelators (HPOs) were designed to treat iron overload and not malaria, hence the need to design and synthesize antimalarial. 3,4-HPOs that act by other mechanisms in addition to abrogation of iron from the intraerythrocytic parasite. 3,4-HPO-quinoline hybrid molecules have not been synthesized nor studied as potential antimalarials. Synthesis and antimalarial evaluation of the hybrids may result in improving the antimalarial activity of this class of compounds.

1.14 Why Haemozoin Inhibitors for Antimalarial Therapy?

The haem detoxification pathway of *P. falciparum* is a particularly attractive drug target because (1) It targets the parasites when they are causing the clinical pathologies (2) Humans detoxify free haem via the haem oxygenase/biliverdin reductase pathway (which is different from the parasites) hence a drug that interferes with haem processing in the parasite will not inhibit haem detoxification in humans. (3) Inhibition of haem detoxification would lead to a built up of high concentration of toxic free haem inside the parasite (Choi *et al,* 2002).

1.15. Synthetic targets

A number of known *N*-alkyl-3, 4-hydroxypyridinones (3,4-HPOs) were targeted for synthesis (Table 1.3). The length of the *N*-alkyl chain varied from one carbon to eight carbon atoms. The objective was to establish the baseline antiplasmodial activity of this class of compounds prior to conjugation with aminoquinolines or artemisinins. Most of the past literature reports gave the the antiplasmodial activity of this type of compounds in qualitative terms i.e. percentage inhibitions rather than quantitatively (IC_{50} values).

Table 1.3. *Target N-alkyl-3,4-hydroxypyridinone compounds and gallium (III) complexes*

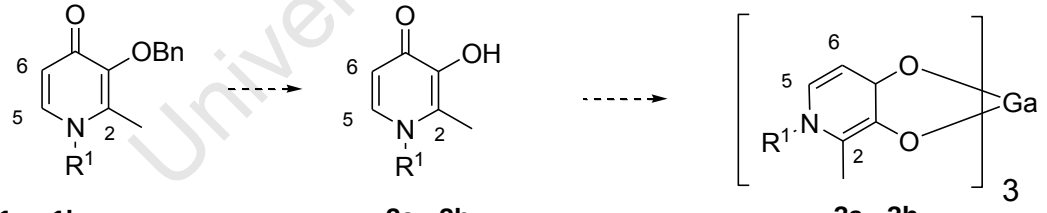

R^1	*methyl*	*ethyl*	*butyl*	*cyclopropyl*	*isopropyl*	*n-propyl*	*n-hexyl*	*n-octyl*
Compound sub-series	**a**	**b**	**c**	**d**	**e**	**f**	**g**	**h**

Gallium (III) complexes of the 3,4-HPOs were prepared and these were tested alongside the corresponding ligands and their benzylated analogues. The aim was to investigate the mode of antiplasmodial activity with respect to iron chelation and or the effect of

complexation on activity against resistant parasites. The most potent compound in the series was targeted for antimalarial combination therapy studies together with chloroquine or artemisinin to justify hybridization of the 3,4-HPOs and aminoquinolines.

Table 1.4. *Target 4-aminoquinoline-3,4-hydroxypyridinone hybrid molecules-Series **A** and **AB***

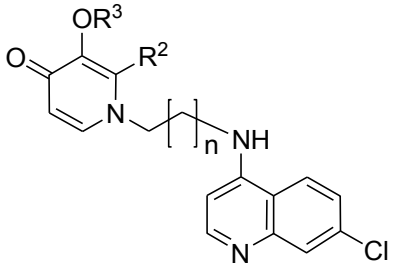

series A: R^2 = Me; series AB: R^2 = Et

Compound	Series	n	R^2	R^3
9	A	1	Me	Benzyl (Bn)
9a	A	1	Me	H
10	AB	1	Et	Bn
10a	AB	1	Et	H
11	A	2	Me	Bn
11a	A	2	Me	H
12	AB	2	Et	Bn
12a	AB	2	Et	H
13	A	3	Me	Bn
13a	A	3	Me	H
13b	A	3	Me	Me
14	AB	3	Et	Bn
14a	AB	3	Et	H
14b	AB	3	Et	Me
15	A	5	Me	Bn
15a	A	5	Me	H
15b	A	5	Me	Me
16	AB	5	Et	Bn
16a	AB	5	Et	H
16b	AB	5	Et	Me

The synergistic antiplasmodial effect of combining compound **2h** with chloroquine motivated the synthesis of the 4-aminoquinoline-3,4-hydroxypyridinone hybrid molecules. The initial targets are depicted in Table 1.4. The 4-aminoquinoline was

incorporated into the hydroxypyridinone via a Michael addition reaction making the targets retain the 3,4-HPO scaffold.

Table 1.5. *Target 4-aminoquinoline-3,4-hydroxypyridinone hybrid molecules-Series **R** and **D***

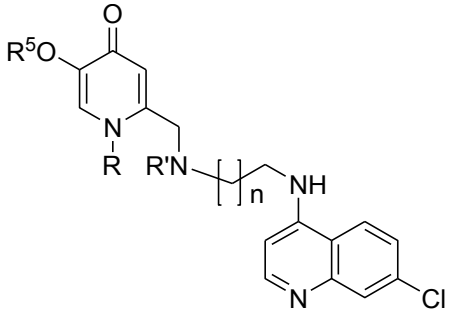

series R: R = Me
series D: R = Cyclopropyl

Compound	Series	n	R	R'	R^5
23	R	1	Me	H	Benzyl(Bn)
23a	R	1	Me	H	H
24	R	2	Me	H	Bn
24a	R	2	Me	H	H
25	R	2	Me	Me	Bn
25a	R	2	Me	Me	H
26	R	3	Me	H	Bn
26a	R	3	Me	H	H
27	R	5	Me	H	Bn
27a	R	5	Me	H	H
28	D	1	cyclopropyl	H	Bn
28a	D	1	cyclopropyl	H	H
29	D	2	cyclopropyl	H	Bn
29a	D	2	cyclopropyl	H	H
30	D	2	cyclopropyl	Me	Bn
30a	D	2	cyclopropyl	Me	H
31	D	3	cyclopropyl	H	Bn
31a	D	3	cyclopropyl	H	H
32	D	5	cyclopropyl	H	Bn
32a	D	5	cyclopropyl	H	H

Preliminary screening indicated that the hybrids **9 - 16** and **9a – 16a** (Series **A** and **AB**) had potential to cause CYP3A4 inhibition in the presence of testosterone. This data prompted structural modification of the initial hybrid molecules to fine tune

physicochemical properties for improved CYP3A4 inhibition profile. As well incorporation of a tertiary amino group was envisaged in order to improve antiplasmodial potency via enhanced accumulation of the target molecules in the parasitic food vacuole. The modified hybrid targets (series **R** and **D**) are shown in Table 1.5 and were derived from kojic acid.

Table 1.6. *Gallium (III) and iron (III) complexes of series **A** and **AB** ligands*

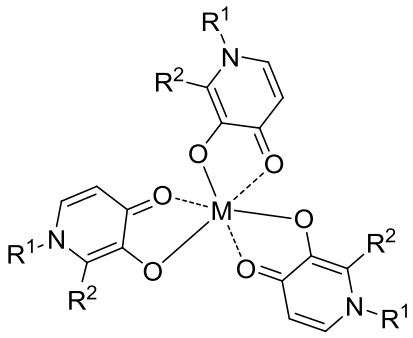

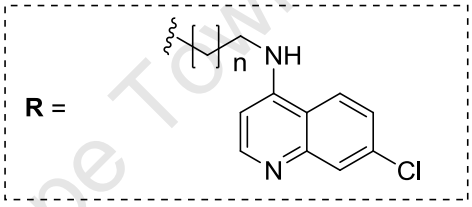

Complex	Ligand	n	R^2	M (III)
13c	13a	3	Me	Fe
13d	13a	3	Me	Ga
15e	15a	5	Me	Fe
15d	15a	5	Me	Ga
16c	16a	5	Et	Ga

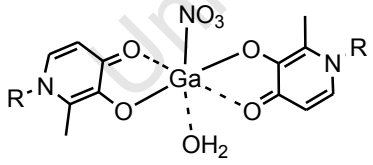

complex **15e**

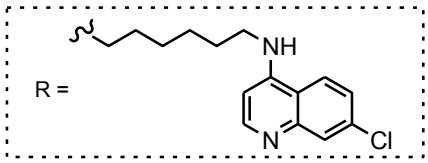

Figure 1.33. *Structure of complex **15e**.*

Gallium (III) and iron (III) complexes of conjugates from series **A** and **AB** were prepared. Selection of the ligand was based on the *in vitro* antiplasmodial potency as well

as availability of the ligand and the latter depended on their respective synthetic yields. On this basis the targets represented in Table 1.6 were prepared.

Further synthetic targets were pursued and in the fifth series the aim was to replace the 3,4-HPO moiety in the hybrid molecules with a biscatecholate group (Figure 1.34). The rationale behind this was to determine if the 3,4-HPO group has influence over the CYP3A4 inhibition property of this hybrid molecules, thus the appropriate bioisostere was used to replace 3,4-HPO.

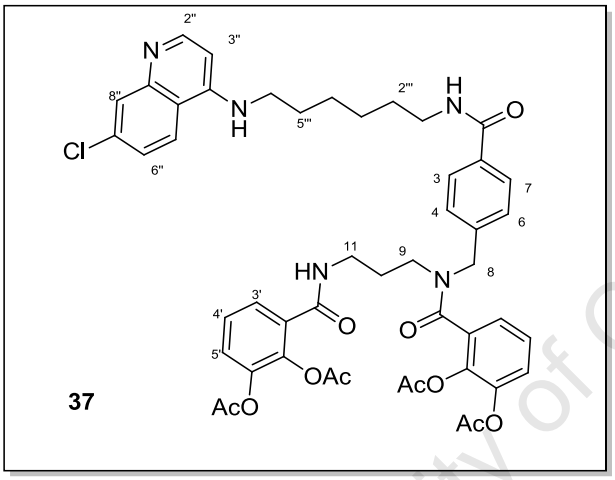

Figure 1.34. *Biscatecholate-4-aminoquinoline conjugate*

In silico predictions, *in vitro* data and synthetic accessibility of the target compounds have in one way or another influenced the design of each series. The design rationales for each series of compounds are systematically considered in the synthesis chapter with respect to the aforementioned factors.

CHAPTER TWO

SYNTHESIS AND CHARACTERIZATION

2.1 Synthesis and Characterization of 1-*N*-alkyl-3,4-Hydroxypyridinones and their Gallium (III) Complexes.

The synthesis of 3,4-hydroxypyridinones involves a double Michael addition reaction between maltol, or ethylmaltol or a kojic acid derivative with a secondary amine as illustrated in Figure 2.1 (Molenda *et al.,* 1994b, c). It involves ring opening and closure. There is competitive formation between the 3,4-hydroxypyridinones and corresponding Schiff bases depending on the solvent used in the reaction, for instance the use of protic solvents favour 3,4-HPO formation, but aprotic solvents promote the Schiff base formation (Fig 2.1).

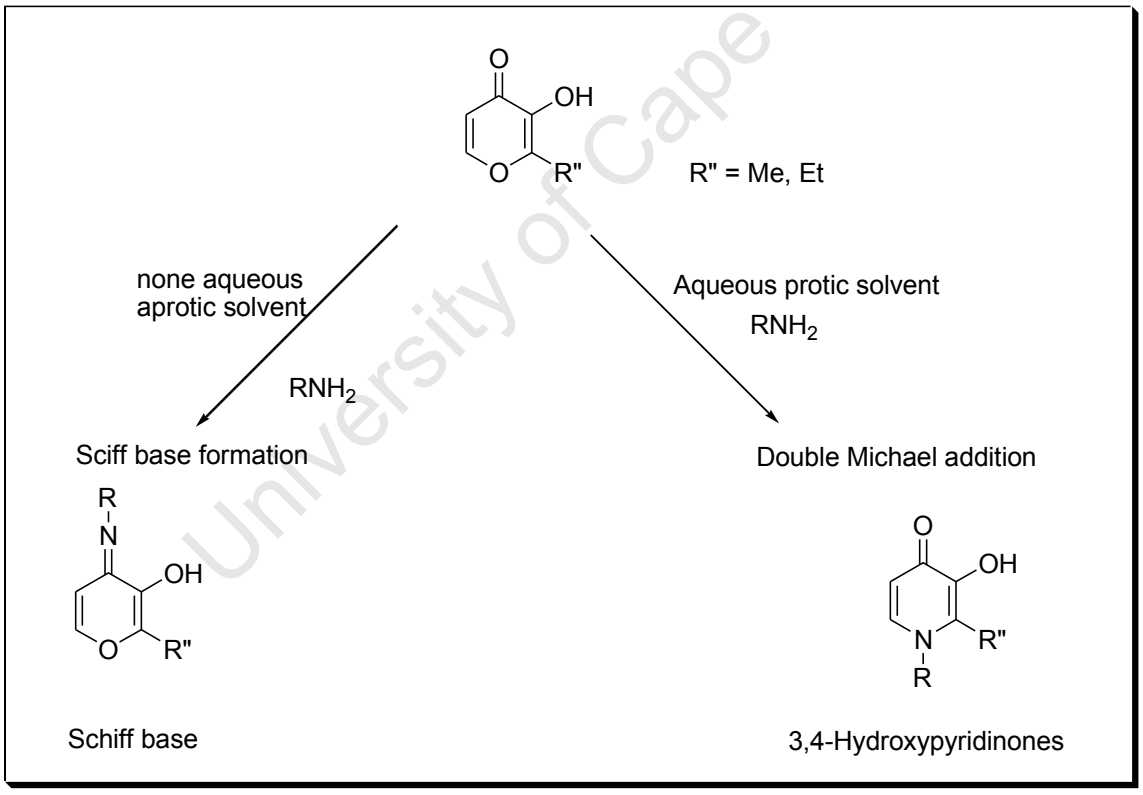

Figure 2.1: *Reaction conditions for Synthesis of 3,4-HPOs*

The two products can be differentiated, in that the Schiff base has a characteristic low melting point and yellow colour unlike the 3,4-HPOs which are white and have relatively

high melting points. More effectively, the UV spectra of their iron complexes differ and this can be used to identify the two. The Schiff base UV spectrum has a relatively low intensity (Molenda *et al* 1994b, c).

2.1.1 Rationale

There was a need to establish the baseline antimalarial activity of known 1-*N*-alkyl-3,4-hydroxypyridinones (3,4-HPO) before synthesis of new structurally modified 3,4-HPOs. Therefore a number of known 3,4-HPOs with variations in the N-alkyl chain length were synthesized and tested for antimalarial activity. The N-alkyl variation was meant to fine tune the lipophilicity of these iron chelators. Lipophilicity directly correlates with the chelators inhibitory activity against the malaria parasite *Plasmodium falciparum* as demonstrated for a number of chelators namely; N-alkyl derivatives of 3,4-hydroxypyridinones (HPOs) and aminothiols. (Shanzer *et al,* 1991, Hershko *et al.,* 1991, Loyevsky and Gorduek, 2001)

Complexation with gallium (III) has been reported to enhance antimalarial activity and to overcome drug resistance in aminophenols (Ocheskey *et al,* 2003; 2005, Goldberg *et al*, 1997). This has not been reported for the antimalarial activity of N-alkyl-3,4-HPOs, hence creating a reason to prepare and study the antimalarial activity of the 3,4-HPO gallium (III) complexes.

2.1.2 Retrosynthesis of the 3,4-HPOs

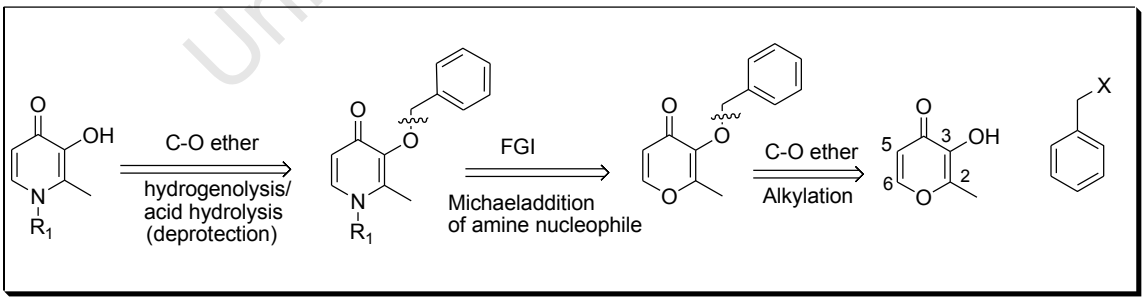

Figure 2.2: *Retrosynthetic analysis of 3,4-HPOs*

The retrosynthesis involves a deprotection of a benzyl ether disconnection C-O of ether formation and a functional group interconversion (FGI) involving a pyrone to a pyridinone via Michael addition and O-alkylation.

The commercially available benzylhalide (BnBr or BnCl) and maltol (3,4-hydroxypyrone) were selected as the starting materials for this synthesis.

The C-3 position in 3-hydroxypyran-4(*H*)-pyranones is known to be highly reactive to electrophilic substitution (Atkinson *et al* 1979) but in benzylmaltol the benzyl protecting group activates the C-2 position making it more prone to a nucleophilic attack. If unprotected the maltol molecule will act it self as a nucleophile rendering it unfavourable for the nucleophilic attack by the primary amine. Lower yields in the synthesis of the hydroxypyridinones are inevitable if the protection of the 3-hydroxy group is excluded.

2.1.3 Synthesis

Benzylmaltol was prepared by refuxing benzylchloride and maltol in the presence of catalytic amounts of NaOH. The reaction progress was monitored by TLC and detection was by UV 254nm/ 330nm and emersion into 0.1M ferric ammonium sulphate solution, to form red colored Fe^{3+} complex for the unreacted maltol and a pale yellow color for the benzylated maltol. (Kruck *et al.,* 2002)

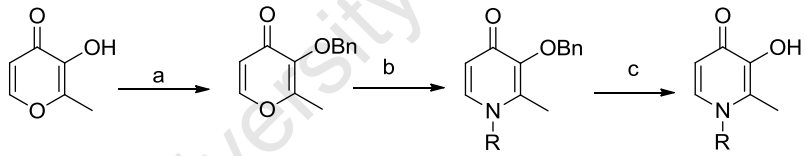

***Conditions and reagents**: (a) BnCl, NaOH, MeOH, reflux, 22h (b) RNH_2 , NaOH, 1:1 EtOH/H_2O, reflux 18h, (c) H_2, Pd/C, 4atm or 2M HCl, reflux 4h.*

Figure 2.3: *Synthesis of 3,4hydroxypyridinones*

The benzylmaltol was subjected to amination using a primary amine to form a benzylated hydroxypyridinone under refluxing conditions (Fig.2.3). This is a Michael addition reaction involving the free nitrogen of the primary amine attacking the pyran resulting in ring opening followed by ring closure mediated by a second nucleophilic attack by the nitrogen (Fig.2.4) This reaction is a thermodynamically controlled S_N2 type reaction such that high temperatures over along period of time in a protic medium favour addition to the conjugated intermediate and not to the carbonyl carbon (Molenda *et al,* 1994,

Clayden, *et al* 2001, Sainsbury, 2001). The unhindered β- carbon and the use of a soft nucleophile favoured the Michael addition at the target site.

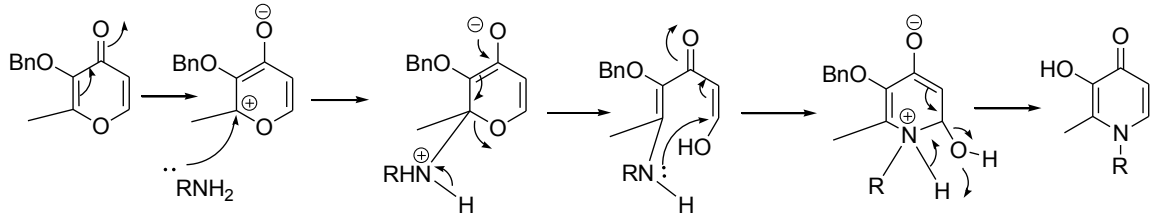

Figure 2.4: *Mechanism of the Michael addition to the benzylmaltol*

The deprotection was achieved by acid catalysed hydrolysis or by hydrogenation (Harris, 1976; Dehkordi *et al.,* 2008), (Fig. 2.3). The hydrolysis phenomenom was also observed during the recrystallization of the benzylated analogues **1c** and **1d** (Table 2.1). The recrystalization procedure involved dissolution in EtOH/HCl (2M), concentration under reduced pressure at 70^{o}C, before recrystalization from EtOH/Et_2O. The acidic conditions and the moderate temperature favoured debenzylation.

The yields of the benzylated 3,4-HPOs appear to be at optimum for compounds with the N-alkyl side chains of intermediate length (3 - 6 carbon atoms), but the yield is lower for compounds with shorter (1 or 2 Carbon atoms) or longer (8 carbon) N-alkyl side chains. It may be assumed that the compounds with shorter side chains are more hydrophilic hence more soluble in the aqueous ethanolic reaction medium unlike the long chain analogues. During the workup, less of the hydrophilic compounds will partion into the organic solvent i.e. dichloromethane and thus more of these compounds will remain in the aqueous layer during the extraction hence poor yields. The opposite effect is assumed for the lipohilic compounds (compounds with longer N- alkyl chain). To rationalize poor yields for the N-octyl analogue, one could consider solubility of the aminoalkane in the aqueous ethanolic reaction mixture/medium. The octylamine which is used to prepare analogue **1h** the may be assumed to less soluble in the reaction mixture hence less available for Michael addition during the reaction time. The other possible reason for the poor yield could be that the Octylamine has a longer chain which poses greater steric hinderance during the Michael addition than amines with shorter chain.

There is no great difference in the yields amongst the deprotected *N*-alkyl-3,4-HPOs.

2.1.4 Characterization

Table 2.1: *Yields of the benzylprotected 3,4-HPOs and their deprotected analogues*

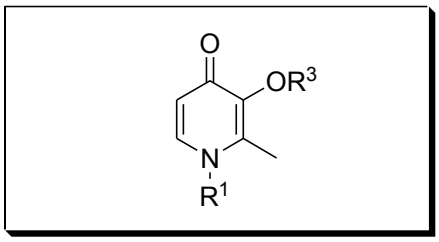

Compound	R^1	R^3	% Yield
1a	Me	Bn	48
1b	Et	Bn	31
1c	n-Bu	Bn	59
1d	cyclopropyl	Bn	57
1e	i-Propyl	Bn	50
1f	n-Propyl	Bn	44
1g	n-Hexyl	Bn	63
1h	n-Octyl	Bn	28
2a	Me	H	75
2b	Et	H	55
2c	n-Bu	H	32
2d	cyclopropyl	H	47
2e	i-Propyl	H	61
2f	n-Propyl	H	83
2g	n-Hexyl	H	74
2h	n-octyl	H	69

The compounds (Table 2.1) were characterized by MS, ^{1}H and ^{13}C NMR, melting point and elemental analysis. None of the compounds was novel except **1d** and **2d**. A typical proton NMR spectrum of these compounds consists of the two diagnostic doublets at δ7-6 ppm corresponding to the pyridinone H-5 and H-6. The multiplet observed in the

region δ 7.4 – 7.0 ppm due to the benzyl aromatic protons as well as the singlet at δ 5 ppm due to the benzyl methylene protons were conspicuously absent in the spectra of the deprotected analogues. The ^{13}C NMR of the deprotected compounds indicated the absence of the peaks in the δ 129-127 ppm region corresponding to the aromatic carbon atoms of the benzyl group.

Table 2.2: *Melting points of the benzylprotected 3,4-HPOs and their deprotected analogues Reported data is from Dobbin et al (1993)*

Compound	Formula	Mp (observed) ^oC	Mp (reported) ^oC
1a	$C_{14}H_{16}ClNO_2.0.5H_2O$	190-192	207-208
1b	$C_{15}H_{18}ClNO_2.2.5H_2O$	151-154	178-179
1c	$C_{17}H_{22}ClNO_2.$	ND	-
1d	$C_{16}H_{18}ClNO_2.$	ND	-
1e	$C_{16}H_{20}ClNO_2.0.5H_2O$	171-173	-
1f	$C_{16}H_{20}ClNO_2.5H_2O$	64-66	-
1g	$C_{19}H_{26}ClNO_2$	46-48	-
1h	$C_{21}H_{30}ClNO_2.H_2O$	55-57	-
2a	$C_7H_{10}ClNO_2.H_2O$	163-165	189-190
2b	$C_8H_{12}ClNO_2.0.5H_2O$	166-168	205-206
2c	$C_{10}H_{16}ClNO_2$	163-166	199-200
2d	$C_9H_{12}ClNO_2$	193-197	-
2e	$C_9H_{14}ClNO_21.5H_2O$	196-197	225-226
2f	$C_9H_{14}ClNO_2$	187-189	206-207
2g	$C_{12}H_{20}ClNO_2.0.5H_2O$	163-164	166-167
2h	$C_{14}H_{24}ClNO_2.1H_2O$	ND	134-135

ND: not determined (oils)

The melting points of the deprotected compounds were found to be much higher than that of the benzylated analogues (Table 2.2). This can be attributed to the presence of intermolecular hydrogen bonding via the hydroxyl group in the deprotected analogues.

The observed melting points are much lower than the ones reported by Dobbin *et al* (1993), however they have a narrow range implying they are pure. The presence of water of hydration as calculated from elemental analyses (Table 2.2) could be the cause of depressed melting points for some compounds. All the compounds reported in earlier reports were isolated as anhydrous salts and their melting points were uncorrected.

2.1.5 Synthesis and Characterization gallium (III) complexes of 3,4-hydroxypyridinones

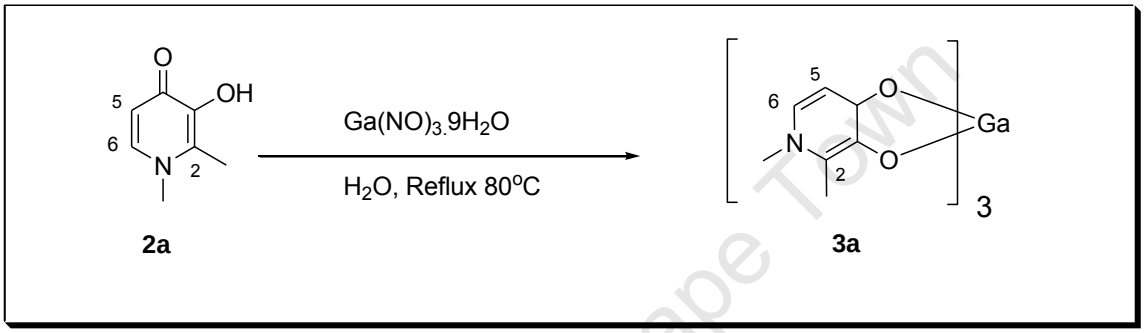

Figure 2.5: *Synthesis of the gallium (III) complexes*

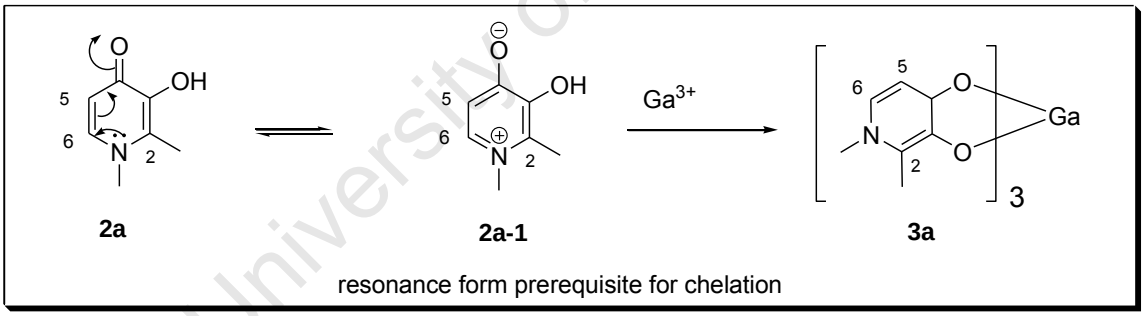

Figure 2.6: *Prerequisite resonance before metal chelation*

The synthesis involved reflux of the ligand with gallium (III) nitrate nonahydrate (Fig. 2.4). Gel filtration on Sephadex LH 20 was used for their purification.

The resonance form **2a-1** (Fig. 2.5) is important for chelation to occur (Dobbin *et al* 1993). The electron withdrawal and the positive charge on the heterocyclic N is

responsible for the co-ordination induced shifts (CIS) observed in their proton and carbon 13 NMR spectra (Fig 2.6, 2.7).

Proton NMR and analytical TLC indicated the absence of the free ligand and the proton NMR spectrum showed only one pair of neat doublets for the H-6 and H-5 pyridinone protons (Fig 2.7) confirming the complete conversion of the ligand to the complex. The presence of co-ordination induced shift (CIS) observed for the pyridinone ring protons confirmed complex formation too (Ferreira *et al.,* 2006; Green *et al.,* 2005; Xiao *et al.,* 1992) such that downfield and upfield shifts were observed for H-5 and H-6 respectively (Fig. 2.7). Some CIS was also observed for the N-alkyl and the 2-methyl protons.

In the ^{13}C NMR spectra CIS was clearly observed for the carbon atoms bound to the coordinating oxygen atoms as expected for bidentate chelation, this is illustrated by the example in figure 2.8. For the carbonyl carbon a CIS of >8 ppm confirmed a dative bond while a similar CIS of similar magnitude for the adjacent hydroxyl carbon verified a covalent metal-oxygen bond. (Green *et al.,* 2005)

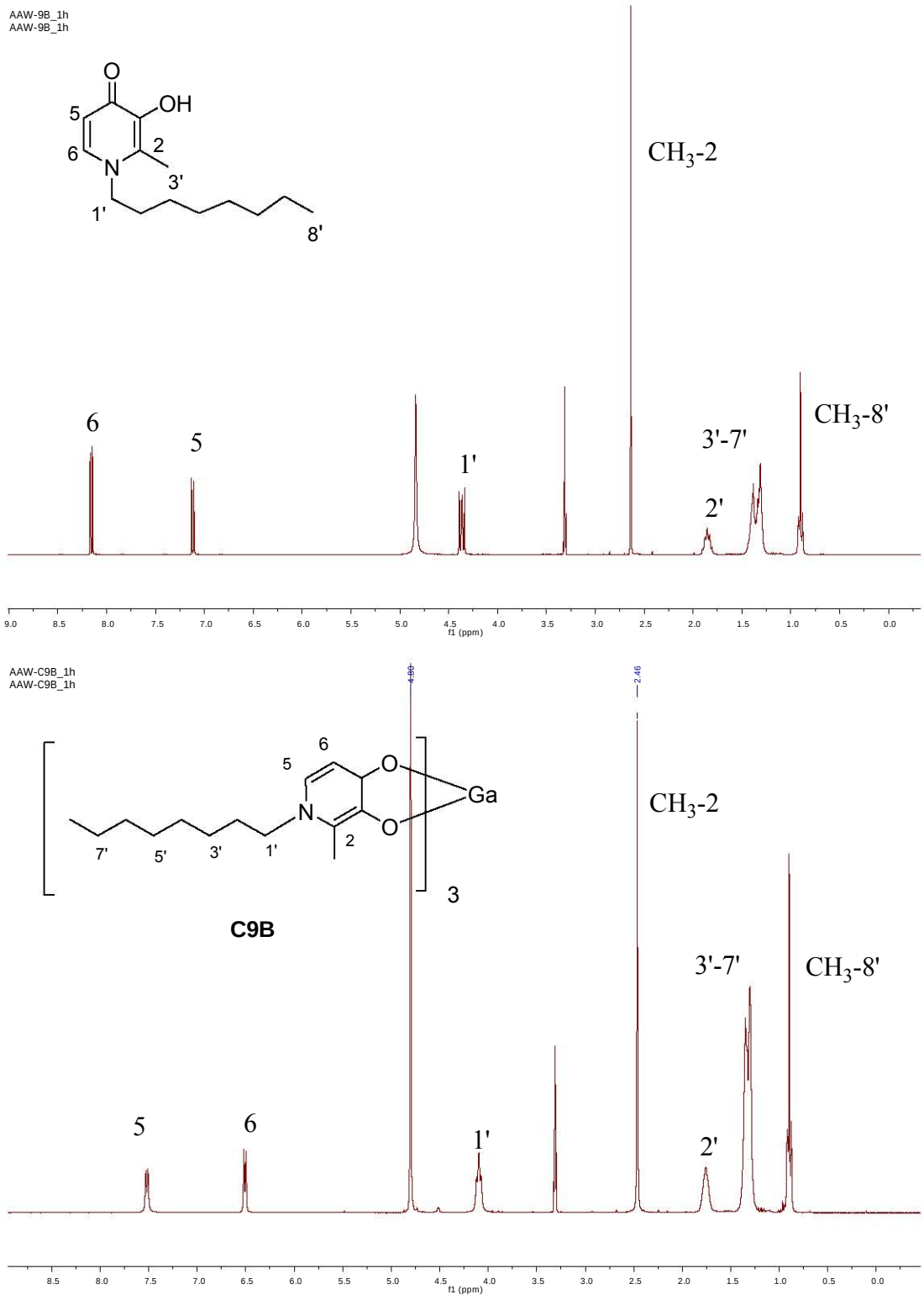

Figure 2.7: *Proton NMR spectra of compound* ***2h*** *and its gallium (III) complex* ***3h (C9B)***

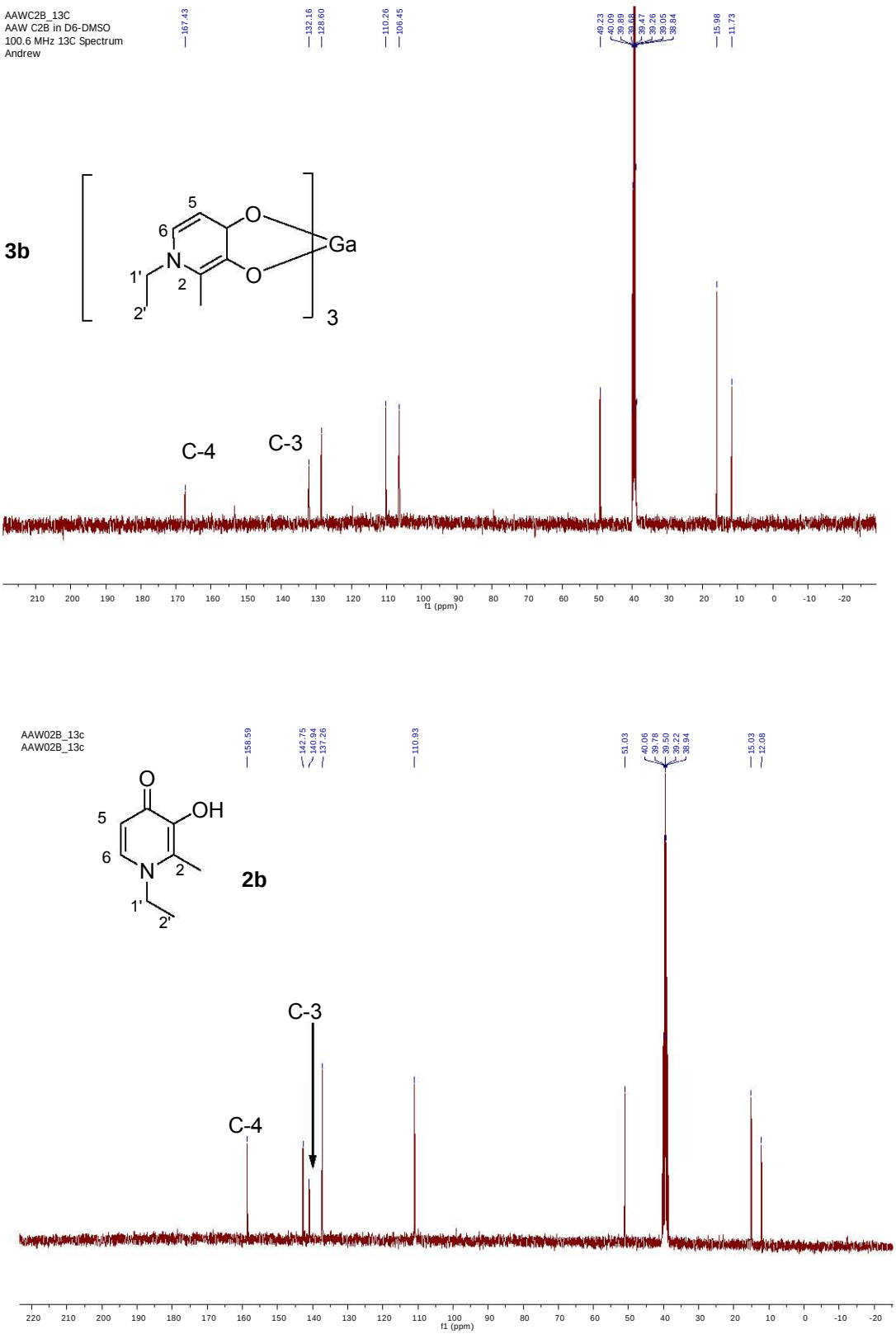

Figure 2.8: *Carbon-13 NMR spectra of compound* ***2b*** *and its gallium complex* ***3b***

Table 2.3: *Melting points of the Ga(III) complexes and the ligands*

Compound	R	Mp Of ligand °C	Mp of gallium complex °C	Mp of gallium complex °C
2a	Me	163-165	326-329	280[a]
2b	Et	166-168	222-225	240[b]
2c	Bu	163-166	303-305	170[c]
2d	cyclopropyl	193-197	237-240	-
2e	isopropyl	196-197	259-260	-
2f	n-propyl	187-189	219-220	290[c]
2g	n-hexyl	163-164	ND	285[a]
2h	n-octyl	ND	ND	--

[a] Nelson *et al.,* 1988; [b] Nelson *et al.,* 1989; [c] Simpson *et al.,* 1991;

In the mass spectra of these complexes the *m/z* observed corresponded to $[ML_3]^+$ or $[ML_3+Na]^+$. ML_2 peaks were also observed and were due to fragmentation and this is consistent with what Nelson and co-workers (1988) have reported.

X-ray crystallographic data of most of these complexes has been reported elsewhere (Xiao, G, 1992). The melting points of the complexes (Table 2.3) were found to be much higher than those of the corresponding ligands due to the strong hydrogen bonding network (Nelson, *et al* 1988). The high melting points are extra proof that complexation occurred. The literature reported melting points for some of the complexes do not compare exactly with the experimental values however the latter values are sharp.

2.2 Synthesis and Characterization of N-(7-chloro-4-quinolyl)-1-(aminoalkyl)-3,4-hydroxypyridinone Double Drugs Derived from Maltol and Ethylmaltol (A and AB series)

2.2.1 Rationale

Multi-therapies associating long acting and short acting compounds with different modes of action offer efficient treatment (Biot and Chibale, 2006). Such double drugs or bifunctional conjugates are known to be more effective against drug resistant organisms than the dual administration of the constituents (Biot and Chibale 2006; Bebbington, *et al,* 2000), in this respect 3,4-HPO-4-amino7-chloroquinolinyl double drugs were designed and synthesized.

2.2.2 Design

The figure below (Fig 2.9) shows the design of these double drugs synthesized by coupling 3,4-HPOs derived from maltol or ethylmaltol to N^1-(7-chloroquinolin-4-yl) diaminoalkanes.

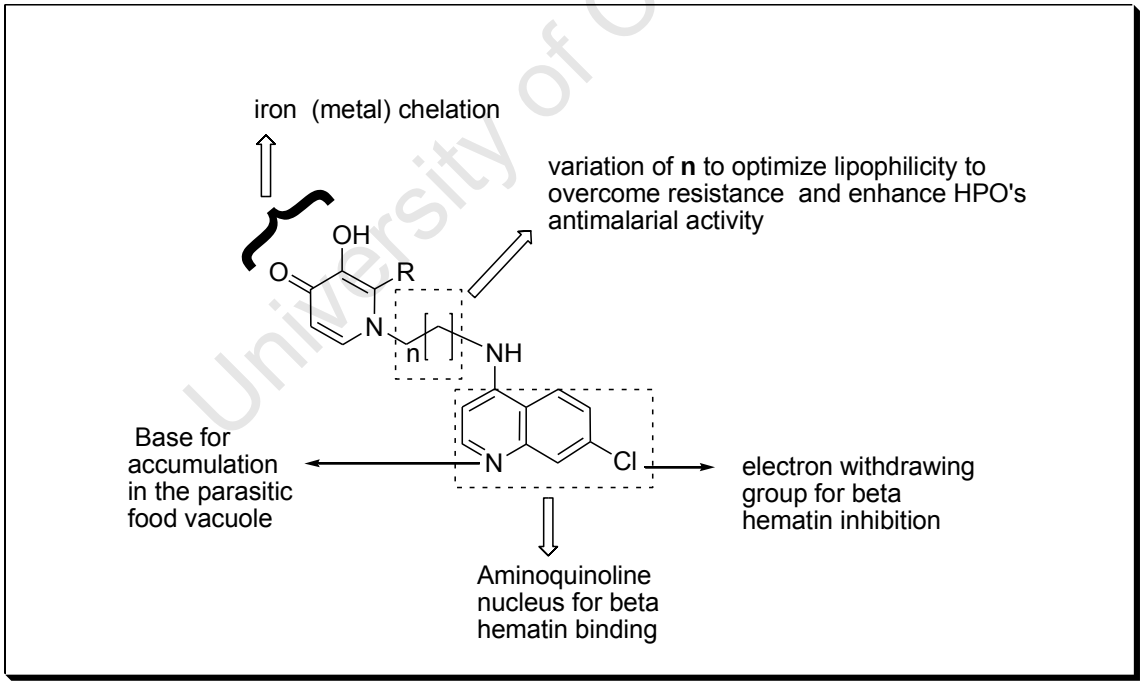

Figure 2.9: *The design of the 3,4-HPO- N^1-(7-chloroquinolin-4-yl) diaminoalkane double drug molecule.*

The double drug was designed to incorporate two modes of antimalarial activity; iron chelation (sequestration) and inhibition of hemozoin formation. The structural features responsible for these biological activities are indicated in figure 2.9.

2.2.3 Retrosynthetic Analysis

One approach was considered and pursued as illustrated in Figure 2.10.

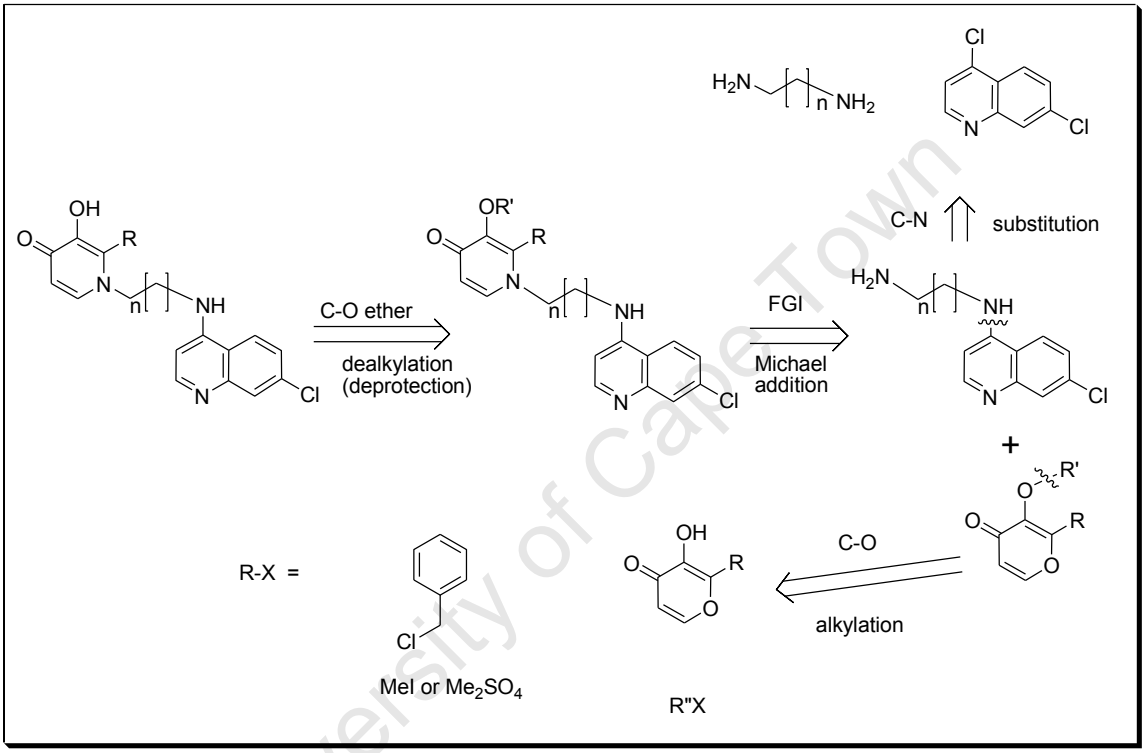

Figure 2.10: *Retrosynthesis analysis of the maltol derived drug conjugates*

The retrosynthetic strategy involved C-O disconnections for an ether formation, a functional group interconvertion (i) involving a pyrone to a pyridinone via Michael addition and (ii) nucleophilic substitution for the 7-chloroquin-4-yl-diaminoalkane intermediates.

2.2.4 Synthesis

All the starting materials (maltol, ethylmaltol, benzylchloride, iodomethane, dimethylsulfate, diaminoalkanes and 4,7-dichloroquinoline) for the synthesis were commercially available The *N*-(7-chloro-4-quinolinyl)-diaminoalkanes were synthesized

using standard procedures as illustrated in Figure 2.11 (Yearick, *et al* 2008; Solomon*, et al*, 2007; Burgess, *et al,* 2006; Blackie, 2002). The reaction for the preparation of *N*-(7-chloro-4-quinolyl)-diaminoalkanes is an addition–elimination reaction and the mechanism is illustrated in Figure 2.10. The methyamine **6a** was synthesised to enable incorporation of a tertiary amine group into the double drugs i.e. the R and D series. The 3-hydroxy-4(1*H*)-pyranones maltol and ethyl maltol were benzylated in 90% aqueous methanol to give compounds **1** and **2** respectively (Fig. 2.12).

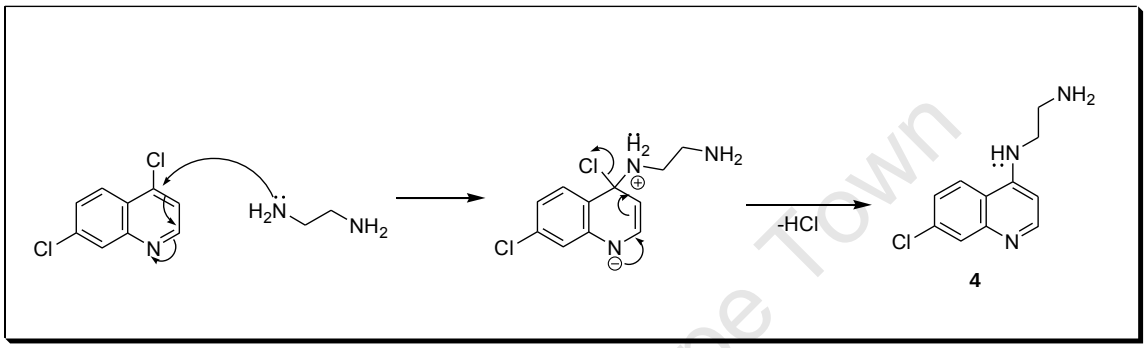

Figure 2.11: *Mechanism for the coupling of 4,7-dichloroquinoline to the diaminoalkane*

A Michael addition of the primary amines (*N*-(7-chloro-4-quinolinyl)-diaminoalkanes) to the benzylated pyranones gave the benzylprotected double drugs as free bases. The workup involved washing off the unreacted benzylmaltol or ethylbenzylmaltol with diethylether at pH 1 and adjusting the pH (using 2M NaOH) to allow precipitation of the target compound leaving the unreacted 4-amino-7-chloroquinoline in solution. The pure compounds were obtained by filtration and washing with deionised water and drying under vacuum. The benzylated double drugs were deprotected by catalytic hydrogenolysis at high pressure or by acid hydrolysis. Catalytic hydrogenation has been observed to convert some aryl halides to aryls (March and Smith, 2007), but in this case such was not observed. Only the target debenzylated hybrid molecules (s) were obtained as supported by evidence from analytical TLC, MS, elemental and NMR data.

The second phase of the synthesis involved the preparation of N-(7-chloro-4-quinolinyl)-1-(aminoalkyl)-3-(methoxy)-2-alkyl-4-(*1H*) pyridinones (3-methoxylated double drugs)

The rationale was to investigate the effect of changing the protecting group at the C-3 position of the pyridinone on the biological activity of these drug conjugates.

The synthetic procedure involved reaction of 3-methoxylated pyranones **17** or **18** with *N*-(7 chloro-4-quinolyl) alkanes (Fig. 2.12) and the products were isolated by precipitation at neutral to basic pH. The methoxylated pyranones were prepared by reacting methyliodide or dimethylsulphate with ethyl maltol and methylmaltol respectively. Dimethylsulphate was unreactive with ethylmaltol presumably due to the steric hinderance by the 2-ethyl group.

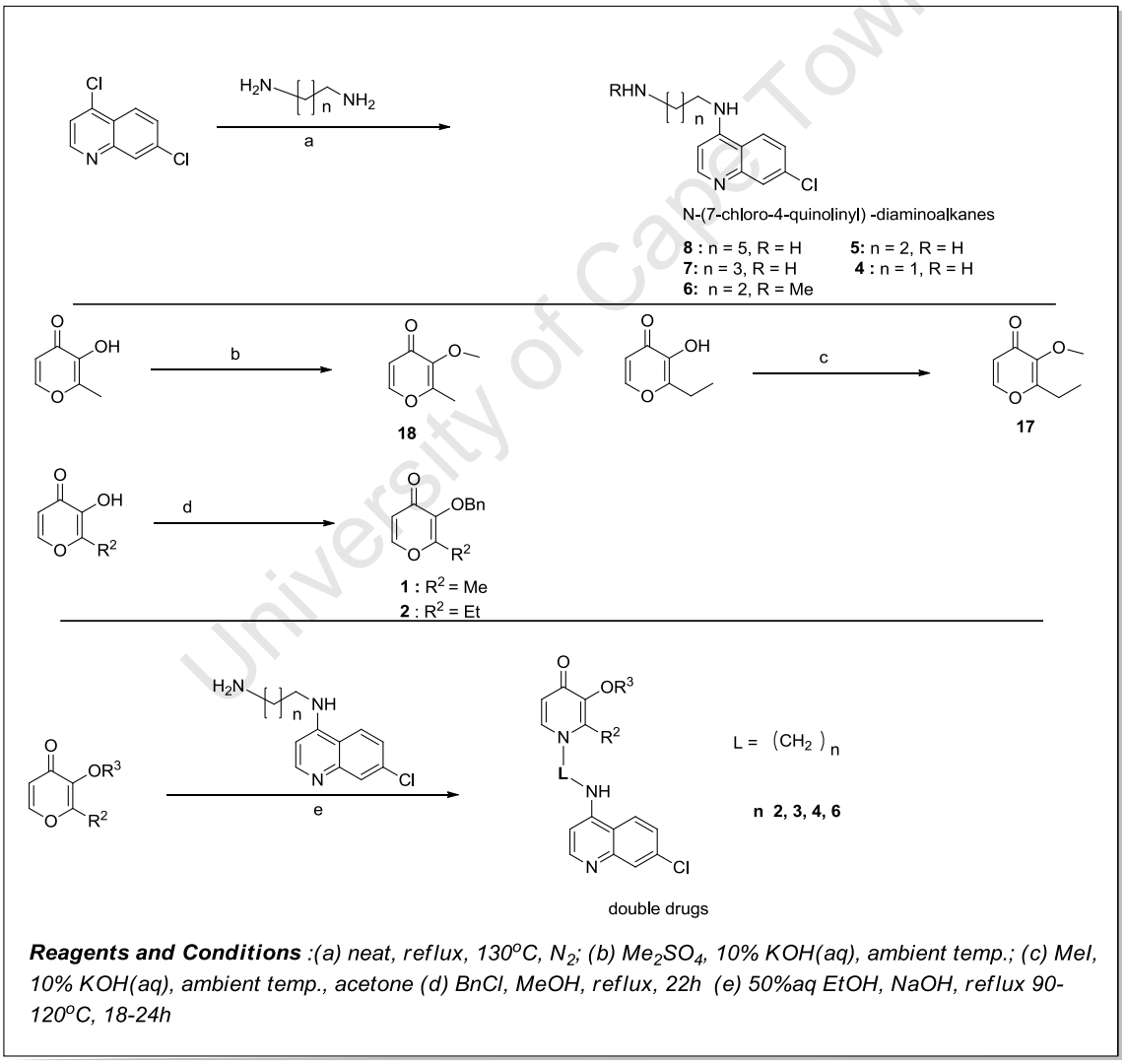

Figure 2.12 *Synthesis of the intermediates and target double drugs*

Table 2.4*: Yields and melting points of the maltol and ethylmaltol derived double drugs*

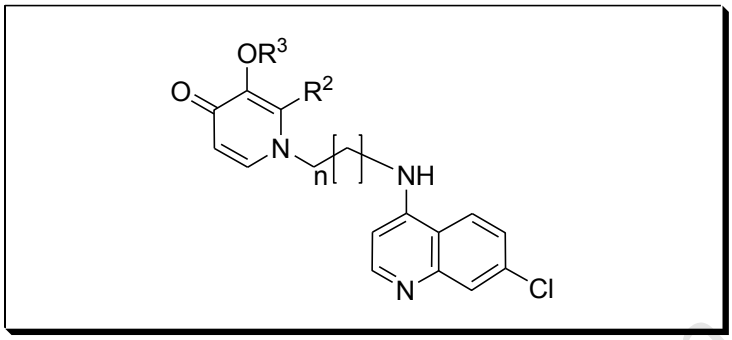

compound	N	R^2	R^3	% Yield	Mp ^oC
9	1	Me	Bn	93	151-152
9a	1	Me	H	68	173-175
10	1	Et	Bn	36	154-157
10a	1	Et	H	30	178-180
11	2	Me	Bn	45	127-129
11a	2	Me	H	50	143-146
12	2	Et	Bn	21	129-130
12a	2	Et	H	40	ND
13	3	Me	Bn	40	128-130
13a	3	Me	H	70	124-25
14	3	Et	Bn	40	112-116
14a	3	Et	H	76	ND
15	5	Me	Bn	27	114-116
15a	5	Me	H	99	134-138
16	5	Et	Bn	34	168-170
16a	5	Et	H	88	ND
16b	5	Et	Me	50	68-69
15b	5	Me	Me	48	96-98
14b	3	Et	Me	70	165-167
13b	3	Me	Me	64	85-87

ND: not determined

The average yield of the 3-methoxylated analogues was higher than those of the corresponding 3-benzyl analogues (Table 2.5) due to the ease of precipitation of the methoxy analogues at neutral to basic pH. The low aqueous solubility of the 3-methoxylated analogues (Table 2.6) was the reason for ease of precipitation. This is illustrated by the difference in the solubility of two related compounds **15b** a methoxylated analog (10μM) and **15** a benzylated analog (20μM) (Table 2.6).

Table 2.5: *Comparison of percentage yields of 3-methoxy and 3-benzyl analogues*

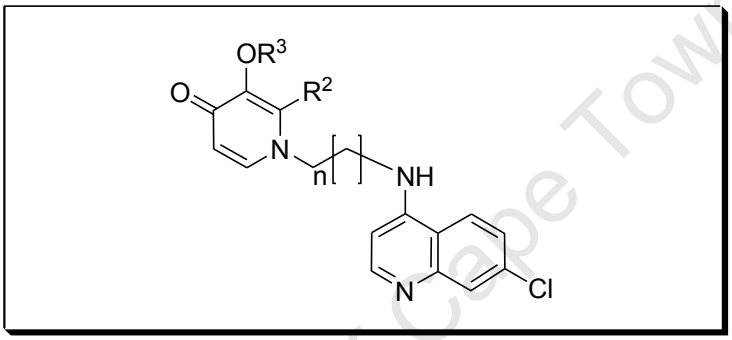

Compound	n	R^2	R^3	% Yield
13b	3	Me	Me	64
13	3	Me	Bn	40
14b	3	Et	Me	70
14	3	Et	Bn	40
15b	5	Me	Me	48
15	5	Me	Bn	27
16b	5	Et	Me	50
16	5	Et	Bn	34

Ordinarily one would expect the less polar (3-methoxylated) analogues to be more soluble than the less polar (benzylated analogues), (Thomas, 2003). Other factors may be contributing to this anomally for example the nature of the lattice packing (Fray *et al*., 2001; Kerns and Di, 2008). An out of plane substituents like the 3-methoxy or the 3-benzyl groups are likely to disrupt the crystal packing thus resulting in a high energy crystal that is more soluble in water. The benzyl group is likely to cause greater

disruption than the methoxy group resulting in greater solubility for the benzylated analogues than the methoxylated analogues. The crystal structure of compound **24** (page 119) shows how the benzyl substituent can be out of plane with the pyridinone or quinoline nucleus at almost perpendicular angles. However there is need to determine crystal structures of the analogues in question for a watertight conclusion. Eventhough melting points can be used to predict the strength of the crystal lattice and hence solubility, in this case it was not appropriate since the most of the compounds in question were not isolated as crystals but as precipitates. Therefore the solubility properties of precipitates cannot be similar to those expected of the crystals.

2.2.5 Characterization

Characterization was by ^{1}H, ^{13}C NMR, MS, IR and elemental analysis. Figure 2.13 and 2.14 show typical examples of a proton and carbon-13 NMR spectra of the benzylated and methoxylated analogues. In the proton NMR spectra of the deprotected analogues the multiplet from the benzyl's aromatic protons and the singlet at δ5 ppm due to the benzyl (methylene) protons being absent. The fingerprint pyridinone H-5 and H-6 peaks are conspicuous as depicted in the Figure 2.13 and can be identified by their *J* value of less than 7Hz. Typical proton NMR peaks for the quinoline protons H-2'' and 3'' appear as doublets with *J* values 5 - 6Hz, (Yearick *et al.,* 2008; Burgess *et al.,* 2006; Sanchez-Delgado *et al.,* 2004). However, this was not true for some of the 3,4-hydroxypyridinone-aminochloroquinoline double drug molecules synthesized in this study

The coupling constants observed for H-2'', H-3'' in some of the double drugs exceeded 7Hz. In most cases H-2'' appeared to be the most deshielded quinoline proton as reported elsewhere. (Yearick *et al.,* 2008; Burgess *et al.,* 2006; Sanchez-Delgado *et al.,* 2004) Comparing the carbon-13 NMR spectra (Fig 2.14) of the 3-methoxylated double drug molecules and that of the benzylated analogues, its clear that the signals due to the benzyl group's aromatic (δ 126-129 ppm) and methylene (δ73ppm) carbons are absent in the former.

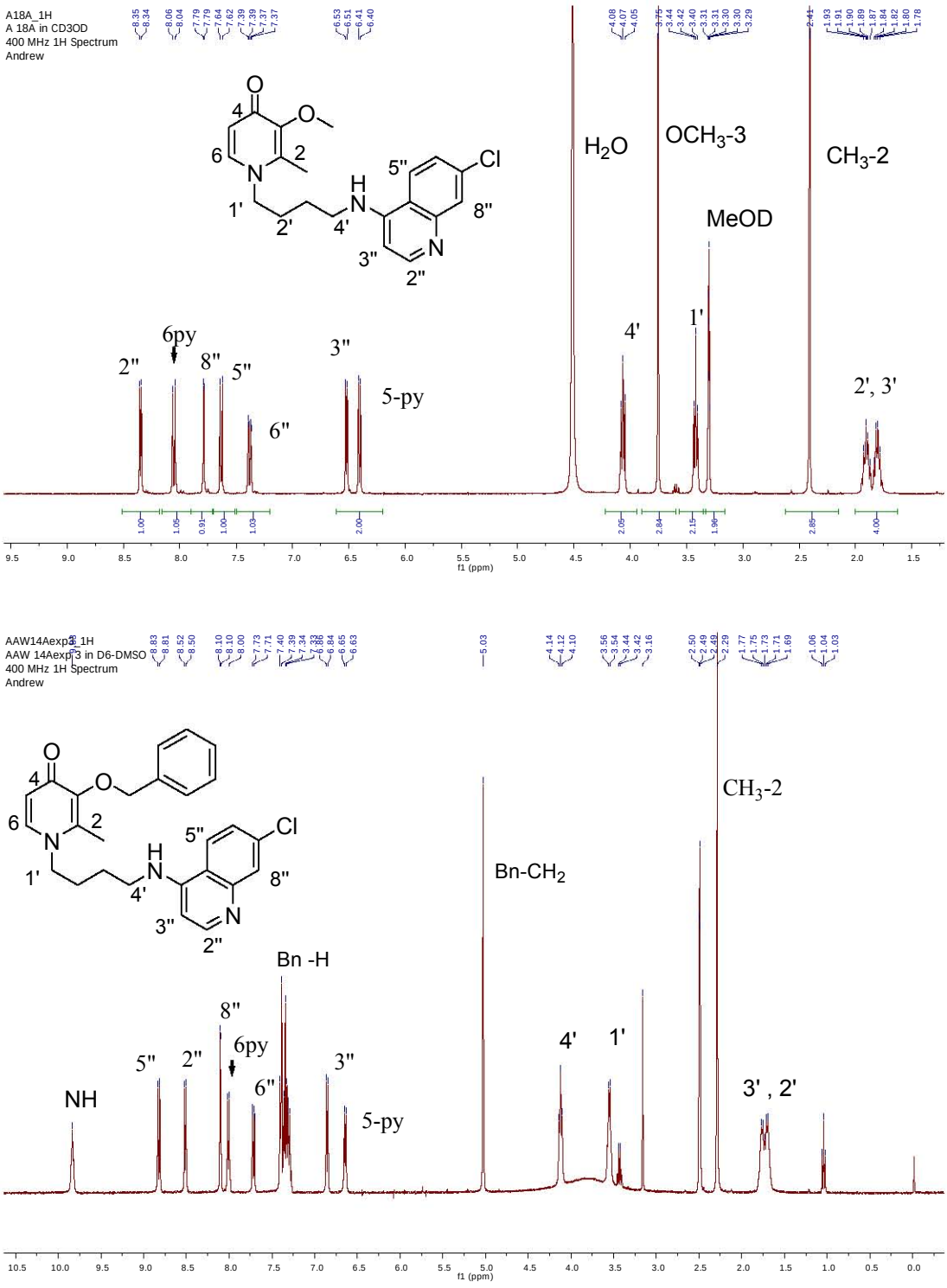

Figure 2.13: *Proton NMR spectra of 3-methoxylated (**13b**) and 3-benzylated (**13**) 3,4-HPO- N^1-(7-chloroquinolin-4-yl) diaminoalkane double drug molecules*

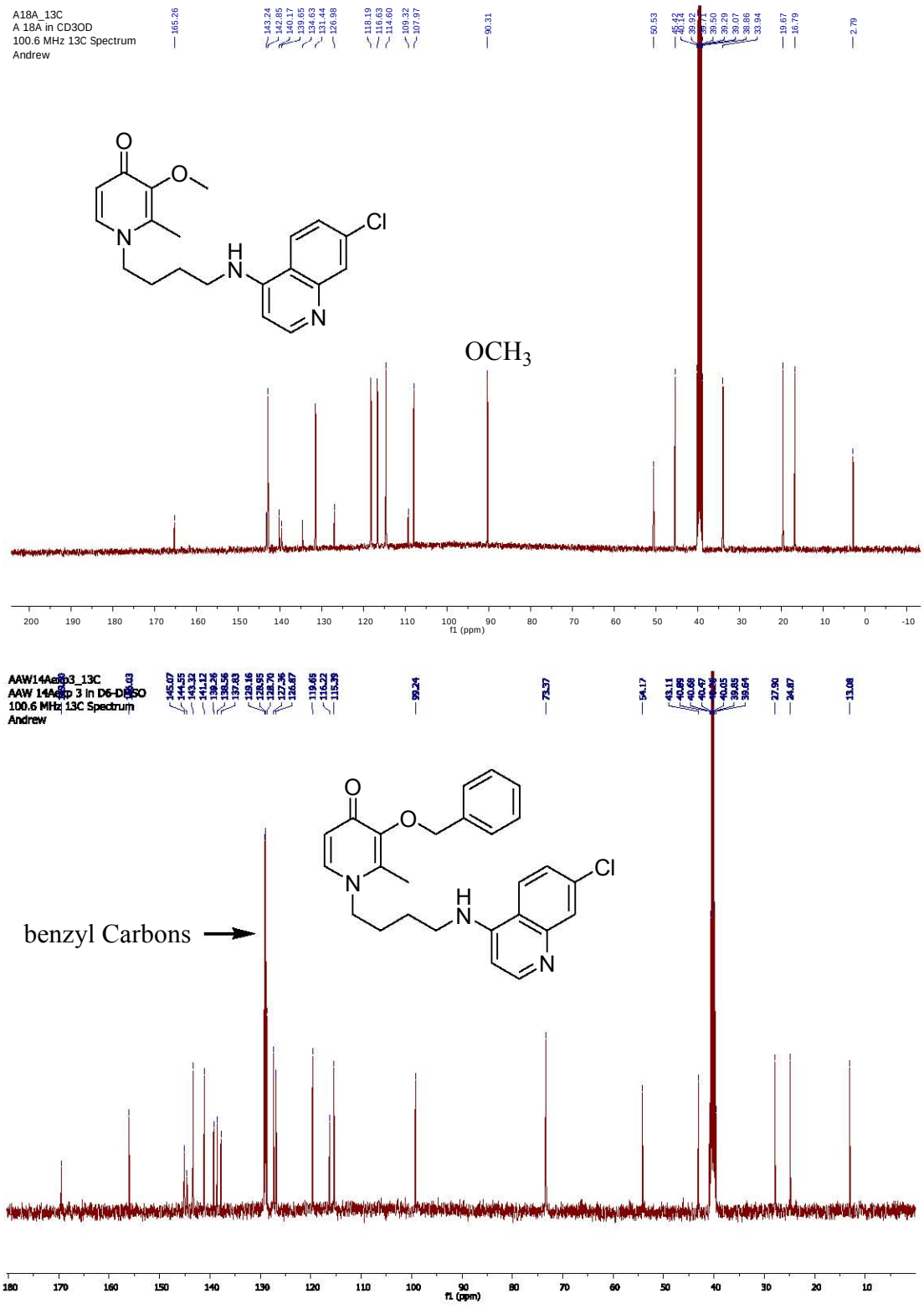

Figure 2.14: *Carbon-13 NMR spectra for 3-methoxylated (**13b**) and 3-benzylated (**13**) 3,4-HPO- N^1-(7-chloroquinolin-4-yl) diaminoalkane double drug molecules.*

^{1}H NMR spectra showed the presence of water in all the samples despite the thorough drying prior to their analysis (Fig. 2.13), this is further observed in the elemental analyses of these compounds. On this basis it may be concluded that these conjugates are hydrated. Indeed the deprotected analogues were highly deliquescent hence required special handling during the elemental analyses which was not available.

Previous reports indicate that the 1-*N*-alkyl-3,4-HPOs are very hygroscopic hence the presence of the same moiety in the 1-*N*-alkyl-3,4-HPO-aminochloroquinoline conjugates may be the cause of the hygroscopic/deliquescent behavior and require very drastic conditions (<0.3Torr, 90^{o}C, 16-48h) to dehydrate them in order to achieve acceptable elemental analyses (Finnegan, *et al* 1987). Facilities to attain such conditions were not available hence most of the compounds were isolated as hydrates as indicated by the elemental analyses.

HR-MS (positive mode) and LR-MS showed protonated molecular ion peaks $(M+H)^{+}$ for all the compounds. The FT-IR confirmed the characteristic features (N-H, C=O, C=N, C=C) of each compound.

2.2.6 Physicochemical properties

The solubility of the double drugs in water was determined using a turdimetric method (Table 2.6). The data was recorded either in 2 or 1 significant figures and no decimal point. Drugs with solubility >100 μM were classified as soluble, those with 50-25 μM were termed partially soluble and those <25 μM insoluble. All the compounds were soluble and their solubility was above the recommended minimum (>20 μg/ml) for drug-like oral compounds (Lipinski CA, 1997), the only exception was **16.** It was demonstrated that conversion of **16** to its dihydrogenchloride salt (13AB2HCl) improved its solubility by more than two fold i.e 28 μg/ml which is above the recommended minimum.

For optimal gastrointestinal absorption by passive diffusion after oral dosing, a drug needs to have a moderate log P (0-3). In this range of log P, there is a good balance of permeability and solubility. (Kerns and Di, 2008) The predicted log P values of these conjugates is in the range 2.6 – 4.5 and they have drug-like solubility i.e >20 μg/ml (Lipinski, 1997) hence these compounds are likely to be orally active *in vivo*.

Lipophilicity was determined using reverse phase HPLC (see experimental section 5.5.6) and standard drugs with known retention times (t_R) and retention capacity were (k') used for calibration. Most of the compounds had log D values in the range $2.46 < \log D_{7.4} > 6.00$ (Table 2.6) and compounds in this range are said to have good permeability but lower absorption owing to lower solubility (Kerns and Di, 2008). Conversely the actual solubility of these compounds is within the acceptable drug-like limits hence no issues are expected with absorption. All the compounds are more soluble than the least soluble standard niclosamide. Data for log D i.e. retention time t_R was recorded to 3 significant figures and as well the k' and log D values for the standards were in 3 significant figures, so it was appropriate to express all the data generated in 3 significant figures.

Table 2.6: *Physicochemical properties of ethylmaltol and maltol derived double drugs.*

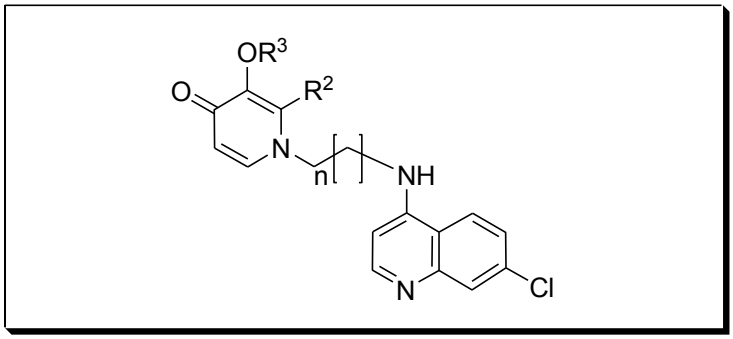

Compound	R^2	n	R^3	Solubility µM	Solubility µg/ml	cLog P	Log D (7.4)
9	Me	1	Bn	>100	> 42	3.80	4.02
9a	Me	1	H	>100	> 32	2.00	1.94
10	Et	1	Bn	>100	> 43	4.20	4.54
10a	Et	1	H	>100	> 34	2.50	2.46
11	Me	2	Bn	>100	> 43	4.30	4.07
11a	Me	2	H	ND	ND	2.50	ND
12	Et	2	Bn	>100	> 44	4.70	4.59
12a	Et	2	H	>100	> 36	3.00	ND
13	Me	3	Bn	>100	> 44	4.80	4.59
13b	Me	3	Me	>100	> 37	4.20	ND
13a	Me	3	H	>100	> 36	3.00	ND
14	Et	3	Bn	>100	> 46	5.20	5.11
14b	Et	3	Me	ND	ND	3.86	ND
14a	Et	3	H	>100	>37	3.50	3.11
15	Me	5	Bn	25	48	5.70	5.48
15b	Me	5	Me	10	40	3.34	ND
15a	Me	5	H	>100	> 38	4.00	3.52
16b	Et	5	Me	ND	ND	4.75	ND
16	Et	5	Bn	25	12	6.2	6.00
16. HCl salt	Et	5	Bn	50	28	6.40	ND
16a	Et	5	H	>100	> 40	4.50	4.05
Paracetamol				>100			
niclosamide				10			

clog P predicted from MoKa ®, ND: not determined

2.3 Preliminary studies on the gallium (III) and iron (III) complexes of N-(7-Chloro-4-quinolyl)-3-(Hydroxy)-4(*1H*)-pyridinone double drugs

2.3.1 Rationale

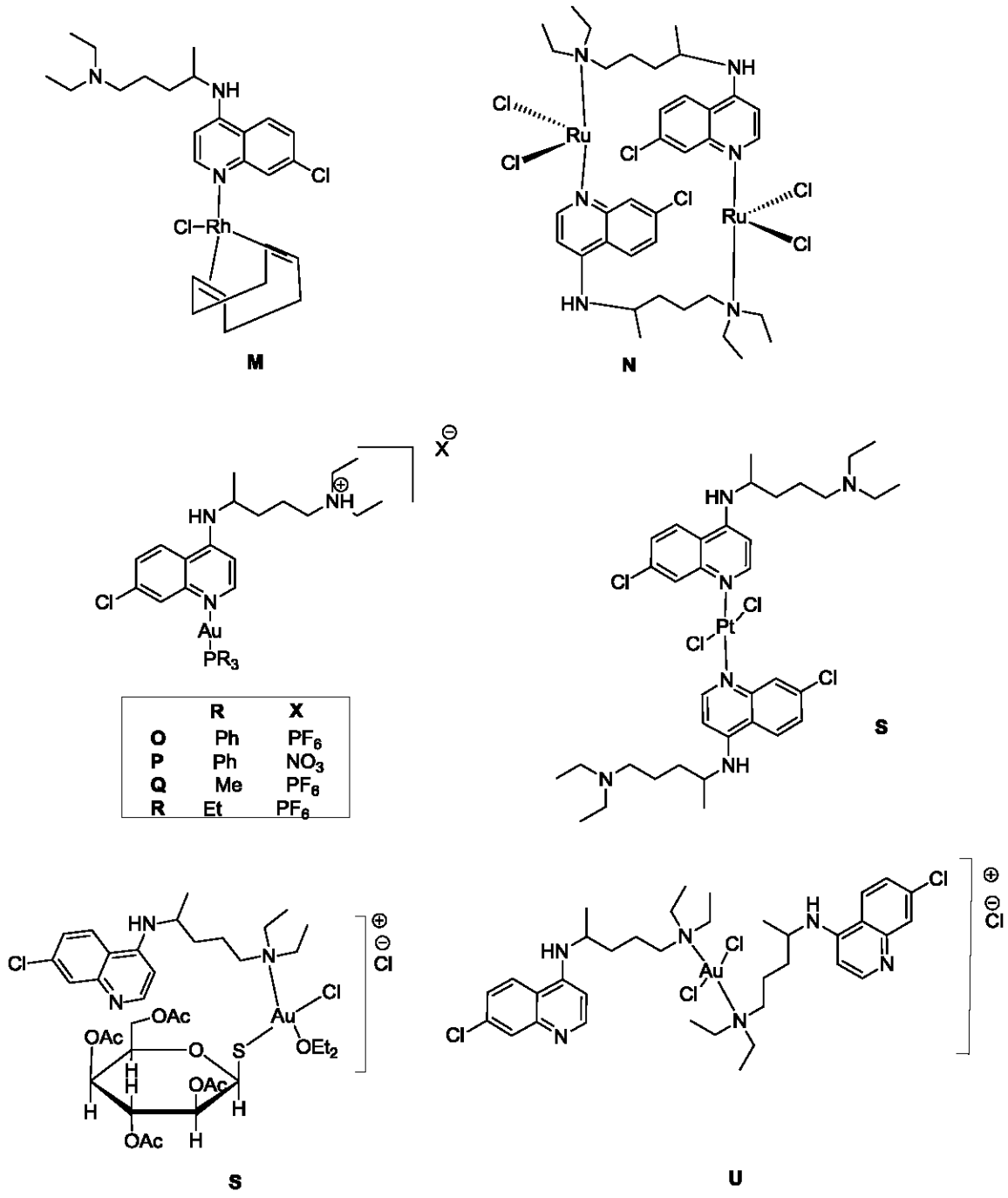

	R	X
O	Ph	PF_6
P	Ph	NO_3
Q	Me	PF_6
R	Et	PF_6

Figure 2.15. *Structures of selected chloroquine based antimalarial metal complexes*

Several reports indicate that metal complexes of chloroquine based ligands have improved activity against CQ sensitive and CQ resistant strains of *P. falciparum* as well good *in vivo* activity against *P. berghei* (Khanye, 2010; Ajibade and Kolawole; Navarro, *et al,* 2004; Blackie, 2002; Sanchez-Delgado, *et. al.,* 1996). The structures of some of the complexes and their respective antiplasmodial activities are depicted in Figures 2.15 and Tables 2.7 and 2.8 respectively.

Table 2.7. *Antiplasmodial activity of some CQ based Ru and Rh complexes against CQ resistant FcB1, K1 and W2 strains of P. falciparum*

Compound	*IC_{50} (μM)*			*Reference*
	FcB1	W2	K1	
M	0.073	ND	ND	Sanchez-Delgado *et. al.,* 1996
N	0.018	ND	ND	Sanchez-Delgado *et .al.,* 1996
CQ	0.072	ND	ND	Sanchez-Delgado *et. al.,* 1996

Table 2.8. *Antiplasmodial activity of some CQ based Au and Pt complexes against CQ resistant FcB1, K1 and W2 strains of P. falciparum*

Compound	IC_{50} (μM)			Reference
	FcB1	W2	K1	
O	0.04	0.07	0.10	Navarro *et. al.,* 2004
P	0.04	0.04	0.06	Navarro *et. al.,* 2004
Q	0.04	0.05	0.09	Navarro *et. al.,* 2004
R	0.01	0.05	0.10	Navarro *et. al.,* 2004
S	ND	ND	0.16	Ajibade and Kolawole., 2008
T	ND	ND	0.05	Navarro *et. al.,* 2004
U	ND	ND	0.04	Navarro *et. al.,* 2004
CQ	0.05	0.07	0.07	Navarro *et. al.,* 2004

2.3.2 Synthesis

The choice of ligands for complexation was based on their *in vitro* antiplasmodial activity and availability of the material; hence ligands **16a**, **15a** and **13a** were used. The synthesis involved the reaction of an aqueous solution of iron (III) nitrate nonahydrate or gallium (III) nonahydrate solution with a methanolic solution of the *N*-(7-chloro-4-quinolyl)-3-(hydroxy)-4(1H)-pyridinone ligand at pH 8

The equivalents of the reactants were varied to explore possibilities of forming ML_3 and ML_2 type of complexes (Fig. 2.16). An assumption was made that the N-1 of the quinoline can participate in the coordination to give a complex with the proposed structure type C (Fig. 2.16) The spectroscopic data, however, ruled out coordination via the quinoline nitrogen and confirmed the sole participation of the 3,4-hydroxypyridinone group in the coordination. This was observed from the molecular ion peaks corresponding to ML_3, and the absence of significant CIS in the proton NMR signals of the quinoline protons. Further details are considered for each complex later in the chapter. Six complexes were prepared, two with iron (III) and four with gallium (III) as their respective metal centres (Table 2.9).

2.3.3 Characterization

The complexes were characterised by ^{1}H and ^{13}C NMR, microanalysis and mass spectrometry. Proton NMR was used to confirm the metal chelation had occurred and that the product was not merely a mixture of the starting materials. The proton NMR spectra of the iron (III) complexes exhibited peak broadening and merging and only two peaks were observed due to the paramagnetic nature of iron (Fig.2.17). The two broad singlets at δ9-6ppm and δ4-2ppm were assigned to the aromatic and aliphatic protons respectively.

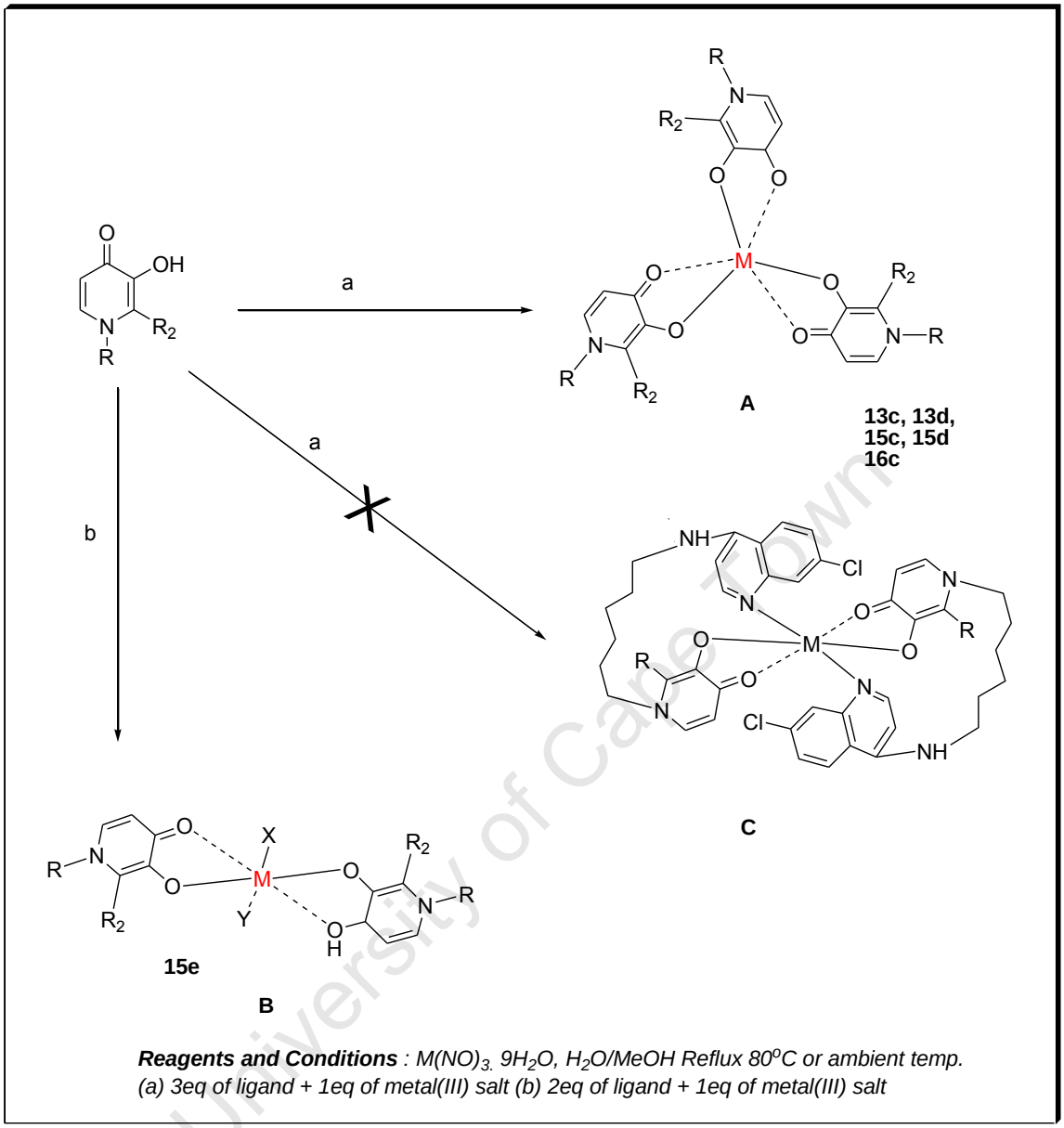

Figure 2.16: *Synthesis of the double drug metal (III) complexes*

For the gallium complexes minimal peak broadening was observed in the proton NMR. However, co-ordination induced shifts (CIS) were observed for the H-5 and H-6 pyridinone protons. In most of the complexes the peaks corresponding to these protons appeared as broad singlets or had diminished *J* values relative to the ligand's (Fig. 2.17 and Table 2.11) and the H-6" signal appeared as a doublet instead of a doublet of doublets.

Table 2.9: *Gallium (III) and iron (III) complexes of the 3,4-HPO-4-amino-7-chloroquinoline conjugates*

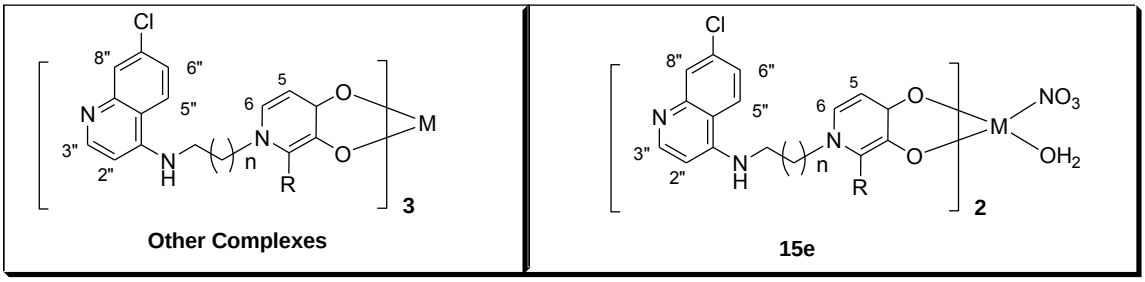

Complex	M (III)	n	R	% Yield	Mp ^{o}C Complex	Mp ^{o}C ligand
13c	Fe	3	Me	72	225-226	124-125
13d	Ga	3	Me	81	215-216	124-125
15c	Fe	5	Me	66	198-200	134-138
15d	Ga	5	Me	81	194-196	134-138
16c	Ga	5	Et	24	202-204	N/A
15e	Ga	5	Et	50	183-184	134-138

When the quinoline moiety participates in the complex formation the main coordination point is via the quinoline N-1 thus the H-2", 3" and 8" are expected to show reasonable CIS on complexation (Blackie M, 2002; Sanchez-Delgado R.A., *et al* 2008), ie 1.8-0.5 ppm for H-8" and >0.6ppm for H-2" and 3" (Sanchez-Delgado *et al* 1996; Lippard *et al*., 1983). These CIS were not observed in any of the double drug complexes except in **13d** (Tables 2.10-2.13). This implied that the quinoline was just a pendant group and was not involved in the metal chelation.

In the case of **13d**, the *Δppm* for H-8" was significant ie >0.5 (Table 2.10) implying that either the quinoline N-1 was involved in the metal chelation or/and a long range electronic disturbance was strongly felt by the quinoline protons due to the reduced distance between the chelating moiety (3,4-HPO) and the quinoline moiety. The MS of

13d showed an ML_3 peak with 100% abundance and this meant complexation via N-1 did not occur because all the six coordination sites on the metal ion were occupied by the three hydroxypyridinone moieties. The double drugs hence behaved as bidentate chelators by using the 3,4- hydroxypyridinone moieties to chelate the metal ions.

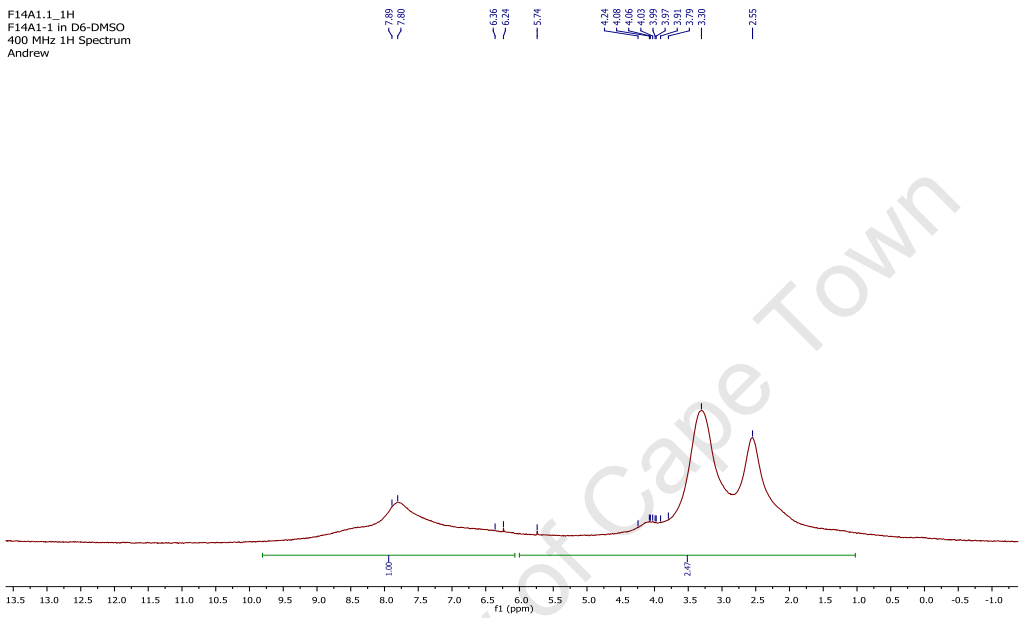

Figure 2.17. *Proton NMR spectrum of the iron (III) complex* ***13c***

Table 2.10: *Coordination induced shift values (CIS Δppm) for* ***13d***

Proton	Ligand **13a** Δppm	Complex **13d** Δppm	Δppm
2”	8.50, *d, J* 7.2	8.41, *d, J* 4.8	0.09
3”	6.86, *d, J* 6.9	6.27, *d, J* 7.2	0.59
5”	8.87, *d, J* 9.3	8.29, *d, J* 7.8	0.58
6”	7.70, *dd, J* 1.8, 9.0	7.46, *m*	0.24
8”	8.10, *d, J* 2.1	7.52, *s*	0.58
5	7.34, *d, J* 6.9	6.56, m	0.78
6	8.36, *d, J* 6.9	7.46, *d, J* 7.2	1.10

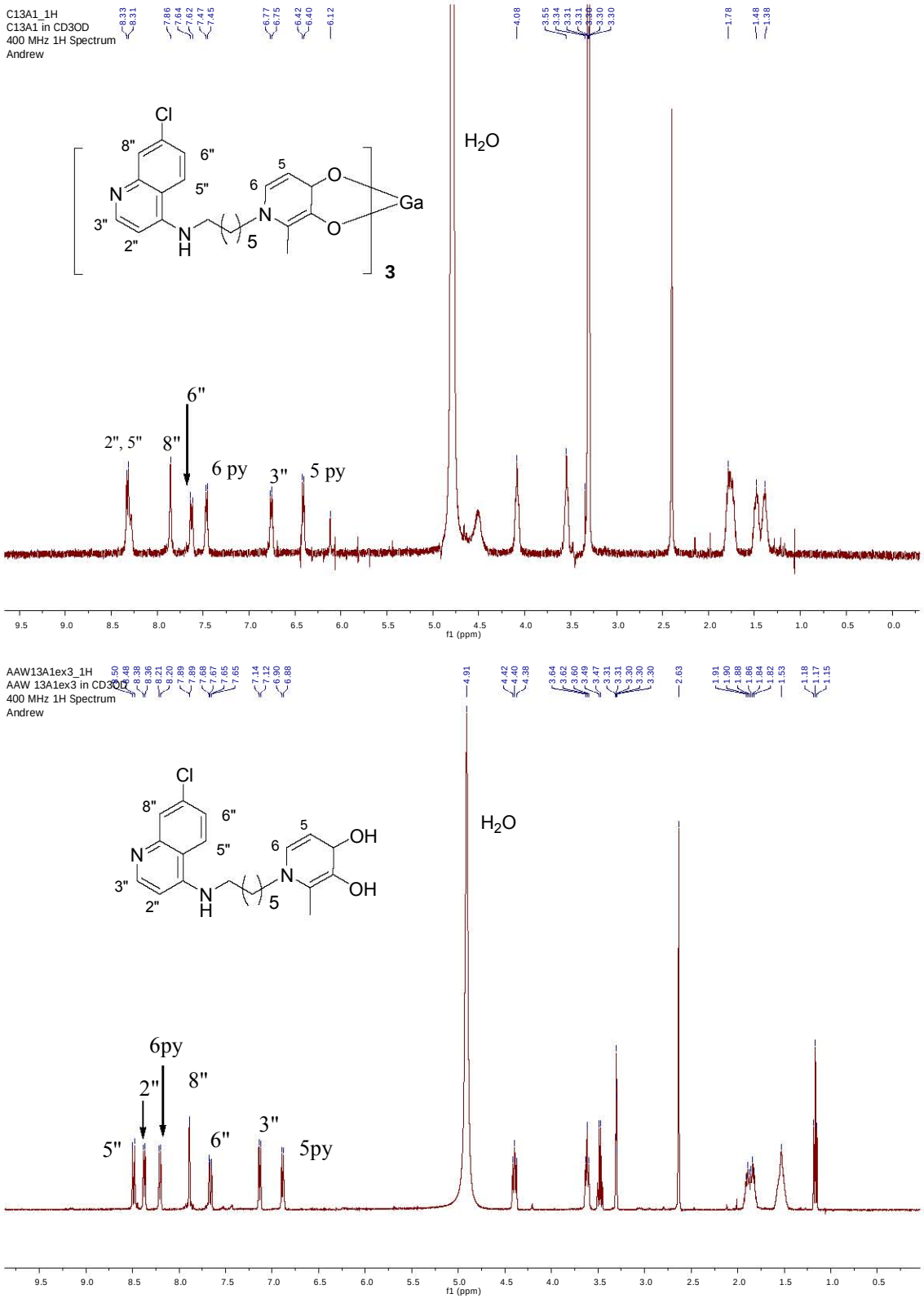

Figure 2.18: *Proton NMR spectra of **15a** and its gallium (III) complex **15d***

Table 2.11: *Coordination induced shift values (CIS Δppm) for* ***15d***

Proton	Ligand **15a** Δppm	Complex **15d** Δppm	Δppm
2”	8.37, *d, J* 7.2	8.32,m	0.05
3”	6.88, *d, J* 7.2	6.76, *d, J* 6.0	0.12
5”	8.48, *d, J* 9.2	8.32, *m,*	0.16
6”	7.66, *d, J* 9.2	7.62, *d, J* 8.7	0.04
8”	7.88, *d, J* 2.0	7.86, *s*	0.02
5	7.10, *d, J* 6.8	6.40, *d, J* 5.4	0.70
6	8.20, *d, J* 6.8	7.46, *d, J* 5.2	0.74

Table 2.12: *Coordination induced shift values (CIS Δppm) for* ***15e***

Proton	Ligand **15a** Δppm	Complex **15e** δppm	Δppm
2”	8.37, *d, J* 7.2	8.41, *d, J* 5.7	0.04
3”	6.88, *d, J* 7.2	6.72, *d, J* 6.4	0.16
5”	8.48, *d, J* 9.2	8.33, *d, J* 9.0	0.15
6”	7.66, *d, J* 9.2	7.50, *d, J* 8.7	0.16
8”	7.88, *d, J* 2.0	7.82, *s*	0.06
5	7.10, *d, J* 6.8	6.53, *m,*	0.57
6	8.20, *d, J* 6.8	7.71, *d, J* 5.4	0.49

In each complex the H-5 and the H-6 had the greatest CIS chemical shifts. Longer NMR runs were required to achieve good carbon-13 NMR spectra for these complexes but for most them good resolution was not achieved even after longer periods.

15e was confirmed to be a ML_2 type of complex with the evidence from HR MS that shows a m/z corresponding to ML_2 and none for ML_3. The positive anion exchange reaction with PF_6^- indicated that **15e** was a cationic complex quite unlike **15d.** The difference in the melting points of **15d** and **15e** was ≈10^oC (Table 2.9); this is extra evidence that the two complexes are not the same. The CIS for the pyridinone protons in the two closely related complexes, **15e** and **15d,** differ by a factor of 2 implying the H-5 and H-6 of the respective complexes are not in similar chemical environments. One can postulate the pyridinone protons in **15e** are less shielded due to the presence of the NO_3^-.

In the preparation of all the above complexes it was proved that the reaction went on to completion and no remnants of the free ligand were detectable from both proton NMR and analytical TLC. None of the complexes showed a positive anion exchange reaction with the PF_6^- except **15e.**

Table 2.13: *Coordination induced shift values (CIS Δppm) for* ***16d***

Proton	Ligand **16a** Δppm	Complex **16c** Δppm	Δppm
2"	8.37, *d, J* 7.2	8.30, *m,*	0.07
3"	6.94, *d, J* 7.2	6.40, *d, J* 6.8	0.54
5"	8.40, *d, J* 9.3	8.30, *m,*	0.10
6"	7.68, *d, J* 8.8	7.64, *dd, J* 1.6, 9.0	0.04
8"	7.87, *d, J* 1.5	7.85, *d, J* 0.8	0.02
5	7.10, *d, J* 7.2	6.76, *d, J* 6.8	0.34
6	8.18, *d, J* 6.9	7.46, *d, J* 6.8	0.72

The MS data of the two iron (III) complexes (**13c**, **15c**) as well as that of **13d** showed *m/z* corresponding to ML_3 the expected molecular ion peak. The mass spectra of **15d** and **16c** did not show the molecular ions for ML_3 but had peaks corresponding to ML_2 and ML and L that were attributed to fragmentation.

It is known that the ML_2 complex species of 3-4-HPOs possess a single charge unlike the neutral ML_3, hence it does not require further protonation or cationization in order to be detected in mass spectrometry. (Xiao *et al,* 2006) As a result, the relative abundance of the ML_2 is overrepresented in the mass spectra of **15d** and **16c** assuming that the two readily fragmented in the MS.

The melting points of all the complexes were found to be higher than those of their respective ligands. This can be attributed to the crystal packing effects due to different co-ordination complexes. This observation in it self is a confirmation of chelation of the metal by the ligand (Dobbin *et al.,* 1993). A similar phenomenon was observed and explained for the gallium complexes of N-alkyl-3,4-HPOs (section 2.1). The melting points of the complexes of **13a** (**13d** and **13c** respectively) and that of **15c** were reported to be much higher than those of their ligands i.e two-fold, but for the other gallium

complexes, **16c** and **15e,** the difference between their melting points and the ligands is not substantial (Table 2.9). This implies that there are relatively stronger bonds in **13d, 13c** and **15c** than in **15d** and **16c.** This data may be used to explain the absence of the molecular ion (ML_3) peaks in the mass spectra of **15d, 16c** and **15c** due to ease of fragmentation.

Crystallization was attempted for purification purposes and for X-ray crystallographic studies but this was unsuccessful. The X-ray crystallography studies would have given accurate data on the structure and formula of these complexes. Ordinary crystallization and crystallization by vapour diffusion using the following solvent pairs was pursued for the six complexes; MeOH/Et_2O, MeOH/EtOAc, MEOH/heptane, MeOH/dichloromethane, dry MeOH/Et_2O, MeOH/ACN, DMSO/dichloromethane but all were unsuccessful.

To ensure that the experimental and calculated elemental analyses were acceptable the following assumptions were made; that traces of $NaNO_3$ were present in most of the complexes, the varied moles of water of hydration where possible for 3,4-HPO complexes was allowed. (Xiao *et al.,* 1992; Nelson *et al.,* 1989) This should be treated as tentative pending X ray crystallographic experimental data. Conductivity measurements may also be used to confirm the cationic nature of **15e.**

The liability observed in these complexes is poor solubility in water, methanol and ethanol which may cause precipitation in bioassay media and impact negatively on evaluation of the biological activity. Similar observations on solubility of metal complexes have been reported by Puerta and co-workers (2006). These complexes were however found to be soluble in a mixture of dichloromethane and methanol (2:8), and in DMSO.

2.4 Synthesis of Kojic acid -Derived Double drugs (R and D series)

2.4.1 Rationale

In order to maximize or retain the antimalarial activity of the previously synthesized double drugs (section 2.2) but minimize their CYP3A4 inhibition (section 3.8.2) in the presence of a substrate (i.e. testosterone), these compounds required structural modification to form the 2-((7-chloroquinolin-4-ylamino)alkylamino)methyl)-1-.alkyl-5-hydroxypyridin-4(1H)-ones (kojic acid derived double drugs).

2.4.2 Design

Two universally accepted strategies for lessening CYP3A4 inhibition were considered when designing the new compounds: (a) Lowering the logD or logP of the drugs (lipophilicity) by introducing more polar groups (Kerns and Di, 2008; Gleeson, 2008), (b) Altering the molecular shape of the series (Yan and Caldwell, 2001). The other strategy was to introduce a tertiary amino group or an extra amino group on the side chain to enhance accumulation of the drugs in the food vacuole of the malaria parasite (Egan and Kaschula, 2007; Yearick, *et al* 2008).

The design represented in Figure 2.20 is similar to that of the maltol/methyl maltol derived double drugs except for the extra basic group in form of a tertiary amine. The pyridinone's N-1 is a weaker base due to the resonance withdrawal of the lone pair of its electrons into the ring and hence has lower pKa of 2-4 (Dekhordi, *et al* 2008) relative to that of the tertiary terminal amino group in chloroquine which has a pKa of 10.21(Volsurf®). Hence the former cannot effectively enhance accumulation of the drug in the parasitic food vacuole. This necessitated the introduction of a tertiary amino group. Tertiary amino groups in 3,4-HPOs have been proposed to enhance targeting of the parasitic lysosomes and other intracellular acidic vacuoles (Dehkordi *et al* 2008). Therefore the presence of the tertiary amino group in the 3,4-HPO-aminoquinoline drug conjugates presents a mimic of the tertiary terminal amino group in chloroquine and related antimalarials. This is backed up by the Volsurf ® predicted pKa values for the extra amino group on the side chain of these novel conjugates (6.78-9.08).

Altering the molecular shape by replacement of the maltol derived substructure with one from kojic acid was envisaged to affect the interraction of these compounds with the CYP3A4 active site. Introduction of steric bulk in the vicinity a heterocyclic nitrogen (especially in pyridines and quinolines) is expected to weaken the coordination of the nitrogen to the P450 prosthetic heme iron (Ridley *et al* 2001; Zlokarnik *et al*, 2005). In this context, the introduction of a bulky group next to the pyridinone heterocyclic nitrogen is not expected to have a significant effect on the compounds interaction with the CYP3A4 active site as it could do for pyridines (Ridley, 2001; Zlokarnik, 2005), because the lone pair on the pyridinone N is not available for this interaction due to its withdrawal into the pyridinone ring via resonance.

In addition predictions using Metasite (Fig.2.18) show that the quinoline moiety **16a** is more exposed to the CYP3A4 active site but remains unreactive, such a prediction implies the quinoline may be responsible for the CYP3A4 inhibition and not the pyridinone moiety. Also it is known that hydroxypyridinones do not directly cause the inhibition of heme containing enzymes (Kayyali *et al,* 1997; 2001). Comparing the predicted exposure and reactivities of **16a**, **27a** and **32a,** it appears that the quinoline moieties of **16a** and **27a** have similar exposure and reactivity but that of **32a** has similar exposure but greater reactivity. This implies that **32a** has a lesser potential to cause CYP3A4 inhibition than the other two. The introduction of the basic amine group increases the electron density (via the lone pair of electrons on N) which enhances enzymatic metabolism of the substrate (Kerns and Di, 2008). For this reason the **R** and **D** series which have an amine group in their side chains are expected to exhibit higher reactivity than the **A**/**AB** series.

The bulky group *ortho* to the pyridinone *N*-1 was envisaged to contribute towards altering the molecular shape of these conjugates and hence proposed to be the cause of the difference in reactivity towards CYP3A4 as predicted in MetaSite output (Fig. 2.19).

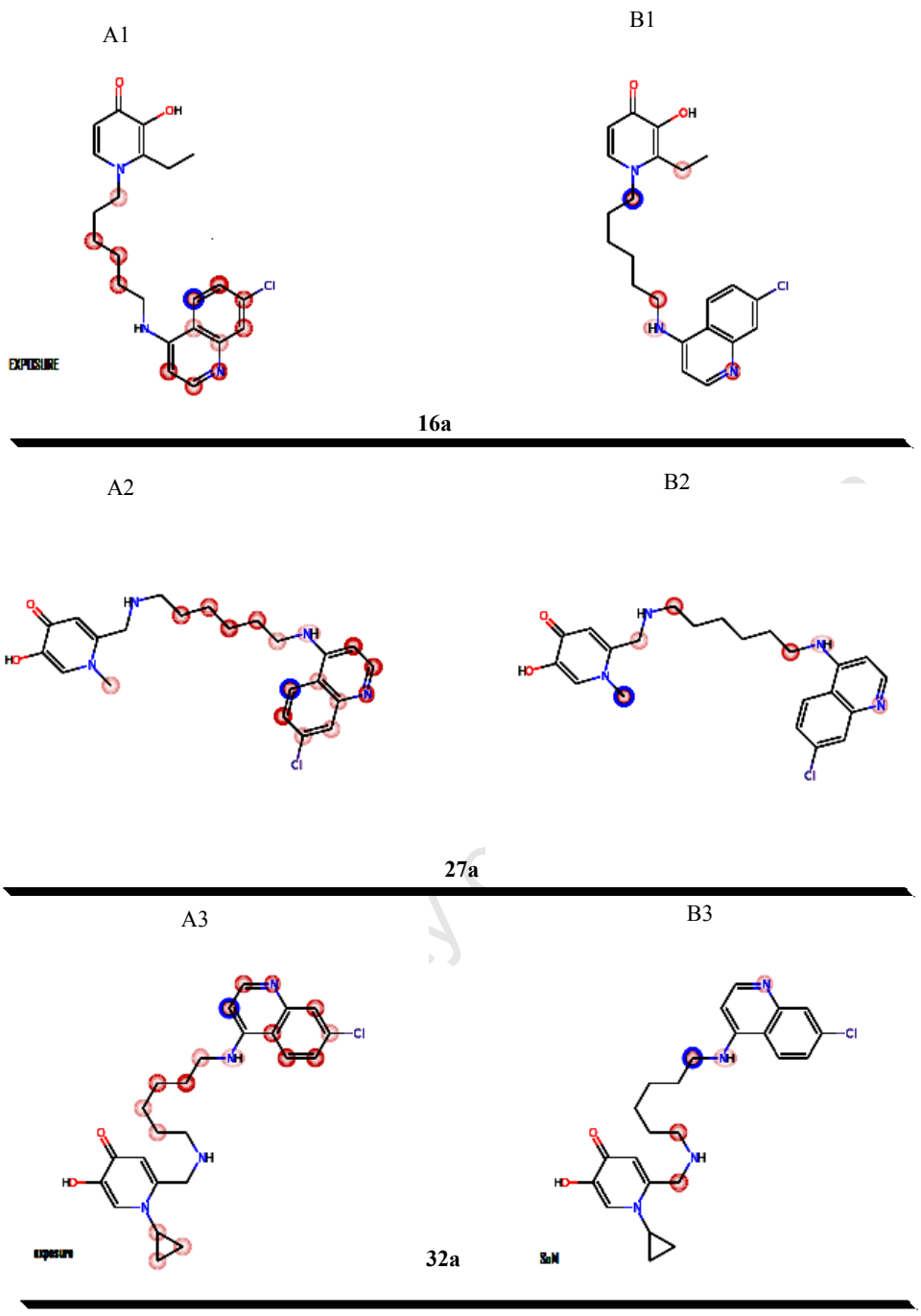

Figure 2.19: *Sites of exposure of the maltol and kojic acid derived double drug to the CYP3A4 active site [A 1,2,3] and sites of metabolism [B 1, 2, 3] from Metasite® The red and blue circles indicate the extent of exposure or reactivity of the highlighted part i.e. blue shows greater exposure or reactivity than red. More intense circle implies greater exposure or reactivity and vice versa. Compound* ***32a*** *quinoline groups appear to be more reactive in the CYP3A4 active site than the other two molecules* ***16a*** *and* ***27a*** *which have similar reactivity.*

2.4.3 Attempted Synthesis of Kojic acid derived double drugs via a Mannich base intermediate

The aim was to introduce tertiary amino groups into this class of conjugate via Mannich bases as envisaged in the design below

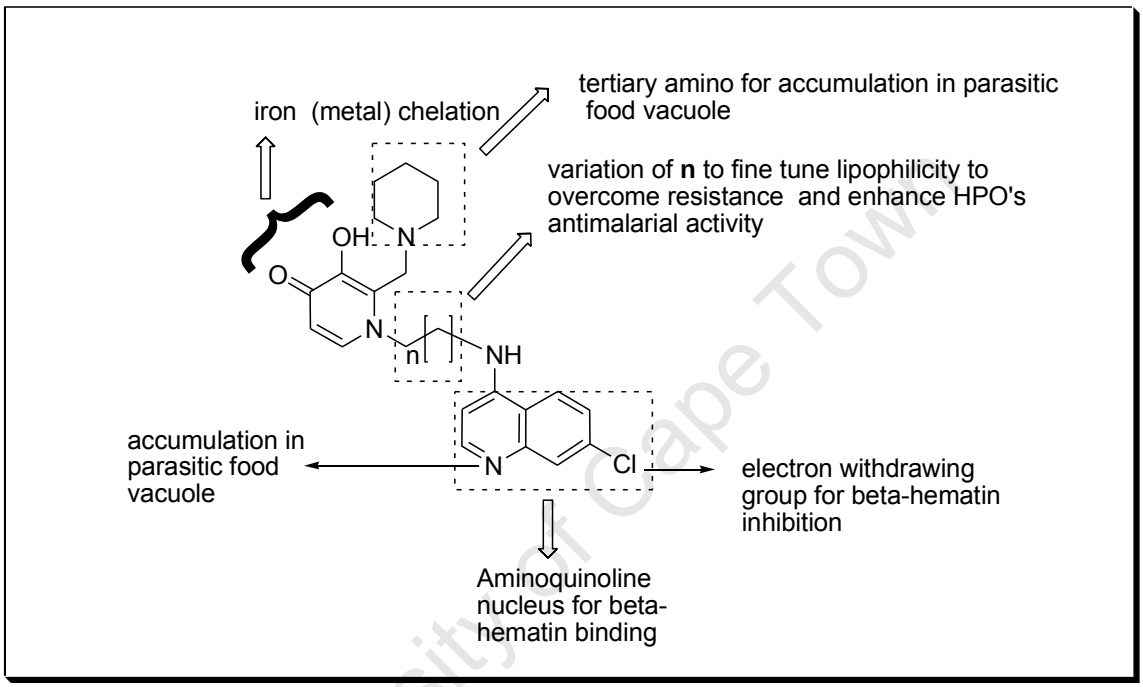

Figure 2.20: *Design of the Kojic acid derived double drugs with a Mannich base group*

2.4.3.1 Retrosynthesis

Before synthesis the retrosynthesis was considered via one route (Fig. 2.21). The strategy involves a a C-O disconnection via dealkylation, FGI of a pyrone to a pyridinone, nucleophilic substitution and a 1,1-diX equivalent requiring a Mannich reaction. The use of kojic acid as the precursor was envisaged, with other main starting reactants being formaldehyde, piperidine, diamines and the 4,7-dichloroquinoline. Kojic acid was chosen as an alternative synthetic precursor for 3,4-HPO–quinoline conjugates because of its high reactivity under Mannich reaction conditions as compared to maltol or ethylmaltol.

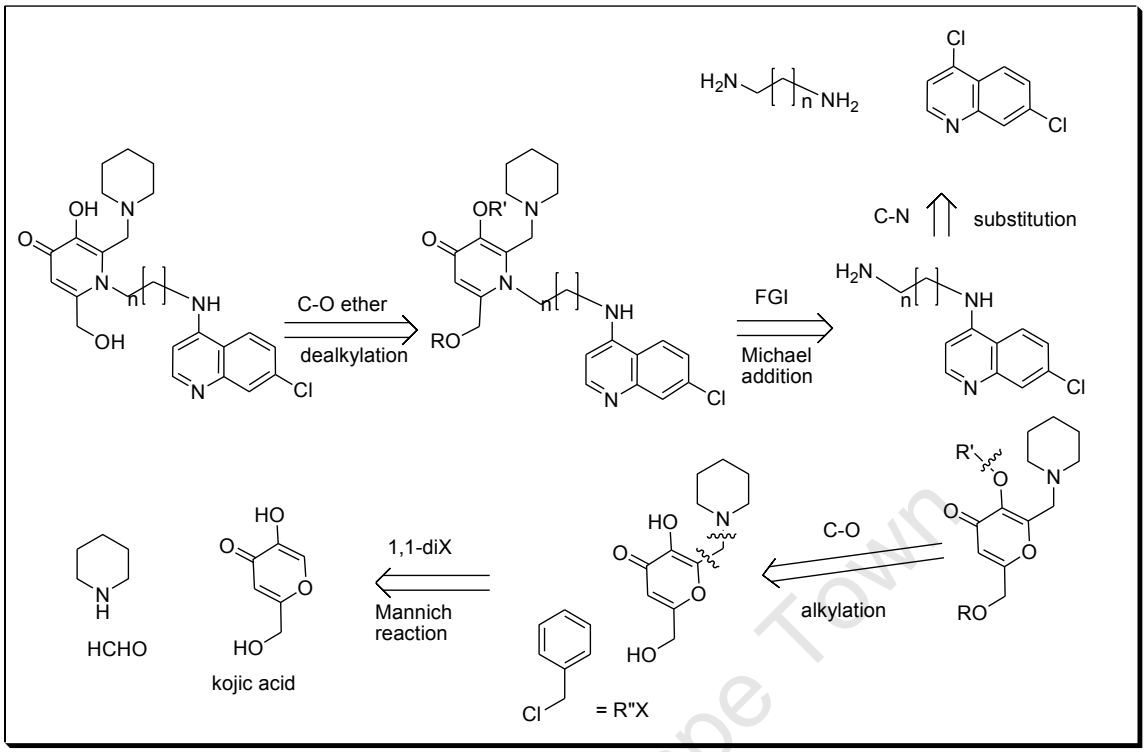

Figure 2.21*: Retrosynthesis of Mannich base intermediates*

The reaction was performed via a one pot direct multi-component protocol. Kojic acid readily reacted at room temperature with piperidine and aqueous formaldehyde to give the crystalline Mannich base. The reaction scheme and mechanism are depicted in figure 2.22 and 2.23 respectively. The reactions proceeded via an iminium ion intermediate which was allowed to react with the unsaturated ketone to form the Mannich base **19**. Selective benzylation of the 3-hydroxy group in **19** was not achieved as the proton NMR indicated benzylation had occurred simultenously at the 6-methylhydroxy and the 3-hydroxy groups (Fig.2.23). Attempts to couple N-(7-chloro-4-quinolinyl) diaminoalkanes to the Mannich base intermediate **19a** via a Michael addition of the amine was unsuccessful probably due steric hindrance by the bulky groups at C-2 and C-6.

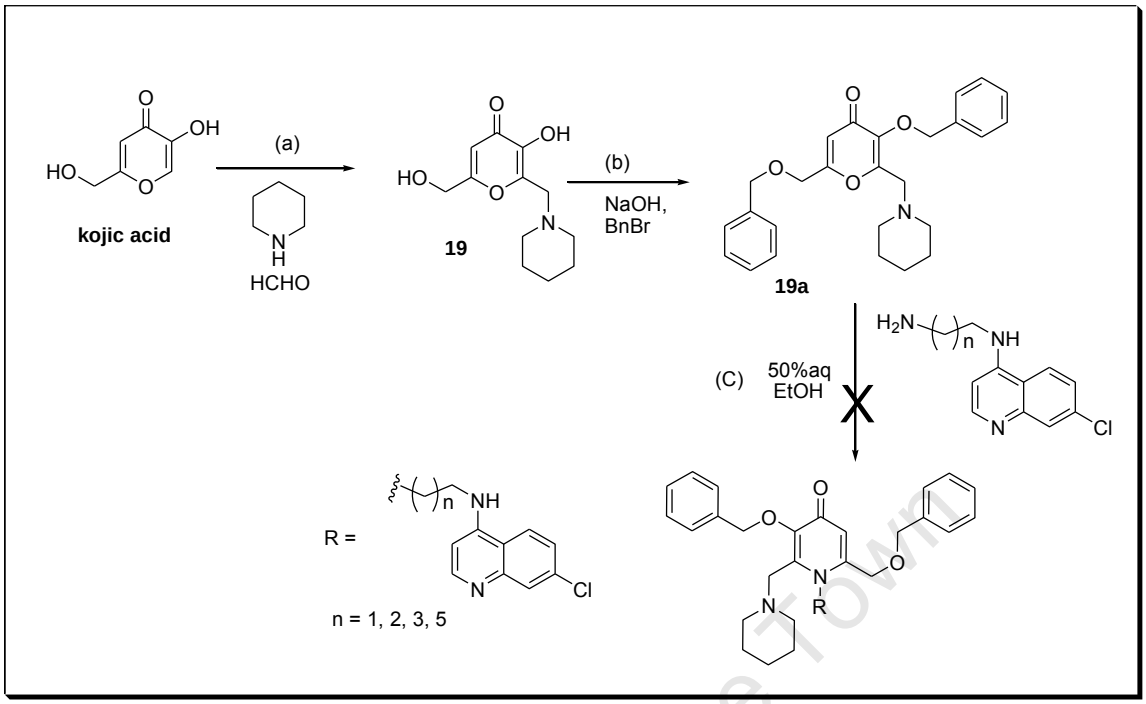

Figure 2.22: *Attempted synthesis of the kojic derived double drugs via Mannich base intermediates*

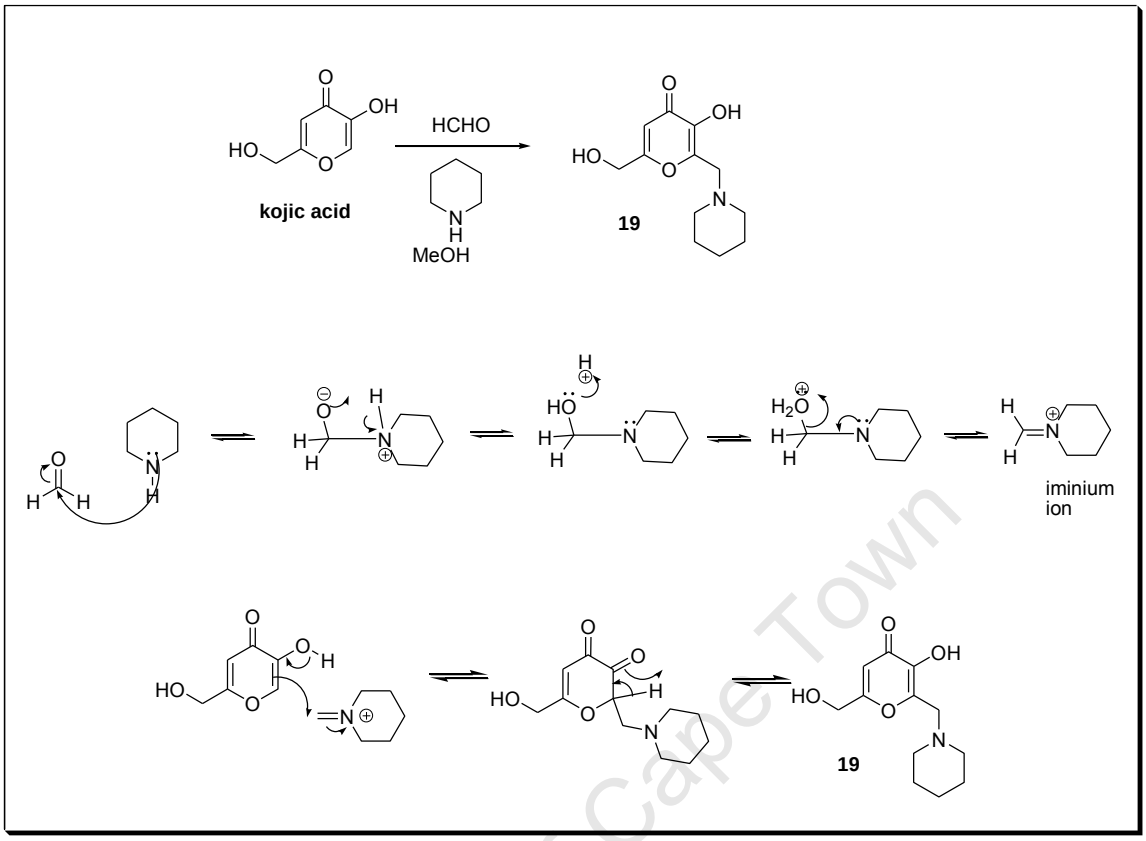

Figure 2.23: *Mechanism for the synthesis of the Mannich base intermediate (Clayden et al 2001; Vogel, A, 1987)*

The mechanism for the formation of the Mannich base intermediate involves a nucleophilic attack on the formaldehyde carbonyl to form the double charged intermediate that undergoes intramolecular proton transfer then dehydration to give the iminium ion intermediate. The acidity of the pyridinone 3-hydroxy group favours the nucleophilic attack of imine by the pyridone's C-6 atom. A second intramolecular proton transfer occurs in the final step.

2.4.4 Synthesis of Kojic acid-derived double drugs via the alkylhalide intermediates

An alternative strategy to kojic acid derived double drugs was adopted and it involved a 2-alkylchloride intermediate of kojic acid on to which *N*-(7-chloro-4-quinolinyl)-diaminoalkanes were coupled via substitution of the chloride.

2.4.4.1 The design

The design of the alternative conjugates is represented in figure 2.24. This design allowed for the simultaneous introduction of the secondary/tertiary amino group and the N(7-chloro-4-quinolinyl) in one step and at the same site of the molecule. This design retained the same functional groups as in the previous design (Fig.2.20).

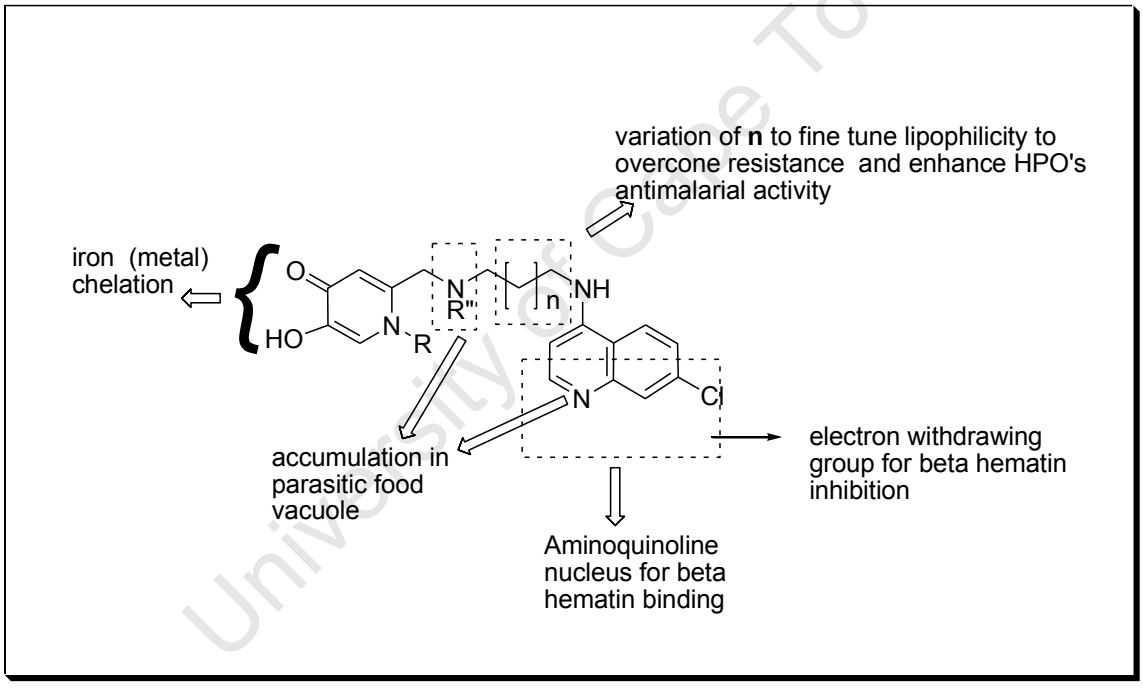

Figure 2.24: *Design of the Kojic acid derived double drugs*

2.4.4.2 Retrosynthesis

In the retrosynthesis (Fig. 2.25) the following were identified as the core reactants; kojic acid, 4,7-dichloroquinoline, diaminoalkanes, benzylchloride, cyclopropylamine or methylamine. Retrosynthesis included C-O ether dealkylation to deprotect the target molecule, and nucleophilic substitution at the pyridinone 2-CH_2 to couple the pyridinone

to the 7-choroquinolin-4-yl-diamine or the 4,7-dichloroquinoline to the diaminoalkanes. Other FGI proceses involved the C-OH to C-Cl and Michael addition.

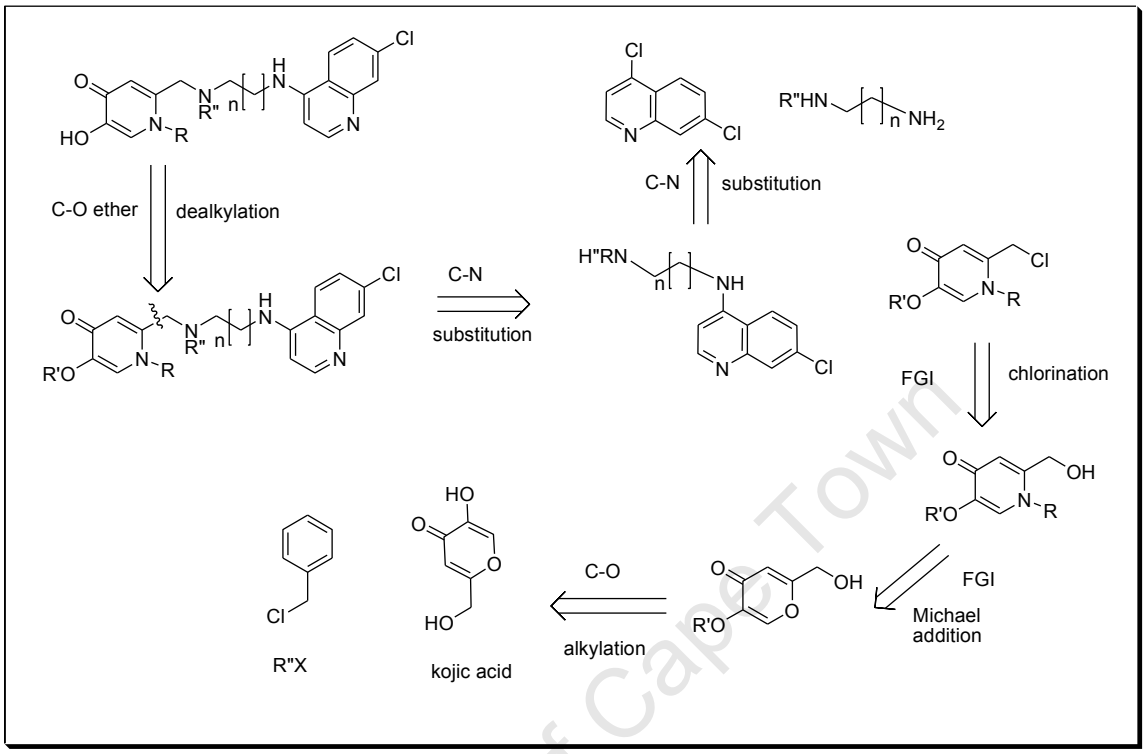

Figure: 2.25*: Retrosynthesis of kojic acid derived double drugs*

2.4.4.3 Synthesis

The initial step involved benzyl protection of the kojic acid. The relatively more acidic 5-hydroxyl group of the pyranone was selected over the 2-methylhydroxyl group to give the desired intermediate (Fig. 2.26). This was followed by Michael addition of methylamine or cyclopropylamine to give the pyridinone **21** or **21a**. Chlorination of the pyridinone (**21** or **21a**) using neat thionylchloride afforded the alkylhalide intermediates **22** or **22a**. These intermediates were easily isolated as precipitates or crystals in moderate to high yields. Chlorination was initially confirmed from the proton NMR as significant deshielding was observed for the protons adjacent to the Cl i.e the signals for methylene protons at C-2 and the protons of the N-1 alkyl groups were shifted by >0.4ppm. Extra evidence was the decrease in the melting point upon chlorination, an example is **21a** (mp 174-175˚C) when compared to **22a** (132-133˚C); its chlorinated analog. The decline in

melting point was due to the absence of H-bonding in **22a**. The chlorination was further confirmed by mass spectrometry. The chlorination mechanism involved substitution of the 5-methylhydroxy by the Cl from thionylchloride. (Fig.2.27)

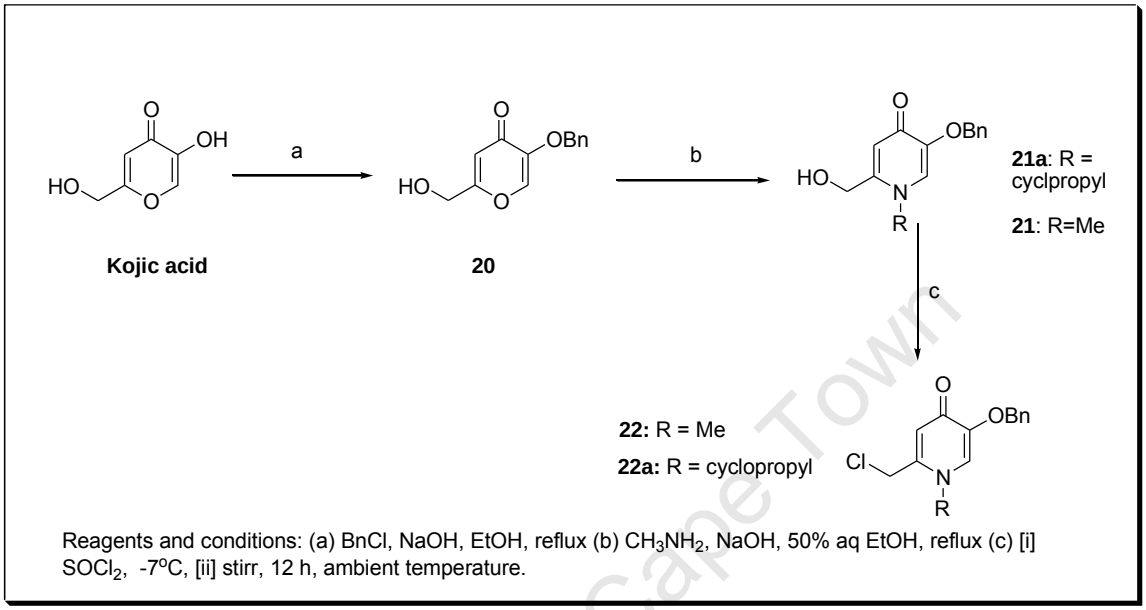

Figure 2.26: *Synthesis of alkyl halide intermediates*

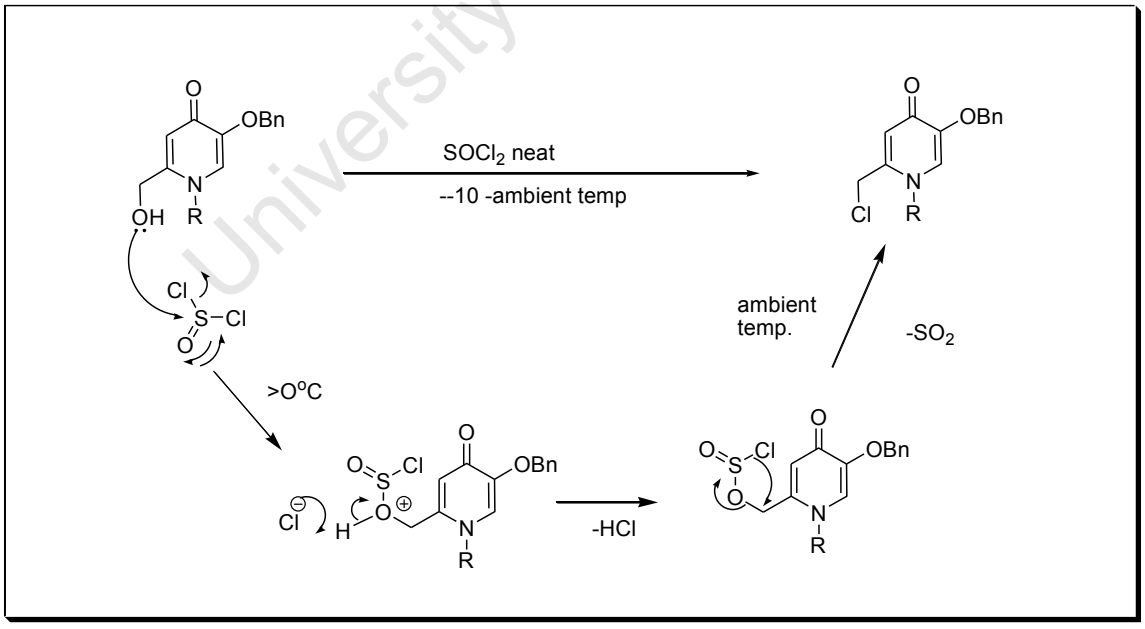

Figure 2.27: *Mechanism for the chlorination step in the alkylhalide intermediate synthesis (Clayden et al 2001; Vogel A, 1987)*

This chlorination involves the 2-hydroxy group of the pyridinone acting as a nucleophile and which attacks the sulfur of the thionylchloride causing the exit of the chloride followed by a proton transfer to the latter to form HCl. The resulting intermediate is thermodynamically unstable and at ambient temperature converts to the most stable product with loss of a molecule of sulfur dioxide.

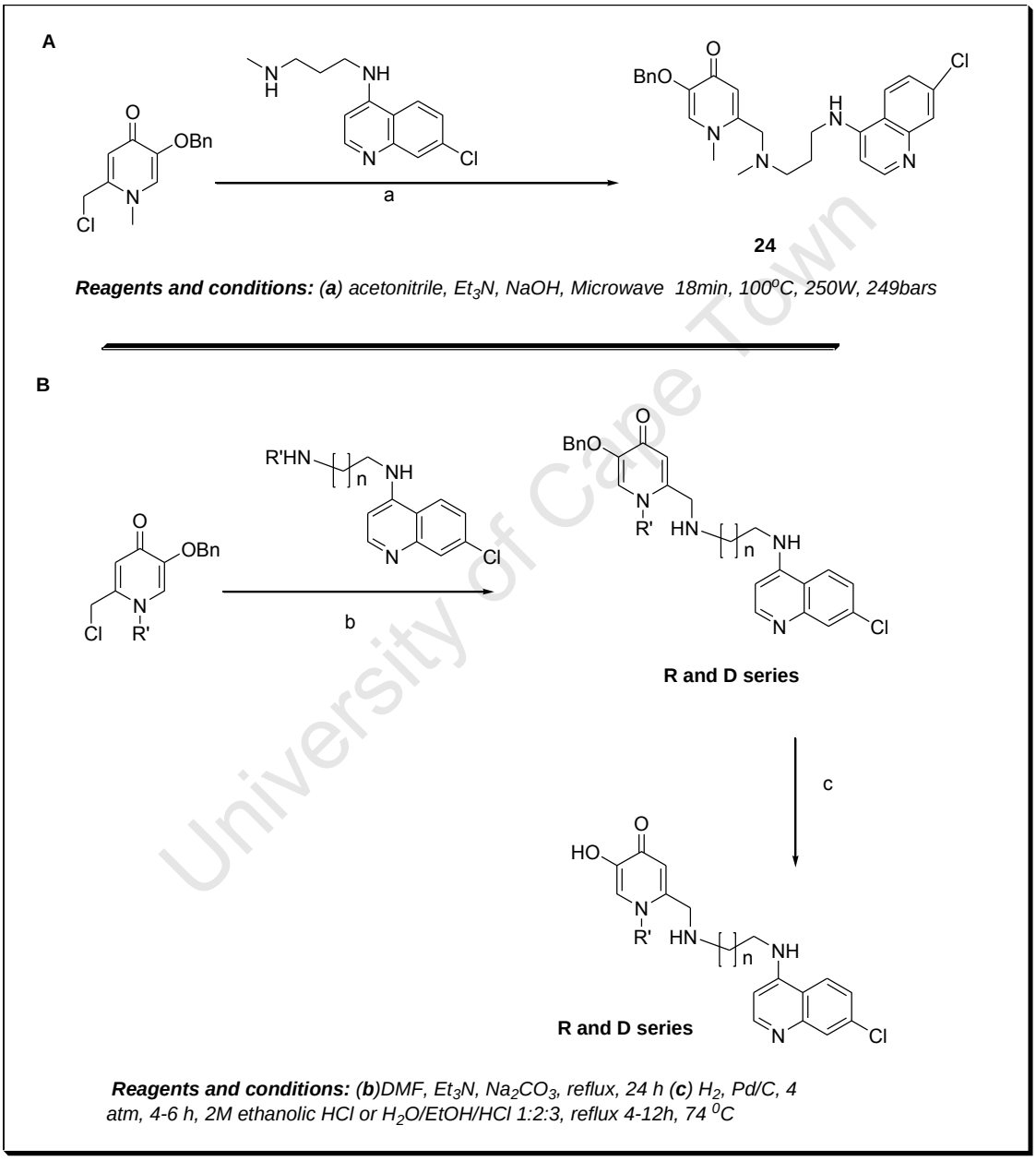

Figure 2.28: *Synthesis of the kojic derived double drugs*

The final step to the benzyl protected conjugates involved reaction of **22** or **22a** with the appropriate *N*-(7-chloro-4-quinolinyl) diaminoalkane (Fig.2.28). The coupling was successful under both microwave and reflux reaction conditions. DMF or acetonitrile were used as solvents because they are polar aprotic and hence appropriate for solubilizing the reactants and for the S_N2 type reaction (Clayden *et al*, 2001), (Fig. 2.29).

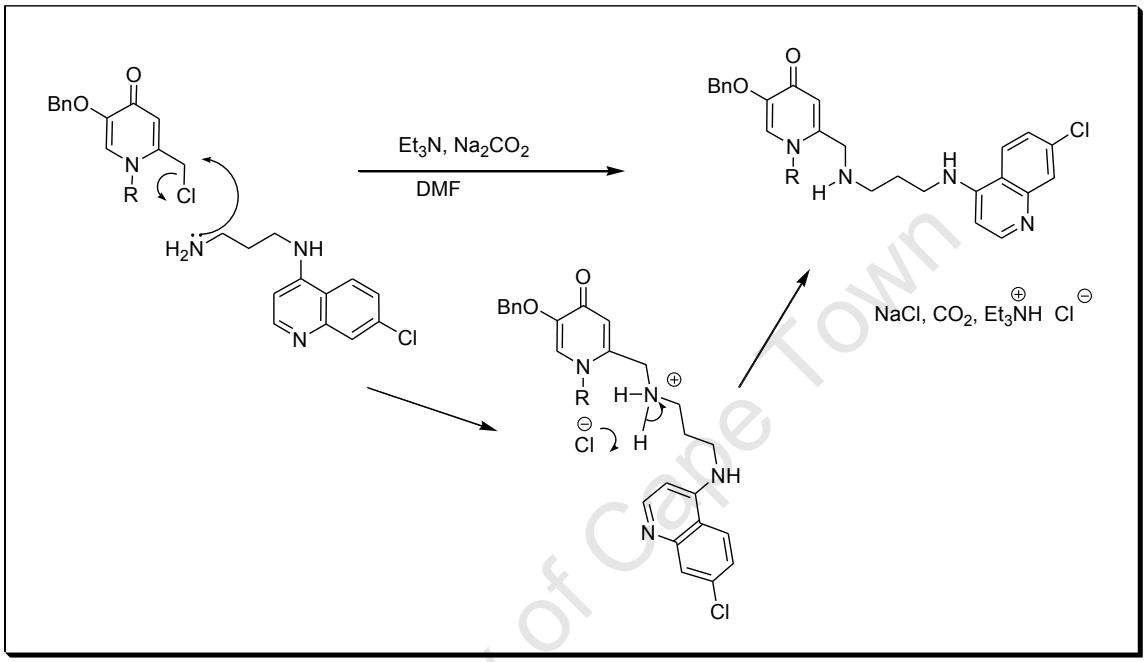

Figure 2.29: *Mechanism for the coupling of the alkylhalide intermediates to the N-(7-chloro-4-quinoyl)diaminoalkane*

The bimolecular substitution of the chlorine on the alkylhalide intermediate by the amine group from the N-(7-chloro-4-quinoyl) diaminoalkane was followed by the deprotonation of the intermediate to give the target molecule. A combination of $NaHCO_3$ and triethylamine were used as bases to optimize the neutralization of HCl which would otherwise protonate the amine and favor the reverse reaction and to optimize the deprotonation of the amine. The purification of the benzylated conjugates was by column chromatography, and where possible, crystallization. An alternative to column chromatography was the precipitation of the unreacted *N*-(7-chloro-4-quinolinyl) diaminoalkane from the dichloromethane solution of the crude product by the addition of brine.

Deprotection was achieved by palladium-catalysed hydrogenolysis or by acid-catalysed hydrolysis. The compounds were isolated in low to moderate yields for the **R** series (Table 2.14) but moderate to high yields in the **D** series (Table 2.15).

Attempts to purify the deprotected compounds by HPLC using a conventional bonded silica stationary phase resulted in poor recovery of the pure compounds. This could be due to the interaction of the chelators with metallic parts of the HPLC instrument or the interaction with the free saturable silanol groups and residual metal impurities on the bonded silica phases. Evidence for this was the multiple peaks and severe tailing in the preparative chromatograms when compared to the analytical chromatograms both under basic and acidic pH. Similar difficulties were reported for the HPLC purification or analysis of *N*-alkyl-3,4-hydroxypyridinones (Guo *et al,* 2001; Epemolu *et al,* 1990). The recommended Hamilton PRP-1 polymer column or porous graphitised carbon (PGC Hypercarb®) columns were not available. Inspite of this, further attempts were pursued to purify two of the compounds using the silica bonded stationary phase.

The purification of compounds **30a** and **32a** were successful but only 10% of the sample was recovered. Different fractions collected from the preparative HPLC showed similar proton NMR profiles indicating the same compound or its metal complexes. Because of this challenge, crystallization was adopted as the most appropriate method for the purification of the deprotected analogs of the kojic acid derived double drugs

Table 2.14: *2-((7-chloroquinolin-4-ylamino)alkylamino)methyl)-5-benzyloxy-1-methylpyridin-4(1H)-ones and deprotected analogues (R series)*

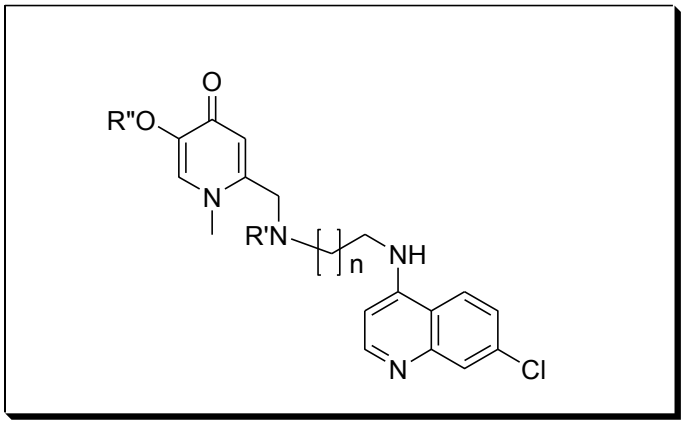

Compound	n	R'	R"	% Yield
23	1	H	Bn	12
23a	1	H	H	74
24	2	Me	Bn	40
24a	2	Me	H	46
25	2	H	Bn	58
25a	2	H	H	43
26	3	H	Bn	48
26a	3	H	H	56
27	5	H	Bn	44
27a	5	H	H	99

2.4.4.4 Characterisation

Characterisation of the compounds was by proton and carbon-13 NMR, high resolution mass spectrometry, elemental analysis, melting point and X-ray crystallography. The aromatic region of the proton NMR spectra of these compounds was similar to that of the maltol-derived double drugs except for the pyridinone protons signals (H-3, H-6), which appeared as two singlets. The aliphatic region of the proton NMR of the kojic acid derived double drugs resembled that of the maltol derivatives except for the following features (a) a singlet at ≈ 3.7- 4.5ppm for the 2-CH_2 protons. (b) a singlet at ≈ 3.5 -

4.5ppm for the N-1-CH_3 group or two multiplets at ≈0.90 - 1.2ppm for H-7 and 3.5 - 4.2ppm for H-8 and H-9 of the cyclopropyl group (Fig. 2.30, 2.31).

Table 2.15: *2-((7-chloroquinolin-4-ylamino)alkylamino)methyl)-5-benzyloxy-1-cyclopropylpyridin-4(1H)-ones and deprotected analogues (D series)*

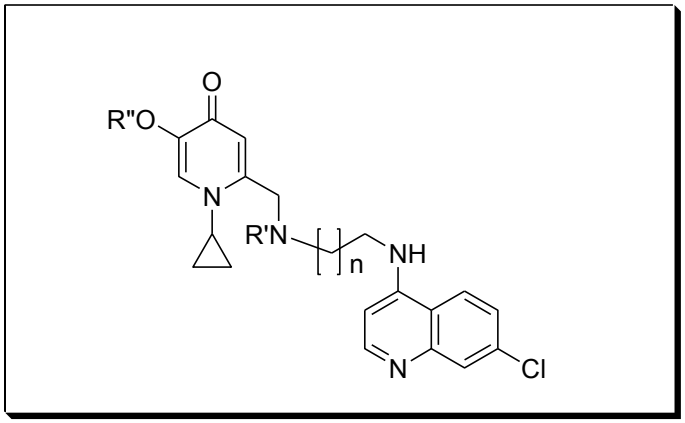

Compound	n	R'	R"	% Yield
28	1	H	Bn	87
28a	1	H	H	56
29	2	H	Bn	91
29a	2	H	H	60
30	2	Me	Bn	89
30a	2	Me	H	
31	3	H	Bn	64
31a	3	H	H	58
32	5	H	Bn	51
32a	5	H	H	51

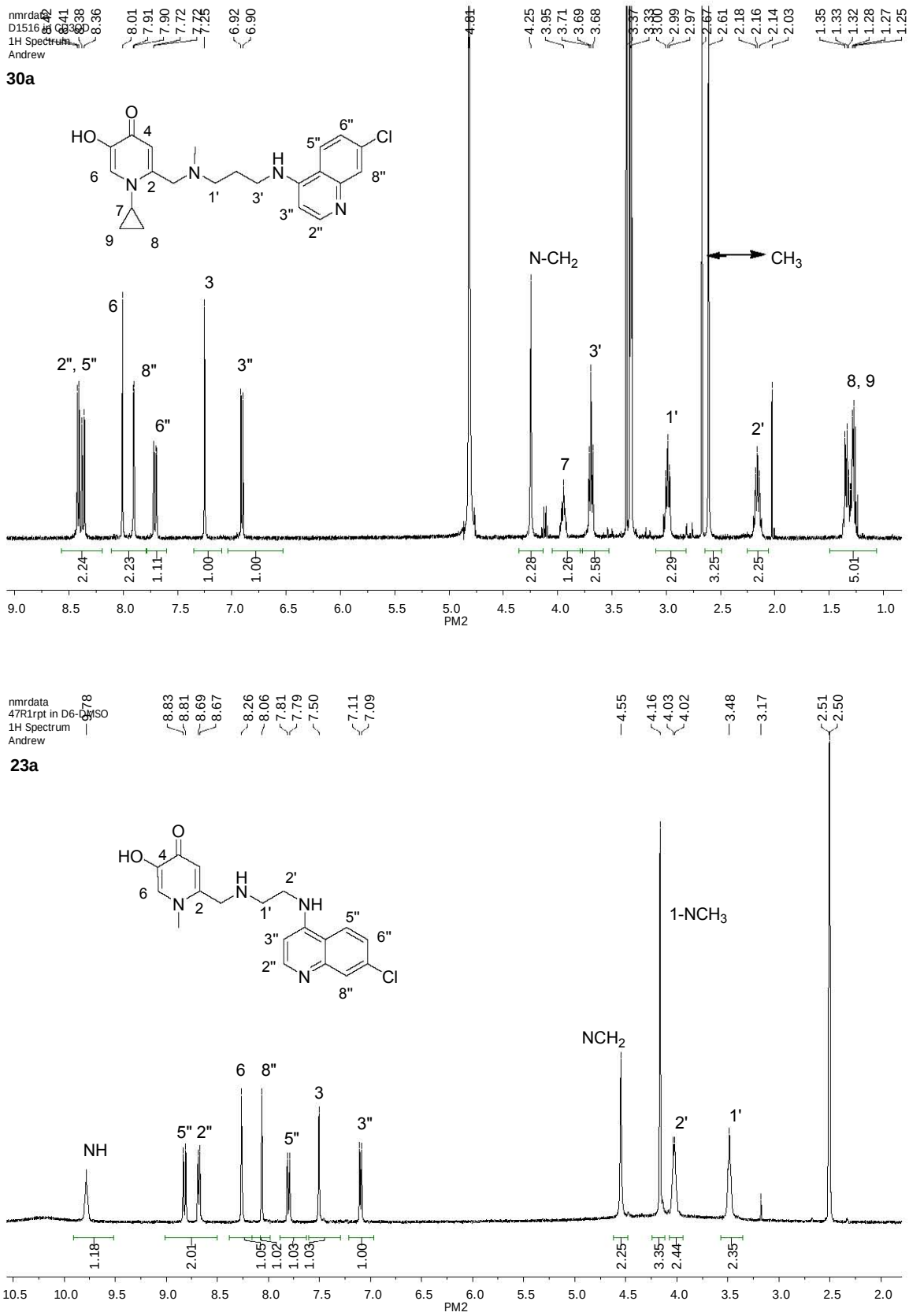

Figure 2.30*: Proton NMR spectrum of kojic acid derived double drugs*

Comparing the carbon-13 spectra of the maltol and kojic acid derived analogs, their spectra were found to have the same number of signals in the aromatic region but extra peaks were observed in the aliphatic region of the kojic derivative signals corresponding to the N-1 alkyl group and the 2-methylene amine.

The HRMS of these compounds indicated *m/z* corresponding to the molecular ion peak. Peaks corresponding to M+H, M+2H and M+3H were also observed due to the protonation of the three amino groups present in each double drug molecule. The elemental analyses indicated the molecules to be hydrated and this was further corroborated by the proton NMR and the X-ray crystallographic data of one of the compounds; **24** (Fig 2.31 and 2.32).

The X-Ray crystallographic analysis of **24** indicated that there was one methanol and three water molecules for each molecule of **24** ($M.3H_2O.CH_3OH$). The methanol molecule is disordered by alternating of the positions of C and O, and the C and O were refined isotropically due to its high thermal motions. Two of the water molecules are disordered with oxygen over two positions. The hydrogens on these disordered methanol and water molecules were excluded form the final structure model.

For the main **24** molecule, all non-hydrogen atoms were refined anisotropically and all hydrogen atoms on carbons were positioned geometrically with C-H distances ranging from 0.95 Å to 1.00 Å and refined as riding on their parent atoms, with U_{iso} (H) = 1.2 - 1.5 U_{eq} (C). The position of amine hydrogen H_2N (on N2) was located in the difference electron density maps and refined with simple bond length constraints. The structure was refined successfully with R factor 0.0579. The parameters for crystal data collection and structure refinements are in Table 1 of the experimental chapter.

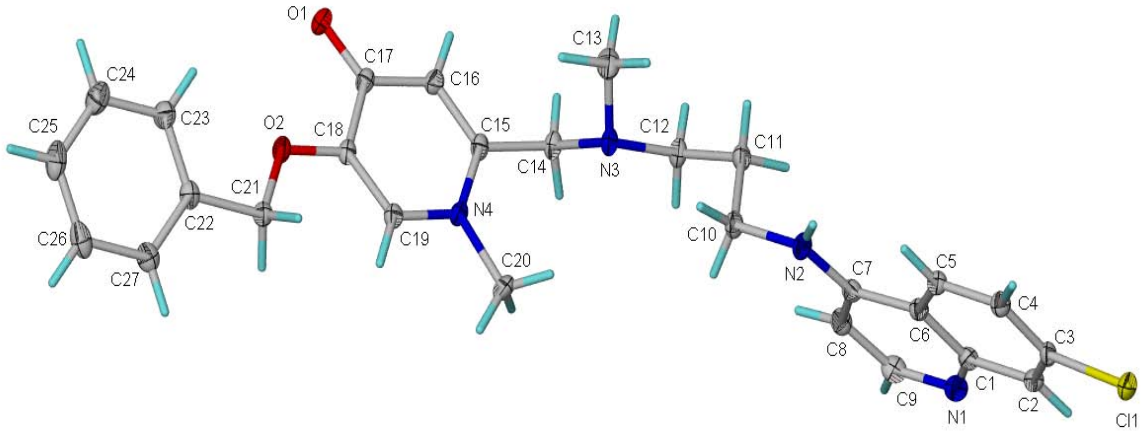

Figure 2.31: *Numbering scheme for* ***24****. Note Solvent molecules excluded.*

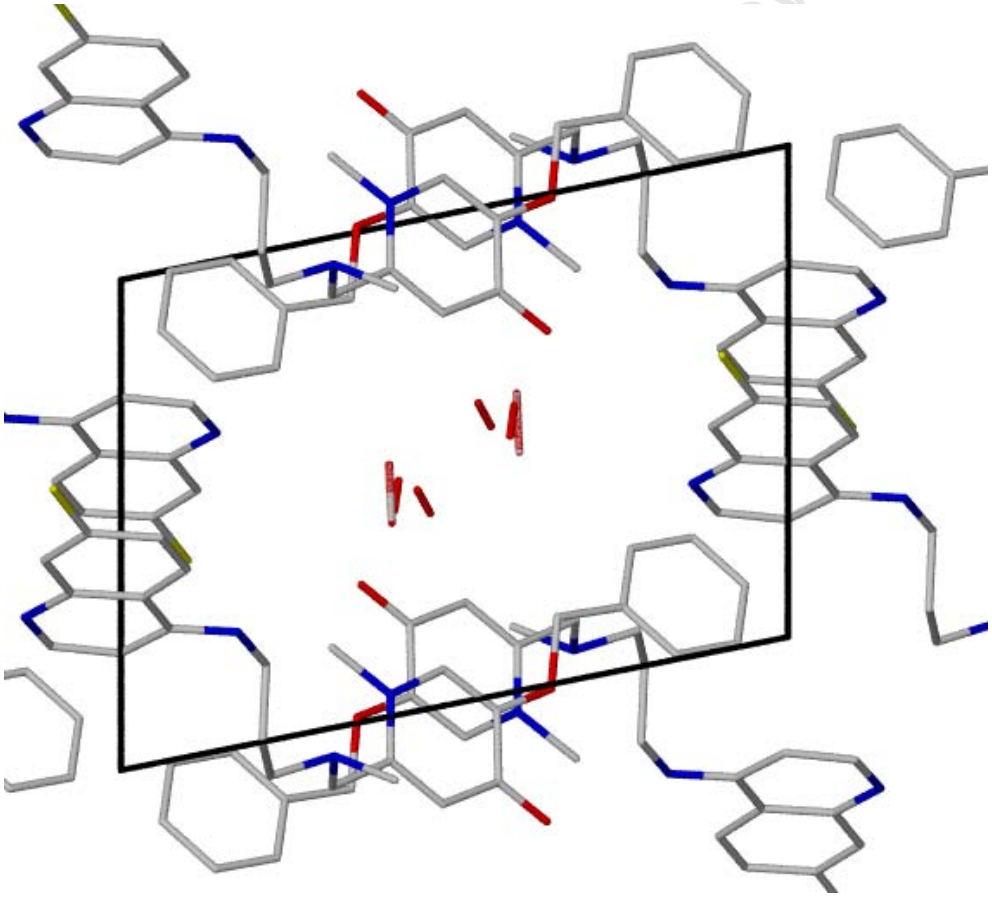

Figure 2.32: *Projection viewed along b. Note the disordered solvent molecules (methanol and waters in the crystal of* ***24****.*

Table 2.16: *Hydrogen bonds for* ***24*** *[A and deg.].*

D-H...A	*d(D-H)*	*d(H...A)*	*d(D...A)*	*<(DHA)*
N(2)-H(2N)...O(1)#1	0.956(10)	2.011(16)	2.908(2)	155(3)
O(1W)-H(1W1)...O(1)	0.966(10)	1.813(14)	2.767(3)	169(4)
O(1W)-H(1W2)...N(1)#2	0.961(10)	1.779(11)	2.740(3)	178(4)

Further analysis show that the heterocyclic ring is not regular as it has two C-C [1.436 (3), 1.419(3)], two C=C [1.364(3), 1.343(2)] and two C-N [1.371(3), 1.353(3)], bonds respectively. The C (17) - O(1) bond (1.276 Å) is significantly longer than a pure ketone C=O bond (1.210 Å) [Dobbin *et al* 1993], this provides the O(1) with a partial negative charge that is used to form strong hydrogen bonds. The C (17) - O(1) bond length is similar to the corresponding bond length in the pyrone precursor kojic acid (1.244Å) and deferiprone **2a** (1.278 Å) a closely related pyridinone [Lokaj *et al* 1991; Clarke *et al,* 1992].

The ketone oxygen O(1) is not protonated because protonation would have resulted in the extension of the C(17)-O(1) bond length to ≈1.346Å, the typical length of a protonated ketonic oxygen in a hydroxypyridinone (Dobbin *et al* 1993). Protonation is not expected since the compound was obtained as a free base and no acid was used in the recrystallization. The water molecules are shown to participate in intramolecular hydrogen bonding along with the ketonic oxygen O(1) and the quinoline nitrogens N(1) and N(2) [Table 2.16]

2.5 Synthesis of Catecholate –aminoquinoline Conjugates

2.5.1 Rationale

The first siderophore-antibiotic double drug to be designed for antimalarial purpose involved a catecholate siderophore conjugated to nalidixic acid and had excellent activity against the resistant *Plasmodium* (Pradines *et al.,* 1996). To overcome membrane mediated resistance synthetic siderophore-drug conjugates may act as a shuttle for active transport of drugs into the microbial cell wall i.e. the "trojan horse antimicrobials" (Braun et al 2009, Ghosh *et al* 1996). The 3,4-hydroxypyridinone is known to be the synthetic bioisostere of the catecholate, the latter is known to be metabolically labile than the former. We envisaged a strategy for novel antimalarials in which the hydroxypyridinone moiety in the 3,4-HPO-aminoquinoline double drugs is replaced with the catecholate with the hope that this may enhance or retain the antimalarial potency and reduce the CYP3A4 inhibition potential of these type of compounds.

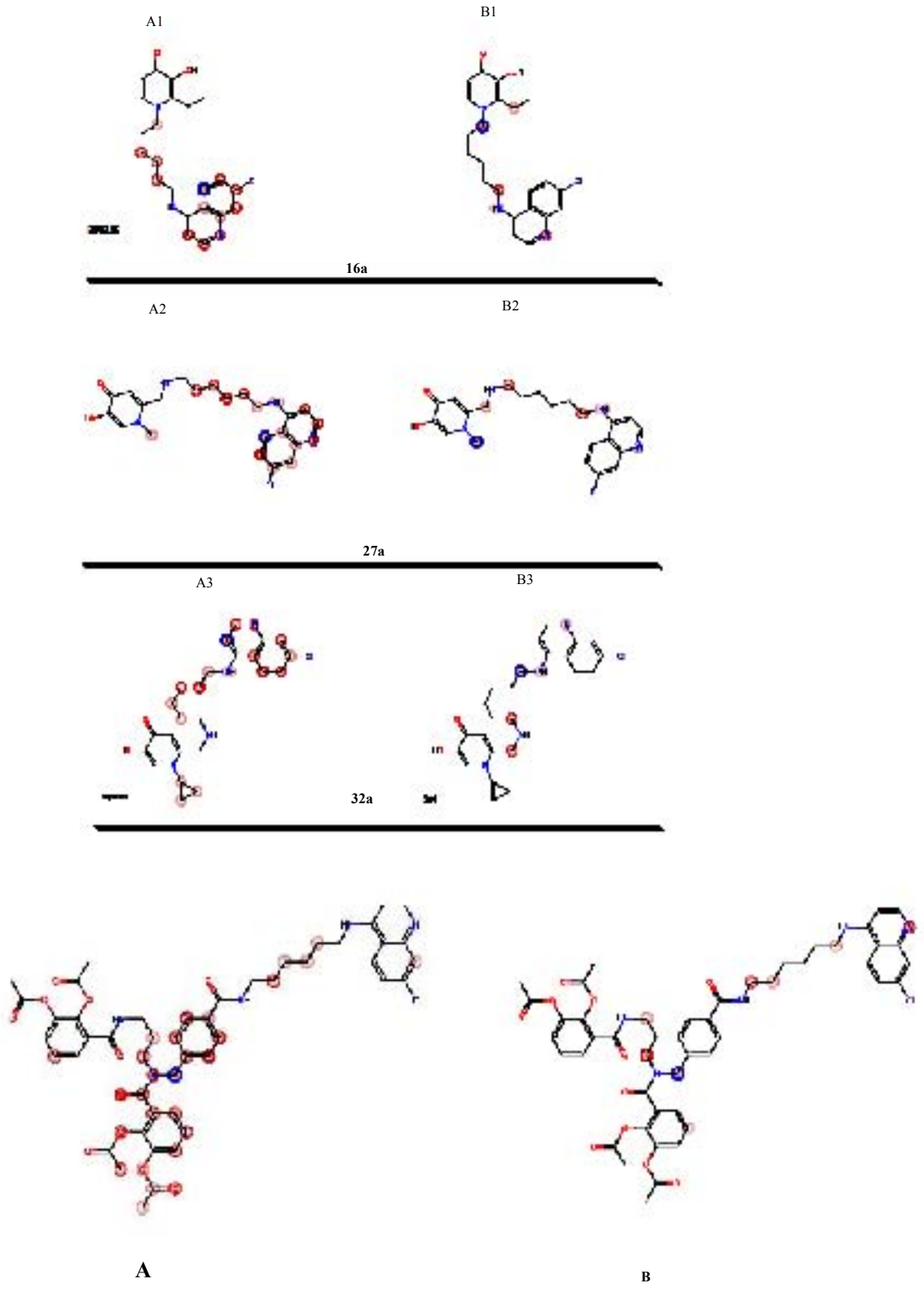

Figure 2.33: *Sites of exposure (A) and reactivity (B) of the biscatecholate double drug from Metasite® prediction. The red and blue circles indicate the extent of exposure or*

reactivity of the highlighted part of the molecule i.e. blue shows greater exposure or reactivity than red. More intense circle implies greater exposure or reactivity and vice versa.

Metasite® prediction showed the quinoline substructure in the novel biscatecholate (Fig 2.32) to be less exposed and more reactive towards the active site (Fig 2.32). Given that the quinoline is associated with CYP3A4 inhibition (Zlokarnik *et al* 2005; Riley and Kenna, 2004), such a prediction implied lesser potential for CYP3A4 inhibition. This contrasts the maltol and kojic derived double drugs profiles in the model in which the quinoline is more exposed but unreactive implying potential to inhibit CYP3A4.

2.5.2 Design

In the design the synthetic tetradentate bis-catecholate siderophore is attached to a *N*-(7-chloro-4-quinoyl) diaminoalkane. The chelator groups are acetyl protected to form a prodrug which can be deprotected under physiological conditions (Braun *et al* 2009, Heinisch *et al,* 2002)

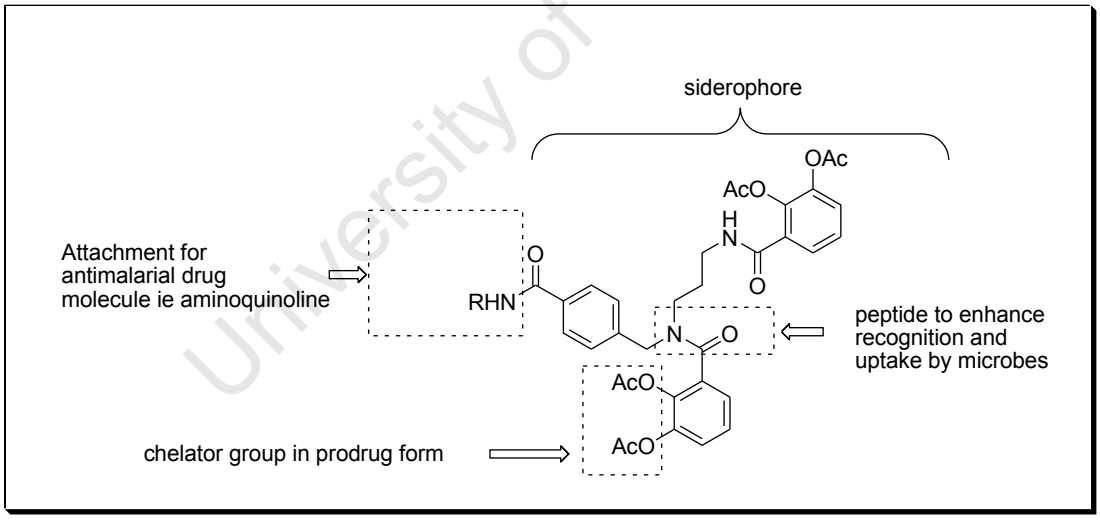

Figure 2.34: *Design of the siderophore-aminoquinolie drug conjugate molecule*

2.5.3 Synthesis

The siderophore fragment **36** was synthesized via several steps as illustrated in Figures 2.35 – 2.37. The initial step was to prepare the **35** which is the backbone on which the

catechols are attached to give the siderophore. The preparation of **35** involved a reductive amination reaction between 1,3-diaminopropane and 4-formylbenzoic acid (Fig. 2.35). The reduction was mediated by hydrogenation catalyzed by palladium on active carbon (Heinisch *et al.,* 2002). The unreacted/excess amine was co-distilled off with toluene.

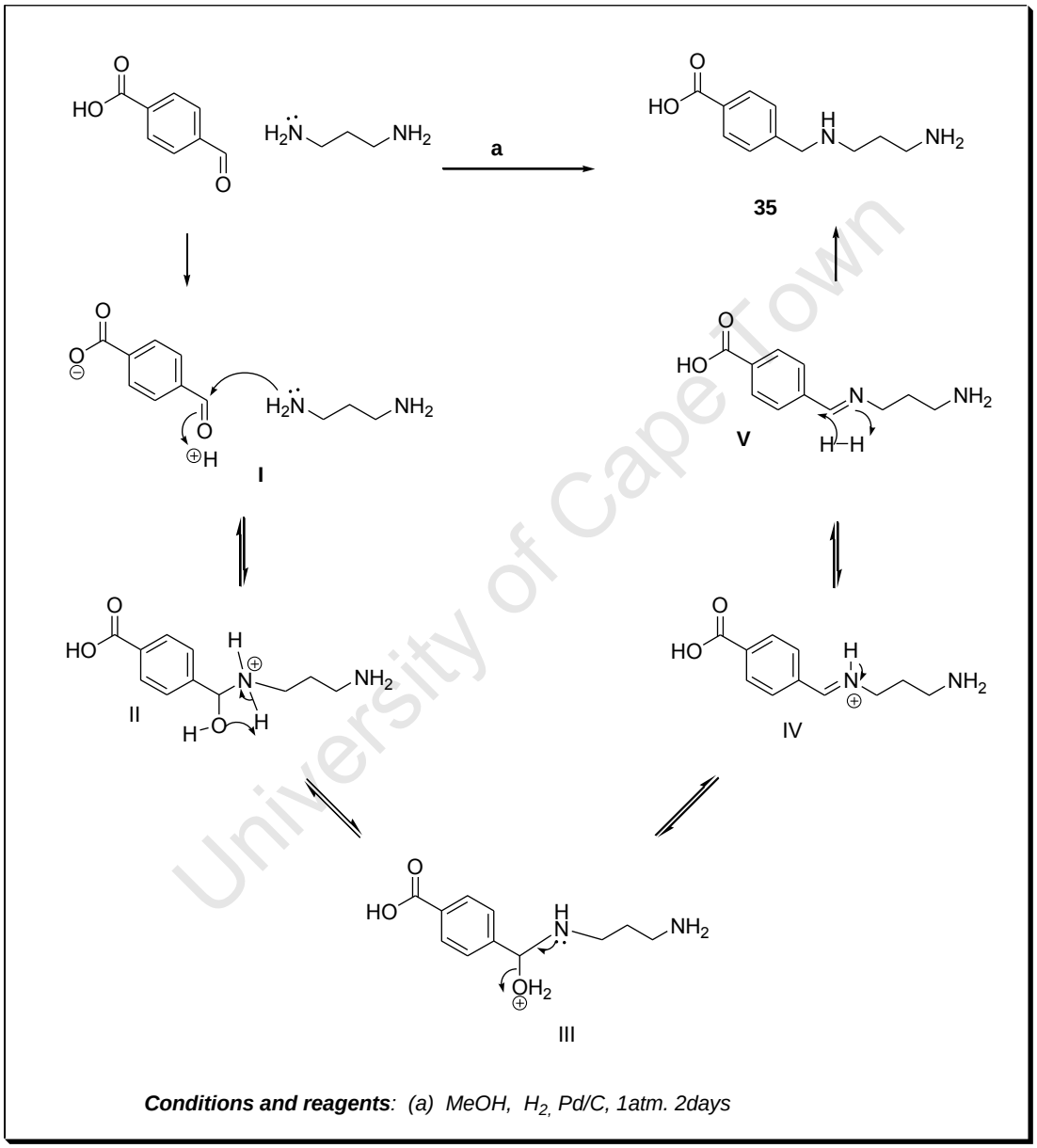

Figure 2.35: *Synthesis of the 4-((3-aminopropylamino)methyl)benzoic acid* ***35*** *and the mechanisms for the reaction.*

The reaction proceeded by the elimination of water from **III** to form the unstable imine intermediate **IV.** (Clayden *et al* 2001) The imine is selectively reduced leaving the carboxylic acid functionality intact to yield the target compound **35.**

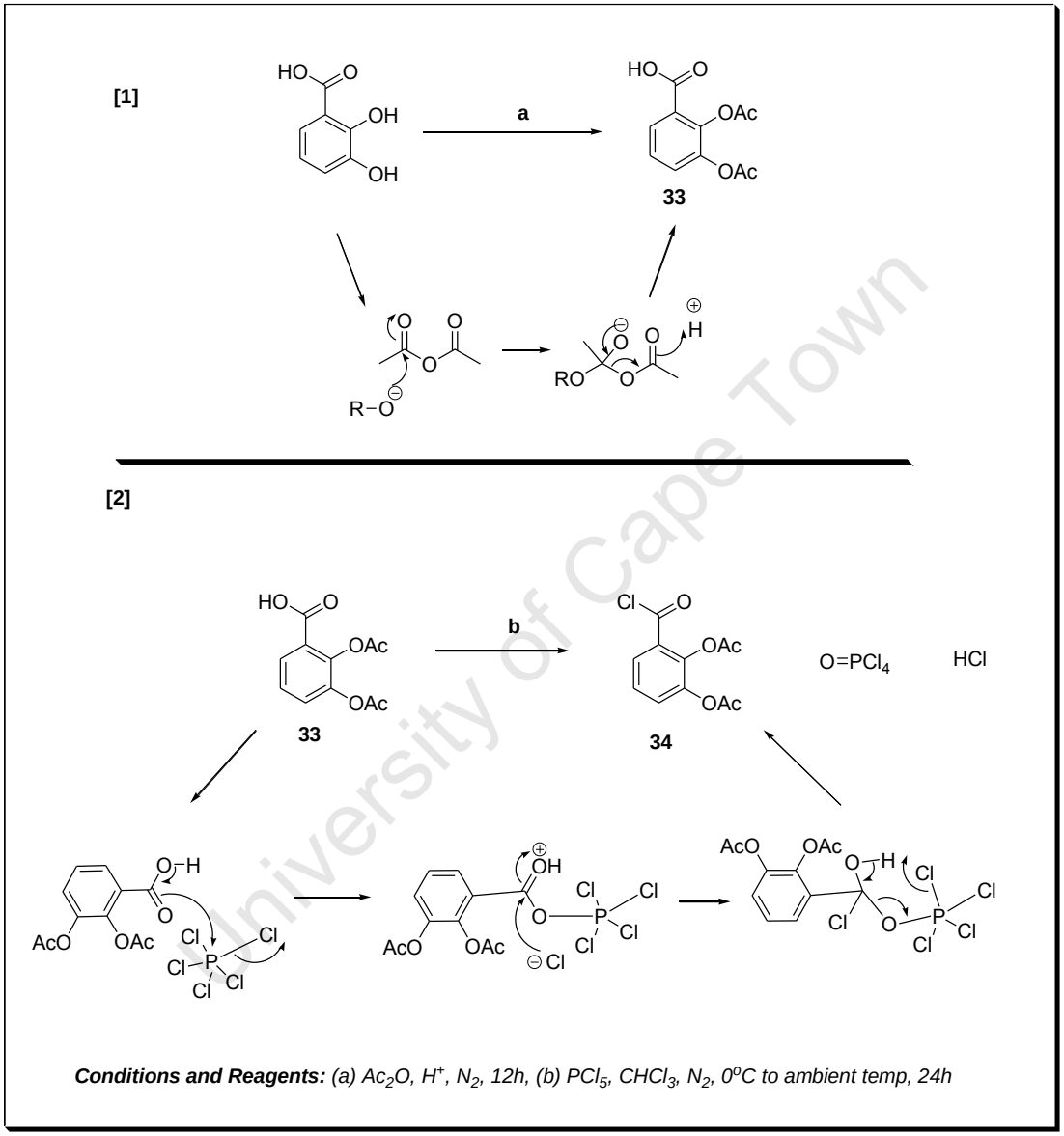

Figure 2.36: *Synthesis of **C4** and mechanisms for the reaction.*

The diacyloxybenzoylchloride **34** was prepared as documented by Bergeron *et al* (1980) Initially the 2,3-dihydroxybenzoic acid was acetylated using acetic anhydride under inert atmosphere and acid catalysis (Fig. 2.36). The final step involved chlorination of **33** with phosphorous pentachloride to give the acid chloride **34**. In all these steps all glass

apparatus were used to avoid contamination from HCl corroding the rubber apparatus. The two compounds (**34** and **33**) were easily separated as crystals or as a solid. Both reactions proceded via unstable tetrahedhral intermediates as illustrated in Figure 2.35. (Clayden *et al.,* 2001)

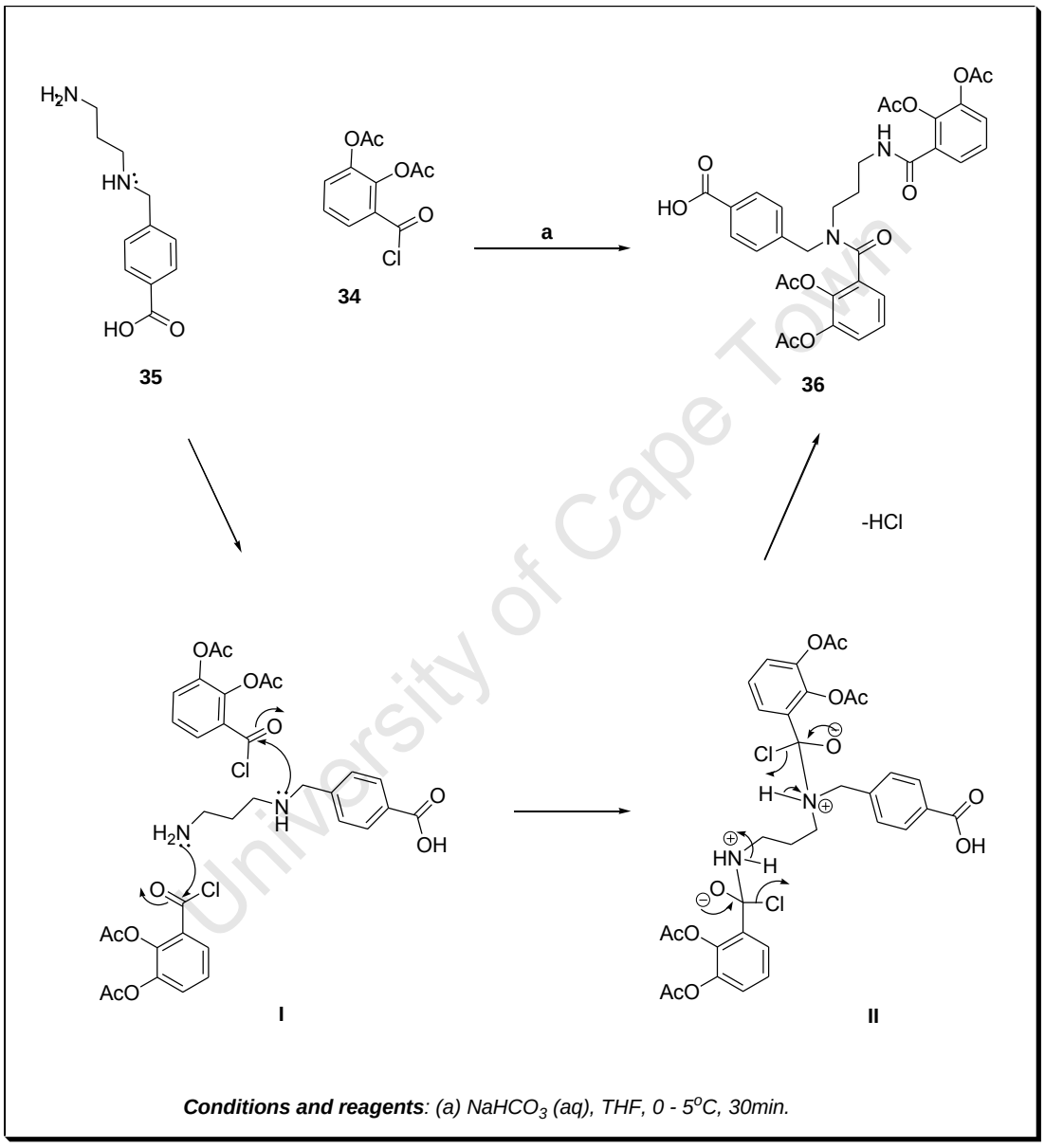

Figure 2.37: *Synthesis of the siderophore* ***36,*** *and mechanisms for the reaction.*

The final step to the siderophore (**36**) was prepared by attaching two molecules of diacylatedbenzyloxychloride **34** to the backbone **35** (Fig. 2.37). Mechanistically it can be

assumed that the first nucleophilic attack occurs on the primary amine which is less hindered. The nitrogen of the amide formed is unreactive towards a second nucleophilic attack since its lone pair is delocalised via resonance with the carbonyl oxygen. Therefore the second nuceophilic attack will certainly occur on the hindered secondary amine to give the target **C6**. The siderophore was purified by recrystallization and preparative HPLC-MS before submitting for physicochemical characterization and biological testing.

The crude form of compound **36** was used in the subsequent step of coupling to the *N*-(7-chloro-4-quinoyl) diaminoalkane **8** (Fig. 2.39). After purification by preparative HPLC-MS (Fig. 2.38), the product was obtained in very low yields. The conjugate **37** was more polar (R_t 6.96min.) than the siderophore **36** (R_t 5.54min.) therefore, it eluted later in the HPLC (Fig. 2.38).

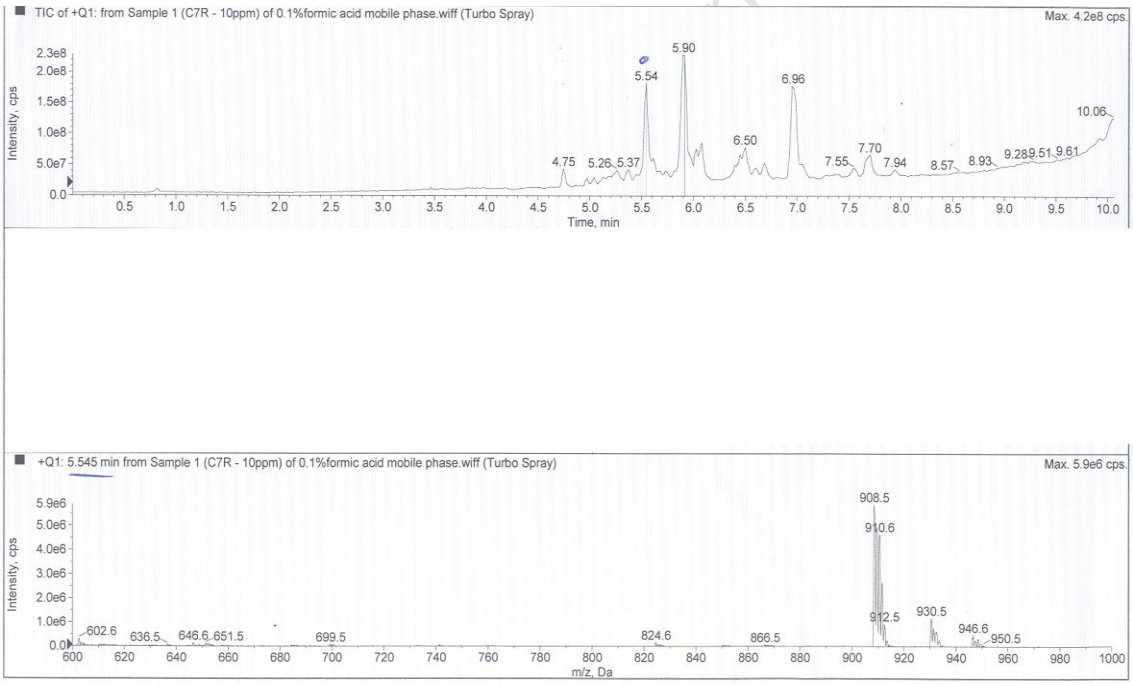

Figure 2.38: *Chromatogram and mass spectrum for the preparative HPLC-MS of* ***37*** *The peaks at retention times 5.54, 5.90 and 6.96 minutes correspond to compounds* ***37,*** *the diamine* ***8*** *and the siderophore* ***36*** *respectively. The mass spectrum peak at m/z 908.5 corresponds to the target compound* ***37****.(bottom plot)*

The synthesis involved the activation of the resonance stabilized unreactive carboxylic acid group in the siderophore. This was achieved by reacting **36** with chloromethylformate in the presence of an acid scavenger (N-methylmorpholine) to form the reactive ester intermediate **VIII** (Clayden *et al.,* 2001; Mackie and Smith, 1985; Wipf, 1999). This intermediate readily underwent nucleophilic attack by the amine to give the target compound and the methylhydrogencarbonate (Fig. 2.39).

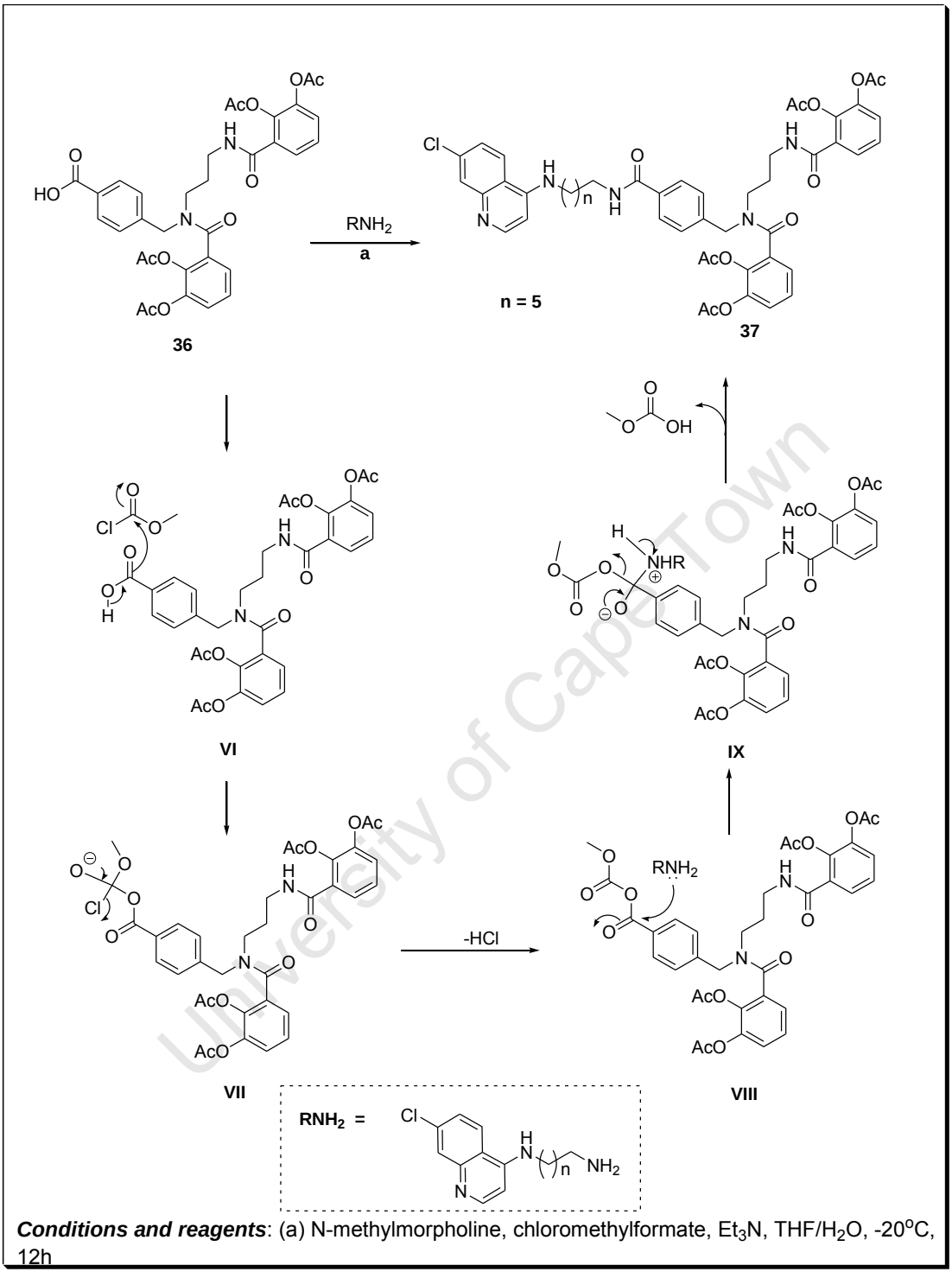

Figure 2.39: *Synthesis of the siderophore-aminoquinoline conjugate **37** and mechanisms for the reaction.*

The terminal methyl group on the mixed anhydride (**VIII**) causes a positive inductive effect which makes the less hindered carbonyl carbon less reactive when compared to the hindered carbonyl (Fig. 2.39). The hindered carbonyl is more reactive towards a nucleophilic attack because of the electron withdrawing effects of the aromatic ring and the oxycarboxylate group attached to it.

2.5.4 Characterization

The compounds were characterised by proton and carbon-13 NMR, elemental analysis, HRMS, and melting point determinations for the solids. HR-MS was important in helping to conclude the target conjugate **37** was isolated since the latter's proton NMR signals were not fully assignable due to high numbers of overlapping multiplets.

CHAPTER THREE
BIOLOGICAL ACTIVITY

3.1 *In vitro* Antiplasmodial Activity of the 3,4-HPOs and their Gallium (III) Complexes

3.1.1 Rationale

There was need to establish the baseline antiplasmodial activity of known 1-*N*-alkyl-3,4-hydroxypyridinones (3,4-HPOs) and confirm the role potential of iron chelation in the antimalarial activity of these compounds before synthesis of new structurally modified 3,4-HPOs. Therefore a number of known 3,4-HPOs with variations in the chain length of the N-alkyl group were synthesized and tested for antiplasmodial activity. The N-alkyl variation was meant to fine tune the lipophilicity of these iron chelators. Lipophilicity has been shown to directly correlate with the inhibitory action of chelators against malaria parasites as demonstrated for a number of chelators namely; *N*-alkyl derivatives of 3,4-hydroxypyridinones (3,4-HPOs) and aminothiols (Shanzer *et al,* 1991, Hershko *et al.,* 1991, Loyevsky *et al.,* 1996).

Complexation with gallium (III) has been reported to enhance antiplasmodial activity and to overcome drug resistance in aminophenols (Ocheskey *et al,* 2003; 2005, Goldberg *et al*, 1997). This has not been reported for the antiplasmodial activity of N-alkyl-3,4-HPOs, hence providing a reason to prepare and study the antiplasmodial activity of the 3,4-HPO-gallium (III) complexes.

3.1.2 Results

The quantitative assessment of *in vitro* antiplasmodial activity in this work was against chloroquine sensitive (CQS) D10 and 3D7 strains and a chloroquine resistant (CQR) K1 strain of *Plasmodium falciparum*.

None of the N-alkyl-3,4-HPOs had activity comparable to CQ against either the resistant or sensitive strains (Table 3.1). The trend of antiplasmodial activity increasing with increase in lipophilicity (*N*-alkyl chain length) was observed in the D10 and K1 strains.

Table 3.1*: In vitro antiplasmodial activity of the N-alkyl- 3,4-HPOs and their 3-benzyl protected analogues*

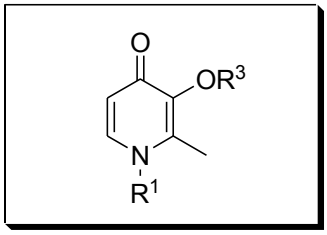

			P. falciparum IC_{50} µM		
Compound	R_1	R_3	D10	3D7	K1
2[a]	Me	H	142	49.1	114.2
1[a]	Me	Bn	>377	>50.0	>87.0
2b	Et	H	67.2	ND	ND
1b	Et	Bn	234	>113	>82.0
2c	Bu	H	35.9	79.2	7.65
1c	Bu	Bn	ND	ND	ND
2d	Cyclopropyl	H	103.9	7.42	>99.5
1d	Cyclopropyl	Bn	ND	>32.0	>78.0
2e	Isopropyl	H	90.1	>77.8	>98.5
1e	Isopropyl	Bn	>343	>35.0	>77.0
2f	n-propyl	H	ND	ND	ND
1f	n-propyl	Bn	256	11.5	>47.0
2g	n-hexyl	H	14.7	3.54	4.16
1g	n-hexyl	Bn	84.0	>98.0	>66.0
2h	n-octyl	H	5.49	2.38	1.80
1h	n-octyl	Bn	48.0	30.8	>61.0
CQ			0.066	0.003	0.21

ND: Not determined.

Table 3.2*: In vitro antiplasmodial activity of the N-alkyl-3,4-HPOs and their gallium (III) complexes*

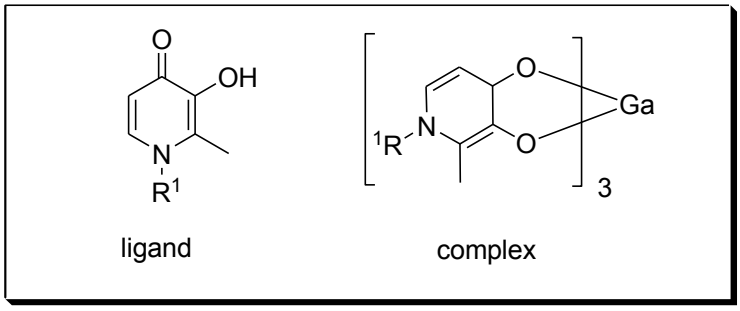

			P. falciparum IC_{50} µM		
Compound	R_1	Ligand or complex	D10	3D7	K1
2[a]	Me	ligand	142	49.1	114.2
3[a]	Me	complex	205	87.4	41.3
2b	Et	ligand	67.2	ND	ND
3b	Et	complex	33.5	7.05	38.0
2c	Bu	ligand	35.9	79.2	7.65
3c	Bu	complex	142	92.1	32.8
2d	Cyclopropyl	ligand	103.9	7.42	>99.5
3d	Cyclopropyl	complex	>177	>99.5	>35.6
2e	Isopropyl	ligand	90.1	>77.8	>98.5
3e	Isopropyl	complex	>175	>98.5	>35.2
2g	n-hexyl	ligand	14.7	3.54	4.16
3g	n-hexyl	complex	38.6	ND	ND
2h	n-octyl	ligand	5.49	2.38	1.80
3h	n-octyl	complex	14.9	2.37	>25.7
CQ			0.066	0.003	0.21

ND: Not determined.

Iron chelation was hypothesised to be the major mode of antimalarial activity for the *N*-alkyl-3,4-HPOs because blocking of the chelator group either by pre-complexation with gallium (III) or by benzyl protection negated the antiplasmodial activity of these compounds (Tables 3.1 and 3.2).

Benzyl protection caused a decrease in the antiplasmodial activity against the sensitive strains but a similar trend was not observed in the resistant strain except for compounds **2g** and **2h** (Table 3.1)

Compounds **2g** and **2h** were the most active as expected since they were the most lipophilic and their antiplasmodial activity was consistent across the three strains of *P. falciparum*. Compound **2h** (IC_{50} = 1.8 μM) was ≈ 30 times more active than its benzylated precursor **1h** (IC_{50}>61 μM) against the CQ resistant isolate K1 (Tables 3.1).

Complexation with gallium (III) caused a decrease in antiplasmodial activity against the sensitive strains except for compound **2b**. A similar trend was not observed in the resistant strain except for compounds **2c** and **2h**. There was a slight improvement in the antiplasmodial activity of some of the 3,4-HPOs on complexation with gallium (III) e.g. **2a**, **2d** and **2e** against K1.

All the compounds were evaluated for β haematin inhibition using the phi-β assay (Ncokazi and Egan, 2005), and none of them showed inhibition at the highest concentration (IC_{50} equivalents = 10).

From the biological data presented, it was concluded that the compounds were not comparable let alone better than CQ and that they had poor activity against the resistant strains of *P. falciparum*. Therefore there was a need for further structural modification to improve their antiplasmodial activity.

3.2 *In vitro* activity of combinations of 2h, 1h, dihydroartemisinin (DHA) and chloroquine diphosphate (CQ-DP).

3.2.1 Rationale

Conjugation of 3,4-HPOs with quinoline or endoperoxide antiplasmodial compounds to form double drugs was envisaged. Prior to synthesizing these double drugs there was need to ascertain whether or not this class of iron chelators synergizes or antagonizes the antiplasmodial activity of the endoperoxides and quinolines. To inform this, the antiplasmodial activity of combinations of selected 3,4-HPOs with dihydoartemisinin and chloroquine diphosphate was studied. Even though iron chelators have been reported to antagonize the *in vitro* antiplasmodial activity of artemisinins (Meshnick *et al* 1993; Stocks *et al.,* 2007) or synergize the antiplasmodial activity of chloroquine CQ (Co *et al.,* 2009) it was important to ascertain this before further work.

Compounds **2h** and **1h,** which had the best *in vitro* antiplasmodial activity among the 3,4-HPOs were selected for drug combination studies. They were combined with chloroquine diphosphate CQ-DP or dihydroartemisinin (DHA) using a method that has been described in literature (Berenbaum 1978; Barquero *et al.,* 1997; Adovelande *et al.,* 1998; Pattanapanyasat *et al.,* 2001; Ohrt *et al.,* 2002), and the combinations were tested *in vitro* against K1 and 3D7 isolates of *P. falciparum.*

The fractional inhibitory concentrations, FICs, were employed to determine synergistic or antagonistic or additive interactions of the drug combinations (He *et al*., 2010, Ohrt *et al* 2002; Berenbaum, 1980; 1978; 1977).

FIC_{50} values were calculated by the formula shown below

$$(1)\ FIC_{50}(B_i) = \frac{IC_{50}(A_i+B_i)}{IC_{50}(B)} \times B_i$$

$$(2)\ FIC_{50}(A_i) = \frac{IC_{50}(A_i+B_i)}{IC_{50}(A)} \times A_i$$

$$(3)\ \Sigma FIC_{50} = FIC_{50}(A_i) + FIC_{50}(B_i)$$

A_i = fraction of A in a given combination

B_i = fraction of B in a given combination

$IC_{50}(A_i+B_i) = IC_{50}$ of fraction combinations of two drugs A and B

$IC_{50}(B) = IC_{50}$ of fraction containing 100% B

$IC_{50}(A) = IC_{50}$ of fraction containing 100% A

Compound **2h** combinations with CQ or DHA were predominantly synergistic in both K1 and 3D7 whereas its benzylated analogue **1h** combinations with DHA and CQ were synergistic and antagonistic respectively

3.2.2 *In vitro* Antiplasmodial Activity of Combinations of 1h or 2h with CQ

The ΣFIC_{50} values for **2h**/CQ-DP combinations are illustrated in Table 3.3 and the interaction was found to be strongly synergistic because the $\Sigma FIC_{50}<1$ when tested against 3D7. A similar interaction was observed for this combination in the K1 strain except for two FIC_{50} values (2.81 and 2.04). If the two data points are treated as outliers then the interaction will be assumed to be synergistic. If the outliers are incorporated then the interaction may be considered additive. In fact additive interaction in combinations between a 3,4-HPO (**2a**) and quinolines (quinine and mefloquine) have been reported (Pattanapanyasat *et al.,* 2002). There is some evidence that the three antimalarials MQ, CQ and QN kill the parasite by similar mechanisms (Tilley *et al.,* 2001) therefore, one could expect the interaction between CQ and 3,4-HPOs to be similar to that of MQ or QN with 3,4-HPOs.

Table 3.3: *In vitro antiplasmodial activity against P. falciparum and FIC_{50} for different combinations of **2h** with CQ-DP*

Fraction of **2h**	Fraction of CQDP	Σ FIC_{50} (3D7)	Σ FIC_{50} (K1)
1	0	1	1
0.788	0.211	0.043	0.08
0.647	0.353	0.007	2.81
0.476	0.524	0.003	0.30
0.35	0.65	0.0015	0.78
0.261	0.739	0.0017	0.02
0.18	0.82	0.0037	2.04
0.115	0.885	0.0005	0.72
0	1	1	1

Table 3.4: *In vitro antiplasmodial activity against P. falciparum and FIC_{50} for different combinations of **1h** with CQ-DP*

Fraction of 1h	Fraction of CQ-DP	Σ FIC_{50} (3D7)	Σ FIC_{50} (K1)
1	0	1	1
0.833	0.277	11.09	2.70
0.7	0.3	1.69	1.94
0.524	0.476	3.46	2.74
0.455	0.545	2.25	5.88
0.283	0.717	0.81	1.49
0.18	0.82	0.31	0.99
0.11	0.89	1.45	0.98
0	1	1	1

Compound **1h** is inactive on its own (IC_{50}^{3D7} = 30.8μM, IC_{50}^{K1} > 61μM) however the **1h**/CQDP combination was observed to be strongly antagonistic in both strains (Table 3.4). Most of the ΣFIC_{50} values for the **1h**/CQDP were >1 in either strain implying that the **1h** and CQ interaction was predominantly antagonistic.

The antagonistic or indifferent interaction observed for **1h**/CQDP implicates competing modes of action between chloroquine and the benzyl protected iron chelator. To explain this one would consider the closeness of the clog P values of CQ and **1h** which are 5.3

and 4.6 respectively. The two compounds have similar lipophilicity hence may access similar intraparasitic compartments and possibly compete for similar pathways leading to antagonism when the two are combined. Such a possibility is minimal for **2h** which is less lipophilic (cLogP of 2.8). The benzyl group on the 3, 4-HPO could be interacting with some of the parasitic targets of CQ possibly by π –π stacking with the heme porphyrin. However, this interaction may be considered weak since the *N*-alkyl 3,4-HPOs were identified were found to be weak β-haematin inhibitors. Another possibility could be that the CQ interaction with its parasitic targets leads to a cascade of events that enables **1h** to access the very targets it could not accesss on its own.

3.2.3 *In vitro* Antiplasmodial Activity of combinations of 2h or 1h with DHA

For the **9B**/DHA all the ΣFIC_{50} values for K1 were less than one implying a synergistic interaction as depicted in Table 3.5, but the ΣFIC_{50} values in the 3D7 data ranged from greater than 1 to less than one suggesting additive interaction.

Table 3.5: *In vitro antiplasmodial activity against P. falciparum and FIC_{50} for different combinations of **2h** with DHA*

Fraction of **2h**	Fraction of DHA	ΣFIC_{50} (3D7)	ΣFIC_{50} (K1)
1	0	1	1
0.857	0.143	0.58	0.013
0.733	0.26	1.70	0.029
0.655	0.3448	0.17	0.001
0.52	0.48	0.96	0.032
0.345	0.655	0.33	0.001
0.286	0.714	1.07	0.046
0.133	0.866	0.87	0.006
0	1	1	1

The synergistic interaction observed for **2h**/DHA was not expected since 3,4-HPOs are known to antagonize endoperoxides (Meshnick *et al,* 1993; Pattanapanyasat *et al*, 2001; Stocks *et al.,* 2007), via sequestration of the endogenous chelatable iron which is claimed to be important in the mechanism of action of all endoperoxide antiplasmodials (Stocks *et*

al, 2007). Combinations of **2h** with other endoperoxides may be investigated in the future to confirm whether the interactions depend on the type of endoperoxide or the type of 3,4-HPO used.

The **1h**/DHA combination resulted in a synergistic interaction in both 3D7 and K1 strains (Table 3.6). The chelating group on **1h** was blocked by the 3-benzyl group, and thus diminishing this compounds ability to act as an iron chelator. As such it was not expected to antagonize the antiplasmodial activity of the endoperoxide. This reaffirms that, apart from iron sequestration being the main mode of action for antiplasmodial *N*-alkyl-3,4-HPOs, these compounds have additional modes of action whose effect may be realized on blocking the chelating group. These findings are comparable to experiments in which pre-complexation with iron (III) was used to block the chelating moiety to prevent the iron chelator from antagonizing the biological activity of artemisinins (Meshnick *et al*, 2002).

Table 3.6: *In vitro antiplasmodial activity against P. falciparum and FIC_{50} for different combinations of **1h** with DHA*

Fraction of **1h**	Fraction of DHA	Σ FIC_{50} (3D7)	Σ FIC_{50} (K1)
1	0	1	1
0.89	0.11	0.0002	0.007
0.813	0.188	0.0005	0.017
0.636	0.364	0.0018	0.015
0.56	0.44	0.0005	0.006
0.41	0.59	0.0002	0.007
0.31	0.69	0.0009	0.008
0.14	0.86	0.002	0.072
0	1	1	1

Given that the **2h**/CQ-DP combination is synergistic in the resistant and sensitive strains of *P. falciparum*, it was felt logical to synthesize 3,4-HPO-4-amino-7-chloroquinolinyl conjugates or hybrid molecules. To synthetically access this type of conjugate, it was inevitable to go through the benzyl protected analogues. Thus the subsequent stage of the work involved synthesis of benzyl protected 4-amino-7-chloroquinolinyl-3,4-HPO

conjugates, which were then deprotected to deliver the target molecules. This direction does not rule out the development of artemisinin-iron chelator conjugates as antiplasmodials to fight drug resistance because Kamchonwongpaisan *et al.,* (1995) demonstrated that an artemisinin-3,4-HPO conjugate retained antiplasmodial activity comparable to that artemisinin.

3.3 Biological activity of the double drugs (hybrids)

The double drugs were evaluated for the inhibition of β-haematin formation, *in vivo* and *in vitro* antiplasmodial activity, cytotoxicity and inhibition of CYP 3A4. The four series of hybrid molecules whose biological activities are considered in this chapter are A, AB, R and D these are predefined in section 1.15.

3.3.1. *In vitro* antiplasmodial activity in CQ sensitive strain 3D7

3.3.1.1. Antiplasmodial and β-haematin inhibition activities of AB series

Table 3.7: *In vitro antiplasmodial activity against CQ sensitive P. falciparum 3D7 strain, and β-haematin inhibition of* ***AB*** *series (ethylmaltol derived) double drugs*

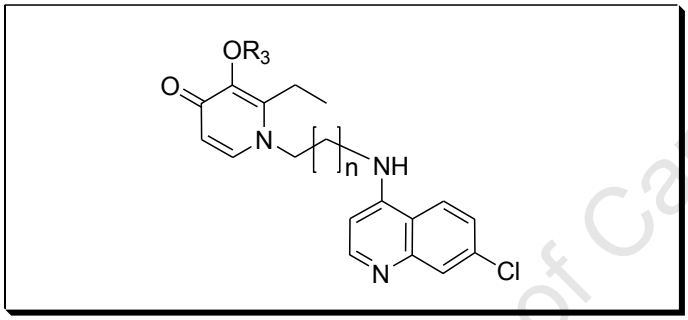

Compound	R^3	n	βHIA IC_{50}/equiv.	*P. falciparum* IC_{50} (μM)
				3D7
10	Bn	1	0.50	0.95
10a	H	1	1.1	0.4
12	Bn	2	0.41	0.12
12a	H	2	1.3	0.12
14	Bn	3	0.19	0.004
14a	H	3	0.98	0.05
16	Bn	5	0.16	0.007
16 HCl salt	Bn	5	---	0.008
16a	H	5	0.49	0.079
CQ			1.9	0.009

In the *in vitro* tests, five isolates of *P. falciparum* were used namely, D10, 3D7 (CQ sensitive) and Dd2, W2 and K1 (CQ resistant). The CQ resistant W2 strain was from the Rosenthal Laboratory, (University of California, San Francisco) and is known to be more susceptible to CQ than other W2 strains from elsewhere (Chibale, 2010: Personal communication) The *in vivo* tests were performed in Swiss Webster female mice infected with *P. berghei.*

The β-haematin inhibition activity assay is used to measure the ability of compounds to inhibit the formation β-haematin, the synthetic equivalent of haemozoin. Haemozoin is produced as an end product of heme released during the digestion of the host haemoglobin and this believed to be a detoxificaion pathway in the parasite (Egan, 2008). Blocking this pathway via haemozoin inhibition kills the parasite. Aqueous pyridine (5% v/v, pH 7.5) forms a low-spin complex with haematin but not with β-haematin. The absorbance of the complex obeys Beer's law, making it useful for quantitating hematin concentration in hematin/β-hematin mixtures, allowing compounds to be investigated for inhibition of β-hematin formation (Ncokazi and Egan, 2004).

For both the benzylated and deprotected analogues, β-haematin inhibition activity appeared to improve with increase in number of carbons in the side chain as depicted in Table 3.7. However, no significant difference was observed between compounds with alkyl linker of 4 or 6 carbons i.e. **14** (0.19 equiv.) and **16** (0.16 IC_{50}/equiv). Deprotection was observed to cause a slight decrease in β-haematin inhibition activity e.g. when **10** (0.5 IC_{50}/equiv.) is compared to its deprotected analogue **10a** (1.1 IC_{50}/equiv.). The β-haematin inhibition activity of all compounds was superior to that of CQ.

The antiplasmodial activity seems to increase with increase with increase in number of carbons in the side chain for both benzylated and deprotected analogues. Deprotection is observed to cause a decrease in antiplasmodial activity against the 3D7 strain e.g. comparing **16** (IC_{50} = 0.007μM) to **16a** (IC_{50} = 0.079μM). Three compounds were observed to be more active than CQ i.e. **14**, **16** and its hydrogenchloride salt. Since compounds **16** and **14** had the best β-haematin inhibition and antiplasmodial activity it

implied that their main mode of action could be by haemozoin inhibition. This is further reinforced by the observation that deprotection caused a decline in both β-haematin inhibition and antiplasmodial activity.

3.3.1.2. Antiplasmodial and β-haematin inhibition activities of A series

For both the benzylated and deprotected analogues, β-haematin inhibition activity appears to increase with increase in the number of carbons in the side chain [Table 3.8]. Deprotection was observed to cause a decrease in β-haematin inhibition activity e.g. comparing **9** (0.93 IC_{50}/equiv.) to its deprotected analogue **9a** (2.9 IC_{50}/equiv.), details are also represented in Figure 3.1. The β-haematin inhibition activity of all compounds in the A series was superior to that of CQ except for **9a** (2.9 IC_{50}/equiv.).

Table 3.8: *In vitro antiplasmodial activity against CQ sensitive P. falciparum 3D7 strain and β-haematin inhibition of the A series (maltol derived) double drugs.*

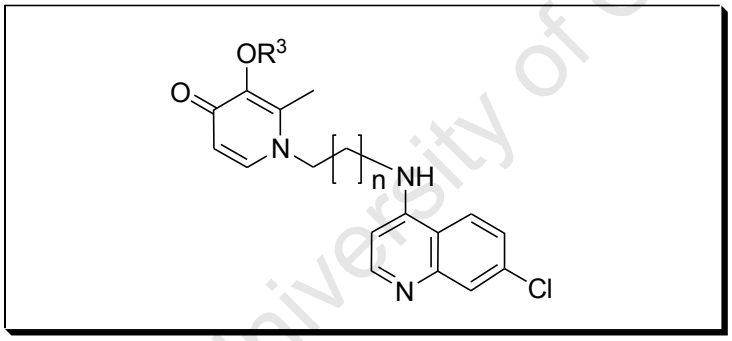

Compound	R^3	n	βHIA IC_{50}/equiv	*P. falciparum* IC_{50} (μM) 3D7
9	Bn	1	0.93	0.49
9a	H	1	2.9	10.8
11	Bn	2	0.49	0.28
11a	H	2	ND	ND
13	Bn	3	0.27	0.05
13a	H	3	0.66	0.03
15	Bn	5	0.25	35.7
15a	H	5	0.47	0.39
CQ			1.9	0.009

β-HIA- *β haematin inhibition activity;*

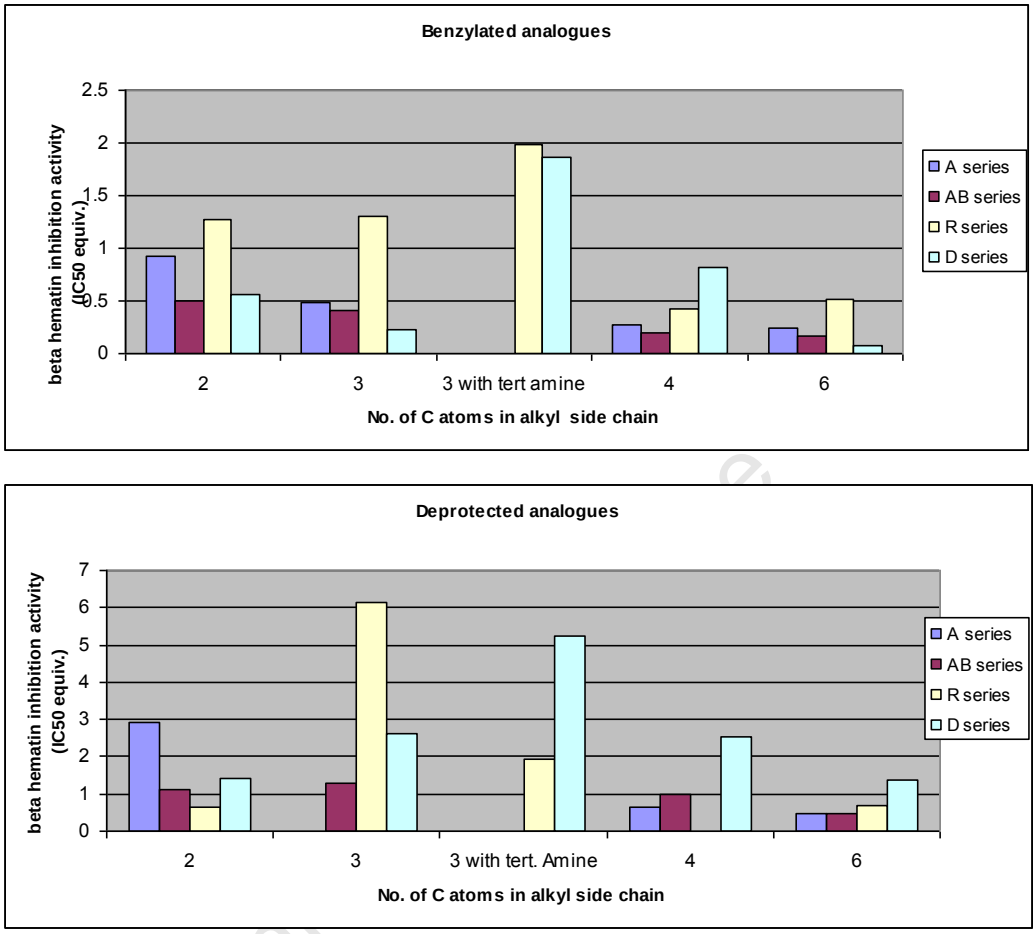

Figure: 3.1 *Comparison of β- haematin inhibition activity among the four series.*

The A and AB series are closely related and data indicates the benzylated AB series to be more potent β-haematin inhibitors than the benzylated A series. R and D series are closely related hence the comparison and it is clear that the benzylated D series are more potent inhibitors than the benzylated R series. Deprotected analogues are seen to be weaker β-haematin inhibitors than the benzylated. No distinct trend was observed in the deprotected analogues. Benzylated analogues with tertiary amine groups were found to be weaker inhibitors than their analogues without a tertiary amino group.

No trend was observed between antiplasmodial activity and lipophilicity in both benzylated and deprotected analogues of the A series. Deprotection was observed to cause either a decrease or an increase in antiplasmodial activity against the 3D7 strain

depending on the compound. Even though deprotection caused a decline in β-haematin inhibition; this did not translate into a drop in antiplasmodial activity for all compounds in the A series. This could mean other mechanisms play part in upholding the antiplasmodial activity of the deprotected compounds despite a decrease in β-haematin inhibition. These mechanisms could be related to iron chelation or access to the site of action or a favorable interaction of the hydroxypyridinone free OH with an intraparasite target.

3.3.1.3. Antiplasmodial and β-haematin inhibition activities of R series

Table 3.9: *In vitro antiplasmodial activity against CQ sensitive P. falciparum 3D7 strain and β-haematin inhibition of kojic derived double drugs (**R** series)*

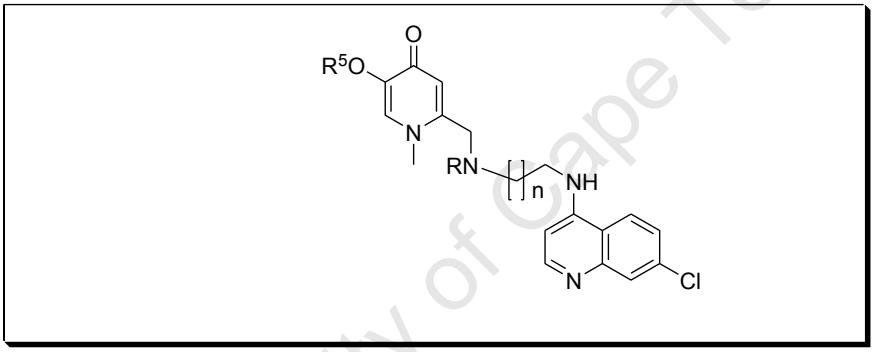

Compound	n	R^5	R	βHIA IC_{50} equiv.	*P. falciparum* IC_{50}(μM) 3D7
23	1	Bn	H	1.27	0.54
23a	1	H	H	0.63	0.58
24	2	Bn	Me	1.98	0.39
24a	2	H	Me	1.95	0.04
25	2	Bn	H	1.30	0.30
25a	2	H	H	6.12	0.12
26	3	Bn	H	0.42	0.24
26a	3	H	H	ND	0.67
27	5	Bn	H	0.51	0.04
27a	5	H	H	0.70	0.19
CQ				1.9	0.016

βHIA: β haematin inhibition activity; ND not determined.

No trend was observed between β-haematin inhibition and lipophilicity in both deprotected and benzylated analogues of the R series (Table 3.9). However, the most

lipophilic compounds (**27** and **27a**) exhibited the best β-haematin inhibition activity. Generally deprotection caused a decrease in β-haematin inhibition activity of these series except for **23**. The β-haematin inhibition activity of all compounds was superior or comparable to that of CQ (1.9 equiv.) except for **25a** (6.12 equiv.). The tertiary amino group was implicated to cause a decrease in the β-haematin inhibition activity for the benzylated analogues e.g. **25** (IC_{50}/equiv. = 1.3) compared to **24** (IC_{50}/equiv. = 1.98). In contrast the tertiary amino group caused an improvement in the β-haematin inhibition activity of the deprotected analogues e.g. **25a** (6.12 equiv.) compared to **24a** (1.95 equiv.), [Fig.3.1].

Antiplasmodial activity was observed to increase with increase in the number of carbons in the side chain. The activity of the R series against the sensitive strain 3D7 was lower than that of chloroquine (IC_{50} = 0.016μM). The most active compounds against 3D7 was **27** (IC_{50} = 0.04μM) and **24a** (IC_{50} = 0.04 μM) and the least potent in the series was **23** (IC_{50} = 0.54μM). Deprotection was observed to cause either a decrease or an increase in antiplasmodial activity against the 3D7 strain depending on the compound. The incorporation of the tertiary amine group caused a drastic improvement in the activity of deprotected analogue but no significant effect on the activity of the benzyl protected analogue. This is clear when the benzylated analogues **24** (IC_{50} = 0.39μM) and **25** (IC_{50} = 0.3μM) are compared and the deprotected analogues **24a** (IC_{50} = 0.04μM) and **25a** (IC_{50} = 0.12μM) are compared. This observation shows the dependence of the antiplasmodial activity of these compounds on β-haematin inhibition. The incorporation of the tertiary amine group in deprotected analogues appeared to cause an increase in β-haematin inhibition activity and as expected it translated into a significant increase in the antiplasmodial activity. In contrast the incorporation of the tertiary amino group in benzylated analogues caused a decline in β-haematin inhibition activity and further translated into a less significant drop in antiplasmodial activity. Structurally it may be hypothesized that the presence of both a tertiary and benzyl group causes steric hindrance thus weakening/interfering with the π-π stacking interactions of the quinoline nucleus or the 3-benzyl group with the heme porphyrin.

3.3.1.4. Antiplasmodial and β-haematin inhibition activities of D series against 3D7

No trend was observed between β-haematin inhibition and increase in the number of carbons in the side chain in both deprotected and benzylated analogues (Table 3.10). Deprotection was found to cause a decrease in both β-haematin inhibition and antiplasmodial activity in all the compounds in the series. Deprotection caused a decline in the β-haematin inhibition for all the D series compounds. The decreased β-haematin inhibition did not translate to lower antiplasmodial activity in all the deprotected analogues. The tertiary amino group was found to cause a decrease in the β-haematin inhibition activity in both the deprotected and benzylated analogues i.e. **29** (0.22 equiv.) when compared to **30** (1.87 equiv.) or **29a** (2.62 equiv.) when compared to **30a** (5.24 equiv.).

Table 3.10: *In vitro antiplasmodial activity against strain against CQ sensitive P. falciparum 3D7 strain and β-haematin inhibition of kojic derived double drugs (**D** series)*

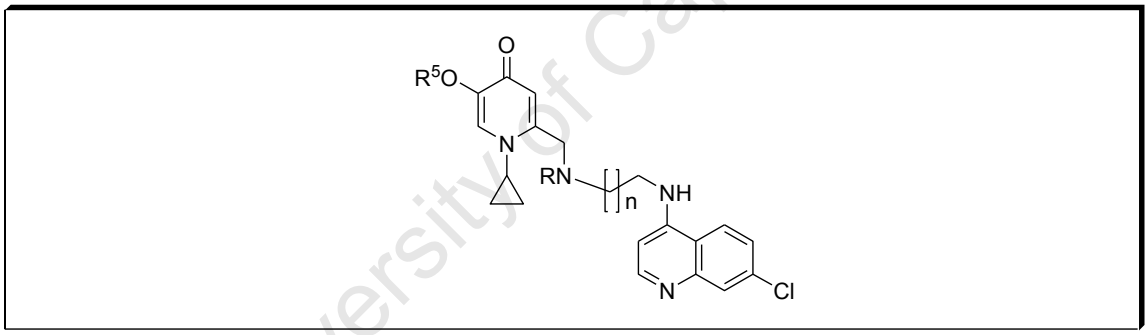

Compound	n	R^5	R	βHIA IC_{50} equiv.	*P. falciparum* IC_{50} (μM)
					3D7
28	1	Bn	H	0.56	0.21
28a	1	H	H	1.41	0.23
29	2	Bn	H	0.22	0.19
29a	2	H	H	2.62	0.20
30	2	Bn	Me	1.87	0.15
30a	2	H	Me	5.24	0.30
31	3	Bn	H	0.82	0.16
31a	3	H	H	2.57	0.17
32	5	Bn	H	0.071	0.004
32a	5	H	H	1.39	0.03
CQ				1.9	0.016

Only compound **32** was more active than CQ against 3D7. The antiplasmodial activity in the 3D7 strain appears to be similar for most compounds except for the compounds with the longest chain (**32** and **32a**). Thus it is postulated that the variation of the side chain begins to have an effect on the antiplasmodial activity when it gets to 6 carbons. The introduction of the chelator group via deprotection did not cause any significant change in the antiplasmodial activity despite causing a significant decrease in the β-haematin inhibition. This may mean the benzyl group is involved in β-haematin inhibition and that the potential contribution of iron chelation towards the activity in the sensitive strain is minimal. In addition it could mean that other factors apart from β-haematin inhibition are important to the overall antiplasmodial potency. Such factors may include enhanced vacuolar accumulation due to the presence of the amino group which may not change on deprotection, or the chelator group may be triggering other mechanisms that compensate activity loss due to decrease in β-haematin inhibition.

The tertiary amino group in the D series appeared to depress the activity in the sensitive strain for the deprotected compounds (**29a** compared to **30a**) possibly due to the decreased β-hematin inhibition caused by the tertiary amine group. Therefore haemozoin inhibition seems to be important for the antiplasmodial activity of these compounds. The tertiary amine group seems to have lesser effect on the antiplasmodial activity of the benzylated analogues in the D series.

3.3.2. *In vitro* antiplasmodial activity in CQ resistant W2 and K1 strain

3.3.2.2.*In vitro* antiplasmodial activity of the AB series in W2 and K1 resistant strains

In both the benzylated and deprotected analogues of the **AB** series, antiplasmodial activity in W2 was found to improve with increase in lipophilicity (Table 3.11). Deprotection was found to enhance activity in the analogues with shorter side chains (less lipophilic analogues) but to cause a decline in the activity of the more lipophilic analogues.

Table 3.11: *In vitro antiplasmodial activity against CQ resistant P. falciparum K1 and W2 strains and β-haematin inhibition of* ***AB*** *series (ethylmaltol derived) double drugs*

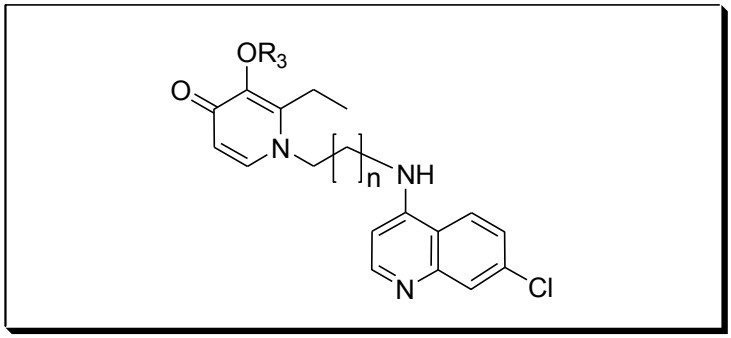

β-HIA- *β haematin inhibition activity;*

Compound	R^3	N	βHIA IC_{50}/equiv.	*P. falciparum* IC_{50} (μM)	
				K1	W2
10	Bn	1	0.50	8.43	2.59
10a	H	1	1.1	0.89	1.24
12	Bn	2	0.41	71.6	2.32
12a	H	2	1.3	0.38	0.54
14	Bn	3	0.19	0.13	0.10
14a	H	3	0.98	0.27	0.16
16	Bn	5	0.16	0.08	0.015
16 HCl salt	Bn	5	ND	0.1	ND
16a	H	5	0.49	0.61	0.09
CQ			1.9	0.44	0.097

In the K1 strain the activity of the benzylated analogues did not show a specific trend. But, the activity of the deprotected analogues increased with increase in lipophilicity. In both resistant K1 and W2 strains, deprotection was found to enhance activity in the analogues with shorter side chains (2 -3 carbon atoms in the side chain) but to cause a decline in activity of analogues with longer side chains (4 – 6 carbon atoms in the side chain)

3.3.2.3. *In vitro* antiplasmodial activity of the A series in resistant W2 and K1 strains

In both the benzylated and deprotected analogues, antiplasmodial activity in W2 was found to improve with increase in lipophilicity (Table 3.12). Deprotection was found to

enhance activity in the analogues with shorter side chains (less lipophilic analogues) but to cause a decline in the more lipophilic analogues. None of the compounds in the A series was more active than CQ in both K1 and 3D7 strains. Compound **13a** (IC_{50} = 0.03μM) had the highest activity in the series against the resistant K1 strain.

In the K1 strain the activity of both the benzylated and deprotected analogues did not show a specific trend. Deprotection was found to enhance activity in K1 except for the least lipophilic compound, **9.**

Table 3.12: *In vitro antiplasmodial activity against CQ resistant P. falciparum K1 and W2 strains and β-haematin inhibition of the A series (maltol derived) double drugs.*

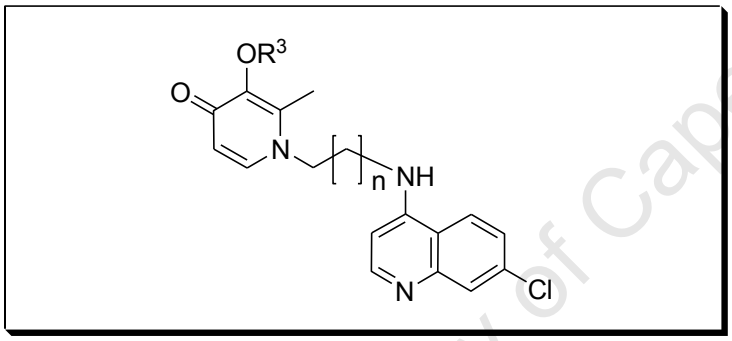

Compound	R^3	N	βHIA IC_{50}/equiv	*P. falciparum* IC_{50} (μM)	
				K1	W2
9	Bn	1	0.93	3.15	9.93
9a	H	1	2.9	32.6	0.28
11	Bn	2	0.49	3.57	2.15
11a	H	2	ND	ND	ND
13	Bn	3	0.27	2.2	1.12
13a	H	3	0.66	0.07	0.08
15	Bn	5	0.25	4.38	0.39
15a	H	5	0.47	0.16	0.07
CQ			1.9	0.44	0.097

β-HIA- *β haematin inhibition activity*

Deprotection is seen to enhance activity in the resistant strain for the series, therefore, it is speculated that, this may be a result of improved access to the site of action, contribution of iron chelation or favorable interaction of the free OH with an intraparasite target.

3.3.2.4. *In vitro* antiplasmodial activity of the R series in resistant K1 strain

In the benzylated analogues antiplasmodial activity was observed to increase with increase in the number of carbons in the side chain, however no trend was observed for the deprotected analogues (Table 3.13). The antiplasmodial activity was found to improve on deprotection for all compounds except **27**. Only two compounds were potent more than CQ and coincidentally they were the deprotected analogues (**24a** and **26a)**.

Table 3.13: *In vitro antiplasmodial activity of kojic derived double drugs (**R** series) against CQ resistant P. falciparum K1 strain and β-haematin inhibition activity*

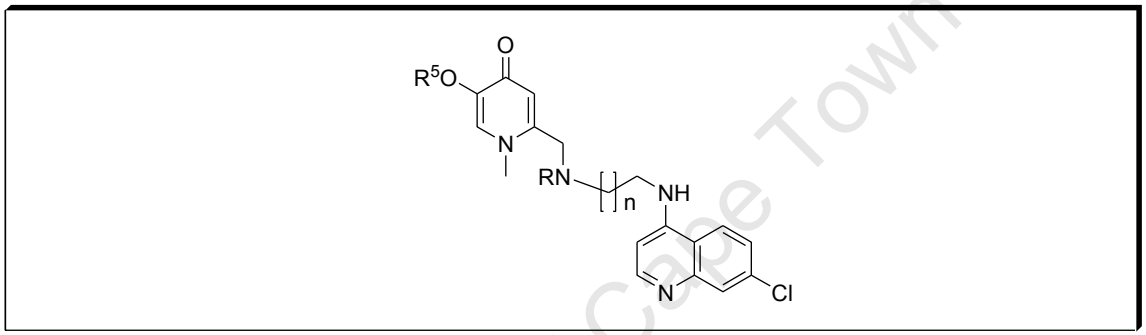

Compound	n	R^5	R	βHIA IC_{50} equiv.	*P. falciparum* IC_{50}(μM)
					K1
23	1	Bn	H	1.27	2.56
23a	1	H	H	0.63	1.75
24	2	Bn	Me	1.98	0.15
24a	2	H	Me	1.95	0.04
25	2	Bn	H	1.30	2.08
25a	2	H	H	6.12	0.27
26	3	Bn	H	0.42	1.71
26a	3	H	H	ND	0.07
27	5	Bn	H	0.51	0.32
27a	5	H	H	0.70	0.32
CQ				1.9	0.20

βHIA: β-haematin inhibition activity; ND not determined.

The introduction of a tertiary amine group enhanced the activity of the **R** series against resistant strain. This is clear when compound **24** (IC_{50} = 0.15μM) is compared to **25** (IC_{50} = 2.08 μM; IC_{50}) or **24a** (IC_{50} = 0.04 μM) to **25a** (IC_{50} = 0.12 μM).

In the previous section it was observed that decline in β haematin inhibition activity for analogues with tertiary amine group caused a decline activity in the sensitive 3D7 strain. However, this did not translate into a decrease in activity in the K1 strain. It shows that other factors may be involved i.e. accumulation in the FV which is important in counteracting the drug export effect of the mutant PfCRT in the resistant strain. It is assumed that accumulation is enhanced by the presence of the tertiary amino group.

All the other compounds in the R series (except **25a**) were stronger β-haematin inhibitors than **24a** but the latter had superior antiplasmodial activity to all. The most potent β-haematin inhibitor (**26**) in the R series was not the most potent antiplasmodial agent. It may be assumed that other factors, other than β-haematin inhibition, are affecting the antiplasmodial activity of **24a**. Probably the accumulation of this compound in the parasitic food vacuole is enhanced by the presence of the tertiary amino group. Furthermore compounds **24** and **24a** exhibited higher antiplasmodial activity in K1 than related analogues that lack the tertiary amine group (**25** and **25a**). This shows that the tertiary amine group in **24** and **24a** enhanced the antiplasmodial activity more than the secondary amine group in **25** and **25a**.

Table 3.14: *In vitro antiplasmodial activity of kojic derived double drugs (**D** series) against CQ resistant P. falciparum K1 strain and β-haematin inhibition activity*

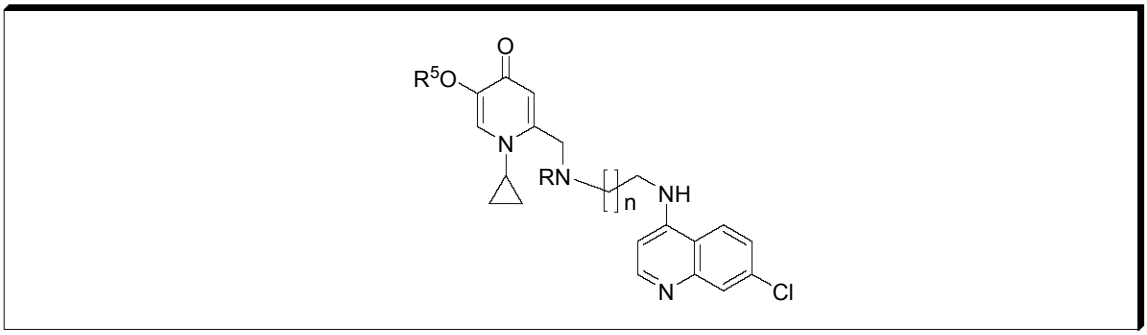

Compound	n	R^5	R	βHIA IC_{50} equiv.	*P. falciparum* IC_{50} (μM)
					K1
28	1	Bn	H	0.56	1.45
28a	1	H	H	1.41	0.36
29	2	Bn	H	0.22	0.27
29a	2	H	H	2.62	0.72
30	2	Bn	Me	1.87	0.97
30a	2	H	Me	5.24	0.46
31	3	Bn	H	0.82	0.85
31a	3	H	H	2.57	0.36
32	5	Bn	H	0.071	0.03
32a	5	H	H	1.39	0.08
CQ				1.9	0.20

3.3.2.5. *In vitro* antiplasmodial activity of the D series in K1 resistant strains

No trend was observed for the variation of the length of the side chain and antiplasmodial activity in both benzylated and deprotected analogues. None of the compounds was as active as CQ except **32** which happen to have the longest side chain (with greatest number of carbons in the side chain). Deprotection caused an increase or a decrease in antiplasmodial activity depending on the compound. Incorporation of the tertiary amine group suppressed the antiplasmodial activity against K1 in the protected analogue i.e. **30** (IC_{50} = 0.97 μM) compared to **29** (IC_{50} = 0.27 μM). Since this was accompanied by a decline in β-hematin inhibition, it may be hypothesized that β-hematin inhibition is an important mode of action of this compounds. The tertiary amine group caused a slight increase in antiplasmodial activity against K1 in the deprotected analogue i.e. **30a** (IC_{50} = 0.46 μM) compared to **29a** (IC_{50} = 0.72 μM)**.**

3.3.2.6. Resistance Indices of compounds from the R, D, A and AB series

Table 3.15*: Resistance indices of compounds in A and AB series*

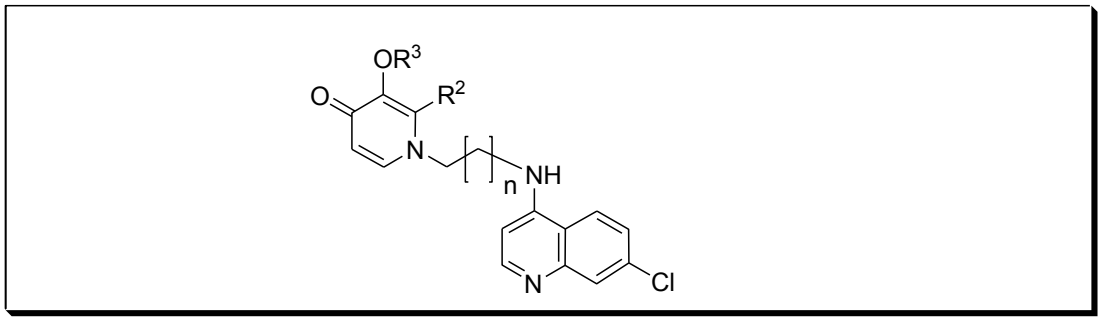

Compound	R^2	R^3	n	K1/3D7	W2/3D7
10	Et	Bn	1	8.9	2.7
10a	Et	H	1	2.2	3.1
12	Et	Bn	2	596	19.3
12a	Et	H	2	3.2	4.5
14	Et	Bn	3	32.5	25
14a	Et	H	3	5.4	3.2
16	Et	Bn	3	11.4	2.1
16. HCl salt	Et	Bn	5	12.5	ND
16a	Et	H	5	7.7	1.1
9	Me	Bn	1	6.4	2.0
9a	Me	H	1	3.0	0.026
11	Me	Bn	2	12.8	7.7
13	Me	Bn	2	44.0	22.4
13a	Me	H	3	2.3	2.7
15	Me	Bn	3	0.12	0.01
15a	Me	H	5	0.4	0.18
CQ				48.9	10.8

In the same laboratory, series A and AB were tested in one assay while the R and D series were tested in a different one. The $RI^{K1/3D7}$ of the standard drug CQ from the two assays was different i.e. 12.2 versus 48.9. (Tables 3.15 and 3.16) Therefore the A and B series are discussed separately from the D and R series.

Most compounds exhibited lower resistance indices than CQ implying that they have potential to act against resistant parasites. The only exceptions were **12, 13,** and **14**.

Table 3.16: *Resistance indices of compounds in the R and D series*

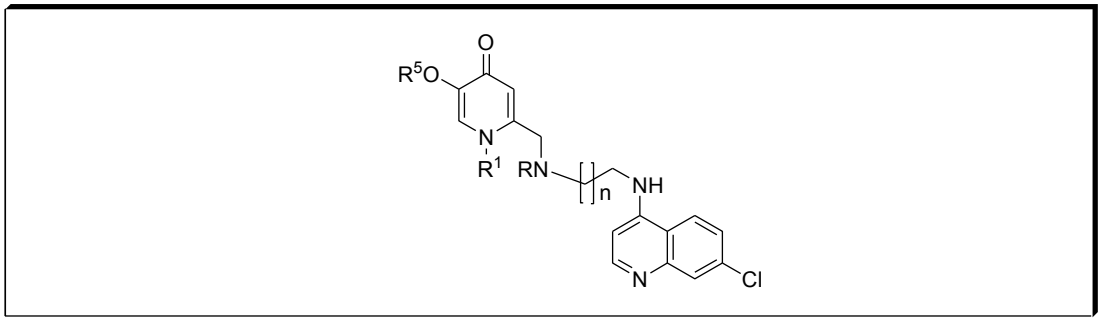

Compound	R^1	R^5	R	N	Resistance index K1/3D7
23	Me	Bn	H	1	4.7
23a	Me	H	H	1	3.0
24	Me	Bn	Me	2	0.4
24a	Me	H	Me	2	1.0
25	Me	Bn	H	2	6.9
25a	Me	H	H	2	2.2
26	Me	Bn	H	3	7.1
26a	Me	H	H	3	0.1
27	Me	Bn	H	5	8
27a	Me	H	H	5	1.7
28	cyclpropyl	Bn	H	1	7.2
28a	cyclpropyl	H	H	1	1.6
29	cyclpropyl	Bn	H	2	1.4
29a	cyclpropyl	H	H	2	3.6
30	cyclpropyl	Bn	Me	2	6.5
30a	cyclpropyl	H	Me	2	1.5
31	cyclpropyl	Bn	H	3	5.3
31a	cyclpropyl	H	H	3	2.1
32	cyclpropyl	Bn	H	5	7.5
32a	cyclpropyl	H	H	5	2.7
CQ					12.2

Generally deprotection was found to lower the resistance indices of most of the compounds. The A series (less lipophilic) had better resistance indices than the AB series (lipophilic), e.g. comparing **10** ($RI^{W2/3D7}$ = 8.9; $RI^{K1/3D7}$ = 2.7) to **9** ($RI^{W2/3D7}$ = 6.4; $RI^{K1/3D7}$ = 2.0) and given that the AB analogues are better β-haematin inhibitors than their A analogues it implies that potency against CQ resistant strains is not dependant on one factor but a combination.

All the compounds in the R and D series had lower RIs, usually much lower RIs than CQ imply good potential to overcome resistant parasites. The general trend indicated that the deprotected analogues had lower RI values than their benzylated analogues. The introduction of the tertiary amine group improves the RI in the R series but not in the D series. The replacement of the N-cyclopropyl group in the D series with a methyl group enhances selectivity for the resistant strain. Tentatively it is proposed that a less bulky N-alkyl group on the pyridinone and a tertiary amine group on the side chain act in concert to confer potency against the resistant strain.

3.3.3. Investigation of the contribution of complexation to antiplasmodial activity

Table 3.17: *Antiplasmodial activity of the double drugs and their metal (III) complexes*

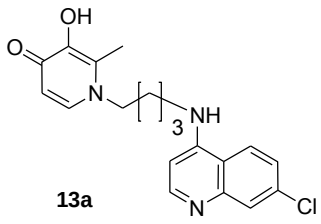

13a

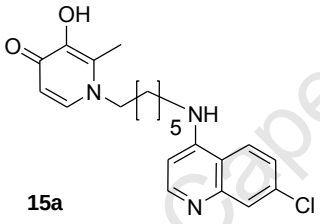

15a

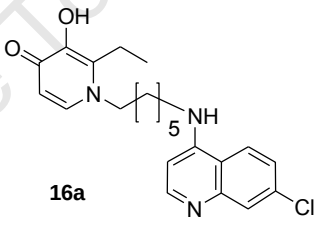

16a

13c: ML_3 M= Fe^{3+} , L = 13a

13d: ML_3 M= Ga^{3+} , L = 13a

15c: ML_3 M= Fe^{3+} , L = 15a

15d: ML_3 M= Ga^{3+} , L = 15a

15e: $ML_2NO_3H_2O$, M= Ga^{3+} , L = 15a

16c: ML_3 M= Ga^{3+}, L =16a

Compound	*P. falciparum* IC_{50} (μM)		Resistance Index
	D10	Dd2	Dd2/D10
13a	0.75	0.53	0.70
13c	0.73	0.6	0.8
13d	0.61	0.34	0.5
15 a	0.49	0.44	0.9
15c	0.26	0.24	0.9
15d	0.26	0.28	1.1
15e	0.44	0.31	0.7
16a	0.15	0.12	0.78
16c	0.48	0.38	0.8
CQ	0.0155	0.194	12.5

Further work was conducted to confirm the effect of complexation on the antiplasmodial activity of these compounds by evaluating the antiplasmodial activity of the gallium (III) and iron (III) complexes of the deprotected analogues in sensitive D10 and resistant Dd2 strains (Table 3.17).

The complexes and their ligands were found to be as active as CQ in the resistant Dd2 strain, but less active than CQ (IC_{50} = 0.0155μM) in the sensitive strain D10, except for compound **16a** (IC_{50} = 0.12 μM). In most cases there was no significant difference between the antiplasmodial activity or the resistance index of a ligand and that of its complex irrespective of the metal core.

In the previous section (3.1.2), it was observed that complexation with gallium greatly reduced the antiplasmodial activity of *N*-alkyl-3,4-hydroxypyridinones, but in this case, the complexation of the aminoquinoline-3,4-HPO conjugates with gallium and iron (III) causes no significant change in antiplasmodial activity. This implies that unlike the *N*-alkyl-3,4-HPOs, potential iron chelation is not the major mode of antimalarial activity for these conjugates. Therefore, other mechanisms predominate even after complexation. Hemozoin inhibition could be one of the mechanisms given the presence of the 7-chloroquinolinyl substructure in these hybrids. It may be concluded that complexation with gallium (III) or iron (III) causes insignificant change in the antiplasmodial activity of these double drug ligands. This casts doubt on whether the presumed iron chelation contributes significantly to the antiplasmodial activity of these compounds.

3.3.4. Involvement of the benzyl group in the β-haematin inhibition

The benzylated double drugs showed better β-haematin inhibition activity than the deprotected analogues. Furthermore, the replacement of the benzyl protecting group with a methoxy group led to a significant decrease in the β-haematin inhibition activity as depicted for related compounds in Table 3.18. This implies involvement of the benzyl group involvement in the inhibition of β-haematin formation probably via the aromatic group of the 3-benzyl participating in a π-π stacking type of interaction with the heme porphyrin.

From the data set in Table 3.18, the benzylated analogues were observed to be better antiplasmodials than the 3-methoxylated analogues against W2. The factors contributing to this could be the superior β-haematin inhibition activity exhibited by the benzylated analogues as well as their high lipophilicity (see clogP and logD values in Table 2.6), enabling them to penetrate cellular membranes easily. This data in itself strongly supports the role of β-haematin inhibition in the mode of action for these hybrid molecules.

Table 3.18: *Comparing the in vitro antiplasmodial activity of the 3-methoxy and 3-benzyl analogues*

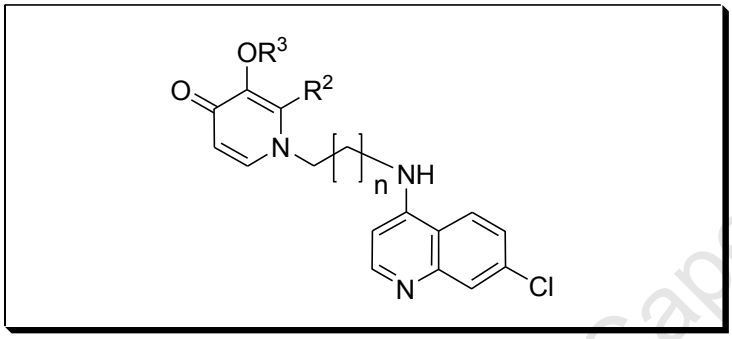

Compound	R^2	N	R^3	B-HIA IC_{50} equiv	*P. falciparum* IC_{50} (μM)		
					3D7	K1	W2
13	Me	3	Bn	0.27	0.05	2.2	0.05
13b	Me	3	Me	0.75	0.07	0.22	0.76
14	Et	3	Bn	0.19	0.004	0.13	0.09
14b	Et	3	Me	1.71	ND	ND	0.21
15	Me	5	Bn	0.25	35.7	4.38	0.08
15b	Me	5	Me	1.07	0.13	2.8	0.09
16	Et	5	Bn	0.16	0.008	0.1	0.07
16b	Et	5	Me	0.47	ND	ND	0.22
CQ				1.9	0.009	0.44	0.097

Table 3.19: *Comparing some potent compounds*

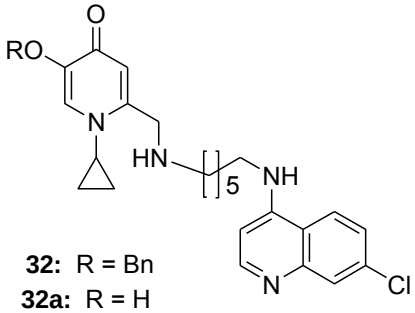

32: R = Bn
32a: R = H

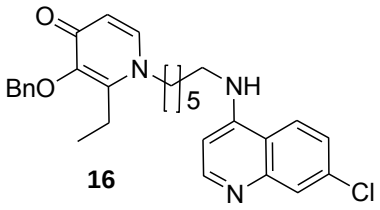

16

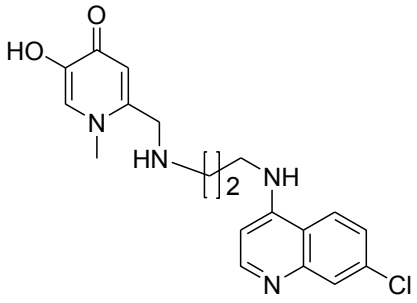

24a

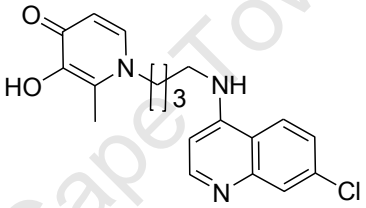

13a

Compound	clogP[a]	pKa[a] of side chain amine	B-HIA IC_{50}/equiv.	*P. falciparum* IC_{50} (μM)		RI Resistance Index K1/3D7
				3D7	K1	
16	6.2	-	0.16	0.007	0.08	11.4
32	5.3	5.47	0.07	0.004	0.03	7.5
32 a	3.6	8.34	1.3	0.03	0.08	2.7
13a	3.0	-	0.66	0.03	0.07	2.3
24a	2.1	6.78	1.95	0.04	0.04	1.0
CQ			1.9	0.013* *(0.009 or 0.016)*	0.32* *(0.44 or 0.20)*	24

clog P[a] and pKa[a] predicted from Volsurf modeller. *Mean values from two assays.

3.3.5 Antiplasmodial activities of the most potent conjugates

The most potent antiplasmodial compounds from the four series i.e. **16**, **32**, **32a**, **13a** and **24a** were compared as illustrated in Table 3.15. This group consists of compounds with a varied number of carbon atoms (3C, 4C and 6C) and the conjugates with 6C in the side chain exhibited stronger antiplasmodial activity against the sensitive strain. However, their activity against the resistant strain was comparable to that of the short side chain conjugates.

The β-haematin inhibition activity of all the compounds was better or similar to that of chloroquine (IC_{50}/equiv = 1.9). On this basis it was hypothesized that, to retain or enhance antiplasmodial activity in this type of compound, β-haematin inhibition activity seems necessary especially for activity against the sensitive strain e.g. the **32** and **16**, the two compounds have the strongest inhibition of β-haematin and the best potency in the sensitive strain.

The introduction of a secondary amine group into **32** appeared to cause the increase β-haematin inhibition and antiplasmodial activities in both strains by 2 fold. Note that this change can not only be attributed to the amino group since several structural differences exist between **16** and **32**. Even though deprotection was seen to cause a decrease in activity in the sensitive strains the consequence were improved resistance indices. Compounds **32, 32a** and **16** were more active in the sensitive strain than the resistant strain implying potential for cross resistance with CQ. Only compound **24** was equipotent in both the resistant and sensitive strains hence can be a good template on which structural modifications may be performed on to improve activity in both resistant and sensitive strains.

Compounds **13a** and **24a** appear to be the best candidates for further development since they have the lowest resistance indices. Structurally, these two molecules contain an iron chelating group and/or a tertiary amine group in the side chain. Presumably the 3,4-HPO chelator moiety enhances activity for the resistant strain possibly via some favourable interaction of the unprotected OH with intraparasitic target(s). The tertiary amino group

may be enhancing drug accumulation in the food vacuole of the resistant strains as discussed earlier. Therefore, it is hypothesized that incorporation of the iron chelator group or the amino group or both in this type of antiplasmodial compounds may enhance activity against resistant strains.

Considering this data, it seemed that lipophilicity is not the only factor involved in overcoming drug resistant malaria parasites in this class of compounds. An optimum balance of lipophilicity and basicity are essential in addition to the type of N-1 alkyl group on the pyridinone moiety.

3.3.6. Antiplasmodial activity of the molecular fragments of the A/AB double drugs

The synthetic intermediates i.e. 7-chloroquinolinyl-4-diaminoalkanes and benzylated pyranones were tested for activity against W2. The rationale was to confirm which fragment of the conjugates contributes more to the activity and whether the conjugation enhances antiplasmodial activity or not.

The three 7-chloroquinolinyl-4-diaminoalkane intermediates showed similar antiplasmodial potency against the CQR strain W2 except for the intermediate **5** and their activity was close to that of chloroquine (Table 3.20). The two benzylated pyranone intermediates were inactive against W2 at the maximum concentration (20μM) tested (Table 3.21).

The IC_{50}^{W2} values of the benzylated double drugs were in the range of 9.92 - 0.015μM (Tables 3.7 and 3.8). This implies that conjugation via covalent bonding to make the double drugs resulted in an additive /synergistic effect unlike the antagonism observed in the combinations (section 3.1.2). This is true if one considers the antiplasmodial activity of the fragments of one of the most active compounds, **16**, it is clear that their respective activities have been enhanced from 0.16μM (for **8**) or >20μM (for **2**) to 0.015μM (for **16**)

Table 3.20: *Antiplasmodial activity of aminoquinoline intermediates*

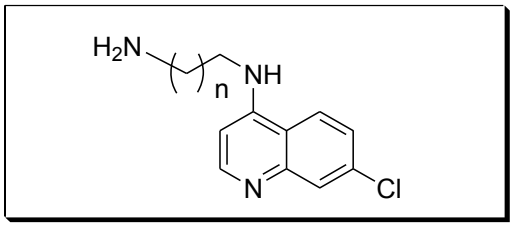

Intermediate/fragment	n	*P.falciparum* IC_{50} (μM) W2
4	1	0.15
5	2	2.01
7	3	0.14
8	5	0.16
CQ		0.097

Table 3.21: *Antiplasmodial activity of benzylated pyranone intermediates*

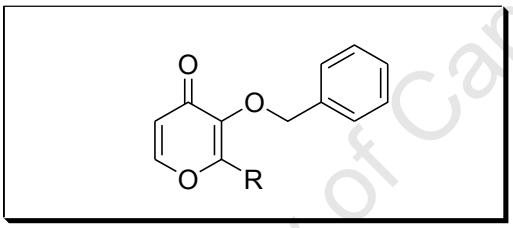

Intermediate/fragment	R^2	*P. .falciparum* IC_{50} (μM) W2
1	Me	>20
2	Et	>20
CQ		0.097

The combination of **1h,** a benzylated N-alkyl-3,4-HPO with CQ-diphosphate, resulted in a predominantly antagonistic interaction (section 3.1.2), whereas the conjugation of a benzylated 3,4-HPO (**1**) and a quinoline (**8**) resulted in synergy. Therefore, the interactions resulting from the individual combination of two therapeutic agents, each as a single entity may not be the only criterion for deciding on whether to conjugate the two or not.

3.3.7 Quantitaive correlations involving β-haematin inhibition and lipophilicity

The lipophilicity of 3,4-HPOs is influenced by the N-1 alkyl group and this is expected to affect the antiplasmodial potency. In addition, it was observed that more lipophilic double drugs displayed better antiplasmodial and β-haematin inhibition activity. To further probe these relationships, correlations between lipophilicity (clog P), and β-haematin inhibition; or antiplasmodial activity were measured. Correlations were only observed for the A/AB series compounds.

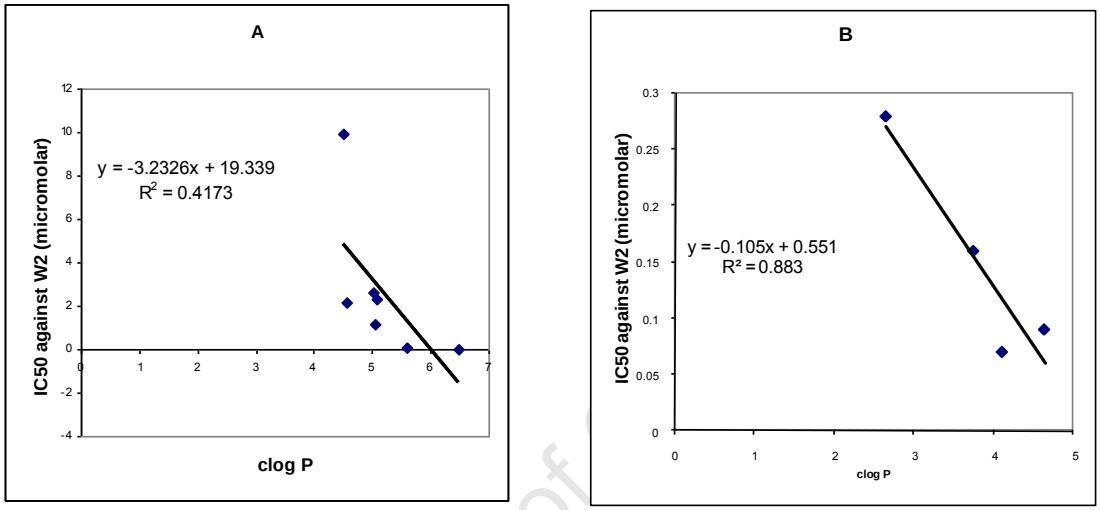

Figure 3.2: *Correlation between Lipophilicy (clog P) and in vitro antiplasmodial activity against W2 parasites for benzylated (A) and deprotected (B) compounds.*

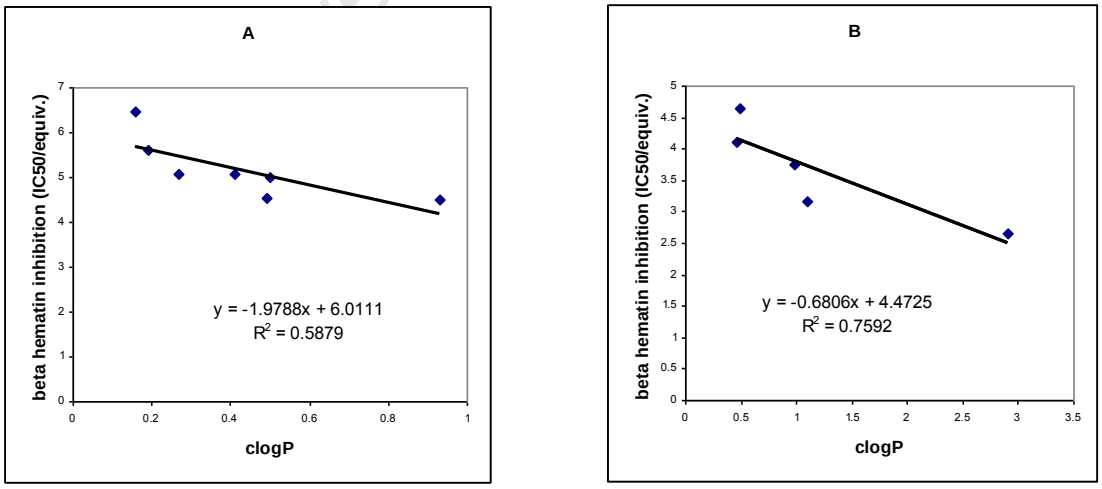

Figure 3.3: *Correlation between β-haematin inhibition and lipophilicity (predicted log P) of benzylated (A) and deprotected double drugs (B).*

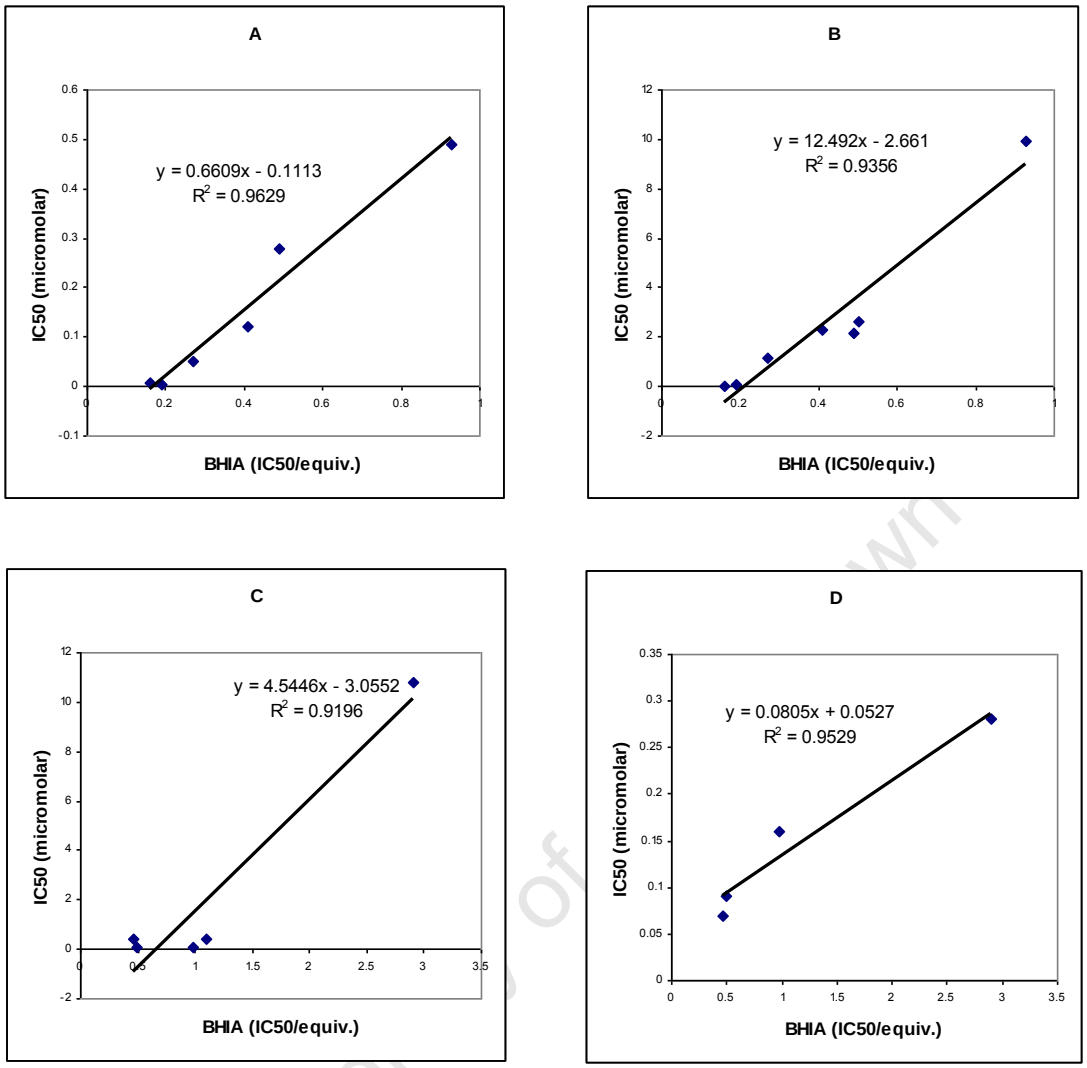

Figure 3.4: *Correlation between β-haematin inhibition activity and antiplasmodial activity for the benzylated series A- against 3D7 & B- against W2 strains and deprotected analogues C- against 3D7 & D- against W2.*

All the double drugs in the **A** and **AB** series were combined together in the analysis and the correlation between their lipophilicity and *in vitro* antiplasmodial activity in 3D7, W2 and K1 were determined. The correlations were not significant in all the resistant and sensitive strains of *P. falciparum*. Further determinations for the separate groups, i.e. protected (nonchelating) and deprotected (chelating), was considered (Fig. 3.2). Significant correlation between lipophilicity and antiplasmodial activity was only observed in the W2 resistant strain for deprotected analogues (R^2=0.41) and benzylated analogues (R^2=0.88). as illustrated in Figure 3.2. The significant correlation in the deprotected compounds is consistent with literature reports indicating that lipophilicity

determines antiplasmodial activity of 3,4-HPOs in resistant strains except that it is single point dependant.

The correlations between β-haematin inhibition and clog P were determined and significant correlations were observed for benzylated ($R^2 = 0.59$) or deprotected ($IC_{50} = 0.76$) analogues (Fig.3.3). This confirmed that lipophilic molecules have the potential of being good β-haematin inhibitors. The data shows β-haematin inhibition of these compounds is related to lipophilicity. It could imply that β-haematin inhibition contributes significantly towards the antiplasmodial activity of these compounds whether the chelator group is protected or not. β-haematin inhibition is considered a major mode of action for quinoline antiplasmodials hence it was important to consider the correlation between β-haematin inhibition and antiplasmodial activity (Fig. 3.4).

Strong correlations were observed between β-haematin inhibition and antiplasmodial activity in 3D7 ($R^2 = 0.96$) and W2 ($R^2 = 0.93$) for the benzylated analogues. At first sight, the correlation also appears to be strong in 3D7 ($R^2 = 0.92$) and W2 ($R^2 = 0.95$) for the deprotected analogues. However, if the data point at (2.9, 10.8) is omitted in the determination of the correlation for deprotected analogues in 3D7, the R^2 value drops to 0.045, strongly suggesting that the correlation is fortuitous. However, the other significant correlations observed may be used as a basis to conclude that β-haematin inhibition is a major mode of action of these conjugates in both resistant and sensitive strains at least for the protected analogues.

For the R series, no significant correlation was observed between the clog P and β-haematin inhibition activity or antiplasmodial activity, and between β-haematin inhibition and antiplasmodial activity for the group as a whole. Even after separating the deprotected and the benzylated compounds, no significant correlations were observed. A similar picture was observed in the D series. This could mean that after the incorporation of the amino groups more factors come into determining the antiplasmodial activity i.e. access to the target which is affected by both lipophilicity and accumulation through pH trapping.

3.3.8. General conclusion on *in vitro* antiplasmodial activity and β-haematin inhibition activity

β-haematin inhibition was found to be an important mode of antiplasmodial action for many if not all of the hybrid molecules. Strong correlations were observed between β-haematin inhibition and antiplasmodial activity for the benzylated conjugates in the A and AB series.

The β-haematin inhibition activities were determined in a cell free assay whereas antiplasmodial activity assays involved a medium containing cells; therefore, good β-haematin inhibition activity did not necessarily translate into good antiplasmodial activity because the effect entirely depends on ability of the conjugates to access the intracellular target. In order to exert optimal antiplasmodial activity, the test compounds have to access their intracellular targets e.g heme. Access to heme is dependent on lipophilicity and the ability to accumulate in the parasitic food vacuole (especially for the resistant strain) through pH trapping. The β-haematin inhibition activity of these hybrids may be attributed to the quinoline nucleus and not the pyridinone substructure since the N-alkyl-3,4-HPOs did not show any inhibition of β-haematin.

Strong haematin inhibition activity was observed to translate into strong antiplasmodial activity in the sensitive 3D7 strain more than in the resistant K1 strain. The explanation to this could be that the mutant PfCRT in the resistant strain was involved in exporting the test compounds out of the FV thus lowering the concentration of the drug at the target site.

Blocking of the iron chelator group in itself was observed not to cause significant antiplasmodial activity this is seen in the dismal potency of the N-alkyl-3,4-HPOs (IC_{50}^{K1} >1.8μM; IC_{50}^{3D7} > 2.38μM) as well as in the assays involving protected or pre-complexed hybrid molecules. It is important to note that deprotection or availability of the chelator moiety seemed to enhance activity in the resistant strains.

3.4. *In vivo* antimalarial activity of 16a (13AB1) and 16. HCl salt (13AB.2HCl)

The dihydrogen chloride salt of compound **16** [**16.2HCl** or 13AB 2HCl] showed the best *in vitro* antiplasmodial potency and was selected for *in vivo* testing. Its deprotected analogue **16a** (13AB1) was also tested to investigate the effect of chelation on *in vivo* antiplasmodial activity. The preliminary findings indicated that iron chelation was not effective against an animal model of malaria. Compound **32** which showed good potency *in vitro* against resistant and sensitive strains of *P. falciparum* is awaiting *in vivo* tests.

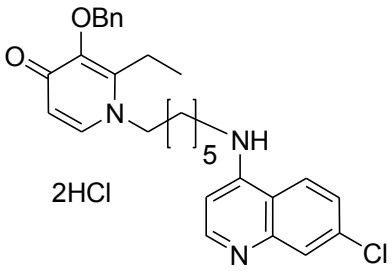

16 .HCl salt (13AB.2HCl)

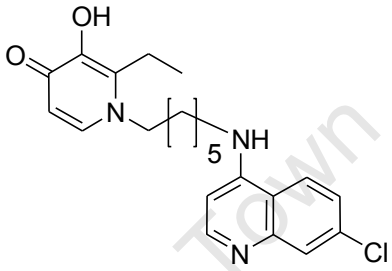

16a (13AB1)

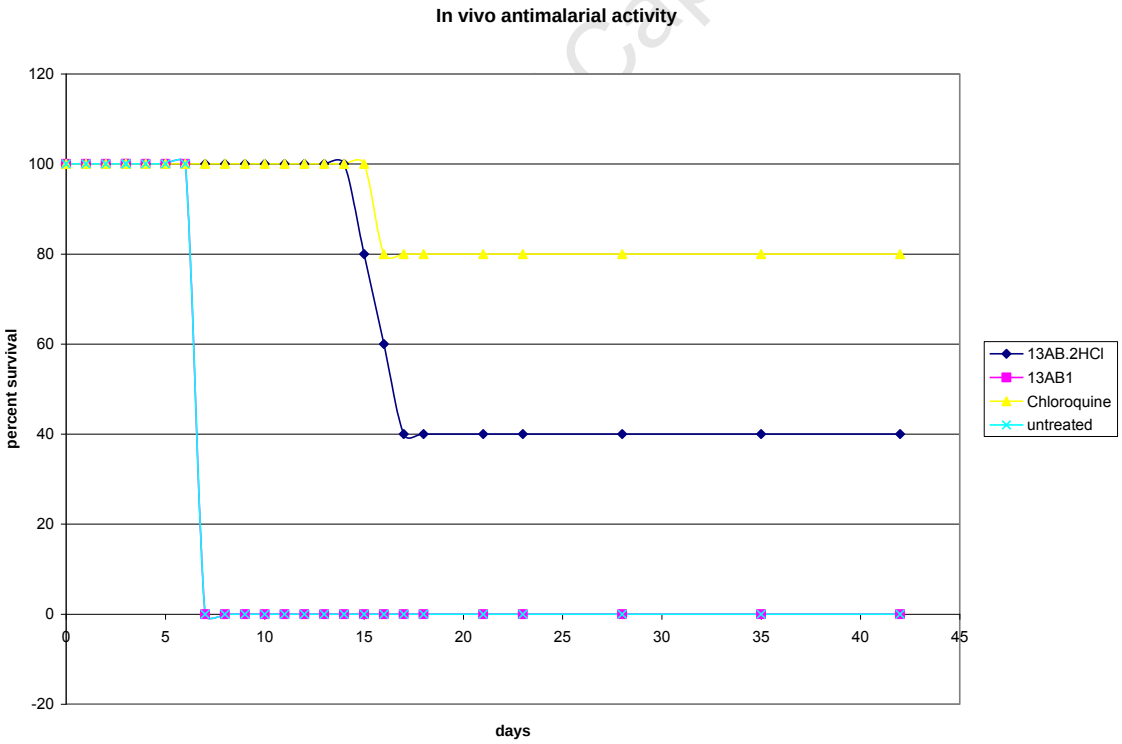

Figure 3.5: *In vivo antiplasmodial activity of* ***16a*** *(13AB1) and* ***16. HCl salt*** *(13AB2HCl)*

The assay involved intra peritoneal administration of the drugs **16. HCl salt** and **16a** to Swiss Webster female mice and chloroquine was used as the standard. Dosage was IP 2x day 50mg/kg and the drugs were dissolved in 5% DMSO/ 5% Cremophor EL in saline.

Considering the data represented in Figure 3.5, the group that was treated with **16a** showed a similar pattern as the untreated group and on day 7 no mice survived in both groups. The mice that were treated with compound **16. HCl salt** behaved like the mice treated with CQ but the percent survival in the presence of the former was lower (40%) compared to chloroquine (80%).

The poor performance of **16a** in the *in vivo* assay could be attributed to the lack of susceptibility of the *P. berghei* to the test compound, absence of the target and poor absorption. Even though **16** and **16a** showed good *in vitro* activity against *P. falciparum*, *In vitro* efficacy against human malaria causing *P. falciparum* does not always translate to *in vivo* efficacy against the rodent malaria causative agent *P. berghei* (S. Wittlin, 2010-Personal Communication). *P. berghei* in mice lacks hemozoin because mice are not their natural hosts (Peters *et al.,* 1986), and since the test compounds **16a** and **16. HCl salt** were confirmed to target haemozoin/β-haematin formation it may be assumed that one of the main targets of these compounds was absent in the test organism. There is a need to confirm the susceptibility of the *P. berghei* to the test compounds by testing the drugs against *in vitro P. berghei* or by use of the humanized SCID mouse model to provide an explanation for the lack of a PK/PD relationship in this case. It may not be assumed that since the test compounds are 4-aminoquinolines then the *P. berghei* parasite will be susceptible to them as it is to chloroquine.

Intra peritoneal (i.p) administration is known to favor the absorption of more lipophilic drugs (Kerns and Di, 2008), since **16** and **16a** have a log D of 6.00 and 4.05 respectively, one would expect **16** absorption to be more favorable than that of **16a** in an i.p administration. Tentatively, it may be hypothesized that **16a** was not effectively absorbed and therefore did not access its targets.

3.7 Antiplasmodial and β-haematin inhibition activity of catecholate double drug 37

The siderophore **36** (IC_{50}/equiv.=5.09), exhibited a lower β-haematin inhibition activity than the siderophore-4-aminoquinoline hybrid **37** (IC_{50}/equiv. =1.04), this 5 fold difference is mainly due to the influence of the 7-chloro-4-aminoquinolinyl moiety which is known to be responsible for β-haematin inhibition in quinoline antiplasmodials (Fig. 3.6).

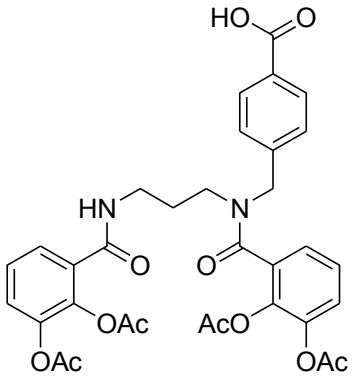

36

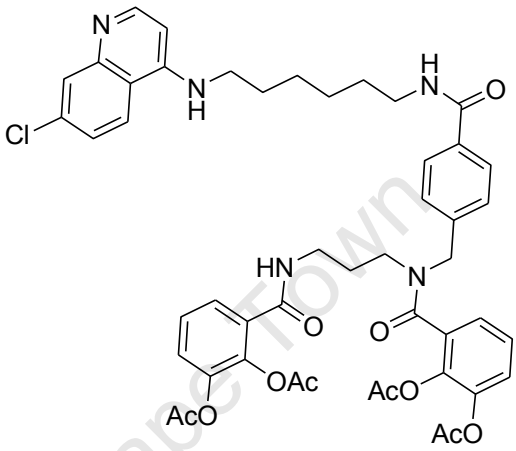

37

Figure 3.6: *Structures of compound **36** and **37***

Table3.22. *In vitro antiplasmodial activity and haematin inhibition activity of catecholates and related D and AB series analogues*

Compound	*BHIA IC_{50}/equiv.*	*P.falciparum. IC_{50} µM against D10*
37	1.04	3.17
36	5.09	29.6
32	0.07	0.15
16	0.16	0.05
16. HCl salt	-	0.22
CQ	1.95	0.04

BHIA β-haematin inhibition activity

The antiplasmodial acivities of the **36** and **37** were evaluated along side related double drugs against CQ sensitive D10 strain (TableS). Compound **37** (IC_{50} = 3.17µM) was found to be about 6 times more potent than **36** (IC_{50} = 29.6µM) this may imply the main mode of activity of the catecholate double drug is via haemozoin inhibition or by mechanisms related to the quinoline substructure.

The β-haematin inhibition activity **37** was 10 times lower than other structurally related 4-aminoquinoline-3,4-HPO double drugs i.e. **16** (IC_{50}/equiv.=0.16; IC_{50}^{D10} = 0.05μM) and **32** (IC_{50}/equiv.= 0.07; IC_{50}^{D10} = 0.15μM) and this was reflected in their antiplasmodial activity i.e. they were more potent. This observation therefore reinforces the importance of hemozoin inhibition in antiplasmodial potency of aminoquinoline based drugs.

3.8. *In vitro* Toxicity Assay

3.8.1. Cytotoxicity

The *in vitro* selectivity index (SI) of these compounds for the parasite over host cells was determined using the KB human nasopharynx carcinoma cell line and the *Plasmodium falciparum* 3D7 and K1 isolates (Table 3.23).

Table 3.23: *In vitro toxicity data; Cytoxicity and CYP3A4 inhibition*

Compound	KB µg/ml	KB µM	3D7 µM	K1 µM	SI KB/3D7	SI KB/K1	CYP3A4 IC_{50} µM
9	22.5	53.7	0.49	3.15	109	17	7.3
9a	ND	ND	10.8	32.6	ND	ND	5.87
10	23.3	52.9	8.43	53.6	6.3	1.0	3.07
10a	ND	ND	0.4	0.89	ND	ND	12.34
11	28.9	66.6	3.57	66.5	18.7	1.0	1.77
11a	ND	ND	ND	ND	ND	ND	14.87
12	6.6	14.7	71.6	14.8	0.21	1.0	1.18
12a	19.5	45.3	0.384	45.4	117	1.0	ND
13	53.2	118.9	0.051	2.17	2331	54.7	1.0
13a	66.3	154.1	0.03	0.07	5136	2201	ND
14	4.16	9.0	0.004	0.13	2250	69	1.21
14a	28.3	63.8	0.054	0.27	1181	236	6.52
15	75.3	158.2	4.38	158.2	36	1.0	2.25
15a	1.38	3.0	0.161	3.2	18	1.0	4.29
16	1.86	3.8	0.011	3.79	345	1.0	1.36
16a	17.7	37.6	0.079	0.61	475.9	61.6	4.04
16.HCl salt	3.27	5.8	0.007	0.089	828.6	65.1	0.29
15b	18.6	46.6	0.13	0.28	358.5	166.4	2.52
13b	10.3	27.7	0.07	0.22	395	125.9	12.8
16b	ND	ND	ND	ND	ND	ND	2.16
14b	ND	ND	ND	ND	ND	ND	6.12
CQ	10.9	34.3	0.009	0.44	3811.1	77.95	ND
POD	0.0003	ND	ND	ND	0.0007	ND	ND
Ketoconazole	ND	ND	ND	ND	ND	ND	0.05

ND: Compound not tested/no data

The assay method considers compounds with IC_{50}< 10 µg/ml to be cytotoxic to mammalian cells (see experimental section), thus more than half of the compounds tested (11 out of 16) were not cytotoxic. Compounds **15a**, **16a**, **16**, **14** and **12** were identified to be toxic. Eleven compounds had a toxicity profile that was comparable or better than that chloroquine. In general the compounds were far less toxic than podophyllotoxin POD (the control drug). POD had IC_{50} of 0.0003µg/ml compared to the most cytotoxic of the test compounds, **15a** which had and IC_{50} of 1.38µg/ml. The cytotoxic compounds appear to be the most lipophilic in the series i.e. with clog P >4

All the compounds tested except **12** (SI = 0.2) had SI greater than one for the 3D7 over KB, implying that the compounds have the desired potential of being more toxic to the target organism than the host's cells. None of the compounds had better selectivity index than CQ (SI = 3811) when 3D7 was considered except **13a**. However, **13**, **14**, **14a** and **16. HCl salt** had selectivity indices close to that of chloroquine.

Ordinarily the CQ sensitive strains of *P. falciparum* are used to assess cytotoxicity, but the resistant strain was also used in this study. The data indicated that the compounds had poor selectivity for the resistant parasites over the mammalian cells with only 3 compounds i.e. **13a** (SI = 2201), **14a** (SI = 236), **15c** (SI = 166), and **13b** (SI =125), showing better selectivity indices than chloroquine (SI = 77.8). Only 9 out of the 16 compounds tested showed SI of greater than one. This was lower than was been observed in the 3D7 strain. This confirmed that most of the compounds were less active against resistant strains (Guetzoyan *et al.,* 2009; Manohar *et al.,* 2010).

3.8.2. *In vitro* CYP3A4 inhibition activity

3.8.2.1 Rationale

CYP3A4 metabolizes over 50% of the drugs on the market and some drugs are known to be inhibitors of CYP3A4 leading to fatal drug-drug interactions (DDIs) when co-administered with other drugs. Such drugs may be withdrawn from the market or their development halted. To avoid such expensive consequences drugs are evaluated for the potential to cause CYP3A4 inhibition in the early stages of lead optimization. The

CYP3A4 inhibition of the compounds was investigated by determining the percent inhibition and the inhibition IC_{50} values. Testosterone was used as the substrate probe. In the first assay the test compounds inhibited CYP3A4 at both high (20 µM) and low concentrations (3µM) and the inhibition was concentration dependent (Fig. 3.7).

3.8.2.2. *In vitro* CYP3A4 inhibition activity of A/AB series

All the compounds tested showed inhibitions in the range 20% - 100% at 3µM concentrations compared to 35% for ketoconazole (Fig. 3.7). This shows that the compounds were moderate to strong CYP3A4 inhibitors (Kerns and Di, 2008). At higher concentration (20 µM) the inhibition rose to over 70% for most compounds compared to 70 % for ketoconazole.

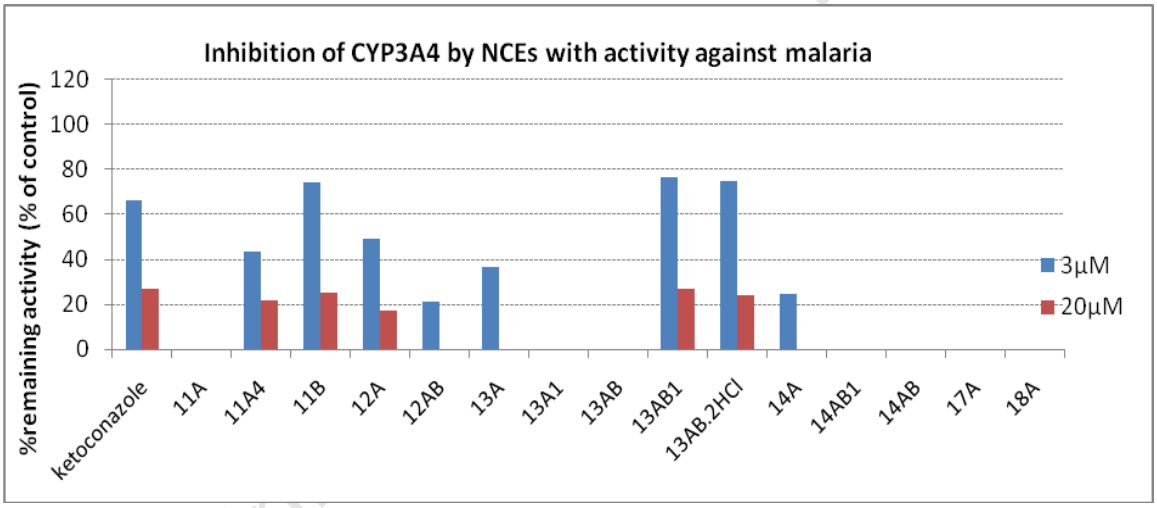

Figure 3.7: *CYP3A4 inhibition by the maltol and ethyl maltol derived double drugs.*

NOTE: Laboratory codes were used in the graph above thus their equivalent numbering in the text are as follows: 11A = ***9;*** *11A4 =* ***9a;*** *11B =* ***10****; 12A =* ***11****; 12AB =* ***12****; 13A =* ***15****; 13A1 =* ***15a;*** *13AB =* ***16****; 13AB1 =* ***16a****; 13AB.2HCl =* ***16. HCl salt****; 14A =* ***13****; 14AB1 =* ***14a****; 14AB =* ***14****; 17A =* ***15b*** *and 18A =* ***13b.*** *Compounds* ***9, 16, 14, 14a, 13b 15a,*** *and* ***16b*** *exhibited 100% inhibition at the two concentrations.*

In the second assay represented in Table 3.23, the trend observed was that the CYP3A4 inhibition increased with increase in the number of carbons in the alkyl linker especially for the benzylated analogues. The methoxylated analogues were relatively less potent

than the benzylated analogues but the former were more potent than the deprotected compounds.

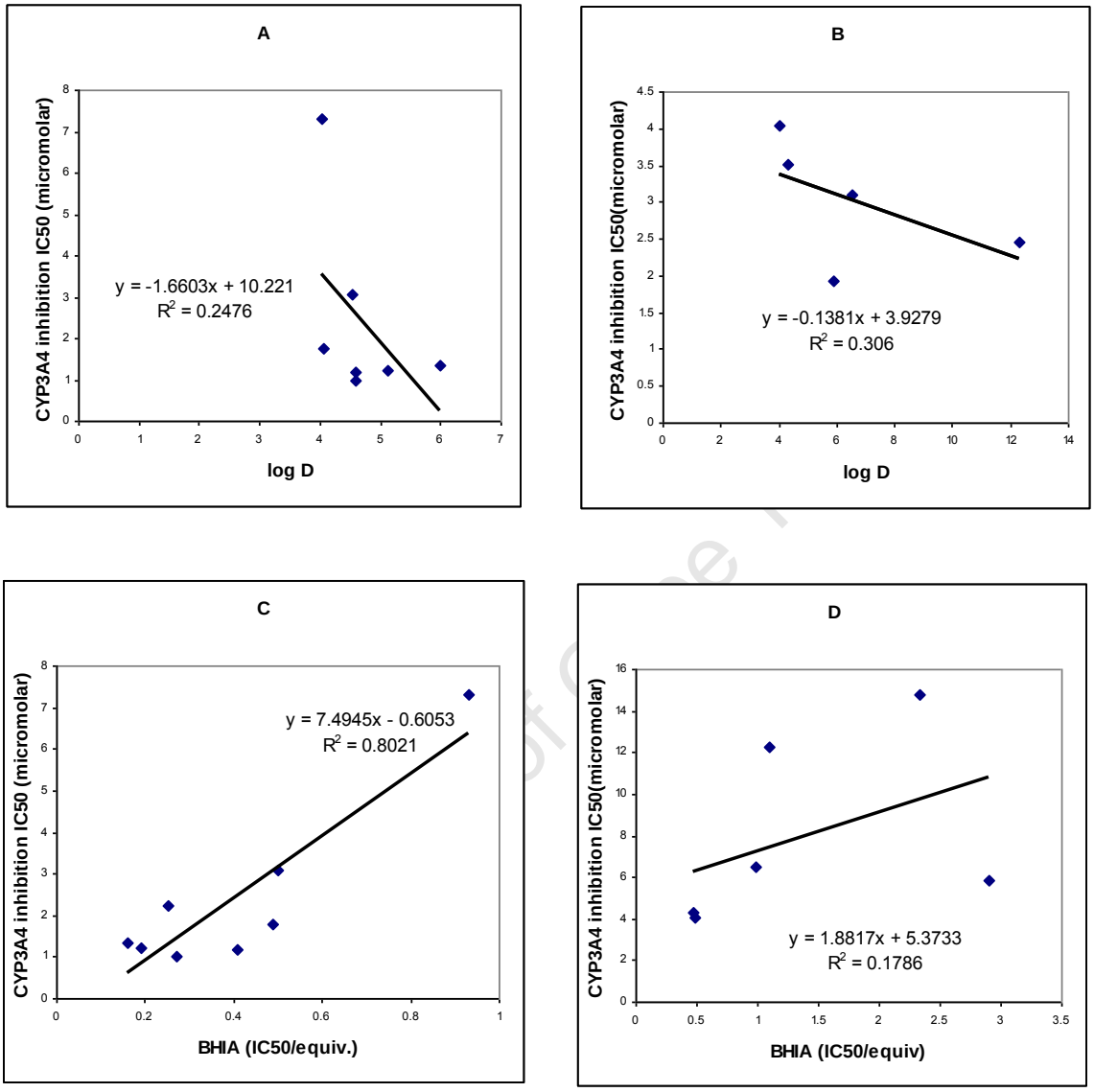

Figure 3.8: *Correlations between CYP3A4 and log P (A and B) or BHIA and CYP3A4 (C and D) for benzylated and deprotected conjugates. When log – log plots was considered for these data similar correlations were observed (same R^2 values were observed).*

The deprotected compounds were found to be weaker CYP3A4 inhibitors when compared to their benzyl protected analogues e.g compounds **11** (IC_{50} = 1.77 µM) when compared to **11a** (IC_{50} = 14.87 µM) or **10** (IC_{50} = 3.07 µM) when compared to **10a** (IC_{50}=12.3 µM).

General rules derived from multiple ADMET assays involving drugs with diverse structures shows that compounds with desirable CYP3A4 inhibitory profiles have molecular weights < 400 and clog P < 4 (Gleeson, 2008). In this respect all the benzylated analogues violated these criteria (MWT > 400 and clog P > 4). The deprotected compounds were found to be relatively less strong inhibitors and this is expected because their clog P and MWT values are within the prescribed limits (Gleeson, 2008).

If a more stringent standard pertaining CYP3A4 inhibition (Kerns and Di, 2008) is applied then all the compounds tested would not pass the test except compounds **10a** and **11a** (IC_{50} > 10 μM). Most of the compounds therefore have a potential to cause drug-drug interaction when co-administered with other drugs since they inhibit CYP3A4 (in the presence of testosterone).

The most potent inhibitor was **16** dihydrogen chloride salt with an IC_{50} of 0.29μM. The other potent inhibitors included **11** (IC_{50} = 1.77μM), **12** (IC_{50} = 1.18μM) and **13** (IC_{50} = 1.0μM); the common structural feature in them being the benzyl group.

In reversible CYP3A4 inhibition, lipophilicity and molecular shape are known to enhance the binding of any ligand to the enzyme's active site, in this case the heme (Yan and Caldwell, 2001). Gleeson, (2008) confirmed that CYP3A4 inhibition depends on the substrate's lipophilicity and found that inhibition increased with increase in the clog P. This prompted investigation of how the log D and predicted log P (clog P) of these compounds correlated with their CYP3A4 inhibition. Correlation between the log D and CYP3A4 inhibition was not significant i.e. < 0.5 (Fig. 3.8 A and B) so was the correlation between CYP3A4 inhibition and clog P. Therefore it was assumed that altering the lipohilicity alone may not confer a favorable CYP 3A4 inhibition profile to these molecules. Thus structural modifications were envisaged so as to confer better physicochemical properties to reduce the CYP3A4 inhibition of these compounds i.e. by synthesis of the R and D series.

The CYP 3A4 binding pocket contains a heme group as the active site and the erythrocytic heme is known to be one of the major targets for quinoline antiplasmodials (Ekins *et al*, 2003; Garrett and Grisham, 2005). Since these double drugs were found to be strong β-haematin inhibitors, it was necessary to investigate whether their interaction with the hemoglobin heme is similar to that of the heme in CYP3A4. To investigate this, the correlation between the β-haematin inhibition and CYP 3A4 inhibition among the benzylated and among the deprotected analogues was separately determined (Fig. 3.8 C and D). The correlation was at first sight found to be significant ($R^2 > 0.8$) in the benzylated analogues and not in the deprotected analogues ($R^2 = 0.18$). However, in the first group it was heavily dependant on a single point (0.93, 7.3). Despite this the benzylated compounds were generally observed to be strong CYP3A4 and β-haematin inhibitors despite the lack of a correlation between the two types of inhibition activities. The benzyl group therefore may be involved in both the CYP3A4 and β-haematin inhibition activities of these compounds. Further work was performed in terms of *in silico* docking of the molecules to the CYP3A4 receptor using Autodock 4.2. to investigate the mode of interaction between the conjugates and the CYP3A4 heme.

The CYP3A4 *in vitro* inhibition data represented in this section may be considered inconclusive because quantitative and qualitative inhibition parameters are dependent on the CYP3A4 substrate (Stresser *et al,* 2000). It is possible that the extensive inhibition of CYP3A4 caused by some drugs under some conditions could be overlooked or underestimated leading to errors in predicting important drug-drug interactions DDIs (Kenworthy *et al.,* 1999). Currently it is recommended that investigators screening for inhibition of CYP3A4-mediated metabolism to highlight potential DDIs should use a substrate probe from each of the three designated groups (Kenworthy *et al.,* 1999) or use two substrate probes from the same group (Lin *et al.,* 2007; Mao *et al.,* 2006). In this case only one substrate probe i.e. testosterone, was used. Because of this the data should be interpreted with caution.

CHAPTER FOUR

IN SILICO ADMET PROFILING

The *in silico* prediction data indicated that structural modifications were likely to enhance the ADMET profile of these hybrid molecules. The R and D series were predicted to have better CYP 3A4 profile than their A/AB analogues. The *in silico* and *in vitro* trends were comparable, however the *in silico* predictions in conjunction with the β-hematin inhibition trend data showed that good β-hematin inhibitors were not necessarily potent CYP3A4 inhibitors. Two unique docking conformations were identified each corresponding to weak (deprotected and 3-methoxylated) and strong inhibitors (benzylated analogues) respectively. Structures responsible for high CYP3A4 affinity were identified and appropriate modifications recommended.

4.1 *In silico* Prediction of Drug-likeness

Physicochemical properties of these compounds such as molecular weight (MWT), clogP, hydrogen bond acceptors (HBA) and hydrogen bond donors (HBD) were studied to identify any violations of the Lipinski guidelines or adherence to drug like properties (Lipinski, 1997), and some of them (cLog P and MWT) were used to predict their potential to inhibit CYP3A4 (Gleeson, 2008). The relevant data is represented in Tables 4.1 and 4.2 and the predictions were conducted with respect to all the four series of the double drugs. Among the benzylated group, the cLog P values predicted for the **D** and **A/AB** series were similar but lower than those for the **R** series (Table 4.1). Half of the benzylated analogues in the **D** and **R** group were found to violate 1 or 2 of the Lipinski guidelines and about 70% of the benzylated analogues in each of the three series have MWT >400, cLogP >4 hence have higher chances of inhibiting CYP3A4 (Gleeson, 2008). Therefore the *in vitro* CYP3A4 inhibition potential of the benzylated compounds was expected not to change significantly after the structural modification. The predicted drug like properties and physicochemical data for the deprotected analogues seem better because all of them complied with the Lipinski guidelines (Table 4.2). The predicted data indicated that the pyranone precursors to the double drugs i.e. kojic acid and maltol had druglike properties.

Table 4.1: *In silico prediction of physicochemical and drug-like properties for benzylated analogues*

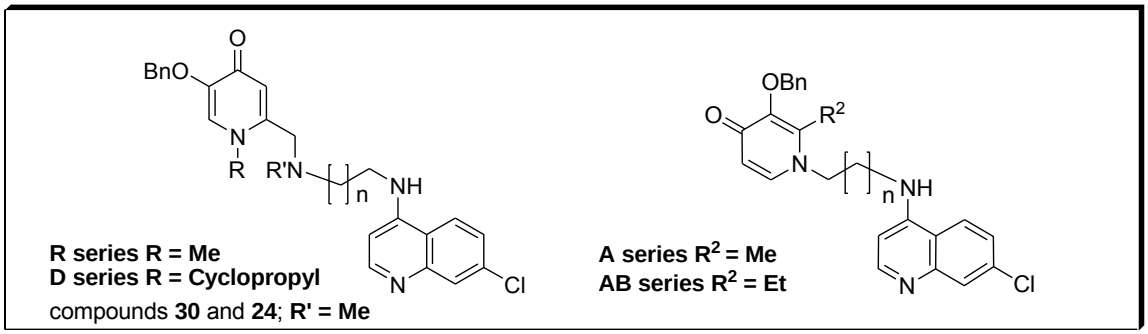

Compound	Series	Linker $(CH_2)_n$	MWT	cLog P*	HBA	HBD	Violations
9	A	1	419.9	3.8	5	2	0
10	AB	1	433.9	4.2	5	2	0
23	R	1	448.1	2.7	6	3	0
28	D	1	474.2	3.4	6	3	0
11	A	2	433.9	4.3	5	2	0
12	AB	2	447.9	4.7	5	2	0
24	R	2	477	3.7	6	2	0
25	R	2	462.2	3.2	6	3	0
29	D	2	489.2	3.9	6	3	0
30	D	2	502.2	4.4	6	2	1 (MWT)
13	A	3	447.9	4.8	5	2	0
14	AB	3	461.9	5.2	5	2	1 (clog P)
26	R	3	477.2	3.7	6	3	0
31	D	3	503.2	4.3	6	3	1 (MWT)
15	A	5	476	5.7	5	2	1 (clog P)
16	AB	5	490	6.2	5	2	1 (clog P)
27	R	5	504.2	4.7	6	3	2 (clog P, MWT)
32	D	5	530.2	5.3	6	3	2 (clog P, MWT)
Kojic acid			142	-1.5	2	2	0
maltol			139	-0.1	2	1	0
Deferiprone			139.2	-0.6	2	1	0
Chloroquine			319	5.3	3	1	1 (clog P)

**Predicted from MoKa*

Table 4.2*: In silico prediction of physicochemical and drug-like properties for deprotected analogues.*

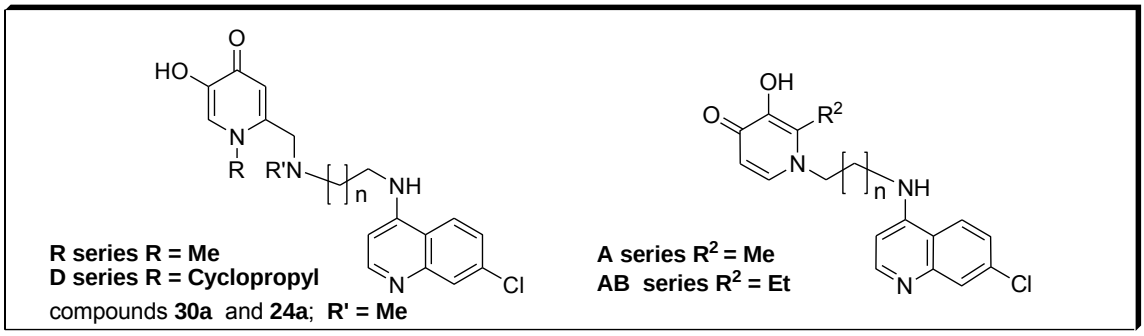

Compound	Linker $(CH_2)_n$	MWT	cLog P*	HBA	HBD	Violations
9a	1	329.8	2.5	5	3	0
10a	1	343.1	2.5	5	3	0
23a	1	358.1	1.0	6	4	0
28a	1	384.1	1.6	6	4	0
11a	2	344.1	2.5	5	3	0
12a	2	357.1	3.0	5	3	0
24a	2	398.1	2.1	6	4	0
25a	2	372.1	1.5	6	4	0
29a	2	387.1	2.0	6	5	0
30a	2	412	2.6	6	5	0
13a	3	357.1	3.0	5	3	0
14a	3	371.9	3.5	5	3	0
26a	3	386.2	2.0	6	4	0
31a	3	412.1	2.6	6	4	0
15a	5	385.9	4.0	5	3	0
16a	5	399.9	4.5	5	3	0
27a	5	414	3.0	6	4	0
32a	5	440	3.6	6	4	0
Kojic acid		142	-1.5	2	2	0
maltol		139	-0.1	2	1	0
Deferiprone		139.2	-0.6	2	1	0
Chloroquine		319	5.3	3	1	1

Violation of the Lipinski guidelines by some of the hybrid molecules does not rule out further development of these series since not all drugs on the market comply with the guidelines fully. An example is chloroquine which does not comply fully with the Lipinski guidelines (clogP>4) yet it was used successfully to treat malaria.

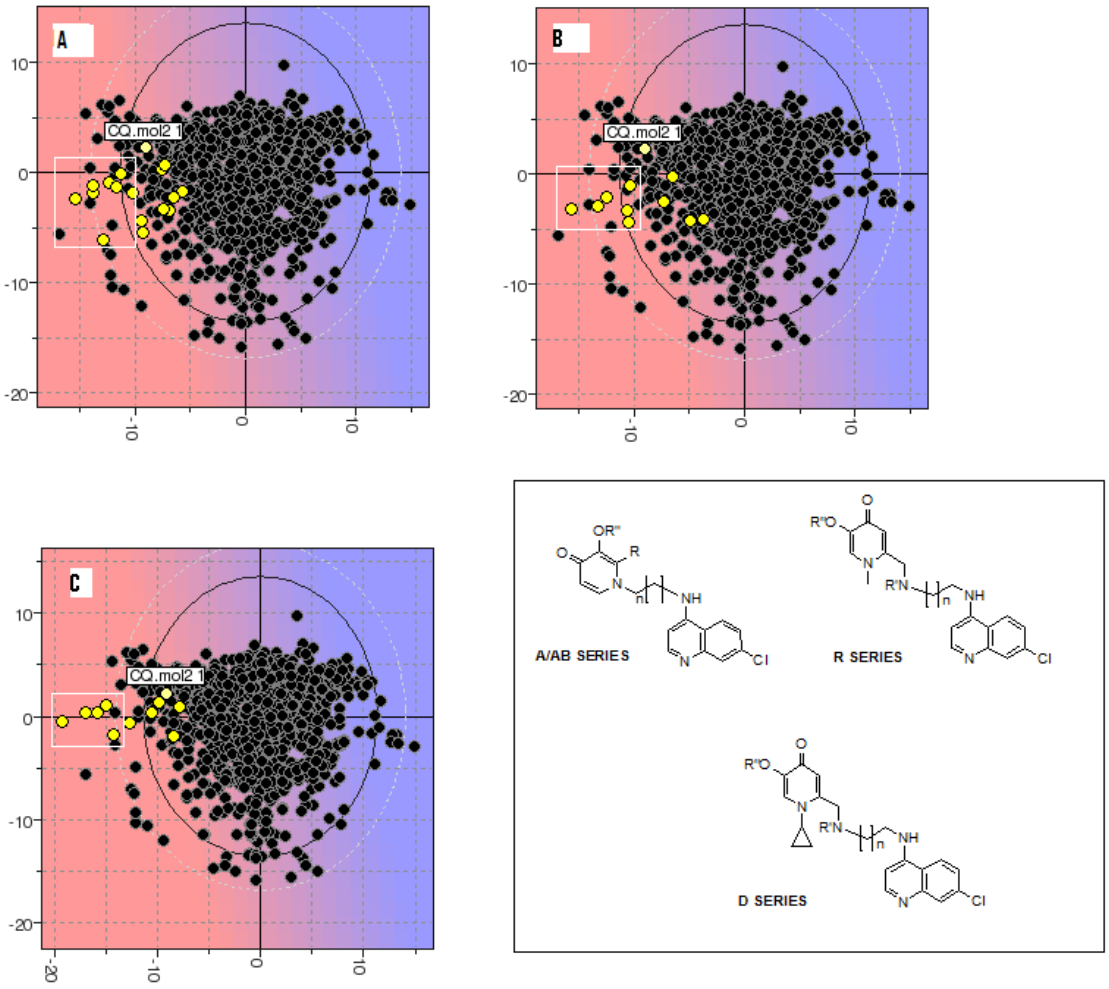

Figure 4.1. *PLS plots for solubility prediction in Volsurf modeller®: The benzylated analogues are enclosed in the white rectangles and deprotected analogues are outside the rectangles. A/AB, R and D series are depicted by plots A, B and C respectively. The extreme right handside or blue zone (x>0) represents highly soluble compounds whereas compounds on the extreme left hand side or magenta zone are less soluble (x<0). The standard drug chloroquine is represented by the yellow dot immediately below the "CQ mol2 1" label.*

In the **R** and **D** series, 77% of the deprotected analogues have cLogP<4 and MWT<400 unlike 23% of the deprotected analogues in the **A/AB** series. Therefore, it was

hypothesized that the structurally modified deprotected analogues from **R** and **D** series are weaker CYP3A4 inhibitors than their analogues in **A/AB** series. Because of their compliance with Lipinski's guidelines, it is presumed that these compounds will be orally bioavailable. It is noteworthy that the Lipinski guidelines are mere guidelines and should be used with caution as they are subject to other factors such as the role of any active transport mechanisms.

Oral administration is a desired route for antimalarials because it maximises patient compliance and reduces ancillary care costs (Ray, 2010). For orally administered drugs adequate aqueous solubility is of paramount importance since dissolution of the active drug (or its prodrug form) in the gastrointestinal fluids precedes its oral absorption from the gastrointestinal system (Kharkar, 2010). Oral bioavailability or the fraction of the active form of an orally administered drug that reaches systemic circulation is thus largely dependent on aqueous solubility as well as membrane permeability especially human intestinal permeability, pKa (ionizability) and presystemic metabolism.

The solubility predictions in Volsurf modeler (Fig. 4.1) did not show any significant shift when series **R** and **D** were compared to the initial series **A** and **AB**. The deprotected analogues in the **A** and **AB** series were predicted to have solubility that was comparable to that of chloroquine. However, the deprotected analogs in the **R** and **D** series were more soluble than chloroquine. This can be attributed to the presence of the extra amine group on the side chain. This group is protonable, thus enhances pH dependant solubility. Therefore, it is anticipated that the **R** and **D** series will have enhanced solubility under gastrointestinal pH (<5). Benzyl protected analogues were predicted to be less soluble than the deprotected analogues. This is attributable to the conversion of a less polar group (O-benzyl) to a more polar one (hydroxyl) via deprotection. Considering that the experimentally determined solubility (turbidimetric) of the **A** and **AB** series was found to be within the druglike limits i.e. 25µg/mL, (Table 2.6) for both benzyl protected and deprotected analogs, it may be stated with some certainty that most compounds in these series do not present potential problems related to solubility albeit this is subject to experimental confirmation.

Note that, although the predicted solubility for the benzylated analogues in the **A** and **AB** series looks poor on the PLS plot, the actual solubility from experimental determinations (Table 2.6), were good and within the drug like limits.

4.2 *In silico* Prediction for CYP3A4 inhibition

4.2.1. Validation of the Accuracy and performance of AutoDock.4.2.

All the docking experiments were done using AutoDock 4.2. The validation of the accuracy and performance was done by inspecting how closely the best docked conformation of a known inhibitor ketoconazole resembled the bound ligand in the experimental crystal structure. The best docked conformation seems to be exactly superimposed on the native bound one (Figure 4.2) and the docked ligand interaction with the amino acid residues in the binding pocket was similar to that of the native bound one

4.2.2 Affinity for the CYP3A4

The affinity of the ligand (substrate or inhibitor) for the enzymes active site is represented by K_i and it is referred to as the affinity constant or the binding constant or the inhibition constant. The K_i experimental was determined in the presence of an inhibitor (a double drug) and the substrate (testosterone). The experiments and data analyses were performed by R. Thelingwani at the AIBST, Harare. The *in vitro* experiments and the data analyses were done as described elsewhere (Shou, 2008; Obach 2008). The data was analysed using the GraphPad Prism software. The predicted K_i was obtained by docking the energy the ligands into the CYP3A4 crystal structure using AutoDock 4.2. The details are given in the experimental section. The inhibition constants of the lowest energy conformation were used in the analyses that follow.

Initial work involved comparing the *in vitro* CYP3A4 inhibition data of **A/AB** series compounds to the AutoDock 4.2 predicted values so as to further confirm the accuracy of the prediction. Of the 20 compounds docked in CY3A4 (PDB code 1TQN), only 6 (30%) had predicted inhibition/affinity constants K_i values similar or very close to the *in vitro* determined K_i values (Table 4.3).

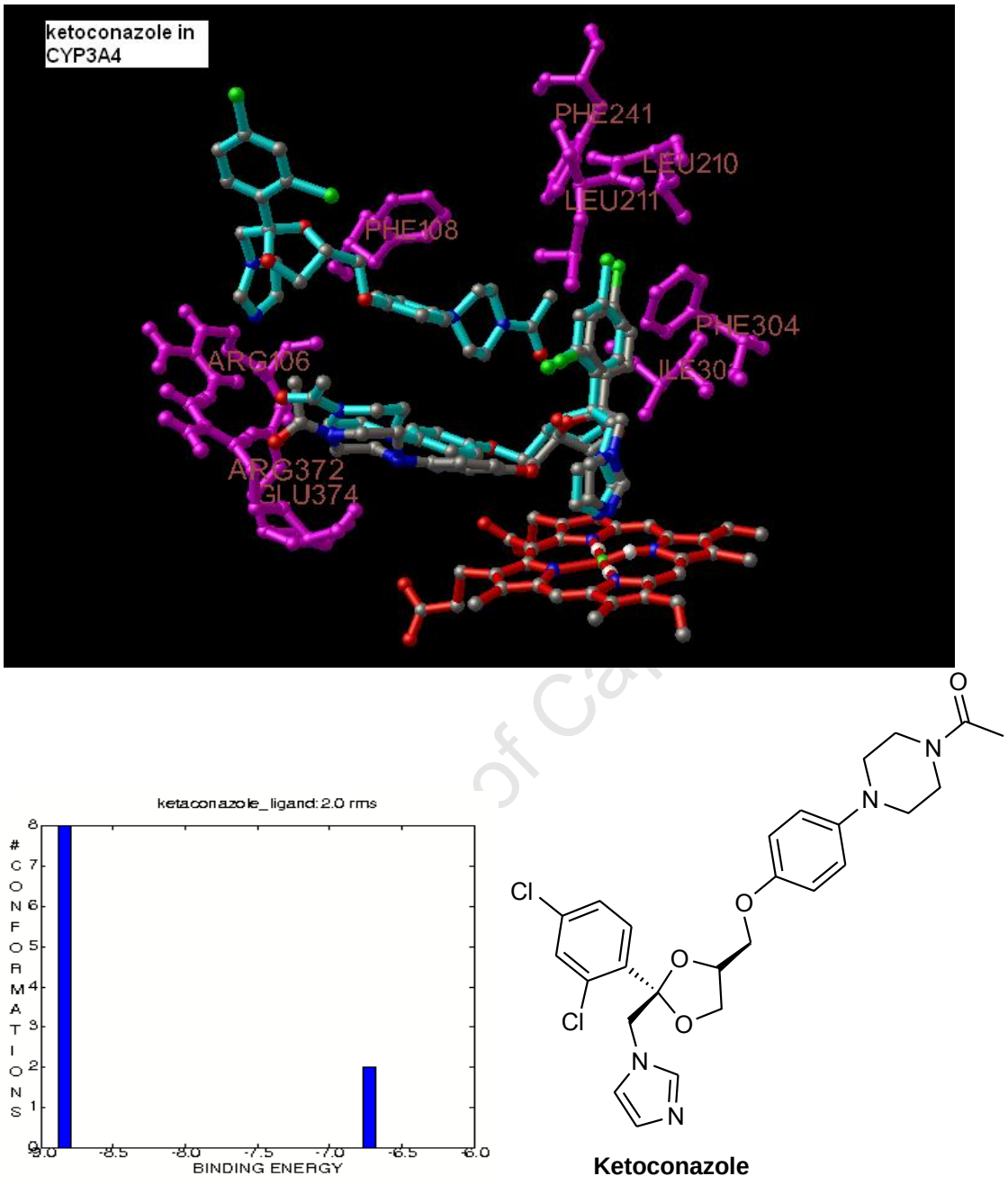

Figure 4.2: *Two ketoconazole molecules binding in to CYP3A4 stacked in an anti-parallel orientation to each other (green) superimposition of the ketoconazole (grey) docked in CYP3A4 active site (PDB code 1TNQ) in AutoDock 4.2 The histogram underneath represents the clustering of the conformations of ketoconazole in AutoDock 4.2.*

In spite of this, significant correlation ($R^2 = 0.6$) was observed between experimental and predicted K_i values for the **A** and **AB** series (Figure 4.3), implying that further optimization of the docking parameters may improve the accuracy of the AutoDock predictions. When the data for the 3-methoxylated analogues was included no significant correlation was observed between the experimental and predicted K_i, thus the correlation depicted in Figure 4.3 excluded data for the methoxylated analogues.

Table 4.3: *Experimental and predicted inhibition constants K_i for some compounds*

Compound	CYP3A4 IC_{50} in μM	K_i *in vitro* in μM	K_i Predicted μM
9	7.3	9.66	1.17
9a	5.87	39.6	2.04
10	3.07	0.97	0.23
10a	12.34	70.9	4.97
11	1.77	0.38	0.59
11a	14.87	5.42	1.49
12	1.18	1.14	0.22
12a	ND	ND	1.05
13	1.0	1.19	1.10
13a	ND	ND	1.03
13b	12.8	3.69	0.23
14	1.21	27.6	0.5
14a	6.52	6.7	1.20
14b	6.12	3.95	1.37
15	2.25	3.73	0.23
15a	4.29	5.81	1.14
15b	2.52	4.38	5.72
16	1.36	0.79	0.97
16a	4.04	3.39	2.71
16b	2.16	3.58	2.79
36	ND	ND	0.06
37	ND	ND	0.44
DFP	ND	ND	426
CQ	ND	ND	5.08
Ketoconazole			0.33

ND: not determined

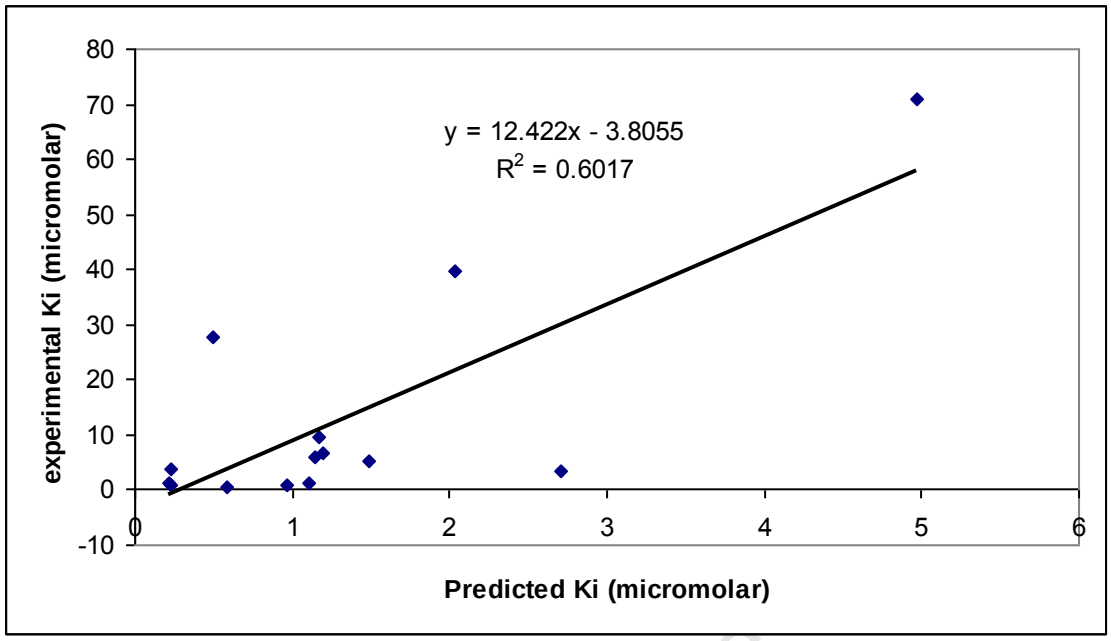

Figure 4.3: *Experimental and predicted inhibition constants correlations for benzylated and deprotected analogues of the **A** and **AB** series*

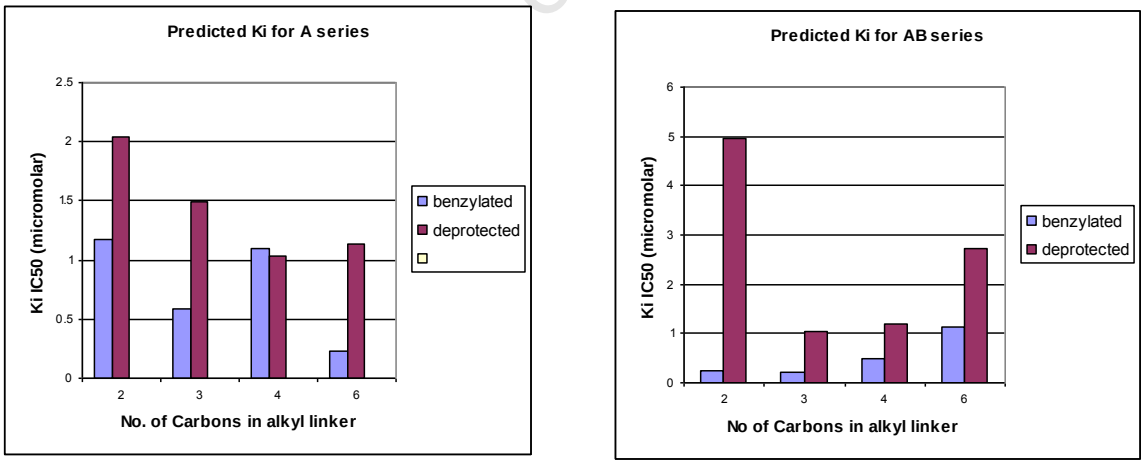

Figure 4.4: *Predicted CYP3A4 inhibition constant K_i trends in the **A** and **AB** series*

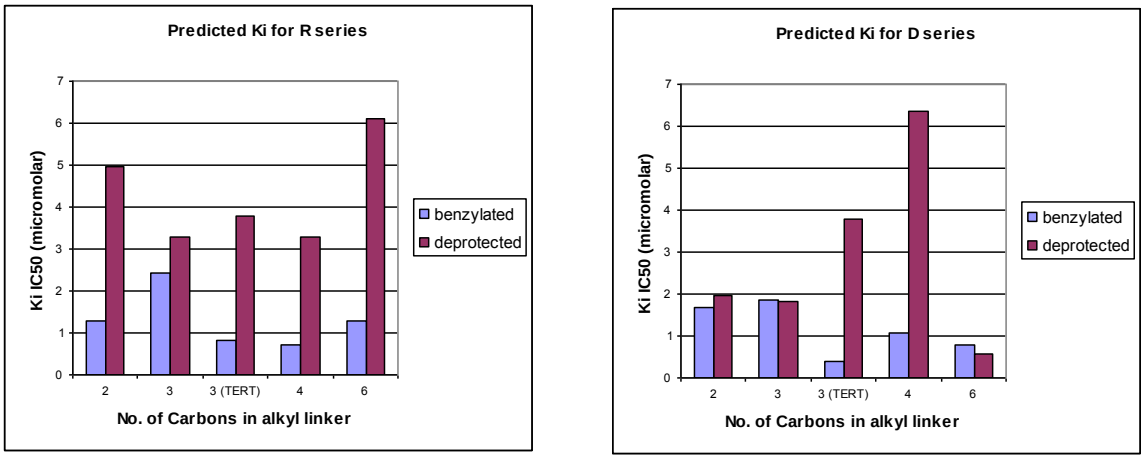

Figure 4.5: *Predicted CYP3A4 inhibition constants K_i trends in the **R** and **D** series*

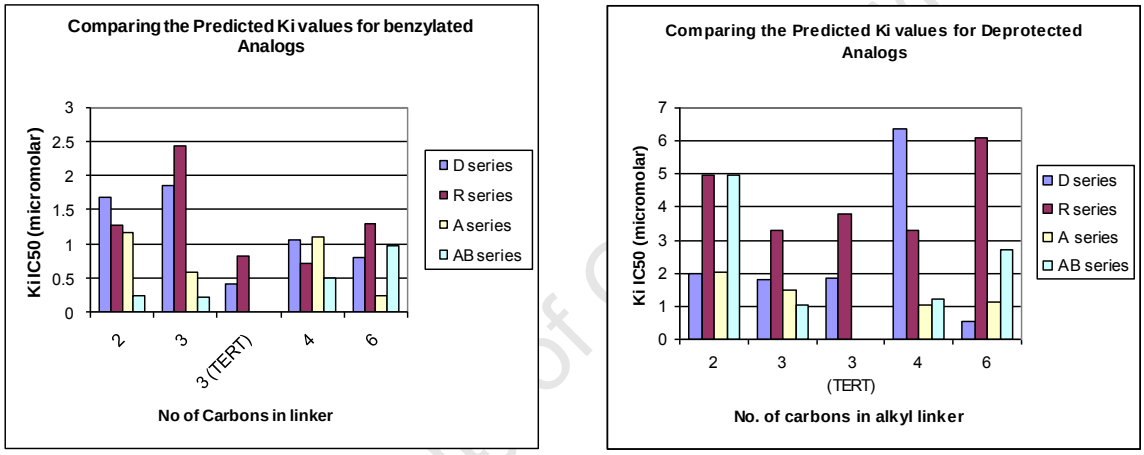

Figure 4.6: *Predicted CYP3A4 inhibition constants K_i trends in all the four series; **A**, **AB**, **R** and **D**. TERT: analogues with tertiary amino group*

Using the predicted inhibition constants from the docking studies it was clear that structural modification may help improve the CYP3A4 profile of these compounds. Most compounds from the **R** and **D** series were predicted to have lower affinity or inhibition potential than their analogues in the **A/AB** series (Fig.4.6). Specifically the **R** series seem to have lower affinities for CYP3A4 than the **D** series and this implies that the former are likely to be weaker CYP3A4 inhibitors. This prediction concurs with predictions obtained using other *in silico* tools i.e. when predicted physicochemical data from Volsurf Modeller and MoKa were used in conjunction with Gleeson criterion (2008) and Lipinski guidelines (section 4.1). All the compounds were predicted to have higher affinity for CYP3A4 than the standard drugs on which their design was based on i.e. DFP (K_i =

426μM) and CQ (K_i =5.08 μM). None was predicted to have higher affinity for CYP3A4 than the potent inhibitor ketoconazole (K_i =0.33μM), except compound **37** (K_i = 0.06μM). Compound **36** (K_i =0.44μM) the synthetic precursor of **37,** showed a low affinity for the CYP3A4 but the affinity increased by more than 10- fold on incorporation of the quinoline moiety to form **37**. This was expected because the quinoline moiety is known to cause CYP3A4 inhibition.

The benzylated double drugs with tertiary amino group: **30 (**K_i =0.41 μM) and **24** (K_i =0.81μM), were predicted to be stronger CYP3A4 inhibitors than their analogues lacking the tertiary amino group: **29** (K_i =1.85 μM) and **25** (K_i =2.43 μM). This trend is not the same as what was observed for β-hematin inhibition since the benzylated compounds with the tertiary amino group were weaker β-hematin inhibitors than their analogues without the tertiary amino group. On deprotection, their predicted CYP3A4 inhibition/affinities were similar or less than that of their analogues without a tertiary amino group i.e. when comparing **30a (**K_i =1.85μM**)** to **29a** (K_i =1.81 μM) and **24a (**K_i =3.79 μM**)** to **25a** (K_i =3.28 μM). This trend is not same for the β-hematin inhibition data of these compounds. These observations also emphasize the point that the chelating/deprotected analogues are likely to have better CYP3A4 inhibition profiles than their protected/benzylated analogues and that β-hematin inhibitors are not necessarily CYP3A4 inhibitors.

4.2.3 Docking conformations in CYP3A4

All the compounds were docked into the templates of the crystal structure of CYP3A4 (Protein Data Bank entry 1TQN). Illustrations that follow are for a few selected compounds, criterion for selection included, accuracy of their predicted K_i values, representative of a series and the magnitude of the affinity/inhibition constants. The docking solutions were groups of conformational clusters in which all-atom root mean square deviation (rmsd) was within 2.0 Å and were ranked by the lowest estimated free energy of docking for analysis. It is hoped that the data generated will help inform future structural modifications of these compounds for a better CYP3A4 inhibition profile.

4.2.3.1 Compounds **16** (13AB) **and 16a** (13AB1)

Both *in vitro* data and docking calculations indicated compound **16** to be among the most potent CYP3A4 inhibitors in the **A/AB** series, and it had the best β-hematin inhibition and antiplasmodial activity in the series. From the docking models, the lowest energy conformation (-8.2Kcal/mol) had a predicted K_i value of 0.97μM versus the experimental value of 0.79 μM. No clustering was observed therefore the docking was repeated using 10 times more evaluations relative to the default evaluations. The resultant lowest energy conformation (-8.5Kcal/mol) had a predicted K_i value of 0.68μM versus the *in vitro* experimental value of 0.79 μM. The conformations in the first and second run were similar and clustering was observed in the second run (Fig 4.7).

The lowest energy cluster conformation for **16** had the benzyl group oriented toward the CYP'3A4 active site (Fig 4.7), and the rest of the ligand was observed to be interacting strongly with the hydrophobic pocket residues (Phe108, Leu210, Leu211, Phe241, Ile301, Phe304). The quinoline nucleus is positioned in a manner that enhances a π bond T stacking with the Phe103 residue. The pyridinone and the benzyl group are seen to interact with Phe304 and Ile301 residues respectively. The described binding mode was observed in most of the molecular models of the benzylated double drugs in the docking calculations.

The abundant cluster conformation for **16** showed the ligand had a higher affinity for the hydrophobic pocket. In both the lowest energy and the abundant cluster conformations, the quinoline appeared to be unexposed to the active site of CYP3A4 i.e. the heme iron.

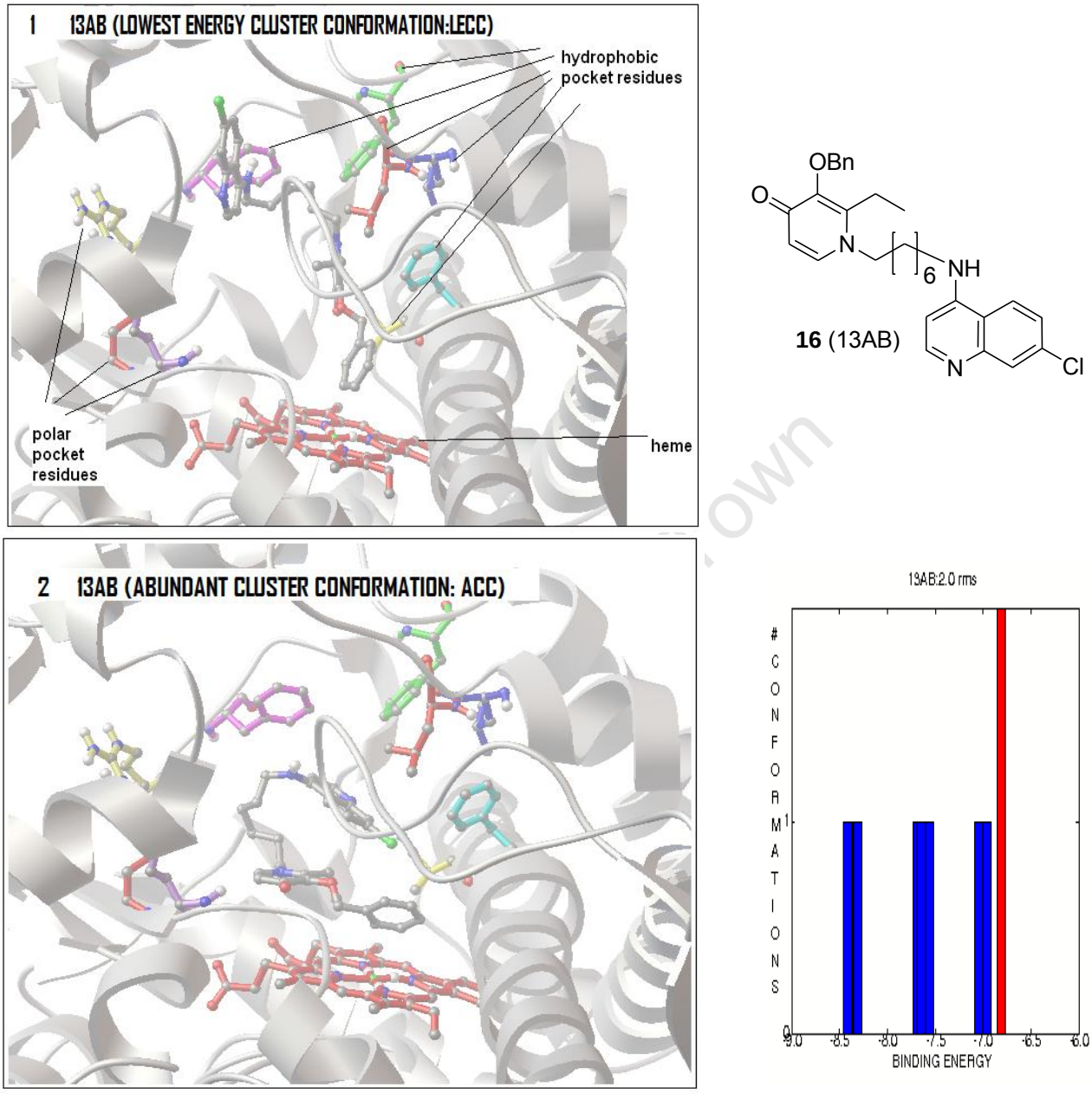

Figure 4.7: *Molecular models of* ***16*** *(13AB) in the active site of CYP3A4 predicted by AutoDock version 4.2. The upper panel (1) depicts a representative conformation from the lowest energy cluster whereas the lower panel (2) depicts a representative conformation from the most abundant cluster. The hydrophobic pocket consists of Phe108 (pink), Leu210 (blue), Leu211 (red), Phe241 (green), Ile301 (yellow), Phe304 (blue-green). The polar pocket residues include Arg372, Arg106 and Glu374. The clusters are shown in the histogram on the right of the lower panel with most abundant*

cluster in red.

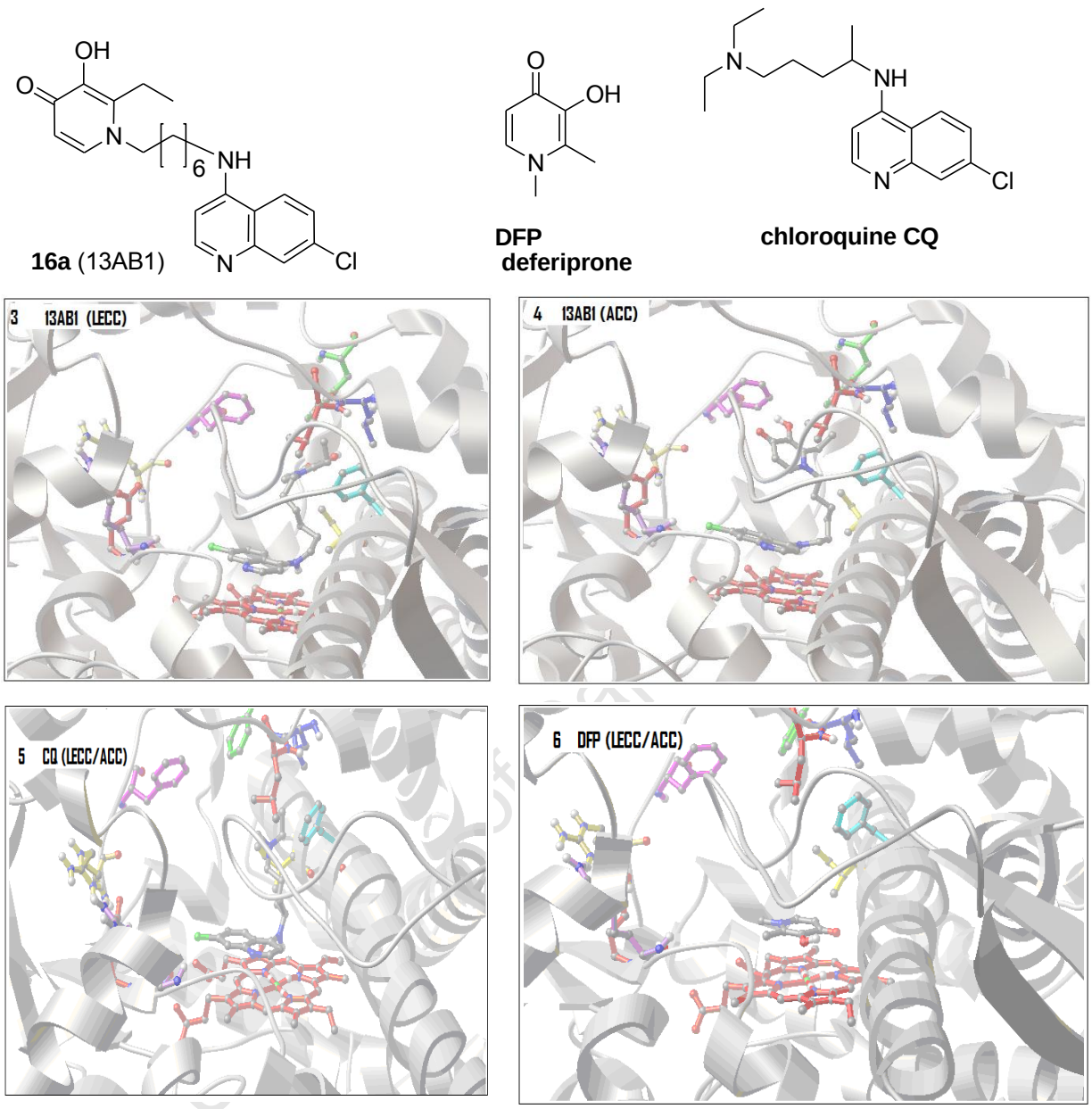

Figure 4.8a: *Molecular models of **16a** (13AB1), **CQ and DFP** in the active site of CYP3A4 predicted by AutoDock version 4.2 .A representative conformation from the lowest energy cluster (LECC) and a representative conformation from abundant cluster conformation (ACC) of **16a** (13AB1) are depicted in panes 3 and 4 respectively. For **CQ** and **DFP** the LECC and ACC were the same for each; see the clustering histograms in Figure 4.8 b*

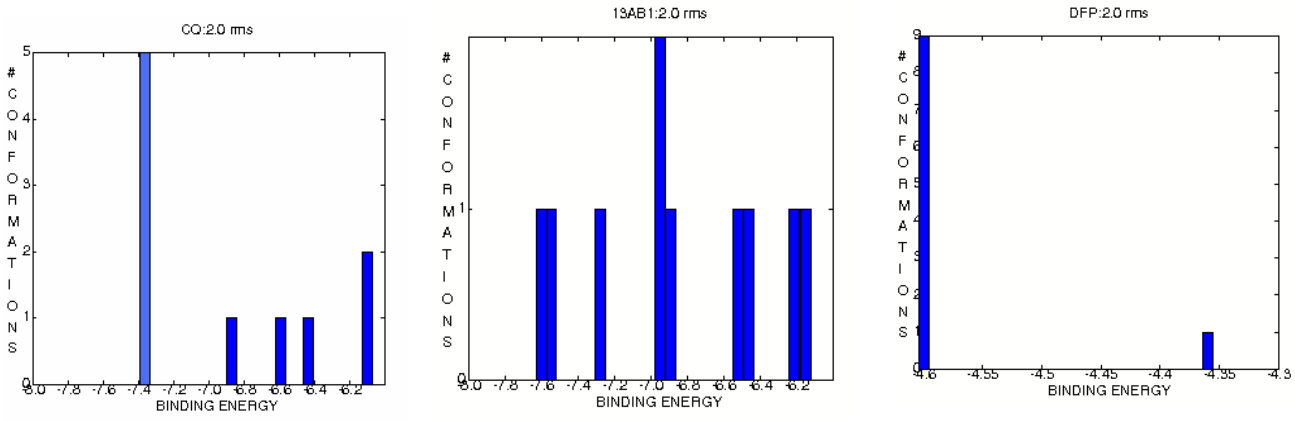

Figure 4.8 b: *Clustering histograms of **16a** (13AB1), **CQ** and **DFP***

Ketaconazole, a known strong inhibitor of CYP3A4, binds simultaneously to the distal and proximal binding sites (Tanaka, *et al* 2004; Fig 4.2). Similarly, compound **16** (13AB) as shown in Figure 4.7 appears to bind simultaneously to the hydrophobic pocket (a distal site) and the heme (a proximal site). This partly explains why 16 (13AB) inhibits CYP3A4 and has a higher affinity for the same.

Compound **16a** (13AB1) [the deprotected analogue of **16** (13AB)] had a predicted K_i of 2.71μM that was closer to the *in vitro* value (3.39 μM). Its binding energy (-7.6 Kcal/mol) was higher than that of **16** (13AB) (-8.5Kcal/mol) implying weak affinity for CYP3A4 than **16** (13AB). The mode of binding which was different from the benzylated analogue is predicted to be via π-π stacking interaction of the quinoline with the porphyrin ring of the heme and the amino group at position 4 of the quinoline ring is closer to the heme iron (Fig. 4.8 a). In this case the quinoline nucleus are more exposed to the active site and are likely to be metabolized hence less CYP3A4 inhibition is expected. In fact, the predicted sites of metabolism from Metasite, indicate that the amino group at position 4 of the quinoline ring as one of the sites of metabolism for this of class compounds (Fig.2.18). From the models the hydroxypyridinone moiety seems to prefer the hydrophobic pocket over the polar pocket.

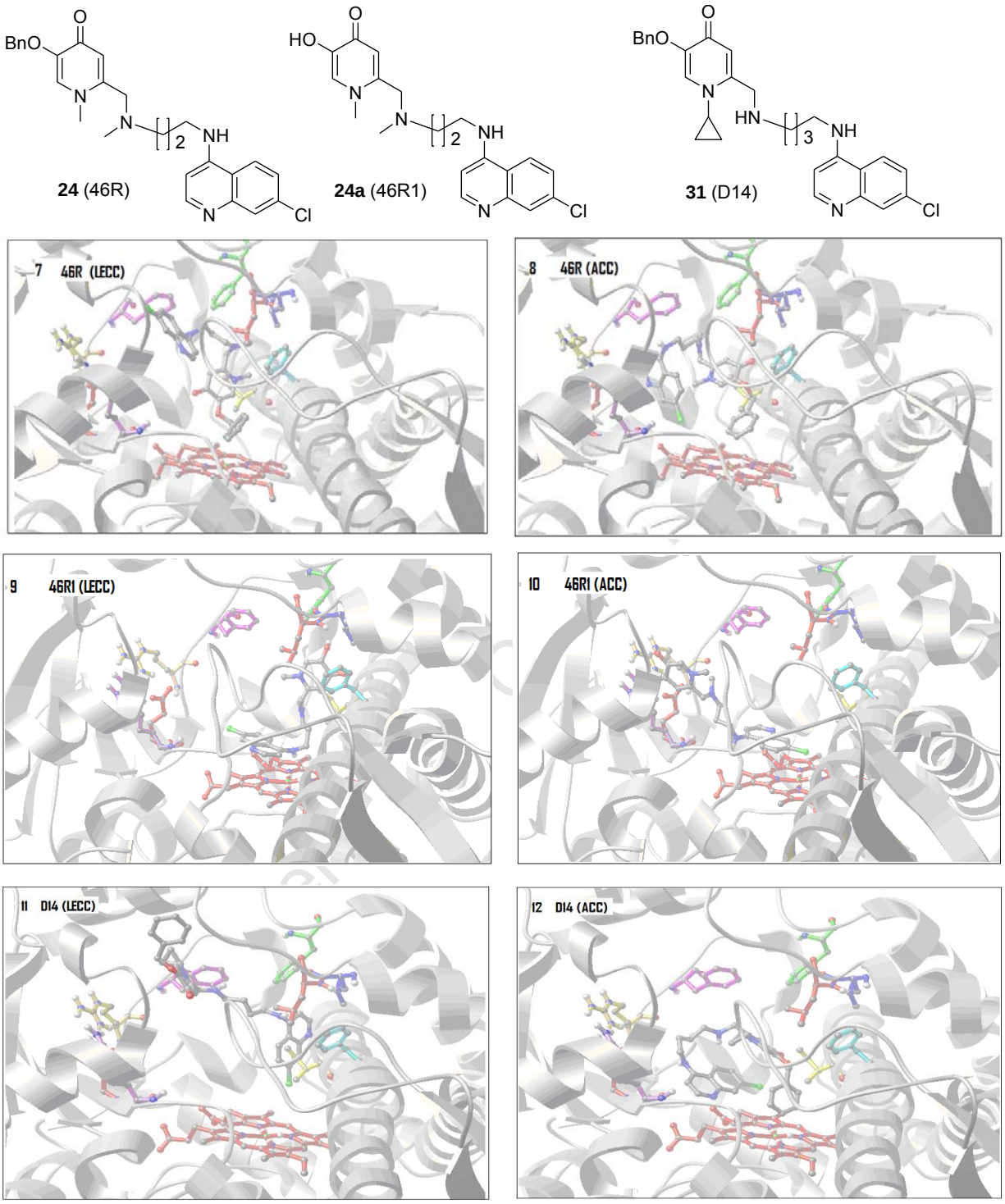

Figure 4.9 a: *Molecular models of **24** (46R), **24a** (46R1) and **31** (D14) in the active site of CYP3A4 predicted by AutoDock version 4.2. A representative conformation from the lowest energy cluster (LECC), in the right hand side panes and a representative conformation from the abundant cluster (ACC), in the left hand side panes. The clustering histograms are shown in Figure 4.9b.*

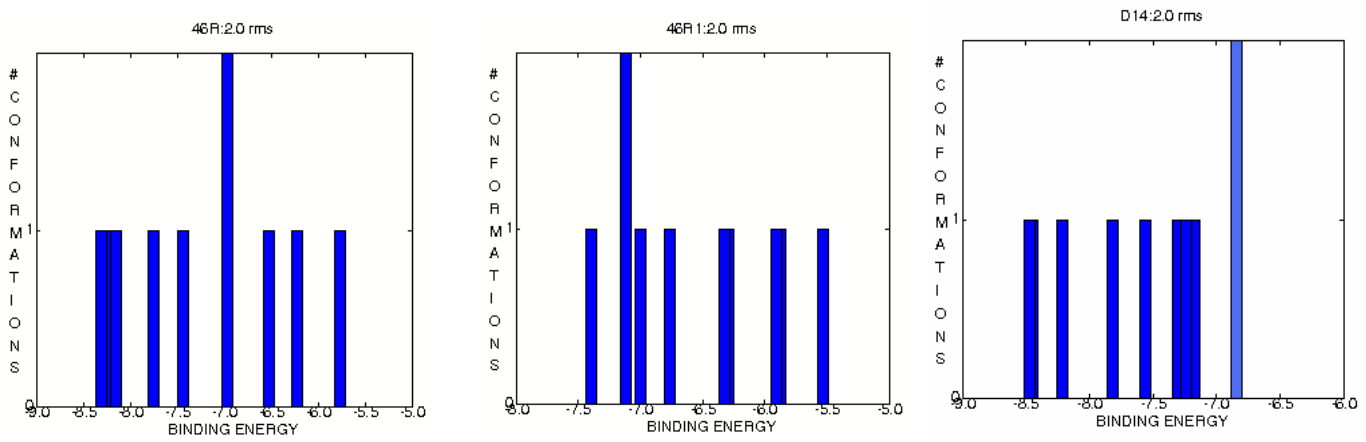

Figure 4.9 b: *Clustering histograms of **24** (46R), **24a** (46R1) and **31** (D14)*

The lowest energy and most abundant conformations for **16a** (13AB1) were similar except for the orientation of the hydroxypyridinone moiety. The clustering observed indicated convergence of the docking data hence adding confidence to the quality of the prediction for **16a** (13AB1) (Fig. 4.8 b).The orientation of the quinoline nucleus towards the CYP3A4 heme in this case, and in all other deprotected analogues, and in 3-methoxy analogues closely resembles the one observed in chloroquine-hematin complexes (Leed *et al.,* 2002). This docking mode also resembles that of chloroquine in CYP3A4 as predicted by the docking models in Figure 4.8 a.

4.2.3.2 Compounds 24 (46R) **and 24a** (46R1)

Compound **24** (46R) was predicted to have a higher affinity for CYP3A4 (K_i = 0.81μM; binding energy -8.3 Kcal/mol) but it was not tested *in vitro*. Visualization of its docking modes was important because its deprotected analogue (**24a** i.e. 46R1) had previously showed excellent antiplasmodial activity and represents the double drugs with a tertiary amino group. The lowest energy and most abundant cluster conformations of **24** (46R) were found to be similar to that of other benzylated analogues (Fig. 4.9 a), i.e. the benzyl group was oriented towards the active site of the CYP3A4 just as in **16** (13AB). For compound **24a** (46R1), its lowest energy conformation showed a π-π stacking interaction between the quinoline nucleus and the heme's porphyrin ring in a manner similar to other deprotected molecules (Fig.4.9 a). The abundant cluster's conformation of **24a** (46R1)

was found to be similar to the lowest energy conformation except that their N-1 groups were oriented differently towards the heme.

4.2.3.3 Compounds **31** (D14) **and 31a** (D141)

Compound **31** (K_i =1.06μM; binding energy -8.15 Kcal/mol) represents compounds from the **D** series and its deprotected analogue **31a** was predicted to have the lowest affinity for CYP3A4 (K_i = 6.4μM; binding energy -7.09 Kcal/mol). The representative conformation from the most abundant cluster for **31** showed an interaction that was similar to other benzylated analogues (Fig 4.10 a), but in the lowest energy conformation the quinoline is involved in π-bond T stacking with the porphyrin ring of the heme. This interaction is long range and the quinoline is far removed from the active site hence one can speculate lower chances of metabolism and higher probability of inhibition. This in a way explains why compound **31** was predicted to have higher affinity for CYP3A4 like the other benzylated analogues. The representative comformation from the abundant cluster indicated a high affinity for the hydrophobic pocket just as observed in other benzylated double drugs.

The lowest energy conformation of **31a** was observed to be similar to other deprotected analogues except that the chloro substituent on the quinoline was oriented towards the heme iron (Fig. 4.10 a). Its most abundant cluster conformation was different from that of the aforementioned deprotected analogues because the pyridinone N-1 (and the cyclopropyl ring) are oriented towards the heme iron. This binding mode is comparable to that of deferiprone (DFP) in Figure 4.8 a. DFP was predicted to have a relatively poor affinity for CYP3A4 (K_i = 426μM; binding energy -4.6 Kcal/mol) and has not been reported to cause any DDIs or CYP3A4 inhibition. It was reported to have no β-hematin inhibition activity in the previous section (3.1), hence it is hypothesized that DFP does not bind heme in the parasitic food vacuole unlike the double drugs reported herein. It can, therefore, be assumed that the binding modes of both the lowest energy and abundant clusters of **31a** (D141) result in metabolism and less inhibition hence the lower affinity predicted for compound **31a** (D141) (K_i = 6.4μM)**.**

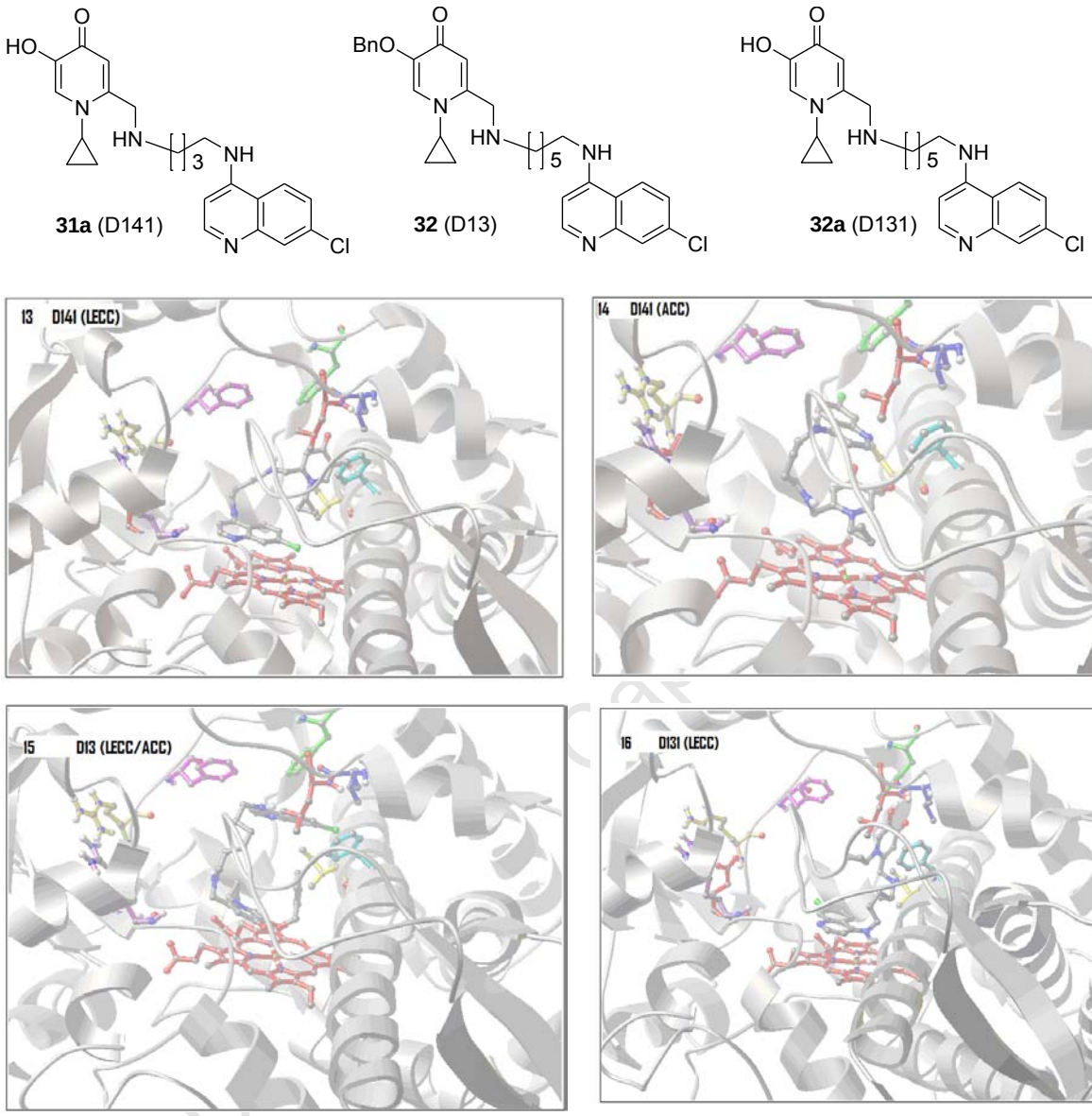

Figure 4.10 a: *Molecular models of **31a** (D141), **32** (D13) and **32a** (D131) in the active site of CYP3A4 predicted by AutoDock version 4.2. The representative conformation from the lowest energy cluster (LECC), in the right hand side panes and the representative conformation from the abundant cluster (ACC), in the left hand side panes for **31a** (D141). The LECC of **32** (D13) was same as its ACC. No abundant cluster was observed for **32a** (D131); see Figure 4.10 b for clustering histograms.*

4.2.3.4. Compounds 32 (D13) and 32a (D131)

32 was found to have the best *in vitro* antiplasmodial activity in D series and the best hematin inhibition activity overall. The compound was predicted to have a very high affinity for CYP3A4 (K_i = 0.8µM; binding energy -9.10 Kcal/mol). The lowest energy conformation of **32** which was the same as the most abundant cluster conformation had the benzylated pyridinone substructure oriented close to the CYP3A4 active site (Fig 4.10). Compound **32a** docks in a manner similar to other deprotected analogues but its quinoline *N*-1 is closer to the heme. However, none of its clustering showed convergence (Fig. 4.10b). It may be assumed that orientation of the quinoline towards the porphyrin ring is a metabolically active orientation since this orientation is adopted mainly by the deprotected analogues which are relatively weaker inhibitors. No abundant cluster was observed for **32a** even after increasing the number of evaluations tenfold.

The lowest energy conformation of **32a** was found to be similar to what has been observed before for other deprotected compounds. However, the pyridinone group appears to be docked deeper into the hydrophobic pocket with a very close interaction with the Phe304 residue more than what was observed for **16a.** This could be due to the presence of the hydrophobic cyclopropyl group that interacts more with the hydrophobic pocket and positions the ligand far from the CYP3A4 active site. This may explain why **32a** has been predicted to have a higher affinity (K_i = 0.56µM) for CYP3A4 than **16a** (K_i = 2.71µM) (Fig 4.10 a).

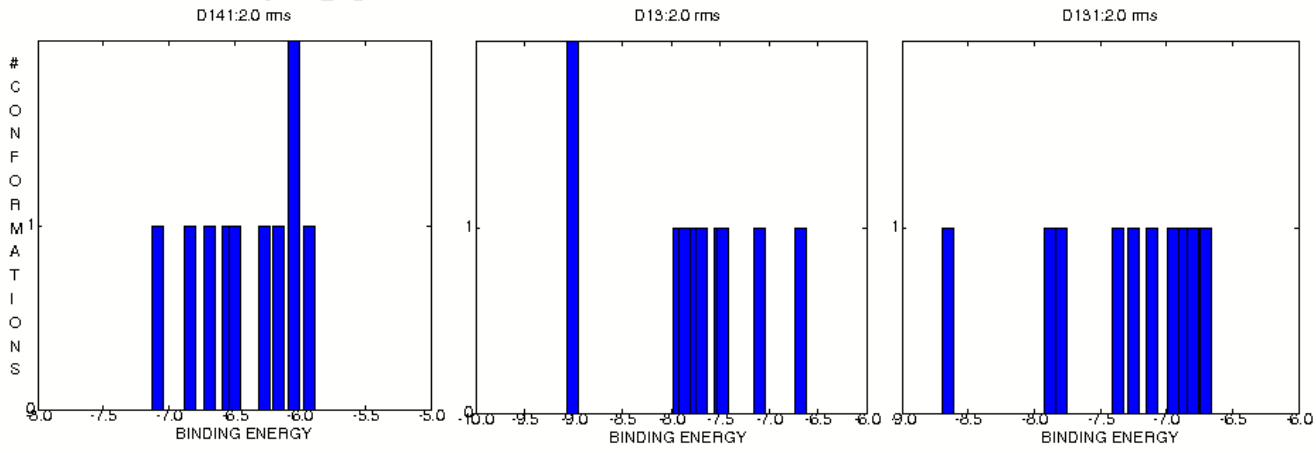

Figure 4.10 b: *Clustering histograms of* ***31a*** *(D141),* ***32*** *(D13) and* ***32a*** *(D131)*

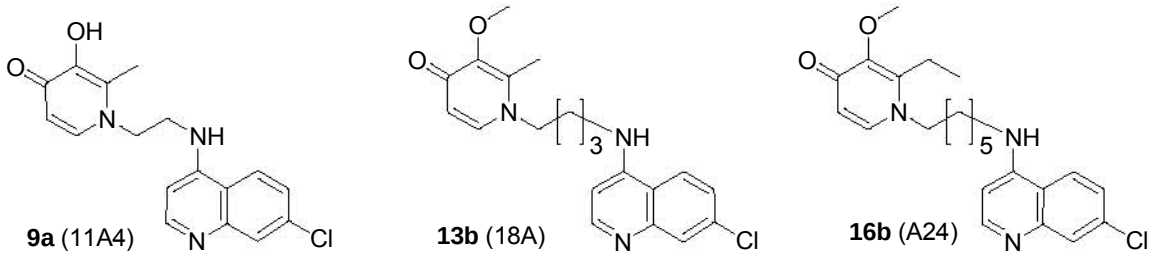

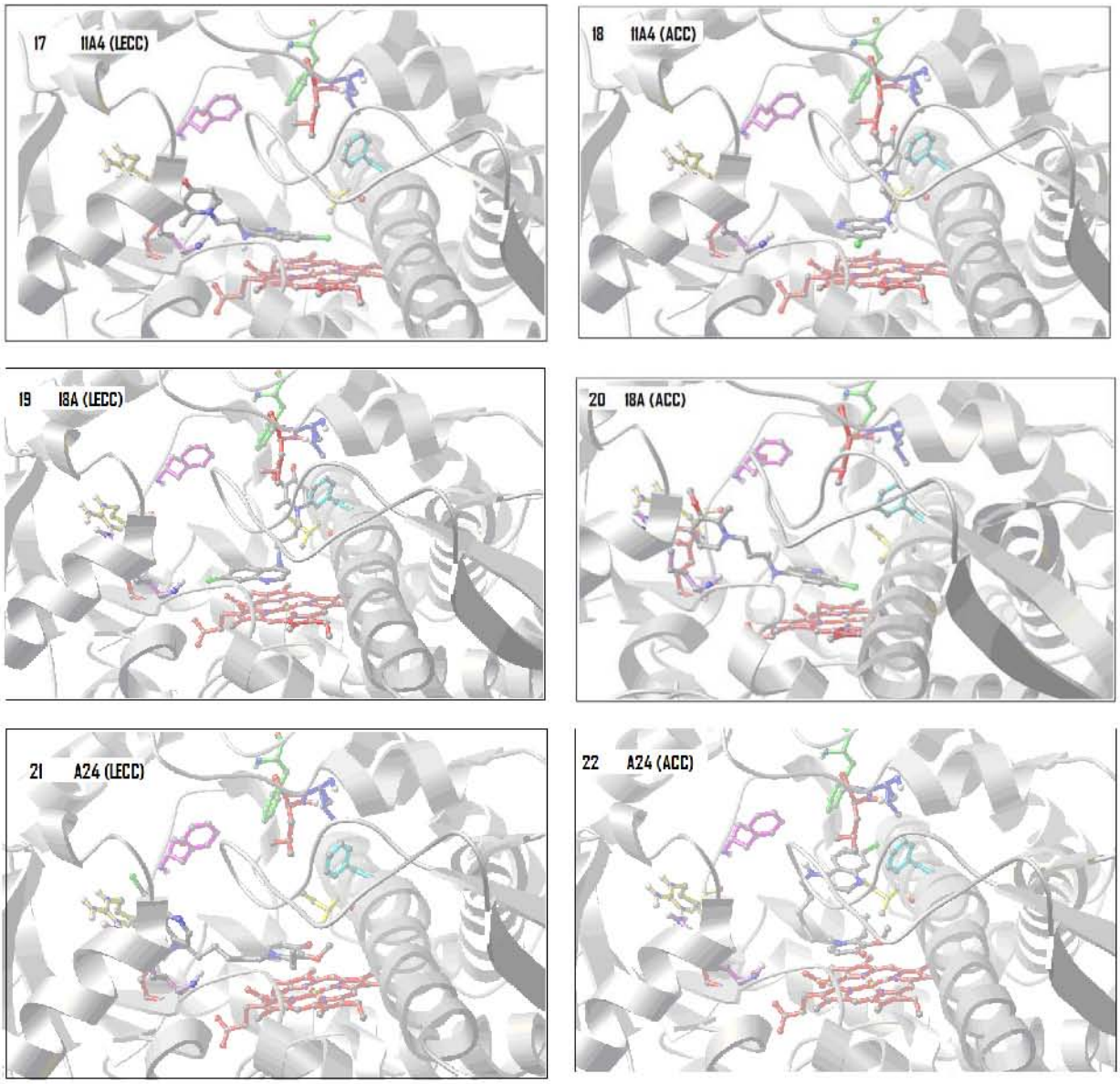

Figure 4.11 a: *Molecular models of* ***9a*** *(11A4),* ***13b*** *(18A) and* ***16b*** *(A24) in the active site of CYP3A4 predicted by AutoDock version 4.2 .A representative conformation from the lowest energy cluster (LECC), in the right hand side panes and a representative conformation from the abundant cluster (ACC), in the left hand side panes. See the clustering histograms in Figure 4.11 b.*

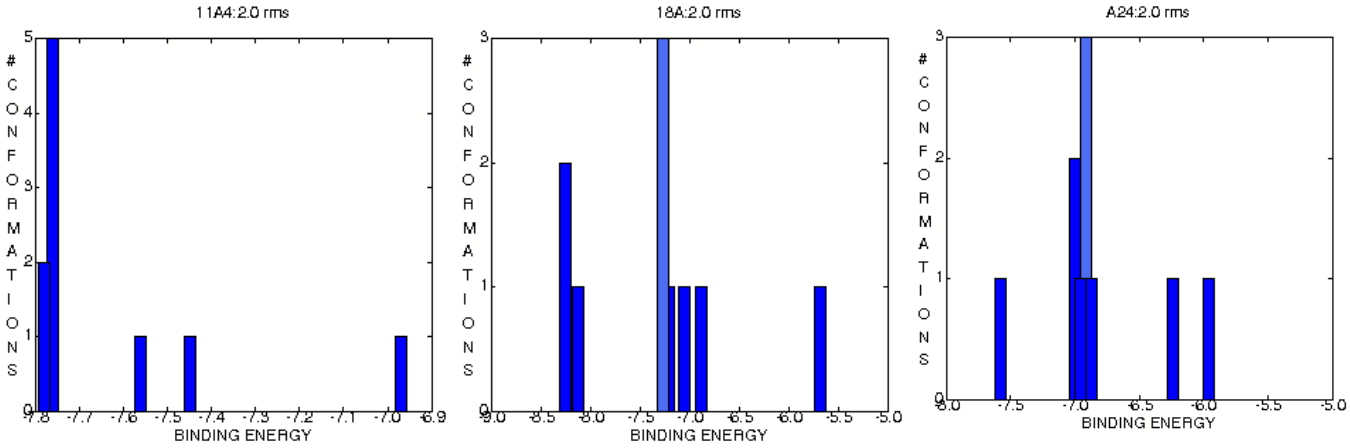

Figure 4.11 b: *Clustering histograms of **9a** (11A4), **13b** (18A) and **16b** (A24).*

In both **16a** (13AB1) and **32a** (D131), the alkyl linker chain seems to contribute to the binding in the hydrophobic pocket via interaction with the Ile 301 residue. Future drug design for these types of molecules may consider use of hydrophilic linkers to reduce this interaction and hence improve the CYP3A4 inhibition profile of the compounds. The hydrophobic alkyl linker prevents the ligand from binding to the polar pocket which is closer to the CYP3A4 active site. Instead it enables it to bind strongly inside the hydrophobic pocket pulling it off the proximity of the active site. The double drugs with smaller alkyl linkers eg **9a** (11A4) interact less with the Ile 301 hence bind easily to the polar pocket (Fig. 4.11 a) and consequently are docked in the proximity of the active site.

4.2.3.5 Compounds 13b (18A), **16b (**A24) **and 9a** (11A4)

Docking conformations of three of the four 3-methoxy protected double drugs were via the quinoline nucleus π-π stacking to the heme's porphyrin rings. This resembles the predicted interactions of the deprotected double drugs in the CYP3A4 active site. For example the conformations of **13b** are similar to that of the deprotected double drugs with short alkyl linkers like **9a** (Fig. 4.11 a). Such conformations as observed for deprotected and methoxylated analogues may be used to distinguish weak inhibitors from potent ones. The conformations of **9a** and **13b**, show the ligands placed very close to the active site and it may be assumed that these results in metabolism rather than inhibition. In fact

9a (K_i =39.6μM) has the lowest *in vitro* affinity constant for CY3A4 in the **A**/**AB** series (Table 4.1)

Compound **16b** docking mode (Figure 4.10) was observed to be similar to that of DFP (Fig. 4.9 a) and compound **31a** (Fig. 4.10 a)**.** Such a mode was assumed to be metabolically active and hypothesized to result in less inhibition of CYP3A4 or less affinity for CYP3A4.

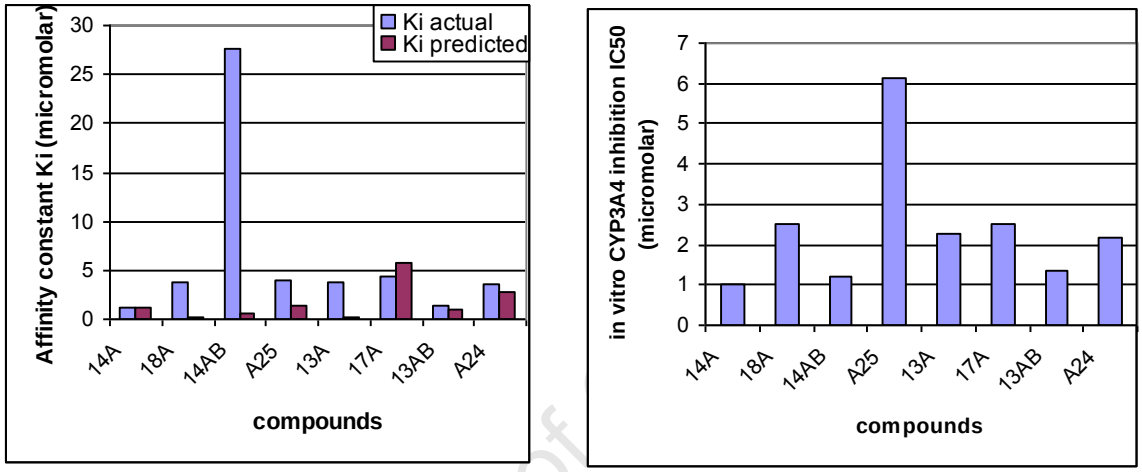

Figure 4.12: *Comparing the in vitro determined (actual) and in silico predicted affinity constants, and the in vitro CYP3A4 inhibition activity of benzylated and methoxylated double drugs from the* ***A/AB*** *series.*

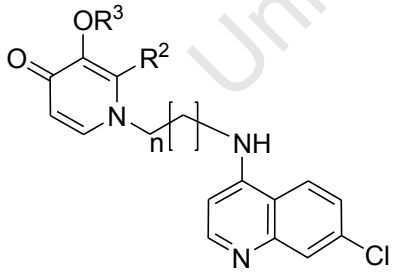

	R^3	n	R^2
14A (**13**)	Bn	3	Me
18A (**13b**)	Me	3	Me
14AB (**14**)	Bn	3	Et
A25 (**14b**)	Me	3	Et
13A (**15**)	Bn	5	Me
17A (**15b**)	Me	5	Me
13AB (**16**)	Bn	5	Et
A24 (**16b**)	Me	5	Et

Figure 4.12b: *Structures of methoxylated double drugs and their benzylated analogues*

The actual affinity of 3-methoxy protected analogues for CYP3A4 was found to be less than that of the benzylated analogues (Fig. 4.12a, b, Table 4.2), the exceptional pair was **14** (14AB) and **14b** (A25). A similar trend was observed in the predicted K_i with one exceptional pair **13** (14A) and **13b** (18A). This shows that to a greater extend there is an agreement between the predicted and actual affinity trends, the deviations noted could be due to *in vitro* experimental error. It is suggested that replacing the benzyl or methoxy groups with smaller and polar protecting groups such as the acetates and use of hydrophilic linkers such as ethers may enhance binding of these ligands into the polar pockets. Such binding would orient the ligand closer to the CYP3A4 active site and hence result in metabolism rather than inhibition.

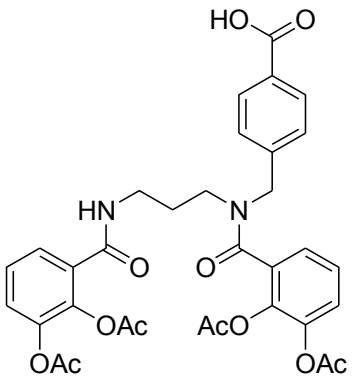

36 (C6)

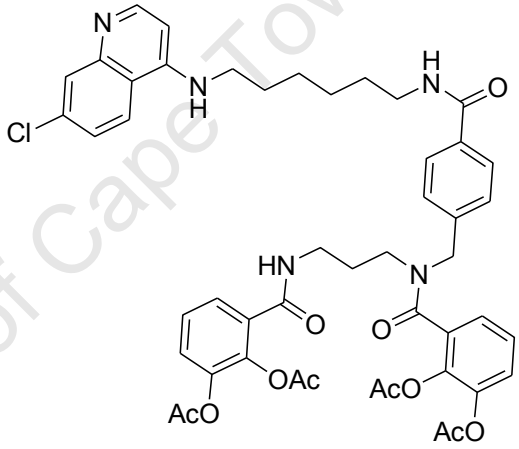

37 (C7R)

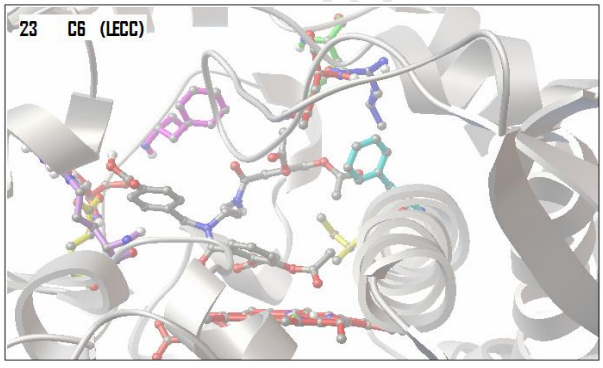

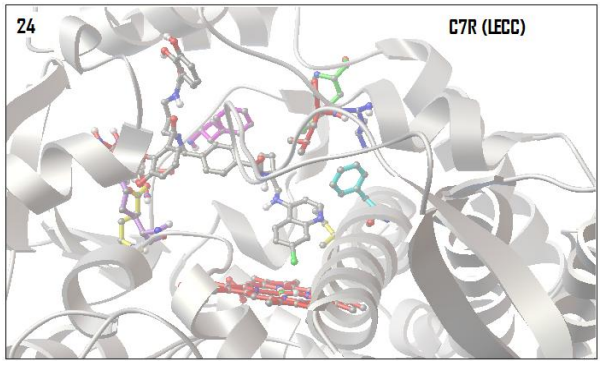

Figure 4.12a: *Molecular models of the **36** (C6) and **37** (C7R) in the active site of CYP3A4 predicted by AutoDock version 4.2. Only a representative conformation from the lowest energy clusterLECC is depicted for each catecholate compound since no abundant cluster was observed in both. See Figure 4.12b.*

4.2.3.5 Compounds **36** (C6) and **37** (C7R)

The docking conformation of compound **36** shows the acetate group is closely docked towards the active site whereas in **37** it is the Cl of the quinoline that is oriented closer to the active site (Fig. 4.13)

The orientation of compound **36** in the active site is assumed to result in metabolism because its binding affinity (K_i = 0.44μM) for CYP3A4 was lower than that of **37** (K_i = 0.06μM**)**. The **37** (C7R) docking mode seems to pull the quinoline group away from the active site into the hydrophobic pocket thus less metabolism and greater inhibition is expected. Since the lowest energy conformation for **37** resembles that of deprotected double drugs, it was hypothesized that decreasing the number of carbon atoms on the alkyl side chain linking the siderophore to the aminoquinoline may lower its CYP3A4 affinity. This strategy is viable because compounds with 6C in the linker have exhibited higher experimental and predicted affinity for CYP3A4 than those with fewer carbons. Since no clustering was observed (Fig. 4.12b) for the two compounds this experiment is inconclusive therefore optimization of the docking parameters should be considered in the future.

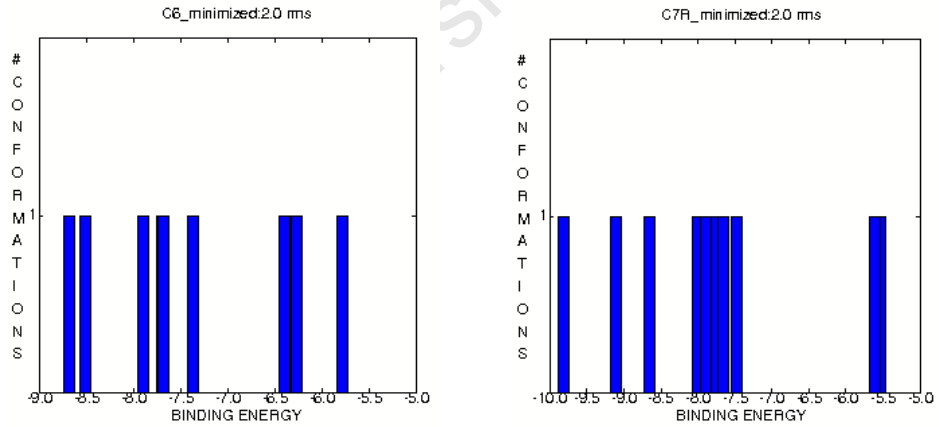

Figure 4.12b: *Clustering histograms of **36** (C6) and **37** (C7R).*

CHAPTER FIVE

EXPERIMENTAL

5.1 Reagents and Purification of solvents

All reagents used in the synthesis were purchased from Sigma Aldrich as analytical grade reagents and were used without further purification. The solvents used were of AR quality and where necessary distilled. Tetrahydrofuran, diethylether and ethanol were dried over sodium wire using benzophenone as indicator.

5.2 Chromatographic separation

Column chromatography was performed using Merck Kieselgel 60: 70-230. Reactions were monitored by thin layer chromatography (TLC) using Merck F_{254} aluminuim backed silica gel 60 pre-coated plates. Detection and visualization of the spots was by ultra violet light (254/366 nm), charring, 0.125 M ferric ammonium sulfate or 2% ninhydrin in methanol. Purification of the compounds by preparative high pressure liquid chromatography (HPLC) and purity analysis was performed on a SPECTRA SYSTEM apparatus with XBridge columns (USA) prep. C18, 5 μ*m,* 19 mm x 250 mm preparative column and XBridge columns (USA) C18, 5μ*m,* 4.6 mm x 150 mm 100A analytical column respectively. Eluents were acetonitrile and water, beginning with ratio of 10:90 (v/v) and reaching 100:0 (v/v) after a period of 15min. (flux rate, 20 or 10mL/min).

5.3 Physical and Spectroscopic characterization

Melting points were determined using a Reichert-Jung Thermovar hot stage microscope and are uncorrected. ^{1}H NMR spectra were recorded using a Varian Mercury spectrometer (300MHz) or on a Bruker spectrometer (400MHz). All spectra were recorded in deuterated chloroform or dimethylsulfate or methanol with tetramethylsilane as an internal standard. ^{13}C NMR was recorded with the same instruments at 75MHz or 100MHz. Chemical shifts (δ) are reported in parts per million (ppm) downfield from the internal standard tetramethylsilane (TMS). High resolution Mass spectrometry (TOF MS ES or ESI) was performed using a Waters API Q-TOF Ultima at Stellenbosch University, Cape Town. Low resolution mass spectrometry (EI+) was performed on a JOEL GC mate III instrument at the University of Cape Town. Microanalyses were performed on a

Fisons EA 1108; C, H, N, S instrument. Infrared spectra were recorded on a Thermo Nicolete FT-IR instrument in the 4000-300 cm^{-1} range using KBr discs.

Single-crystal X-ray diffraction data were collected on a Bruker KAPPA APEX II DUO diffractometer using graphite-monochromated Mo-Kα radiation (χ = 0.71073 Å). Data collection was carried out at 100(2) K. Temperature was controlled by an Oxford Cryostream cooling system (Oxford Cryostat). Cell refinement and data reduction were performed using the program SAINT[1]. The data were scaled and empirical absorption corrections were performed using SADABS. The structure was solved by direct methods using SHELXS-97 and refined by a full-matrix least-squares methods based on F^2 using SHELXL-97 and using the graphics interface program X-Seed. The programs X-Seed and POV-Ray were both used to prepare molecular graphic images.

Solubility was determined using a turbidimetric method at pH 7.4 and was carried out at the AiBST, Harare, Zimbabwe.

5.4 Synthesis

Synthesis of the 3,4-hydroxypyridinones followed documented procedures as described elsewhere (Dobbin P, *et al* 1994; Storr *T,* et al 2003; Ma Y *et al* 2004; Dehkordi *et al* 2008) with some modification. Aminoquinoline intermediates were synthesized as described by Solomon *et al*, 2007. The metal complexes were prepared as described in various references (Green, DE, *et al,* 2005 and Xiao, G. *et al* 1993) with some modifications. Hydrogenation was performed on a Parr instrument at pressures of 1-4 atm. at ambient temperature. Compound purification included crystallization, solvent extraction, precipitation, freeze drying, and column chromatography and HPLC.

5.4.1 Synthesis of *N*-alkyl-3,4-hydroxypyridinones and their gallium (III) complexes

***2-methyl -3-(benzyloxy)-4-pyranone (benzylmaltol)* (1)**

To a solution of 3-hydroxy-2-methylpyranone (maltol) (5.00g; 39.70mmol) in MeOH (38ml) was added NaOH (5ml; 10M) followed by benzylmaltol (6.70g; 52mmol) dropwise. The mixture was refluxed for 22h at 92°C. Complete removal of the solvent under reduced pressure yielded a residue which was mixed with water (80mL) then

extracted into CH_2Cl_2 (80mL×3). The combined organic extracts were washed with 5% (aq) NaOH (80ml×2) followed by water (80ml ×1). The extract was dried over anhydrous Na_2SO_4 and concentrated to give orange oil (**1**).

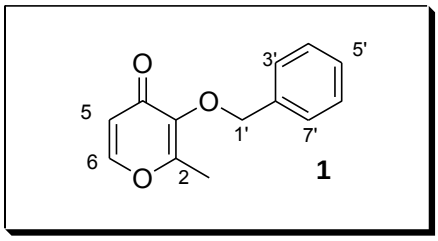

1

Orange oil, (9.45g, 69%). R_f (10% MeOH/CH_2Cl_2) 0.64; δ_H (300MHz, $CDCl_3$) 7.58 (1H, *d, J* 4.8, H-6), 6.36 (1H, *d*, 5.0 H-5), 7.27-7.25(2H, *m*, H- 4', 6'), 7.42-7.30(3H, *m*, H-3',5',7'), 5.16 (2H, *s*, H-1'), 2.09 (3H*, s,* CH_3-2); δ_c (75MHz, $CDCl_3$) 174.9, 159.5, 153.3, 143.7, 136.8, 128.9, 128.6 (2C), 128.3, 128.2, 117.0, 73.4, 14.6;

Synthesis of 1-Ethyl-2-methyl-3-(benzyloxy)-4(1*H*)-pyridinone (2)

Ethylmaltol (l7.84g, 56mmol) was dissolved in MeOH, 10M NaOH (6.9ml, 60mmol) was followed by addition of benzylchloride (6.9ml, 60mmol). The mixture was refluxed at 99^{o}C for 7h. A solid residue (NaCl) was filtered off and the filtrate concentrated to dryness. The resultant oily residue was taken up in CH_2Cl_2 (25ml), washed with 5% w/v NaOH (aq) (3×13ml), finally with water (21×3ml) and dried over anhydrous Na_2SO_4 to give 10.335g of bright orange oil.

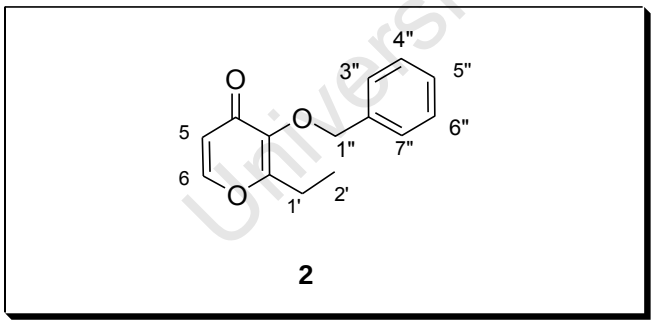

2

Bright orange oil (10.335g, 80%), δ_H (400MHz, $CDCl_3$) 7.6 (1H, *d, J* 5.6, H-6), 7.39 (2H, *dd, J* 2, 7.8 H-4", 6"), 7.35-7.31 (3H, *m,* H-3", 5", 7"), 6.3 (1H, *d, J* 5.6, H-5), 5.2 (2H, *s,* H-1"), 2.5 (2H, *q, J* 7.6 C**H**$_2$-2), 0.99 (3H, *t, J* 7.6, C**H**$_3$-2); δ_C (100MHz, $CDCl_3$) 176, 164, 144, 138, 129 (2C) 128.4 (2C), 128.3 (2C), 117, 73, 21.8, 10.9.

Synthesis of 1,2-Dimethyl-3-(benzyloxy)-4(1H)- pyridinone hydrochloride (1a)

To a solution of benzylmaltol (1.25g; 5.80mmol) in 50% (aq) EtOH (20ml) was added 40% (aq) methylamine (0.8ml; 9.00mmol). Afterwards a catalytic amount of 2N NaOH (0.05ml; 0.01mmol) was added. The mixture was refluxed for 18h at 105°C. The pH of the resultant mixture was ad*j*usted to 7 using NaOH (10N) then extracted into CH_2Cl_2 (50ml×3). The organic layer was dried over anhydrous Na_2SO_4, filtered and concentrated under reduced pressure. The green oil obtained was dissolved in 35ml EtOH/HCl (1:1)), concentrated then recrystalised from EtOH/Et_2O to give a white soli*d,* compound **2**. The other benzylprotected HPOs were synthesized using a similar procedure. Ethylamine, *n*-butylamine, cyclopropylamine, *tert*-propylamine, *n*-propylamine, *n*-hexylamine and *n*-octylamine were used in place of methylamine for the preparations of compounds **1b**, **1c**, **1d**, **1e**, **1f**, **1g**, and **1h** respectively.

1,2-Dimethyl-3-(benzyloxy)-4(1H)- pyridinone hydrochloride **(1a)**

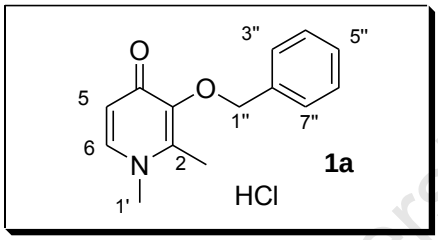

White solid (793mg, 48%); m.p. 190-192; R_f (10% MeOH/CH_2Cl_2) 0.32; V_{max} (KBr) cm^{-1} 3448 (H_2O), 3280 (NH) 1628 (C=O), 843 (py C-H); δ_H (300MHz, $CDCl_3$) 7.38 (2H, *dd, J* 2.1, 7.3, H-4", 6"), 7.3-7.2 (3H, *m,* H-3", 5", 7") 7.14 (1H, *d*, *J* 7.5, H-6), 6.34 (1H, *d, J* 7.4, H-5), 5.16 (2H, *s,* H-1"), 3.48 (3H, *s*, NC**H**$_3$), 2.07 (3H, *s,* CH_3-2); Anal.Calcd (found) for $C_{14}H_{16}ClNO_2.0.5H_2O$: C, 61.2 (62.9); H, 6.24(5.8); N 5.1(5.1).

1-ethyl-2methyl-3-(benzyloxy)-4(1H)-pyridinone hydrochloride **(1b)**

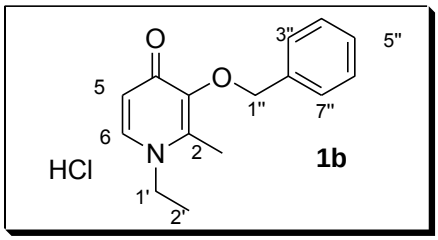

Cream crystals (600mg, 31%); m.p. 151-154°C; R_f (10%MeOH/CH_2Cl_2) 0.25; δ_H (400MHz, $CDCl_3$) 7.4(2H, *dd, J* 1.8, 7.8, H-4", 6"), 7.3(3H, *m,* H-3", 5", 7"), 7.2 (1H, *d, J* 7.5, H-6), 6.4(1H, *d, J* 7.5, H-5), 5.2(2H, *s,* H-1"), 3.8(2H, *q, J*7.25, H-1'), 2.1(3H, *s,* C**H**$_3$-2), 1.3(3H, *t, J* 7.5 NCH_2C**H**$_3$-2'). δc (100MHz, $CDCl_3$) 146.2, 140.2, 137.8, 137.4, 136.8, 129.5, 129.3, 129.1, 128.2,

127.9, 117.7, 72.97, 48.6, 15.79, 12.2; Anal. Calcd (found) for $C_{15}H_{18}ClNO_2.2.5H_2O$: C 55.47 (55.2), H,7.14 (6.4), N 5.4 (4.31).

1-butyl-2-methyl-3(benzyloxy)-4(1H)-pyridinone hydrochloride **(1c)**

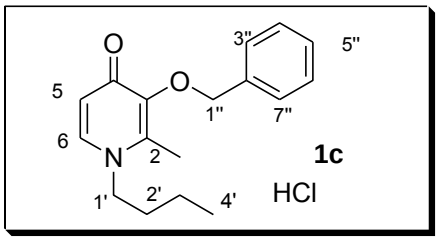

Orange oil (1.1g, 59%); R_f (10%MeOH/CH_2Cl_2) 0.25; δ_H (300MHz, $CDCl_3$) 7.2 (1H, *d, J* 7.5, H-6), 6.4 (1H, *d, J* 7.5 H-5), 7.42-7.37 (2H, *m,* H-4", 6"), 7.35-7.24 (3H, *m,* H-3", 5", 7"), 5.2 (2H, *s,* CH_2-1"), 3.65 (2H, *t, J* 7.4 H-1'), 2.1 (3H, *s,* C**H$_3$**-2), 1.6 (2H, *q* 7.4*,* H-2'), 1.3 (2H, *m,* H-3'), 0.93(3H, *t, J* 7.28 H-4'); δ_C (75MHz, $CDCl_3$) 173.3, 146.1, 140.5, 138, 137.7(2C), 129.1 (2C), 128.2 (2C), 127.9, 72.9, 53.5, 32.7, 20.0, 13.6, 12.4.

1-cyclopropyl-2-methyl-3(benzyloxy)-4(1H)-pyridinone hydrochloride **(1d)**

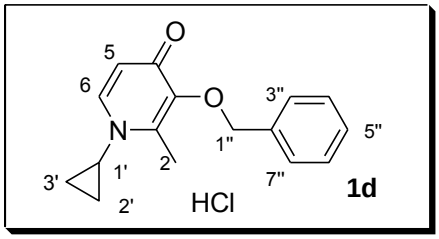

Yellow oil (989.3mg, 47%) R_f (10%MeOH/CH_2Cl_2) 0.38; δ_H (400MHz, $CDCl_3$) 7.41 (2H, *dd, J* 1.6, 7.8, H-4", 6"), 7.3 (3H, *m,* H-3", 5", 7"), 7.2 (1H, *d,* 7.5, H-6) 6.33(1H, *d, J* 7.7, H-5), 5.2 (2H, *s,* H-1"), 3.2 (1H, *septet, J* 4.0 H-1'), 2.15 (3H, *s,* C**H$_3$**-2), 1.01(2H, *m,* H-2'), 0.93(2H, *m,* H-3'); δ_C (100MHz, $CDCl_3$)145.8, 142.9, 138.1, 137.8 (2C), 129, 128.4 (2C), 128.2, 127.9, 116.7, 72.9, 35.4, 12.7, 8.3, 6.5, 5.2. HR-MS (ESI+) found 256.1338 (M+H) $C_{16}H_{18}NO_2$ [M+H] requires 256.1338.

1-isopropyl-2-methyl-3-(benzyloxy)-4(1H)-pyridinone hydrochloride **(1e)**

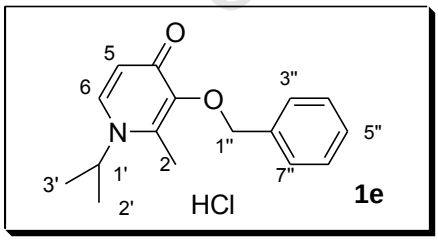

Orange crystals (800mg, 50%), m.p. 171-173^{o}C); Rf (10%MeOH/CH_2Cl_2) 0.54; δ_H (300MHz, $CDCl_3$) 7.4(2H, *dd, J* 7.6, 1.9, H-4", 6"), 7.31(1H, *d, J* 7.8, H-6), 7.7(1H, *d, J* 7.7, H-5), 7.32-7.26 (3H, *m*, H-3", 5", 7"), 5.2 (2H, *s*, H-1''), 4.3(1H, *septet, J* 6.6, H-1'). 2.3 (3H, *s,* C**H$_3$**-2), 1.36 (6H, *d J, 6.6,*H-2', 3'); δ_C (75MHz, $CDCl_3$) 173.1, 145.9, 140.4, 137.7, 132.6, 129.1, 128.2, 127.9, 117.7, 73, 51.6, 22.7, 12.1 (2C).; Anal.Calcd (found) for $C_{16}H_{20}ClNO_2.0.5H_2O$: C 63.47 (64.68); H 6.99 (6.1); N, 4.63 (4.33).

***1-propyl-2-methyl-3(benzyloxy)-4(1H)-pyridinone hydrochloride* (1f)**

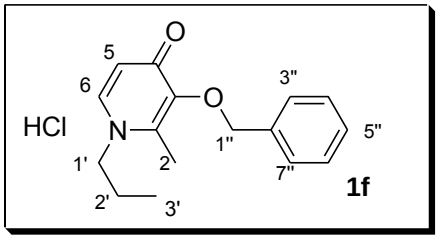

Golden brown crystals (977mg, 44%); m.p. 64-66^{o}C; R_f (10% MeOH/CH_2Cl_2) 0.5; δ_H (400MHz, DMSO) 8.44 (1H, *d, J* 7.14, H-6), 7.52 (1H, *d, J* 7.14, H-5), 7.4 (2H, *d* , *J*, 1.7, 7.8, H-4", 6"), 7.38-7.36 (3H, *m,* H-3", 5", 7"), 5.09 (1H, *s,* H-1"), 4.3 (2H, *t,* 7.4, H-1'), 2.4 (3H, *s,* C**H$_3$**-2), 1.71(2H, *sextet J* 7.5 H-2'), 0.89(3H, *t, J* 7.4, H-3'); δ_C (100MHz, DMSO) 163.7, 149.1, 142.7, 141.9, 136, 128.7 (2C), 128.4 (2C), 128.38, 112.5, 74.1, 57.1, 22.7, 12.95, 10.2. Anal.Calcd (found) $C_{16}H_{20}ClNO_2.5H_2O$: C 61.63 (60.97): H 7.11 (6.97); N 4.49 (4.14).

***1-Hexyl-2-methyl-3(benzyloxy)-4(1H)-pyridinone hydrochloride* (1g)**

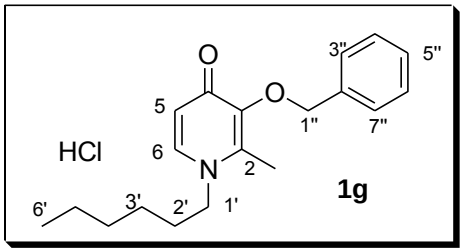

Colourless needles (1.2g, 63%); m.p. 46-48^{o}C. Rf (10% MeOH/ CH_2Cl_2) 0.43; δ_H (300MHz, $CDCl_3$) 7.4 (2H, *dd, J* 2.7, 7.2, H-4", 6"), 7.3 (1H*, d, J* 7.2, H-6), 7.3-7.23(3H, *m,* H-3", 5", 7"), 6.68(1H, *d, J* 7.32, H-5), 5.2 (1H, *s,* H-1"), 3.75 (2H, *t, J* 7.5, H-1'), 2.09 (3H*, s,* C**H$_3$**-2), 1.6 (2H, *quintet, J* 7.2, H-2'), 1.25 (6H, *m,* H-3', 4', 5'), 0.88 (3H, *t, J* 6.6, H-6'); δ_C (75MHz, $CDCl_3$) 171.1, 145.6, 142, 138.7, 137.2, 129.1, 128.3 (2C),128.1 (2C), 116.6, 73.3, 54.4, 31.2, 30.6, 25.9, 22.4, 13.8, 12.5. Anal.Calcd (found) for $C_{19}H_{26}ClNO_2$: C 67.94 (67.73); H 7.8 (6.55); N 4.17 (3.78).

***Octyl-2-methyl-3(benzyloxy)-4(1H)-pyridinone hydrochloride* (1h)**

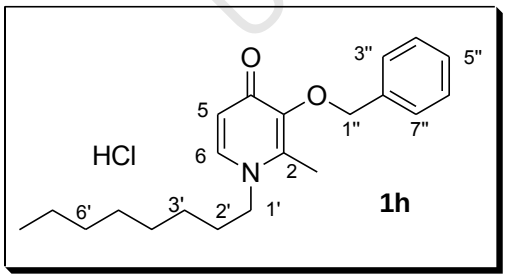

Colourless crystals (630mg, 28%); m.p. 55-57^{o}C; R_f (5%MeOH/CH_2Cl_2) 0.36; δ_H (400MHz, $CDCl_3$) 8.38 (1H, *d, J* 7.02, H-6), 7.99 (1H, *d, J* 7.06, H-5), 7.36-7.31(5H, *m,* H-benzyl), 5.18 (2H, *s,* H-1"), 4.28(2H, *t, J 7.5,* H-1'), 2.38(3H, *s,* H-2), 1.8-1.67(2H, *m*, H-2'), 1.37-1.18(10H, *m,* H-3'- 7'), 0.87(3H, *t, J* 6.75, H-8'); δ_C (100MHz, $CDCl_3$) 164.7, 147.9, 143.4, 141, 135.8, 129.1, 128.8 (2C), 128.6 (2C), 113.5, 74.9, 56.95, 31.6, 30.5, 29.0, 28.9, 26.2, 22.5, 14, 13.3;

Anal.Calcd (found) for $C_{21}H_{30}ClNO_2.H_2O$: C 67.63 (67.48); H 8.38 (8.16); N 3.76 (3.79).

Hydrogenolysis of compound 1a

A solution of compound **1a** (155mg, 0.57mmol) was dissolved in 90% (aq) EtOH and transferred into a 250ml hydrogenation flask, to it was added 8g Pd/C (10%w/w) suspension in 90% (aq) EtOH. The pH was adjusted to 1 (conc. HCl) before hydrogenation at 4bars (58psi) for 4h. Afterwards the mixture was filtered concentrated and recrystalised from EtOH/Et_2O to give a white powder 1C2. A similar method was applied in the deprotection of the other 3,4-HPOs.

Deprotection of compound 1f by acid hydrolysis.

Compound **1f** (39mg, 0.125mmol) was dissolved in ethanolic HCl~2*M,* (4mL, 8mmol) and refluxed at 90^oC for 4h. The solvent was removed by evaporation under reduced pressure followed by recrystalization from EtOH/Et_2O to give yellow crystals of compound, **2f**.

***1,2-Dimethy-3-hydroxy4-(1H)-pyridinone hydrochloride* (2a)**

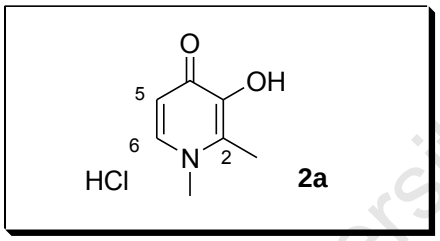

White solid (84mg, 75%); m.p. 163-165^oC; R_f (10%MeOH/CH_2Cl_2) 0.25; V_{max} (KBr) cm^{-1} 3448 (H_2O), 3300 (OH), 3287 (NH), 1632 (C=O), 809 (py C-H); δ_H (300MHz, $CDCl_3$) 8.21 (1H, *d, J* 6.95, H-6), 7.32(1H, *d, J* 6.95, H-5), 3.99(3H, *s,* NC**H**$_3$), 2.5(3H, *s,* C**H**$_3$-2); δ_C (75MHz, $CDCl_3$) 158.6, 142.5, 141.9, 138.3, 110.4, 43.7, 12.6. Anal. Calcd (found) for $C_7H_{10}ClNO_2.H_2O$: C 43.42(43.17); H 6.25(5.54); N 7.24 (7.03).

***1-Ethyl-2-methyl-3-hydroxy-4(1H)-pyridinone Hydrochloride* (2b)**

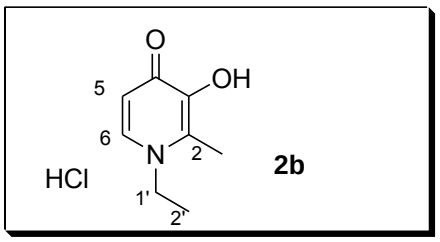

White solid (60mg, 55%); R_f (10%MeOH/ CH_2Cl_2) 0.36; m.p. 166-168^oC; δ_H (300MHz, DMSO) 8.24(1H, *d, J* 6.95, H-6), 7.36(1H, *d, J* 6.93, H-5), 4.34(2H, *q, J* 7.23, H-1'), 2.53 (3H, *s,* C**H**$_3$-2), 1.37(3H, *t, J* 7.2 H-2'); δ_C (75MHz, DMSO) 158.6, 142.8, 140.95, 137.3, 110.9, 51, 15, 12.1; Anal. Calcd. (found) for $C_8H_{12}ClNO_2.0.5H_2O$: C 48.37 (47.95), H 6.6 (6.29), N 7.05 (6.84).

***1-Butyl-2-methyl-3-hydroxy-4(1H)-pyridinone hydrochloride* (2c)**

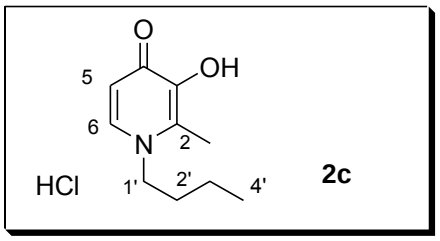

White crystals (350mg, 32%); R_f (10%MeOH/ CH_2Cl_2) 0.38; m.p. 163-166^oC; δ_H (300MHz, DMSO) 8.23(1H, *d, J* 6.97, H-6), 7.38 (1H, *d, J* 6.9, H-5), 4.35(2H, *t, J* 7.5, H-1'), 2.5(3H, *s,* CH_3-2), 1.8-1.64(2H, *m,* H-2') 1.3 (2H, *sextet, J* 7.3 H-3') 0.9(3H, *t, J* 7.2 H-4'); δ_C (75MHz, DMSO) 158.6, 142.8, 141, 137.8, 110.7, 55.5, 31.3, 18.7, 13.1, 12.3; Anal. Calcd. (found) for $C_{10}H_{16}ClNO_2$: C 55.17(55.35), H 7.4 (6.99), N 6.43(6.17)

***1-Cyclopropyl-2-methyl-3-hydroxy-4(1H)-pyridinone Hydrochloride* (2d)**

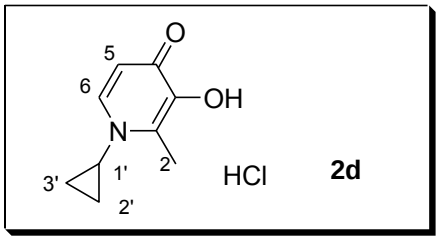

Colourless crystals (467mg, 47%); m.p. 193-197^oC; R_f (10%MeOH/ CH_2Cl_2) 0.47; δ_H (300MHz, DMSO) 8.2 (1H, *d, J* 6.3, H-6), 7.30 (1H, *d, J* 7.2 H-5), 3.87 (1H, *q, J* 5.7, H-1'), 2.6(3H*, s,* C**H$_3$**-2), 1.2(4H, *d, J* 5.4, H-2', 3'); δ_C (75MHz, DMSO) 159.1, 143.5, 142.3, 137.8, 110.1, 40.3, 12.8, 7.4 (2C).; Anal. Calcd. (found) for $C_9H_{12}ClNO_2$: C 53.6 (52.99), H 6.00(5.81), N 6.95 (6.84). HR-MS (ESI+) found 166.0852 (M+H) $C_9H_{12}NO_2$ [M+H] requires 166.0852

***1-isoPropyl-2-methyl-3-hydroxy-4(1H)-pyridinone hydrochloride* (2e)**

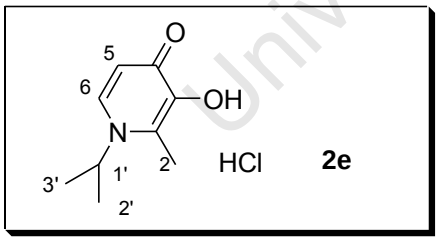

White crystals (85mg, 61%); m.p. 196-197; R_f (10%MeOH/ CH_2Cl_2) 0.45; δ_H (300MHz, DMSO) 8.32 (1H, *d, J* 7.2, H-6), 7.38(1H, *d, J* 6.9. H-5), 4.9 (1H, *septet, J* 6.6, H-1'), 2.58 (3H, *s,* C**H**$_3$-2), 1.46 (6H, *d, J* 6.6, H-2', 3'); δ_C (75MHz, DMSO) 158.4, 142.5, 141.0, 133.7, 111.2, 55.5, 22, 12 (2C); Anal. Calcd. (found) for $C_9H_{14}ClNO_2 1.5H_2O$: C 46.8 (47.9); H 7.73 (6.91); N 6.07 (6.01).

***1-Propyl-2-methyl-3-hydroxy-4(1H)-pyridinone hydrochloride* (2f)**

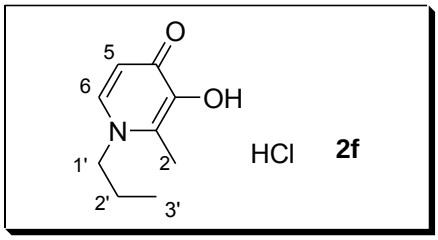

Yellow crystals (86.1mg, 83%* or 23.7mg, 78 %**); m.p. 187-189°C; R_f (10%MeOH/ CH_2Cl_2) 0.45; δ_H (300MHz, DMSO) 8.22 (1H, *d, J* 6.9, H-6), 7.33 (1H, *d, J* 6.9, H-5), 4.27 (2H, *t, J* 7.5, H-1'), 2.52 (3H, *s,* C**H**$_3$-2), 1.76 (2H, *sextet, J* 7.44, H-2'), 0.89(3H, *t, J* 7.4); δ_C (75MHz, DMSO) 158.7, 142.8, 141.1, 137.9, 110.6, 57, 22.7, 12.3, 10.1; . Anal. Calcd. (found) for $C_9H_{14}ClNO_2$: C 53.08 (53.03); H 6.93 (5.2); N 6.88 (6.77). *Hydrogenation produc*t,* **hydrolysis product.

***1-Hexyl-2-methyl-3-hydroxy4-(1H)-pyridinone hydrochloride* (2g)**

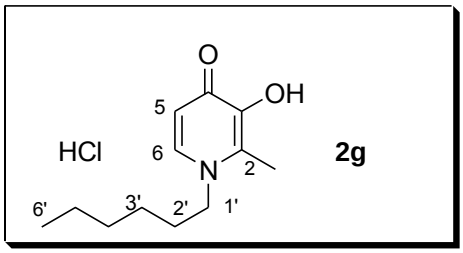

White crystals(77.3mg, 59%); m.p. 163-164°C; R_f (10%MeOH/ CH_2Cl_2) 0.55; δ_H (300MHz, DMSO) 8.2(1H, *d, J* 7.2, H-6), 7.27 (1H, *d, J* 7.2, H-5), 4.3 (2H, *t, J* 7.5, H-1'), 2.4(3H, *s,* C**H**$_3$-2) 1.7 (2H, *quintet, J* 7.6, H-2'), 1.28 (6H, *m,* H-3', 4', 5'), 0.85 (3H, *t, J* 4.5); δ_C (75MHz, DMSO) 158.8, 142.9, 140.9, 137.8, 110.7, 55.7, 30.4, 29.3, 25.0, 21.7, 13.5, 12.3; Anal. Calcd. (found) for $C_{12}H_{20}ClNO_2.0.5H_2O$: C 56.58 (57.8); H 8.31 (7.2); 5.5 (5.19).

***Octyl-2-methyl-3hydroxy-4(1H)-pyridinone hydrochloride* (2h)**

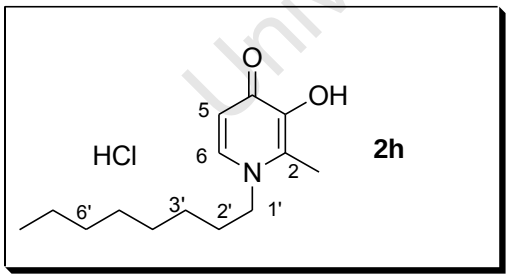

White crystals (155mg, 69%) from EtOH/Et_2O; m.p. 55-57°C; R_f (50%MeOH/EtOAc) 0.73; δ_H (300MHz, CD_3OD) 8.15 (1H, *d, J* 6.9, H-6), 7.1 (1H, *d, J* 6.9 H-5), 4.37(2H,*t, J 7.5,* H-1'), 2.6(3H, *s,* C**H**$_3$-Py), 1.86 (2H, *sextet*, *J* 7.8 H-7'), 1.36 (10H, *m,* H-2'- 6'), 0.9(3H, *t, J* 6.9, H-8'); δ_C (75MHz, CD_3OD) 159.6, 145, 143, 139, 111, 57, 32.8, 31.3, 30.2, 30.1, 27.3, 23.6, 14.4, 12. Anal. Calcd. (found) for $C_{14}H_{24}ClNO_2.1H_2O$: C 57.62 (57.26); H 8.98 (8.97); 4.80 (3.34).

Synthesis of Tris (3-hydroxy-1,2-dimethyl-4-pyridinonato) gallium (III) [3a]

To a solution of compound **2b, (**46mg, 0.3mmol) in MeOH (1ml), was added an aqueous solution of $Ga(NO)_3.9H_2O$ (41.8mg, 0.121mmol) while stirring for 3min.The pH was adjusted to 8 (0.1M NaOH), before refluxing (4h at 80°C). Evaporation to dryness under reduced pressure gave a white powder (68mg), which was dissolved in 1:1 H_2O/MeOH and purified by gel filtration on Sephadex LH 20 with MeOH as the mobile phase. Analogous procedures were used to prepare all the other 3,4-HPO-gallium (III) complexes.

***Tris(3-hydroxy-1,2-dimethyl-4-pyridinonato) gallium (III)*, (3a)**

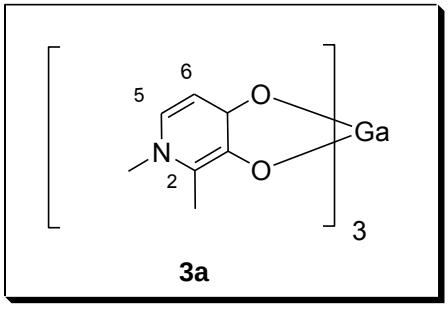

3a

White solid (62mg, 72.1%) m.p. 326-329°C; R_f (10%MeOH/ CH_2Cl_2) 0.07 δ_H (400MHz, DMSO) 7.45 (1H, *d, J* 6.7, H-6), 6.26 (1H, *d, J* 6.7, H-5), 3.7 (3H, *s,* C**H$_3$**-1), 2.28 (3H, *s,* C**H$_3$**-2); MS found 506.11 (ML_3 + Na), 569 (ML_3 + $NaNO_3$)

***Tris(3-hydroxy-2-methyl-1-(ethyl)-4-pyridinonato) gallium (III),* (3b)**

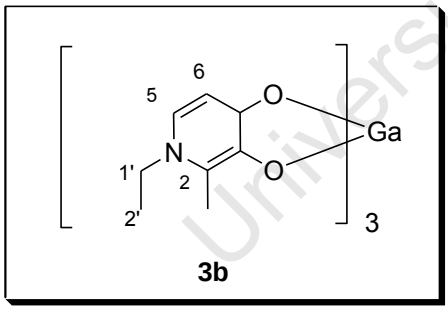

3b

Pink solid 69.7 mg (85%) m.p. 222- 225°C; R_f (10%MeOH/ CH_2Cl_2) 0.08; δ_H (400MHz, DMSO) 7.5 (1H, *d, J* 6.16, H-6), 6.3 (1H, *d, J* 6.29, H-5), 4.1 (2H, *t, J*, 7.2, H-1'), 2.3 (3H, *s,* C**H$_3$**-2), 1.27 (3H, *t, J* 6.8, H-2'); δ_C (100MHz, DMSO) 167.4, 132.2, 128.6, 119.7, 110.2, 106.5, 49.0, 16.0.

***Tris(3-hydroxy-2-methyl-1-(butyl)-4-pyridinonato) gallium (III)* (3c)**

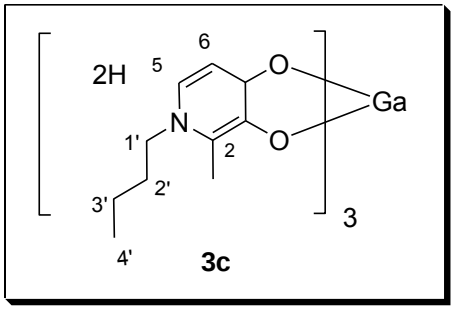

3c

White solid (40.8mg, 59.1%) m.p. 303-305°C; R_f (10%MeOH/ CH_2Cl_2) 0.41 or (EtOAc/MeOH, 1:1) 0.21; δ_H (400MHz, DMSO) 7.5 (1H, *d, J* 6.8, H-6), 6.29 (1H, *d, J* 6.4, H-5), 4.0 (2H, *t, J*, 7.2, H-1'), 2.3 (3H, *s,* C**H$_3$**-2), 1.6 (2H, *q, J* 7.2, H-2'), 1.3 (2H,

septet, J 7.6, H-3'), 0.9(3H, *t,* 7.7, H-4'); δ_C (100MHz, DMSO) 164.7, 153.5, 132.7, 128.3, 105, 53.9, 32.1, 19.0, 13.4, 11.7 Anal. Calcd. (found) for $C_{30}H_{42}GaN_3O_6.4.5H_2O$: C 52.11(52.45); H 7.43 (7.11); N 6.08 (5.54). HR-MS (ESI+) found 610.2408 (ML_3 -2H) $C_{30}H_{30}GaN_3O_6$ [ML_3-2H] requires 610.2408.

***Tris(3-hydroxy-2-methyl-1-(cyclopropyl)-4-pyridinonato) gallium (III),* (3d)**

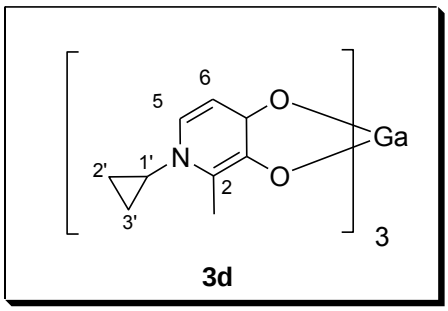

3d

White solid (87mg, 69%); m.p. 237-240 ^oC; R_f (30%EtOAc/MeOH) 0.18; δ_H (300MHz, DMSO) 7.5 (1H, *d,* 6.9, H-6) 6.2 (1H, *d, J* 6.9, H-5), 3.6 (1H, *septet, J* 4.5 H-1'), 2.4 (3H, *s*, C**H**$_3$-2), 1.1 (4H, *m*, H-2',3'); δ_C (100MHz,DMSO)167.9, 152.8, 132.3, 130.9, 105.7, 36.5, 12.2, 12.4 (2C). MS found 397.08 (ML_2), 586.15 (ML_3+Na+2H)

***Tris(3-hydroxy-2-methyl-1-(isopropyl)-4-pyridinonato) Gallium (III)* (3e)**

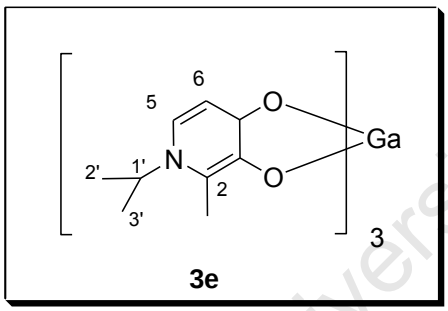

3e

Golden brown crystals (85mg, 75%), m.p. 259-260^oC); R_f (7:1MeOH/EtOAc) 0.29; δ_H (400MHz, DMSO) 7.6 (1H, *d, J* 6.99, H-6), 6.32 (1H, *d, J* 6.9, H-5), 4.6 (1H, *septet, J* 6.5, H-1'), 2.3 (3H, *s,* C**H**$_3$-2), 1.37 (6H, *d J,* 6.6*,* H-2', 3'); δ_C (100MHz, DMSO) 167.2, 128.7, 128.67, 128.1, 110.3, 52.7, 22.4, 11.8 (2C); MS found 401.11 (ML_2), 590.19 (ML_3 + Na).

***Tris(3-hydroxy-2-methyl-1-(propyl)-4-pyridinonato) gallium (III)* (3f)**

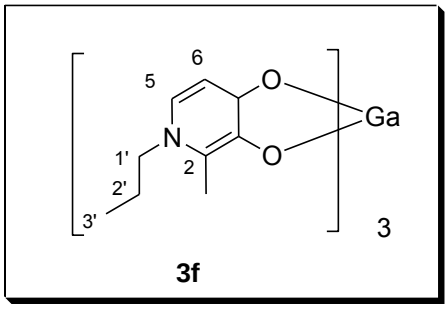

3f

Pink powder (53mg, 47%); m.p. 219-220^oC; R_f (30%EtOAc/MeOH) 0.29; δ_H(300MHz, DMSO) 7.5 (1H, *d, J* 6.7, H-6), 6.26 (1H, *d, J* 6.8, H-5), 3.98 (2H, *t,* 6.7, H-1'), 2.3 (3H, *s,* C**H**$_3$-2), 1.67 (2H, *sextet J* 7.49, H-2'), 0.87 (3H, *t, J* 7.36, H-3'); δ_C (100MHz, DMSO) 167.5, 153.4, 132.6, 128.3, 105.8, 55.4, 23.3, 11.8, 10.3; MS found 403 (ML_2), 590.19 (ML_3+Na).

***Tris(3-hydroxy-2-methyl-1-(hexyl)-4-pyridinonato) gallium (III)* (3g)**

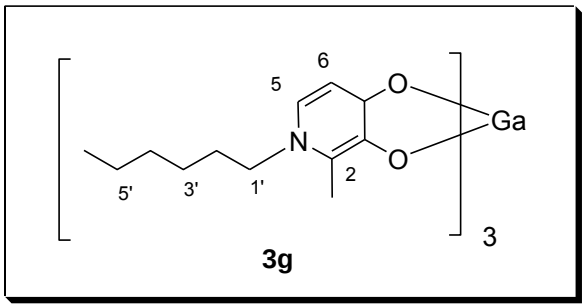

3g

White solid (25mg, 21%); R_f (30%EtOAc/MeOH) 0.77; δ_H (300MHz, DMSO) 7.5 (1H, *d, J* 6.7, H-6), 6.27 (1H, *d, J* 6.7 H-5), 4.01(2H, *t, J 6.9,* H-1'), 2.3 (3H, *s,* C**H$_3$**-2), 1.67(2H, *m*, H-2'), 1.3 (6H, *m,* H-3'- 5'), 0.86 (3H, *t, J* 6.8, H-6'); δ_C (100MHz, DMSO) 168, 128 (2C), 110, 106, 54.1, 30.6, 30.1, 25.4, 21.8, 13.7, 11.9; MS 485.20 (ML_2), 716.33 (ML_3 + Na).

***Tris(3-hydroxy-2-methyl-1-(octyl)-4-pyridinonato) Gallium (III)* (3h)**

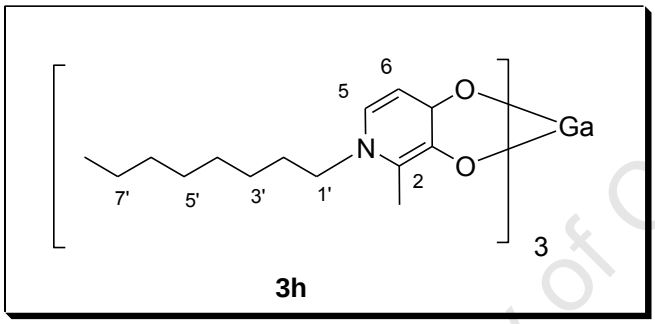

3h

pink resin (73.5mg, 96%) R_f (50%EtOAc/MeOH) 0.83; δ_H (300MHz, CD_3OD) 7.51 (1H, *d, J* 6.6, H-6), 6.51 (1H, *d, J* 6.6 H-5), 4.1 (2H, *t, J* 7.4, H-1'), 2.4 (3H, *s,* CH_3-2), 1.76 (2H, *m*, H-2'), 1.33 (10H, *m,* H-3'- 7'), 0.9 (3H, *t, J* 6.9, H-8'); δ_C (75MHz, CD_3OD) 168.6, 154, 134.8, 133, 108.6, 56.4, 32.9, 31.9, 30.3, 27.4, 23.7, 14.4 (2C), 12.; MS 541.27(ML_2), 778.46 (ML_3+H), Anal. Calcd. (found) for $C_{42}H_{66}GaN_3O_6H_2O$ [ML_3H_2O] C 63.62 (63.10); H 8.82 (8.20); N 5.18 (4.85).

5.4.2. Synthesis of 4-aminoquinoline-3,4-hydroxypyridinone hybrids (A/AB series)

Synthesis of *N*-(7-chloro-4-quinolyl)-1,3-diaminopropane (4)

A mixture of 1,3-diaminopropane (3.7g, 50mmol) and 4,7-dichloroquinoline (2.293g, 11.6mmol) was heated to 80^{o}C for 1.5h under nitrogen atmosphere and subsequently at 145^{o}C for 4h with continuous stirring. After cooling, 2M NaOH (10ml) was added and stirred to precipitate the product, this was washed with water before drying to give 2.83g of the product. Analogous procedures were used to prepare compounds **4, 5**, **6, 7** and **8**.

N-(7-chloro-4-quinolyl)-1,2-diaminoethane (4)

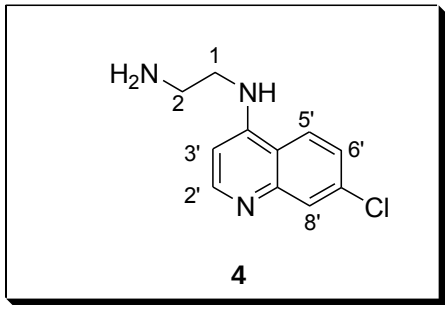

4

Creme solid (1.62g, 97%) R_f (10%MeOH/ CH_2Cl_2) 0.32; δ_H (300MHz, DMSO) 8.4 (1H, *d, J* 8.4, H-5'), 7.8 (1H, *d, J* 5.4, H-2'), 7.8 (1H, *d, J* 2.1, H-8'), 7.4 (1H, *dd, J* 2.4, 9.0, H-6'), 6.6 (1H, *d, J* 5.2, H-3'), 3.57 (2H, *t, J* 6, H-1), 3.1 (2H, *t, J* 6.3, H-2).

N-(7-chloro-4-quinolyl)-1,3-diaminopropane (5)

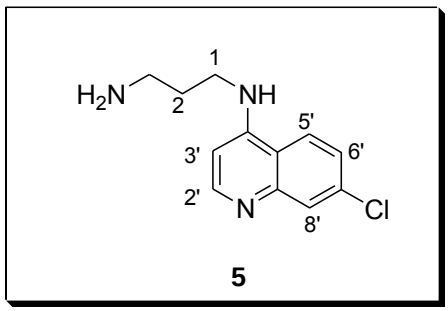

5

White solid (2.83g, 90%); R_f (20%MeOH/ EtOAc) 0.15; V_{max} (KBr) cm^{-1} 3279w (NH), 1575s (C=N), 1532m (C=C), δ_H (400MHz, DMSO) 8.38, (1H, *d, J* 5.2, H-2'), 8.3(1H, *d, J* 8.8, H-5'), 7.7 (1H, *d, J* 2.4, H-8'), 7.38 (2H, *dd, J* 2.4, 9.0, H-6'), 6.47 (1H, *d, J* 5.6, H-3'), 3.36 (2H, *t, J* 6.8, H-1) 1.88 (2H, *t, J* 6.8, H-3), 1.6 (2H, *quintet, J* 6.8, H-2).

***N-(7-chloroquinolin-4-yl)propane -1,3-diamine* (6)**

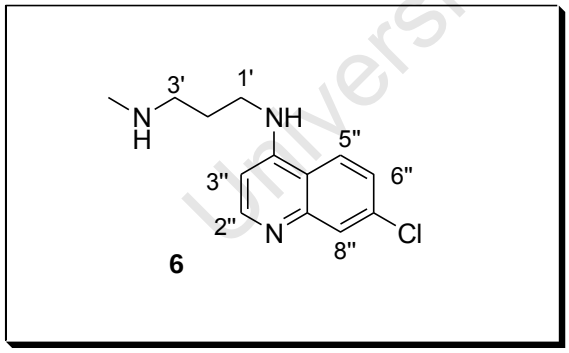

6

Pale brown solid (1g, 98.3%) Rf 0.11 (MeOH/CH_2Cl_2)), δ_H (DMSO d_6), 8.4 (1H, *d, J* 5.2, H-2"), 8.2 (1H, *d, J* 8.8, H-5"), 7.8 (1H, *br.s*, H-8"), 7.52 (1H, *br.s*,1'- NH), 7.43 (1H, *d, J* 8.8, H-6") 6.46 (1H, *d, J* 5.2, H-3") 3.3 (2H, *m,* H-3' obscured by H_2O peak) 2.61 (2H, *t, J* 6.4, H-3'), 2.52 (1H, *br.s*, 3'-NH), 2.31 (3H, *s,* 1-NC**H$_3$**) 1.8 (2H, q, *J* 6.4, H-2'); δ_C (DMSO d_6, 100MHz), 152.6, 150.8, 149.8, 133.9, 128.2, 124.7, 124.6, 118.2, 99.2, 50.2, 41.8, 36.9, 28.

***N-(7-chloro-4-quinolyl)-1,4-diaminobutane* (7)**

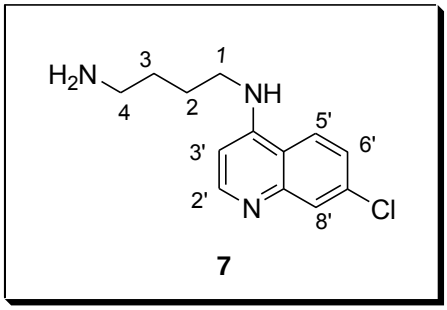

7

Pale yellow solid (2.158g, 79%) ; δ_H (400MHz, DMSO) 8.37 (1H, *d, J* 5.6, H-2'), 8.2 (1H, *d, J* 8.8, H-5'), 7.7 (1H, *d, J* 2.0, H-8'), 7.4 (1H, *dd, J* 2.0, 9.0, H-6'), 6.45 (1H, *d, J* 5.2, H-3'), 3.2 (2H, *t, J* 6.9, H-1), 2.6 (2H, *t, J* 6.4, H-4), 1.7 (2H, *q, J* 7.2, H-2), 1.47 (2H, *q, J* 6.9, H-3); δ_C (75MHz, DMSO) 151.7, 149.99, 148.98, 133, 127.3, 123.9, 123.7, 117.4, 98.5, 42.3, 41.1, 30.5, 25.

***N-(7-chloro-4-quinolyl)-1,6-diaminohexane* (8)**

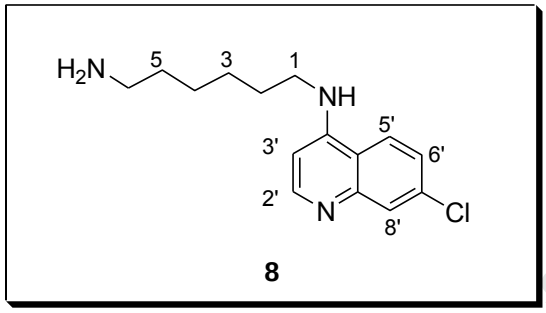

8

White solid (3.823g, 92%) ,δ_H ; (400MHz, DMSO) 8.37 (1H, *d, J* 5.6, H-2'), 8.25 (1H, *d, J* 8.8, H-5'), 7.7 (1H, *d, J* 2.0, H-8'), 7.4 (1H, *dd, J* 2.4, 9.0, H-6'), 6.4 (1H, *d, J* 5.2, H-3'), 3.2 (2H, *q, J* 6.0, H-1), 1.67 (2H, *quintet, J* 6.4, H-6), 1.4 (8H, *m*, H-2,3,4,5); δ_C (100MHz, DMSO) 152.5, 150.9, 149.9, 134, 128.2, 124.7, 124.6, 118, 99.3, 43.2, 28.6, 27.2, 27.1, 26.9 (2C).

Synthesis of *N*-(7-chloro-4-quinolinyl)-aminoalkyl-3-benzyloxy-2-alkyl-4(*1H*)-pyridinones

Ethylbenzylmaltol (**2**, 552mg, 2.4mmol) and *N*-(7-chloro-4-quinolyl)-1,2-diaminobutane (**7,** 1.0g, 3.7mmol) were dissolved in ethanol, then water (25ml) was added to the mixture to obtain a 50% aqueous EtOH solution. The pH of the solution was ad*j*usted to 13 (2M NaOH) before refluxing at 110^{o}C for 24h. Afterwards the pH was ad*j*usted to 1 (2M HCl) before washing with diethylether (50mlx2). On ad*j*ustment of the pH to 7 (2M NaOH), a yellow precipitate formed which was filtered and washed with water and dried under vacuum to give 425mg (36%) of the pure compound **14**.

Analogous procedures were used for preparation of the compounds **9**, **10**, **11**, **12**, **13**, **15** and **16**.

***3-(benzyloxy)-1-(2-(7-chloroquinolin-4-lyamino)ethyl)-2-methylpyridin-4(1H)-one* (9)**

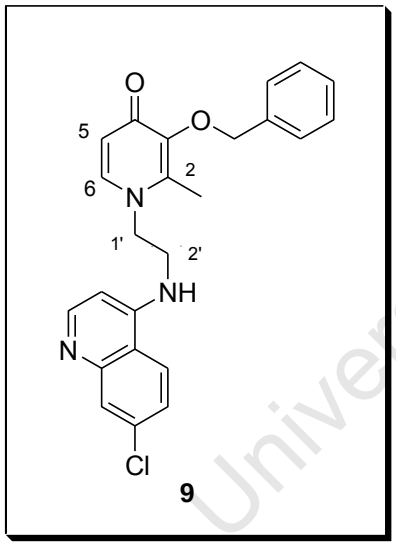

9

Bright yellow crystal*s,* (366mg, 93%), from EtOH/EtOAc; mp. 151-152 ^{0}C. R_f (50%MeOH/ CH_2Cl_2) 0.5; V_{max} (KBr) cm^{-1} 3448w (H_2O), 3280w (NH) 1628s (C=O), 1624s (C=N), 1600s (C=N), 1491m (C=C), 822m (py C-H); δ_H (400MHz, DMSO) 8.77 (1H, *d, J* 9.0, H-5"), 8.6 (1H, *d, J* 7.2, H-2"), 8.34 (1H, *d, J* 7.2, H-6), 8.16 (1H, *d, J* 2.0, H-8"), 7.65 (1H, *dd, J* 2.0, 9.0, H-6"), 7.45-7.28 (5H, *m,* H-benzyl),7.27 (1H, *d, J* 7.27, H-5), 6.99 (1H, *d, J* 7.2, H-3"), 4.92 (2H, *s,* CH_2-Bn), 4.7 (2H, *t, J* 7.2, H-1'), 4.04 (2H, *q, J,* 7.2, H-2'), 2.5 (3H, *s,* C**H**$_3$-2); δ_C(100MHz, DMSO) 164, 156.9, 151.8 (2C), 139.5, 128.1 (2C), 128 (2C), 127.6, 127.5 (2C), 124.3, 124 (2C), 123.8, 123.6, 115.99, 110, 98.7, 71.8, 70.1 (2C), 21.6; HRMS *m/z* calculated for $C_{24}H_{23}N_3O_2Cl$ [M+H] 420.1490 found 420.1479; Anal. Calcd. (found) for C 44.2 (45.23), H 5.7 (4.73), N 8.6 (7.73), $C_{24}H_{22}ClN_3O_2$ 4H_2O; HPLC purity analysis >98%

***3-(benzyloxy)-1-(2-(7-chloroquinolin-4-lyamino)ethyl)-2-ethylpyridin-4(1H)-one* (10)**

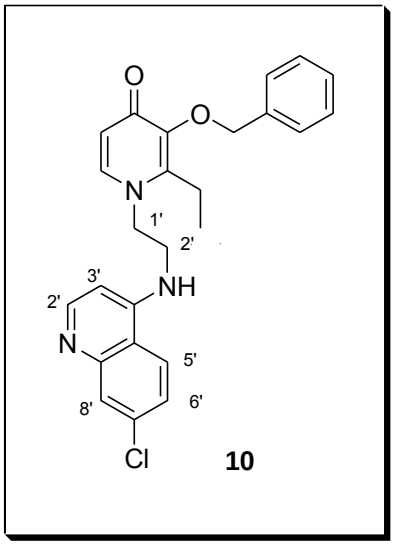

10

Yellow-orange crystals (220mg, 36%), from $CHCl_3/Et_2O$; mp 154-157 ^oC; R_f (50%MeOH/ CH_2Cl_2) 0.6; V_{max} (KBr) cm^{-1} 3400w (H_2O), 3212w (NH) 1629s (C=O), 1607s (C=N), 1582m (C=C), 834m (py C-H); δ_H (400MHz, DMSO) 8.37 (1H, *d, J* 5.6, H-2"), 8.32 (1H, *d, J* 8.9, H-5"), 7.83 (1H, *d, J* 2.2, H-8"), 7.63 (1H, *d, J* 7.6, H-6), 7.5 (1H, *dd, J* 2.2, 8.99, H-6"), 7.32-7.29 (5H, *m,* H-benzyl), 6.5 (1H, *d, J* 5.66, H-3"), 6.1 (1H, *d, J* 7.2, H-5), 4.92 (2H, *s,* CH_2-Bn) 4.18 (2H, *t, J* 6.3, H-2'), 3.6 (2H, *t, J* 7 H-1'), 2.64 (2H, *q, J,* 7.2, $CH_3C\mathbf{H}_2$-2), 0.98 (3H, *t, J* 7.6, $C\mathbf{H}_3CH_2$-2); δ_C (100MHz, DMSO) 209, 150.5, 150.4, 150.39, 145.38, 145.3, 145, 139.8, 139.74,139.78, 139.71, 124.7(2C), 124.6(2C), 116, 98.5 (2C), 71.9, 71.8, 50.5, 42.8, 18.7, 13.1; HRMS *m/z* calculated for $C_{25}H_{25}N_3O_2Cl$ [M+H] 434.1635 found 434.1645. Anal. Calcd. (found) for C 55.41 (55.51), H 6.69 (5.47), N 7.75 (7.83) $C_{25}H_{24}ClN_3O_2$ $6H_2O$; HPLC purity analysis >98%

***3-(benzyloxy)-1-(3-(7-chloroquinolin-4-lyamino)propyl)-2-methylpyridin-4(1H)-one* (11)**

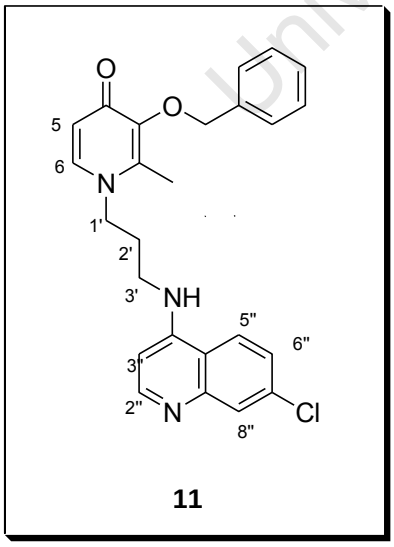

11

White powder (675mg, 45%); m.p 125-127 ^0C; R_f (Et_3N/MeOH/ CH_2Cl_2 ; 0.1:2:8) 0.27; V_{max} (KBr) cm^{-1} 3433w (H_2O), 3224w (NH) 1617s (C=O), 1544s (C=N), 1506m (C=C), 815m (py C-H); δ_H (400MHz, DMSO) 9.4 (1H, *s,* NH), 8.69 (1H, *d, J* 9.2, H-5"), 8.53 (1H, *d, J* 6.8, H-2"), 8.04 (1H, *d, J* 1.6, H-8"), 7.6 (2H, *m,* H-6, 6"), 7.38-7.29 (5H, *m,* H-benzyl), 6.81 (1H, *d, J* 6.8, H-3"), 6.15 (1H, *d, J* 7.2, H-5), 4.99 (2H, *s,* CH_2-Bn) 4.06 (2H, *t, J* 7.2, H-1'), 3.5 (2H, *q, J* 5.6 H-3'), 2.1 (3H, *s,* $C\mathbf{H_3}$-Py), 2.05 (2H, *quintet, J,* 6.8, H-2'). δ_C (100MHz, DMSO) 172.4, 155.5, 146, 144.5, 141.4, 140, 138.4, 138 (2C),

129.2 (2C), 129.1 (2C), 129, 128, 127, 126.6 (2C), 120.6, 116.7, 99.3, 72.5, 51.1, 29.2, 12.6; HRMS *m/z* calculated for $C_{25}H_{25}N_3O_2Cl$ [M+H] 434.1635 found 434.1652. Anal. Calcd. (found) for C 55.41 (55.51), H 6.69 (5.47), N 7.75 (7.83) $C_{25}H_{24}ClN_3O_2$ $6H_2O$; HPLC purity analysis >98%.

***3-(benzyloxy)-1-(3-(7-chloroquinolin-4-lyamino)propyl)-2-ethylpyridin-4(1H)-one* (12)**

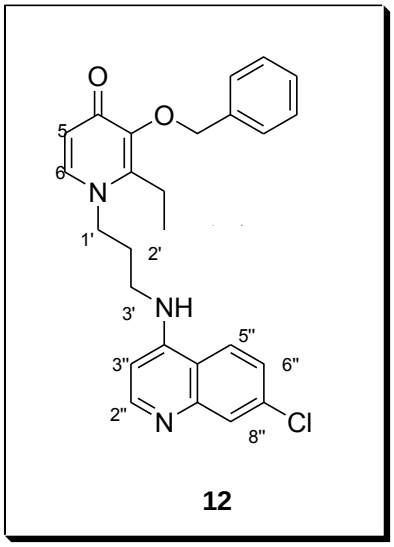

12

Yellow powder (319mg, 21%); m.p 129-130°C R_f (Et_3N/MeOH/ CH_2Cl_2 ; 0.1:2:8) 0.36; V_{max} (KBr) cm^{-1} 3430w (H_2O), 3233w (NH) 1614s (C=O), 1541s (C=N), 1502m (C=C), 818m (py C-H); δ_H (400MHz, DMSO) 9.6 (1H, *s,* NH), 8.73 (1H, *d, J* 8.8, H-5"), 8.54 (1H, *d, J* 7.2, H-2"), 8.06 (1H, *d, J* 2, H-8"), 7.75-7.71 (2H, *m*, H-6, 6"), 7.39-7.28 (5H, *m,* H-benzyl), 6.85 (1H, *d, J* 7.2, H-3"), 6.19 (1H, *d, J* 7.6, H-5), 5.06 (2H, *s,* CH_2-Bn), 4.06 (2H, *t, J* 7.2, H-1'), 3.56 (2H, *q, J* 5.6, H-3'), 2.57 (2H, *q, J* 7.6, $CH_3C\mathbf{H}_2$-Py), 2.08 (2H, *quintet, J* 7.2 H-2') ,0.97 (3H, *t, J* 7.6, $C\mathbf{H}_3CH_2$-Py), δ_C (100MHz, DMSO) 172.5, 155.8, 146, 145, 144, 140, 139.7, 138.5, 138.4, 128.9(2C), 128.8(2C), 128.4, 127, 126.7, 120, 117, 108, 99, 72, 50, 30 (2C), 19, 14.; HRMS *m/z* calculated for $C_{26}H_{27}N_3O_2Cl$ [M+H] 448.1972 found 448.1774 Anal. Calcd. (found) for C 56.16 (56.57), H 6.89 (6.24), N 7.56 (7.65), $C_{26}H_{26}ClN_3O_2$ $6H_2O$; HPLC purity analysis >98%.

***3-(benzyloxy)-1-(4-(7-chloroquinolin-4-lyamino)butyl)-2-methylpyridin-4(1H)-one* (13)**

Cream powder (403mg, 40%); mp 128-130°C; R_f (Et_3N/MeOH/ CH_2Cl_2 ; 0.1:2:8) 0.36; V_{max} (KBr) cm^{-1} 3400w (H_2O), 3034w (NH) 1614s (C=O), 1544s (C=N), 1494m (C=C), 811m (py C-H); δ_H (400MHz, DMSO) 9.8 (1H, *m,* NH), 8.8 (1H, *d, J* 9.2, H-5"), 8.5 (1H, *d, J* 7.2, H-2"), 8.1 (1H, *d, J* 2, H-8"), 8.0 (1H, *d, J* 7.6, H-6), 7.7 (1H, *dd, J* 2, 9.2, H-6"), 7.4-7.33 (5H, *m,* H-benzyl), 6.8 (1H, *d, J* 7.2, H-3"), 6.6 (1H, *d, J* 7.2, H-5), 5.03 (2H, *s,* CH_2-Bn),4.12 (2H, *t, J* 7.2, H-1'), 3.55 (2H, *q, J* 6, H-4'), 2.8 (3H, *s,* $C\mathbf{H}_3$-2), 1.77 (4H, *m,* H-2', 3'); δ_C (100MHz, DMSO) 169.5, 156, 145, 144.5, 143, 141.2, 139, 138, 137.8,

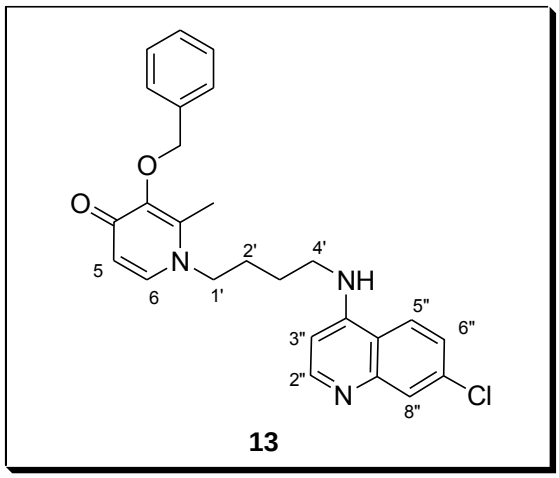

13

129.4, 129.3, 129.1, 128.9, 128.7, 127.4, 126.8, 119.7, 116, 115, 99, 74.2 54, 43, 27.9, 24.9, 13; HRMS *m/z* calculated for $C_{26}H_{27}N_3O_2Cl$ [M+H] 448.1792 found 448.1777; Anal. Calcd. (found) for C 56.16(56.69), H 6.89 (5.84), N 7.56 (7.62) $C_{26}H_{26}ClN_3O_26H_2O$: HPLC purity analysis >98%.

***3-(benzyloxy)-1-(4-(7-chloroquinolin-4-lyamino)butyl)-2-ethylpyridin-4(1H)-one* (14)**

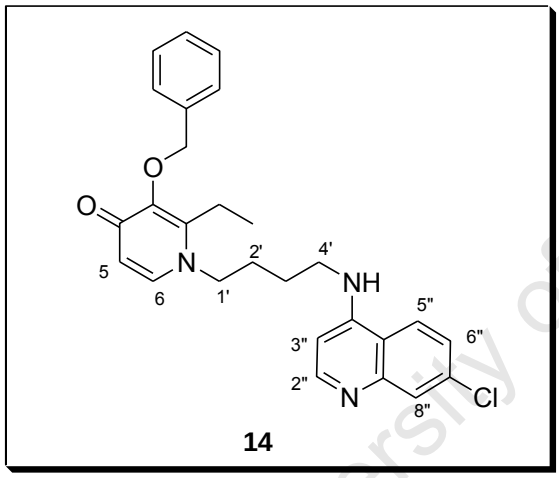

14

Bright yellow powder (403mg, 40%); Mp 112-116^{o}C R_f (Et_3N/MeOH/ CH_2Cl_2 ; 0.1:2:8) 0.36; V_{max} (KBr) cm^{-1} 3392w (H_2O), 3226w (NH) 1613s (C=O), 1575s (C=N), 1540m (C=C), 809m (py C-H); δ_H (400MHz, DMSO) 8.6 (1H, *d, J* 8.8, H-5"), 8.47 (1H, *d, J* 6.8, H-2"), 7.96 (1H, *d, J* 2, H-8"), 7.64. (1H, *d, J* 7.2 H-6), 7.63. (1H, *dd, J* 2, 9.2, H-6"),7.5-7.4 (5H, *m,* H-benzyl), 6.73 (1H, *d, J* 6.4, H-3"), 6.15 (1H, *d, J* 7.2, H-5), 5.1 (2H, *s,* C**H**$_2$-Bn), 3.92 (2H, *t, J* 6.4, H-1'), 3.46 (2H, *m*, H-4'), 2.9 (2H, *q, J* 7.2, CH_3C**H**$_2$ Py), 1.78-1.68 (4H, *m,* H-2', 3') 0.98 (3H, *t , J 7.2,* CH_2C**H**$_3$-2); δ_C (100MHz, DMSO) 174, 146, 145, 140, 137 (2C), 128.9, 128.84 (2C), 128.1 (2C), 128.3(2C), 126.6, 126.5, 126, 122, 116.9, 99 (2C), 72.4, 52.5, 43.3, 29.1, 25, 19.6, 14.1; HRMS *m/z* calculated for $C_{27}H_{29}N_3O_2Cl$ [M+H] 462.1948 found 462.1951; Anal. Calcd. (found) for C 65.12 (65.86), H 6.48 (6.35), N 8.44 (8.65) $C_{27}H_{28}ClN_3O_2$ $2H_2O$; HPLC purity analysis >98%.

***N-(7-chloro-4-quinolinyl)-1-(6-aminohexyl)-3-(benzyloxy)-2-methyl-4(1H)-pyridinone* (15)**

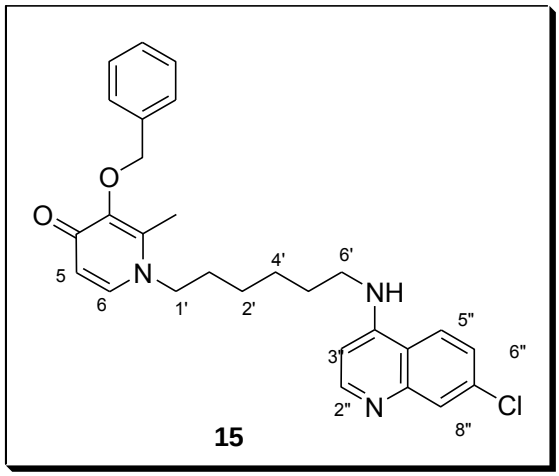

15

Orange oil (330mg, 27%); R_f (Et_3N/MeOH/ CH_2Cl_2 ; 0.1:2:8) 0.69; V_{max} (KBr) cm^{-1} 3400w (H_2O), 3943w (NH) 1630s (C=O), 1618s (C=N), 1580m (C=C), 800m (py C-H); δ_H (300MHz, $CDCl_3$) 8.45 (1H, *d, J* 5.4, H-2"), 7.95 (1H, *d, J* 2.1, H-8"), 7.85 (1H, *d, J* 9, H-5"), 7.32-7.25 (6H, *m,* H-benzyl, H-6"), 7.1 (1H, *d, J* 7.5, H-6), 6.4 - 6.33 (2H, *d, J* 7.5, H-5, 2"), 5.16 (2H, *s,* CH_2-Bn), 3.68 (2H, *t, J* 7.5, H-1'), 3.25 (2H, *q, J* 6.6, H-6'), 2.09 (3H, *s,* C**H**$_3$-2), 1.7 (2H, *quintet, J* 7.2 H-2') 1.57 (2H, *quintet, J* 7.2 H-5'), 1.41-1.22 (2H, *m,* H-3', 4') δ_C (75MHz, $CDCl_3$) 173, 151.7, 150, 149, 140.6, 138, 134.6, 128.8(2C), 128.3 (2C), 128.2, 128, 127.9 (2C), 124.9, 121.8, 117, 98.8 (2C), 72.9, 53.6, 42.9, 30.5, 28.6, 28.4, 26.9, 12.3; HRMS *m/z* calculated for $C_{28}H_{31}N_3O_2Cl$ [M+H] 476.2105 found 476.2094; Anal. Calcd. (found) for C 66.85 (66.91), 6.61 (6.58), 8.35 (5.09), $C_{28}H_{30}ClN_3O_2$ $1.5H_2O$; HPLC purity analysis >98%.

***N-(7-chloro-4-quinolyl)-1-(6-aminohexyl)-3-(benzyloxy)-2-ethyl-4(1H)-pyridinone* (16)**

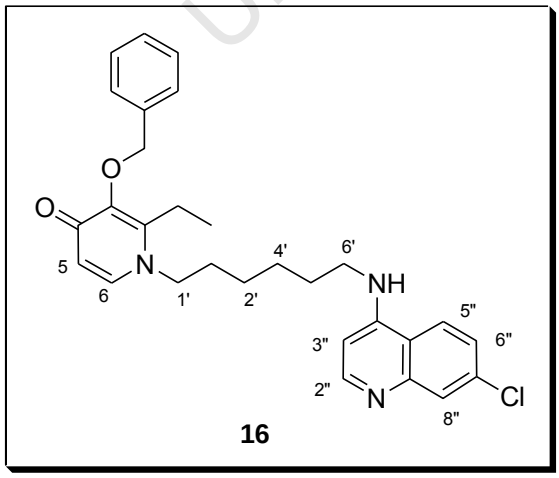

16

Yellow powder (360mg, 34%); Mp 168-170^oC R_f (Et_3N/MeOH/ CH_2Cl_2 ; 0.1:2:8) 0.65; V_{max} (KBr) cm^{-1} 3302w (H_2O), 3103w (NH) 1609s (C=O), 1575s (C=N), 1532m (C=C), 870m (py C-H); δ_H (300MHz, $CDCl_3$) 8.47 (1H, *d, J* 6, H-2"), 7.92 (1H, *d, J* 3, H-8"), 7.78 (1H, *d, J* 9, H-5"), 7.41-7.13 (6H, *m,* H-benzyl, H-6"), 7.14 (1H, *d, J* 6, H-6), 6.38 (1H, *d, J* 6, H- 3"), 6.34 (1H,

d, J 6, H- 5), 5.24 (2H, *s,* CH_2-Bn), 3.73 (2H, *t, J* 6, H-1'), 3.28 (2H, *m,* H-6'), 2.56 (2H, *q, J* 7.5, $CH_3C\mathbf{H}_2$-2), 1.78- 1.62 (4H, *m,* H-2', 5') 1.53 – 1.3 (4H, *m,* H-3',4'), 1.41-1.22 (2H, *m,* H-3', 4'), 1.01 (3H, *t, J* 7.5, $CH_2C\mathbf{H}_3$-2) δ_C (75MHz, $CDCl_3$) 173.5, 151.5, 150, 148.7, 145.9, 145.6, 138.1, 137.7, 134.9, 128.5(2C), 128.2 (2C), 127.9, 125, 121.4, 117.4, 117.2, 98.8 (2C), 72.8, 53.1, 43, 31.2, 29.6, 28.5, 26.7, 19.5, 13.3; HRMS *m/z* calculated for $C_{29}H_{33}N_3O_2Cl$ [M+H] 490.2261 found 490.2265; HPLC purity analysis >98%.

***N-(7-chloro-4-quinolyl)-1-(6-aminohexyl)-3-(benzyloxy)-2-ethyl-4(1H)-pyridinone dihydrogenchloride* (16.HCl salt)**

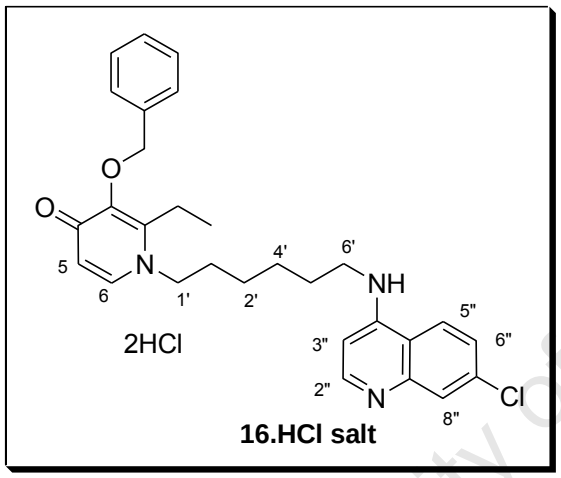

16.HCl salt

0.6ml of 1.25 M HCl (0.75mmol) in MeOH solution was added to **16** (101mg, 0.207mmol) and stirred overnight in a sealed flask. Ethylacetate was added until precipitation was complete, solvent was removed and the white solid dried under vacuum for 2h to give the dry salt Yellow deliquescent solid (550mg, 86%) ; δ_H (300MHz, CD_3OD) 8.48 (1H, *d, J* 8.8, H-5"), 8.38 (2H, *m*, H-2", 6), 7.88 (1H, *d, J* 1.5, H-8"), 7.65 (1H, *dd, J* 2, 9.2, H-6"), 7.60 (5H, *m,* H-benzyl), 7.25 (1H, *d, J* 7.2, H- 3"), 6.88 (1H, *d, J* 7.2, H- 5), 5.25 (2H, *s,* CH_2-Bn), 4.37 (2H, *t, J* 7.6, H-1'), 3.62 (2H, *t, J* 7.2, H-6'), 2.92 (2H, *q, J* 7.6, $CH_3C\mathbf{H}_2$-2), 1.85 (4H, *m,* H-2', 5') 1.51 (4H, *m,* H-3',4'), 1.48 (3H, *t, J* 7.6, $C\mathbf{H_3}CH_2$-2), δ_C (100MHz, CD_3OD) 155.8, 148.1, 146.1(2C), 135.2, 134.2, 133.7, 131.5, 130.5, 127.9, 120.4 (2C), 120.2 (2C), 119.1, 116.8, 110.7, 107.4, 104.8, 90.3, 66.7, 47.9, 35.2, 22.7, 19.4, 17.9, 17.4, 12.1, 3.45; HR-MS m/z calculated for 490.2557 $C_{29}H_{33}Cl_3N_3O_2$. [M + H] found 492.2278; Anal. Calcd. (found) for C 56.45 (56.77), H 6.53 (6.51), N 6.81 (6.41) $C_{29}H_{34}Cl_3N_3O_2.3H_2O$.

Representative procedure for the synthesis of *N*-(7-chloro-4-quinolinyl)-diaminoalkyl-3-(hydroxy)-2-alkyl-4(*1H*)-pyridinones (deprotection)

237mg (0.48mmol) of compound **16** was dissolved in 30ml 2M ethanolic-HCl then subjected to hydrogenation in the presence of Pd/C 40mg (10 %w/w), 4 atmospheres pressure for 6.5h. Then the catalyst was filtered off and the solvent removed by rotary evaporation to give 169mg (88%) of a brown resin, **16a**. Similar procedures were used to deprotect the other compounds with recrystalisation where possible.

***N-(7-chloro-4-quinolinylaminoethyl)-3-(hydrox)y-2-methyl-4(1H)-pyridinone dihydrogen chloride* (9a)**

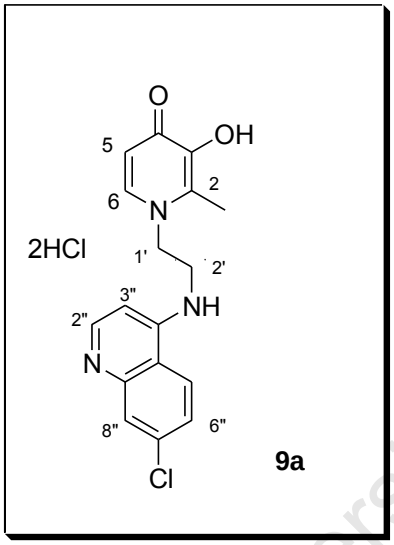

9a

White crystals (42mg, 68%), from EtOH/EtOAc; Mp 173-175°C R_f (20%MeOH/ CH_2Cl_2) 0.35; V_{max} (KBr) cm^{-1} 3398br.w (OH), 3224w (NH) 1624s (C=O), 1606s (C=N), 1588m (C=C), 825m (py C-H); δ_H (300MHz, CD_3OD); 8.5 (1H, *d, J* 7.6, H-2"), 8.4 (1H, *d, J* 9.3, H-5"), 8.16 (1H, *d, J* 6.9, H-6), 7.95 (1H, *d, J* 1.8, H-8"), 7.7 (1H, *dd, J* 1.8, 9.3, H-6"), 7.06 (1H, *d, J* 6.9, H-5 Py), 7.01 (1H, *d, J* 7.2, H-3"), 4.8 (masked by H_2O peak, H-1'), 4.17 (2H, *t, J,* 6, H-2'), 2.7 (3H, *s,* C**H**$_3$-2); δ_C (75MHz, CD_3OD) 160, 144.6, 141.5, 139.9, 132, 129.3 (2C), 129.3 (2C), 126.2, 126.1, 120.6, 111.9, 99.9, 55.4 25, 13. MS. *m/z* calculated for $C_{17}H_{16}N_3O_2Cl$ [M+H] 329.78 found 330.1 (100%); Calcd. (found) for C 39.97 (40.08), H 5.92 (5.03), N 8.23 (9.19) $C_{17}H_{18}Cl_3N_3O_26H_2O$; HPLC purity analysis >98%.

***N-(7-chloro-4-quinolyl)-1-(2-aminoethyl)-3-(hydroxy)-2-ethyl-4(1H)-pyridinone dihydrogen chloride* (10a)**

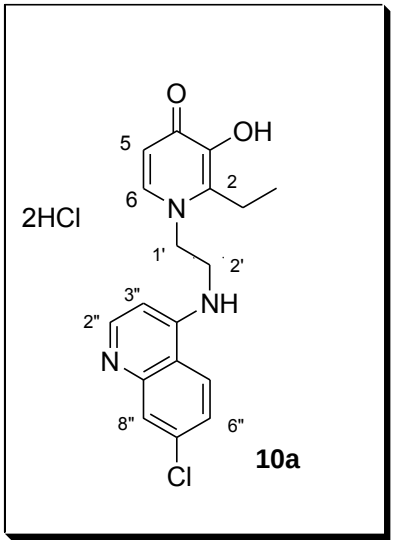

10a

Cream crystals (33mg, 30%), from Et_2O; Mp 178-180^oC R_f (50%MeOH/ CH_2Cl_2) 0.22; V_{max} (KBr) cm^{-1} 3411br.w (OH), 3212w (NH) 1624s (C=O), 1602s (C=N), 1582m (C=C), 815m (py C-H); δ_H (400MHz, CD_3OD) 8.5 (1H, *d, J* 6.8, H- 2"), 8.4 (1H, *d, J* 9.2, H-5"), 8.17 (1H, *d, J* 6.8, H-6), 7.95 (1H, *d, J* 2, H-8"), 7.7 (1H, *dd, J* 2.0, 9.0, H-6"), 7.07 (1H, *d, J* 6.8, H-5 Py), 6.98 (1H, *d, J* 7.2, H-3"), 4.18 (2H, *t, J* 6.0, H-1'), 3.3 (masked by H_2O peak H-2'), 3.14 (2H, *q, J,* 7.6, CH_3 C**H**$_2$-2), 1.3 (3H, *t, J* 7.6, CH_2C**H**$_3$-Py); δ_C (75MHz, CD_3OD) 160, 157, 148, 145, 144, 141, 140, 129(2C), 126, 120, 117,112, 99, 54, 44, 21, 12; HPLC purity analysis >98%.

***N-(7-chloro-4-quinolyl)-1-(4-aminoethyl)-3-(hydroxy)-2-methyl-4(1H)-pyridinone* (11a)**

The benzylated analogue **11**, (45mg 0.104mmol) was dissolved in a solvent mixture (water, conc. HCl, EtOH, 1:3:2) and the resultant slurry refluxed at 74^oC, for 12h. Solvent removal by evaporation in vacuo afforded compound **11a.** Which was further dried under vacuum. Bright orange powder (25mg, 50%); mp. 143-146 ^0C; Rf 0.24 (MeOH/ CH_2Cl_2 1:1), V_{max} (KBr) cm^{-1} 3422br.w (OH), 3226w (NH) 1636s (C=O), 1613s (C=N), 1590m (C=C), 759m (py C-H); δ_H (CD_3OD, 400MHz) 8.5 (1H, *d, J* 9.2, H-5"), 8.45 (1H, *d, J* 6.8, H-2"), 8.31 (1H, *d, J* 6.4, H-6), 7.9 (1H, *d, J* 2, H-8"), 7.71 (1H, *dd, J* 1.6, 9.0, H-6"), 7.1 (1H, *d, J* 6.4, H-3"), 6.99 (1H, *d, J* 6.4, H-5), 4.6 (2H, *t, J* 5.6, H-3'), 3.79 (2H, *t, J* 6.4, H-1') 2.66 (3H, *s,* CH_3-2), 2.39 (2H,

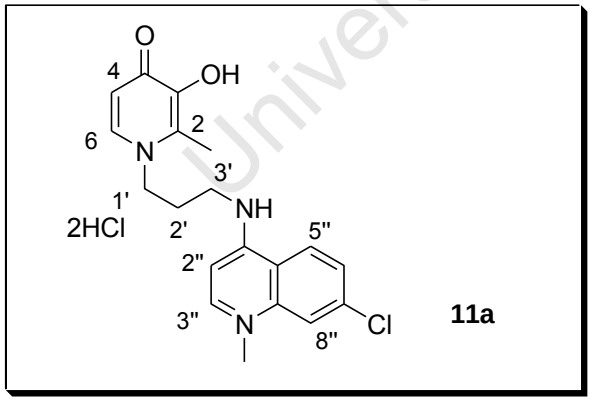

11a

m, H-2').; δ_C (CD_3OD, 100MHz), 158, 156, 142, 140 (2C), 136, 126 (2C), 123.6 (2C), 117.6, 109, 114, 97.3, 54, 39, 26.9, 10.1; MS. *m/z* calculated for $C_{18}H_{18}N_3O_2Cl$ [M+H] 344.11 found 344.1 (100%); Anal. Calcd (found) for $C_{18}H_{20}Cl_3N_3O_2$ $4H_2O$, C 44.23 (43.95), H 5.77 (5.24), N 8.60 (9.31); HPLC purity analysis >98%

***N-(7-chloro-4-quinolyl)-1-(3-aminopropyl)-3-(hydroxy)-2-ethyl-4(1H)-pyridinone dihydrogen chloride* (12a)**

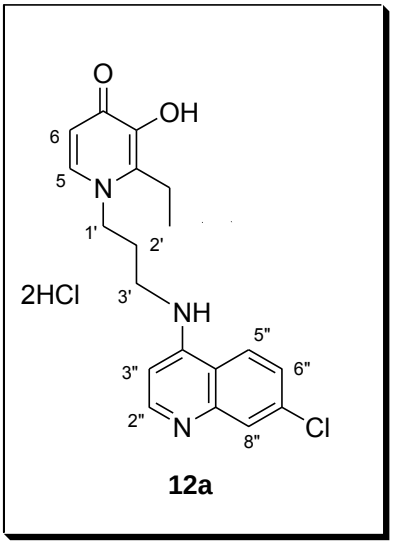

12a

Brown powder (70mg, 40%); mp.180 - 184°C R_f (50% MeOH/ CH_2Cl_2) 0.54; V_{max} (KBr) cm^{-1} 3443br.w (OH), 3241w (NH) 1632s (C=O), 1613s (C=N), 1586m (C=C), 820m (py C-H); δ_H (400MHz, CD_3OD) 8.5 (1H, *d, J* 9.2, H-5"), 8.4 (1H, *d, J* 7.2, H-2"), 8.3 (1H, *d, J* 7.2, H-6), 7.9 (1H, *d, J* 1.6, H-8"), 7.7 (1H, *dd, J* 2.0, 8.8, H-6"), 7.1 (1H, *d, J* 6.8, H-3"), 7.0 (1H, *d, J* 7.2, H-5), 4.6 (2H, *t, J* 7.6, H-1'), 3.8 (2H, *t, J* 6.8, H-3'), 3.1 (2H, *q, J* 7.6, $CH_3C\mathbf{H}_2$-2), 2.4 (2H, *quintet, J* 6.8, H-2'), 1.27 (3H, *t, J* 7.6 $CH_2C\mathbf{H}_3$-2); δ_C (75MHz, CD_3OD) 159.9, 157.7, 147.9, 144.9, 144.1, 139.9, 139.5, 128.8(2C), 126.5, 120.3, 117, 112, 100, 54, 30.7, 41.7, 21.2, 12.2.; MS. *m/z* calculated for $C_{19}H_{21}N_3O_2Cl$ [M+H] 358.13 found 358.1. Anal. Calcd. (found) for C 42.35 (41.76), H 6.36 (5.58), N 7.8 (8.10), $C_{19}H_{22}ClN_3O_2$ $6H_2O$; HPLC purity analysis >98%

***N-(7-chloro-4-quinolyl)-1-(4-aminobutyl)-3-(hydroxy)-2-methyl-4(1H)-pyridinone dihydrogen chloride* (13a)**

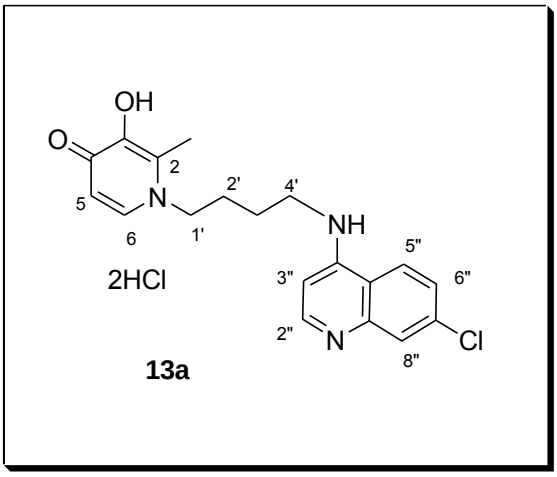

13a

Brown crystals (100mg, 70%) from hot Et_2O; R_f (50% MeOH/ CH_2Cl_2) 0.3; V_{max} (KBr) cm^{-1} 3399br.w (OH), 3239w (NH) 1632s (C=O), 1609s (C=N), 1577m (C=C), 813m (py C-H); δ_H (400MHz, DMSO) 9.9 (1H, *m,* NH), 8.87 (1H, *d, J* 9.3, H-5"), 8.5 (1H, *d, J* 7.2, H-2"), 8.36 (1H, *d, J* 6.9, H-6), 8.1 (1H, *d, J* 2.1, H-8"), 7.7 (1H, *dd, J*

1.8, 9.0, H-6"), 7.34 (1H, *d, J* 6.9, H-5), 6.86 (1H, *d, J* 6.9, H-3"), 4.43 (2H, *t, J* 7.2, H-1'), 3.58 (2H, *q, J* 6, H-4'), 2.5 (3H, *s,* C**H**$_3$-2) 1.92-1.77 (4H, *m,* H-2', 3'); δ_C (100MHz, DMSO) 159, 156, 143.6, 143.3 142, 139, 138.8, 127 (2C), 126.9, 119, 116, 111, 99, 70.8, 56, 42.9, 24.8, 13.2.; MS. *m/z* calculated for $C_{19}H_{21}N_3O_2Cl$ [M+H] 358.13 found 358.1 (100%); HPLC purity analysis >98%

***N-(7-chloro-4-quinolyl)-1-(4-aminobutyl)-3-(hydroxy)-2-ethyl-4(1H)-pyridinone dihydrogen chloride* (14a)**

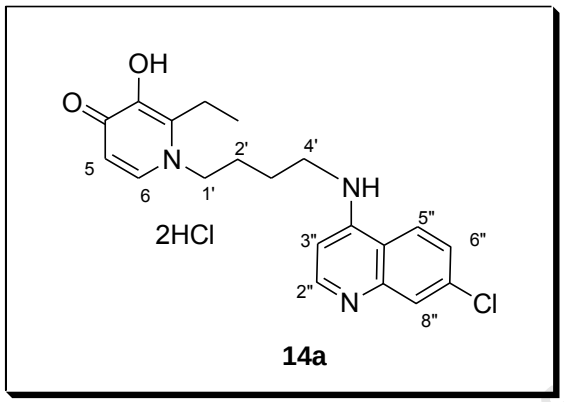

14a

Brown sticky solid (163mg, 76%); R_f (50% MeOH/ CH_2Cl_2 ; 1:2:8) 0.48; V_{max} (KBr) cm^{-1} 3391br.w (OH), 3272w (NH) 1632s (C=O), 1615s (C=N), 1594m (C=C), 797m (py C-H); δ_H (400MHz, CD_3OD) 8.5 (1H, *d, J* 8.8, H-5"), 8.4 (1H, *d, J* 7.2, H-2"), 8.25 (1H, *d, J* 7.2, H-6), 7.89 (1H, *d, J* 2.0, H-8"), 7.69 (1H, *dd, J* 2.0, 8.2, H-6"), 7.1 (1H, *d, J* 7.2, H-5), 6.9 (1H, *d, J* 7.2, H-3"), 4.47 (2H, *t, J* 7.6, H-1'), 3.67 (2H, *t, J* 7.2, H-4'), 3.08 (2H, *t, J* 7.6, CH_3C**H**$_2$-2), 2.05-1.9 (4H, *m,* H-2', 3') 1.29 (3H, *t , J* 7.6, CH_2 C**H**$_3$-2); δ_C (100MHz, CD_3OD) 158.7, 146.7, 142.6 (2C), 138.2, 133.8, 127.5 (2C), 122.9, 119.9, 115.8, 110.8, 98.7, 98.1, 55.7, 42.9, 28.6, 24.7, 19.9, 11.0: MS. *m/z* calculated for $C_{20}H_{23}N_3O_2Cl$ [M+H] 372.15 found 372.1 (100%); Anal. Calcd. (found) for C 44.91 (44.16), H 6.41 (6.01), N 7.84 (8.05), $C_{20}H_{24}Cl_3N_3O_25H_2O$: HPLC purity analysis > 98%

***N-(7-chloro-4-quinolyl)-1-(6-aminohexyl)-3-(hydroxy)-2-methyl-4(1H)-pyridinone dihydrogen chloride* (15a)**

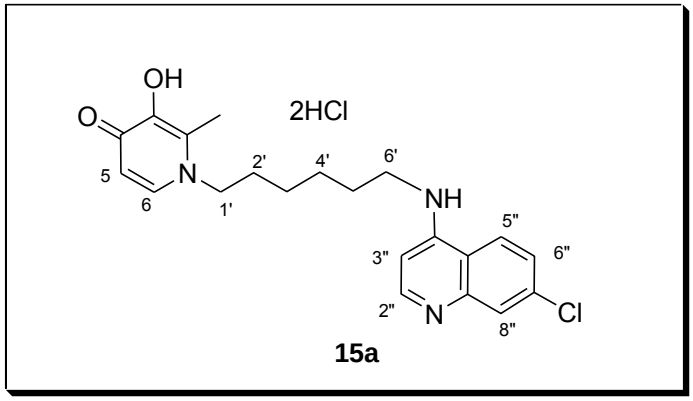

15a

White powder (179mg, 90%), from hot Et_2O; Mp 134-138^oC R_f (50% MeOH/ CH_2Cl_2) 0.61; V_{max} (KBr) cm^{-1} 3425br.w (OH), 3226w (NH) 1632s (C=O), 1613s (C=N), 1586m (C=C),

816m (py C-H); δ_H (400MHz, CD_3OD) 8.48 (1H, *d, J* 9.2, H-5"), 8.37 (1H, *d, J* 7.2, H-2"), 8.2 (1H, *d, J* 6.8, H-6), 7.88 (1H, *d, J* 2, H-8"), 7.66 (1H, *dd, J* 2.0, 9.2 H-6"), 7.1 (1H, *d, J* 6.8, H-5), 6.88 (1H, *d, J* 7.2 H-3"), 4.4 (2H, *t, J* 8.0, H-1'), 3.6 (2H, *t, J* 7.2, H-6'), 2.6 (3H, *s,* C**H**$_3$-2), 1.9 – 1.8 (4H, *m,* H-2',5') 1.56 – 1.48 (4H, *m,* H-3', 4'); δ_C (100MHz, CD_3OD) 158.3, 156.4, 143.9, 142.5, 142, 138.8, 138, 127.4 (2C), 125, 119.8, 115.7, 110.7, 98.6, 65.7, 56.7, 43.6, 30, 27.7, 25.8, 11.6.; MS. *m/z* calculated for $C_{21}H_{25}N_3O_2Cl$ [M+H] 386.16 found 386.0 (100%); Anal. Calcd. (found) for C54.97 (54.87), H 5.71 (5.94), N 9.16 (9.35), $C_{21}H_{26}Cl_3N_3O_2$; HPLC purity analysis >98%.

***N-(7-chloro-4-quinolyl)-1-(6-aminohexyl)-3-(hydroxy)-2-ethyl-4(1H)-pyridinone dihydrogen chloride* (16a)**

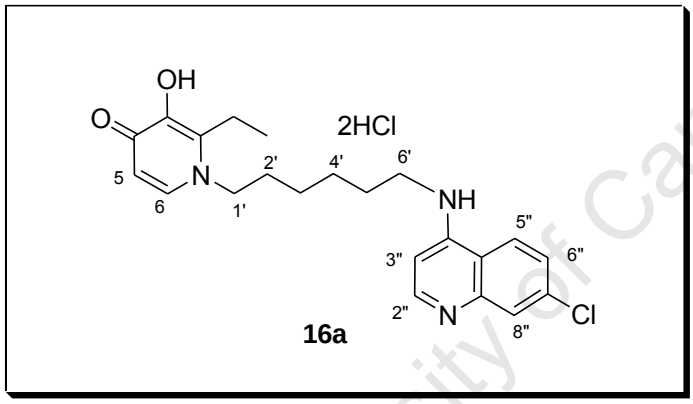

16a

Brown resin (169mg, 88%); R_f (50% MeOH/CH_2Cl_2) 0.64; V_{max} (KBr) cm^{-1} 3302br.w (OH), 3103w (NH) 1624s (C=O), 1616s (C=N), 1609m (C=C), 862m (py C-H)δ_H (400MHz, CD_3OD) 8.4 (1H, *d, J* 9.3, H-5"), 8.37 (1H, *d, J* 7.2, H-2"), 8.18 (1H, *d, J* 6.9, H-6), 7.87 (1H, *d, J* 1.5 H-8"), 7.68(1H, *d, J* 8.8, H-6"), 7.1 (1H, *d, J* 7.2, H-5), 6.94 (1H, *d, J* 7.2, H-3"), 4.39 (2H, *t, J* 7.5, H-1'), 3.62 (2H, *J* 7.5, H-6'), 3.06 (2H, *q, J* 7.5, $CH_3C\mathbf{H}_2$ -2), 1.97-1.79 (4H, *m,* H-2', 5'), 1.55-1.15 (4H, *m,* H-3', 4'), 1.29 (3H, *t , J* 7.5, $CH_2C\mathbf{H}_3$-2); δ_C (100MHz, DMSO) 159, 156, 146.7, 143.6, 143.4, 139.1, 138.9, 138.7, 127.5 (2C), 126.2, 119.8, 111.7, 99.3, 56.1, 43.9, 31.3, 28.2, 26.7, 26.2, 20.3, 12.6; MS. *m/z* calculated for $C_{22}H_{26}N_3O_2Cl$ [M+H] 400.18 found 400.2 (100%); HPLC purity analysis > 98%.

5.4.3. Synthesis of 4-aminoquinoline-3,4-hydroxypyridinone hybrids (3-OMe analogues)

2- Ethyl-2-methoxy-pyranone **(17)**

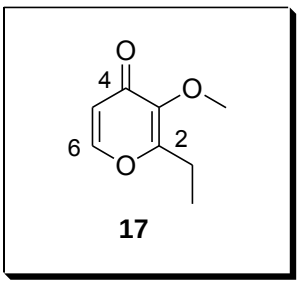

17

To a solution of ethylmaltol (7.0g, 50mmol) in acetone (20ml), was added 2.5M KOH (20ml, 50mmol) followed by methyliodide (7.76g, 55mmol) drop wise. After a 12h stirring, the solvent was removed under pressure and the product extracted into CH_2Cl_2. The organic extract was dried over anhydrous $MgSO_4$ then concentrated to give **17.**

Pale orange oil (4.46g, 58%) R_f 1.6 (CH_2Cl_2) δ_H ($CDCl_3$, 300MHz), 7.61 (1H, *d, J* 5.7, H-6), 6.3 (1H, *d, J* 5.7 H-5), 3.82 (3H, *s,* 3-OCH_3), 2.66 (2H, q, *J* 7.5, 2- $C\mathbf{H_2}CH_3$) 1.19 (3H, *t, J* 7.5, 2-$CH_2C\mathbf{H_3}$).

2-Methyl-2-methoxy-pyranone **(18).**

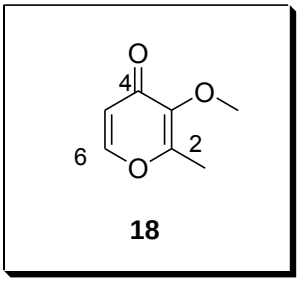

18

Compound **18** was prepared using a method similar to that of **17** using dimethylsulphate as the methylating agent. Orange oil (5.7g, 41%) R_f 0.44 (10% MeOH /CH_2Cl_2) δH (CD_3OD, 300MHz), 7.95 (1H, *d, J* 5.7, H-6), 6.41 (1H, *d, J* 5.7 H-5), 3.94 (3H, *s,* OCH_3-3), 2.35 (3H, *s,* CH_3-2).

Synthesis of N-(7-chloro-4-quinolinyl)-1-(6-aminohexyl)-3-(methoxy)-2-ethyl-4(1H)-pyridinone

To a solution of **17** (200mg, 1.3mmol) in EtOH was added *N*-(7-chloro-4-quinolinyl)-1,6-diaminohexane (**8**), (555mg, 1.85mmol) then water was added to make a 50% aq EtOH solution. After pH adjustment to 13 (2M NaOH) the mixture was refluxed for 24h. Removal of the solvent under reduced pressure, was followed by addition of 25ml of water, pH adjustment to 1 (Concentrated HCl) and washing with Et_2O (50ml ×2). The pH was adjusted to 8 and the compound extracted into CH_2Cl_2 (50ml ×3), the organic extract was dried over anhydrous $MgSO_4$ before concentration to give a yellow resin which was titurated in ethylacetate to give compound **16b** as a yellow powder when dry.

N-(7-chloro-4-quinolinyl)-1-(6-aminohexyl)-3-(methoxy)-2-ethyl-4(1H)-pyridinone

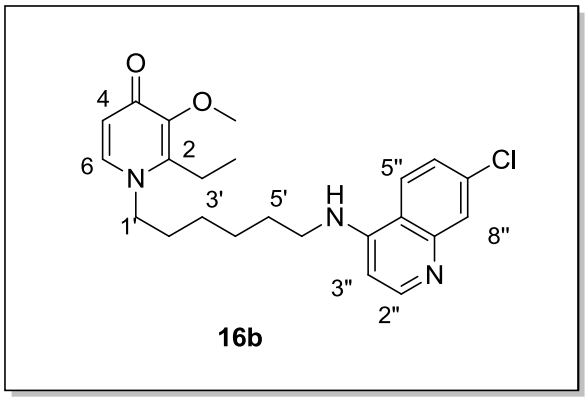

16b

(16b) Yellow powder (226mg, 50%); mp. 68 - 69 ^{0}C. R_f 0.6 (MeOH/ CH_2Cl_2 1:1), δ_H (DMSO d_6, 300MHz), 8.38 (1H, *d, J* 5.4, H-2''), 8.25(1H, *d, J* 9.0, H-5"), 7.77 (1H, *d, J* 2.4, H-8"), 7.54 (1H, *d, J* 7.5, H-6 Py) 7.41 (1H, *dd, J* 2.1, 9.0, H-6"), 7.19 (1H, *br.s*, N-H), 6.44 (1H, *d, J* 5.7, H- 3"), 6.1 (1H, *d, J*, 7.5, H-5 Py), 3.86 (2H, t*, J,* 7.5, H-6'), 3.75 (3H, *s,* 3- OCH_3), 3.25 (DMSO, masking H-1'), 2.64 (2H, q, *J,* 7.5, C**H**$_2$CH$_3$-2), 1.67 (4H, *m,* H-2,' 5'-H), 1.40 (4H, *m,* H- 3', 4'), 1.1 (3H, t*, J* 7.5, CH_2C**H**$_3$-2); δ_C (DMSO d_6, 100MHz), 172.6, 152.6, 150.9, 149.8, 147.3, 145.7, 140.1, 134.1, 128.2, 124.9, 124.7, 118.2, 117.0, 99.4, 59.4, 52.9, 43.1, 31.7, 28.4, 26.9, 19.6 (2C), 14.4; HR MS. *m/z* calculated for $C_{23}H_{27}$ Cl N_3O_2 [M-H] 412.1792 found 414.1792; Anal. Calcd (found) for $C_{23}H_{28}ClN_3O_2$ H_2O, C 62.45 (62.28), H 6.49 (6.79), N 10.4 (9.55); HPLC purity analysis >98%

Synthesis of N-(7-chloro-4-quinolinyl)-1-(4-aminobutyl)-3-(methoxy)-2-ethyl-4(1H)-pyridinone (14b)

To a solution of **17** (200mg, 1.3mmol) in EtOH was added *N*-(7-chloro-4-quinolinyl)-1,4-diaminobutane (**7**), (522mg, 1.85mmol) followed by water to make a 50% aq EtOH solution. After pH adjustment to 13 (2M NaOH) the mixture was refluxed for 24h. Removal of the solvent by evaporation, was followed by addition of an equal amount of water, pH adjustment to 1 (Concentrated HCl) and washing with Et_2O (50ml×2). Further pH adjustment to 8 resulted in precipitatation of the product, which was filtered and washed with water and recrystallised from methanol/ ethylacetate. This method was used to synthesize compounds **13b** and **15b.**

***N-(7-chloro-4-quinolyl)-1-(4-aminobutyl)-3-(methoxy)-2-methyl-4(1H)-pyridinone* (13b)**

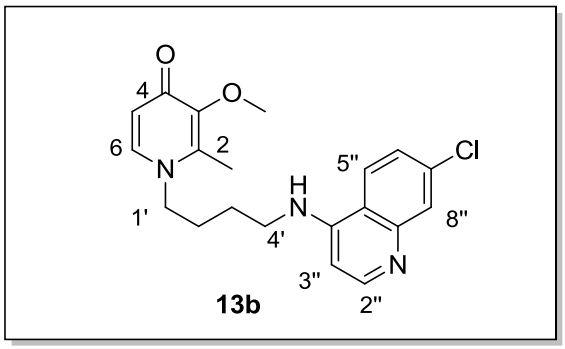

13b

Pale yellow powder (1.02g, 64%); mp. 87 – 87 ^{0}C; R_f 0.35 (MeOH/ CH_2Cl_2 1:1), δ_H (CD_3OD d_4, 400MHz), 8.34 (1H, *d, J* 5.6, H-2''), 8.05(1H, *d, J* 9.2, H-5"), 7.78 (1H, *d, J* 2.4, H-8"), 7.63(1H, *d, J* 7.2 H-6), 7.38 (1H, *dd, J* 2.0, 9.2, H-6"), 6.5 (1H, *d, J* 5.6, H- 3"), 6.4 (1H, *d, J*, 7.6, H-5), 4.07 (2H, t, *J,* 7.5, H-4'), 3.75 (3H, *s,* OCH_3-3), 3.4 (2H, *t, J* 6.8, H-1'), 2.41 (3H, *s,* CH_3-2), 1.8 (4H, *m,* H-2', 3'); δ_C (CD_3OD, 100MHz), 165.3, 143.2, 142.8, 142, 140.2, 135, 131.4, 126.9, 118.2, 116.7, 114.6, 109.3, 107.9, 90.3, 50.5, 45.4, 33.9, 19.7(2C), 16.8; HR MS. *m/z* calculated for $C_{20}H_{23}$ Cl N_3O_2 [M-H] 372.1479 found 372.1471; Anal. Calcd (found) for $C_{20}H_{22}ClN_3O_2$ $6H_2O$, C 52.01 (52.35), H 7.54 (6.63), N 8.27 (9.08); HPLC purity analysis >98%.

***N-(7-chloro-4-quinolinyl)-1-(4-aminobutyl)-3-(methoxy)-2-ethyl-4(1H)-pyridinone* (14b)**

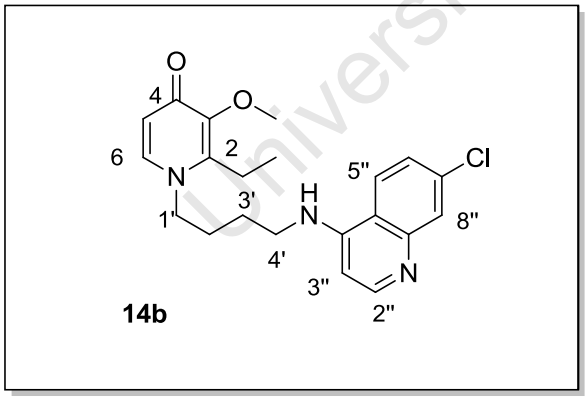

14b

Yellow powder (400mg, 70%); mp. 166 - 165 ^{0}C; R_f 0.45 (MeOH/ CH_2Cl_2 1:1), δ_H (DMSO d_6, 300MHz), 8.4 (1H, *d, J* 5.4, H-2''), 8.26 (1H, *d, J* 9.0, H-5"), 7.78 (1H, *d, J* 2.1, H-8"), 7.58(1H, *d, J* 7.5 H-6 py), 7.44 (1H, *dd, J* 2.1, 9.0, H-6"), 7.34 (1H, *br.s*, N-H), 6.5 (1H, *d, J* 5.4, H-3"), 6.1 (1H, *d, J*, 7.5, H-5), 3.93 (2H, t, *J,* 6.9, H-4'), 3.75 (3H, *s,* OCH_3-3), 2.65 (2H, q, *J,* 7.5, C**H**$_2$$CH_3$-2), 1.74 (6H, *m,* H-1', 2', 3'-H), 1.1 (3H, t, *J* 7.5, 2- CH_2C**H**$_3$); δ_C (DMSO d_6, 75MHz), 171.7, 151.1, 150.2, 148.4, 146.4, 144.7, 139.1, 133.5, 126.9, 124.0, 123.9, 117.2, 116.1, 98.6, 58.5, 51.8, 43.8, 28.4, 24.5, 18.7, 13.4; HR MS. *m/z* calculated for $C_{21}H_{23}$ Cl N_3O_2 [M-H] 384.1479

found 384.1482; Anal. Calcd (found) for $C_{21}H_{24}ClN_3O_2$ $1.5H_2O$, C 60.22 (60.15), H 6.32 (6.65), N 10.53 (10.11); HPLC purity analysis >98%

***N-(7-chloro-4-quinolyl)-1-(6-aminohexyl)-3-(methoxy)-2-methyl-4(1H)-pyridinone* (15b)**

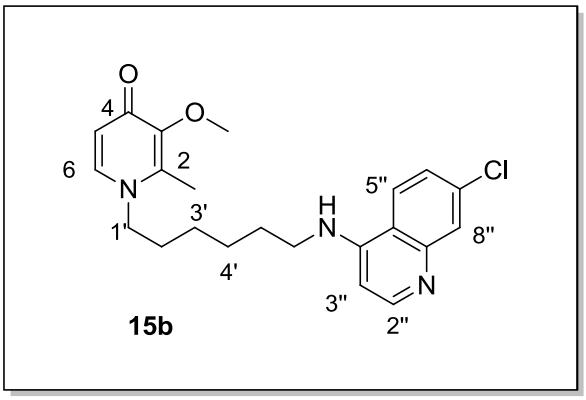

15b

Yellow powder (883mg, 48%); mp. 96 – 98 ^{0}C; R_f 0.54 (MeOH/ CH_2Cl_2 1:1), δ_H (CD_3OD d_4, 400MHz), 8.34 (1H, *d, J* 6.4, H-2''), 8.24 (1H, *d, J* 9.2, H-5"), 7.8 (1H, *d, J* 2.0, H-8"), 7.67 (1H, *d, J* 7.2 H-6), 7.53 (1H, *dd, J* 2.0, 9.2, H-6"), 6.68 (1H, *d, J* 6.8, H- 3"), 6.41 (1H, *d, J*, 7.6, H-5), 4.03 (2H, t, *J,* 6.9, H-6'), 3.75 (3H, *s,* OCH_3-3), 3.48 (2H, *t, J* 7.2, H-1'), 2.43 (3H, *s,* CH_3-2), 1.78 (4H, *m,* H-2', 5'), 1.5 (4H, *m,* H-3', 4'); δ_C (CD_3OD, 100MHz), 165.1, 145, 135, 138, 131.7, 129.4, 117.9 (2C), 115.7 (2C), 114, 108.2, 107.8, 90.2, 50.6, 45.7, 38.9, 34.9, 22.0, 19.6, 18.2, 17.6; HR MS. *m/z* calculated for $C_{22}H_{25}$ Cl N_3O_2 [M-H] 398.1635 found 398.1644; Anal. Calcd (found) for $C_{22}H_{26}ClN_3O_2.5H_2O$, C 52.0 (52.13), H 6.98 (6.74), N 9.10 (8.22); HPLC purity analysis >98%

5.4.4. Attempted Synthesis of Kojic derived 4-aminoquinolines-3,4-hydroxypyridinone via Mannich base intermediates

Synthesis of 3-hydroxy-6-hydroxymethyl-2-piperidinomethylpyran-4-(1H)-one (19)

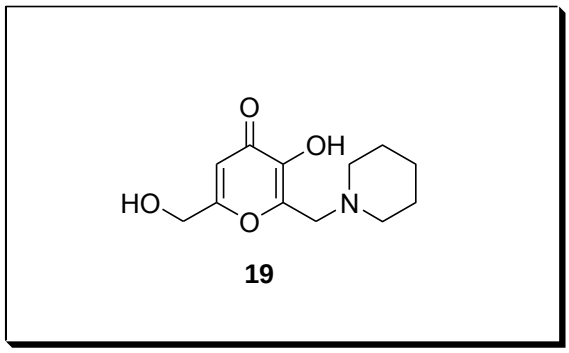

19

To a solution of formaldehyde 37% (1.8g, 60mmol), and piperidine (3.4g, 40mmol) in EtOH (96%), was added ko*j*ic acid (4.26g, 30mmol), in 40ml in EtOH, 96%), then stirred for 1h before overnight refrigeration. The resultant white crystals were filtered off, washed with EtOH, then diethylether before

drying under vacuum to afford compound **19** as white crystals. Positive reaction with 4% methanolic ninhydrin confirmed piperidine incorporation.

White solid (5.788g, 85%), Rf 0.38 (MeOH/ CH_2Cl_2 1:1) δ_H (DMSO d_6, 400MHz) 6.33 (1H, *s,* H-5), 4.32 (2H, *s,* C**H$_2$**OH-6), 3.5 (2H, *s,* C**H$_2$**N(CH_3)CH_2-2), 2.43 (4H, *m,* -CH_2-N-CH_2-(piperidine)), 1.52 (6H, *m,* -CH_2-CH_2-CH_2-(piperidine)); δ_C (DMSO d_6, 100MHz), 173.4, 167.4, 146.8, 143.6, 108.9, 59.6, 54.4, 53.6 (2C), 25.4 (2C), 23.6.

Synthesis of 3-Hydroxy-6-hydroxymethyl-2-piperidinomethylpyran-4-(H)-one (19a)

To a solution of **19** (4.12g, 18mmol) in MeOH was added 4.5M NaOH (5ml, 22.5mmol). The mixture was heated to reflux (83^{o}C) before addition of benzylbromide (3.926g, 22.5mmol) drop wise then refluxed further for 6h. The mixture was later evaporated coole*d,* and water (50ml) adde*d,* before extraction into dichloromethane (50ml ×3). The combined organic extracts were washed with 5% NaOH (aq) (50ml ×2), and water (50ml×2) then dried over anhydrous $MgSO_4$ filtered and concentrated to afford **19a** orange oil which was further dried under vacuum.

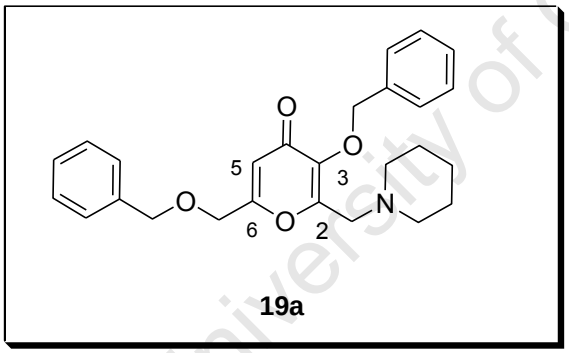

19a

Orange oil (3.313g, 58%) Rf 0.8 (MeOH/ CH_2Cl_2 1:1); δ_H (DMSO d_6, 400MHz), 7.5-7.3 (10H, *m,* H-benzyl) 6.48 (1H, *s,* H-5), 5.12 (2H, *s,* C**H$_2$**Bn-3), 4.41(2H, *s,* C**H$_2$**OCH_2Bn-6), 3.50 (2H, *s,* CH_2OC**H$_2$**Bn-6), 3.45 (2H, *s,* C**H$_2$**N(CH_3)CH_2-2), 2.38 (4H, *m,* -CH_2-N-CH_2-(piperidine)), 1.56 (4H, *m,* -C**H$_2$**-CH_2-C**H$_2$**-(piperidine)), 1.56 (2H, *m,* -CH_2-C**H$_2$**-CH_2-(piperidine)),

5.4.5. Synthesis of kojic derived 4-aminoquinoline -3,4-hydroxypyridinone hybrids via alkylhalide intermediates (R series)

Synthesis of *5-(benzyloxy)-2-(hydroxymethyl)-4-(1H)-pyran-4-one* (20)

To a solution of ko*j*ic acid (7.3g, 50mmol) in MeOH was added 11M NaOH (5ml, 55mmol). The mixture was heated to reflux (80^{o}C) before addition of benzylchloride (6.43g, 55mmol) dropwise then refluxed at 84^{o}C for 12h. White crystals formed on cooling to room temperature and were washed in water and cold MeOH then dried under vacuum to give **20.**

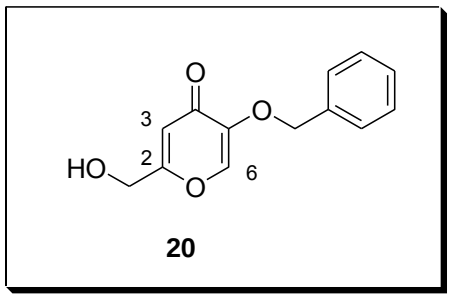

20

White needles (8.55g, 74%); mp. 119-122 ^{0}C; R_f 0.93 (MeOH/ CH_2Cl_2 1:3), δ_H (DMSO d_6, 400MHz), 8.15 (1H, *s,* H-6), 7.37 (5H, *m,* Bn C-H), 6.32 (1H, *s,* H-3), 4.94 (2H, *s,* C**H$_2$**-Bn-5), 4.28 (2H, *s,* C**H$_2$**OH-2), δ_C (DMSO d_6, 100MHz), 173.2, 167.9, 146.6, 141.3, 136.1, 128.4 (2C), 128.1, 128, 111.2, 111.1, 70.6, 59.3.

Synthesis of *5-(benzyloxy)-2-(hydroxymethyl)-1-methypyridin-4 (1H)-one* (21)

5ml of 40% methylamine (1.8g, 11mmol) was added to a solution of **20** (1.4g, 6.03mmol) in EtOH, refluxed at 70 ^{o}C in a sealed tube for 12h. pH ad*j*ustment to 1 (concentrated HCl) gave a thick precipitate, the solvent was removed by evaporation before washing the residue with diethylether. More water was added (25ml) to the residue and pH ad*j*usted to 9 followed by washing with water and drying the product under vacuum.

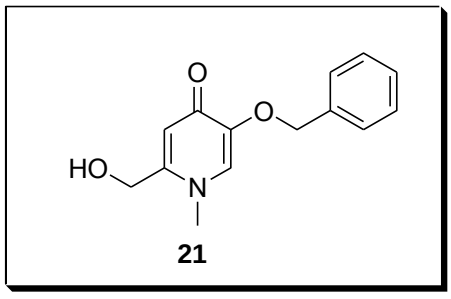

21

White needles (1.359g, 91%); mp. 205-207 ^{0}C R_f 0.72 (MeOH/ CH_2Cl_2 1:1)), δ_H (DMSO d_6, 300MHz), 7.54 (1H, *s,* H-6), 7.36 (5H, *m,* Bn C-H), 6.26 (1H, *s,* H-3), 5.01 (2H, *s,* C**H$_2$**-Bn-5), 4.36 (2H, *s,* C**H$_2$**OH-2), 3.58 (3H, *s,* NC**H$_3$**-1) δ_C (DMSO d_6, 75MHz), 172, 148.5, 146.7, 137.1, 129.7, 127.9 (2C), 127.6 (2C) , 127.5 (2C), 115.1, 70.7, 59.2.

***2-(chloromethyl)-5-(benzyloxy)- 1-methypyridin-4 (1H)-one* (22)**

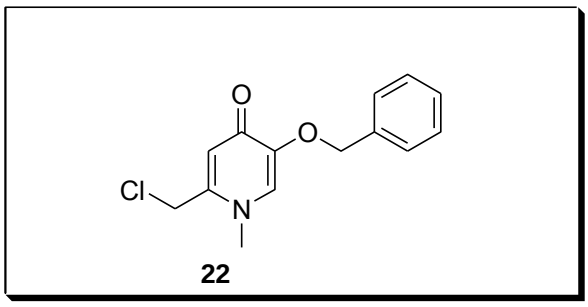

22

To neat thionyl chloride (9.82g, 82mmol) below 0°C (ice/acetone mixture) was added **21** (2.45g, 9.9mmol) then stirred at room temperature overnight in a sealed flask. The crystals formed were washed with petroleum ether and dried under vacuum to give white **22**. White crystals (2.55g, 97%); mp. 168-169 ^{0}C R_f 0.47 (MeOH/ CH_2Cl_2 1:1), δ_H (DMSO d_6, 300MHz), 8.86 (1H, *s,* H-6),), 7.7 (1H, *s,* H-3), 7.41 (5H, *m,* Bn C-H) 5.24 (2H, *s,* 5-C**H$_2$**-Bn), 5.1 (2H, *s,* 2-C**H$_2$**Cl), 4.15 (3H, *s,* 1-NC**H$_3$**).

Synthesis of *5-(benzyloxy)-2-((2-(7-chloroquinolin-4-ylamino)hexylamino)methyl)-1-methylpyridin-4 (1H)-one* (27) –Method A

To a solution of **22** (193mg, 0.73mmol), and **8** (244mg, 0.88mmol) in 3ml dimethylformamide , was added triethylamine (87mg, 0.86mmol) and anhydrous Na_2CO_3 (92.4mg, 0.88mmol) before refluxing at 80°C for 24h. After adding dichloromethane (6ml) the mixture was washed with water (6ml ×2) then the solvent was removed under reduced pressure. The residue was subjected to column chromatography on silica gel via gradient elution with 0, 10, 20, 30, 50% MeOH/EtOAc. The title compound was eluted by 30-50% MeOH/EtOAc. Evaporation under reduced pressure afforded a yellow oil which was titurated in EtOAc to give a white solid on drying under vacuum. Further drying was done under vacuum at 60°C for 6h. Compounds **26, 25** and **23** were synthesized using a similar procedure. White solid (220mg, 44%); mp. 116 – 117 ^{0}C; R_f 0.17 (MeOH/ EtOAc 1:1)) δ_H (CD_3OD, 400MHz), 8.3 (1H, *d, J* 5.6, H-2"), 8.08 (1H, *d, J* 8.8, H-5"), 7.76 (1H, *br.s*, H-8"), 7.5 (1H, *s,* H-6) 7.40 (6H, *m,* benzylCH, H-6"), 6.5 (1H, *s,* H-

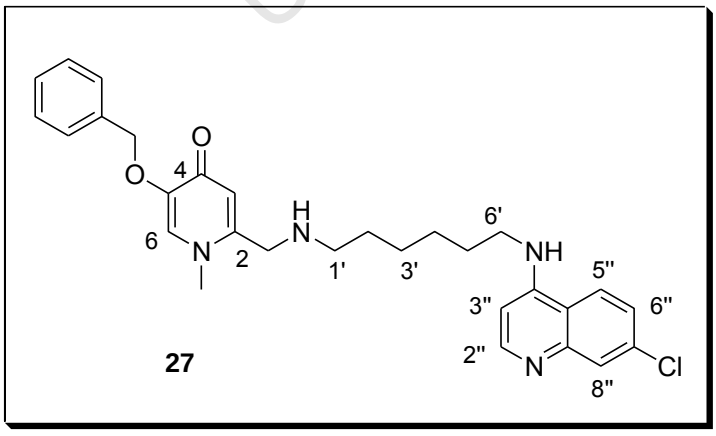

27

3), 6.46 (1H, *d, J* 5.6, H-3"), 5.05 (2H, *s,* 5-C**H$_2$**Bn), 3.73 (3H, *s,* 1-C**H$_3$**), 3.67 (2H, *s,* 2-C**H$_2$**NH), 2.6 (2H, *t, J* 7.2, H-6'), 1.73 (2H, *t, J* 7.2, H-1'), 1.48 (8H, *m,* H-2'- 5'). δ_C (CD_3OD, 100MHz),172.5, 151.4, 150.9, 148.5, 146.8, 136.5, 134.9, 129, 128.9, 128.1(2C), 127.7(2C), 127.6, 126.1, 124.5, 123.1, 117.4, 115.9, 98.2, 71.2, 55.2, 49.4, 48.9, 42.6, 39.9, 29.3, 27.9, 26.7; MS. *m/z* calculated for $C_{29}H_{34}ClN_4O_2$ [M+H] 505.23 found 505.2 (100%); Anal. Calcd (found) for $C_{29}H_{33}ClN_4O_2$ $2H_2O$. C 64.37(64.99), H 6.89 (6.46), N 10.35 (9.95).HPLC purity 99%, R_t 10.43 min.

***5-(benzyloxy)-2-((2-(7-chloroquinolin-4-ylamino)butylamino)-1-methylpyridin-4-(1H)-.one* (26)**

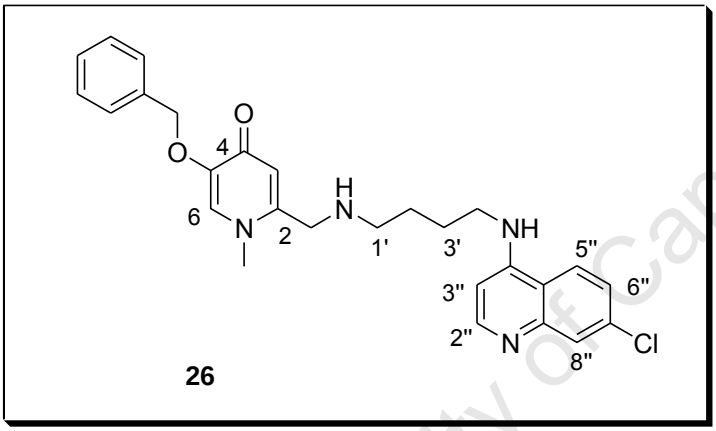

26

22 (263mg, 1mmol) and **7** (299mg, 1.2mmol) were used to prepare compound **26** using a method similar to the one described for **27**, above. White solid (218mg ,48%); mp. 80-81 ^{0}C; R_f 0.1 **(**MeOH/ EtOAc, 1:1) δ_H (CD_3OD, 400MHz), 8.3 (1H, *d, J* 5.6, H-2"), 8.06 (1H, *d, J* 8.8, H-5"), 7.74 (1H, *d, J* 2, H-8"), 7.5 (1H, *s,* H-6) 7.3 (6H, *m,* benzylCH, H-6"), 6.5 (1H, *s,* H-3), 6.48 (1H, *d, J* 5.6, H-3"), 5.03 (2H, *s,* 5-C**H$_2$**Bn), 3.71 (3H, *s,* 1-NC**H$_3$**), 3.70 (2H, *s,* 2-C**H$_2$**N), 3.36 (2H, *t, J,* 7.2, H-4'), 2.67 (2H, *t, J* 7.2, 2-H-1'), 1.7 (4H, *m,* H-2', 3'); δ_C (CD_3OD, 75MHz),173.8, 157.6, 152.8, 152.1, 149.4, 146.7, 137.7, 136.4, 130.1, 129.5 (2C), 129.2, 129 (2C), 127.3, 125.9, 124.4, 116.7, 116.6, 99.7, 72.4, 62.3, 43.7, 41.6, 41.3, 28.4, 26.5; MS. *m/z* calculated for $C_{27}H_{30}ClN_4O_2$ [M+H] 477.2 found 477.2 (100%); Anal. Calcd (found) for $C_{27}H_{29}ClN_4O_2$ $2H_2O$. C 63.21(63.71), H 6.48 (6.78), N 10.92 (11.76). HPLC purity 99% R_t 13.80 min.

Method-B: To a solution of **7** (250mg, 1mmol) in 3ml dimethylformamide triethylamine (101mg, 1mmol) and anhydrous $NaHCO_3$ (168mg, 2mmol) was added compound **22** (263mg, 1mmol) before refluxing at 90^{o}C for 20h., After adding dichloromethane (15ml) the mixture was washed with brine (15ml ×3) [precipitation of remnants of **7** were

observed on addition of brine] and water (10mlx2) The solution was filtered to remove **7**, then dried over anhydrous sodiumsulphate. The solvent was removed under reduced pressure to give a bright orange oil (280mg, 59%). Further drying was done under vacuum at 30-60^{o}C for 6h to get the pure compound. The elemental analysis data of the dry compound was similar to the product from method A. This method was applied successfuly in the repeated syntheses of compounds **25, 24** and **30**.

***5-(benzyloxy)-2-((2-(7-chloroquinolin-4-ylamino)propylamino)-1-methylpyridin-4 (1H)-one* (25)**

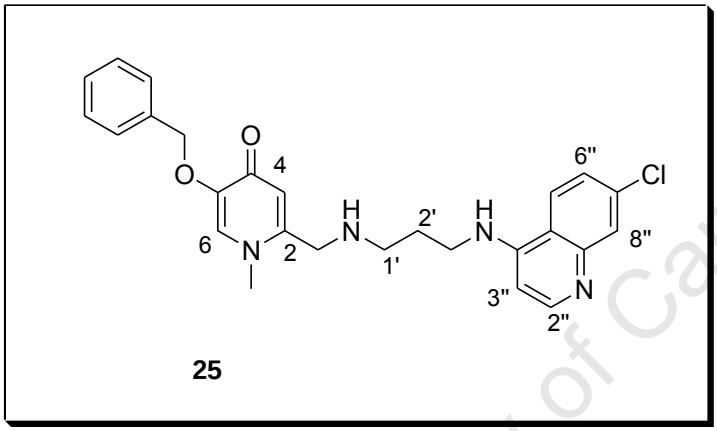

25

Yellow solid (270mg, 58%), R_f 0.37 (MeOH/ EtOAc 1:1) δ_H (CD_3OD, 400MHz), 8.26 (1H, *d, J* 6.0, H-2"), 7.9 (1H, *d, J* 8.8, H-5"), 7.69 (1H, *br.s*, H-8"), 7.41(1H, *s,* H-6) 7.3(6H, *m,* benzyl-CH, H-6"), 6.48 (1H, *s,* H-3), 6.42 (1H, *d, J* 5.2, H-3"), 4.95,(2H, *s,*5-C**H$_2$**Bn), 3.65 (3H, 1-NC**H$_3$**), 3.36 (2H, *t, J,* 6.8, H-3'), 3.23 (2H, *s,* 2-C**H$_2$**NH), 2.72 (2H, *t, J* 6.4, H-1'), 1.86 (2H, q, *J* 6.4, H-2'); δ_C (CD_3OD, 75MHz), 173.9, 152.8, 152.4, 149.8, 149.6, 149.3, 148.9, 137.8, 136.4, 130.2, 129.9, 129.5, 129.2, 129.1, 127.6, 126, 124.2, 118.8, 117.2, 117.1, 99.6, 72.4, 50.9, 42.4, 41.2, 29.2; MS. *m/z* calculated for $C_{26}H_{28}ClN_4O_2$ [M+H] 463.19 found 463.2 (100%); Anal. Calcd (found) for $C_{26}H_{27}ClN_4O_2$ H_2O . C 64.92(64.11), H 6.04 (6.64), N 11.65 (11.91). HPLC purity 92% R_t 13.39 min.

***5-(benzyloxy)-2-(((3-(7-chloroquinolin-4-ylamino)propyl)(methyl)amino)methyl)-1-methypyridin-4(1H)-one.* (24)**

To a solution of **6** (250mg, 1mmol) in acetonitrile (10ml) was added **22** (263mg, 1mmol) followed by NaOH (44mg, 1.1mmol), sonicated to dissolve then su*j*ected to microwave conditions (250W, 100^{o}C, 249 bar*s,* 18min.) MeOH was added to dissolve the precipitate, solvent evaporated off under vacuum and the residue sub*j*ected to column

chromatography on silica gel via gradient elution with 0; 20; 30% MeOH/EtOAc. **24** was eluted by 30% MeOH/EtOAc and the fraction was subsequently rotaevaporated to give a white hygroscopic solid which was recrystalised from methanol/water.

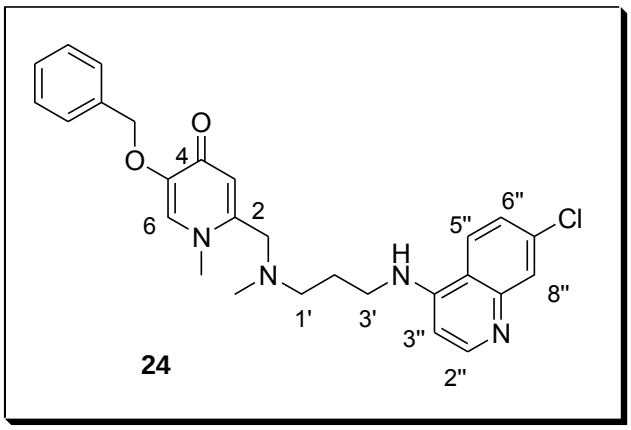

24

Colourless needles from methanol/H_2O (190mg, 40%); mp. 84-87 ^{0}C; R_f 0.4 (MeOH/ EtOAc 1:1) δ_H (CD_3OD, 300MHz), 8.33 (1H, *d, J* 5.6, H-2"), 8.01 (1H, *d, J* 8.8, H-5"), 7.74 (1H, *d, J* 1.6, H-8"), 7.32 (7H, *m,* benzylCH**,** H-6, H-6"), 6.5 (1H, *d, J* 6.0, H-3"), 6.45 (1H, *s,* H-3), 4.87 (2H, *s,* 5-C**H$_2$**Bn), 3.71 (3H, *s,* 1-C**H$_3$**), 3.44 (2H, *s,* 2-C**H$_2$**NH), 3.36 (2H, *t, J* 6.8, H-3'), 2.56 (2H, *t, J* 6.4, H-1'), 2.70 (3H, *s,* C**H$_3$**-N(CH_2)CH_2), 1.90 (2H, *m,* H-2'). δ_C (CD_3OD, 75MHz), 173.4, 153.6, 150.9, 149.1, 148.3, 147.9, 137.7, 129.9, 129,5(2C), 129.1(2C), 129.0(2C), 126.5, 126.3, 124.6, 118.8, 118.4, 99.6, 72.2, 60.3, 55, 42.1, 41.9, 26.7; MS. *m/z* calculated for $C_{27}H_{30}ClN_4O_2$ [M+H] 477.21 found 477.2 (100%); Anal. Calcd (found) for $C_{27}H_{29}ClN_4O_2$ $2H_2O$ C 63.21 (63.57), H 6.48 (6.13), N 10.92 (11.09); HPLC purity analysis 95%.

Alternative method B was used to prepare more of the compound **24**; 300mg, (65% yield) of orange oil.

***5-(benzyloxy)-2-((2-(7-chloroquinolin-4-ylamino)ethylamino)-1-methylpyridin-4 (1H)-one* (23)**

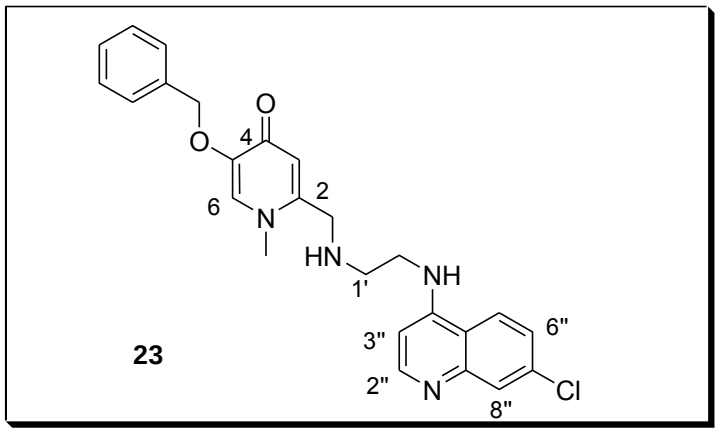

23

Orange resin (56mg, 12.5%); mp. R_f 0.1 (MeOH/ EtOAc 1:1) δ_H (CD_3OD, 300MHz), 8.34 (1H, *d, J* 5.7, H-2"), 8.05 (1H, *d, J* 9.0, H-5"), 7.77 (1H, *d, J* 2.1, H-8"), 7.42 (7H, *m,* benzylCH, H-6, 6"), 6.53 (1H, *s,* H-3), 6.52 (1H, *m,* H-3, 3"), 5.0 (2H, *s,* C**H$_2$**Bn), 3.78 (2H, *s,* 2-C**H$_2$**NH), 3.74 (3H, 1-NC**H$_3$**), 3.48 (2H, *t, J,* 6.3, H-2'), 2.98 (2H, *t, J* 6.3, H-1'); δ_C (DMSO, 100MHz): 171.9, 151.8, 150.3, 147.8, 147.4, 147.2, 137.7, 134.9, 129.9, 128.7 (2C), 128.4(2C), 128.3, 126.1, 125.1, 124.9, 117.5, 116.9, 99.2, 71.1, 49.5, 47.0 (2C), 43.0; MS. *m/z* calculated for $C_{27}H_{30}ClN_4O_2$ [M+H] 449.17 found 449.2 (100%); Anal. Calcd (found) for $C_{25}H_{25}ClN_4O_2$ $3H_2O$. C 60.79 (60.50), H 6.12 (5.50), N 11.34 (12.04); HPLC purity analysis 98%, R_t 11.52 min.

Deprotection of 2-((7-chloroquinolin-4-ylamino)alkylamino)methyl)-5-benzyloxy-1-methylpyridin-4(1H)-ones

A solution of **24** (221mg, 0.46mmol) in 2M ethanolic HCl was sub*j*ected to hydrogenolysis in the presence of Pd/C 30mg (10 %w/w), 4 atm pressure for 4h. Then the catalyst was filtered off on celite and the solvent removed by evapouration under reduced pressure to give an orange oil which was titurated in MeOH/EtOAc to give a 100mg of a yellow solid (**24a**) on drying under vacuum. Extra drying was done at 30-60^{o}C for 6h. Similar procedures were used to prepare compounds **25a, 24a** and **23a.** Compound **27a** was prepared using acid hydrolysis as described for compound **11a.**

***2-((3-(7-chloroquinolin-4-ylamino)hexylamino)methyl)-5-hydroxy-1-methylpyridin-4(1H)-one*.(27a)**

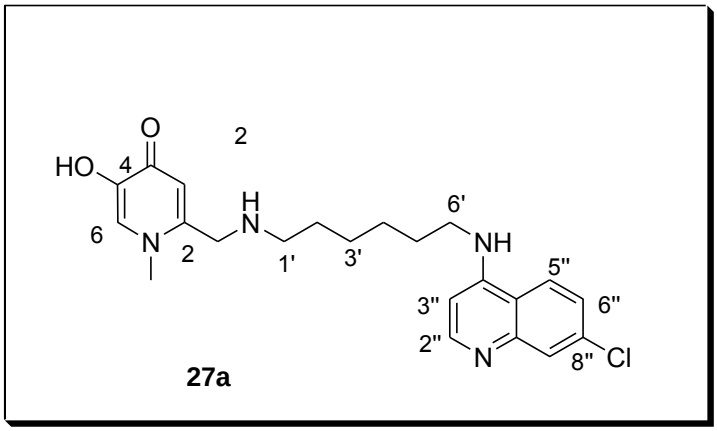

27a

Off white powder (110mg, 99%).; δ_H (CD_3OD, 300MHz); mp. 177-180 ^{0}C; R_f 0.1 (**(**NH_3/MeOH/EtOAc, 0.01:1:9); 8.45 (1H, *d, J* 6, H-2"), 8.32 (1H, *d, J* 9, H-5"), 8.20 (1H, *d, J* 2.8, H-8"), 7.86 (1H, *s,* H-6) 7.63 (1H, *dd, J* 9, 3, H-6"), 7.59 (1H, *s,* H-3), 6.88 (1H, *d, J* 6, H-3"), 4.19 (3H, *s,* C**H$_3$**-1), 3.61 (2H, *t, J* 6, H-6'), 3.28 (4H, *m,* C**H$_2$**NH-2, H-1'), 1.86 (4H, *m,* H-2', 5'), 1.55 (4H, *m,* H-3'- 4'); δ_C (CD_3OD, 75MHz) 160.8, 156.3, 145.9, 142.3, 140.4, 139.7, 138.6, 133.8, 127.3, 124.8, 118.9, 115.6, 115.3, 198.5, 48.7, 45.7, 43.9, 43.4, 27.3, 25.8, 25.7, 25.5; HRMS. *m/z* calculated for $C_{22}H_{26}ClN_4O_2$ [M-2H] 413.1744 found 413.1734; Anal. Calcd (found) for $C_{22}H_{35}Cl_4N_4O_2$ $3H_2O$, C 45.77 (45.93), H 6.11 (6.08), N 9.70 (9.84); HPLC purity analysis 98%.

***2-((4-(7-chloroquinolin-4-ylamino)butylamino)methyl)-5-hydroxy-1-methylpyridin-4(1H)-one*.(26a)**

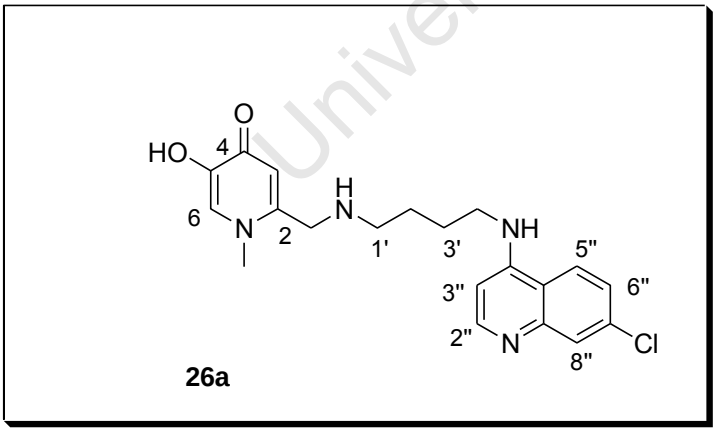

26a

White solid (100mg, 56%), mp. 183-184 ^{0}C R_f 0.21 **(**NH_3/MeOH/EtOAc, 0.01:1:9) δ_H (DMSO, 300MHz), 10.1 (1H, br*s,* OH), 9.79 (1H, *s,* NH), 8.87 (1H, *d, J* 9.0, H-5"), 8.51 (1H, *d, J* 6, H-2"), 8.31 (1H, *s,* H-6), 8.14 (1H, *s,* H-8") 7.72 (1H, *dd, J* 9.0, 3.0, H-6"), 7.6 (1H, *s,* H-3), 6.90 (1H, *d, J* 6, H-3"), 4.41(2H, *s,* C**H$_2$**NH-2), 4.17 (3H, *s,* NC**H$_3$-**1), 3.58 (2H, *m,* H-1'), 3.15 (2H, *t, J* 9, (H-4"), 1.86 (4H, *m,* 2', 3'); δ_C (DMSO, 75MHz) 160.5, 155.8, 145.9, 143.2, 140.9, 139.0, 138.4, 133.1, 127.2, 126.6, 119.5, 116.4, 115.9, 99.2, 47.4, 45.5, 44.6, 42.8, 25.1, 23.2. MS. *m/z* calculated for

$C_{20}H_{24}ClN_4O_2$ [M+H] 387.1588 found 387.1 (90%); Anal.Calcd (found) for $C_{20}H_{26}Cl_4N_4O_2$ $4H_2O$. C 42.27 (41.96), H 6.03 (5.11), N 9.86 (9.85); HPLC purity analysis 98% R_t 12.36 min. .

***2-((6-(7-chloroquinolin-4-ylamino)propylamino)methyl)-5-hydroxy-1-methylpyridin-4(1H)-one*.(25a)**

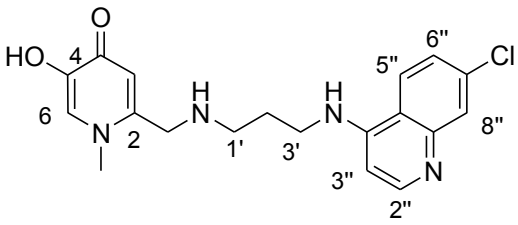

25a

White solid (21mg, 43%), mp. 163-165 ^{0}C R_f 0.09 (**(**NH_3/MeOH/EtOAc, 0.01:1:9) δ_H (CD_3OD, 300MHz), 8.57 (1H, *d, J* 9.0, H-5"), 8.43 (1H, *d, J* 6, H-2"), 8.26 (1H, *s,* H-6), 7.90 (1H, *d, J* 3, H-8") 7.67 (2H, *m*, H-3, 6"), 7.0 (1H, *d, J* 6, H-3"), 4.6 (2H, *s,* C**H**$_2$NH-2), 4.25 (3H, *s,* NC**H**$_3$ -1), 4.09 (2H, *m,* H-1'), 3.82 (2H, *m,* H-3'), 3.47 (2H, *m,* H-2'); δ_C (CD_3OD, 75MHz), 160.4, 156.3, 145.8, 142.7, 140.3, 139.7, 138.6, 133.9, 127.4, 125.1, 118.9, 115.7, 115.4, 98.7, 46.1, 45.8, 44.2, 40.3, 24.5. MS. *m/z* calculated for $C_{19}H_{19}ClN_4O_2$ (M+K-2H) 409.0834 found 409.1 (100%); Anal. Calcd (found) for $C_{19}H_{34}Cl_4N_4O_2$ $5H_2O$. C 39.87 (40.21), H 5.99 (5.39), N 9.79 (9.88); HPLC purity analysis 99% R_t 11.91 min. .

***2-(((3-(7-chloroquinolin-4-ylamino)propyl)(methyl)amino)methyl)-5-hydroxy-1-methylpyridin-4(1H)-one* (24a)** Colourless needles (MeOH/EtOAc), (37mg, 46%); mp. 154-156 ^{0}C; δ_H (CD_3OD, 300MHz), 8.50 (1H, *d, J* 9, H-5"), 8.40 (1H, *d, J* 6, H-2"), 8.27 (1H, *s,* H-6), 7.89 (1H, *s,* H-8"), 7.67 (2H, *m,* H-3, 6"), 6.99 (1H, *d, J* 6.0, H-3"), 4.27 (2H, *s,* 2-C**H**$_2$NH), 3.76 (2H, *m,* H-3'), 3.57 (2H, *m,* H-1'), 3.32 (3H, *s,* 1-C**H**$_3$), 2.97 (3H, *s,* CH_2NC**H**$_3CH_2$) , 2.4 (2H, *m,* H-2'). δ_C (CD_3OD,

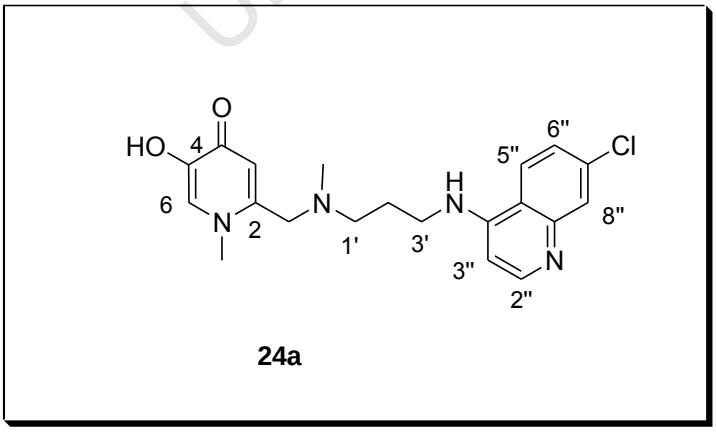

24a

75MHz), 160.2, 156.4, 146.2, 142.7, 139.7, 138.6, 134.6, 127.4(2C), 125.2, 118.9, 117.1, 115.7, 98.8, 54.5, 54.2, 44.7, 40.4, 39.6, 22.4.; MS. *m/z* calculated for $C_{20}H_{24}ClN_4O_2$ (M+H) found 387.1 (100%); Anal. Calcd (found) for $C_{20}H_{26}Cl_4N_4O_2$ 2.5H_2O, C 44.38 (44.05), H 5.77(5.90), 10.35 (10.35); HPLC purity analysis 99% R_t 9.66 min. .

***2-(((2-(7-chloroquinolin-4-ylamino)ethyl)(methyl)amino)methyl)-5-hydroxy-1-methylpyridin-4(1H)-one* (23a)**

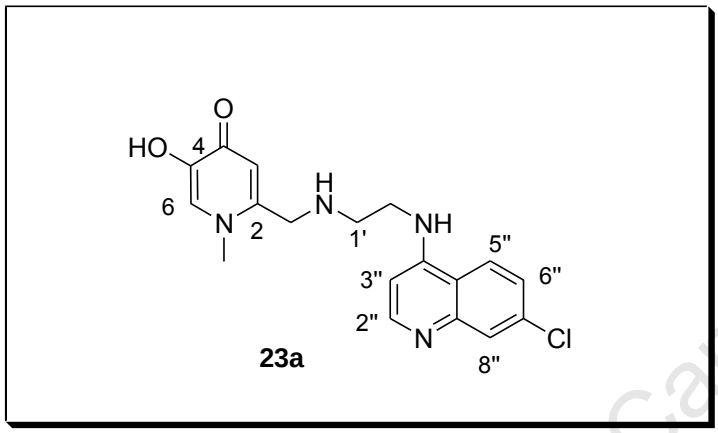

23a

Colorless needles (1.25M methanolic HCl/H_2O/EtOAc), (23mg, 74%); mp. 174-175 ^{0}C R_f 0.04 (NH_3/MeOH/EtOAc, 0.01:1:9) δ_H (DMSO, 300MHz), 10.3 (1H, *br.s* OH), 9.78 (1H, *s,* NH), 8.82 (1H, *d, J* 9, H-5"), 8.68 (1H, *d, J* 6, H-2"), 8.26 (1H, *s,* H-6), 8.06 (1H, *s,* H-8"), 7.81 (1H, *d, J* 9, H-6"), 7.50 (1H, *s,* H-3), 7.10 (1H, *d, J* 6, H-3"), 4.55 (2H, *s,* C**H$_2$**NH-2), 4.16 (3H, *s,* NC**H$_3$**-1), 4.0 (2H, *m,* H-2'), 3.17 (2H, *m,* H-1'); δ_C (DMSO, 75MHz), 162.4, 156.2, 145.9, 143.8, 141.1, 138.9, 138.7, 133.2, 127,4 (2C), 126.9, 119.5, 116.2, 99.5, 45.8 (2C), 45.6, 44.6; MS. *m/z* calculated for $C_{18}H_{20}ClN_4O_2$ (M+H) 359.1275 found 359.1 (100%); Anal. Calcd (found) for $C_{18}H_{19}Cl_4N_4O_2$,2H_2O C 42.88 (43.07), H 5.20 (6.17), 11.11 (10.53); HPLC purity analysis 97.7% R_t 9.76 min..

5.4.6. Synthesis of kojic derived 4-aminoquinoline -3,4-hydroxypyridinone hybrids via alkylhalide intermediates (D series)

***5-(benzyloxy)-2-(hydroxymethyl)-1-cyclopropylpyridin-4 (1H)-one,* (21a)**

3.4ml 98% cyclopropylamine (2.775g, 48mmol) was added to a solution of **20** (5.813g, 25mmol) in 50% aq EtOH, refluxed at 70 ^{o}C in a sealed tube for 12h. pH adjustment to 1 (conc. HCl) then put in the freezer to maximize precipitation (4h). The precipitate was filtered and the residue washed with cold water and diethylether to give 3.4g of an off white solid on drying in the oven at 50^{o}C for 8h.

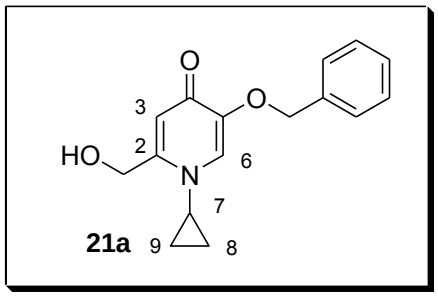

Off white solid (3.444g, 50%); mp. 174 – 175 ^{o}C δ_H (DMSO d_6, 400MHz), 8.28 (1H, *s,* H-6), 7.56 (1H, *s,* H-3), 7.40 (5H, *m,* Bn C-H), 5.26 (2H, *s,* 5-C**H$_2$**-Bn), 4.86 (2H, *s,* 2-C**H$_2$**OH), 2.5 (1H, *m*, H-7), 1.30-1.17 (4H, *m*, H-8, 9) δ_C (DMSO d_6, 100MHz), 162, 155.4, 143.7, 135.5, 130.7, 128.3 , 128.2 (2C) , 127.9 (2C),, 110.5, 71.6, 57.9, 37.1, 7.35(2C); HRMS. *m/z* calculated for $C_{16}H_{18}ClNO_3$ [M+H] 272.1299 found 272.12887; Anal. Calcd (found) for $C_{16}H_{17}ClNO_2$ $3H_2O$, C 59.06 (60.00), 7.13 (8.03), 4.31 (1.82).

***5-(benzyloxy)-2-(chloromethyl)-1-cyclopropylpyridin-4 (1H)-one hydrogenchloride*, (22a)**

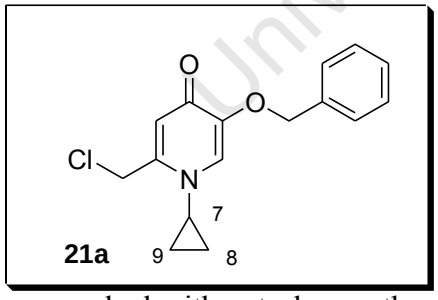

To neat thionyl chloride (11.42g, 96mmol) below 0^{o}C (ice /acetone mixture) was added **21a** (3.3g, 12.08mmol) then stirred further at ambient temperature for 1h. Diethylether was added to the preformed solid then put in a freezer for 1h, the solid was washed with petroleum-ether to give brown sticky/hygroscopic crystals. These were further dried in a dessicator under vacuum to give the product. Brown crystals (3.444g, 83%); mp. 132 – 133 ^{o}C; δ_H (DMSO d_6, 400MHz), 8.39 (1H, *s,* H-6), 7.37 (5H, *m,* Bn C-H), 6.34 (1H, *s,* H-3), 5.27 (2H, *s,* C**H$_2$**-Bn-5), 5.17 (2H, *s,* C**H$_2$**Cl-2), 3.99 (1H, *m*, H-7), 1.39-1.19 (4H, *m*, H-8, 9) δ_C (DMSO d_6, 100MHz), 162, 149.3, 145.2, 135.8, 132.4,

129.1 , 128.9 (2C) , 128.6 (2C), 114.4, 72.2, 40.6, 39.1, 8.44 (2C); HRMS. *m/z* calculated for $C_{16}H_{17}ClNO_2$ [M+H] 290.0948 found 290.0930; Anal. Calcd (found) for $C_{16}H_{17}Cl_2NO_2\,H_2O$, C 55.83 (56.28), H 5.56 (5.51), N 4.07 (3.66).

Synthesis of *5-(benzyloxy)-2-((6-(7-chloroquinolin-4-ylamino)hexylamino)methyl)-1-cyclopropylpyridin-4(1H)-one*. (32)

22a (290mg, 0.89mmol) was added to a solution of **8** (277mg, 1mmol) in DMF followed by triethylamine (100mg, 1mmol) and sodiumhydrogencarbonate (84mg, 1mmol) then refluxed at 110°C for 24h. After cooling the reaction mixture was diluted with water (15ml)and extracted with dichloromethane (15ml×3) before washing with water (15ml×1). This was dried over anhydrous sodium sulphate and concentrated to give an orange residue which was subjected to column chromatography (with MeOH/EtOAc/0.05%NH_3 as the eluant). Compound **32** was eluted in the 15%MeOH/EtOAc fraction and evaporated to give a white solid. Further drying was done under vacuum at 30-60°C for 6h to get the pure compound. This procedure was employed for the preparation of the successive compounds.

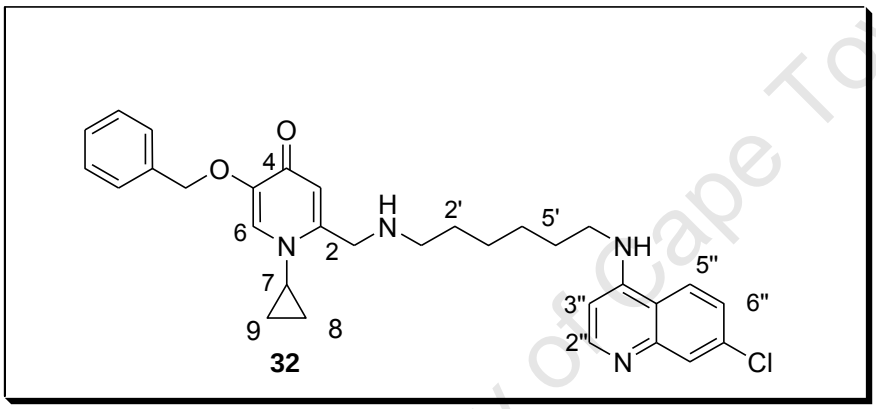

32

White solid (250mg, 51%); mp. 138-141 ^{0}C R_f 0.82 (NH_3/MeOH/ EtOAc 0.01:1:1) δ_H (DMSO, 300MHz), 8.38 (1H, *d, J* 6.0, H-2"), 8.28 (1H, *d, J* 9.0, H-5"), 7.76 (1H, *d, J* 3, H-8"), 7.35 (7H, *m,* benzylCH, H-6, H-6"), 7.21 (1H, *m*, NH), 6.44 (1H, *d, J* 6.0, H-3"), 6.29 (1H, *s,* H-3), 5.01 (2H, *s,* 5-C**H$_2$**Bn), 3.78 (2H, *s,* 2-C**H$_2$**NH), 3.49 (1H, *m,* H-7), 2.56 (obscured by DMSO, H-6'), 1.99 (2H, *t, J* 6.0, H-1'), 1.39 (8H, *m,* H-2'- 5'), 1.0 (4H, *m*, H-8, 9). δ_C (DMSO, 75MHz) 171.7, 151.7, 149.9, 149.8, 148.9, 146.0, 137.2, 133.1, 128.0 (2C), 127.7, 127.6 (2C), 127.5, 127.3 (2C), 123.9, 123.7, 115.5, 98.4, 70.6, 48.6, 48.3, 42.2, 33.9, 29.3, 27.7, 26.4, 26.3, 7.41 (2C); HRMS. *m/z* calculated for $C_{31}H_{36}ClN_4O_2$ [M+H] 531.2527 found 531.2543; Anal. Calcd (found) for $C_{31}H_{33}ClN_4O_2$

H_2O . C 67.81 (67.68), H 6.79 (6.90), N 10.20 (10.05); HPLC purity analysis 91% R_t 14.63. .

***5-(benzyloxy)-2-((4-(7-chloroquinolin-4-ylamino)butylamino)methyl)-1-cyclopropylpyridin-4(1H)-one*. (31)**

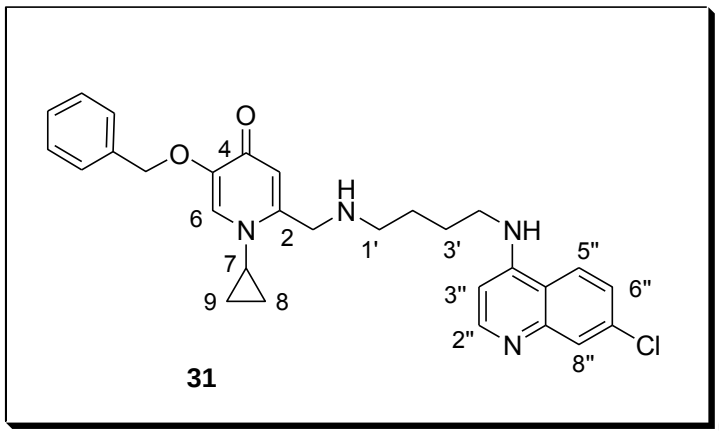

31

Bright yellow resin (300mg, 64%); mp. 73-74 ^{0}C R_f 0.75 (NH_3/MeOH/ EtOAc 0.01:1:1) δ_H (DMSO, 300MHz), 8.39 (1H, *d, J* 6.0, H-2"), 8.27 (1H, *d, J* 9.0, H-5"), 7.7 (1H, *d, J* 3, H-8"), 7.36 (7H, *m,* benzylCH, H-6", H-6), 7.33 (1H, *m*, NH), 6.46 (1H, *d, J* 6.0, H-3"), 6.31 (1H, *s,* H-3), 5.01 (2H, *s,* C**H$_2$**Bn-5), 4.25 (1H, *br.s*, NH), 3.8 (2H, *s,* C**H$_2$**NH-2), 3.42 (3H, *m,* H-4', 7), 1.65 (4H, *m,* H-2'- 3'), 1.05 (4H, *m*, H-8, 9). δ_C (DMSO, 75MHz) 172.2, 152.4, 150.1, 150.5, 149.6, 146.7, 137.8, 133.8, 128.7 (2C), 128.4 (2C), 128.2, 127.5, 127.3, 124.6, 124.4, 117.9, 115.9, 99.1, 71.1, 49.1, 48.9, 40.2, 34.6, 26.1, 22.9, 8.09 (2C); HRMS. *m/z* calculated for $C_{29}H_{31}ClN_4O_2$ [M+H] 503.2214 found 503.2225; Anal. Calcd (found) for $C_{29}H_{31}ClN_4O_2$ $2H_2O$. C 64.61 (64.54), 6.54(6.20), N 10.39 (10.88); HPLC purity analysis 91.5% R_t 9.79 min. .

***5-(benzyloxy)-2-(((3-(7-chloroquinolin-4-ylamino)propyl(methyl)amino)methyl)-1-cyclopropylpyridin-4(1H)-one*. (30)**

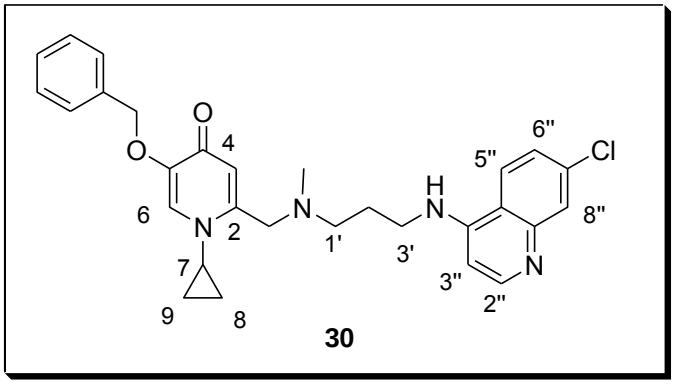

30

A solution of **6** (250mg, 1mmol) triethylamine (196mg, 2mmol), and sodiumhydrogencarbonate (168mg, 2mmol) in DMF 3ml was heated to 50^{o}C before adding **22a** (300mg, 0.9mmol), then refluxed at 90 ^{o}C for 12h. After a workup similar to that described for **32,** a brown oil was obtained which was recrystalized to colorless cubes

from MeOH/EtOAc. **Alternatively method B** was used to prepare more of this compound using **6** (112mg, 0.448mmol) and compound **22a** (100mg, 1mmol),and sodium hydrogencarbonate (84mg, 1mmol) to give a brown oil (200mg, 88%) .Colourless cubes (MeOH/ EtOAc 1:1), (427 mg, 89%); mp. 76 - 77 ^{0}C Rf 0.84 (NH_3/MeOH/ EtOAc 0.01:1:1) δ_H (DMSO, 300MHz), 8.39 (1H, *d, J* 6.0, H-2"), 8.23 (1H, *d, J* 9.0, H-5"), 7.76 (1H, *d, J* 3, H-8"), 7.37 (7H, *m,* benzylCH, H-6", H-6), 7.14 (1H, *t, J* 6, NH), 6.44 (1H, *d, J* 6.0, H-3"), 6.25 (1H, *s,* H-3), 4.96 (2H, *s,* C**H$_2$**Bn-5), 3.57 (2H, *s,* C**H$_2$**NH-2), 3.52 (1H, *m,* H-7), 2.56 (2H, *t, J* 6, H-3'), 2.22 (3H, *s,* C**H$_3$**N), 2.71 (2H, *t, J* 6, H-1'), 1.89 (2H, *m,* H-2'), 0.91 (4H, *m*, H-8, 9). δ_C (DMSO, 75MHz) 171.9, 152.4, 150.6, 149.6, 148.4, 146.9, 137.7, 133.8, 128.7 (2C), 128.4 (2C), 128.2, 128.1, 127.9, 124.5, 124.4, 117.9, 117.7, 99.1, 71.0, 58.4, 55.1, 42.0, 40.8, 34.9, 25.9, 7,95 (2C); HRMS. *m/z* calculated for $C_{29}H_{32}ClN_4O_2$ [M+H] 503.2214 found 503.2228; Anal. Calcd (found) for $C_{29}H_{31}ClN_4O_2$ 3.5H_2O, C 61.53 (61.40) H 6.77 (6.08), N 9.90 (9.84)**;** HPLC purity analysis 99.4% R_t 10.8 min. .

***5-(benzyloxy)-2-((3-(7-chloroquinolin-4-ylamino)propylamino)methyl)-1-cyclopropylpyridin-4(1H)-one.* (29)**

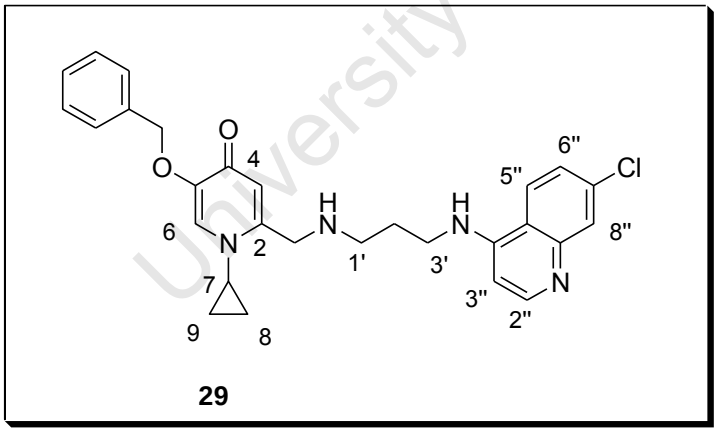

29

Yellow foam (420 mg, 91%); mp. 58 - 60^{0}C; R_f 0.75 (NH_3/MeOH/ EtOAc 0.01:1:1) δ_H (DMSO, 300MHz), 8.39 (1H, *d, J* 6.0, H-2"), 8.21 (1H, *d, J* 9.0, H-5"), 7.7 (1H, *d, J* 3, H-8"), 7.36 (8H, *m,* benzyl-CH, H-6", H-6, NH), 6.48 (1H, *d, J* 6.0, H-3"), 6.33 (1H, *s,* H-3), 5.01 (2H, *s,* 5-C**H$_2$**Bn), 3.82 (2H, *s,* 2-C**H$_2$**NH), 3.50 (1H, *m,* H-7), 3.37 (2H, *t, J* 6, H-3'), 2.71 (2H, *t, J* 6, H-1'), 1.85 (2H, *m,* H-2'), 0.98 (4H, *m*, H-8, 9). δ_C (DMSO, 75MHz) 172.2, 152.4, 150.6, 150.4, 149.5, 146.7, 137.8, 133.8, 128.7 (2C), 128.4 (2C), 128.2, 128.1, 127.9, 124.5 (2C), 117.9, 116.0, 99.1, 71.1, 48.9, 47.3, 40.3, 34.6, 28.5, 8.09 (2C); HRMS. *m/z* calculated for $C_{28}H_{30}ClN_4O_2$ [M+H] 489.2057 found 489.2071; Anal. Calcd (found) for

$C_{28}H_{29}ClN_4O_2$ $1H_2O$, C 66.33(66.08) H 6.16 (6.16), N 11.04 (11.47); HPLC purity analysis 95% R_t 13.95 .

***5-(benzyloxy)-2-((2-(7-chloroquinolin-4-ylamino)ethylamino)methyl)-1-cyclopropylpyridin-4(1H)-one.* (28)**

Orange foam (390 mg, 87%); mp. 56-57^{0}C R_f 0.74 (NH_3/MeOH/EtOAc 0.01:1:1) δ_H (DMSO, 300MHz), 8.40 (1H, *d, J* 6.0, H-2"), 8.23 (1H, *d, J* 9.0, H-5"), 7.78 (1H, *d, J* 3, H-8"), 7.37 (7H, *m,* benzylCH, H-6", H-6), 7.17 (1H, *m,* NH), 6.52 (1H, *d, J* 6.0, H-3"), 6.33 (1H, *s,* H-3), 5.01 (2H, *s,* C**H$_2$**Bn-5), 3.87 (2H, *s,* C**H$_2$**NH-2), 3.50 (1H, *m,* H-7), 3.40 (2H, *t, J* 6, H-2'), 2.89 (2H, *t, J* 6, H-1'), 0.95 (4H, *m*, H-8, 9). δ_C (DMSO, 75MHz) 172.2, 152.3, 150.6, 150.3, 149.6, 146.7, 137.8, 133.8, 128.7(2C), 128.4 (2C), 128.2 (2C), 127.9, 124.5(2C), 117.9, 116.0, 99.2, 71.1, 48.7, 47.3, 43.0, 34.6, 8.04(2C); MS. *m/z* calculated for $C_{27}H_{28}ClN_4O_2$ [M+H] 475.19 found 475.2(100%); Anal. Calcd (found) for $C_{27}H_{27}ClN_4O_2$ $1H_2O$, C 65.78 (65.00) H 5.93 (5.97), N 11.36 (12.20); HPLC purity analysis 95.6% R_t 10.28 min.

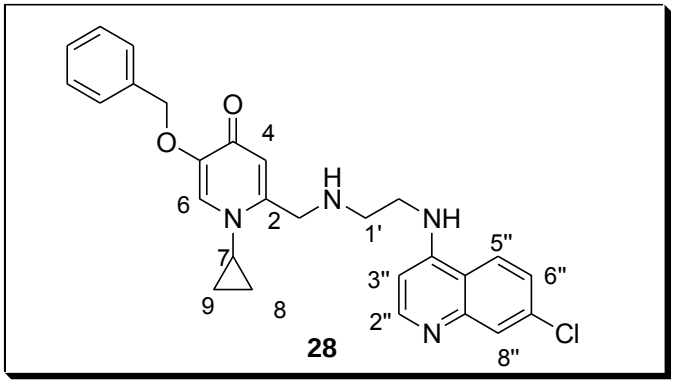

28

***2-((6-(7-chloroquinolin-4-ylamino)hexylamino)methyl)-1-cyclopropyl-5-hydroxypyridin-4(1H)-one.* (32a)**

White solid (250mg, 51%); R_f 0.12 (NH_3/MeOH/ EtOAc 0.01:1:1) δ_H (DMSO, 300MHz), 10.2 (1H, *br.s*, OH), 9.72 (1H, *m,* NH), 8.82 (1H, *d, J* 9.0, H-5"), 8.49 (1H, *d, J* 6, H-2"), 8.33 (1H, *s,* H-6), 8.12 (1H, *d, J* 3,

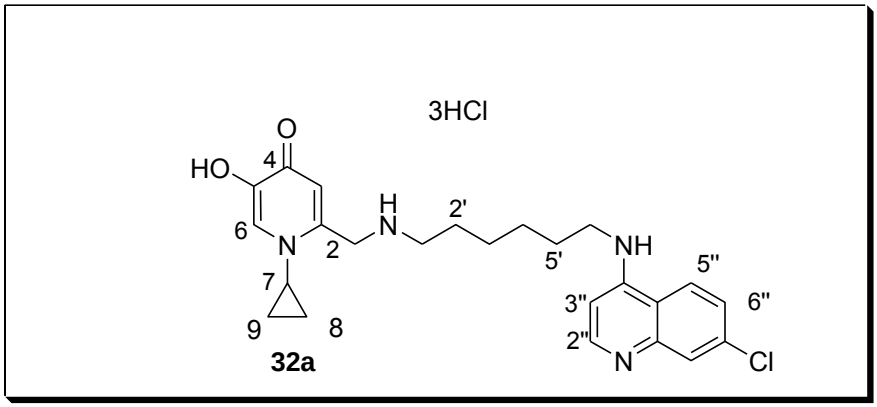

32a

H-8"), 7.70 (1H, *dd, J* 3.0, 9.0, H-6"), 7.67 (1H, *s,* H-3), 6.87 (1H, *d, J* 6.0, H-3"), 4.55 (2H, *s,* 2-C**H$_2$**NH), 4.23 (1H, *m,* H-7), 3.56 (1H, *m,* H-6'), 3.08 (2H, *m,* H-1'), 1.76 (4H, *m,* H-2', 5'), 1.38 (4H, *m*, H-3', 4'), 1.3 (4H, *m,* H-8, 9). δ_C (DMSO, 75MHz) 161.2, 155.8, 145.2, 143.1, 139.1(2C), 138.4, 132.4, 127.2, 126.6(2C), 119.5, 115.8, 99.04, 48.1, 45.2, 43.4, 27.8, 26.2, 26.1, 25.6, 22.9, 8.53 (2C); HRMS. *m/z* calculated for $C_{24}H_{30}ClN_4O_2$ [M+H] 441.2057 found 441.2074; Anal. Calcd (found) for $C_{24}H_{32}Cl_4N_4O_2$ $4H_2O$, C 46.31 (45.72), H 6.48 (6.74), N 9.00(9.69); HPLC purity analysis 98% R_t 15.70 min. .

***2-((4-(7-chloroquinolin-4-ylamino)butylamino)methyl)-1-cyclopropyl-5-hydroxypyridin-4(1H)-one* (31a)**

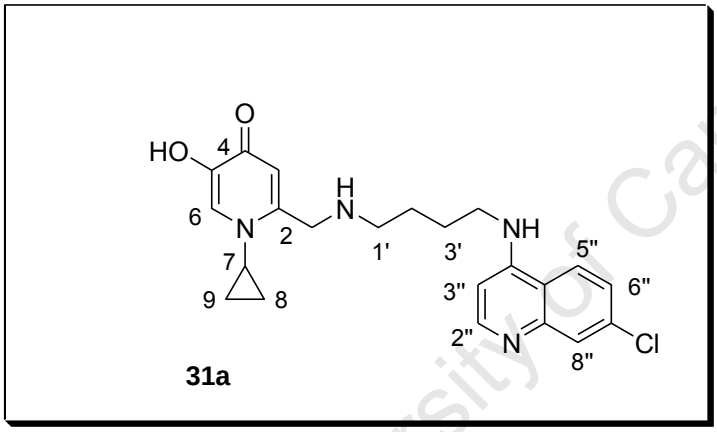

31a

Sticky white solid (100mg, 58%) Rf 0.1 (NH_3/MeOH/ EtOAc 0.01:1:1) δ_H (CD_3OD, 300MHz), 8.55 (1H, *d, J* 9.0, H-5"), 8.40 (1H, *d, J* 6.0, H-2"), 8.27 (1H, *s,* H-6), 7.89 (2H, *m,* H-8", NH), 6.46 (2H, *m,* H-3, 6"), 6.95 (1H, *br.s,* H-3"), 4.95 (obscured by H_2O, C**H$_2$**NH-2), 4.19 (1H, *br.s*, H-7), 3.42 (2H, *m*, H-4'), 2.0 (4H, *m,* H-2'- 3'), 1.19 (4H, *m*, H-8, 9); δ_C (CD_3OD, 75MHz) 162.3, 157.7, 146.6, 144, 143.8, 140.9, 139.9, 134.3, 128.6, 126.5, 124.2, 120.4, 115.8, 100.1, 47.1, 44.0, 40.5 (2C), 26.1, 24.6, 9.34 (2C); HRMS. *m/z* calculated for $C_{22}H_{26}ClN_4O_2$ [M+H] 413.1744 found 413.1763; Anal. Calcd (found) for $C_{22}H_{28}Cl_4N_4O_2$ $4.5H_2O$ C 43.79 (44.58), H 6.18 (6.96), N 9.26 (8.04); HPLC purity analysis 98%. R_t 12.66 min.

***2-(((3-(7-chloroquinolin-4-ylamino)propyl(methyl)amino)methyl)-1-cyclopropylhydroxypyridin-4(1H)-one trihydrogenchloride* (30a)**

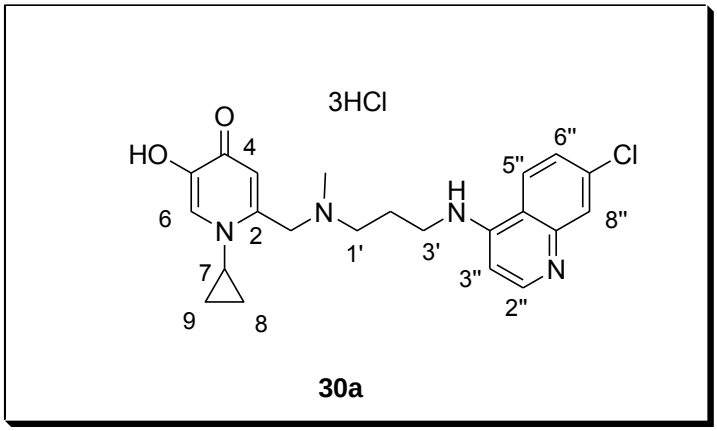

30a

Brown oil (20mg, 24%), Rf 0.21 (NH_3/MeOH/EtOAc 0.01:1:1) δ_H(CD_3OD, 300MHz), 8.43 (1H, *d, J* 7.2, H-2"), 8.37 (1H, *d, J* 8.1, H-5"), 8.01 (1H, *s,* H-6), 7.90 (1H, *d, J* 4, H-8"), 7.71 (1H, *dd, J* 9.1, 2.0, H-6"), 7.25 (1H, *s,* H-3), 6.91 (1H, *d, J* 7.2, H-3"), 4.25 (2H, *s,* 2-C**H$_2$**NH), 4.12 (1H, *m,* H-7), 3.69 (2H, *t, J* 7, H-3'), 2.99 (1H, *t, J* 7.8, H-1'), 2.61 (3H, *s,* C**H$_3$**N), 2.16 (2H, *m,* H-2'), 1.30 (4H, *m*, H-8, 9). δ_C (CD_3OD, 75MHz) 156.3, 145.1, 142.5, 139.8, 138.6, 130.2, 127.4 (2C), 124.4, 119.0 (2C), 115.5, 114.1, 98.3, 56.5, 54.3, 41.1, 40.7, 37.5, 24.7, 7.56 (2C); HRMS. *m/z* calculated for $C_{22}H_{26}ClN_4O_2$ [M+H] 413.1744 found 413.1753; Anal. Calcd. (found) for $C_{22}H_{30}Cl_4N_4O_2$, C50.40 (36.53), H 5.77 (4.26), N 10.61 (6.79); HPLC purity analysis 98% R_t 9.70min .

***2-((3-(7-chloroquinolin-4-ylamino)propylamino)methyl)-1-cyclopropyl-5-hydroxypyridin-4(1H)-one* (29a)**

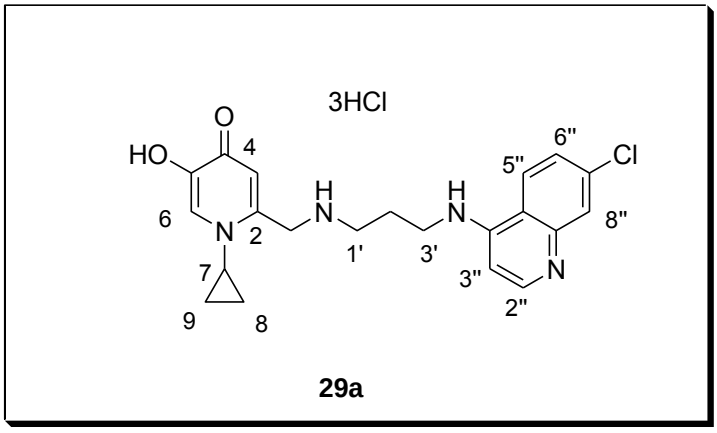

29a

Yellow foam (150mg, 60%); mp. 89-91 ^{0}C Rf 0.15 (NH_3/MeOH/ EtOAc 0.01:1:1) δ_H (DMSO, 300MHz), 10.3 (1H, *br.s*, OH), 9.92 (1H, *s,* NH), 8.86 (1H, *d, J* 9.0, H-5"), 8.56 (1H, *d, J* 6.0, H-2"), 8.30 (1H,*s,* H-6), 8.14 (1H, *d, J* 3.0, H-8"), 7.74 (1H, *dd, J* 9.0,

3.0, H-6"), 7.47 (1H, *s,* H-3), 6.96 (1H, *d, J* 6, H-3"), 4.59 (2H, *s,* 2-C**H$_2$**NH), 4.22 (1H, *m,* H-7), 3.75 (2H, *m,* H-3'), 3.28 (2H, *t, J* 6, H-1'), 2.25 (2H, *m,* H-2'), 1.31 (4H, *m*, H-8, 9). δ_C (DMSO, 75MHz) 161.7, 155.2, 145.0, 142.6, 142.2, 138.4, 137.8, 130.9, 126.6, 126.0, 118.8, 118,8, 115.5, 98.6, 45.1(2C), 44.8, 38.1, 18.3, 7.92(2C); HRMS. *m/z* calculated for $C_{21}H_{24}ClN_4O_2$ [M+H] 399.1583 found 399.1598; Anal. Calcd (found) for $C_{21}H_{26}Cl_4N_4O_22H_2O$. C 46.34 (46.26), H 5.56 (5.74), N 10.29 (10.22); HPLC purity analysis 98% R_t 12.55min .

***2-((2-(7-chloroquinolin-4-ylamino)ethylamino)methyl)-1-cyclopropyl-5-hydroxypyridin-4(1H)-one* (28a)**

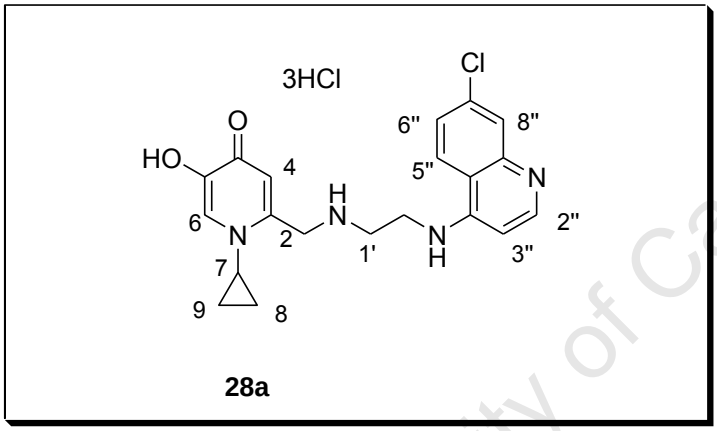

28a

Cream solid (108 mg, 56%); mp. 215-217 ^{0}C Rf 0.11 (NH_3/MeOH/ EtOAc 0.01:1:1); δ_H (DMSO, 300MHz), 9.55 (2H, *br.s* OH, NH), 8.93 (1H, *d*, *J* 9.0, H-5"), 8.63 (1H, *d, J* 6.0, H-2"), 8.32 (1H, *s,* H-6), 8.17 (1H, *d, J* 3, H-8"), 7.75 (1H, *dd, J* 3.0, 9.0, H-6"), 7.48 (1H, *s,* H-3), 7.11 (1H, *d, J* 6, H-3"), 4.71 (2H, *s,* C**H$_2$**NH-2), 4.25 (1H, *m*, H-7), 4.07 (2H, *m,* H-2'), 3.54 (2H, *m,* H-1'), 1.27 (4H, *m*, H-8, 9). δ_C (DMSO, 75MHz) 144.9, 142.9, 142.2, 138.3, 137.9, 131.0, 126.6 (2C), 126.4 (2C), 118.8, 115.6, 115.1, 98.8, 45.4 (2), 44.8, 38.2, 7.93 (2C); HRMS. *m/z* calculated for $C_{20}H_{22}ClN_4O_2$ [M+H] 385.1400 found 385.1405; Anal. Calcd (found) for $C_{20}H_{24}Cl_4N_4O_21.5H_2O$. C 46.08 (45.45), H 5.22 (5.21), N 10.75 (11.70); HPLC purity analysis 93% R_t 12.34min. .

5.4.7. Synthesis of gallium (III) and iron (III) complexes of A/AB series

Tris(3-hydroxy-2-methyl-N-(7-chloro-4-quinoinlyl)-1-(6-aminobutyl)-3-(hydroxy)-2-methyl-4(1H)-pyridinonato iron (III) **(13d)**

A solution of iron (III) nitrate nonahydrate (20.2mg, 0.05mmol) in 1ml deionised water was added to a stirred solution of **13a** (67.8mg, 0.15mmol), in 2ml MeOH at pH 8 (2M NaOH). The mixture was refluxed at 80^{o}C for 4h. The resultant precipitate was washed with water, MeOH/H_2O 5:1 and cold MeOH in that order then freeze dried for 3h at -57^{o}C to obtain a brick red solid.

Analogous procedure was applied to synthesize complexes **13e, 15d** and **15e** using compounds ligands **13a** and **15a** respectively.

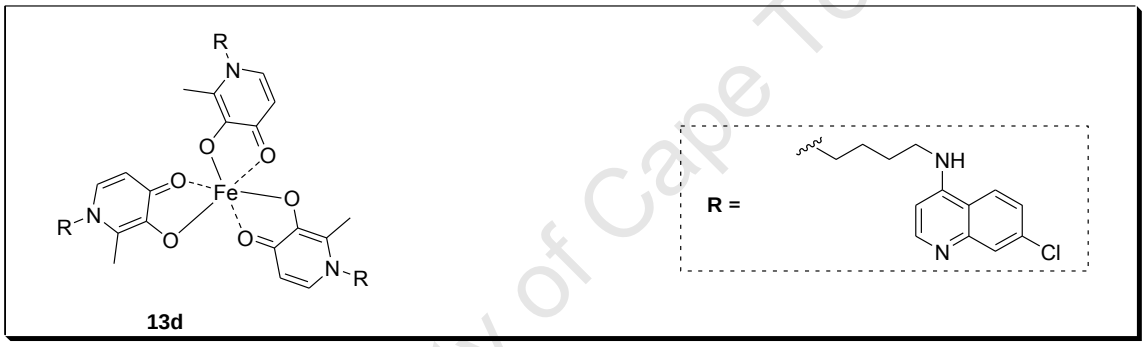

13d

Brick red solid (48mg, 72%); mp. 225-226 ^{o}C; R_f 0.04 (MeOH/CH_2Cl_2 1:1) δ_H ($DMSOd_6$, 400MHz), 9-6 (*br.s* – quinolinyl, pyridinone C-H), 4-2 (*br.s*, aliphatic C-H); δ_C ($DMSOd_6$, 100MHz) no peaks observed (30^{o}C); Anal. Calcd (found) for $C_{57}H_{57}Cl_3FeN_9O_6$ $10H_2O$ $NaNO_3$. C 48.71(49.73), H 5.52 (5.00), N 9.97 (9.46); MS found 1173 ([ML_3 +2Na+H , 25%), 1171 ([ML_3 +2Na - H], 100%), 858.7 ([ML_2 2Na - H], 18%)

Tris (N-(7-chloro-4-quinolinyl)-1-(6-aminobutyl)-3-(hydroxy)-2-methyl-4(1H)-pyridinonato gallium (III) **(13e)**

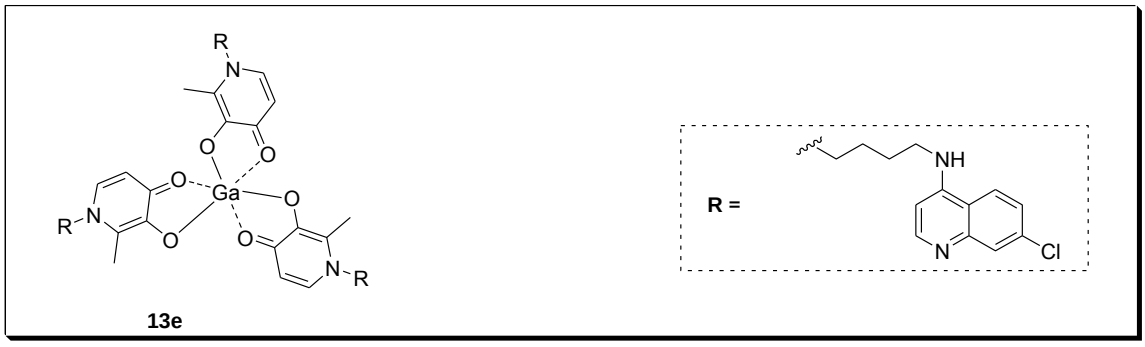

Dark brown solid (117mg, 81%); mp. 215 – 216 ^{o}C; R_f 0.14 (MeOH/ CH_2Cl_2, 1:1). δ_H ($DMSOd_6$, 400MHz) 8.41 (1H, *d, J* 4.8, H-2"), 8.29 (1H, *d, J* 7.8, H-5"), 7.52 (1H, *s,* H-8"), 7.46 (2H, *m,* H-6, 6"), 6.56 (1H, *m*, H-5), 6.27 (1H, *d, J* 7.6, H-3"), 4.18 (2H, *m,* H-1'), 3.38 (masked by H_2O, H-4'), 2.31 (3H, *s,* C**H$_3$**-py), 1.79 (4H, *m,* H-2', 3'), δ_C ($DMSOd_6$, 100MHz) , 168.5, 167.1 (2C), 154.0 (3C), 152.6, 152.5 (2C), 151.9 (2C), 151.7 (2C), 151.4 (2C), 148.9 (2C), 148.7, 135.1 (2C), 134.7, 131.6 (3C), 129.5, 127.6 (2C), 127.3, 125.1 (6C), 118.1 (2C), 107.8 (2C), 106.9, 99.5 (3C), 55.1 (2C), 54.7, 42.8 (2C), 42.7, 28.7, 28.5 (2C), 25.5, 25.4 (2C), 12.7 (3C).. Anal. Calcd (found) for $C_{57}H_{57}Cl_3GaN_9O_6$ $NaNO_3$ $12H_2O$. C 47.50(47.63), H 5.66 (5.04), N 9.72 (9.53); MS found 1140.28 (ML_3, 42%), 783.13 (ML_2 +2H, 100%),

Tris(3-hydroxy-2-methyl-N-(7-chloro-4-quinolinyl)-1-(6-aminohexyl)-3-(hydroxy)-2-methyl-4(1H)-pyridinonato iron (III) **(15d)**

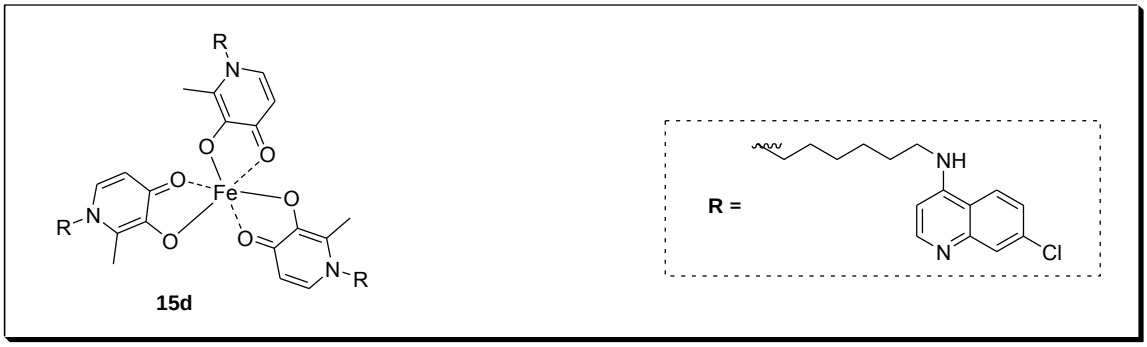

Brick red solid (90mg, 66%); 196 – 200 ^{o}C; R_f 0.1 (MeOH/ $CH_2Cl_2$1:1) δ_H ($DMSOd_6$, 400MHz), 9-6 (*br.s* – quinolinyl, pyridinone C-H), 4-2 (*br.s,* aliphatic C-H); δ_C ($DMSOd_6$, 100MHz) no peaks observed (30^{o}C); Anal. Calcd (found) for $C_{63}H_{69}Cl_3FeN_9O_6$ $7H_2O$. C 56.61(56.34), H 6.26(5.81), N 9.43(10.06); MS found 1233 ([ML_3 +2H + Na, 100%).

Bis-(N-(7-chloro-4-quinolinyl)-1-(6-aminohexyl)-3-(hydroxy)-2methyl-4(1H)-pyridinonato gallium (III) **(15e)**

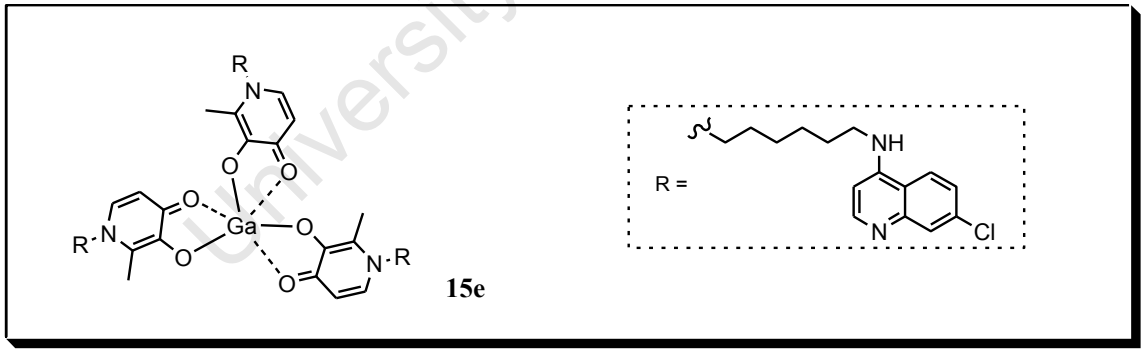

Pink shiny solid (101mg, 81%); mp. 194 – 196 ^{o}C; R_f 0.14 (MeOH/ CH_2Cl_2,1:1) δ_H (CD_3OD, 400MHz) 8.32 (2H, *m,* H-2", 5"), 7.86 (1H, *s,* H-8"), 7.62 (1H, *d, J* 8.7, H-6"), 7.46 (1H, *d, J* 5.2, H-6 py), 6.76 (1H, *d, J* 6.0, H-3"), 6.40 (1H, *d, J* 5.4, H-5 py), 4.08 (2H, *m,* H-1'), 3.55 (2H, *m*, H-6'), 2.40 (3H, *s,* C**H$_3$** py), 1.78 (4H, *m,* H-2', 5'), 1.43 (4H, *s,* H-3', 4'). Anal. Calcd (found) C 50.80 (50.77), H 6.02 (5.91), N 9.40 (10.20) for

$C_{63}H_{69}Cl_3GaN_9O_6$ $10H_2O$;$NaNO_3$ MS found 946 (ML_2 + 2Na + NO_3, 100%). ML_3 (absent).

Aqua-bis-(3-hydroxy-2-methyl-N-(7-chloro-4-quinolinyl)-1-(6-aminohexyl)-3-(hydroxy)-2-methyl-4(1H)-pyridinonato-nitrato- gallium (III) **(15f)**

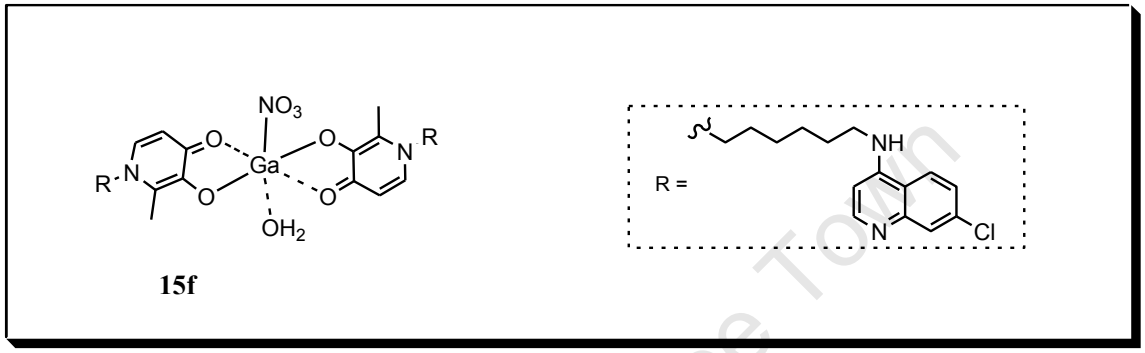

15f

A solution of gallium (III) nitrate nonahydrate (31.2mg, 0.075mmol) in 1ml deionised water was added dropwise to a solution of compound **15a** (66mg, 0.15mmol)**,** in 2ml MeOH, pH was adjusted to 8 (2M NaOH). The resultant precipitate was washed with water, MeOH/H_2O 5:1 then cold MeOH and freeze dried for 1.5h at -57^oC to obtain a pale pink solid. To confirm anion exchange in **15f,** an aqueous solution of sodium hexafluoride phosphate was added to a hot solution of the complex in DMSO, a precipitate formed afterwards. This test was repeated for the other complexes and none of them formed a precipitate.

Pale pink solid (40mg, 50%); mp. 183 – 184 ^oC; R_f 0.14 (MeOH/ CH_2Cl_2,1:1); δ_H ($DMSOd_6$, 300MHz) 8.41 (1H, *d, J* 5.7, H-2"), 8.33 (1H, *d, J* 9, H-5"), 7.82 (1H, *d, J* 1.5, H-8"), 7.71 (1H, *d, J* 5.4, H-6 py), 7.50 (1H, *dd, J* 9, 1.8, H-6"), 6.72 (1H, *d, J* 6.4, H-3"), 6.53 (1H, *m,* H-5 py) , 4.13 (2H, *t, J* 7.2, H-1'), 3.44 (obscured by H_2O, H-6'), 2.44 (3H, *s,* C**H**$_3$ py), 1.69 (4H, *m,* H-2', 5'), 1.40 (4H, *s,* H-3', 4'). δ_C ($DMSOd_6$, 75MHz) 169.3, 151.8, 146.8, 143.1, 135.9, 134.3, 130.8, 126.5, 126.2, 122.8, 120.9, 117.2, 106.9, 98.5, 54.5, 39.7, 29.9, 27.5, 25.9, 25.4, 12.2. Anal. Calcd (found) for [$C_{42}H_{46}Cl_2GaN_6O_4^+$ NO_3^-

] $3H_2O$ $NaNO_3$. C 48.48 (48.52), H 5.04 (5.62), N 10.77(10.04); HRMS. *m/z* calculated for $C_{42}H_{46}Cl_2GaN_6O_4$ [M+H] 837.2213 found 837.2210.

Bis(N-(7-chloro-4-quinolyl)-1-(6-aminohexyl)-3-(hydroxy)-2-ethyl-4(1H)-pyridinonato gallium (III) **(16d)**

A solution of gallium (III) nitrate nonahydrate (21mg, 0.5mmol) was added dropwise while stirring to an aqueous solution of **16a** (45mg, 0.1mmol). After pH adjustment to 7 (0.1M NaOH), the mixture was refluxed for 4h at 85°C, then left to cool overnight. TLC indicated all the ligand had been used up in the reaction. Drying by rotary evaporation afforded an orange powder, which was washed with water to give orange crystal*s,* which were further dried under vacuum.

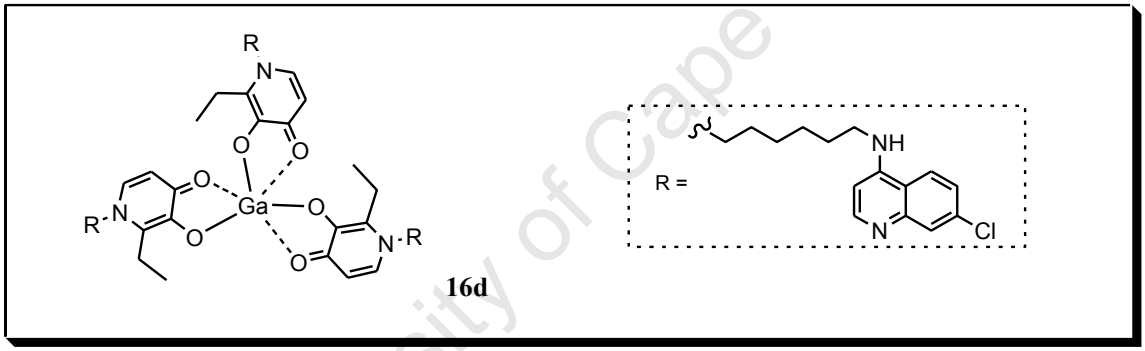

16d

Orange crystals (10mg, 24%), from H_2O; mp. 200 – 204 °C; R_f (50% MeOH/ CH_2Cl_2) 0.24; δ_H (400MHz, CD_3OD) 8.3 (2H, *m*, H2"-5"), 7.85 (1H, *d, J* 0.8, H-8"), 7.64 (1H, *dd, J* 1.6, 9.0, H-6"), 7.46 (1H, *d, J* 6.8, H-6), 6.76 (1H, *d, J* 6.8, H-5), 6.4 (1H, *d, J* 6.8, H-3"), 4.09 (2H, *t, J* 8.7, H-1'), 3.56 (2H, *t, J* 7.6, H-6'), 3.41 (2H*, m,* C**H₂**CH_3-Py), 2.4 (3H, *br.s,* CH_2C**H**$_3$-Py), 1.8–1.72 (4H, *m,* H-2',5'), 1.5–1.38(4H, *m,* H-3', 4'); MS found 974 (ML_2 +2Na + NO_3, 100%), ML_3 (absent); Anal. Calcd (found) for $C_{66}H_{75}Cl_3GaN_9O_6$ $12H_2O$ $2NaNO_3$. C 47.97 (48.04), H 6.04 (5.67), N 9.32 (8.47).

5.4.8. Synthesis of 4-aminoquinoline-biscatecholate hybrids

***2, 3-Diacetoxybenzoic acid* (33)**

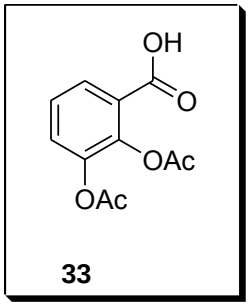

33

To 2,3-dihydroxybenzoic acid 99% (4.70g, 30mmol) was added acetic anhydride (6.16g, 60mmol), followed by 3drops of conc. Sulphuric acid then the mixture was stirred under nitrogen, a white precipitate was observed after 20minutes. After 12h of reaction the slurry was poured over ice (200g) and extracted with dichloromethane (100ml ×7). The organic layer was back-extracted with ice water (50mL × 3), dried over anhydrous Na_2SO_4, filtered and reduced in vacuo to the product. White solid (5.945, 82%); mp. 145-148^{0}C, R_f 0.49 (EtOAc) δ_H ($CDCl_3$, 300MHz), 7.97 (1H, *d, J* 7.6, H-3), 7.37 (2H, *m,* H-4, 5), 2.33(3H, *s,* C**H$_3$**OCO), 2.32 (3H, *s*, C**H$_3$**OCO).

***2,3-Diacetobenzoylchloride* (34)**

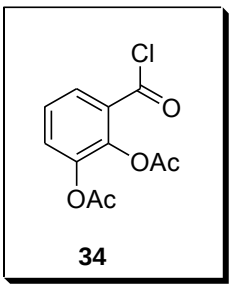

34

A solution of **33** (5.428g, 32mmol) in dry ethanol-free chloroform (120ml), was cooled to 0^{o}C under nitrogen before adding phosphorous(V) pentachloride (10g, 48mmol), the mixture was allowed to warm to ambient temperature and stirred for 24h. After concentration in vacuo the residue was redissolved in benzene (250mL), washed with 5% $NaHCO_3$, (w/v) (20ml×3), dried over anhydrous $MgSO_4$, filtere*d,* evaporated under vacuo to give a yellow oil that crystalised on standing. White crystals (5.456, 67%); mp. 116-118 ^{0}C Rf 0.71 (EtOAc) δ_H ($CDCl_3$, 300MHz), 7.91 (1H, *dd, J* 7.6, 1.7, H-3), 7.61-7.08 (2H, *m,* H-4, 5), 2.26 (3H, *s*, C**H$_3$**OCO), 2.24 (3H, *s,* C**H$_3$**OCO).

***4-((3-aminopropylamino)methyl)benzoic acid* (35)**

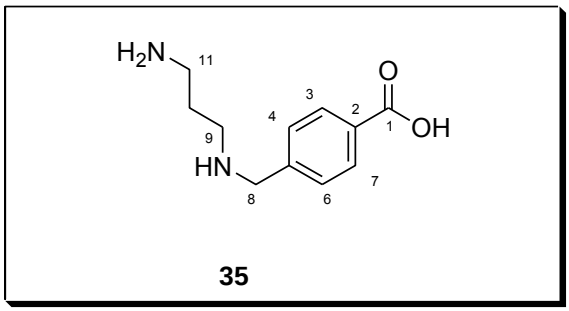

35

4-Formylbenzoic acid 97% (7.5g, 50mmol) was dissolved in MeOH (15ml) followed by the addition of 1,3-diaminopropane (4.4g, 60mmol), then Pd/C (1.0g) was added under nitrogen. The mixture was hydrogenated at ambient temperature and atmospheric pressure for 2days. TLC showed incomplete convertion hence further hydrogentaion was done at 1 atmosphere on the Parr hydrogenator for complete reduction. Then, the reaction mixture was filtered over celite and the solvent evapourated to give thick oil that solidified on standing. The residue was co-distilled with toluene (10ml×10) to remove the amine residue. This yielded a golden solid.

Golden solid (7.45g, 67%); mp. 78-81 ^{0}C δ_H (D_2,O, 300MHz), 7.72 (2H, *d*, *J* 8.2, H-3, 7), 7.23 (2H, *d*, *J* 8.2 H-4, 6), 3.65 (2H, *s,* H-8), 2.82 (2H, *m,* H-9), 2.56 (2H, *m,* H-11), 1.71 (2H, *m,* H-10). δ_C (D_2,O, 75MHz) 175.0, 140.8, 135.8, 129.5, 129.3, 129.1, 128.9, 51.9, 45.8, 38.0, 26.9. Anal. Calcd (found) for $C_{11}H_{16}N_2O_2$ H_2O, C 58.39 (59.24), H 8.02 (9.23), 12.38 (14.05)

***4-((2,3-Diacetoxy-N-(3-(2,3-diacetoxybenzamido)propyl)benzamido)methyl)benzoic acid* (36)**

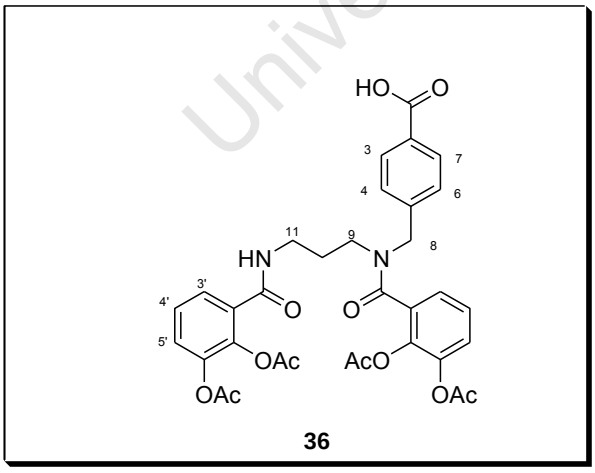

36

A solution of **35** (1.846g, 7.21mmol) in 0.5M $NaHCO_3$ (60ml, 30mmol) was sonicated at 0-5^{o}C, then a solution of **34** (3.580g, 14mmol**)** in dry THF (20ml) was added to it dropwise with stirring for 30 minutes. The mixture was reduced in vacuum to remove THF, cooled to 0^{o}C, then acidified to pH 1 (6N, HCl). The resultant white sticky precipitate was extracted into ethylacetate (30ml x 3). The organic layer was washed with brine (50ml x 2), dried over anhydrous $MgSO_4$, evaporated under vacuum to give the target compund

as an off white solid which was recrystalised from Methanol. White powder (3.02g, 65%); mp.168 - 170 ^{o}C; R_f 0.74 (MeOH/ EtOAc 1:1) δ_H ($CDCl_3$, 300MHz), 8.03-7.91 (4H, *m,* H-3, 4, 6, 7), 7.23 (6H, *m,* 3", 4", 5"), 3.46 (2H, *s,* H-8), 2.24-2.39 (16H, C**H$_3$**OCO, H-9, 11), 1.78 (2H, *m,* H-10).). δ_C ($CDCl_3$, 75MHz), 191.3, 169.7, 168.9, 168.2, 167.6, 167.4, 165.1, 143.5, 142.7, 139.1, 131.0, 130.7, 130.6, 129.9, 129.4, 128.3, 128.1, 127.0, 126.6, 126.4, 126.3, 125.7, 124.6, 124.1, 123.8, 60.3, 52.11, 47.9, 46.4, 41.9, 36.8, 29.6, 26.9. HRMS. *m/z* calculated for $C_{33}H_{33}N_2O_{12}$ [M+H] 649.2034 found 649.2029; Anal. Calcd (found) for $C_{33}H_{32}N_2O_{12}$ H_2O, C 59.46 (59.17), H 5.14 (5.51), 4.20 (2.92).

***3-((4-(6-(7-chloroquinolin-4-ylamino)hexylcarbamoyl)benzyl)(3-(2,3-diacetoxybenzamido)propyl)carbamoyl)-1, 2-phenylene diacetate.* (37)**

A solution of **36** (519mg, 0.8mmol) and N-methylmorpholine (99µl) was dissolved in dry THF (8ml) and cooled to -20^{o}C, methylformate (116 µl) was added then stirred for 1h at -10^{o}C. To the mixture a solution of **8** (243mg, 0.88mmol), triethylamine (123 µl, 0.88mmol) in 5ml THF/water (4:1) was added and stirred at -10^{o}C for 12h. The solvent was removed under vacuum, attempts to redissolve the residue in EtOAc failed; hence it was redissolved in MeOH/ACN dried over Na_2SO_4, evapourated under vacuum to give 200mg of the crude product as a white foam. 100mg of this was purified by HPLC to give 30mg of the pure compound. White hygroscopic solid (30mg, 8%); mp. 117–120 ^{o}C: R_f 0.22 (MeOH/EtOAc1:1); δ_H (CD_3OD, 300MHz), 8.31 (2H, *m*), 7.99 (3H, *m,* H-5", H-3, 7), 7.82 (1H, *d, J* 2.1, H-8"), 7.45 (3H, *m*), 7.28 (9H, *m*), 3.55 (2H, *m,* H-6"'), 3.34 (2H, *s,* H-8), 3.15 (2H, *m,* H-1"'), 2.30-2.27 (4H, *m,* H-9, 11), 2.25-2.14 (12H, *m,* C**H$_3$**OCO), 1.82 (4H, *m,* H-2"' 5"'), 1.65

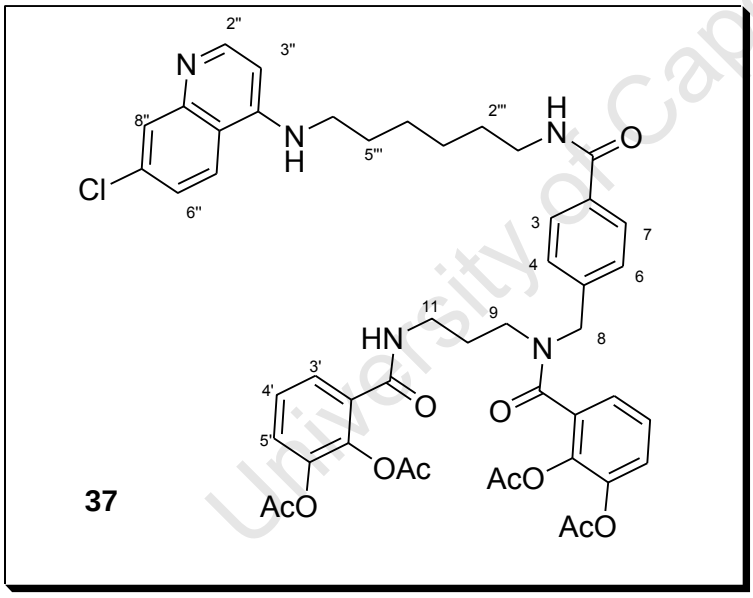

37

(2H, *m,* H-10), 1.50 (4H, *m,* H-3''', 4'''); HRMS. *m/z* calculated for $C_{48}H_{50}ClN_5O_{11}$ [M+H] 908.3274 found 908.3275.

5.5. Procedures for biological assays

5.5.1 phiβ-Haematin Inhibition Assay

The assay is based on the ability of haematin, but not β-haematin to form a low spin complex with aqueous pyridine at pH 7.5. The assay has been fully described by Ncokazi and Egan, 2005. It involves serial dilution of the drug solutions in triplicate in a 96 well plate using a multichannel pipette. The test drugs (compounds) were dissolved in DMSO or methanol. Drug concentrations varied from 1-10 equivalents relative to haematin, each well containing 10.12μL in the final mixture. 101.2 μL of haematin stock solution (1.68mM in 0.1M NaOH) was added to each well followed by 10.12 μL of 1.0M HCl. The 58.7 μL of acetate solution (12.9*M,* pH 5.0) which was preincubated at 60^{o}C was added and the plate incubated at 60^{o}C for 60 minutes. The mixture was quenched with 80 μL of 30% (v/v) pyridine solution in 20mM HEPE*S,* pH 7.5 and allowed to settle at ambient temperature. Afterwards 30 μL of the supernatant was transferred to another plate and diluted to 250 μL with 30% (v/v) pyridine solution (pH 7.5, 20mm HEPES). The absorbance was read at 450nm using an ASYS UVM 340 plate reader. The IC_{50} values for β-haematin inhibition were determined by fitting the absorbance data to a sigmoidal dose response curve by non-linear least squares fitting using GraphPadPrism software.

5.5.2 *In vitro* Antiplasmodial assays:

In vitro* Antiplasmodial assays: Dd2 and D10 strains of *Plasmodium falciparum

Compounds were tested in duplicate on one occasion against D10 Chloroquine sensitive (CQS) and Dd2 Chloroquine resistant (CQR) strains. Continuous *in vitro* cultures of asexual erythrocyte stages of *P. falciparum* were maintained using a modified method of Trager and *J*ensen (1976). The quantitative assessment of antiplasmodial activity in vitro was determined via the parasite lactate dehydrogenase assay using a modified method by Makler (1993). The samples were prepared to a 2mg/ml stock solution in 10% DMSO or

10% methanol and were sonicated to enhance solubility. The samples were tested as a suspension if not completely dissolved. The stock solutions were stored at -20^{o}C and further dilutions were prepared on the day of the experiment. Chloroquine (CQ) was used as the reference drug in all experiments. A full dose-response was performed for all compounds to determine the concentration inhibiting 50% parasite growth (IC_{50} value). Compounds were tested at a starting concentration of 100µg/ml, which was then serially diluted 2-fold in complete medium to give 10 concentrations; with the lowest concentration being 0.2µg/ml. The same dilution technique was used for all the samples. CQ was tested at a starting concentration of 100ng/ml. The highest concentration of solvent to which the parasites were exposed had no measurable effect on parasite viability (data not shown). The IC_{50} values were obtained using a non-linear dose-response curve fitting analysis via GraphPad Prism v.4.0 software.

In vitro* Antiplasmodial assays: W2 strain of *Plasmodium falciparum

The protocol to this assay is as described by Rosenthal, *et al*, 1996. The W2 (CQ resistant) strain of *P. falciparum* (1% parasitemia, 2% hematocrit), were cultured in 0.5ml of medium in 48-well culture dishes. Stock solutions of inhibitors (10mM) in DMSO were added to cultured parasites to a final concentration of 20µM. From the 48-well plate*s,* 125µM of culture was transferred to two 96-well plates (duplicates). Serial dilutions (1%) of inhibitors were made to final concentrations of 10µ*M,* 2µ*M,* 0.4µ*M,* 80n*M,* 16n*M,* and 3.2nM. Cultures were maintained at 37^{o}C for 2 days after which the parasites were washed and fixed with 1% formaldehyde in PBS. After 2 days parasitemia was measured by flow cytometry using the DNA stain YOYO-1 as a marker of cell survival (Greenbaum, 2004).

In vitro* Antiplasmodial assays: 3D7 and K1 strains of *Plasmodium falciparum

The 3D7 clone is known to be sensitive to all antimalarials whereas the K1 which originates from Thailand is resistant to CQ and pyrimethamine, but sensitive to mefloquine. The cultures are naturally, asynchronous (65-75% ring stage) and are maintained in continuous log phase growth in RPMI 1640 supplemented with 5% washed human A+ erythrocytes , 25mM HEPE*S,* 32nM $NaHCO_3$ and AlbuMAXII (lipid rich

bovine serum albumin) (GIBCO, Grand Islan*d,* NY) (CM). All cultures and assays were conducted at 37^{o}C under an atmosphere of 5% CO_2 and 5% O_2 with the balance N_2. ges This assay was performed in various stages i.e. the primary and secondary screens.

Stock solutions were prepared in 100% DMSO at 20mg/ml and futher dilutions were done using complete medium RPMI 1640 supplemented with 15nM cold hypoxanthine and AlbuMAXII. Assays were performed in sterile 96-well microtitre plates; each plate containing 100µl of parasite culture (0.5% parasitemia, 2.5% hematocrit). Each drug was tested in triplicate and parasite growth compared to the control and blank (uninfected erythrocytes) wells. After 24h incubation at 37^{o}C, 3.7 Bq of [^{3}H] hypoxathine was added to each well. Cultures were incubated for a further 24h before harvesting them onto glass fibre filter mats. Radioactivity was counted using a Wallac Microbeta 1450 scintillation counter. The results were recorded as counts per minute (CPM) per well at each drug concentration, control and blank. Percentage inhibition was calculated from comparison to blank and control well*s,* and IC_{50} values were calculated using Microsoft XLFit line fitting software (IDB*S,* UK).

(a) Primary Screen

The primary screen used the 3D7 strain. The test compounds are tested at 4 concentrations (30, 10, 3, 1, 0.3, and 0.1µg/ml). Compounds that did not affect parasite growth at 10µg/ml are considered inactive, between 10 and 11µg/ml are designated as partially active and if <1µg/ml the compound was classified as active and was further evaluated by 3-fold serial dilutions in a repeat test.

(b) Secondary Screen

In this screen both 3D7 and K1 were used. The test drug was diluted 3-fold over at 12 diffierent concentrations with appropriate starting concentrations based on the primary screen. The IC_{50} was determined by sigmoidal dose response analysis using Microsoft XLFit (IDB*S,* UK). For each assay, the $IC_{50,}$ and IC_{90} values for each parasite line were determined against CQ and other standard compounds appropriate for the assay.

5.5.3. Mammalian cell toxicity Assay

KB cells is a cell line derived from a human carcinoma of the nasopharynx, typically is used as an assay for antineoplastic agents. The KB cells were maintained as monolayers in RPMI 1640 + 10% HIFC. All cultures and assays were conducted at 37^{o}C under an atmosphere of 5%CO_2/ 95% air mixture. The Assay takes upto 5days.

(a) Day 1:

KB cells are harvested, counted and washed in serum free medium (2000rpm, 10 minutes. 4^{o}C), and resuspended in fresh medium (RPMI 1640 + 10% HIFC) at a concentration of 4 x 10^4/ml. 100µl is added to wells on a 96- well plate (4 x 10^3/well). The plate was incubated overnight at 37^{o}C under an atmosphere of 5%CO_2/ 95% air mixture to allow cells to adhere.

(b) Day 2:

Test compounds were prepared in 100% DMSO 20mg/ml and diluted to a starting concentration of 600µg/ml (2 x top concentration) with RPMI + 10% HIFC. The control wells had no drug. A 10-fold serial dilution was performed across the plate ie 300, 30, 3, etc. The plate was then incubated for 72h at atmosphere of 5%CO_2/ 95% air mixture.

Podophyllotoxin was used as the reference drug.

(c) Day 5:

Each well was assessed by microscopic observation. 20µl Alamar Blue was added to each well then the plates were incubated for 2-4h before reading (Gemini, EX/EM 530/580, cut-off 550nm) IC_{50} values were calculated using sigmoidal regression analysis (MS XLFit)

5.5.4. *In vivo* antiplasmodial assay against *P. berghei*

The *in vivo* tests were performed in Swiss Webster female mice infected with *Plasmodium berghei.* It involved intra peritoneal administration of the drugs **16.HCl salt**, **16a** and chloroquine as the reference at a dosage of 2x day 50mg/kg. The drugs were dissolved in 5% DMSO 5% Cremophor EL in saline before administration. The control consisted of the untreated animals. Parasitemia was monitored for upto 40 days.

5.5.5. *In silico* ADME studies

The *insilico* studies included prediction of compliance to the Lipinski guidelines (drugability), physicochemical properties and ADME properties. The drugability predictions were performed using Volsurf modeller and Chemaxon calculator plugins (www.chemaxon.com) whereby a set of 4 guidelines predicting for a compound to have good oral absorption and permeation i.e. < hydrogen bond donor*s,* <10 hydrogen bond acceptor*s,* <500 molecular weight*,* and a calculated logP (ClogP) of <5. MoKa software (www.moldiscovery.com) was used to predict pKa. Solubilities of the compounds were profiled in Volsurf (www.moldiscovery.com) and this was projected onto a model of known drugs. The sites of metabolism in CYP3A4 were predicted using MetaSite (www.moldiscovery.com).

In silico Docking in the CYP 3A4 active site

The study employed a cytochrome P450 (CYP3A4) crystal structure [protein data bank; PDB code 1TQN] to predict the modes of binding and the affinity constants of the synthesised ligands/substrates at the lowest binding energy conformation. The ligand docking program Autodock 4.2.3 was used and no partial charges were added to the P450 heme moiety. The Autodock 4.2.3 was obtained from the Scripps institute (La Jolla, CA). In AutoDock 4.3.2 all the substrates were treated as flexible ligands by modifying their rotatable torsions but the CYP3A4 template was considered to be a rigid receptor. The 3D coordinates of the CYP3A4 structure (1TQN) was acquired from the PDB and was used without further modification. The structures of the substrates were built using Chemdraw 12 then converted to SYBL MOL2 format using Chem3D Ultra 10 (CambridgeSoft Corp., Cambridge, MA). The substrates were modified with Gasteiger atomic charges assignment and flexible torsions were defined. The default settings were used for docking. The grid box was centered at 18.599, 7.921 and 57.938, with dimensions of 30×36×60. Docking was accomplished on a Linux workstation with 64bit Dual Core Intel Xenon Enterprise Linux WS4 operating system. The maximum number of energy evaluations and the maximum number of generations was set at the default values of 250,000 and 27,000 respectively. The rest of the parameters were set at their default values. AutoDock 4.2.3 searched the globally optimised genetic algorithm (LGA)

and 10 LGA runs were conducted for each template and docking solutions were groups of conformational clusters in which all atom root mean square deviations (rmsd) within 2.0Å of each other were clustered together using Autodock 4.2.3 tools.

5.5.6. Physicochemical and *In Vitro* ADMET Studies

Purity Analysis

Initially the purity of the test compounds was determined using reversed phase HPLC according to published methods (de Aquino Ribeiro, 2007, Patel, P 2004, Xie 2003) on a Zorbax C18, 4.6x150mm, 5µm column, with mobile phase of **A**; water/acetonitrile/trifluoroacetic acid (95:5:0.1) and **B:** acetonitrile/trifluoroacetic acid (100:0.1). The gradient elution started with 10% **B** attaining 90% in 10min and back to 10% in another 5 min.

Lipophilicity

Lipophilicity was determined using reverse phase HPLC and standard drugs with known retention times (t_R) and retention capacity were (k') were used for calibration. A Zorbax C18, 4.6 x 150mm, 5µm column, with a mobile phase of **A:**10mM ammonium acetate in acetonitrile/water (5:95), **B:**10mM ammonium acetate in water/acetonitrile (95:5) starting with 0% **B,** attaining 100% **B** in 20minutes were the chromatographic conditions used. Linear regression curves with accurate k' values on the Y axis and t_R on the X axis for the reference compounds were used to estimate the k' values for the test compound [i.e t_R of the test compounds were used to extrapolate their k' values on the curves]. A second curve plotted from published logD values against t_R of reference compounds was used to estimate the logD of the test compounds.The reference compounds used were metroprolol, propanolol, testosterone and felodipine.

Solubility

A turbidimetric method was used to determine solubility. Compounds were pre-diluted from stocks in 100% DMSO before dilution in 0.1M buffered saline pH 7.4 to desired concentrations. Serial dilutions from the highest concentrations were made to obtain 2.5, 1.25, 0.63, 0.31, 0.16 and 0.08mM working concentrations. Working stocks were further diluted in PBS to make the required concentrations (100, 50, 25, 12.5, 6.25, 3.125 and 1.56µM). A control plate, where the final dilutions were performed in DMSO, was also

prepared to determine if the increase in absorbance was due to the compound itself with increase in concentration and not due to the formation of a precipitate. The plates were incubated at 37^{o}C for 2hours followed by UV detection at 595nm. Two compounds were used as controls: one poorly soluble compound (niclosamide solubility < 1μM) and one very soluble compound (paracetamol solubility>100μM).

Lower limits of solubility were estimated as values at which a rise in absorbance from baseline/blank is observed. Absorbance values above 0.05 were also used as a complimentary diagnostic tool for formation of precipitate. The compounds were classified into three broad categories according to their aqueous solubility. Compounds with solubility below 20μM were classified as poorly soluble, between 20 and 100μM as partially soluble and above 100μM as soluble. The lower bound solubility (the solubility at which the compound begins to precipitate) was used in classifying the compounds. As expected the two controls (niclosamide and paracetamol) gave values which were consistent with previously reported literature.

CYP3A4 inhibition

In this assay, testosterone was used as a probe substrate and its β hydroxylation was used as a marker reaction. Two concentrations were used, 3μM and 20μM to investigate if the inhibition was concentration dependent. The inhibition effects were investigated using ketoconazole (known potent inhibitor of CYP3A4) and the uninhibited reaction as references. Components in the incubation mixture (total volume = 200μl) were HLM 0.5mg/ml, phosphate buffer pH7.4 0.1*M,* NADPH 1m*M,* test compound 320μM and 20μM and testosterone 100 μM.

DMSO concentrations were kept constant in all the reactions (0.2%) and the substrate was dissolved in methanol giving a final concentration of 40% methanol in the incubation mixture. The reaction was stopped by addition of a double volume of ice cold methanol. The mixture was vortexed for a minute followed by centrifugation at 0^{0}C for 15minutes. Supernatant was collected and the centrifugation repeated. The supernatant was evaporated under a gentle stream of nitrogen gas followed by reconstitution in mobile phase. The metabolite (6β-hydroxytestosterone) was detected by HPLC-UV using the

following conditions Zorbax C18, 4.6 x 150m*m,* 5µm diameter sample solvent 50% methanol/water (v/v), mobile phase **A**: 50mM KH_2PO_4 **B**: methanol, by isocratic elution 50% **A**:50% **B** at 1ml/min flow rate. The in*j*ection volume of 100µl with uncontrolled temperature detection at 254nm and a running time of 15minutes.

The extent of CYP3A4 inhibition was also shown by the IC_{50}. The IC_{50} is the amount of compound that is required to cause 50% inhibition. One point IC_{50} calculation was used to estimate the IC_{50} for both the test compounds and the control. Estimations were done using inhibition data at 3µM using the relationship below.

$$IC_{50} = x\left[\frac{100 - \text{percent control at } x}{\text{percent control at } x}\right]^{1/h}$$

Where x = 3µM and h = -1

CHAPTER SIX

CONCLUSION AND RECOMMENDATIONS

The main aim of this project was to synthesise novel hybrid structures of 3,4-HPOs with 4-aminoquinolines and screening of the synthesized compounds for biological activity i.e. *in vitro* and *in vivo* antimalarial activity, β-haematin inhibition and cytotoxicity. Alongside this, *N*-alkyl-3, 4-HPOs and their gallium (III) complexes were synthesised. Iron (III) and gallium (III) complexes of selected hybrid molecules were also prepared to investigate the contribution of iron chelation or complexation to antiplasmodial activity. In addition to these one biscatecholate -4-aminoquinoline conjugate **37** was prepared. All the compounds were characterised using ^{1}H and ^{13}C NMR spectroscopy, IR spectroscopy, MS and elemental analysis. The purity of the hybrids/conjugates was ascertained by analytical HPLC. The X-ray structure of one of the kojic acid derived hybrids, **24,** was determined. Solubility profiles were determined for some of the compounds using turbidimetry and the log D values of selected compounds were also determined.

All the compounds were tested for *in vitro* antiplasmodial activity and only two (**16** and **16a**) were evaluated for *in vivo* antiplasmodial efficacy in mice. The simple *N*-alkyl-3,4-HPOs were found to be less active compared to CQ and their main mode of action was linked to iron chelation. Their potency was observed to increase with increase in lipophilicity and none of them inhibited β-haematin formation at the highest concentration (10μM) tested.

Even though β-haematin inhibition was identified as one of the major modes of action for the synthesised 4-aminoquinoline-3,4-HPO conjugates, a free 3-hydroxy group on the hydroxypyridinone moiety was found to play an important role in enhancing activity against the resistant strain. The 4-aminoquinoline-3,4-HPO conjugates were found to be stronger β-haematin inhibitors than CQ and the benzyl group was identified to be involved in β-haematin inhibition. Most of the compounds had better

resistance indices than CQ indicating potential to act against resistant malaria. The tertiary amine was identified to be more effective in enhancing the activity of the conjugates against the resistant strain.

The most potent conjugates **13a**, **16**, **24a**, **32** and **32a,** were identified and all were more potent than CQ in the resistant strain. Of these only the ones with the longest side chain (6 carbon atoms) were more potent than CQ in the sensitive strain. Therefore modification of the side chain was found to be important in enhancing activity against the sensitive strains. All the compounds had significantly similar activity in the resistant strain but **24a** and **13a** had the best resistance indices.

Increasing the length of the alkyl side chain did not enhance activity against the resistant strain significantly as well this strategy caused an increase in the potential to cause CYP3A4 inhibition or drug-drug interactions (DDIs). Consequently among the most potent compounds only **24a** and **13a** were identified as the best candidates because they were equipotent in both the resistant and sensitive strains showed reduced potential to cause CYP3A4 inhibition as deduced from *in vitro* and/or *in silico* data. Therefore, controlled lipophilicity is important in designing potent antimalarials with acceptable ADMET/physicochemical properties. Future synthetic work should consider conjugates that are structurally related to compound **24a** i.e. containing both chelator and tertiary amino groups. Crystal structures of complexes of haematin and such compounds may help elucidate the role or interaction of the two groups with respect to β-hematin inhibition.

Both *in silico* and *in vitro* data alongside correlation studies showed that the CYP3A4 and haematin inhibition activities of the drug conjugates are independent from each other and that a strong inhibitor of CYP3A4 is not necessarily a strong inhibitor of β-haematin.

Protection of the iron chelation group by benzylation was found to enhance inhibition of CYP3A4 in the presence of testosterone. Compounds that were evaluated for *in*

vitro CYP3A4 inhibition i.e. A/AB series, were found to have greater potential to cause DDIs in the presence of testosterone but this data should be treated with caution until the assay is repeated using other substrate probes. The structural modification strategies of alteration of the molecular shape and incorporation of extra polar groups was found to have potential to improve the CYP3A4 inhibition profile of the 4-aminoquinoline -3,4-HPO hybrids. This was deduced from the *in silico* and *in vitro* data.

Docking conformations of the conjugates in AutoDock 4.2 were found to be reliable in distinguishing strong CYP3A4 inhibitors from weak CYPA4 inhibitors. The N-alkyl side chain and the benzyl group were identified to be the main substructures whose interaction with the CYP binding pockets was predicted to influence inhibition. Thus the docking experiments may be used to screen designed molecules prior to synthesis. A strategy of modification of the alkyl side chain via its functionalization to incorporate hydrophilic groups and the use of less lipophilic hydroxyl-protecting groups or the use of shorter alkyl side chains may be adopted in future to synthesise hybrids with better CYP3A4 profiles.

Structural features incorporated into antiplasmodial molecules aimed at improving potency may suppress or enhance each others effect or affect the ADME profile of the new chemical entity. The tertiary amine group together with the chelator group (hydroxypyridinone), were observed to enhance activity against the CQ resistant strain, but they caused a decrease in β-haematin inhibition for compound **24a**. The same tertiary amino group was predicted to enhance CYP3A4 inhibition in the conjugates. Similarly aromatizing of the protecting group at the 3-position was identified to enhance CYP3A4 and β-haematin inhibition. Incorporation of the benzyl group to enhance haematin inhibition in future work may require adoption of uniquely designed structures that have an iron chelating group and some extra polar groups to counteract the lipophilicity of the aromatic ring so as to avoid high affinity for CYP3A4. Therefore, the search for potent antimalarials could be effective and

efficient if *in silico* tools are employed to detect and avoid potential ADMET liabilities and undesired physicochemical properties prior to synthesis.

Preliminary synthesis of the gallium (III) and iron (III) complexes of the conjugates was important in studying the potential contribution of iron chelation towards the antiplasmodial activity of the conjugates. However, the characterization was incomplete. Therefore, future work should aim at the preparation of X-Ray quality crystal of complexes of the **A**/**AB**, **R** and **D** series to enhance complete structural elucidation. Metallation of the quinoline heterocyclic N-1 which is known to enhance potency against resistant strains may be pursued for the aminoquinoline-3,4-HPO hybrids with or without complexation of the hydroxypyridinone moiety.

In vivo screening of these double drugs was performed for **16a** and **16.HCl salt** and their efficacy against *P.berghei* in mice was dismal when compared to CQ. The cause of the failure of the *in vitro* potency of these compounds to translate to *in vivo* potency was not resolved fully. Future work in different animal models or against different strains of *Plasmodia* is important. Currently *in vivo* screening for related compounds to study their PK/PD interactions is under way. It is recommended that compounds **24a** and **13a** which were identified to have the best antiplasmodial and ADMET profiles be evaluated *in vivo*.

CHAPTER SEVEN

REFERENCES

Adachi, Y; Yoshida, J; Kodera, Y; Katoh, A; Takada, J; Sakurai, H. *J. Med. Chem.* (2006), 49(11), 3251-3256.

Adovelande J, Deleze J, Schrevel J. *Biochem. Pharmacol.* (1998) 55, 433-440

Ajibade PA; Kolawole GA.*Transition Met Chem* (2008) 33; 493-497.

Albert, A,. Selective Toxicity. New York: Chapman & Hall, 1981.

Ali, H.I.; Ashida, N; Nagamatsu, T. *Bioorg. Med. Chem.* (2007), 15(19), 6336-6352

Ali, H.I.; Tomita, K; Akaho, E; Kambara, H; Miura, S; Hayakawa, H; Ashida, N;

Amelia Santos M; Gama Sofia; Gano Lurdes; Cantinho Guilhermina; Farkas Etelka *Dalton Transactions* (Cambridge, England : 2003) (2004), (21), 3772-81.

Amelia Santos, M.. *Coord. Chem. Rev.* (2002), 228(2), 187-203.

Atkinson, J.G., Girard, Y., Rokach, J., Rooney, C.S., McFarlane, C.S., Rackham, A., Share, N.N..*J. Med Chem,* (1978), 22, 1:99-106.

Atwood J. L. and Barbour, L. J. , *Cryst. Growth Des*., (2003), 3, 3.

Aytemir, M. D., Hider, R. C., Erol, D. D., Ekizoglu M, Ozalp, M. *Turk J Chem.* (2003) 27, 445-452.

Azzaoui, K.; Diaz-Perez, M.J.; Price, G.B.; Wainer, I.W. *Book of Abstracts, 214th ACS National Meeting*, (1997). Las Vegas, NV, September 7-11

Barat LM; Bloland PB; *Infect. Dis. Clin. North Am.* (1997), 11, 969-987.

Barbour L. J., *J. Supramol. Chem.*, (2001), 1, 189-191;

Barnerjee R; Goldberg DE (2001) in Rosenthal PJ (ed) Antimalarial Chemotherapy:mechanisms of action resistance and new directions in drug discovery. Humana press, New Jersey. PP 43-63

Barquero AA; Alche LE; Coto CE. *Int. J. Antimicrob. Agents* (1997) 9, 49-55

Barral K., Balzarini, J., Neyt*s, J*., DeClerq, E., Hider, R.C., Camplo, M.**.** *J. Med. Chem.*, (2006); 49:43-50.

Barret JF; Whittaker PG; Williams JG; Lind T. *Br. Med. J.* (1994), 309, 79-82.

Basco LK; Le Bras J. *Jpn. J. Med. Sci. Biol.(*1994), 47, 59-63.

Bebbington, D; Monck, N. J. T.; Gaur S; Palmer, A M.; Benwell K; Harvey, V., Malcolm, C. S.; Porter, Richard H. P. *J. Med. Chem.*, (2000), 43(15), 2779-2782.

Behere, D.V., Goff, H.M., *J. Am. Chem. Soc.* (1984), 106, 4945-4950.

Berenbaum MC. *J. Infect. Dis*. (1978), 137, 122-130.

Berenbaum MC.; Norden CW; Moellering Jr RC; *J. Infect. Dis.* (1980) 142, (3) 476-480

Berenbaum, M. C. *Clin. Exp. Immunol.* (1977), 28(1), 1-18.

Berger J; Dyek JL; Galou P; Aplogan A; Schneider D; Traissac P. *Eur. J. Clin. Med*.(2000)54, 29-35.

Bergeron, R.J., McGovern, K.A., Channing, M.A., Burton, P.S.. *J. Org. Chem* (1980), 45, 1589-1592.

Bickel, H.; Hall, G. E.; Keller-Schierlein, W.; Prelog, V.; Vischer, E.; Wettstein, A. *Helvetica Chimica Acta* (1960), 43 2129-38.

Biot C, Pradines B, Sergeant M H, Gut J., Rosenthal P.J., Chibale K. *Bioorg. Med. Lett*. (2007), 17, 6434-6438.

Biot C; Chibale K. *Infectious Disorders: Drug Targets* (2006), 6(2), 173-204.

Biot C; Glorian G; Maciejewiski LA; Brocard JS. J. *Med. Chem.* (1997), 40, 3715-3718

Bitonti AJ; McCann PP; Kyle DE; Oduola AM; Rossan RN. *Science* (1988), 242, 1301-1303.

Blackie, M.A.L. PhD Thesis (2002) University of Cape Town.

Bloomer, J. C.; Clarke, S. E.; Chenery, R. J. *Drug Met.Disp.* (1997), 25(7), 840-844.

Bohle, D. Scott; Dinnebier, Robert E.; Madsen, Sara K.; Stephens, Peter W. *J.Biol. Chem.* (1997), 272(2), 713-716.

Borsnik, K., Paik, I., Shapiro, T.A., Posner, G.H., (2002). *Int. J.Parasitol.,* 32, 1661-1667.

Braun V; Pramanik A; Gwinner T; Koeberle M; Bohn, E. *BioMetals* (2009), 22(1), 3-13.

Bray PG; Ward SA; O'Neil PM. *Curr. Trop. Microbiol. Immunol*. (2005), 295, 3- 38.

Bray PG and Ward SA. *Pharmacol Ther.* (1998), 77, 1-28.

Bray PG; Hawley SR; Ward SA. *Mol. Pharmacol*. (1996), 50, 1551-1558.

Bray PG; Howells RE; Ritchie GY; Ward SA. *Biochem. Pharmacol*. (1992), 44, 1317-1324.

Bray PG; Mungthin M; Ridley RG; Ward S. *Mol. Pharmacol* (1998), 54, 170.

Bray, P G.; Mungthin M; Hastings I M.; Biagini, G A.; Saidu, D K.; Lakshmanan V; Johnson, D. J.; Hughes R H.; Stocks P A.; O'Neill P M.; Fidock, D.A.; Warhurst, D C.; Ward S.A. *Mol. Microbiol.* (2006), 62(1), 238-251.

Brown, W. H. *J. Exp.l Med.* (1911), 13 290-9.

Bruce-Chwatt LJ; *Br. Med. J.* (1983), 286, 1457-1458.

Brueckner RP; Ohrt C; Baird JK; Milhous WK. 8-Aminoquinolines. In Rosenthal PJ (ed) Antimalarial Chemotherapy:mechanisms of action resistance and new directions in drug discovery. Humana press, New Jersey.pp 3-14

Buller R; Peterson M.L.; Almarsson O; Leiserowitz L. *Cryst. Growth Des.* (2002), 2(6), 553-562.

Burgess SJ, Selzer A, Kelly X.J, Smilkstein M.J, Riscoe M.K, Peyton D.H. Byk G., Gilon C.**.** *J. Org Chem.,* (1992), 57, 5687-5692.

Bzik JD; li WB; Horii T. Inselburg J. *Proc. Natl. Acad. Sci USA.*(1987) 84, 8360-8364.

Cabantchik Z.I, Glickstein H, Golenser J, Loyevsky M, Tsafack A. *Acta Haematol* (1996); 95:70-77

Cabantchik ZI**.** *Parasitol Today* (1995);11:73-78.

Cabantchik, Z. I.; Moody-Haupt, S.; Gordeuk, V. R. *FEMS Immunology and Medical Microbiology* (1999), 26(3-4), 289-298.

Cazzola M, Arioso P, Barosi G, Bergamaschi G, Dezza L, Ascari E,. *Br J Haematol* (1983); 53:659-665.

Chen, M. M.; Shi, L.; Sullivan, D. J. *Mol. Biochem. Parasitol.* (2001), 113(1), 1-8.

Chevion M, Chuang L, Golenser J,**.** *Antimicrob Agents Chemother*., (1995);39:1902-1905.

Chibale K (2010) Personal Communication. University of Cape Town.

Chibale K. *IUBMB Life* (2002), 53(4,5), 249-252.

Chiyanzu I; Clarkson C; Smith PJ.; Lehman J; Gut J; Rosenthal P.J.; Chibale K. *Bioorg. Med. Chem.* (2005), 13(9), 3249-3261.

Choi C.H.Y, Schneider EL, Kim JM, Gluzman IY, Goldberg DE, Elman JA, Marletta MA.. *Chem. Biol*. (2002);9:881-889.

Chou A C; Chevli R; Fitch C D. *Biochemistry* (1980), 19(8), 1543-9.

Clarke CK, Eaton JM.. *Clin Res* (1990);38:300A.

Charman Susan A; Arbe-Barnes Sarah; Bathurst Ian C; Brun Reto; Campbell Michael; Charman William N; Chiu Francis C K; Chollet Jacques; Craft J Carl; Creek Darren J; Dong Yuxiang; Matile Hugues; Maurer Melanie; Morizzi Julia; Nguyen Tien; Papastogiannidis Petros; Scheurer Christian; Shackleford David M; Sriraghavan Kamaraj; Stingelin Lukas; Tang Yuanqing; Urwyler Heinrich; Wang Xiaofang; White Karen L; Wittlin Sergio; Zhou Lin; Vennerstrom Jonathan L *PNAS.* (2011), United States of America 108(11), 4400-5.

Clarke, ET.; Martell, AE.; Reibenspies, J. *Inorganica Chimica Acta* (1992), 196(2), 177-83.

Clayden J, Worthers P, Greeves N, Warren S. Organic Chemistry, London; Oxford: 2001.

Co, E A.; Dennull, RA.; Reinbold, D D.; Waters, NC.; Johnson, J D. *Antimicrob. Agents Chemother.* (2009), 53(6), 2557-2563.

Constantinidis, I.; Satterlee, James D. (1988) *J. Am. Chem. Soc.*, 110(3), 927-32.

Coppens I; Vielemayer O. *Int. J. Parasitol*.(2005) 35, 597-615.

De Aquino, R., De Campos, J. A., Alves, L.M.M., Lages, G.P., Pianetti, G.A., *J. of Pharmaceutical and Biomedical Analysis* (2007), 43, 298-303.

De D; Krogstad FM; Cogswell FB; Krogstad DJ. *Am J. Trop. Med. Hyg.* (1996).

De Groot M, Ackland M.J., Home V.A., Alex A, Jones B.C., *J. Med. Chem.* (1999) 42, 1515-1524.

de Villiers, K.A.; Egan, T.J.. *Molecules* (2009), 14(8), 2868-2887.

de Villiers, K.A.; Marques, H.M., Egan, T.J. *J. Inorg. Biochem*.(2008), 102, 1660-1667

Dehkordi L. S., Liu, Z. D., Hider R.C., *Eur. J. Med. Chem.* (2008) 43, 1035-1047.

Diro M; Beydoun SN. *South. Med. J.* (1982), 75, 959-963.

Dobbin P, Hider RC, Hall AD, Taylor PD, Sarpong P, Porter JB, Xiao G, Helm D. *J. Med. Chem.* (1993); 36: 2448 – 2458.

Domanski T; He Y; Khan K.K.; Roussel F; Wang Q; Halpert J.R. *Biochemistry* (2001), 40(34), 10150-10160.

Dondorp, A.M.; Nosten F; Yi P; Das D; Phyo A.P; Tarning J; Lwin K.M; Ariey F; Hanpithakpong W, Lee S.J.; Ringwald P; Silamut K; Imwong M; Chotivanich K; Lim, P; Herdman T; Sam A.S; Yeung, S; Singhasivanon P; Day N.P. J.; Lindegardh N; Socheat D; White N.J. *N. Eng. J. Med.* (2009), 361(5), 455-467.

Dorn, A; Vippagunta S.R; Matile H; Jaquet C; Vennerstrom J.L.; Ridley R.G. *Biochem.l Pharmacol.* (1998), 55(6), 727-736.

Dorsey G; Fidock DA; Wellems TE; Rosenthal PJ (2001) in Rosenthal PJ (ed) Antimalarial Chemotherapy:mechanisms of action resistance and new directions in drug discovery. Humana press, New Jersey. PP 153-172

Dunne, W.; Singh N; Shukle M; Valecha N; Bhattacharyya P. C.; Dev V; Patel K; Mohapatra M.K.; Lakhani J; Benner, R; Lele C; Patki K. *J. Infect. Dis.* (2005), 191(10), 1582-1588.

Dzekunov SM; Ursos LMB; Roepe PD; *Mol. Biochem. Parasitol.* (2000), 110, 107-124.

Egan T.J.; Ncokazi K.K. *J. Inorg. Biochem.* (2005), 99(7), 1532-1539.

Egan W.J.; Zlokarnik G; Grootenhuis, P.D. J. *Drug Discovery Today: Technologies* (2004), 1(4), 381-387.

Egan, T.J. *J.Inorg. Biochem.*(2008), 102(5-6), 1288-1299.

Egan, T.J.; Chen, J Y-J.; de Villiers, K A.; Mabotha, T.E.; Naidoo K.J.; Ncokazi, K.K.; Langford S.J.; McNaughton D; Pandiancherri S; Wood, B.R. *FEBS Lett*. (2006), 580(21), 5105-5110.

Egan, T.J.; Combrinck, J.M.; Egan J; Hearne G.R.; Marques H.M.; Ntenteni S; Sewell B. T; Smith, Peter J.; Taylor D; van Schalkwyk D.A.; Walden J.C. *Biochem. J.* (2002), 365(2), 343-347.

Egan, T.J.; Kaschula, C.H *Current Opinion in Infectious Diseases* (2007), 20(6), 598-604.

Ekcthawatchai, S., Kamachonwongpaisan, Kongsaerea, P., Tarnchompoo, B., Elford, B.C., Roberts, M.F., Wilson, R.J.F., (1985). *Trans Soc Trop Med Hyg.,* 81, 434.

Ekins S, Bravi G, Gillespie J S, Ring B J, Wikel J.H., Wrighton S.A. (2000) *Drug Metab Disp* 28 994-1002

Ekins S, De Groot M and Jones J.P., *Drug. Metab. Disp*. (2001) 29, 936-944

Ekins, S.; Mestres, J.; Testa, B. *Br. J. Pharmacol.* (2007), 152(1), 21-37.

Ekins, S; Stresser, David M.; Andrew W.J. *Trends in Pharmacological Sciences* (2003),24(4), 161-166.

Ekroos, M; Sjoegren, T. *Proc. Natl Acad Sci of* (USA) (2006), 103(37), 13682-13687.

Ellis B.L.; Duhme A.K.; Hider, R.C.; Hossain, M. B; Rizvi, S; van der Helm, D. *J. Med. Chem.* (1996), 39(19), 3659-3670.

Epemolu RO; Singh S; Hider RC; Damani LA. *J. Chromatogr* (1990) 519, 171.

Evans, W. E.; Relling, M.V. *Science* (Washington, D. C.) (1999), 286(5439), 487-491.

Ferreira, CL.; Bayly, SR.; Green, DE.; Storr, T; Barta, CA.; Steele, J; Adam, M J.; Orvig, C. *Bioconjugate Chemistry* (2006), 17(5), 1321-1329.

Fidock D.A.; Nomura T; Talley A. K.; Cooper R.A.; Dzekunov S.M.; Ferdig M.T.; Ursos L.M. B.; Sidhu A.B. S; Naude B; Deitsch K.W.; Su Xin-Zhuan; Wootton J.C.; Roepe, P.D.; Wellems T.E. *Molecular Cell* (2000), 6(4), 861-871.

Finnegan, MM.; Lutz, TG.; Nelson, WO.; Smith, A; Orvig, C. *Inorg. Chem*. (1987), 26(13), 2171-6.

Fitch CD. *Science* (1970), 169, 289-290.

Foley M; Tilley L; *Pharmacol. Ther*. (1998) 79, 55-87

Francis S.E, Banerjee R, Goldberg D.E. *J. Biol. Chem.* (1997); 272:14, 961-14, 968.

Fray, M. Jonathan; Bull, David J.; Carr, Christopher L.; Gautier, Elisabeth C. L.; Mowbray, Charles E.; Stobie, Alan. *J. Med. Chem.* (2001), 44(12), 1951-1962.

Fritsch G, Sawatski G, Treumer J, Jung A, Spira D.T.. *Exp. Parasitol.* (1987);63:1-9. Gabay T, Ginsburg H. *Exp. Parasitol.* (1993);77:261-272.

Gabresselassie H. PhD Thesis (1996), McGill University.

Gallup J L; Sachs J D . *Am. J. Trop. Med. Hyg.* (2001), 64(1-2 Suppl), 85-96.

Gamboa de Dominguez N, Rosenthal P.J. *Blood* (1996); 87: 4448-4454.

Gardner M.J. *et al*., *Nature* (2002), 419. 498-511

Geary TG; Divo Ad; Jensen JB; Zangwil M; Ginsburg H. *Biochem Pharmacol*.(1990), 40, 685-691.

Gessner RK. PhD Thesis (2008) University of Cape Town.

Ghosh M; Lambert L.J.; Huber P.W.; Miller M.J. *Bioorg. Med. Chem. Lett.* (1995), 5(20), 2337-40.

Ghosh, A., Ghosh, M., Niu, C., Malouin, F., Moellmann, U.,Miller, *J*. M., *Chem. Biol*., (1996), 3:1011-1019.

Ginsburg, H; Kanaani, J. *Trends in Biomembranes & Bioenergetics* (1990), 1(1), 111-17.

Gleeson M.P. *J. Med Chem.* (2008), 51(4), 817-834.

Goldberg D.E.; Sharma V.; Oksman A.; Gluzman I.Y.; Wellems T.E.; Piwnica-Worms D. *J. Biol. Chem.* (1997), 272(10), 6567-6572.

Gorduek VR, Thuma PE, Brittenham GA, Biemba G, Zulu S, Simwanza, *Am J Trop Med Hyg* (1993);48:193-197

Gorduek VR, Thuma PE, Brittenham GM, McLaren C, Parry D, Backenstose AR., *N. Eng. J. Med.* (1992a);327:1473-1477.

Gorduek VR, Thuma PE, Brittenham GM, Zulu S, Simwanza G, Mhangu A, *Blood* (1992b);79:308-312.

Gorduek VR, Thuma PE, McLaren CE, Biemba G, Zulu S, Poltera A.A, *Blood* (1995b);85:3297-3301.

Green D.E.; Ferreira C.L.; Stick, R.V.; Patrick B.O.; Ada*m* M.J.; Orvig C. *Bioconjugate Chem.* (2005), 16(6), 1597-1609

Greenbaum, D.C., Mackery, Z., Hansell, E., Doyle, P., Gut, J., Caffrey C.R., Lehman, J., Rosenthal, P.J., McKerrow, J.H., Chibale, K. *J. Med. Chem.,* (2004), 47, 3212-3219.

Gross, G. A.; Grueter, A.; Heyland, S. *Food. Chem. Toxicol.* (1992), 30(6), 491-8.

Guantai, E.M.; Ncokazi K; Egan, T.J.; Gut J; Rosenthal P.J.; Smith P.J.; Chibale K. *Bioorg. Med. Chem.*(2010), 18(23), 8243-8256.

Guengerich, F.F. *Advances in Pharmacology* (San Diego) (1997), 43(Drug-Drug Interactions: Scientific and Regulatory Perspectives), 7-35.

Guetzoyan, L; Yu, Xiao-M; Ramiandrasoa, Fl; Pethe, S; Rogier, C; Pradines, B; Cresteil, T; Perree-Fauvet, M; Mahy, *J. Bioorg.Med. Chem.* (2009), 17(23), 8032-8039.
Guo F; Thiessen JJ; Tesoro A; Spino M. *J. Chromatogr.* (2001) B 75, 107-115.

Hammadi A., Ramiandrasoa F; Sinou V; Rogier C; Fusai T; Le Bras J; Parzy D; Kunesch G; Pradines B. *Biochem. Pharmacol.* (2003), 65(8), 1351-1360.

Harris L.N. R. *Aust.J.Chem* 1976; 29:1329-1334.

Hasinoff B.B, Reiders FX, Clark V. *Drug. Metab. Disp.* (1991);19:74-80.

Hawley SR; Bray PG; mungthin M; Atkinson JD; O'Neil PM; Ward SA. *Antimicrob. Agents Chemother.* (1998) 42, 682-686.

Hayward, Rhys; Saliba, Kevin J.; Kirk, Kiaran. *Journal of Cell Science* (2006), 119(6), 1016-1025.

He Z; Chen L; You J; Qin L; Chen X. *Int. J. Antimicrob. Agents* (2010), 35, 191-193.

Heinisch, L., Whittmann, S., Stoiber, T., Berg, A., Ankel-Fuchs, D., Mollmann, U. . *J. Med Chem* (2002), 45, 3032-3040.

Heppner DG, Hallaway PE, Kontoghiorghes GJ, Eaton JW. *Blood.,* 1988;72:358-361.

Hershko C, Peto T.E. *J. Exp. Med.* (1988); 168:375-387

Hershko C, Theanacho EN, Spira D*T,* Peter HH, Dobbin P, Hider RC**.** *Blood* (1991a);77:637-643

Hershko, C.; Link, G.; Pinson, A.; Peter, H. H.; Dobbin, P.; Hider, R. C. *Blood* (1991b), 77(9), 2049-53.

Hider R.C; Kong X. *Natural Product Reports* (2010), 27(5), 637-57.

Hider, R C.; Lerch, K**.** *Biochem. J.* (1989), 257(1), 289-90.

Hider, R.C.; Liu, Z. *J. Pharm. and Pharmacol.* (1997), 49(Suppl. 2), 59- 64.

Hider, R.C.; Liu, Z.D. *Curr. Med. Chem*. (2003), 10(12), 1051-1064.

Hider, R.C.; Zhou, T. *Annals of the New York Academy of Sciences* (2005), 1054(Cooley's Anemia), 141-154.

Hoang, A.N.; Sandlin, R.D.; Omar A; Egan, T.J.; Wright, D.W. *Biochemistry* (2010), 49(47), 10107-10116

Hsieh W, Liu S.. *Inorg. Chem.,* (2005);44:2031-2038.

Hsieh, MM, Everhart JE, Byrd-Holt DD, Tisdale JF, Rodgers GP. (2007). *Ann. Intern. Med*. 146(7) 436-492.

Hyde JE. *Acta Trop*. (2005), 94, (3) 191-206.

Imap, K., Limura, S., Hasegawa, T., Okita, T., Hirano, M., Kamachi, H., Kamei, H., *J. Antibiotic*. (1993), 840-849

Kalinowski, D.S.; Yu Y; Sharpe P.C.; Islam M; Liao, Yi-Tyng; Lovejoy D.B.; Kumar N; Bernhardt P V.; Richardson D.R. *J. Med. Chem.* (2007), 50(15), 3716-3729.

Kamchonwongpaisan, S; Paitayatat, S; Thebtaranonth, Y; Wilairat, P; Yuthavong, Y. *J. Med. Chem.* (1995), 38(13), 2311-16.

Kaschula C.H.; Egan T.J.; Hunter R; Basilico N; Parapini S; Taramelli D; Pasini E; Monti, D. *J. Med Chem.* (2002), 45(16), 3531-3539.

Kawashima, Y; Yamagishi, T., Ikeya, H; Yoneda, F; Nagamatsu, T. *Bioorg. Med. Chem.* (2007), 15(1), 242-256.

Kayyali, R. S.; Porter, *J*. B.; Hider, R. C.**.** *J. Inorg. Biochem.* (1997), 67(1-4), 331.

Kayyali, R; Porter, J.B.; Liu, Z.D; Davies, N.A.; Nugent, J.H.; Cooper, C.E.; Hider, R.C. *J. Biol. Chem.*(2001), 276(52), 48814-48822.

Kellenberger E; Rodrigo, J; Muller, P; Rognan, D. *Proteins: Structure, Function, and Bioinformatics* (2004), 57(2), 225-242.

Kenworthy, K.E, Bloomer J.C, Clarke, S.E., Houston, J.B. (1999).*Br. J Clin. Pharmacol.,* 48, 716-727

Kerns EH; Di L. (2008) Drug-like Properties: Concepts, Structures Design and Methods from ADME to Toxicity Optimization. Academic Press, London

Khanye D.S. PhD Thesis (2010) University of Cape Town.

Kitchen, D.B.; Decornez, H; Furr, J.R.; Bajorath, J. *Nature Reviews Drug Discovery* (2004), 3(11), 935-949.

Kolakovitch KA, Gluzman IY, Duffin KL, Goldberg DE. *Mol. Biochem. Parasitol.* (1997); 87:123-135.

Kontoghiorghes, G. J.; Pattichis, K.; Neocleous, K.; Kolnagou, A. *Curr. Med. Chem.* (2004), 11(16), 2161-2183.

Kontoghiorghes, G. J.;Eracleous. E, Economides C, Kolnagou A. *Curr. Med. Chem.* (2005);12;2663- 2681.

Krogstad DJ; Schlesinger PH. *N Eng. J. Med.* (1987), 317, 542-549.

Krogstad, D.J.; Schlesinger, P.H.; Gluzman, I.Y. *J. Cell Biol.* (1985), 101(6), 2302-9.

Kronbach T, Mathys D, Umeno M, Gonzalez, F.J**.,** *Mol. Pharmacol.* (1989), 36, 89-96.

Kruck, Theo P. A.; Burrow, Timothy E. *J. Inorg. Biochem.* (2002), 88(1), 19-24.

Kulkami AY; Yi H; Hopfinger AJ. *J. Chem. Inf. Comput. Sci.* (2002), 42; 331-342.

Kuter D. MSc Thesis (2009). University of Cape Town.

Leed A; Dubay K; Ursos LM; Sears D; De Dios AC; Roepe PD . *Biochemistry* (2002), 41 (32) 10245-10255

Leeson, P.D.; Springthorpe, B. *Nature Reviews Drug Discovery* (2007), 6(11), 881-890.

Lehane AM; Kirk K. *Antimicrob. Agents Chemother.* (2008), 52, 4374

Lin, T; Pan, K; Mordenti; Pan, L. *Journal of Pharmaceutical Sciences* (2007), 96(9), 2485-2493.

Lipinski C. A., Lombardo, F., Dominy B W., Feeney P. *J*., *Advanced drug Delivery Reviews*, (1997) 23, 3-25.

Lipinski, C.A. *Drug Discovery Today: Technologies* (2004), 1(4), 337-341.

Liu DY; Liu ZD; Lu SL; Hider RC. *J. Chromatogr* (1999) B, 730, 135-139.

Liu Z D; Khodr H H; Liu D Y; Lu S L; Hider R C. *J. Med. Chem.* (1999), 42(23), 4814-23.

Liu, Z.D.; Kayyali, R; Hider, R.C.; Porter, J.B.; Theobald, A.E. *J. Med. Chem.* (2002), 45(3), 631-639.

Liu, Zu D.; Piyamongkol, S.; Liu, Ding Y.; Khodr, Hicham H.; Lu, Shu L.; Hider, Robert C. *Bioorg. Med. Chem.* (2001), 9(3), 563-573

Lokaj J; Kozisek J; Koren B; Uher M; Vrabel V. *Acta Cryst*. (1991), C47, 193-194.

Loyevsky M, John C, Dickens B, Hu V, Gorduek V.R. *Mol Biochem. Parasitol.* (1999);101:43-59.

Loyevsky M, Lytton SD, Mester B, Libman J, Shanzer A, Cabantchik ZI.. *J Clin Invest* (1993); 91: 218-224.

Loyevsky M, Sacci JB Jr, Boehme P, Weglicki W, John C, Gorduek VR. *Exp. Parasitol* (1999a); 91:105-114.

Loyevsky,M and Gorduek, V.R. Iron chelators. In: Rosenthal PJ, MD. (ed). Antimalarial Chemotherapy: Mechanisms of Action , Resistance and New Directions in Drug Discovery, Totowa New Jersey: Humana Press,pp.307-346, 2001.

Lytton, S.D.; Mester, B; Libman, J; Shanzer, A; Cabantchik, Z. I. *Blood* (1994), 84(3), 910-15.

Ma, Y; Luo, W; Quinn, P.J.; Liu, Z; Hider, R.C. *J.Med. Chem.* (2004), 47(25), 6349-6362.

Mabeza G F; Loyevsky M; Gordeuk V R; Weiss G**.** *Pharmacol. Ther.* (1999), 81(1), 53-75.

Madden, J.C.; Cronin, M.T. D**.** *Expert Opinion on Drug Metabolism & Toxicology* (2006), 2(4), 545-557.

Makler M T; Ries J M; Williams J A; Bancroft J E; Piper R C; Gibbins B L; Hinrichs D J. *Am. J. Trop. Med. Hyg.* (1993), 48(6), 739-41.

Manohar, S; Khan, S I.; Rawat, DS. *Bioorg. Med. Chem. Lett.* (2010), 20(1), 322-325.

Mao, B; Gozalbes, R; Barbosa, F; Migeon, J; Merrick, S; Kamm, K; Wong, E; Costales, C; Shi, W; Wu, C; Froloff, N. *Journal of Chemical Information and Modeling* (2006), 46(5), 2125-2134.

March J; Smith MB. (2007). Advanced Organic Chemistry Reactions, Mechanisms and Structure 5th edition. Wiley InterScience, New Jersey. pp 11-42.

Margout, Delphine; Wein, Sharon; Gandon, Hermine; Gattacceca, Florence; Vial, Henri J.; Bressolle, Francoise M. M. (2009). *Journal of Separation Science*, 32(11), 1808-1815.

Marques, H.M., Voster K., Egan, T.J., *J. Inorg. Biochem.* (1996), 64, 7-23.

Martin RE; Marchetti RV; Cowan AI; Howitt SM; Broer S; Kirk K. *Science* (2010), 325, 1680-1682.

Martin SK; Oduola AMJ; Milhous WK. *Science* (1987), 235, 899-901.

Martin, R.E.; Kirk, K. *Mol. Biol. Evol.* (2004), 21(10), 1938-1949.

Martinez A; Rajapakse C.S.K; Naoulou B; Kopkali Y; Davenport L; Sanchez-Delgado R.A. *J. Biol Inorg Chem* (2008), 13, 703 – 712.

Matsumura, Y; Shirai, K; Maki, T; Itakura, Y; Kodera, Y. *Tetrahedron Lett.* (1998), 39(16), 2339-2340.

Meshnick S R. *Medecine Tropicale : revue du Corps de sante colonial* (1998), 58(3 Suppl), 13-7.

Meshnick SR; Yang Y-Z; Lima V; Kuypers F; Kamchonwongpaisan S; Yuthavong Y. Antimicrob. Agents Chemother. (1993), 37, 1108-1114.

Meshnick, S.R. (2002). *Int. Journal for Parasit*. 32: 1655-1660

Meunier B; Robert A. *Accounts of Chemical Research.* (2010), 43 (11) 1444 -1451

Miller, M.J. *Chem. Rev.* (Washington, DC, United States) (1989), 89(7), 1563-79.

Miller, M.J.; Malouin, F. *Accounts of Chemical Research* (1993), 26(5), 241-9.

Molenda, J.J; Basinger, M.A.; Hanusa, T.P.; Jones, M.M. *J. Inorg. Biochem.* (1994a), 55(2), 131-46.

Molenda, J.J; Jones, M.M.; Basinger, M.A. *J. Med. Chem.* (1994b), 37(1), 93-8.

Molenda, J.J; Jones, M.M.; Johnston, D.S.; Walker, E.M., Jr.; Cannon, D.J. *J. Med. Chem.* (1994c), 37(25), 4363-70.

Mollmann U; Heinisch L; Bauernfeind A; Kohler T; Ankel-Fuchs D *Biometals*: (2009), 22(4), 615-24.

Moore C.D, Shahrokh K, Sontum, S.F., Cheatam III, T.E., and Yost G.S. (2010) *Biochemistry*, 49, 9011-9019

Moore, C.D.; Shahrokh, K; Sontum, S.F.; Cheatham, T.E., III; Yost, G. S. *Biochemistry* (2010), 49(41), 9011-9019.

Moreau S; Perly B; Chachaty C; Deleuze C. *Biochemie* (1982), 64, 1015-1025.

Morris GM; Huey R; Pique M; Hart WL; Chang M; Gillet A; Forli S; Godsell DS; Olson AJ. (2008) AutoDock 4.2. Scripps Institute, La Jolla.

Murray MJ; Murray MB; Murray CJ. *Br. Med. J.* (1978), 2, 1113-1115.

Musonda, C.C.; Yardley, V; Carvalho de Souza, R.C.; Ncokazi K; Egan, T.J.; Chibale, K. *Organic & Biomolecular Chemistry* (2008), 6(23), 4446-4451.

Mzayek, Fawaz; Deng, Haiyan; Mather, Frances J.; Wasilevich, Elizabeth C.; Liu, Huayin; Hadi, Christiane M.; Chansolme, David H.; Murphy, Holly A.; Melek, Bekir H.; Tenaglia, Alan N.; Mushatt, David M.; Dreisbach, Albert W.; Lertora, Juan J. L.; Krogstad, Donald J. (2007), PLoS Clinical Trials 2(1),

Naude, B; Brzostowski, J.A.; Kimmel, A.R.; Wellems, T.E. *J. Biol. Chem.* (2005), 280(27), 25596-25603.

Navarro M; Vasquez F; Sanchez-Delgado RA; *J. Med. Chem*. (1997), 40, 1937-1939.

Navarro, M. *Coordination Chemistry Reviews* (2009), 253(112), 1619-1626.

Navarro, M; Perez, H; Sanchez-Delgado, RA. *J. of Med. Chem*. (1997), 40(12), 1937-1939.

Navarro, M; Vasquez, F; Sanchez-Delgado, RA.; Perez, H; Sinou, V; Schrevel, J. *J. Med. Chem.* (2004), 47(21),

Ncokazi K.K; Egan T.J. *Anal. Biochem.* (2005), 338(2), 306.

Nelson, W.O.; Karpishin, T.B.; Rettig, S.J.; Orvig, C. *Can. J. Chem.*(1988), 66(1), 123-31.

Nelson, W.O.; Rettig, S.J.; Orvig, C. *Inorg. Chem.* (1989), 28(16), 3153-7.

Nikam, Sham S.; Cordon, John J.; Ortwine, Daniel F.; Heimbach, Tycho H.; Blackburn, Anthony C.; Vartanian, Mark G.; Nelson, Carrie B.; Schwarz, Roy D.; Boxer, Peter A.; Rafferty, Michael F. (1999), *J. Med. Chem.* 42(12), 2266-2271.

Nosten F; ter Kuile F; Chongsuphajaisiddhi T; Luxemburger C; Webster H K; Edstein M; Phaipun L; Thew K L; White N J. *Lancet* (1991), 337(8750), 1140-3.

Novak I. *J. Org. Chem.*, (2004); 69: 5005-5010.

Novak, I; Harrison, L.J.; Kovac, B; Pratt, L.M.(2005) *J. Org. Chem.*.

Nuefeld EJ. *Blood.* 107, 3439-3441.

Obach SR (2007) Inhibition of drug Metabolizing Enzymes and Drug – Drug Interraction in Drug Discovery and Development. In: P. Li. (ed). Drug – Drug Interractions in Pharmaceutical Development.New Jersey, Wiley, pp. 76 – 91

Ocheskey, J.A.; Harpstrite, S.E.; Oksman, A; Goldberg, D.E.; Sharma, V. *Chemical Communications*, (Cambridge, United Kingdom) (2005), (12), 1622-1624.

Ocheskey, J.A.; Polyakov, V.R.; Harpstrite, S.E.; Oksman, A; Goldberg, D.E.; Piwnica-Worms, D; Sharma, V. *J. Inorg. Biochem.* (2003), 93(3-4), 265- 270.

Ohrt, C; Willingmyre, G.D.; Lee, P; Knirsch, C; Milhous, W. *Antimicrob. Agents Chemother.* (2002), 46(8), 2518-2524.

Oliveira M F; Silva J R; Dansa-Petretski M; de Souza W; Lins U; Braga C M; Masuda H; Oliveira P L**.** *Nature* (1999), 400(6744), 517-8.

Oliveira, M. F.; d'Avila, J. C. P.; Torres, C. R.; Oliveira, P. L.; Tempone, A. J.; Rumjanek, F. D.; Braga, C. M. S.; Silva, J. R.; Dansa-Petretski, M.; Oliveira, M. A.; de Souza, W.; Ferreira, S. T. *Mol. Biochem. Parasitol.* (2000), 111(1), 217-221.

Oliveira, M.F.; Kycia, S.W.; Gomez, A; Kosar, A.J.; Bohle, D. S; Hempelmann, E; Menezes, D; Vannier-Santos, M.A; Oliveira, P.L.; Ferreira, S.T. *FEBS Lett.* (2005), 579(27), 6010-6016.

Oliveira, M.F.; Timm, B.L.; Machado, A.; Miranda, K; Attias, M; Silva, J.R.; Dansa-Petretski, M; de Oliveira, M.A.; de Souza, W; Pinhal, N.M.; Sousa, J.J. F.; Vugman, N.V.; Oliveira, P.L. *FEBS Lett.* (2002), 512(1-3), 139-144.

Olliaro, PL.; Haynes, RK.; Meunier, B; Yuthavong, Y. *Trends in Parasitology* (2001), 17(3), 122-126

Olliaro P; Wells T.N.C. *Clinical Pharmacology and Therapeutics*, 85, 6, 584-595

Omara-Opyene, A. L; Moura, P.A.; Sulsona, C.R.; Bonilla, J. A; Yowell, C.A.; Fujioka, H; Fidock, D.A.; Dame, J.B. *J. Biol. Chem.* (2004), 279(52), 4088-54096.

O'Neill, P.M.; Bray, P.G.; Hawley, S.R.; Ward, S.A.; Park, B. K. *Pharmacol. Ther.* (1998), 77(1), 29-58.

O'Neill, P.M.; Willcock, D J; Hawley, S.R.; Bray, P.G.; Storr R.C; Ward, S.A.; Park, B. K. *J. Med. Chem.*(1997), 40, 437-448.

O'Neill, Paul M.; Shone, Alison E.; Stanford, Deborah; Nixon, Gemma; Asadollahy, Eghbaleh; Park, B. Kevin; Maggs, James L.; Roberts, Phil; Stocks, Paul A.; Biagini, Giancarlo; Bray, Patrick G.; Davies, Jill; Berry, Neil; Hall, Charlotte; Rimmer, Karen; Winstanley, Peter A.; Hindley, Stephen; Bambal, Ramesh B.; Davis, Charles B.; Bates, Martin; Gresham, Stephanie L.; Brigandi, Richard A.; Gomez-de-las-Heras, Federico M.; Gargallo, Domingo V.; Parapini, Silvia; Vivas, Livia; Lander, Hollie; Taramelli, Donatella; Ward, Stephen A. (2009). *J. Med. Chem*. 52(7), 1828-1844.

Pagola, S; Stephens, P.W.; Bohle, D. S; Kosar, A.D.; Madsen, S.K. *Nature* (London) (2000), 404(6775), 307-310.

Painter HJ; Morrisey JM; Mather MW; Vaidya AB. *Nature*. (2007) 446, 88 – 91.

Patel P., Oschinskiy, S., Koehler *J*., Zhang L., Vajjhala S., Philips C., Hobb*s,* S**.** *Journal of Association for Laboratory Automation* 9, 185-191.

Pattanapanyasat K, Thaithong S, Kyle DE, Udomsangpetch R, Yongvanichit K, Hider RC. *Cytometry* (1997);27 (Abstract).

Pattanapanyasat, K; Kotipun, K; Yongvanitchit, K; Hider, R.C.; Kyle, D.E.; Heppner, D. G; Walsh, D.S. *Southeast Asian J. Trop. Med. and Public Health* (2001), 32(1), 64-69.

Peters,W.; Ze-Lin, Li; Robinson, B. L.; Warhurst, D. C. *Ann. Trop. Med. Parasitol.* (1986),80(5), 483-9.

Petersen I; Eastman R Lanzer M. *FEBS Letters* (2011) 585, 1551-1562.

Phillipe, P., and Miller, R.S., (2002). *Lancet Infectious Diseases*., 2, 206–207.

Pisciotta, J.M.; Coppens, I; Tripathi, A.K.; Scholl, P.F.; Shuman, J; Bajad, S; Shulaev, V; Sullivan, D.J. *Biochem. J.l* (2007), 402(1), 197-204.

Pisciotta, J.M.; Ponder, E.L.; Fried, B; Sullivan, D. *Int. J. Parasitol.* (2005), 35(10), 1037-1042.

Pollack S, Flemming J. *Br. J. Haematol* (1984); 58: 289-293

Pollack S, Schnelle V. *Br. J. Haematol.* (1988); 68: 125-129

Porter J.B, Gyparaki M, Huehns E.R, Hider R.C. *Biochem Soc Trans* 1986;14:1180 (abstract)

Porter, J.B.; Hider, R.C.; Huehns, Ernst R. *Semin. Hematol.* (1990), 27(2), 95-100.

Posner G.H, Cumming J.N, Ploypradith P, Oh C.H. *J Am Chem Soc* 1995;117: 5885-5886.

Pooley, Sophie; Fatih, Farrah A.; Krishna, Sanjeev; Gerisch, Michael; Haynes, Richard K.; Wong, Ho-Ning; Staines, Henry M (2011) *Antimicrob. Agents Chemother*. 55(2), 550-556.

Pradines B; Ramiandrasoa F; Basco L K; Bricard L; Kunesch G; Le Bras. *Antimicrob. Agents Chemotherapy* (1996), 40(9), 2094-8.

Price, R.N., 2002. *Expert Opinion on Investigational Drugs.* 9,1815.

Puerta, DT.; Botta, M; Jocher, CJ.; Werner, EJ.; Avedano, S; Raymond, KN.; Cohen, SM. *J. Am. Chem. Soc*. (2006), 128(7), 2222-2223.

Rai, B.L.; Dekhordi, L.S.; Khodr, H; Jin, Y; Liu, Z; Hider, R.C. *J. Med. Chem.* (1998), 41(18), 3347-3359.

Raventos-Suarez C, Pollack S, Nagel R.L. *Am. J. Trop. Med. Hyg.* 1982; 31:919-922

Ray,S., *J. Med. Chem.* (2010), 53, 3685 – 3695.

Raynes K. *Int J. Parasitol*. (1999), 29, 367-379.

Raynes, Kaylene. *Int. J. Parasitol.* (1999), 29(3), 367-379.

Riley RJ; Parker AJ; Trigg S; Manners CN. (2001). *Pharmaceutical Research.* 18, 652-655

Riley, R.J.; Kenna, J. G. *Current Opinion in Drug Discovery & Development* (2004), 7(1), 86-99.

Roepe PD. *Biochemistry* (2011), 550, 163-171

Roosenberg II, J.M., Li Y., Lu Y., Miller MJ. *Curr. Med. Chem.* (2000), 7, 159 – 197

Rosenthal PJ (ed) Antimalarial Chemotherapy:mechanisms of action resistance and new directions in drug discovery. Humana press, New Jersey.

Rosenthal P.J., and Miller L.H. In Rosenthal P.J., (ed) Antimalarial Chemotherapy: mechanisms of action resistance and new directions in drug discovery. Humana press, New Jersey.pp 3-14

Rosenthal, P.J.; Sijwali, P.S.; Singh A; Shenai, B.R. *Curr. Pharm. Des.*(2002), 8(18), 1659-1672.

Rotheneder, A; Fritsche, G; Heinisch, L; Mollmann, U; Heggemann, S; Larcher, C; Weiss, G. *Antimicrob. Agents Chemother.* (2002), 46(6),

Russo, I; Babbitt, S; Muralidharan, V; Butler, T; Oksman, A; Goldberg, DE. *Nature* (London, United Kingdom) (2010), 463(7281), 632-636.

SAINT Version 7.60a, Bruker AXS Inc., Madison, WI, USA, 2006.

Sakurai H; Adachi, Y. *BioMetals* (2005), 18(4), 319-323.

Sanchez, C.P.; McLean, J.E.; Rohrbach, P; Fidock, D.A.; Stein .D.; Lanzer, M. *Biochemistry* (2005), 44(29), 9862-9870.

Sanchez, C.P.; Rohrbach, P; McLean, J.E.; Fidock, D.A.; Stein, W.D.; Lanzer, M. *Mol. Microbiol.* (2007), 64(2), 407-420.

Sanchez-Delgado R A ; Martinez A; Rajapakse CS K; Naoulou B; Kopkalli Y; Davenport L;. *J. Biol. Inorg. Chem* (2008), 13(5), 703-12.

Sanchez-Delgado, R.A.; Anzellotti, A. *Mini-Reviews in Medicinal Chemistry* (2004), 4(1), 23-30.

Sanchez-Delgado, RA.; Navarro, M; Perez, H; Urbina, J A. *J. Med. Chem*. (1996), 39(5), 1095-9.

Santos AM, Gil M, Marques S, Gano L, Cantinho G, Chaves S. *J. Inorg. Biochem.*. (2002); 92: 43-54.

Santos, M. A; Gil, M; Gano, L; Chaves, S. *J. Biol. Inorg. Chem.*(2005),

Scheibel LW, Rodriguez S. *Prog Clin Biol Res* (1989); 313: 119-149.

Scheibel LW, Stanton GG. *Mol. Pharmacol.* (1986);30:364-369.

Scott MD, Ranz A, Kuypers FA, Lubin BH, Meshnick SR . *Br. J. Haematol.*(1990)

Sendagire, H; Kaddumukasa, M; Ndagire, D; Aguttu, C; Nassejje, M; Pettersson, M; Swedberg, G; Kironde, F. *Acta Tropica* (2005), 95(3), 172-182.

Sergio Wittlin (2010), Swiss Institute of Tropical Health.

Sevrioukova, I.F.; Poulos, T.L. *Proc. Natl Acad. Sci.* (USA). (2010), 107(43), 18422-18427.

Shanzer A, Libman J, Lytton S.D, Glickstein H, Cabantchik Z.I. *Proc Natl Acad Sci USA* (1991);88:6585-6589.

Share, N.N. *J. Med Chem,* (1978), 22, 1:99-106.

Sharma, V; Piwnica-Worms, D. *Chem. Rev.* (Washington, D. C.) (1999), 99(9), 2545-2560.

Sharma, V; Piwnica-Worms, D; Sharma, V; Beatty, A; Goldberg, D E. *Chemical Communications* (Cambridge) (1997), (22), 2223-2224.

Sheldrick, G. M. SHELXS-97, SHELXL-97 and SADABS version 2.05, University of Göttingen, Germany, 1997.

Sherman IW. *Microbiol. Rev.* (1979), 43, 453-495.

Shou M (2007) Mechanism based CYP inhibition: Enzyme Kinetics, Assays and Prediction of Human Drug-Drug Interractions. In: P. Li. (ed). Drug – Drug Interractions in Pharmaceutical Development.New Jersey, Wiley, pp. 95– 108

Sidhu, A.B.S; Verdier-Pinard, D; Fidock, D.A. *Science* (Washington, DC, United States) (2002), 298(5591), 210-213.

Simpson, L; Rettig, S.J.; Trotter, J; Orvig, C. *Can. J. Chem.* (1991), 69(5), 893-900.

Slater AF, Cerami A. *Nature* (1992);355:167-169.

Solomon, V. R; Haq, W.; Srivastava, K; Puri, S.K.; Katti, S. B. *J. Med. Chem.*, (2007); 50(2): 394-398.

Spek, A.L. *J. Appl. Crystallogr*., (2003), 36, 7-13

Stahel, E; Mazier, D; Guillouzo, A; Miltgen, F; Landau, I; Mellouk, S; Beaudoin, R.L.; Langlois, P; Gentilini, M. *Am. J. Trop. Med. Hyg.* (1988), 39(3), 236-40.

Stenberg, Patric; Norinder, Ulf; Luthman, Kristina; Artursson, Per. *Journal of Medicinal Chemistry* (2001), 44(12), 1927-1937.

Stocks, PA.; Bray, PG.; Barton, V E.; Al-Helal, M; Jones, M; Araujo, NC.; Gibbons, P; Ward, SA.; Davies, J; Amewu, R; Mercer, A E.; Ellis, G; O'Neill, M. *Angewandte Chemie, International Edition* (2007), 46(33), 6278-6283.

Storr T, Mitchell D, Buglyo P, Thompson K.H, Yuen, G. V, McNeill J.H., Ovig C. *Bioconjugate Chem.* (2003)14, 212-221.

Stresser D.M., Blanchard, A.,P, Turner S.D, Erve J.C., Dandeneau A.A., Miller V.P, Crespi C.L., Charles L.(2000) *Drug. Metab. Disp*. 28 (12) 1440-1448

Su X; Kirkman LA; Fujioka H; Wellems TE. *Southeast Asia and Africa Cell*. (1997), 91, 593-603.

Sullivan, D.J. *Int. J. Parasitol.* (2002), 32(13), 1645-1653.

Tanaka, T; Okuda, T; Yamamoto, Y. *Chem.Pharm. Bull.* (2004), 52(7), 830-835.

Taylor W R; Richie T L; Fryauff D J; Picarima H; Ohrt C; Tang D; Braitman D; Murphy G S; Widjaja H; Tjitra E; Ganjar A; Jones T R; Basri H; Berman J. *Clin. Infect. Dis.*(1999), 28(1), 74-81.

Thomas G. (2003). Fundamentals of Medicinal Chemistry. W. Sussex, Wiley.

Thompson, K.H.; Barta, C.A.; Orvig, C. *Chem. Soc. Rev.* (2006), 35(6), 545-556.

Thompson, KH.; Chiles, J; Yuen, VG.; Tse, J; McNeill, JH.; Orvig, C. *J. Inorg. Biochem*. (2004), 98(5), 683-690.

Thompson, KH.; Liboiron, BD.; Sun, Y; Bellman, KD. D.; Setyawati, IA.; Patrick, B O.; Karunaratne, V; Rawji, G; Wheeler, J; Sutton, K; Bhanot, S; Cassidy, C; McNeill, JH.; Yuen, VG.; Orvig, C. *J. Biol. Inorg. Chem.* (2003), 8(1-2), 66-74.

Thuma PE, Mabeza GF, Biemba G, Bhat GJ, McLaren C, Moyo VM. *Trans R Soc Trop Med Hyg* (1998);92:214-218.

Thuma PE, Olivieri, NF, Mabeza GF, Biemba G, Parry D, Zulu S *et al*. *Am J Trop Med Hyg* (1998);58:358-364.

Tilley L ; Loria P; Foley M (2001) in Rosenthal PJ (ed) Antimalarial Chemotherapy:mechanisms of action resistance and new directions in drug discovery. Humana press, New Jersey. PP 87-121

Triglia T; Cowman AF. *Proc. Natl. Acad. Sci USA*. (1994), 91 (15) 7149-7153.

Tsafack A, Loyevsky M, Ponka P, Cabantchik Z.I. *J. Lab. Clin. Med.* (1996);127:575-582.

Ueng, Y, Kawabara T, Chu Y., Geungerich P.F.**.** *Biochemistry* (1997) 36 (2), 370-381.

Van de Waterbeemd, H; Gifford, E. *Nature Reviews Drug Discovery* (2003), 2(3), 192-204.

Van Schalkwyk, D.A.; Egan, T.J. *Drug Resistance Updates* (2006), 9(4-5), 211-226.

Van Zyl RL, Havlik I, Hempelman E, Macphail AP, McNamara L. *Biochem Pharmacol* (1993);45:1431-1436.

Vennerstrom, Jonathan L. (2011) Abstracts, 42nd Central Regional Meeting of the American Chemical Society, Indianapolis, IN, United States, June 8-10 ,2011.

Verdier F; Le Bras J; Clavier F; Hatin I; Blayo MC. *Antimicrob. Agents. Chemother.*(1985), 27, 561-564.

Verdonk, M.L. *Proceedings of the European Symposium on Structure-Activity Relationships (QSAR) and Molecular Modelling,* 15th, Istanbul, Turkey, Sept. 5-10, 2004 (2006), 265-269.

Vippagunta SR; Dorn A; Matile H; Bhattacharjee AK; Karle JM; Ellis WY; Ridley RG; Vennerstrom JL. *J. Med. Chem.* (1999), 42, 4630-4639.

Vogel I.A. Elemental Practical Organic Chemistry. Part 1:small scale preparations. (2004)CBS publishers New Delhi.

Von Kohler H., Eichler B, and Salewski R. *Z. anog. Chem,* (1970), 379, 183.

Von Wallenfels K., Friedrich, K., Reiser J., Ertel W, and Thieme H.K., *Angew. Chem. Internat.* Edn (1976), 15, 261.

Wang R.W, Newton D.J., Liu N., Atkins W.M., Lu A.Y.H.,. *Drug Metab. Disp*.(2000) 28, 360-366

Warhurst, D.C., *Biochem. Pharmacol.* (1981), 30, 3323-3327.

Watanabe, N; Nagasu, T; Katsu, K; Kitoh, K. *Antimicrob. Agents Chemother.* (1987), 31(4), 497-504.

Weinberg ED; Moon J. *Drug Met. Rev.* (2009) 41, (4) 644-662.

Weinberg, E.D.; Moon, J. *Drug Met. Rev.* (2009), 41(4), 644-662.

Weissbuch I; Leiserowitz L. *Chem. Rev.* (2008), 108(11), 4899-914.

Wellems TE; Panton LJ; Gluzman IY. *Nature* (1990), 345, 253-255.

Wellems, T.E., (2002). *Science* 298, 124-126.

Wells, T.N.C.; Alonso, P.L.; Gutteridge, W.E. *Nature Reviews Drug Discovery* (2009), 8(11), 879-891.

Wermsdorfer, W.H., (1994).*Acta Trop.,* 56, 143-156.

White, N. J. *Parasitologia* (Roma, Italy) (1999), 41(1-3), 301-308.

White, N. *Philosophical Transactions of the Royal Society of London, Series B: Biological Sciences* (1999), 354(1384), 739-749.

WHO. Antimalarial drug combination Therapy. Report of a Technical consultation. (2001) Geneva.

WHO. *Bull World Health Organ.*(1996), 74, 47-54

WHO. Guidelines on Treatment of Malaria, 2006. Geneva.

WHO., (2000). Bench aids for diagnosis of malaria infections. WHO. Geneva.

WHO., 1996. *Bull World Health Organ.,* 74, 47-54.

WHO.World Malaria www.who.int/malaria/wmr2008/malaria2008.pdf

Wiesner, J; Ortmann, R; Jomaa, H; Schlitzer, M. *Angewandte Chemie,* International Edition (2003), 42(43), 5274-5293.

Willairantana, P., Krudsood, S., prastertsuk, S., chalermrut, K., Looareeswan, S., (2002). *Archives of Medical Research* 33, 416-421.

Williams, P.A.; Cosme, J; Vinkovic, D.M; Ward, A; A, Hayley C.; Day, P.J.; Vonrhein, C; Tickle, I.J.; Jhoti, H. *Science* (Washington, DC, United States) (2004), 305(5684), 683-686

Winstanley, P.A., (2001). *The Lancet Infectious Diseases* 1, 243-250.

Winstanley, P.A., Ward, S.A., and Snow, R.W., (2002). *Microbes Infect* 4, 157.

Wipf P (1995) Handbook for Reagents for organic synthesis reagents for high throughput solid phase and solution phase organic synthesis. Vol. 6. John Wiley and sons. London. Pp. 162; 263; 276.

Wiwanitkit Viroj.,. *International Journal of General Medicine* (2010), 3 327-9.

Wongsrichanalai, C., Lin, K., Pang, L.W. (2001). *Am J Trop Med Hyg.* 65, 450-455.

Wongsrichanalai, C., Picker, L.A. Wernsdorfer, H.W., Meshnick. R.S., (2002). *The Lancet Infectious Diseases*. 2, 209-217.

World Bank . The World Bank Booster Report for Malaria Control in Africa (2007).

www.povray.org.

www.tulane.edu/~wiser/malaria/mal

Xiao, G; Van der Helm, D; Hider, R.C.; Dobbin, P.S. *Journal of the Chemical Society, Dalton Transactions: Inorganic Chemistry* (1972-1999) (1992), (22), 3265-71.

Xie, Y., jiang, Z. Zhou, H., Cai, X., Wong, Y., Liu, Z., Bain, Z., Xu, H., Liu, L., *J. of Pharmaceutical and Biomedical Analysis* (2007), 43, 204-212.

Yan Z and Yan GW. *Curr. Topics In Med Chem*.(2001), 1, 403-425.

Yan, Z; Caldwell, GW. *Current Topics in Medicinal Chemistry* (Hilversum, Netherlands) (2001), (5), 403-425.

Yano, J.K.; Wester, M.R.; Schoch, G.A.; Griffin, K.J.; Stout, C. D; Johnson, E.F. *J. Biol. Chem.* (2004), 279(37), 38091-38094.

Yayon, A.; Cabantchik, Z. I.; Ginsburg, H. *EMBO Journal* (1984), 3(11), 2695-700.

Yearick, K; Ekoue-Kovi, K; Iwaniuk, D.P.; Natarajan, J.K.; Alumasa, J; de Dios, A,C.; Roepe, P.D.; Wolf, C. *J. Med Chem.* (2008); 51(7): 1995-1998.

Yinnon A.M, Theanacho EN, Grady R.W, Spira D.T, Hershko C. *Blood* (1989);74:2166-2171.

Zahner H; Diddens H; Keller-Schierlein W; Nageli H U. *The Japanese Journal of Antibiotics* (1977), 30 Suppl 201-6.

Zaihui Z; Rettig, S.J.; Orvig, C. *Inorg. Chem.* (1991), 30(3), 509-15.

Zhou Shu-Feng. *Current Drug Metabolism* (2008), 9(4), 310-22.

Zlokarnik, G; Grootenhuis, P.D.J.; Watson, J.B. *Drug Discovery Today* (2005), 10(21), 1443-1450.

APPENDICES

Appendix 1

Antiplasmodial Data for Combinations of 2h and 1h with Chloroquine-Diphosphate or Dihydroartemisinin

Table A1.1

Table A1: *In vitro activity and FIC_{50} for different combinations of **2h** to CQ-DP*

Fraction of 2h	Fraction of CQDP	IC_{50} (µg/mL) against 3D7	IC_{50} (µg/mL) against K1	Σ FIC_{50} (3D7)	Σ FIC_{50} (K1)
1	0	3.512	3.306	1	1
0.788	0.211	0.183	0.095	0.043	0.08
0.647	0.353	0.036	2.281	0.007	2.81
0.476	0.524	0.02	0.18	0.003	0.30
0.35	0.65	0.012	0.388	0.0015	0.78
0.261	0.739	0.015	0.009	0.0017	0.02
0.18	0.82	0.04	0.831	0.0037	2.04
0.115	0.885	0.007	0.273	0.0005	0.72
0	1	20	0.3413	1	1

Table A1.2: *In vitro activity and FIC_{50} for different combinations of **1h** to CQ-DP*

Fraction of 1h	Fraction of CQ-DP	IC_{50} (µg/mL) against 3D7	IC_{50} (µg/mL) against K1	Σ FIC_{50} (3D7)	Σ FIC_{50} (K1)
1	0	20	20	1	1
0.833	0.277	0.32	2.659	11.09	2.70
0.7	0.3	0.045	1.778	1.69	1.94
0.524	0.476	0.058	1.608	3.46	2.74
0.455	0.545	0.033	3.028	2.25	5.88
0.283	0.717	0.009	0.586	0.81	1.49
0.18	0.82	0.003	0.343	0.31	0.99
0.11	0.89	0.013	0.311	1.45	0.98
0	1	0.008	0.284	1	1

Table A1.3: *In vitro activity and FIC_{50} for different combinations of **2h** and DHA*

Fraction of 2h	Fraction of DHA	IC_{50} (µg/mL) against 3D7	IC_{50} (µg/mL) against K1	ΣFIC_{50} (3D7)	ΣFIC_{50} (K1)
1	0	0.684	0.463	1	1
0.857	0.143	0.008	0.002	0.58	0.013
0.733	0.26	0.013	0.003	1.70	0.029
0.655	0.3448	0.001	0.0001	0.17	0.001
0.52	0.48	0.004	0.002	0.96	0.032
0.345	0.655	0.001	0.0001	0.33	0.001
0.286	0.714	0.003	0.002	1.07	0.046
0.133	0.866	0.002	0.0002	0.87	0.006
0	1	0.002	0.032	1	1

Table A1.4: *In vitro activity and FIC_{50} for different combinations of **1h** to DHA*

Fraction of 1h	Fraction of DHA	IC_{50} (µg/mL) against 3D7	IC_{50} (µg/mL) against K1	Σ FIC_{50} (3D7)	Σ FIC_{50} (K1)
1	0	8.55	0.716	1	1
0.89	0.11	0.002	0.003	0.0002	0.007
0.813	0.188	0.005	0.005	0.0005	0.017
0.636	0.364	0.019	0.003	0.0018	0.015
0.56	0.44	0.006	0.001	0.0005	0.006
0.41	0.59	0.003	0.001	0.0002	0.007
0.31	0.69	0.013	0.001	0.0009	0.008
0.14	0.86	0.029	0.007	0.002	0.072
0	1	20	0.857	1	1

Appendix 2

X-Ray Crystallography Data

Table A2.1. *Crystal data and structure refinement for* ***24****.*

Empirical formula	C28 H39 Cl N4 O6
Formula weight	563.08
Temperature	100(2) K
Wavelength	0.71073 A
Crystal syste*m,* space group	Triclinic, P-1
Unit cell dimensions	a = 9.5389(15) A alpha = 67.050(2) deg. b = 11.3729(17) A beta = 78.186(3) deg. c = 14.358(2) A gamma = 86.383(3) deg.
Volume	1403.7(4) A^3
Z, Calculated density	2, 1.332 Mg/m^3
Absorption coefficient	0.185 mm^-1
F(000)	600
Crystal size	0.17 x 0.16 x 0.15 mm
Theta range for data collection	1.94 to 28.39 deg.
Limiting indices	-12<=h<=12, -15<=k<=15, -19<=l<=19
Reflections collected / unique	22961 / 7020 [R(int) = 0.0389]
Completeness to theta = 28.39	99.5 %
Absorption correction	Semi-empirical from equivalents
Max. and min. transmission	0.9728 and 0.9692
Refinement method	Full-matrix least-squares on F^2
Data / restraints / parameters	7020 / 5 / 372
Goodness-of-fit on F^2	1.074
Final R indices [I>2sigma(I)]	R1 = 0.0579, wR2 = 0.1648
R indices (all data)	R1 = 0.0772, wR2 = 0.1790
Extinction coefficient	n/a
Largest diff. peak and hole	0.490 and -0.886 e.A^-3

Table A2.2. *Atomic coordinates (x 10^4) and equivalent isotropic displacement parameters (A^2 x 10^3) for* ***24****. U(eq) is defined as one third of the trace of the orthogonalized Uij tensor.*

	x	y	z	U(eq)	
Cl(1)	6001(1)	14554(1)	-987(1)	25(1)	
O(1)	-2793(2)	779(1)	6392(1)	22(1)	
O(2)	-108(2)	-29(1)	6458(1)	21(1)	
N(1)	3509(2)	11075(2)	-1429(1)	22(1)	
N(2)	2346(2)	8943(2)	1761(1)	21(1)	
N(3)	-578(2)	5565(2)	3204(1)	19(1)	
N(4)	442(2)	2792(2)	4046(1)	19(1)	
C(1)	3822(2)	11512(2)	-732(2)	19(1)	
C(2)	4594(2)	12688(2)	-1133(2)	20(1)	
C(3)	4967(2)	13152(2)	-472(2)	20(1)	
C(4)	4582(2)	12520(2)	606(2)	20(1)	
C(5)	3834(2)	11384(2)	1003(2)	19(1)	
C(6)	3442(2)	10845(2)	355(2)	17(1)	
C(7)	2697(2)	9632(2)	740(2)	18(1)	
C(8)	2391(2)	9220(2)	6(2)	22(1)	
C(9)	2819(3)	9959(2)	-1038(2)	23(1)	
C(10)	1569(2)	7721(2)	2182(2)	21(1)	
C(11)	-16(2)	7880(2)	2131(2)	22(1)	
C(12)	-720(3)	6654(2)	2247(2)	22(1)	
C(13)	-1311(3)	5812(2)	4110(2)	30(1)	
C(14)	-1194(2)	4433(2)	3176(2)	20(1)	
C(15)	-912(2)	3223(2)	4046(2)	18(1)	
C(16)	-2007(2)	2558(2)	4830(2)	19(1)	
C(17)	-1787(2)	1421(2)	5664(2)	18(1)	
C(18)	-320(2)	1041(2)	5641(2)	18(1)	
C(19)	737(2)	1715(2)	4841(2)	19(1)	
C(20)	1630(3)	3416(2)	3170(2)	27(1)	
C(21)	1335(2)	-392(2)	6550(2)	20(1)	
C(22)	1272(2)	-1556(2)	7539(2)	20(1)	
C(23)	84(3)	-1811(2)	8337(2)	25(1)	
C(24)	60(3)	-2872(2)	9254(2)	31(1)	
C(25)	1221(3)	-3672(2)	9375(2)	31(1)	
C(26)	2402(3)	-3422(2)	8583(2)	29(1)	
C(27)	2432(3)	-2364(2)	7662(2)	24(1)	
O(1A)	-6062(7)	5642(5)	4065(5)	128(2)	
C(1A)	-4868(5)	5089(5)	4024(4)	101(1)	
O(1B)	-4868(5)	5089(5)	4024(4)	101(1)	
C(1B)	-6062(7)	5642(5)	4065(5)	128(2)	
O(1W)	-5265(2)	2163(2)	6519(1)	40(1)	
O(2WA)	-4768(6)	-523(5)	5837(4)	42(1)	

O(3WA)	-3977(5)	-2618(5)	5361(4)	37(1)
O(2WB)	-4183(6)	-951(5)	5899(4)	42(1)
O(3WB)	-4497(7)	-3104(5)	5550(4)	51(1)

Table A2.3. *Bond lengths [A] and angles [deg] for* ***24****.*

Cl(1)-C(3)	1.744(2)	O(1)-C(17)	1.276(2)
O(2)-C(18)	1.360(2)	O(2)-C(21)	1.428(3)
N(1)-C(9)	1.325(3)	N(1)-C(1)	1.366(3)
N(2)-C(7)	1.345(3)	N(2)-C(10)	1.462(3)
N(2)-H(2N)	0.956(10)	N(3)-C(13)	1.466(3)
N(3)-C(14)	1.466(3)	N(3)-C(12)	1.472(2)
N(4)-C(15)	1.353(3)	N(4)-C(19)	1.371(3)
N(4)-C(20)	1.480(3)	C(1)-C(2)	1.419(3)
C(1)-C(6)	1.423(3)	C(2)-C(3)	1.362(3)
C(2)-H(2)	0.9500	C(3)-C(4)	1.407(3)
C(4)-C(5)	1.370(3)	C(4)-H(4)	0.9500
C(5)-C(6)	1.414(3)	C(5)-H(5)	0.9500
C(6)-C(7)	1.443(3)	C(7)-C(8)	1.395(3)
C(8)-C(9)	1.389(3)	C(8)-H(8)	0.9500
C(9)-H(9)	0.9500	C(10)-C(11)	1.525(3)
C(10)-H(10A)	0.9900	C(10)-H(10B)	0.9900
C(11)-C(12)	1.521(3)	C(11)-H(11A)	0.9900
C(11)-H(11B)	0.9900	C(12)-H(12A)	0.9900
C(12)-H(12B)	0.9900	C(13)-H(13A)	0.9800
C(13)-H(13B)	0.9800	C(13)-H(13C)	0.9800
C(14)-C(15)	1.509(3)	C(14)-H(14A)	0.9900
C(14)-H(14B)	0.9900	C(15)-C(16)	1.373(3)
C(16)-C(17)	1.419(3)	C(16)-H(16)	0.9500
C(17)-C(18)	1.436(3)	C(18)-C(19)	1.364(3)
C(19)-H(19)	0.9500	C(20)-H(20A)	0.9800
C(20)-H(20B)	0.9800	C(20)-H(20C)	0.9800
C(21)-C(22)	1.510(3)	C(21)-H(21A)	0.9900
C(21)-H(21B)	0.9900	C(22)-C(27)	1.388(3)
C(22)-C(23)	1.391(3)	C(23)-C(24)	1.393(3)
C(23)-H(23)	0.9500	C(24)-C(25)	1.383(4)
C(24)-H(24)	0.9500	C(25)-C(26)	1.381(4)
C(25)-H(25)	0.9500	C(26)-C(27)	1.395(3)
C(26)-H(26)	0.9500	C(27)-H(27)	0.9500
O(1A)-C(1A)	1.267(6)	O(1W)-H(1W2)	0.961(10)

O(1W)-H(1W1)	0.966(10)	O(2WA)-O(2WB)	0.713(5)
O(3WA)-O(3WB)	0.699(6)	C(18)-O(2)-C(21)	117.91(16)
C(9)-N(1)-C(1)	116.14(18)	C(7)-N(2)-C(10)	122.16(19)
C(7)-N(2)-H(2N)	119.2(19)	C(10)-N(2)-H(2N)	118.5(19)
C(13)-N(3)-C(14)	110.89(18)	C(13)-N(3)-C(12)	110.68(18)
C(14)-N(3)-C(12)	107.76(16)	C(15)-N(4)-C(19)	120.43(18)
C(15)-N(4)-C(20)	121.49(17)	C(19)-N(4)-C(20)	117.99(19)
N(1)-C(1)-C(2)	117.14(19)	N(1)-C(1)-C(6)	123.70(19)
C(2)-C(1)-C(6)	119.1(2)	C(3)-C(2)-C(1)	119.58(19)
C(3)-C(2)-H(2)	120.2	C(1)-C(2)-H(2)	120.2
C(2)-C(3)-C(4)	122.28(19)	C(2)-C(3)-Cl(1)	118.55(16)
C(4)-C(3)-Cl(1)	119.15(17)	C(5)-C(4)-C(3)	118.8(2)
C(5)-C(4)-H(4)	120.6	C(3)-C(4)-H(4)	120.6
C(4)-C(5)-C(6)	121.45(19)	C(4)-C(5)-H(5)	119.3
C(6)-C(5)-H(5)	119.3	C(5)-C(6)-C(1)	118.77(19)
C(5)-C(6)-C(7)	123.29(18)	C(1)-C(6)-C(7)	117.93(19)
N(2)-C(7)-C(8)	122.82(19)	N(2)-C(7)-C(6)	120.47(19)
C(8)-C(7)-C(6)	116.70(19)	C(9)-C(8)-C(7)	120.0(2)
C(9)-C(8)-H(8)	120.0	C(7)-C(8)-H(8)	120.0
N(1)-C(9)-C(8)	125.5(2)	N(1)-C(9)-H(9)	117.2
C(8)-C(9)-H(9)	117.2	N(2)-C(10)-C(11)	112.51(17)
N(2)-C(10)-H(10A)	109.1	C(11)-C(10)-H(10A)	109.1
N(2)-C(10)-H(10B)	109.1	C(11)-C(10)-H(10B)	109.1
H(10A)-C(10)-H(10B)	107.8	C(12)-C(11)-C(10)	112.45(18)
C(12)-C(11)-H(11A)	109.1	C(10)-C(11)-H(11A)	109.1
C(12)-C(11)-H(11B)	109.1	C(10)-C(11)-H(11B)	109.1
H(11A)-C(11)-H(11B)	107.8	N(3)-C(12)-C(11)	113.56(18)
N(3)-C(12)-H(12A)	108.9	C(11)-C(12)-H(12A)	108.9
N(3)-C(12)-H(12B)	108.9	C(11)-C(12)-H(12B)	108.9
H(12A)-C(12)-H(12B)	107.7	N(3)-C(13)-H(13A)	109.5
N(3)-C(13)-H(13B)	109.5	H(13A)-C(13)-H(13B)	109.5
N(3)-C(13)-H(13C)	109.5	H(13A)-C(13)-H(13C)	109.5
H(13B)-C(13)-H(13C)	109.5	N(3)-C(14)-C(15)	112.13(17)
N(3)-C(14)-H(14A)	109.2	C(15)-C(14)-H(14A)	109.2
N(3)-C(14)-H(14B)	109.2	C(15)-C(14)-H(14B)	109.2
H(14A)-C(14)-H(14B)	107.9	N(4)-C(15)-C(16)	119.89(18)
N(4)-C(15)-C(14)	119.13(18)	C(16)-C(15)-C(14)	121.0(2)
C(15)-C(16)-C(17)	122.8(2)	C(15)-C(16)-H(16)	118.6
C(17)-C(16)-H(16)	118.6	O(1)-C(17)-C(16)	123.7(2)
O(1)-C(17)-C(18)	121.60(18)	C(16)-C(17)-C(18)	114.67(18)
O(2)-C(18)-C(19)	124.6(2)	O(2)-C(18)-C(17)	114.52(17)
C(19)-C(18)-C(17)	120.88(18)	C(18)-C(19)-N(4)	121.3(2)
C(18)-C(19)-H(19)	119.4	N(4)-C(19)-H(19)	119.4
N(4)-C(20)-H(20A)	109.5	N(4)-C(20)-H(20B)	109.5
H(20A)-C(20)-H(20B)	109.5	N(4)-C(20)-H(20C)	109.5
H(20A)-C(20)-H(20C)	109.5	H(20B)-C(20)-H(20C)	109.5

O(2)-C(21)-C(22)	107.28(17)	O(2)-C(21)-H(21A)	110.3
C(22)-C(21)-H(21A)	110.3	O(2)-C(21)-H(21B)	110.3
C(22)-C(21)-H(21B)	110.3	H(21A)-C(21)-H(21B)	108.5
C(27)-C(22)-C(23)	119.6(2)	C(27)-C(22)-C(21)	119.5(2)
C(23)-C(22)-C(21)	120.9(2)	C(22)-C(23)-C(24)	120.1(2)
C(22)-C(23)-H(23)	120.0	C(24)-C(23)-H(23)	120.0
C(25)-C(24)-C(23)	120.1(2)	C(25)-C(24)-H(24)	119.9
C(23)-C(24)-H(24)	119.9	C(26)-C(25)-C(24)	119.9(2)
C(26)-C(25)-H(25)	120.1	C(24)-C(25)-H(25)	120.1
C(25)-C(26)-C(27)	120.3(2)	C(25)-C(26)-H(26)	119.8
C(27)-C(26)-H(26)	119.8	C(22)-C(27)-C(26)	120.0(2)
C(22)-C(27)-H(27)	120.0	C(26)-C(27)-H(27)	120.0
H(1W2)-O(1W)-H(1W1)	101(3)		

Table A2.4. *Anisotropic displacement parameters (A^2 x 10^3) for **24**. The anisotropic displacement factor exponent takes the form: -2 pi^2 [h^2 a*^2 U11 + ... + 2 h k a* b* U12]*

	U11	U22	U33	U23	U13	U12
Cl(1)	26(1)	16(1)	27(1)	-5(1)	0(1)	-5(1)
O(1)	21(1)	21(1)	18(1)	-2(1)	-2(1)	-5(1)
O(2)	22(1)	17(1)	19(1)	-1(1)	-5(1)	-1(1)
N(1)	24(1)	25(1)	19(1)	-9(1)	-6(1)	1(1)
N(2)	24(1)	16(1)	20(1)	-6(1)	-4(1)	-6(1)
N(3)	26(1)	13(1)	17(1)	-3(1)	-6(1)	-3(1)
N(4)	20(1)	16(1)	17(1)	-4(1)	-1(1)	-3(1)
C(1)	18(1)	18(1)	20(1)	-6(1)	-5(1)	2(1)
C(2)	20(1)	18(1)	19(1)	-4(1)	-2(1)	2(1)
C(3)	18(1)	12(1)	25(1)	-4(1)	-3(1)	-1(1)
C(4)	22(1)	17(1)	22(1)	-8(1)	-4(1)	-1(1)
C(5)	20(1)	17(1)	18(1)	-6(1)	-4(1)	0(1)
C(6)	17(1)	16(1)	19(1)	-7(1)	-3(1)	0(1)
C(7)	17(1)	17(1)	21(1)	-7(1)	-4(1)	1(1)
C(8)	23(1)	18(1)	27(1)	-11(1)	-6(1)	-2(1)
C(9)	25(1)	27(1)	24(1)	-14(1)	-9(1)	2(1)
C(10)	23(1)	15(1)	25(1)	-5(1)	-5(1)	-3(1)
C(11)	22(1)	15(1)	26(1)	-4(1)	-4(1)	-1(1)
C(12)	24(1)	16(1)	22(1)	-2(1)	-7(1)	-3(1)
C(13)	45(2)	23(1)	21(1)	-10(1)	-4(1)	-1(1)
C(14)	24(1)	15(1)	19(1)	-4(1)	-7(1)	-4(1)

C(15)	24(1)	14(1)	18(1)	-6(1)	-5(1)	-3(1)
C(16)	19(1)	18(1)	20(1)	-6(1)	-4(1)	-2(1)
C(17)	22(1)	16(1)	16(1)	-6(1)	-3(1)	-5(1)
C(18)	23(1)	15(1)	16(1)	-5(1)	-5(1)	-2(1)
C(19)	22(1)	16(1)	19(1)	-6(1)	-4(1)	-1(1)
C(20)	24(1)	23(1)	22(1)	-1(1)	3(1)	-2(1)
C(21)	21(1)	17(1)	19(1)	-6(1)	-4(1)	0(1)
C(22)	26(1)	17(1)	21(1)	-7(1)	-9(1)	-1(1)
C(23)	27(1)	23(1)	21(1)	-5(1)	-7(1)	2(1)
C(24)	34(1)	30(1)	23(1)	-2(1)	-7(1)	-4(1)
C(25)	39(1)	22(1)	30(1)	0(1)	-19(1)	-6(1)
C(26)	32(1)	20(1)	41(1)	-10(1)	-22(1)	3(1)
C(27)	25(1)	22(1)	29(1)	-12(1)	-10(1)	0(1)
O(1W)	45(1)	47(1)	21(1)	-9(1)	-6(1)	19(1)
O(2WA)	38(3)	38(3)	63(3)	-31(2)	-19(2)	5(2)
O(3WA)	41(3)	31(2)	36(2)	-5(2)	-15(2)	-12(2)
O(2WB)	39(3)	33(3)	57(3)	-21(2)	-12(2)	5(2)
O(3WB)	74(4)	45(3)	41(3)	-17(3)	-25(3)	9(3)

Table A2.5. *Torsion angles [deg] for* ***24.***

C(9)-N(1)-C(1)-C(2)	178.3(2)
C(9)-N(1)-C(1)-C(6)	-0.3(3)
N(1)-C(1)-C(2)-C(3)	-178.3(2)
C(6)-C(1)-C(2)-C(3)	0.4(3)
C(1)-C(2)-C(3)-C(4)	-1.6(3)
C(1)-C(2)-C(3)-Cl(1)	176.54(16)
C(2)-C(3)-C(4)-C(5)	1.5(3)
Cl(1)-C(3)-C(4)-C(5)	-176.60(17)
C(3)-C(4)-C(5)-C(6)	-0.3(3)
C(4)-C(5)-C(6)-C(1)	-0.8(3)
C(4)-C(5)-C(6)-C(7)	177.9(2)
N(1)-C(1)-C(6)-C(5)	179.4(2)
C(2)-C(1)-C(6)-C(5)	0.8(3)
N(1)-C(1)-C(6)-C(7)	0.5(3)
C(2)-C(1)-C(6)-C(7)	-178.07(19)
C(10)-N(2)-C(7)-C(8)	-2.1(3)
C(10)-N(2)-C(7)-C(6)	178.96(19)
C(5)-C(6)-C(7)-N(2)	-0.6(3)
C(1)-C(6)-C(7)-N(2)	178.2(2)
C(5)-C(6)-C(7)-C(8)	-179.6(2)
C(1)-C(6)-C(7)-C(8)	-0.8(3)
N(2)-C(7)-C(8)-C(9)	-178.1(2)

C(6)-C(7)-C(8)-C(9)	0.9(3)
C(1)-N(1)-C(9)-C(8)	0.4(4)
C(7)-C(8)-C(9)-N(1)	-0.7(4)
C(7)-N(2)-C(10)-C(11)	-75.1(3)
N(2)-C(10)-C(11)-C(12)	162.18(18)
C(13)-N(3)-C(12)-C(11)	63.2(3)
C(14)-N(3)-C(12)-C(11)	-175.41(19)
C(10)-C(11)-C(12)-N(3)	56.6(3)
C(13)-N(3)-C(14)-C(15)	-67.1(2)
C(12)-N(3)-C(14)-C(15)	171.61(19)
C(19)-N(4)-C(15)-C(16)	-2.0(3)
C(20)-N(4)-C(15)-C(16)	174.6(2)
C(19)-N(4)-C(15)-C(14)	178.21(19)
C(20)-N(4)-C(15)-C(14)	-5.3(3)
N(3)-C(14)-C(15)-N(4)	-68.8(3)
N(3)-C(14)-C(15)-C(16)	111.4(2)
N(4)-C(15)-C(16)-C(17)	0.5(3)
C(14)-C(15)-C(16)-C(17)	-179.69(19)
C(15)-C(16)-C(17)-O(1)	-178.8(2)
C(15)-C(16)-C(17)-C(18)	1.9(3)
C(21)-O(2)-C(18)-C(19)	7.6(3)
C(21)-O(2)-C(18)-C(17)	-173.47(18)
O(1)-C(17)-C(18)-O(2)	-1.2(3)
C(16)-C(17)-C(18)-O(2)	178.15(18)
O(1)-C(17)-C(18)-C(19)	177.8(2)
C(16)-C(17)-C(18)-C(19)	-2.9(3)
O(2)-C(18)-C(19)-N(4)	-179.52(19)
C(17)-C(18)-C(19)-N(4)	1.6(3)
C(15)-N(4)-C(19)-C(18)	0.9(3)
C(20)-N(4)-C(19)-C(18)	-175.7(2)
C(18)-O(2)-C(21)-C(22)	177.12(17)
O(2)-C(21)-C(22)-C(27)	158.3(2)
O(2)-C(21)-C(22)-C(23)	-23.3(3)
C(27)-C(22)-C(23)-C(24)	0.0(4)
C(21)-C(22)-C(23)-C(24)	-178.4(2)
C(22)-C(23)-C(24)-C(25)	0.3(4)
C(23)-C(24)-C(25)-C(26)	-0.4(4)
C(24)-C(25)-C(26)-C(27)	0.1(4)
C(23)-C(22)-C(27)-C(26)	-0.3(3)
C(21)-C(22)-C(27)-C(26)	178.2(2)
C(25)-C(26)-C(27)-C(22)	0.2(4)

Table A2.6. *Hydrogen bonds for* ***24*** *[A and deg.].*

D-H...A	d(D-H)	d(H...A)	d(D...A)	<(DHA)
N(2)-H(2N)...O(1)#1	0.956(10)	2.011(16)	2.908(2)	155(3)
O(1W)-H(1W1)...O(1)	0.966(10)	1.813(14)	2.767(3)	169(4)
O(1W)-H(1W2)...N(1)#2	0.961(10)	1.779(11)	2.740(3)	178(4)

Symmetry transformations used to generate equivalent atoms:#1 -x,-y+1,-z+1 #2 x-1,y-1,z+1